

GRANITIDS OF THE WESLEYVILLE AREA  
IN NORTHEASTERN NEWFOUNDLAND:  
A STUDY OF THEIR EVOLUTION  
AND GEOLGICAL SETTING

CENTRE FOR NEWFOUNDLAND STUDIES

**TOTAL OF 10 PAGES ONLY  
MAY BE XEROXED**

(Without Author's Permission)

N. R. JAYASINGHE





National Library of Canada  
Collections Development Branch

Canadian Theses on  
Microfiche Service

Bibliothèque nationale du Canada  
Direction du développement des collections

Service des thèses canadiennes  
sur microfiche

## NOTICE

The quality of this microfiche is heavily dependent upon the quality of the original thesis submitted for microfilming. Every effort has been made to ensure the highest quality of reproduction possible.

If pages are missing, contact the university which granted the degree.

Some pages may have indistinct print especially if the original pages were typed with a poor typewriter ribbon or if the university sent us a poor photocopy.

Previously copyrighted materials (journal articles, published tests, etc.) are not filmed.

Reproduction in full or in part of this film is governed by the Canadian Copyright Act, R.S.C. 1970, c. C-30. Please read the authorization forms which accompany this thesis.

THIS DISSERTATION  
HAS BEEN MICROFILMED  
EXACTLY AS RECEIVED

Ottawa, Canada  
K1A 0N4

## AVIS

La qualité de cette microfiche dépend grandement de la qualité de la thèse soumise au microfilmage. Nous avons tout fait pour assurer une qualité supérieure de reproduction.

S'il manque des pages, veuillez communiquer avec l'université qui a conféré le grade.

La qualité d'impression de certaines pages peut laisser à désirer, surtout si les pages originales ont été dactylographiées à l'aide d'un ruban usé ou si l'université nous a fait parvenir une photocopie de mauvaise qualité.

Les documents qui font déjà l'objet d'un droit d'auteur (articles de revue, examens publiés, etc.) ne sont pas microfilmés.

La reproduction, même partielle, de ce microfilm est soumise à la Loi canadienne sur le droit d'auteur, SRC 1970, c. C-30. Veuillez prendre connaissance des formules d'autorisation qui accompagnent cette thèse.

LA THÈSE A ÉTÉ  
MICROFILMÉE TELLE QUE  
NOUS L'AVONS REÇUE

GRANITOIDS OF THE WESLEYVILLE AREA IN NORTHEASTERN  
NEWFOUNDLAND: A STUDY OF THEIR EVOLUTION  
AND GEOLOGICAL SETTING

by

N.R. Jayasinghe, B.Sc., M.Sc.



A Thesis submitted in partial fulfillment  
of the requirements for the degree of  
Doctor of Philosophy

Department of Geology  
Memorial University of Newfoundland

July, 1979

St. John's

Newfoundland



## ABSTRACT

Granitic rocks occupy more than three quarters of the Wesleyville area. They consist of eight granitoids, namely, the Wareham Quartz Monzonite and the Cape Freels, Lockers Bay, Deadman's Bay, Newport, North Pond, Business Cove and Big Round Pond granites. The first five of these intrusions are megacrystic -- characterized by  $\geq 2$  cm long microcline crystals set in a finer grained "matrix". The North Pond and the Business Cove granites are garnetiferous, two-mica granites. The Big Round Pond pluton is a medium-grained biotite granite. Radiometric ages, field relationships and structural evidence indicate that the granitoids have been emplaced in the Silurian to Carboniferous times.

The country rocks of the granitoids are represented by two gneissic units: the Square Pond Gneiss and the Hare Bay Gneiss. The Square Pond Gneiss consists of psammitic to semi-pelitic gneiss, schist and metasediment with an eastward prograding metamorphism from greenschist to amphibolite facies. The Hare Bay Gneiss consists mostly of migmatite in the amphibolite facies. The contact between the two gneiss terrains is marked by a "migmatite front".

The gneisses have been deformed at least twice before the migmatization. The peak metamorphism and the migmatization have occurred during a third deformation event, the latter part of which has also included the emplacement of the Wareham, North Pond and the Business Cove plutons. A fourth deformation event has produced two major, north-northeast-trending sinistral shear zones in the area. The western one cuts through the North Pond, Wareham and the Lockers Bay plutons. The easterly shear zone has

deformed the western margin of the Cape Freels Granite and the adjacent Hare Bay Gneiss. Age relationships between these shear zones and the Dover Fault are not known. The Deadman's Bay Granite post-dates the shear zone and pre-dates a suite of north-south trending alkalic basalt dikes. The dikes are truncated by the Newport and the Big Round Pond granites.

Geochemical work indicates that the North Pond Granite could have been derived by the fractionation of feldspars and biotite from a Wareham Quartz Monzonite-type magma. The initial  $^{87}\text{Sr}/^{86}\text{Sr}$  ratios and the chemistry of the megacrystic granitoids and the Big Round Pond Granite suggest that they could have been produced by the partial melting of greywacke.

None of the plate-tectonic models so far proposed adequately explain the development of the Gander Zone. No new plate-tectonic model has been proposed in the present study but it adds a few more constraints to future plate-models dealing with the Gander Zone in Newfoundland.

ACKNOWLEDGEMENTS

Special thanks are due to Dr. A.R. Berger who supervised the thesis and who was a constant source of advice and encouragement throughout the study. T.J. Calon, B.J. Fryer, C.J. Hughes, V.S. Papezik, D.F. Strong, H. Williams and many others at Memorial University of Newfoundland are gratefully acknowledged for useful discussion and constructive criticism. R.V. Gibbons, I. Knight, S.P. Colmann-Sadd, R.F. Blackwood, B.F. Kean and K. Byrne at the Newfoundland Department of Mines and Energy are thanked for their cooperation.

T. Lomax and R. Parsons provided able assistance in the field; F. Thronhill, L. Warford, G. Ford and W. Marsh prepared thin sections and photographs; J. Vahtra, G. Andrews, D. Press, A. Thompson and H. Longerich assisted in analytical and computer work; G. Woodland and L. Murphy typed the final draft of the thesis; all of these are thanked for their help. My wife Shelia is thanked for her encouragement, for drafting the figures and for typing the early drafts of the thesis.

The work was carried out during the tenure of a Memorial University Fellowship. A part of the field work was supported by the Newfoundland Department of Mines and Energy.

## TABLE OF CONTENTS

	<u>Page</u>
ABSTRACT .....	ii
ACKNOWLEDGEMENTS .....	iii
LIST OF FIGURES .....	ix
LIST OF TABLES .....	xviii
CHAPTER 1 - INTRODUCTION .....	1
1.1 Access and topography .....	1
1.2 Geological setting .....	2
1.3 Previous work .....	7
1.4 Purpose of the present study .....	14
CHAPTER 2 - THE COUNTRY ROCKS .....	17
2.1 Square Pond Gneiss .....	17
2.1.1 Structural Geology .....	19
2.1.2 Petrography .....	26
2.1.3 Metamorphism .....	28
2.1.4 Chronological analyses of metamorphism and deformation .....	35
2.1.5 Geochemistry .....	44
a. Garnet-Biotite geothermometry .....	47
2.2 Hare Bay Gneiss .....	49
2.2.1 Structural Geology .....	50
2.2.2 Petrography .....	60
2.2.3 Metamorphism .....	62
2.2.4 Geochemistry and origin .....	64
2.3 Summary .....	69
CHAPTER 3 - INTRUSIVE ROCKS: GRANITOIDS AND GABBRO .....	71
3.1 Classification .....	72
3.2 Lithology of the megacrystic plutons .....	77
3.3 Descriptions of the individual plutons .....	82
3.3.1 Wareham Quartz Monzonite .....	82
a. Distribution and contact relationships .....	82
b. Lithology and structure .....	83
3.3.2 North Pond Granite .....	87
a. Distribution and contact relationships .....	87
b. Lithology .....	88
c. Structure .....	89

	<u>Page</u>
3.3.3 Business Cove Granite .....	94
a. Distribution and contact relationships .....	94
b. Lithology .....	95
c. Structure .....	95
d. Relationships between the fabrics in the Wareham, North Pond and Business Cove plutons .....	97
3.3.4 Cape Freels Granite .....	100
a. Distribution and contact relationships .....	100
b. Lithology .....	101
c. Structure .....	101
3.3.5 Lockers Bay Granite .....	107
a. Distribution and contact relationships .....	107
b. Lithology and structure .....	110
3.3.6 Deadman's Bay Granite .....	111
a. Distribution and contact relationships .....	111
b. Lithology and structure .....	115
3.3.7 Newport Granite .....	117
a. Distribution and contact relationships .....	117
b. Lithology .....	118
c. Structure .....	122
3.3.8 Big Round Pond Granite .....	123
a. Distribution and contact relationships .....	123
b. Lithology and structure .....	123
3.3.9 Gabbro .....	125
3.4 Deformation in the shear zones .....	125
3.4.1 Method .....	126
3.4.2 Results .....	128
3.5 Ages of the granitoids .....	136
3.6 Summary .....	143
CHAPTER 4 - THE MICROCLINE MEGACRYSTS .....	145
4.1 Structural state of the megacrysts .....	145
4.2 Chemical composition .....	150
4.3 Origin of the microcline megacrysts .....	155
4.4 Summary .....	163
CHAPTER 5 - THE DIABASE DIKES .....	164
5.1 Petrography .....	166
5.2 Chemistry .....	168
5.3 Origin and tectonic implications .....	172

	<u>Page</u>
CHAPTER 6 - GEOCHEMISTRY OF THE GRANITOIDS: A MAGMATIC ORIGIN .....	176
6.1 Major and minor element oxides and trace elements .....	176
6.2 Element ratios .....	206
6.3 Wareham Quartz Monzonite - North Pond Granite relationship .....	214
6.4 Genetic classifications of the granitoids based on their composition .....	227
6.4.1 I-type and S-type granitoids .....	227
6.4.2 Orogenic and non-orogenic granitoids .....	280
6.5 Summary .....	231
CHAPTER 7 - ORIGIN OF THE GRANITOIDS .....	233
7.1 Introduction .....	233
7.2 Differentiation of basaltic magma .....	234
7.3 Partial melting of mantle lithologies .....	234
7.4 Contamination of basaltic magma by sialic crustal rocks .....	237
7.5 Partial or complete melting of crustal rocks .....	239
7.6 Cause of the melting of the source rocks .....	245
7.7 H <sub>2</sub> O content: Crystallization sequence .....	248
7.8 The garnets and the muscovites: Leucogranites and megacrystic granites .....	256
7.9 Summary .....	261
CHAPTER 8 - SUMMARY, PLATE TECTONIC MODELS AND FUTURE WORK .....	262
8.1 Summary .....	262
8.1.1 Field relationships, rock types, metamorphism and structure .....	262
8.1.2 Geochemistry and the origin of the granitoids ...	267
8.2 Plate-tectonic models .....	268
8.3 Future work .....	271
REFERENCES .....	273
APPENDIX 1.1 .....	291
APPENDIX 2.1 .....	293
APPENDIX 3.1 .....	297
APPENDIX 3.2 .....	299
APPENDIX 3.3 .....	302
APPENDIX 4.1 .....	310



	<u>Page</u>
APPENDIX 4.2 .....	312
APPENDIX 6.1 .....	319
APPENDIX 6.2 .....	336
APPENDIX 7.1 .....	343
APPENDIX 8 .....	350

## LIST OF FIGURES

	<u>Page</u>
Figure 1.1 Tectonic stratigraphic zones of Newfoundland .....	4
2.1 General geology of the thesis area .....	18
2.2 Convolute lamination in the metasedimentary rocks ...	20
2.3 Profile of an $F_2$ fold .....	20
2.4 Stereoplot showing lineations, minor fold axes and poles to $S_2$ and $S_3$ structures in the Square Pond Gneiss .....	22
2.5 Traces of $S_1$ in $S_2$ in the Square Pond Gneiss .....	23
2.6 $F_2$ folds of $S_1$ in the Square Pond Gneiss .....	24
2.7 $S_2$ crenulation cleavage .....	24
2.8 $F_3$ folds in the Square Pond Gneiss .....	25
2.9 Granite sheet truncating $S_2$ in the Square Pond Gneiss .....	25
2.10 Photomicrograph showing garnets in a garnet- quartz layer .....	29
2.11 Photomicrograph of a mafic inclusion in the Square Pond Gneiss .....	29
2.12 ACF diagrams for the Square Pond Gneiss .....	31
2.13 Sketch map showing greenschist facies and amphibolite facies metamorphic rocks in the study area .....	32
2.14 Pressure-Temperature grid of some of the equilibrium curves mentioned in the text .....	34
2.15a Garnet porphyroclast with straight inclusion trails .....	36
2.15b Garnet porphyroblast with curved inclusion trails .....	36
2.15c Staurolite porphyroblasts with crenulated inclusion trails .....	37
2.15d Crenulated inclusion trails in a staurolite porphyroblast .....	37

(x)

	<u>Page</u>
Figure 2.15e Staurolite porphyroblast with straight inclusion trails .....	38
2.15f Helicitic inclusion trails in an andalusite porphyroblast .....	38
2.16 Inclusion trails in garnets on the limbs and the crest of an $F_3$ fold in a garnet-quartz layer .....	40
2.17 Schematic illustration of the interpreted progressive development of the fold shown in Fig. 2.16 .....	42
2.18 Graph showing possible chronological relationship between metamorphism and deformation phases in the Square Pond Gneiss .....	43
2.19 Composition of garnets in the Square Pond Gneiss ....	46
2.20 Composition of coexisting garnet and biotite in the Square Pond Gneiss. Plotted on Perchuck's (1970) graph .....	46
2.21 Hare Bay Gneiss on the northern shore of Indian Bay .....	51
2.22 $F_3$ folds in the Hare Bay Gneiss .....	53
2.23 Stereoplot showing minor fold axes, lineation and poles to $S_3$ , $S_4$ and crenulation cleavage in the Hare Bay Gneiss .....	55
2.24 Square Pond Gneiss inclusions in the Hare Bay Gneiss .....	56
2.25 $F_4$ folds in the Hare Bay Gneiss .....	56
2.26 Transposition of $S_3$ in the Hare Bay Gneiss .....	58
2.27 $F_3$ folds refolded by $F_4$ folds .....	58
2.28 Broad warps of $S_4$ in the Hare Bay Gneiss .....	59
2.29 Fibrolite in the Hare Bay Gneiss .....	63
2.30 ACF diagram for the Hare Bay Gneiss .....	63
2.31 Enrichment or depletion of major and minor element oxides and trace elements in the Hare Bay Gneiss relative to the Square Pond Gneiss .....	66

	<u>Page</u>
Figure 3.1 Modal classification of the granitoids according to Streckeisen (1973) .....	73
3.2 Normative classification of the granitoids according to Hietanen (1963) .....	74
3.3 Undeformed microcline megacrysts in the Cape Freels Granite .....	79
3.4 Clusters of microcline megacrysts in the Deadman's Bay Granite .....	79
3.5 Compositional zones in a microcline megacryst .....	81
3.6 An Apophysis of the Wareham Quartz Monzonite truncating $F_3$ folds in the Hare Bay Gneiss .....	81
3.7 A sphene grain in the Wareham Quartz Monzonite .....	84
3.8 Stereoplot showing poles to structures in the Wareham Quartz Monzonite .....	86
3.9 Folded gneissic xenolith in Wareham Quartz Monzonite .....	86
3.10 Apophyses of the North Pond Granite truncating $S_2$ and $S_3$ in the Square Pond Gneiss .....	89
3.11 The porphyritic phase and the medium-grained phase of the North Pond Granite .....	89
3.12 Stereoplot showing poles to structures in the North Pond Granite .....	92
3.13 $NP_1$ cutting across a pegmatite and $NP_1$ axial planar to a minor fold of a quartz vein in North Pond Granite .....	92
3.14 A xenolith of the Wareham pluton in the North Pond Granite .....	93
3.15 Feldspar alignment, $NP_2$ and crenulation cleavage in the North Pond Granite. Possible sense of shear along $NP_2$ .....	93
3.16 An apophysis of the Business Cove Granite truncating $D_3$ structures in the Hare Bay Gneiss .....	96
3.17 Pegmatites in the Business Cove Granite cut by $BC_1$ ...	96

	<u>Page</u>
Figure 3.18 Gneissic xenolith in the Business Cove Granite folded with sheets of the host .....	99
3.19 Schematic illustration of the emplacement of the Wareham, North Pond and Business Cove plutons and the development of $S_3$ , $W_1$ , NP and BC, during $D_3$ .....	99
3.20 Alignment of rectangular microcline megacrysts (CF.) in the Cape Freels Granite .....	103
3.21 Granitic minor intrusions in the Cape Freels Granite outside the shear zone .....	103
3.22 Deformed Cape Freels Granite .....	105
3.23 Stereoplot showing lineation related to $CF_2$ and poles to $CF_2$ and circulation cleavage in the Cape Freels Granite .....	106
3.24 Schematic diagram showing the difference in extension of feldspars on horizontal surfaces and vertical surfaces perpendicular to $S_4$ in Cape Freels Granite .....	108
3.25 Fold in mylonitized migmatite .....	108
3.26 Lockers Bay Granite .....	109
3.27 An apophysis of the Deadman's Bay Granite .....	112
3.28 "spotted" metasediments adjacent to the Deadman's Bay Granite .....	112
3.29 Andalusite porphyroblast overprinting microcrenul- ations ( $F_2$ or $F_3$ ) in the Square Pond Gneiss adjacent to the Deadman's Bay Granite .....	113
3.30 An apophysis of the Deadman's Bay Granite cutting a deformed ( $D_4$ ) megacrystic granite sheet in the Hare Bay Gneiss .....	113
3.31 Granophyric matrix in inclusions of chilled granite in the Deadman's Bay pluton .....	116
3.32 Remobilized Cape Freels Granite near the contact of the Newport pluton .....	116

	<u>Page</u>
Figure 3.33 A sheet-like xenolith of equigranular granite in the Newport pluton .....	119
3.34 Banding in hornblende monzodiorite patches in the Newport Granite .....	119
3.35 Plagioclase-rich patches in hornblende monzodiorite Newport pluton .....	121
3.36 Schematic interpretation of the development of round feldspar-rich patches shown in Fig. 3.35 .....	121
3.37 Contact of the Big Round Pond Granite cutting across microcline megacrysts in the Newport Granite .....	124
3.38 Subhedral quartz grains in the Big Round Pond Granite .....	124
3.39 The change in shape and orientation of an initial elliptical particle subject to a finite strain .....	127
3.40 Curves showing variation in $R_f/\phi$ for initial elliptical ratios ( $R_2$ ) subject to various finite strain ratios ( $R_5$ ) .....	127
3.41 Sketch map of the Cape Freels Granite showing location of strain analyses .....	129
3.42a $R_f/\phi$ diagrams for the locations within the shear zone .....	131
3.42b $R_f/\phi$ diagrams for the locations in the granite outside the shear zone .....	132
3.43 Axial ratios of the strain ellipsoid for three locations within the shear zone plotted on the Flinn diagram .....	133
3.44 Formation of conjugate shear fractures due to differences in lateral compression along a shear zone .....	133
3.45 Formation of secondary shear fractures oblique to primary shear fractures in a shear zone .....	135
3.46 (A) Diagram showing angular relationships between feldspar shape alignment, mylonitic foliation ( $S_4$ ) and circulation cleavage in the Cape Freels Granite .....	135



	<u>Page</u>
Figure 3.46 (B) Possible sense of shear along $S_4$ .....	135
3.47 The sequence of intrusive events in the area based on field relationships and structural evidence .....	138
3.48 Diagrammatic representation of the radiometric data from the granitoids in the area .....	141
4.1 $2\theta$ angles of the 060 and 304 diffractions of the microcline megacrysts plotted on a reference diagram from Wright (1968) .....	147
4.2 Diffractograms between $22.5^\circ$ and $24.5^\circ$ $2\theta$ (CuL ) for the megacrysts .....	149
4.3 Composition of feldspars from rock units in the area .....	152
4.4 Distribution of $K_2O$ , $Na_2O$ , $BaO$ and $CaO$ across a zoned microcline megacryst in the Newport Granite ...	153
4.5 Ba and Sr contents in feldspars from the Newport Granite .....	154
4.6 Microcline megacrysts overgrowing a gneissic xenolith in the Deadman's Bay Granite .....	156
4.7 Microcline megacrysts overgrowing a granitic minor intrusion in the Cape Freels Granite .....	156
4.8 Nucleation density and rate of growth of plagioclase, alkali feldspar and quartz in a synthetic granite composition .....	159
4.9 Albite content of plagioclase feldspars in the plutons plotted against that of coexisting potassium feldspars .....	161
5.1 Rose diagram shearing dominant trend of the diabase dikes .....	165
5.2 A diabase dike in the Deadman's Bay pluton .....	167
5.3 Plots of alkali versus silica and potash versus silica, of the diabase dikes .....	170
5.4 Plot of the dikes in $TiO_2 - K_2O - P_2O_5$ diagram .....	171
5.5 Plot of the dikes in the $(Ti/100) - Y \times 3 - Zr$ triangle .....	171

	<u>Page</u>
Figure 5.6 Plot of silica versus alumina of the pyroxenes from the dikes .....	174
5.7 Plot of $Al_2$ versus $TiO_2$ of the pyroxenes from the dikes .....	174
6.1 (a to k) Major and minor element variation diagrams .....	180 - 190
6.2 (a to m) Trace element variation diagrams .....	192 - 204
6.3 (a to e) K/Rb, Ba/Rb, Rb/Sr, Ba/Sr, and Sr.Ca ratios versus Thornton-Tuttle Differentiation Index .....	208 - 212
6.4 Analyses from the granitoids plotted in the $(Na_2O + K_2O) - FeO - MgO$ , (AFM) diagram .....	216
6.5 Analyses from the granitoids plotted in the $Al_2O_3 - FeO - MgO$ , (A'FM) diagram .....	218
6.6 Analyses from the granitoids plotted in the $CaO - FeO - MgO$ (CFM) diagram .....	220
6.7 The distribution of Ba, Sr and Rb between solid phase and melt .....	225
6.8 Schematic representation of the possible differentiation sequence that produced the North Pond Granite from a magma similar to the Wareham Quartz Monzonite in composition .....	226
6.9 Plots of $Na_2O$ vs. $K_2O$ and Mole $Al_2O_3/(Na_2O + K_2O + CaO)$ of the granitoids in the area .....	229
7.1 Diagram showing the melting behaviour of mantle compositions .....	236
7.2 $(Na_2O + K_2O)$ , $MgO$ , $TiO_2$ and $SiO_2$ contents in Mixtures between (1) basalt and granodiorite, (2) basalt and Hare Bay Gneiss .....	238
7.3 Hypothetical Ba and Sr contents of partial melts derived from the "average" greywacke in equilibrium with a solid phase containing plagioclase and biotite .....	243
7.4 Pressure and Temperature grid of some melting and reaction relations pertinent to the generation of the granitoids .....	246

	<u>Page</u>
7.5 Phase relationships in granitic melts at differing pressure, temperatures and $P_{H_2O}$ .....	250
7.6 Plutons represented in the $Q_3$ -Ab -Or -An - $H_2O$ system (5kb) .....	254
7.7 Compositions of the granitoid plotted in the (2Ca _ Na + K ) - Al - FM diagram .....	259
8.1 Relative time relationships between metamorphic deformational and intrusive vents in the area .....	266

## LIST OF TABLES

	<u>Page</u>
Table 2.1 Chemical analyses of the Square Pond Gneiss .....	45
2.2 Temperatures estimated using garnet-biotite pairs in the Square Pond Gneiss .....	48
2.3 Modal analyses of the Hare Bay Gneiss .....	61
2.4 Chemical analyses of the Hare Bay Gneiss .....	65
3.1 Modal analyses of the granitic plutons in the thesis area .....	75
3.2 Radiometric data from the granitoids in the thesis area .....	140
4.1 2 $\theta$ CuK values of the diffraction used in determining the structural state of the microcline megacrysts .....	146
5.1 Major and trace element contents and the CIPW norms of the diabase dikes .....	169
5.2 Analyses of the pyroxenes from the diabase dikes .....	173
6.1 Average compositions of the granitoids .....	177
6.2 Distribution coefficients used in the geochemical modelling .....	222
7.1 The degree of melting of the source rocks (greywacke) and the plagioclase and biotite contents in the residue required to produce the parent magmas of the plutons .....	242
7.2 Crystallization sequences in granitic melts at 5 and 8 kb and with varying H <sub>2</sub> O contents .....	251
7.3 Average compositions of the plutons expressed in terms of their normative (mesonorm) quartz, anorthite, albite and orthoclase contents .....	253

## CHAPTER I

### INTRODUCTION

The northeastern part of Newfoundland is characterized by a complex of metamorphic and granitic rocks. The present study deals with petrology, structure and petrogenesis of a number of these granitoids and their country rocks. However, the main emphasis in this study is the evolution of the granitoids in this part of Newfoundland.

The study area is covered by the Wesleyville, Musgrave Harbour (east half) and the St. Brendan's (northwest portion) map sheets (Nos. 2F/4, 2F/5 and 2C/13) of the Canadian National Topographic 1:50,000 series. Most of the conclusions and the descriptions in this thesis are based on work carried out in the Wesleyville and the east half of the Musgrave Harbour map areas. The writer has done only reconnaissance studies in the northwest portion of the St. Brendan's map area, where descriptions of the geology are based on reconnaissance studies by the writer and on detailed studies by Blackwood (1977).

#### 1.1. Access and Topography

The thesis area is accessible by Routes 320 and 330 which branch off the Trans-Canada Highway at Gambo and Gander, respectively. An older road between Indian Bay and Valleyfield and a number of logging roads provide further access within the area. Some of the area inland can be reached by canoe and all of the coastline is accessible by small boat.

The area has a subdued topography and for the most part lies below the 100 m contour. Away from the coast, especially in the southern

half of the area, scattered hills which may reach up to 200 m above sea level are present. Ponds and bogs of various sizes are common. The larger bogs generally have a convex surface due to the faster accumulation of organic debris in the poorly drained central parts, than in the better drained peripheral parts. Numerous small brooks drain the ponds and the bogs and contribute to four major streams, Anchor Brook, Windmill Brook, Northwest River and Indian Bay Brook. The drainage pattern is not generally influenced by bedrock structure. However, the coastline, especially in the southern part of the study area, is controlled by joints and minor shear zones; a number of long, deep bays (Loo Cove, Indian Bay and Trinity Bay) parallel the strikes of the latter.

The area shows effects of extensive glaciation. A veneer of till, variable in thickness covers much of the inland area. Boulder fields composed of erratics of local rock types are common, e.g. south of Ten Mile Pond and north and east of North West Pond. Glacial striations, roches moutonnees and crag and tail structures in the area indicate that the ice movement was from west to east.

An extensive forest fire in 1961 destroyed most of the vegetation in the area. Thus, apart from a few stream valleys and islands, it is not forested densely. At places, dead fall and secondary growth make traversing extremely difficult. Exposure near the coast, where vegetation is sparse, is excellent.

#### 1.2. Geological Setting

Newfoundland represents the northeast termination of the Appalachian Orogen which is continuous for 3000 km along the Atlantic



seaboard south to Alabama. Wilson (1966) suggested that the Appalachian Orogen developed through the opening and closing of an Early Paleozoic ocean named Iapetus by Harland and Geyer (1972).

In 1978, Williams divided Newfoundland into four major geologic divisions and extrapolated each division over the entire length of the Appalachian system. These broad divisions are distinguished from each other by differences in their Ordovician and/or earlier stratigraphy and structural history. From west to east, these divisions are: the Humber Zone, the Dunnage Zone, the Gander Zone, and the Avalon Zone (Figure 1.1). An additional zone, the Meguma Zone of the Nova Scotia, lies to the east of the Avalon Zone, in the northern Appalachians. The four zones in Newfoundland are described briefly below.

The Humber Zone consists of a Grenvillian continental basement of gneisses and granites. This is intruded by mafic dikes and is locally overlain by plateau basalts of Precambrian age (Williams and Stevens, 1969; Stukas and Reynolds, 1974). The mafic rocks are considered to indicate distension related to the development of Iapetus. The mafic rocks are overlain by a Late Precambrian - Early Cambrian sandstone and shale sequence and a prominent Cambrian-Ordovician carbonate succession. The latter passed upwards into Middle Ordovician flysch facies that immediately preceded the emplacement of a number of thrust slices from the east. Limestone breccia and shale that are contemporaneous with the autochthonous carbonate succession above, constitute the structurally lower slices. A variety of volcanic rocks, schists, gabbros, granites and ophiolites form the structurally higher slices (Williams, 1975). At places, Middle Ordovician limestones overlie the transported rocks and set an upper limit to their emplacement.

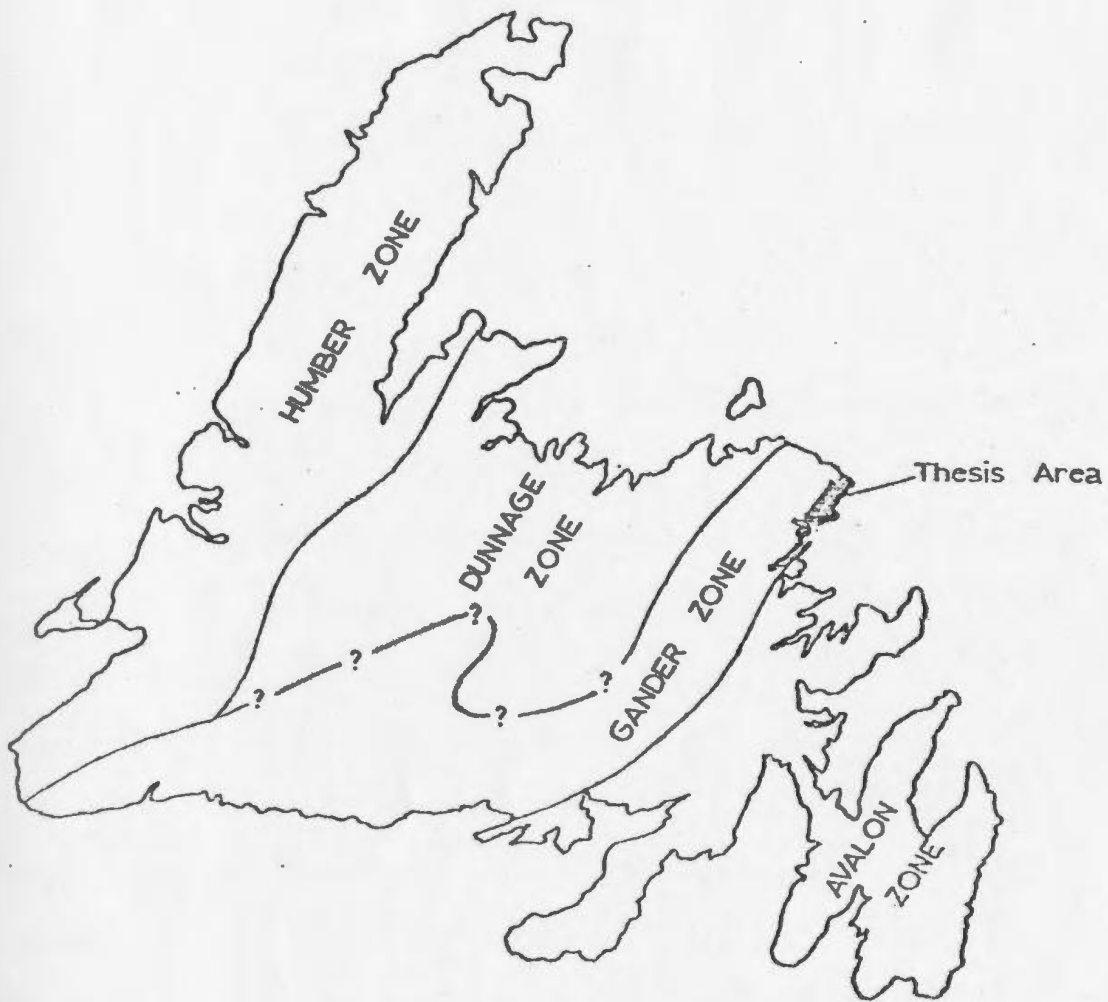


Fig. 1.1. Tectonic stratigraphic zones of Newfoundland (after Williams, 1978).

Toward the east, the autochthonous carbonate sequence is progressively more deformed and metamorphosed and it is bordered farther east by the polydeformed and metamorphosed Precambrian to Early Cambrian Fleur de Lys Supergroup. The eastern margin of the Humber Zone is defined by the Baie Verte - Brompton Line (Williams and St. Julien, 1978; Williams, 1979). This is a steep structural zone marked by deformed ophiolites. The eastern part of the zone is intruded by younger, Silurian-Devonian granitoids (Williams et al., 1974; Strong, 1979).

The Dunnage Zone mostly represents Ordovician oceanic crust and volcanic and sedimentary rocks that were deposited upon it. Fragments of the oceanic crust occur in the ophiolites within the zone (Upadhyay, Dewey and Bird, 1971). Volcanic rocks overlying the ophiolites consist of a pre-Caradocian early arc sequence and a post-Caradocian late arc sequence separated from each other by a Middle Ordovician and younger sedimentary sequence (Kean et al., in press). In places, the post-Caradocian volcanic rocks are overlain by Silurian sandstone and conglomerate. A belt of discontinuous basic-ultrabasic bodies, called the Gander River Ultrabasic Belt (Jenness, 1954), occurs in the eastern part of the zone. These basic-ultrabasic bodies have been interpreted as dismembered ophiolites (Williams, 1978, 1979; Currie et al., 1979). The Dunnage-Gander Zone boundary in Newfoundland is not very clear but has been considered to lie to the east of the Gander River Ultrabasic Belt.

The Dunnage Zone has been intruded by a variety of granitoids. They range from tonalitic to granitic in composition. The latter includes both peraluminous and peralkaline granites. The granitoids range from Ordovician to Jurassic in age but are predominantly of Silurian-Devonian age.

The Gander Zone consists of a gneissic, migmatitic terrain and a thick succession of polydeformed, psammitic and semipelitic meta-sedimentary rocks of pre-Middle Ordovician age called the Gander Group (McGonigal, 1973). The relationships between the metasedimentary rocks and the gneisses and migmatites are not well known. The gneisses and migmatites have been interpreted either as basement to the Gander Group (Kennedy and McGonigal, 1972; Kennedy, 1976; Blackwood, 1977) or as deeper, more highly metamorphosed levels of the metasediments (Jenness, 1963; Blackwood, 1978).

Granitoid rocks underlie about 50 percent of the Gander Zone in Newfoundland. These comprise two broad divisions: megacrystic granites<sup>1</sup> and biotite muscovite granites<sup>2</sup>. Despite arguments for a Precambrian age for some of the granitoids in the Gander Zone (Kennedy and McGonigal, 1972; Blackwood and Kennedy, 1975; Kennedy, 1975, 1976), radiometric dates from the plutons in the Gander Zone indicate that they were emplaced in Silurian-Devonian times (Bell, Blenkinsop and Strong, 1977; Bell *et al.*, 1979; see also Currie and Pajari, 1977).

The Avalon Zone is separated from the Gander Zone by the Dover-Hermitage Bay Fault (Blackwood and O'Driscoll, 1976). The Avalon Zone consists mainly of Late Precambrian volcanic and sedimentary rocks that can be divided into three broad groups: a lower assemblage of

---

<sup>1</sup>Characterized by microcline megacrysts greater than 2 cm in length, set in a finer-grained matrix of quartz, plagioclase, microcline and biotite.

<sup>2</sup>Also contain minor garnet. These rocks have been referred to as "leucogranites" by some authors (Williams, 1968; Strong, 1977, 1979).

predominantly volcanic rocks (Harbour Main and Love Cove groups), an intermediate assemblage of dominantly sedimentary rocks (Conception Group) and an upper assemblage of sedimentary and volcanic rocks (Cabot, Hodgewater and Musgravetown Groups). These are in places overlain by Cambrian and Ordovician shales and sandstones. The Avalon Zone is intruded by granitoids with either Precambrian or Devonian-Carboniferous ages (Strong, 1979).

The present thesis area lies in the northeastern corner of the Gander Zone (Figure 1.1). Approximately three-fourths of the area is underlain by granitoids, the remainder is occupied by gneisses and migmatites. The geology, good exposure and the easy accessibility makes the area an excellent place to study the evolution of granitoid rocks in northern Gander Zone.

### 1.3. Previous Work

In 1975, the writer mapped the coastal-strip between Lumsden and Trinity Bay in the present study area for an M.Sc. thesis at Memorial University of Newfoundland (Jayasinghe, 1976). The Cape Freels Granite was mapped and some of the other intrusions in the area and their country rock migmatites were partly mapped. The metamorphism and structure of the rocks were described and preliminary conclusions were drawn on their geologic history. Results of this study formed the basis of a research paper (Jayasinghe and Berger, 1976). In 1976 and 1977, the writer completed the mapping of Wesleyville and Musgrave Harbour (East half) map area. The result of this is a 1:50,000 scale geologic map and a short report (Jayasinghe, 1978a). A swarm of diabase dikes that occur in the eastern part of the study area was studied in detail in 1978 (Jayasinghe, 1978b). Conclusions and some of the data in these

studies are discussed in the following chapters. Brief descriptions of previous and current geological studies in the area by others are given below.

The first systematic study in the area was done by Jenness who mapped a large area to the south of the Wesleyville map sheet (Jenness, 1963). Jenness named the metasediments, gneisses and migmatites that underlie the northern Gander Zone as the Gander Lake Group and interpreted them as a conformable sequence that underwent metamorphism prograding eastward. The Group was divided into three broad units, from west to east, the Upper Unit, the Middle Unit and the Lower Unit. Based on brachiopods and graptolites in the Middle and Upper units, Jenness assigned a Middle Ordovician age to the Gander Lake Group.

Jenness considered the granitoid plutons intruding the Gander Lake Group as granitized equivalents of the Lower Unit and the Love Cove Group (a thick sequence of Precambrian volcanic rocks and volcaniclastic sediments in the Avalon Zone) or as apophyses of a large granitic intrusion, the Ackley Batholith, which occurs farther to the south. Based on a few K/Ar age determinations, Jenness assigned a Devonian age to the plutons.

In 1968, Williams mapped the Wesleyville and the Musgrave Harbour east map area. He showed that the area is underlain by sedimentary rocks, metasediments, migmatites and granites. The sedimentary rocks were noted to occur in the southwest corner of the map area succeeded by metasediments and migmatites respectively to the east. The sedimentary rocks and the metasediments were found to continue



southwards into the Lower Unit of Gander Lake Group (Jenness, 1963). The migmatites were regarded to have formed by migmatization of meta-sediments under the influence of the granites.

Williams recognized two main types of granites in the area; porphyritic biotite granites and garnetiferous muscovite leucogranites. He noticed sheets of garnetiferous leucogranites intruding the porphyritic biotite granites and concluded that the latter must be the older of the two. He found areas of both foliated and unfoliated porphyritic granites and concluded that these granites were emplaced during more than one intrusive event. On the basis of field relationships and isotopic dates in adjoining map-areas (Jenness, 1963; Williams, 1964), all the plutons in the area were assigned a Devonian age.

Younce in 1970 mapped the southeastern corner of the thesis area as a part of a Ph.D. study at Cornell University. The migmatites and the granites of the Gander Lake Group were found to be separated from the sedimentary and volcanic rocks of the Love Cove Group and the Musgravetown Group to the east, by a zone of mylonites and brecciation which he called the Dover Fault. He related the granites in his study area to the Ackley Batholith.

Kennedy and McGonigal (1972) studied rocks farther to the west and southwest of the present thesis area. This study formed a part of an M.Sc. thesis at Memorial University (McGonigal, 1973). They observed that the changes in metamorphic grade and structural complexity across the Gander Lake Group are not gradational as proposed by Jenness (1963) but occur at two distinct "levels". Thus, they divided the Gander Lake Group into three distinct divisions, named respectively from east to west

the gneissic terrane, the metasedimentary terrane and the sedimentary and volcanic terrane. The gneissic terrane was considered to be unconformably overlain by the metasedimentary terrane which in turn was regarded to be unconformably overlain by or separated by a melange zone from the sedimentary and volcanic terrane. They referred to the metasedimentary terrane as the Gander Lake Group and to the Middle Ordovician sedimentary and volcanic terrane as the Davidsville Group.

Kennedy and McGonigal found garnetiferous leucogranites intruding the metasedimentary terrane as pre-tectonic pre-Middle Ordovician intrusions. Since garnetiferous leucogranite sheets cut the porphyritic biotite granites in the Wesleyville area (Williams, 1968), this discovery led Kennedy and McGonigal to suggest that both the leucogranites and the megacrystic granites in the northern Gander Zone are pre-Middle Ordovician in age.

Brückner (1972) pointed out that use of the name "Gander Lake Group" by Kennedy and McGonigal for a redefined part of the original Gander Lake Group of Jenness (1963) violated a section of the American Commission of Stratigraphic Nomenclature. Consequently, McGonigal (1973) renamed the reduced Gander Lake Group, the Gander Group.

Blackwood and Kennedy (1975) studied the shores of Freshwater Bay just to the south of the present study area. They referred to the gneissic terrane of Kennedy and McGonigal (1972) as the Bonavista Bay Gneiss Complex. They also partly mapped and named a deformed, megacrystic microcline granite intruding the gneiss complex, the Lockers Bay Granite. They described the Dover Fault as a 300-500 m wide mylonitic zone that separates the Gander Zone from the Avalon Zone,

in northeast Newfoundland. Blackwood and Kennedy correlated the mylonitic foliation in the fault zone with the steep northeasterly trending foliation in the Bonavista Bay Gneiss Complex, the Lockers Bay Granite and in the Precambrian Love Cove Group of the Avalon Zone.

Blackwood in 1976 divided the Bonavista Bay Gneiss complex into two main north-northeast trending belts that are separated from each other by a "migmatite front". The western belt consisting of "paragneisses" was called the Square Pond Gneiss and the eastern belt consisting of "granitic gneisses" was called the Hare Bay Gneiss. A part of the latter was referred to as the Traverse Brook Gneiss. Based on structural evidence he interpreted the age of the Lockers Bay Granite as Precambrian.

In 1977, Blackwood mapped the Gambo and the northwestern part of the St. Brendan's map area. He confirmed Kennedy and McGonigal's idea (Kennedy and McGonigal, 1972) that the Gander Group forms a cover sequence to the gneissic rocks. The term Traverse Brook Gneiss was abandoned and the rocks that were placed under it were included in the Hare Bay Gneiss. He described the Hare Bay Gneiss as a "complexly folded, banded, tonalitic orthogneiss and migmatite" and the Square Pond Gneiss as a "grey, thinly banded, psammitic gneiss". Subsequently, working in an area farther to the west, he changed his previous idea and accepted the conclusion reached by Jenness fifteen years before that the Gander Group, Square Pond Gneiss and Hare Bay Gneiss constitute a conformable sequence which underwent prograde metamorphism from west to east (Blackwood, 1978).

Strong et al., in 1974, included samples from granitoid bodies in the present thesis area in an extensive geochemical survey of granitic

rocks in northeastern Newfoundland. Two of the granites in the area were named the Cape Freels Granite and the Newport Granite. All the other granitoids in the area were grouped under the term Deadman's Bay Granite. Dickson (1974) described the chemistry and petrography of some of the granitoid intrusions in the area. Based on an eastward  $K_2O$  increase in the granitoid plutons and metal zonation in northeastern Newfoundland, Strong et al. (1974) and Dickson (1974) attributed the origin of the granites to processes related to an eastward dipping Paleozoic subduction zone. Later, Strong and Dickson (1978) indicated that granitoid intrusions in the Gander Zone resulted by anatexis of crustal rocks. The garnetiferous muscovite biotite leucogranites were regarded as water-rich anatectic melts of crustal rocks and were considered to be unrelated to the megacrystic granites.

Kennedy (1975) proposed that the Gander Group and the Bonavista Bay Gneiss Complex were deformed and metamorphosed by a Late Hadrynian event which he referred to as the Ganderian Orogeny. The Ganderian Orogeny was attributed to activity within a continental margin, involving opening and subsequent closure of a marginal basin. The granites in the Gander Zone were considered to have formed by the partial melting of the Bonavista Bay Gneiss Complex as a result of processes associated with a subduction zone. He implied that the granites are Precambrian in age.

Wanless et al. (1965) obtained a K/Ar date of  $335 \pm 14$  m.y. from biotites in the Deadman's Bay Granite. Their sample location ( $49^{\circ}13'20''N$ ,  $54^{\circ}03'75''W$ ) lies slightly outside the present thesis area.

In 1969, Fairbairn and Berger obtained a tentative Rb/Sr whole-rock isochron date of 600 m.y. for the Deadman's Bay pluton. Cormier (in Kennedy, 1975) recalculated their data to produce an age of  $580 \pm 120$  m.y. Berger and Naylor (1974) reported a few preliminary zircon dates ranging from  $510 \pm 10$  to  $385 \pm 10$  m.y. for the same pluton. However, owing to the preliminary nature of the studies, not much significance could be attached to the above Rb/Sr and zircon dates.

In 1975, Bell and Blenkinsop obtained a Rb/Sr whole-rock isochron date of  $400 \pm 15$  m.y. from the Cape Freels Granite. Later, Bell *et al.* (1977) refined this date to  $400 \pm 5$  m.y. and reported a  $^{87}\text{Sr}/^{86}\text{Sr}$  initial ratio of  $0.7078 \pm 0.008$  for the granite. Bell and Blenkinsop (1977) reported a whole-rock isochron age of  $300 \pm 18$  m.y. and a  $^{87}\text{Sr}/^{86}\text{Sr}$  initial ratio of  $0.7146 \pm 0.0013$  for the Lockers Bay Granite which they reaffirmed in 1978 (K. Bell, 1978, personal communication) after analysing additional rock and mineral samples from the pluton. Bell *et al.* (1979) obtained a Rb/Sr whole-rock isochron age of  $332 \pm 42$  m.y. and a  $^{87}\text{Sr}/^{86}\text{Sr}$  initial ratio of  $0.7059 \pm 0.002$  for the Newport Granite. All of the above dates have been calculated with a decay constant of  $1.47 \times 10^{-11} \text{ yr}^{-1}$  for  $^{87}\text{Rb}$ .

The area has not been examined in detail for mineralization. Gale (1967) assessed the economic potential of the pegmatites in the area. He found that most of the pegmatites especially in the eastern part of the area carry beryl and chrysoberyl in quantities of no present economic value.

#### 1.4. Purpose of the Present Study

Previous studies have indicated that the area has a complex structural and intrusion history. However the detailed structural and intrusive sequence in the area is not known. Furthermore, none of the granitoids in the area has been completely mapped. This has led to serious complications. For example, Strong *et al.* (1974) and Dickson (1974) considered a number of chronologically and lithologically different plutons as belonging to one intrusion, and names and boundaries of some of the plutons have been changed repeatedly (Jayasinghe and Berger, 1976; Jayasinghe, 1978). In addition, the origin of the granitoids or the genetic relationships between the biotite muscovite granites and the megacrystic granites in the area is not very clear. Therefore the principal aims of this study are:

1. to produce a detailed geological map of the area,
2. to establish the detailed metamorphic, structural and intrusive sequence in the area,
3. to determine the origin of the granitoids, and
4. to investigate the genetic relationship between the biotite muscovite granites and the megacrystic granites in the area.

It is hoped that this study would throw light on similar problems in other parts of the Gander Zone. However, before proceeding to the subsequent chapters, the general geology of the area is outlined below.

#### 1.5. Brief Outline of Geology

The thesis area is underlain by metasediments<sup>1</sup>, schists<sup>1</sup>,

gneisses<sup>1</sup>, migmatites<sup>1</sup> and granitic bodies (see geological map in back pocket). The metasediments, schists, and the gneisses occur in the southwestern part of the area and are a continuation of Blackwood's (1977) Square Pond Gneiss<sup>2</sup>. The migmatites occur to the east of the Square Pond Gneiss and are a continuation of Blackwood's (1977) Hare Bay Gneiss.

The contact between the Square Pond Gneiss and the Hare Bay Gneiss in the thesis area is gradational and represents a "migmatite front". The migmatites contain numerous inclusions of the Square Pond Gneiss lithologies.

At least three major deformations can be recognized in the Square Pond Gneiss and two can be seen in the Hare Bay Gneiss. The metamorphic grade in the Square Pond Gneiss increases from greenschist facies in the west to amphibolite facies in the east. The Hare Bay Gneiss has an amphibolite facies metamorphic grade.

There are nine main granitic intrusions in the area. Most of them occur within the Hare Bay Gneiss. Five of these intrusions, the Wareham Quartz Monzonite and the Lockers Bay, Cape Freels, Deadman's Bay

---

<sup>1</sup>In this thesis the terms schist, gneiss, and migmatite are used in the context of the definitions given in the Glossary of the American Geological Institute. See Appendix 1.1 for definitions. The term metasediment refers to a sedimentary rock without foliation and/or banding but shows evidence of having been subject to metamorphism.

<sup>2</sup>The terms Square Pond Gneiss and Hare Bay Gneiss are used here in the sense of Blackwood (1977). These units do not consist entirely of gneisses, but no attempt is made to rename them on the basis of their dominant lithology due to two main reasons: (1) the areas of the Square Pond Gneiss and the Hare Bay Gneiss studied by Blackwood are much larger than those included in the present thesis area, and (2) the terms Square Pond Gneiss and the Hare Bay Gneiss have already been accepted and have appeared in a number of publications on the geology of northern Gander Zone and renaming of these units may lead to confusion.

and the Newport granites are characterized by microcline megacrysts<sup>1</sup>. Two of the remaining plutons, the North Pond and the Business Cove granites, are characterized by the presence of muscovite and sporadic garnets. The other, the Big Round Pond pluton consists dominantly of medium-grained biotite granite.

The Wareham, North Pond and the Cape Freels plutons have been partly deformed by two north-northeast trending shear zones which post-date a northeast trending mineral alignment in parts of the North Pond and the Business Cove granites. The Deadman's Bay, Newport and the Big Round Pond granites do not have penetrative mineral alignments.

A north-south trending swarm of diabase dikes pre-dates the Newport and the Big Round Pond granites and post-dates all the other plutons in the area. A few small gabbros occur associated with the granitoids.

In the following chapters, firstly the structure and the metamorphism of the country rocks of the granitoids are described; secondly, the petrology and the structure of the granitoids are discussed. The later chapters deal with the geochemistry and the origin of the granitoids.

---

<sup>1</sup> In this study the term megacrysts refers to crystals greater than 2 cm in length, set in a finer grained "matrix".



## CHAPTER 2

### THE COUNTRY ROCKS

The pre-granite emplacement rock types in the area are represented by two gneissic units: the Square Pond Gneiss and the Hare Bay Gneiss (Figure 2.1). They have suffered a complex history of deformation and metamorphism. It is the aim of this chapter to unravel this history in order to establish the period of granite emplacement relative to the structural and metamorphic events in the area.

#### 2.1. Square Pond Gneiss

The Square Pond Gneiss consists mainly of grey, medium grained gneiss. Associated with the gneiss are areas of schists and psammitic metasediments. The schists are common in the eastern part of the gneiss terrane and the psammites are common in the west, especially to the east and north of First Pond in the southwest corner of the Wesleyville map area.

The gneissic rocks are characterized by a 1 to 3 mm wide banding produced by alternating quartz-rich layers and micaceous layers. The latter are always thinner than the former. The schists are rich in biotite and usually contain coarse, dark brown staurolite and pink to grey andalusite. Also present in the schists are 0.5 to 2 cm wide greyish-pink bands composed wholly of fine grained quartz and garnet in the ratio of about 60:40. The psammitic metasediments are mostly massive but in places have a weak banding produced by thin (< 1 mm) discontinuous mica films separating thicker psammitic layers.

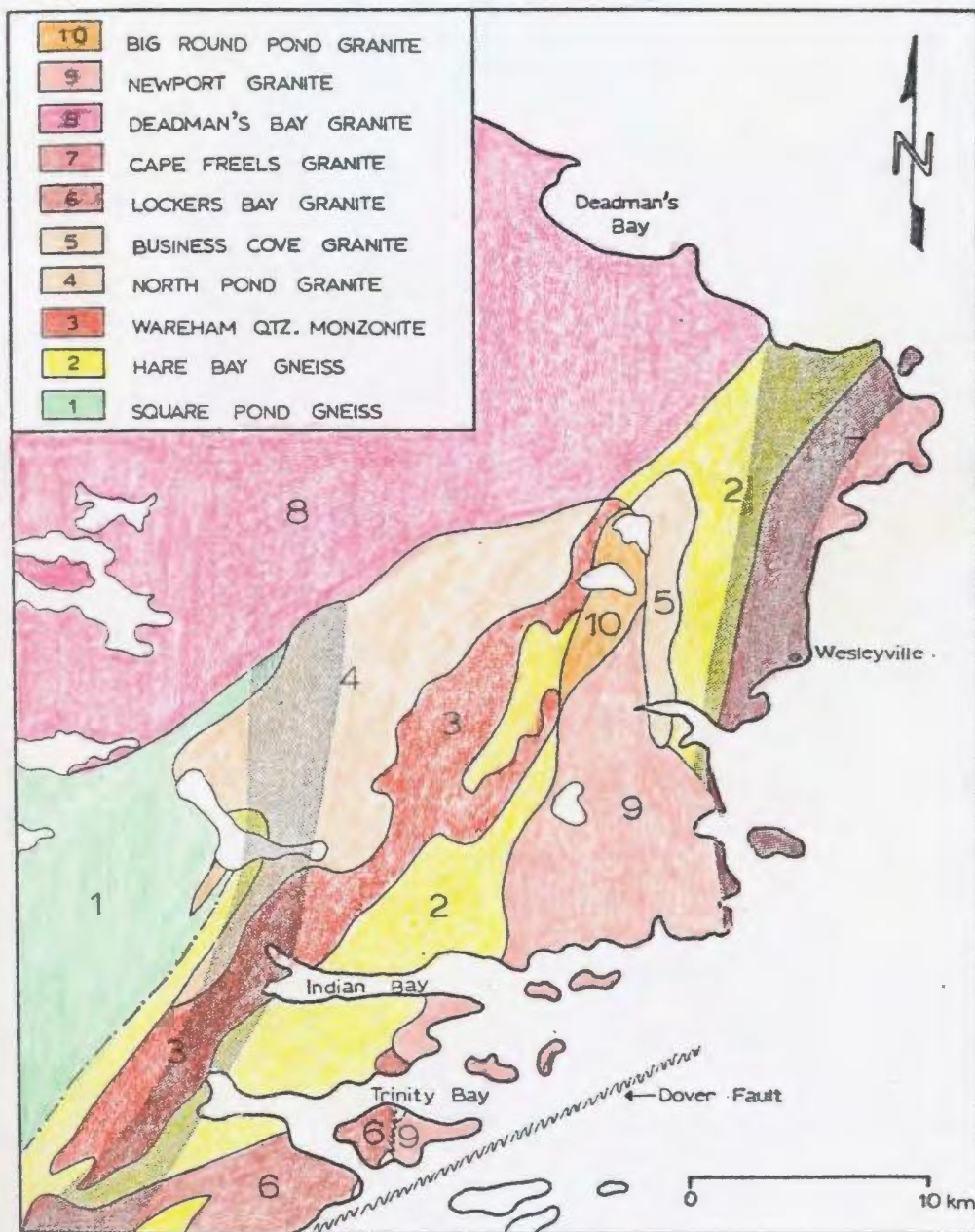


Fig. 2.1. General geology of the thesis area. Shaded bands denote shear zones.

The Square Pond Gneiss can be divided into two regions on the basis of the distribution of the index minerals garnet, staurolite and andalusite. The rock types around and to the north of First Pond do not contain these minerals and have a lower metamorphic grade than the rest of the gneiss terrane.

#### 2.1.1. Structural Geology

The Square Pond Gneiss has undergone polyphase deformation as can be seen from the common superposition of two or more structures. A chronological sequence of deformation events can be constructed by correlating the structures from outcrop to outcrop based on their local age relationships and similarities in geometric style and attitude. Although such a correlation may not be valid when applied to a large area, it does seem to be significant within the relatively small area of gneiss described here. In a few outcrops, on the road to First Pond, the metasedimentary rocks show very complex folds of psammitic and more pelitic horizons (Figure 2.2). These probably represent soft-sediment deformation.

There is evidence for three main deformations in the Square Pond Gneiss. These are designated as  $D_1$ ,  $D_2$  and  $D_3$  respectively.  $D_1$  has produced a gneissic banding ( $S_1$ ) characterized by alternating 1 to 5 mm wide quartz-rich horizons and thinner micaceous films. The banding has a muscovite-biotite foliation parallel to it. In places,  $S_1$  is axial planar to minor folds ( $F_1$ ) of a thicker (10 to 20 cm) compositional banding that probably represents original sedimentary bedding (Figure 2.3). However, both  $S_1$  and  $F_1$  folds are rare in the

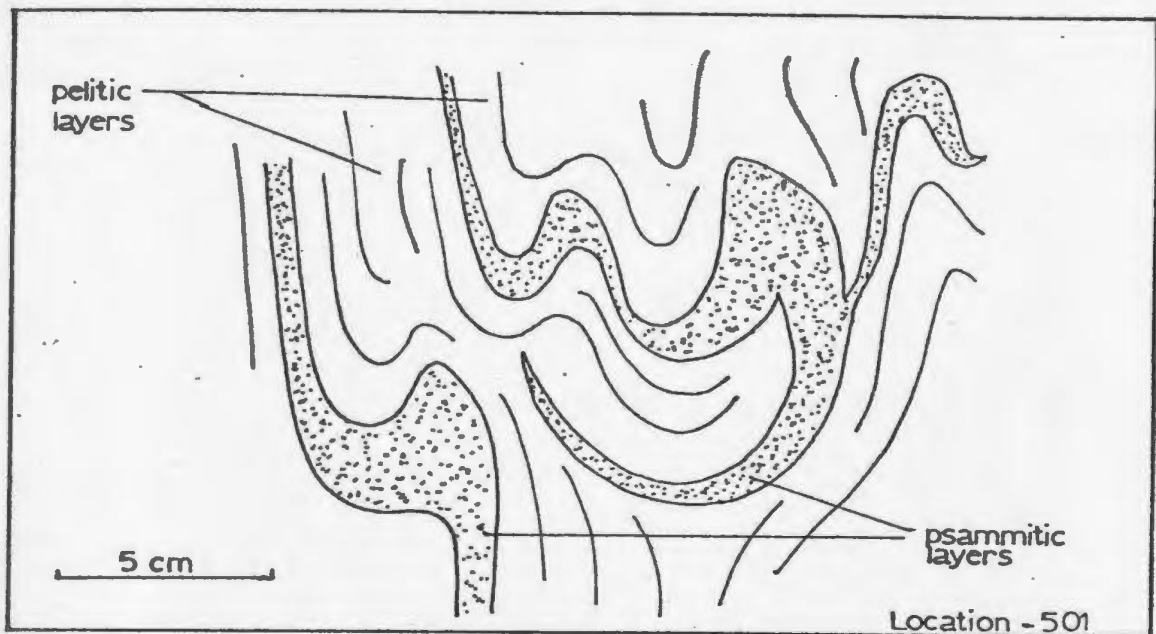


Figure 2.2. Convolute lamination in the metasedimentary rocks. (See location map in back pocket for locations mentioned in the figures and figure captions.)

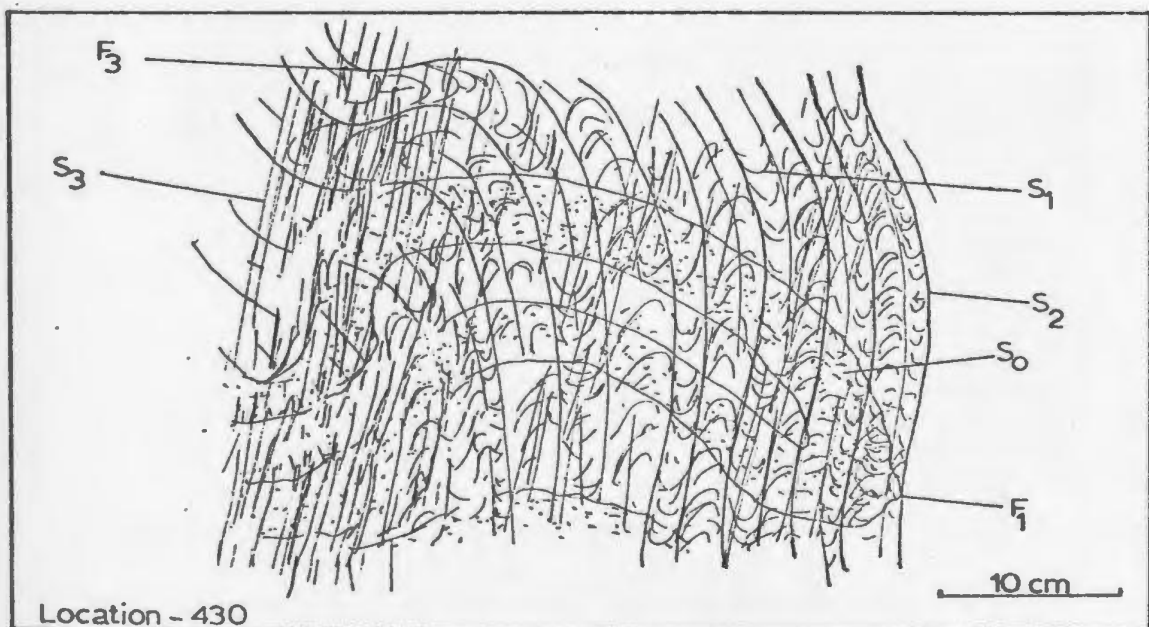


Figure 2.3. Profile of an  $F_1$  fold cut by later structures ( $S_2$ ,  $S_3$ ).

area because they have been obliterated during the later deformations; where they are present, they have been refolded by later structures.

$D_2$  has resulted in a second gneissic banding ( $S_2$ ).  $S_2$  is the most prominent structure seen in the Square Pond Gneiss. Like  $S_1$ ,  $S_2$  is also characterized by alternating 0.1 to 1 cm wide quartz-rich layers and less than 0.5 cm thick micaceous layers and a muscovite-biotite foliation parallel to the layering.  $S_2$  strikes in an east-northeast direction and dips at moderate angles mostly to the northwest (Figure 2.4). In places, it contains curved traces of  $S_1$  (Figure 2.5). In a few outcrops at First Pond,  $S_2$  is axial planar to open to tight minor folds of  $S_1$  (Figure 2.6) or forms a crenulation cleavage (Figure 2.7). The  $F_2$  folds have northeast trends and plunge at shallow to moderate angles in both northeasterly and southwesterly directions (Figure 2.4). Intersection of  $S_1$  and  $S_2$  has resulted in a lineation with a variable attitude. Commonly  $S_2$  is axial planar to isoclinal  $F_2$  folds of quartz veins, in most of which only separated fold noses remain.

$D_3$  has produced a northeast striking, steeply dipping foliation ( $S_3$ ) (Figure 2.4) defined by aligned muscovite and biotite.  $S_3$  is axial planar to  $F_3$  minor folds of the  $S_2$  gneissic banding (Figure 2.8). Commonly, the  $F_3$  folds refold the  $F_2$  folds resulting in type 3 interference patterns (Ramsay, 1967). In places,  $S_3$  cuts across minor granitic intrusions that have truncated the  $S_2$  gneissic banding (Figure 2.9). The  $D_3$  structures are well developed in the eastern part of the gneiss terrane where the rocks are semi-pelitic to pelitic in composition, but less so in the west where psammitic rock types are predominant.

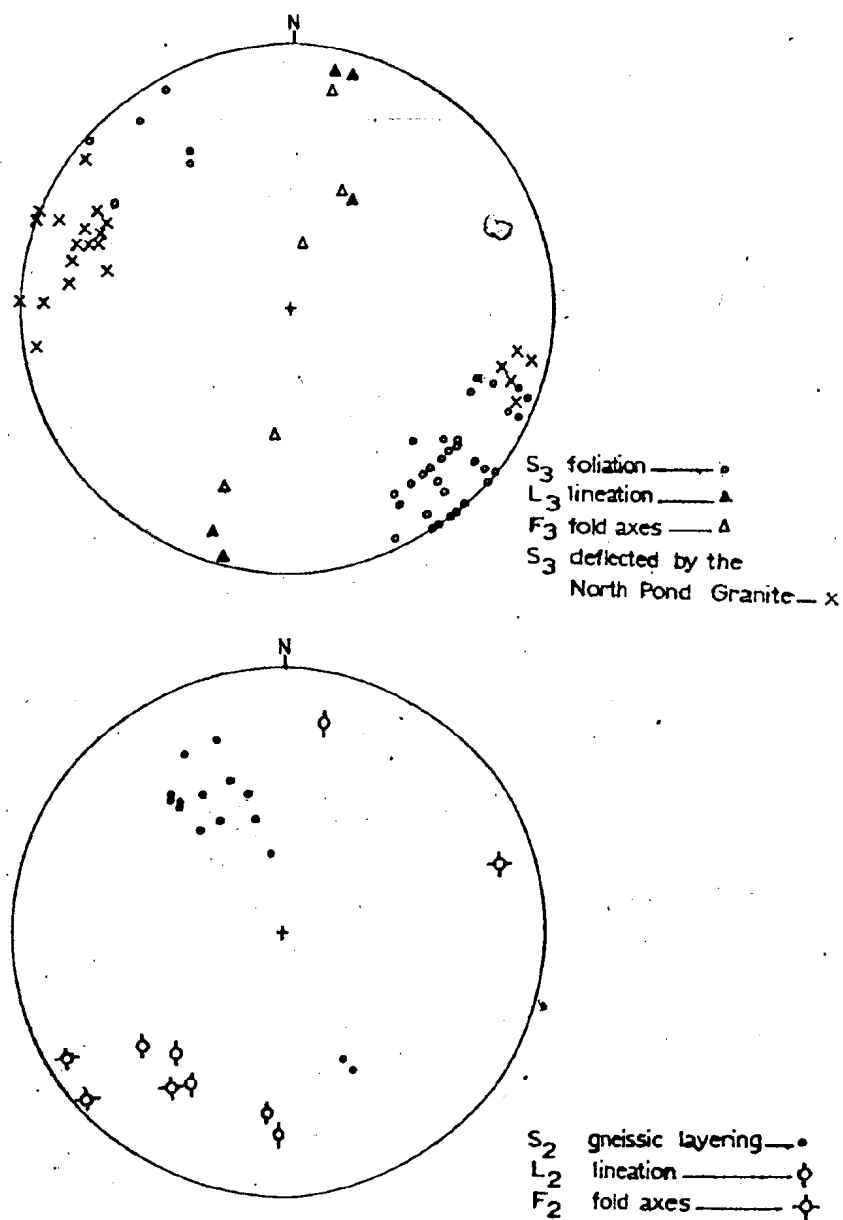


Fig. 2.4. Stereoplots showing  $L_2$  and  $L_3$  lineations,  $F_2$  and  $F_3$  minor fold axes and poles to  $S_2$  and  $S_3$  structures in the Square Pond Gneiss. (Trends of structures in the Square Pond Gneiss were noted in many places but it was not possible to measure the three dimensional attitude of the structures at all the locations.)

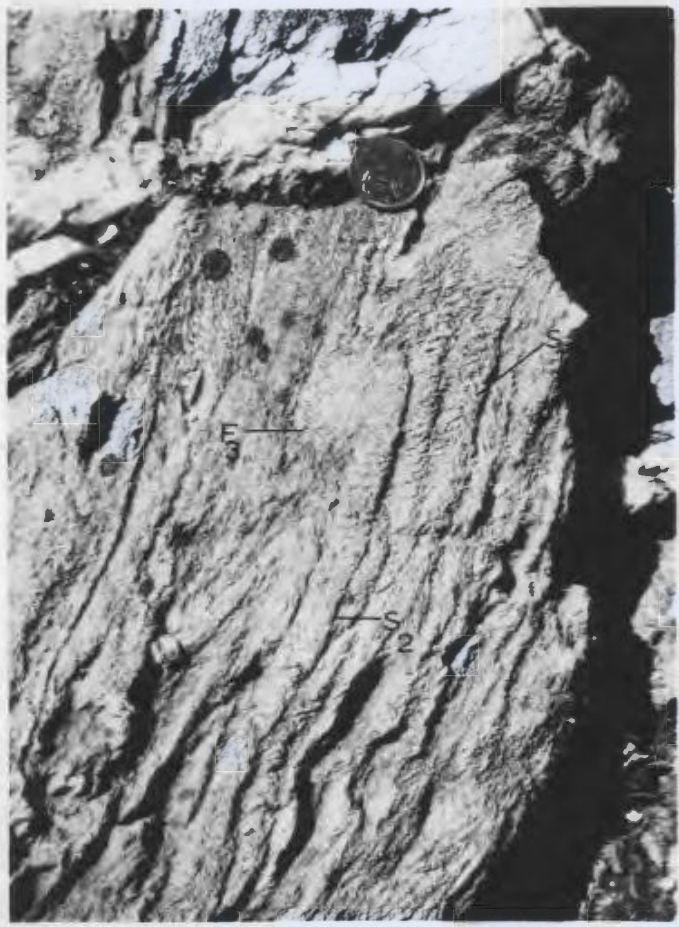


Fig. 2.5. Traces of  $S_1$  in  $S_2$  in the Square Pond Gneiss.  
Location -430.





Fig. 2.6.  $F$  folds of  $S_1$  in the Square Pond Gneiss.  $S_2$  occurs axial planar to the folds. Location -572, First Pond.

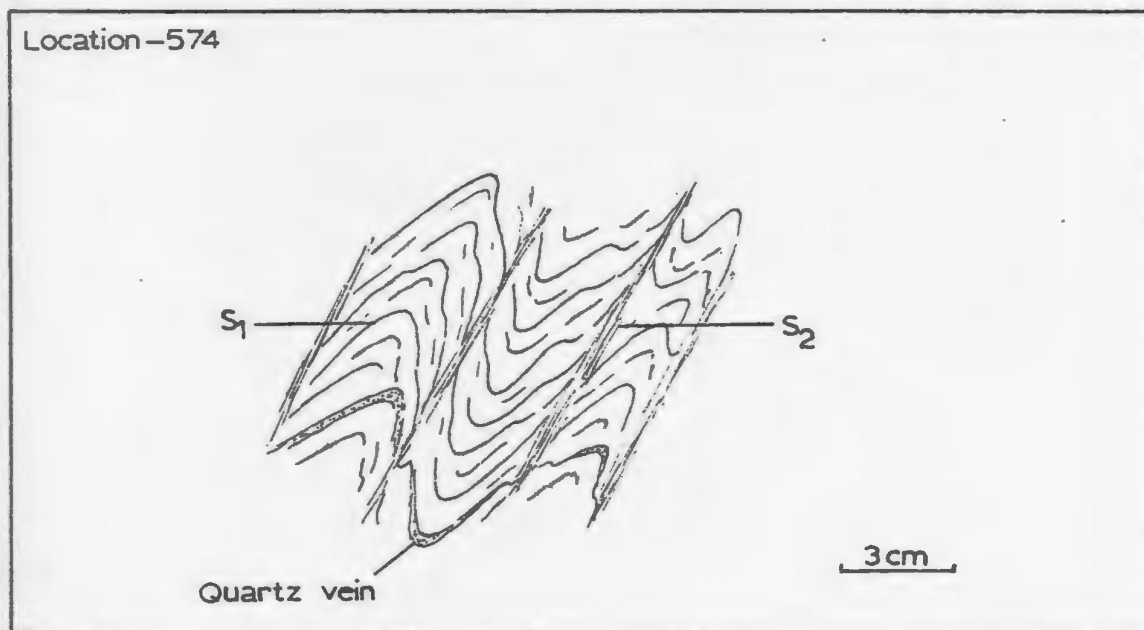


Fig. 2.7.  $S_2$  crenulation cleavage.



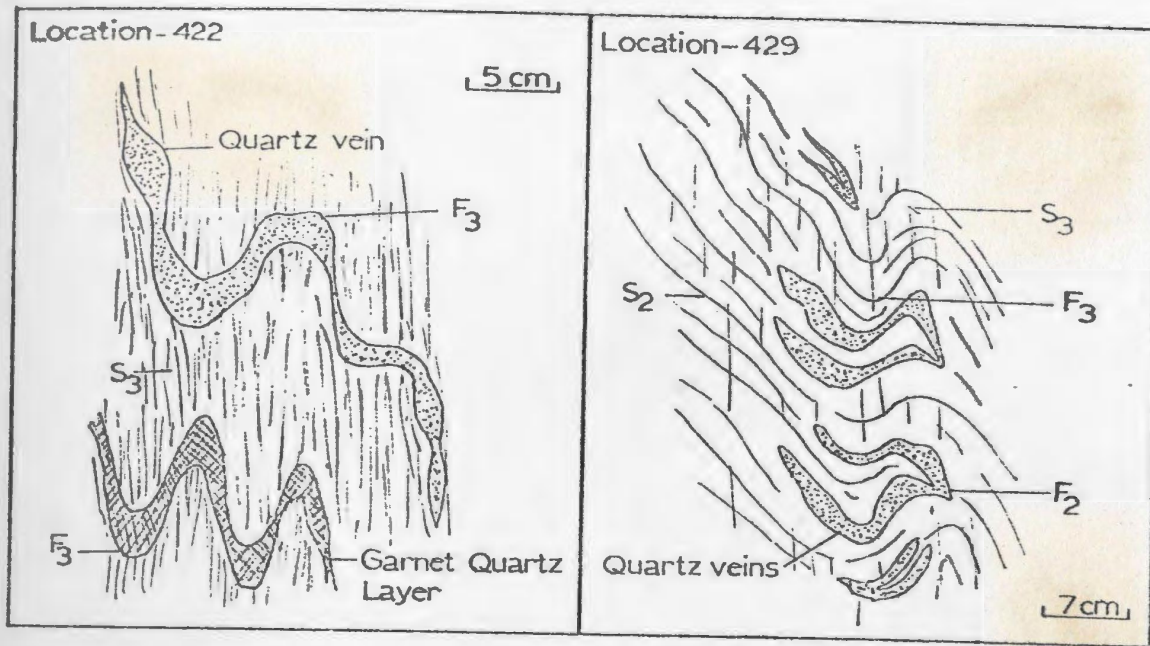


Fig. 2.8.  $F_3$  folds in the Square Pond Gneiss.  $F_2$  folds refolded by  $F_3$  folds. Location - 429.



Fig. 2.9. Granite sheet truncating  $S_2$  in the Square Pond Gneiss and truncated by  $S_3$ . Location - 430.

Within 1 km of the western contact of the North Pond Granite,  $S_3$  has assumed a more northerly orientation. This could be the result of either forceful intrusion of the granite or moulding of the  $S_3$  against the granite by a later deformation event ( $D_4$ ). The central part of the North Pond Granite is cut by a north-northeasterly trending shear zone that marks the  $D_4$  deformation in the area.

In a few outcrops  $S_2$  and  $S_3$  in the gneiss are affected by crenulations with horizontal axial planes. The significance of these crenulations is not well understood. East-southeast striking, steeply dipping kink bands in  $S_2$  and  $S_3$  are common throughout the gneiss terrain. These kink bands are believed to be the same age as kink bands of similar orientation that deform the  $S_4$  fabric elsewhere in the area.

#### 2.1.2. Petrography

Quartz, muscovite and biotite are the chief constituent minerals in the Square Pond Gneiss. Plagioclase is generally minor (<10%) but garnet, staurolite and andalusite constitute 25 to 50 percent of some horizons in a few outcrops. The accessory minerals in the Square Pond Gneiss include chlorite, ilmenite, zircon, apatite and tourmaline. Accurate modal analysis of this lithologic unit was not possible because of its fine-grained nature.

Quartz grains in the gneiss show a gradual coarsening from west (average 0.1 mm close to the western margin of the area) to east (up to 4 mm). They have straight, curved or embayed grain boundaries. Undulatory extinction is common.

Muscovite and biotite are associated with each other and are generally aligned parallel to the planar structures ( $S_1$ ,  $S_2$ ,  $S_3$ ) in the host. Like quartz, the micas show a gradual coarsening from west (0.04 to 0.12 mm in length) to east (up to 0.4 mm) in the gneiss terrain. Biotite has pale brown to dark brown or greenish brown pleochroism. The greenish brown type is dominant in the western part of the gneiss. Rarely, randomly oriented porphyroblastic biotite has overgrown the finer parallel aligned micas. Most of the biotite has been altered to chlorite. In addition, fine grained chlorite occurs together with mica in rocks around First Pond, and probably represent primary chlorite.

Where present plagioclase (0.1 to 0.3 mm) is highly altered, probably to sericite and epidote. The plagioclase grains show albite twins and have compositions ranging from  $An_8$  to  $An_{14}$ <sup>2</sup>.

Garnet is pinkish in colour, ranges from 0.4 to 1.6 mm in diameter and is idiomorphic to hypidiomorphic. Some grains have inclusion rich cores and clear rims, others are clean or have inclusion trails ( $S_2$ ) extending right across the host crystal. (The inclusion trails in the garnet, staurolite and the andalusite grains are described in detail in section 2.1.4.). The inclusions consist mostly of ilmenite<sup>1</sup>. Garnet

---

<sup>1</sup>Identified in polished sections.

<sup>2</sup>Determined optically by the extinction method.

grains in the garnet-quartz layers have cores richer in inclusions than elsewhere in the gneiss. The cores of these garnet grains contain, in addition to ilmenite inclusions, numerous tiny dark inclusions (Figure 2.10) that are probably chlorite produced by alteration of garnet.

Staurolite occurs in the mica-rich parts of the Square Pond Gneiss. It ranges from 0.1 to 1 cm in length; average length is between 1 and 1.5 mm. It is hypidiomorphic and has pale yellow to yellowish pleochroism. Some of the grains show interpenetrant twins. Inclusion trails ( $S_2$ ) consisting of ilmenite<sup>1</sup> are common. A few staurolite grains contain helicitic inclusion trails ( $S_2$ ) of small elongate quartz.

Like the staurolite, andalusite is generally found in the mica-rich parts of the Square Pond Gneiss. It ranges from 1 mm to 3 cm in length. Andalusite grains are idiomorphic to hypidiomorphic in shape and contain inclusion trails ( $S_2$ ) similar to those in the staurolite.

On a few outcrop surfaces at First Pond, the Square Pond Gneiss contains elongated, roughly rectangular inclusions of a lithology darker than the host. In thin section, these appear to consist of epidote, biotite, quartz and actinolite (Figure 2.11). These may represent remnants of some mafic dikes that pre-dated the deformation and the metamorphism of the gneiss.

#### 2.1.3. Metamorphism

The ACF diagrams for the Square Pond Gneiss (Figure 2.12) suggest that it consists of rock types of two metamorphic grades. Rock

---

<sup>1</sup>Identified in polished sections.

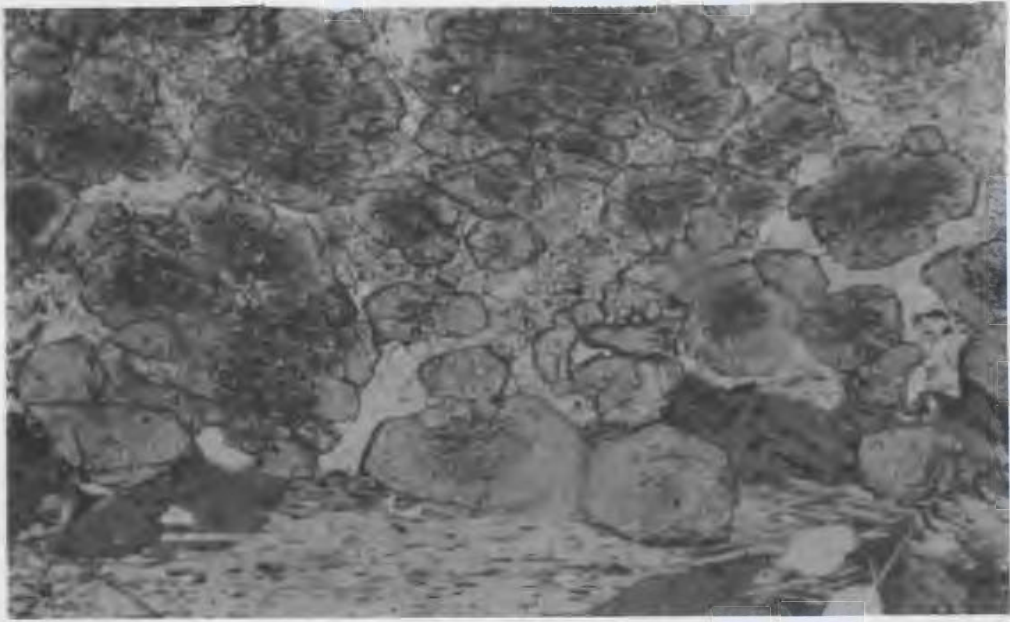


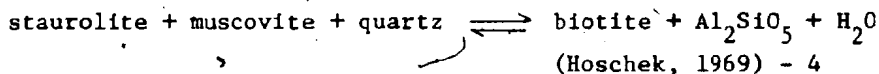
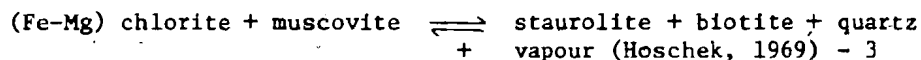
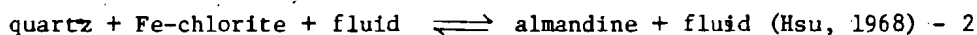
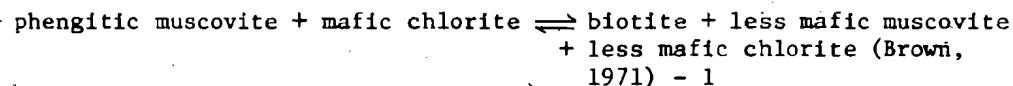
Fig. 2.10. Photomicrograph showing inclusion-rich cores and clear rims in garnets in a garnet-quartz layer. (X10). Location - 422.



Fig. 2.11. Photomicrograph of a mafic inclusion in the Square Pond Gneiss. A - actinolite, B - biotite, E - epidote, Q - quartz, (X40). Location - 575.

types<sup>1</sup> around and to the north of First Pond consist of quartz, plagioclase (albite), biotite, muscovite and chlorite and contain mafic inclusions with epidote, biotite, quartz and actinolite. Thus they are in the greenschist facies (Miyashiro, 1973). The rest of the gneiss terrain has developed garnet, staurolite and andalusite in addition to quartz, plagioclase (albite-oligoclase), biotite and muscovite and is in the amphibolite facies (Miyashiro, 1973). The areas that fall into each of these facies are shown in Figure 2.13. The general eastward coarsening of the minerals observed agrees with the eastward increasing metamorphic grade in the gneiss terrain. The presence of andalusite and the absence of kyanite indicate that the metamorphism of the Square Pond Gneiss in the thesis area is of the low-pressure type<sup>2</sup> (Miyashiro, 1973).

Listed below are a few reactions that could have produced biotite, garnet, staurolite and andalusite in the Square Pond Gneiss.



<sup>1</sup>These rock types contain "thermal" andalusite within the contact aureole of the Deadman's Bay Granite.

<sup>2</sup>Blackwood (1977) reported the presence of all three minerals kyanite, andalusite and sillimanite in the Square Pond Gneiss, to the south and west of the present study area. Thus the metamorphism in the Square Pond Gneiss in northern Gander Zone must have ranged from low-pressure to medium-pressure types. A similar variation in metamorphic conditions were reported by Colman-Sadd (1979) for rock types in southern Gander Zone.

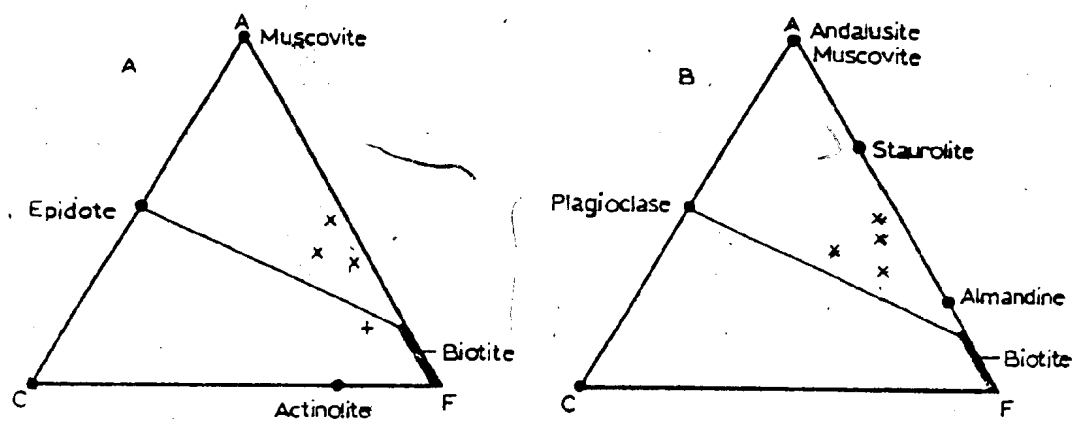


Fig. 2.12. ACF diagrams for the Square Pond Gneiss. A - rock types around and to the north of First Pond, B - rest of the gneiss terrain.

x - chemical analyses of the Square Pond Gneiss.  
 + - chemical analysis of a mafic inclusion in the Square Pond Gneiss.



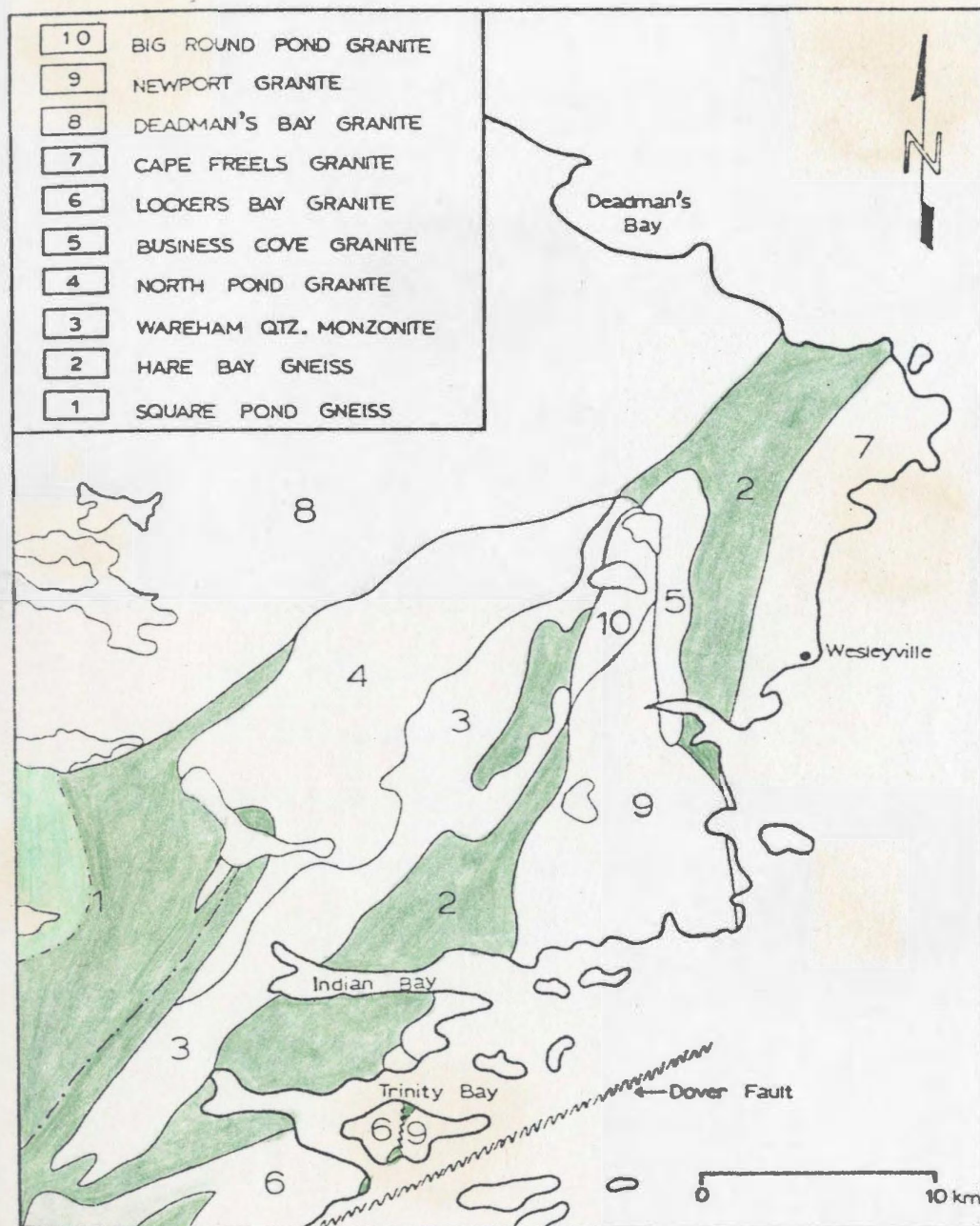


Fig. 2.13. Sketch map showing greenschist facies (light green) and amphibolite facies (dark green) metamorphic rocks in the study area.



Equilibrium curves for the reactions 2, 3, and 4 are shown in Figure 2.14. These equilibrium curves have been determined under  $fO_2$  conditions controlled by the fayalite - magnetite - quartz (FMQ) buffer. Pelitic rocks undergoing metamorphism generally have  $fO_2$  values similar to those defined by the FMQ buffer (Miyashiro, 1973). Therefore the above equilibrium curves can be used to obtain approximate pressure, temperature conditions of the metamorphism in the Square Pond Gneiss in the present study area. The stability of most metamorphic minerals is a function of not only P and T but also of the bulk chemistry. However, since insufficient chemical analyses from the mineral phases in the gneisses are available the effect of their composition on the equilibrium curves is not discussed.

Andalusite is the only  $Al_2SiO_5$  polymorph observed in the Square Pond Gneiss. Therefore the pressure during the metamorphism must have been below that of the andalusite-sillimanite-kyanite triple point which occurs at 5.5 kb and 622°C according to Richardson *et al.* (1969). The "staurolite in" reaction curve (No. 3 in Figure 2.14) intersects the andalusite-kyanite field boundary at 4.7 kb and 545°C. The "staurolite out" reaction curve (No. 4 in Figure 2.14) cuts the andalusite-sillimanite field boundary at 4.3 kb and 650°C. Therefore the amphibolite facies metamorphism in the Square Pond Gneiss probably occurred at temperatures between 550 and 650°C and pressures below 5.5 kb. The greenschist facies metamorphism of the gneiss probably took place at temperatures between 550°C and 350°C (see Mueller and Saxena, 1977).

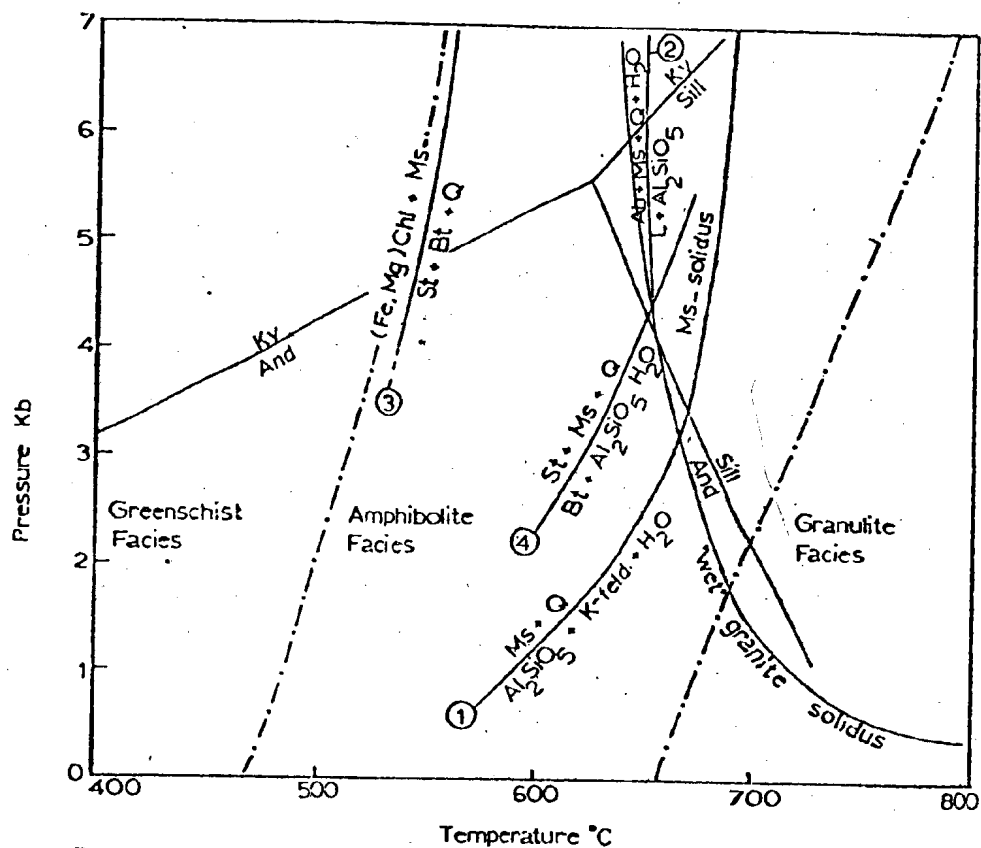


Fig. 2.14. Pressure-temperature grid of some of the equilibrium curves mentioned in the text. 1 - Day (1973), 2 - Storre and Karotke (1977), 3 and 4 - Hoschek (1969).<sup>\*</sup> Al<sub>2</sub>SiO<sub>5</sub> data from Richardson *et al.* (1969). Facies boundaries from Saxena (1977). "Wet" granite solidus from Wyllie (1977).

<sup>\*</sup>P-T values of the Al<sub>2</sub>SiO<sub>5</sub> triple point are controversial (see Miyashiro, 1973; Mueller and Saxena, 1977).

#### 2.1.4. Chronological Analyses of Metamorphism and Deformation

Several authors (Rast, 1958; Zwart, 1962; Spry, 1962; Harte and Johnson, 1969; Zwart and Calon, 1977) have demonstrated that microstructural relationships between porphyroblasts and matrix can be used to infer the relative timing between mineral growth and deformation. The most commonly used criteria in such chronological analyses are: (1) relationships between margins of porphyroblasts and fabrics in the matrix, and (2) relationships between inclusion trails in porphyroblasts and fabrics outside. These criteria do not yield unequivocal time relationships between mineral growth and deformation (Olsen, 1978; Vernon, 1978). However, the microstructural relationships between garnets, staurolites and andalusites, and the fabrics in the Square Pond Gneiss are consistent with the preceding structural analysis and provide some additional though not unequivocal evidence for the relationship between metamorphism and deformation. According to the usual convention the inclusion trails in the minerals are referred to as Si and the "external" fabrics in the matrix are called Se.

Garnets, staurolites and andalusites in the Square Pond Gneiss show both straight and crenulated inclusion trails. In addition, garnets also show curved inclusion trails (Figure 2.15). The inclusion trails consist mostly of ilmenite. The crenulated inclusion trails in staurolite and andalusite consist of ilmenite and quartz stringers. The quartz stringers are considerably smaller in size than quartz outside.

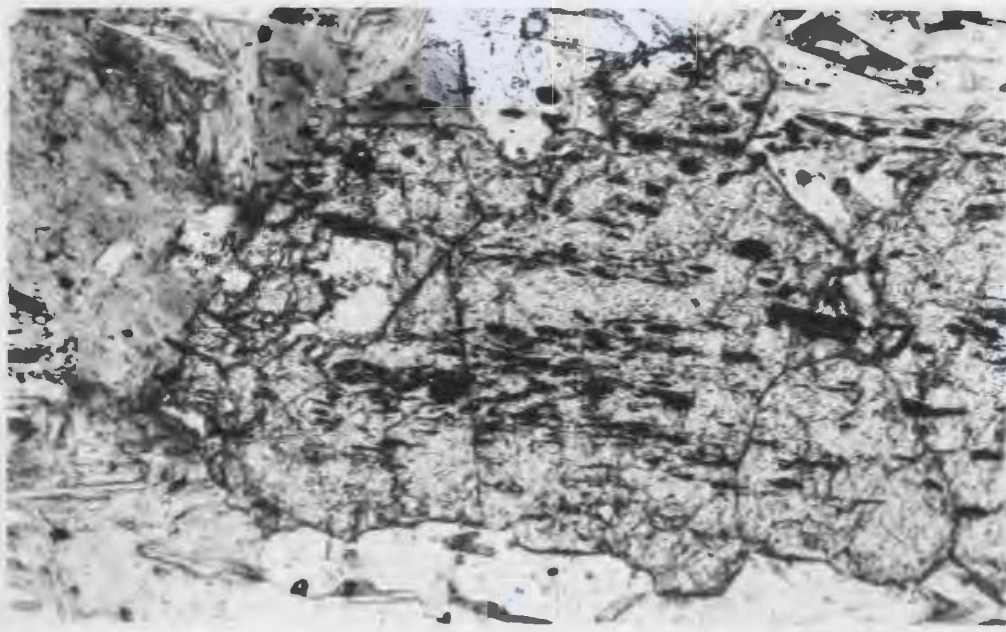


Fig. 2.15a. Garnet porphyroblast with straight inclusion trails (X40). Location - 435.

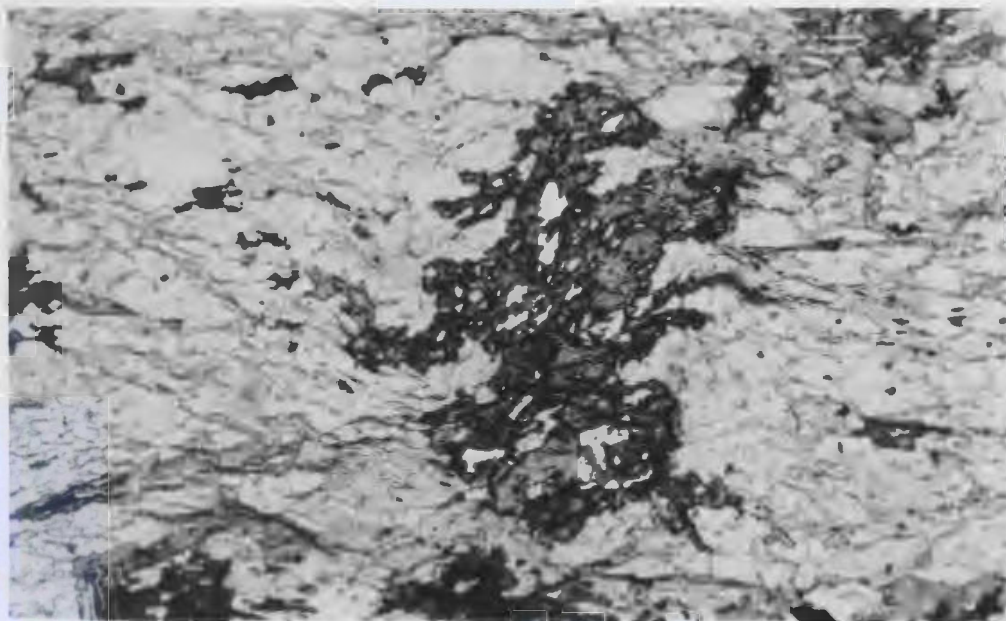


Fig. 2.15b. Garnet porphyroblast with curved inclusion trails (X40). Location - 547.

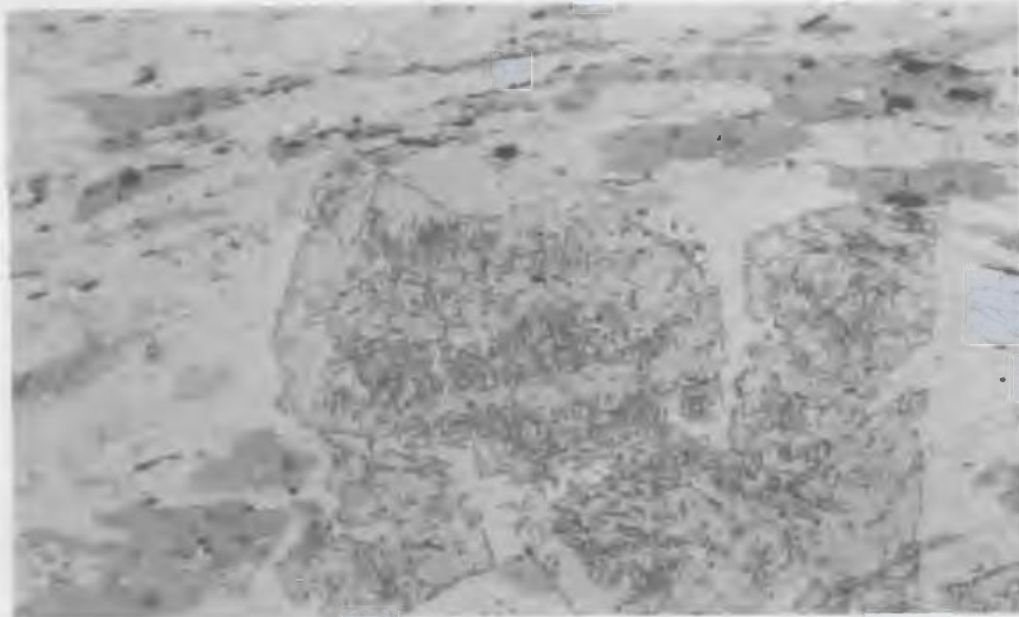


Fig. 2.15c. Staurolite porphyroblasts with crenulated inclusion trails (X10). Location - 712.

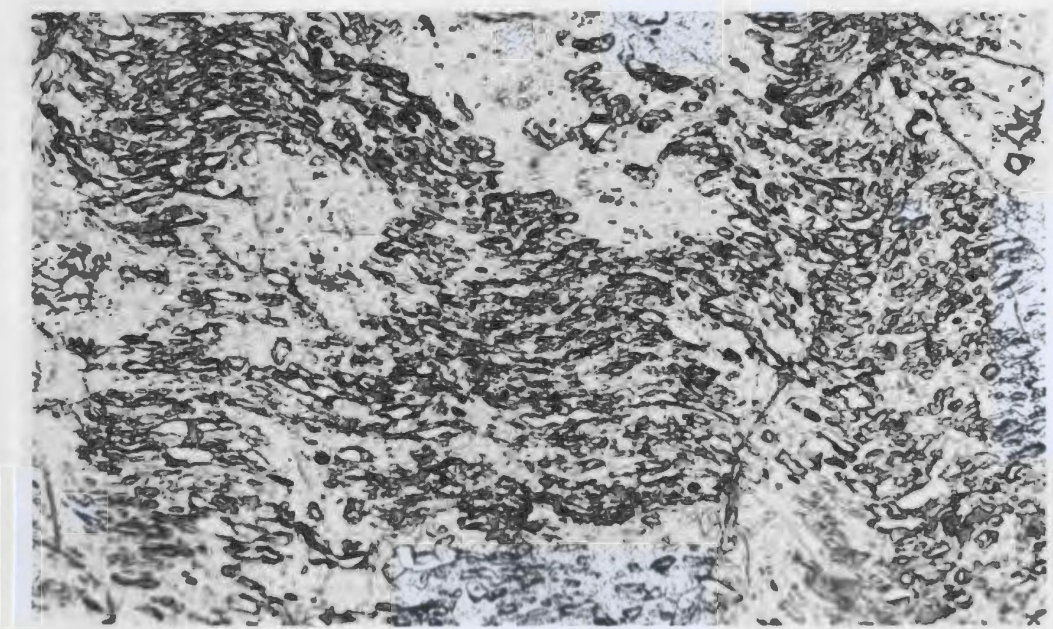


Fig. 2.15d. Crenulated inclusion trails in a staurolite porphyroblast shown above (X40).



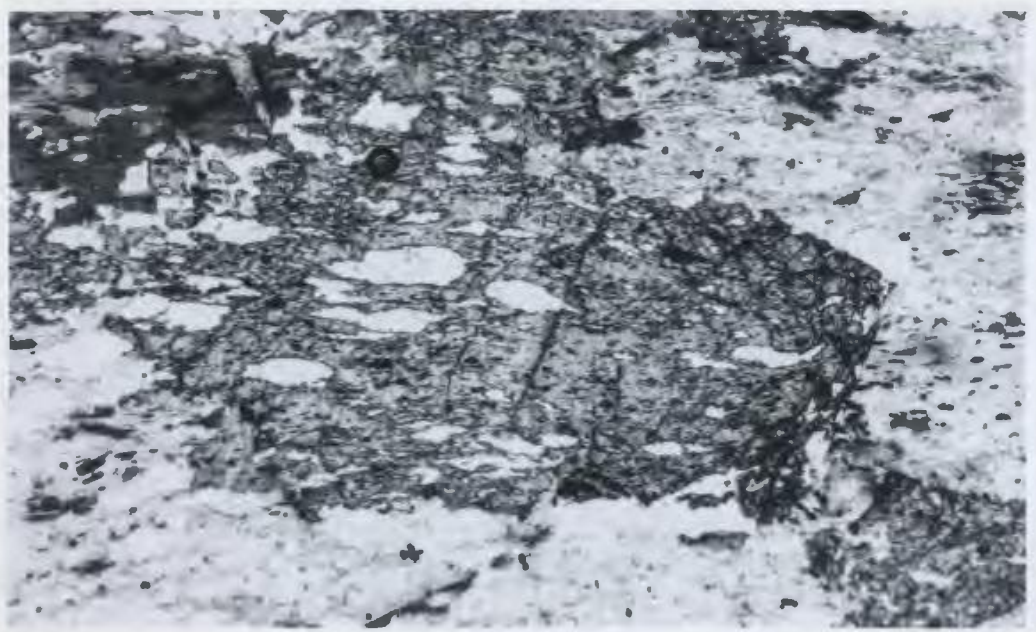


Fig. 2.15e. Staurolite porphyroblast with straight inclusion trails (X40). Location - 547.



Fig. 2.15f. Helicitic inclusion trails in an andalusite porphyroblast (X40). Location - 422.

The straight inclusion trails in garnets either occur in the core of the garnets surrounded by an inclusion-free garnet rim or extend right across the crystal. They are either parallel or inclined at various angles to the external fabric which is the  $S_3$  foliation in the gneiss. Inclusion trails oriented oblique to  $S_3$  are assumed to represent  $S_2$ . The straight inclusion trails in the staurolites and the andalusites extend right across the host crystals. They trend parallel to the length of the host crystal which in turn lies parallel to or at low angles to the external fabric,  $S_3$ . These inclusion trails are also assumed to represent  $S_2$ .

The parallelism between the inclusion trails and the long axis of staurolite and andalusite crystals may be related to the preferential growth of these minerals in the direction of already existing anisotropy (in this case  $S_2$ ) of the host rocks. Diffusion of components needed for their growth would certainly be faster along the anisotropy than across it.

The crenulated inclusion trails are rare. In the case of garnets, crenulated inclusion trails were only found in one of the garnet-quartz layers in an outcrop approximately 2 km to the northwest of Northwest (First) Pond. This garnet-quartz layer has been folded by  $D_3$  with  $S_3$  axial planar to the folds. The crenulated  $S_1$  occurs in the core of the garnets, surrounded by a clear garnet rim. The  $S_1$  in garnets at the hinge of the  $F_3$  fold of the garnet-quartz layer shows an "M" shaped pattern whereas the  $S_1$  in garnets on the two limbs shows asymmetrical "S" and "Z" patterns (Figure 2.16). The axial traces of the "M" shaped crenulations are parallel to the external

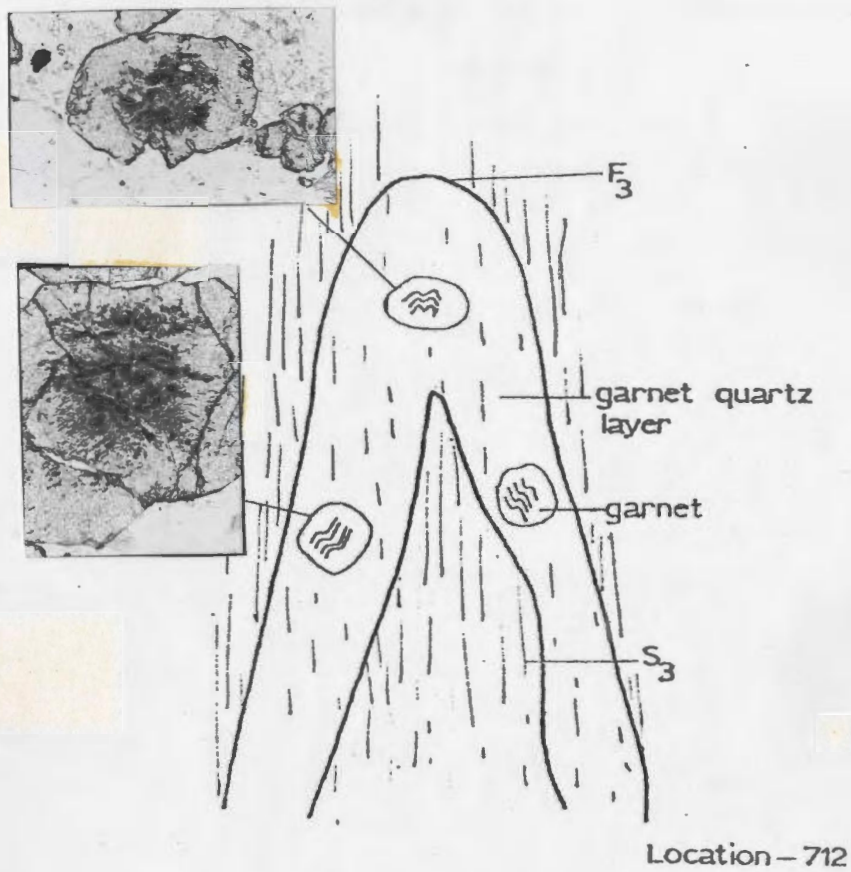


Fig. 2.16. Inclusion trails in garnets on the limbs and the crest of an  $F_3$  fold in a garnet-quartz layer. (Garnets X10, fold<sup>3</sup> is not to scale). Location - 712.



fabric which is the  $S_3$  in the gneiss. The  $S_1$  that define the "S" and "Z" shaped crenulations trend oblique to the external fabric. The garnets probably overgrew  $S_2$  during the early part of  $D_3$ . With progressive deformation the fold has been flattened and  $S_2$  has rotated towards the axial plane of the fold (i.e. towards  $S_3$ ) while the circular garnets remained fixed in orientation thus giving an angle between  $S_1$  and  $S_2$  (Figure 2.17).

The curved inclusion trails in the garnet continue into  $S_3$  in the gneiss. These inclusion trails are believed to represent garnet growth during  $D_3$ . The inclusion-rich cores and clear rims may indicate fast and slow rates of growth of garnet grains respectively (Rast and Sturt, 1957).

The crenulated inclusion trails in staurolite and andalusite occur either in the cores or extend across the host crystals. The axial traces of the crenulations are generally oriented parallel to or at low angles to  $S_3$ . As in the case of garnet, no  $F_3$  crenulations were seen in the micas outside staurolite and andalusite grains. The micas are aligned parallel to  $S_3$  and appear to have been flattened against the staurolite and andalusite. Therefore the crenulated  $S_1$  in these are believed to represent  $F_3$  crenulations of  $S_2$ . The grain size difference between the external quartz and the quartz inclusions in the staurolite and andalusite porphyroblasts is probably a result of matrix coarsening subsequent to the growth of these porphyroblasts.

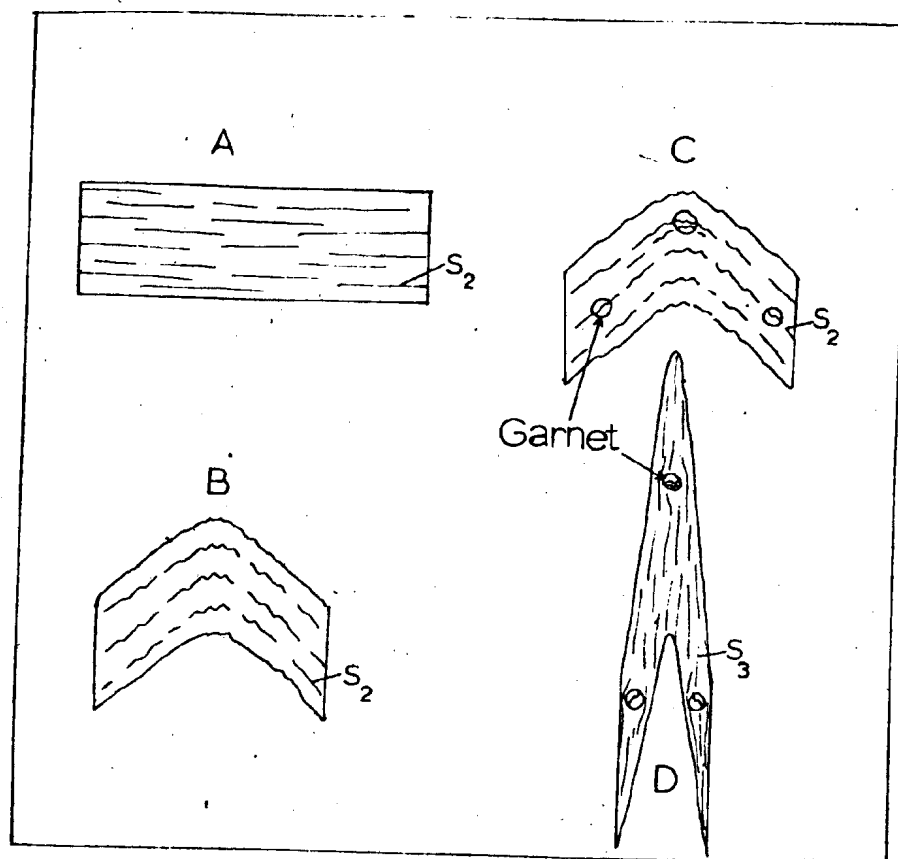


Fig. 2.17. Schematic illustration of the interpreted progressive development of the fold shown in Fig. 2.16.

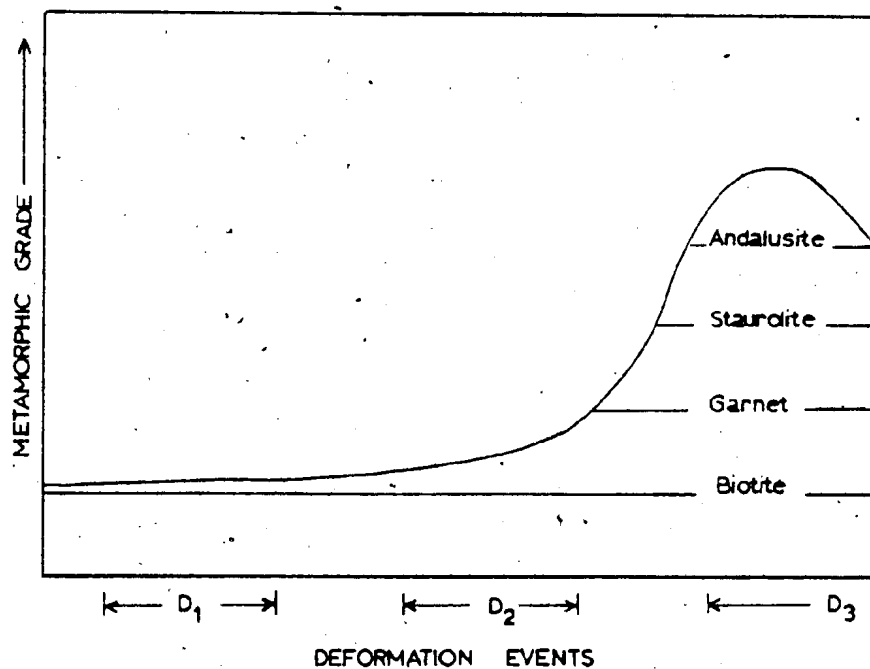


Fig. 2.18. Graph showing deduced chronological relationship between metamorphism and deformation phases in the Square Pond Gneiss.

[Biotite defines  $S_1$ ,  $S_2$  and  $S_3$  fabrics and thus appears to have been stable from  $D_1$  through to  $D_3$ . Some garnet, staurolite and andalusite contain straight  $S_2$  inclusion trails; others contain inclusion trails showing  $F_3$  crenulations. Thus these minerals appear to have grown post  $D_2$ .]

The chronological relationships between the growth of garnet, staurolite and andalusite (metamorphism) and deformation events in the Square Pond Gneiss are shown in Figure 2.18.

#### 2.1.5. Geochemistry<sup>1</sup>

Eight rock samples from the Square Pond Gneiss were analysed for major and minor element oxides and thirteen trace elements. The results are shown in Table 2.1 and attest to the dominantly psammitic nature of the gneiss terrain. The main reason for analysing these rocks is to investigate whether the Square Pond Gneiss could have produced the migmatites and the granitic intrusions in the area and the analyses will be used toward this end in the appropriate sections of the thesis.

In addition to the above whole-rock analyses, garnet and biotite from two locations within the Square Pond Gneiss were analysed for major element oxides,  $TiO_2$  and  $MnO$ . The garnet cores and rims were analysed separately. The individual mineral analyses are listed in Appendix 2.1. The composition of garnet is shown in Figure 2.19. It is rich in almandine. Garnet cores appear to be richer in spessartine than the rims. The highest spessartine contents of the analysed garnet

---

<sup>1</sup>The analytical techniques used in this study and the precision and accuracy of the results are given in Appendix 6.1. A sample location map is given in back pocket.

Table 2.1 Chemical analyses of the Square Pond Gneiss

Sample #	429	436	455	501	502	542	552	575*	$\bar{x}$	S
SiO <sub>2</sub> wt.%	76.6	80.5	80.7	72.6	77.5	78.4	73.4	53.5	77.1	3.2
TiO <sub>2</sub>	0.65	0.54	0.49	0.80	0.62	0.55	0.80	1.01	0.64	0.12
Al <sub>2</sub> O <sub>3</sub>	11.00	9.07	8.53	11.80	9.25	10.80	12.80	13.40	10.46	1.57
Fe <sub>2</sub> O <sub>3</sub>	1.15	0.61	0.45	0.49	0.57	1.27	1.20	3.01	0.82	0.37
FeO	2.58	2.52	1.91	4.60	2.84	2.18	3.22	4.89	2.84	0.89
MnO	0.06	0.08	0.04	0.10	0.08	0.06	0.10	0.18	0.07	0.02
MgO	1.12	0.98	0.71	1.65	1.14	1.04	1.41	8.96	1.15	0.30
CaO	1.04	0.51	1.30	0.56	0.88	0.45	0.56	6.16	0.76	0.32
Na <sub>2</sub> O	2.80	1.51	2.24	1.39	1.72	2.22	1.68	0.87	1.94	0.50
K <sub>2</sub> O	2.16	2.02	1.17	2.26	2.78	2.28	2.95	3.85	2.23	0.58
P <sub>2</sub> O <sub>5</sub>	0.09	0.06	0.10	0.15	0.09	0.15	0.09	0.38	0.10	.03
H <sub>2</sub> O	1.12	1.21	0.93	2.76	1.22	1.37	1.98	2.80	1.51	
Total	100.37	99.61	98.57	99.16	98.69	100.77	100.19	99.01	99.62	
Zr (ppm)	238	258	236	244	200	222	254	470	236	20
Sr	84	62	114	54	93	81	60	394	78	21
Rb	118	105	51	79	112	94	121	225	98	23
Zn	55	47	42	78	53	54	70	93	57	13
Cu	10	7	12	53	16	14	15	19	18	16
Ba	363	303	215	518	560	484	551	822	428	135
Nb	13	13	13	15	14	13	17	15	14	2
Ca	12	12	13	18	15	16	16	23	15	2
Pb	22	7	17	15	15	5	14	35	14	6
Ni	16	14	15	32	19	19	20	249	19	6
Cr	61	54	39	65	47	40	58	533	52	10
V	89	70	50	109	87	74	90	204	81	19
Y	34	31	24	27	31	28	39	45	31	5

$\bar{x}$  - average composition

S - standard deviation

\* - mafic inclusion (not included in the mean)

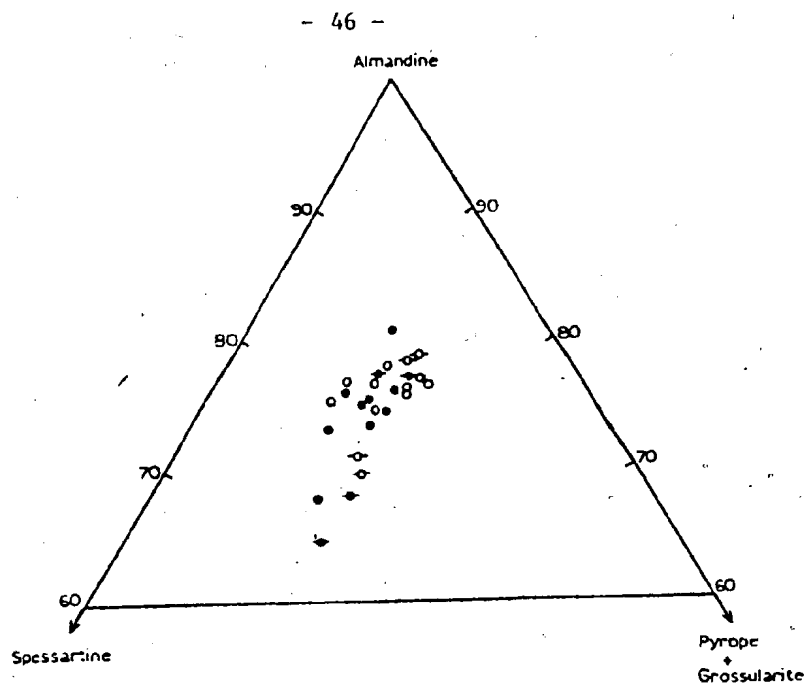


Fig. 2.19. Composition of garnets in the Square Pond Gneiss. Open circles - garnet rims, solid circles - garnet cores, circles with horizontal bars - garnets from a garnet-quartz layer.

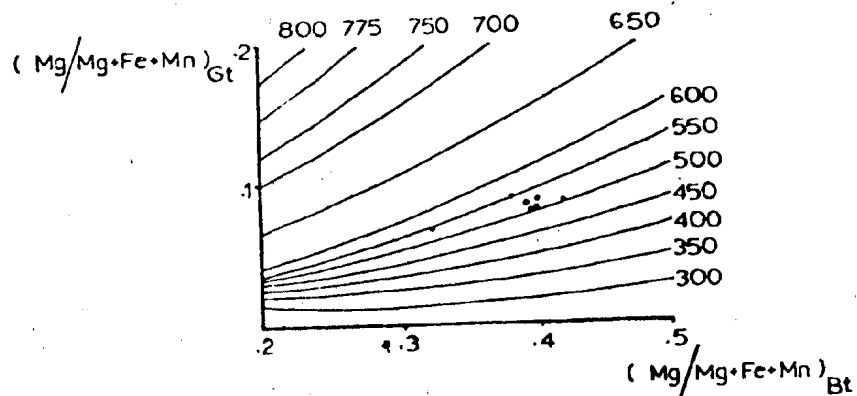


Fig. 2.20. Compositions of coexisting garnet and biotite in the Square Pond Gneiss, plotted on Perchuk's (1970) graph for garnet-biotite geothermometry.

crystals were found among those from the garnet-quartz layers in the gneiss.

The MnO content in garnet is known to decrease with increasing metamorphic grade at the time of formation (Miyashiro, 1973). Thus the garnet cores, richer in spessartine than the rims, may indicate that the garnet grew at different times in the metamorphic history of the gneiss as suggested by the chronological analysis presented previously. The high spessartine content in garnet from the garnet-quartz layers probably indicates higher Mn contents in the latter than in the adjacent rocks.

#### 2.15a. Garnet-Biotite Geothermometry

Several authors have shown that the partitioning of Fe and Mg between coexisting garnet and biotite can be used successfully as a geothermometer (Perchuk, 1970; Ahlin, 1976; Goldmann and Albee, 1977; Ferry and Spear, 1978). In order to apply this geothermometer to the metamorphism of the Square Pond Gneiss, several biotite and garnet grains were analysed from two localities within the gneiss terrain. The analyses were done using a JEOL JXA - 50A electron microprobe. Results are listed in Appendix 2.1. It is assumed that the garnet rim, but not necessarily the garnet core, is in equilibrium with the adjacent biotite grain (Hollister, 1966). Thus only the analyses of the garnet rims and the biotite grains adjacent to them were used in the following calculations.

Perchuk gave a graph indicating equilibrium temperatures for coexisting garnet and biotite with different  $Mg/(Mg + Fe + Mn)$  ratios. The  $Mg/(Mg + Fe + Mn)$  ratios of garnet-biotite pairs from the

Table 2.2 Temperatures estimated using garnet-biotite pairs in the Square Pond Gneiss  
(Fe, Mg and Mn values are from the structural formula)

	Fe	Mg	Mn	$K = (\text{Mg/Fe})_{\text{Gt}} / (\text{Mg/Fe})_{\text{Bt}}$	$T_1^{\circ}\text{C}$	$T_2^{\circ}\text{C}$
R <sub>1</sub>	4.24	0.45	0.73	0.1598	533	500
B <sub>1</sub>	2.62	1.74	0.02			
R <sub>2</sub>	4.44	0.47	0.64	0.1608	535	575
B <sub>3</sub>	2.75	1.81	0.02			
R <sub>3</sub>	4.41	0.49	0.62	0.1648	543	575
B <sub>3</sub>	2.73	1.84	0.02			
R <sub>4</sub>	4.24	0.48	0.77	0.1547	523	500
B <sub>4</sub>	2.57	1.88	0.02			
R <sub>6</sub>	4.64	0.53	0.71	0.1823	576	550
B <sub>6</sub>	2.89	1.81	0.02			
R <sub>7</sub>	4.56	0.47	0.69	0.1501	514	500
B <sub>7</sub>	2.49	1.79	0.01			
R <sub>9</sub>	4.05	0.35	0.93	0.1825	576	550
B <sub>9</sub>	3.21	1.52	0.02			

$T_1$  = temperature estimated using the equation given by Ferry and Spear (1978)  $\ln K = \frac{-2109}{T^{\circ}\text{K}} + 0.782$

$T_2$  = temperature estimated using Perchut's (1970) graph (Figure 2.20).

R<sub>i</sub> and B<sub>i</sub> denote garnet rim (Gt) and adjacent biotite (Bt).



Square Pond Gneiss are shown in Table 2.2 and are plotted on Perchuk's graph (Figure 2.20).

Ferry and Spear gave the following expression for the equilibrium temperature (T) of coexisting garnet and biotite:

$$\ln k = \frac{-2109}{T^{\circ}\text{K}} + .782 \text{ where } k = \frac{(\text{Mg/Fe})_{\text{garnet}}}{(\text{Mg/Fe})_{\text{biotite}}}$$

The  $\ln k$  values of garnet and biotite from the Square Pond Gneiss and temperatures calculated using the above expression are shown in Table 2.2. Temperatures determined by both Perchuk's and Ferry and Spears' methods range from 500 - 575°C. This is only a minimum estimate of the temperature of the peak of metamorphism of the Square Pond Gneiss because both Perchuk's ratios and  $k$  are functions of Ca and Mn, both of which are present in the garnet and biotite. The actual temperature of metamorphism may have been around 550 - 650°C (Ferry and Spear, 1978), which agrees well with the temperatures determined above on the grounds of mineral assemblages.

## 2.2. Hare Bay Gneiss

The Hare Bay Gneiss outcrops in three separate northeast-trending bands in the map area. The most westerly of these adjoins the Square Pond Gneiss (Figure 2.1, page 18). The contact between the Square Pond Gneiss and the Hare Bay Gneiss is a "migmatite front" which is an approximately 1 km wide zone where paragneisses have been progressively converted into migmatites. Within the migmatite front, the rock types in the west have developed sodic plagioclase porphyroblasts

and small lenses of (2-3 cm long) quartzofeldspathic material that parallel the gneissic banding, the amount of quartzofeldspathic segregations and the sodic plagioclase blastesis increase towards the east gradually giving rise to migmatite (Blackwood, 1977; Jayasinghe, 1978), which constitutes the major part of the Hare Bay Gneiss.

The Hare Bay Gneiss is characterized by alternating quartzofeldspathic layers (leucosome\*) and mica-rich layers (melanosome\*) that range from less than a millimeter to about four centimeters in width. The layers of leucosome and melanosome are mostly parallel to each other and have diffuse margins which at places are marked by biotite selvages. The megascopic appearance of the migmatite is variable; from place to place it has phlebitic, stromatic, folded and locally schlieren and nebulitic structures\* (Figure 2.21). Inclusions of the Square Pond Gneiss, ranging from a few centimeters to several meters across, occur throughout the migmatite and represent the paleosome. Most of the inclusions are psammitic to semi-pelitic in composition with the former predominating over the latter. Also present are minor, lensoid inclusions of amphibolite. The structural geology and the petrology of the neosome are described in detail below.

#### 2.2.1. Structural Geology

The Hare Bay Gneiss is characterized by three main structural features, the layering, a foliation that occurs axial planar to the folds of the layering and a second foliation that is related to the shear zones in the area.

---

\*migmatite terminology from Mehnert (1968).



Fig. 2.21. Hare Bay Gneiss on northern shore of Indian Bay.  
Location - 413.

The layering in the Hare Bay Gneiss was described previously. It has a biotite-muscovite alignment parallel to it. Field evidence, for example the gradational contact between the Square Pond Gneiss and the Hare Bay Gneiss, and the presence of numerous inclusions of the former in the latter, indicate that the Hare Bay Gneiss was probably derived by the migmatization of a gneiss terrain, a part of which is represented by the Square Pond Gneiss (see section 2.2.4. on the origin of the migmatite). The layering in the migmatite may be largely inherited from the predominant layering in the parent gneiss terrain. The peak metamorphism in the area, which is probably the cause of the migmatization, post-dates  $D_2$  (see Figure 2.18, page 43). Thus  $D_2$  structures in the parent gneiss may have largely controlled the layering in the migmatite. Therefore the layering in the Hare Bay Gneiss is correlated with  $S_2$  in the Square Pond Gneiss.

At places the layering in the Hare Bay Gneiss is tightly folded with the development of an axial planar foliation defined by biotite and muscovite (Figure 2.22). Elsewhere this foliation parallels the layering. Since the layering in the migmatite correlates with  $S_2$  in the Square Pond Gneiss, the foliation in the former is probably equivalent to the regional schistosity  $S_3$  recognized in the latter. Therefore the folds of the layering in the migmatite are called  $F_3$  folds and the foliation that occur axial planar to these folds is termed  $S_3$ .



Fig. 2.22.  $F_3$  folds in the Hare Bay Gneiss, south of Indian Bay.

The  $F_3$  folds in the Hare Bay Gneiss plunge at moderate angles in both northeasterly and southwesterly directions (Figure 2.23).  $S_3$  has a northeasterly strike and dips at shallow to steep angles mostly to the northwest except south of Indian Bay where  $S_3$  strikes in a east-northeast direction; there,  $S_3$  dips at steep angles mostly to the south-southwest. During the  $D_3$  deformation, the banding and  $S_3$  foliation in the migmatite have been flattened against the Square Pond Gneiss inclusions. The inclusions themselves have been deformed, either into boudins or else folded or rotated towards  $S_3$  (Figure 2.24). The axial planes of the folded inclusions are parallel with  $S_3$  in the host. Commonly the inclusions contain a layering that in many cases is oriented oblique to  $S_3$  in the host. This layering is believed to be  $S_2$  in the Square Pond Gneiss.

The Hare Bay Gneiss, to the north and south of North West Pond and adjacent to the Cape Freels Granite, is deformed by the two main shear zones (Figure 2.1) that mark the  $D_4$  deformation in the area.

Within the shear zones, the Hare Bay Gneiss shows a strong mylonitic fabric,  $S_4$ . In these zones, the biotite in the migmatite has been stretched out to form "streaks" that wrap around lenticles of feldspar (Jayasinghe, 1976; Jayasinghe and Berger, 1976). The feldspar grains are less than 0.8 mm in diameter. Quartz occurs in bands that parallel the anastomosing foliation defined by the biotite. The quartz grains range from 0.08 to 0.24 mm in diameter and have sutured grain boundaries. Also present are a few, larger, elongated quartz grains with well-developed subgrains.

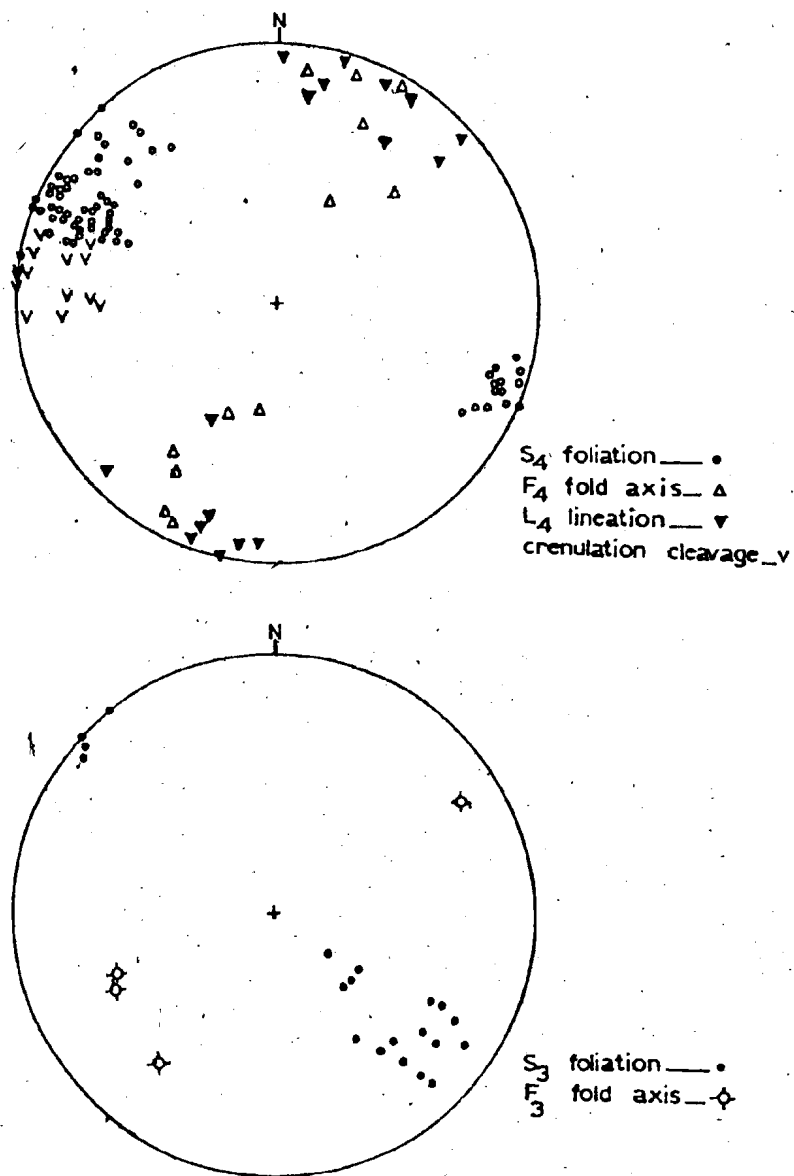


Fig. 2.23. Stereoplot showing  $F_3$  and  $F_4$  minor fold axes,  $L_4$  lineation and poles to  $S_3$ ,  $S_4$  and crenulation cleavage in the Hare Bay Gneiss. (Trends of structures in the Hare Bay Gneiss were noted in many places but it was not possible to measure the three dimensional attitude of the structures at all the locations.)

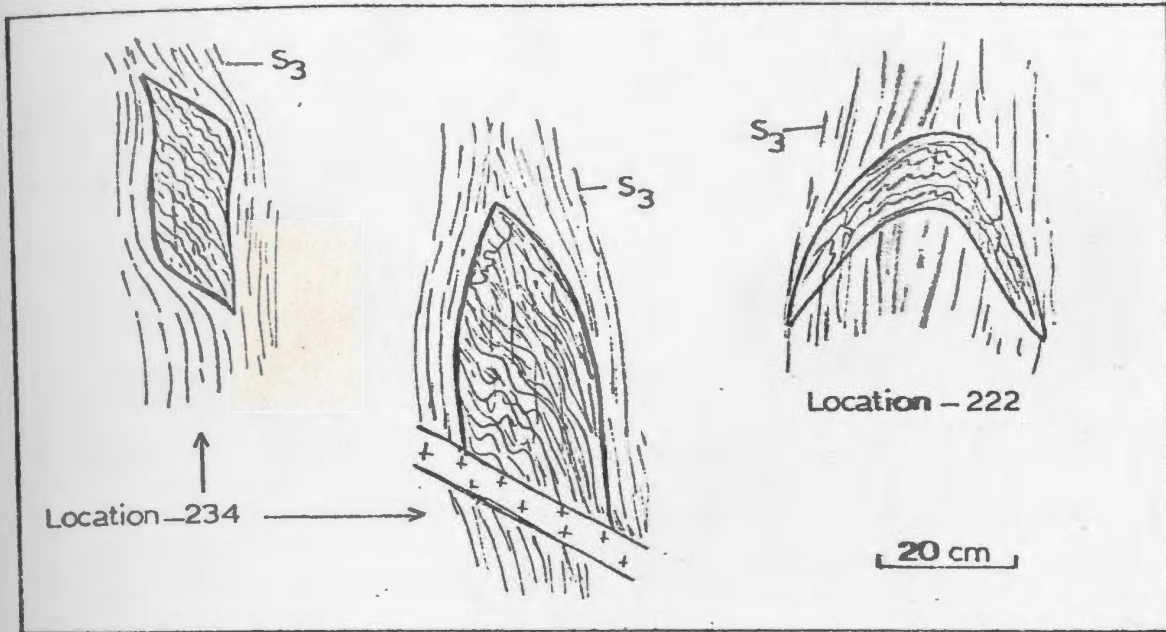


Fig. 2.24. Square Pond Gneiss inclusions in the Hare Bay Gneiss. The inclusions have been deformed by  $D_3$ :

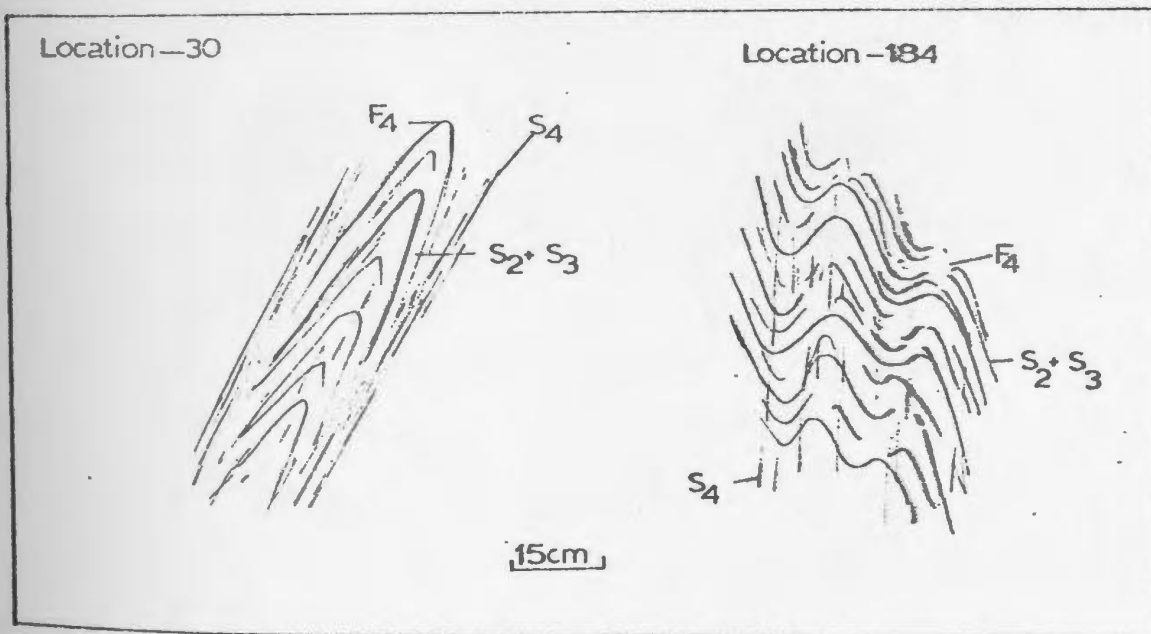


Fig. 2.25.  $F_4$  folds in the Hare Bay Gneiss.



The  $S_4$  foliation strikes in a north-northeasterly direction except in the northern part of the migmatite adjoining the Cape Freels Granite. There the strike is more northeasterly (Figure 2.23). The dips are mostly steep.  $S_4$  foliation planes contain a lineation ( $L_4$ ) marked by elongated quartz grains, that plunges at shallow angles to the northeast and southwest. Generally the  $D_4$  structures trend parallel to the margins of the shear zones.

$S_4$  is axial planar to close to tight minor folds ( $F_4$ ) of  $S_3$  and the migmatitic layering (Figure 2.25).  $F_4$  folds are not very common. In places the layering and  $S_3$  occur as curved traces between  $S_4$  foliation planes (Figure 2.26).  $F_4$  fold axes have attitudes similar to those of  $L_4$ .  $F_4$  folds have refolded  $F_3$  folds in the migmatites as well as in the gneissic inclusions resulting in type-1 and type-3 interference patterns (Figure 2.27).

A widespread, steeply dipping and northerly-trending crenulation cleavage can be seen offsetting  $S_4$  in the migmatite. This cleavage is marked by thin ( $< 1$  mm thick) discontinuous micaceous layers. Broad warps of  $S_4$  with east-west axial traces occur in places (Figure 2.28). These post-date the crenulation cleavage. East-southeast striking, steeply dipping kink bands have deformed  $S_4$  and the crenulation cleavage and cut across the broad warps. These kink bands are believed to be of the same age as the kink bands that deformed the composite schistosity in the Square Pond Gneiss.

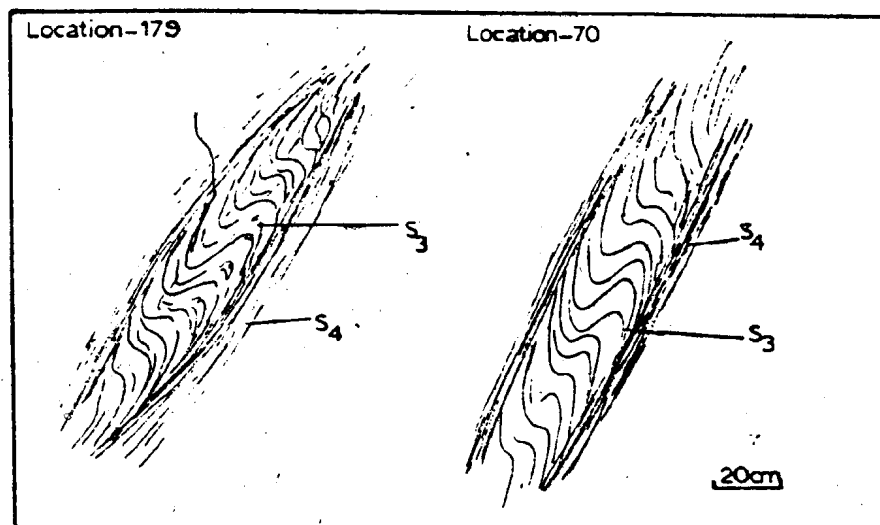


Fig. 2.26. Transposition of  $S_3$  in the Hare Bay Gneiss.

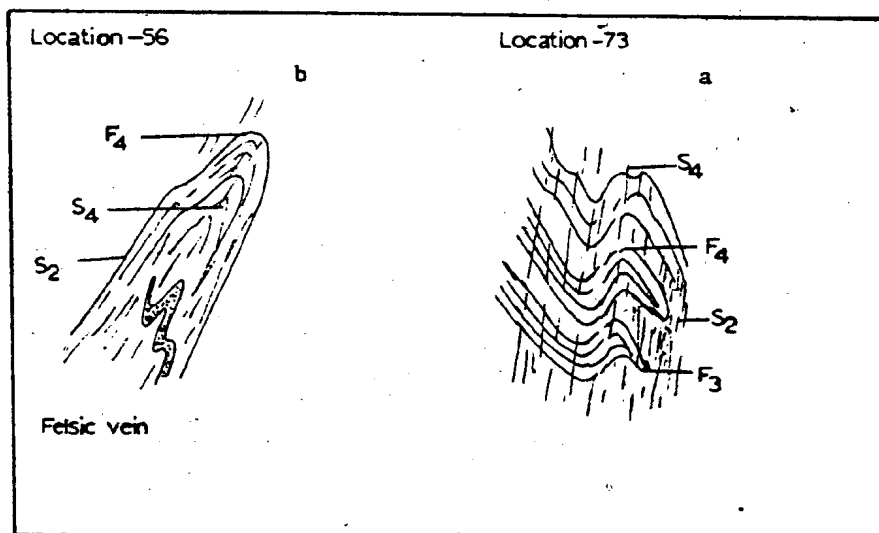


Fig. 2.27. a)  $F_3$  folds refolded by  $F_4$  folds. Hare Bay Gneiss.  
b)  $F_4$  fold in Hare Bay Gneiss.

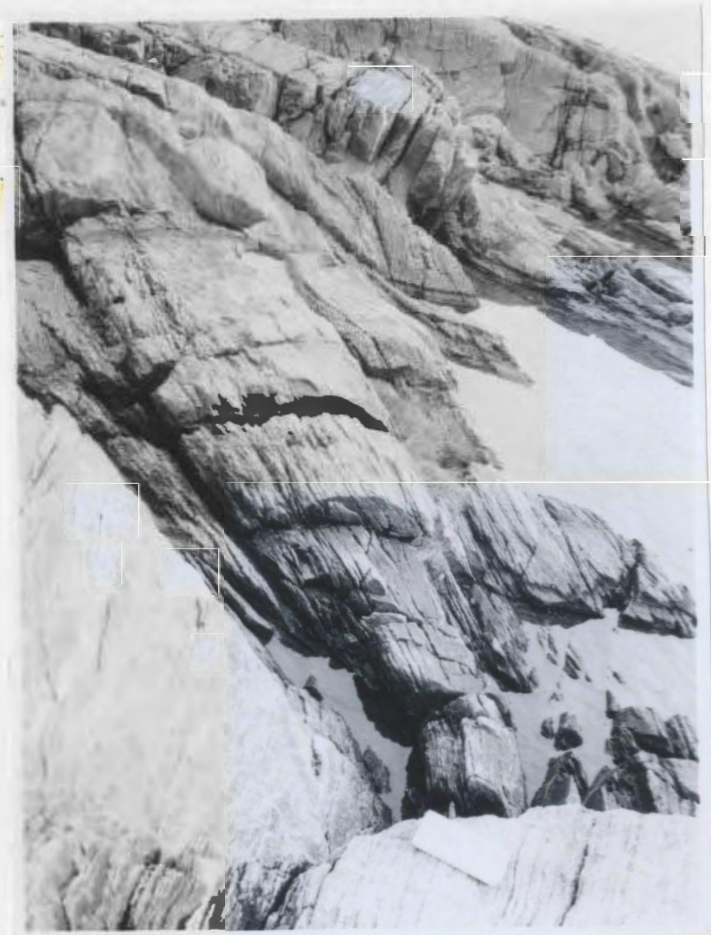


Fig. 2.28. Broad warps of  $S_4$  in the Hare Bay Gneiss.

### 2.2.2. Petrography\*

The main mineral constituents in the Hare Bay Gneiss are quartz, plagioclase, biotite and muscovite. Small amounts of orthoclase are locally present. Microcline porphyroblasts are common in the gneiss adjacent to some of the megacrystic granites in the area and will be discussed later, together with the microcline megacrysts in the plutons (Chapter 3). Accessory minerals include ilmenite, magnetite, zircon, apatite and tourmaline. Table 2.3 shows the modal composition of the Hare Bay Gneiss.

Quartz grains range from 0.4 to 2 mm in diameter and are xenomorphic in shape. Some quartz grains show elongation in the direction of mica alignment ( $S_3$ ) in the gneiss. The grain boundaries of the quartz are either embayed or sutured. Undulatory extinction is common.

Biotite flakes range from 0.2 to 2 mm in length and commonly show pale brown to dark brown pleochroism; a few show pale brown to greenish brown pleochroism. The biotite is partly chloritized.

Muscovite occurs associated with the biotite but is everywhere subordinate to the latter. In places, mats of fibrolite are associated with the muscovite (Figure 2.29). The micas occur both as aligned grains defining the  $S_3$  schistosity in the gneiss and as randomly oriented flakes. The opaque minerals in the gneiss tend to occur with the biotite.

---

\* descriptions of microstructures in this section apply to the gneiss outside the shear zones.

Table 2.3. Modal analyses of the Hare Bay Gneiss.

Sample #	413	51	54	56
quartz	30.9	47.8	48.2	45.7
microcline	9.4	5.2	---	---
plagioclase	46.9	34.6	36.4	38.2
biotite	21.1	10.4	10.3	8.3
muscovite	12.1	2.0	4.1	6.8
accessory minerals	Tr	Tr	Tr	Tr
No. of points	800	550	650	700

Tr - trace amounts

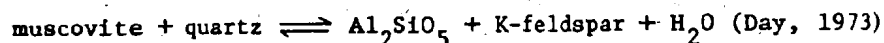
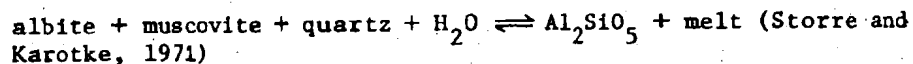
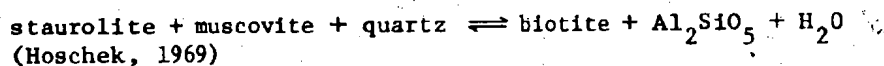
Plagioclase grains range from 0.4 to 2.5 mm in size and are highly altered to sericite and epidote. They have hypidiomorphic to xenomorphic shapes and curved and embayed grain boundaries. Polysynthetic twinning is common; a few grains show pericline twinning in addition to the albite twinning. The composition ranges from  $An_8$  to  $An_{16}$ . Some of the plagioclase shows oscillatory zoning.

Plagioclase commonly has developed a myrmekitic structure adjacent to orthoclase. Orthoclase grains are similar in shape to the plagioclase but are smaller in size (0.4 to 1 mm in diameter).

Small (<1 mm across), idiomorphic to hypidiomorphic, pinkish to reddish, garnet grains occur in places. Coarse tabular sillimanite crystals occur in some micaceous parts of the gneiss.

#### 2.2.3. Metamorphism

The mineralogy of the Hare Bay Gneiss is shown in the ACF and AFM diagrams in Figure 2.30. The mineral parageneses suggest that metamorphism of the Hare Bay Gneiss has reached amphibolite facies. Sillimanite and orthoclase in the Hare Bay Gneiss may have been produced by the following reactions. Equilibrium curves of these reactions are shown in Figure 2.14.



No staurolite or andalusite was found in the Hare Bay Gneiss. The staurolite "out" equilibrium curve (Hoschek, 1969) cuts the



Fig. 2.29. Fibrolite in the Hare Bay Gneiss. Location - 310, northern shore of Indian Bay.

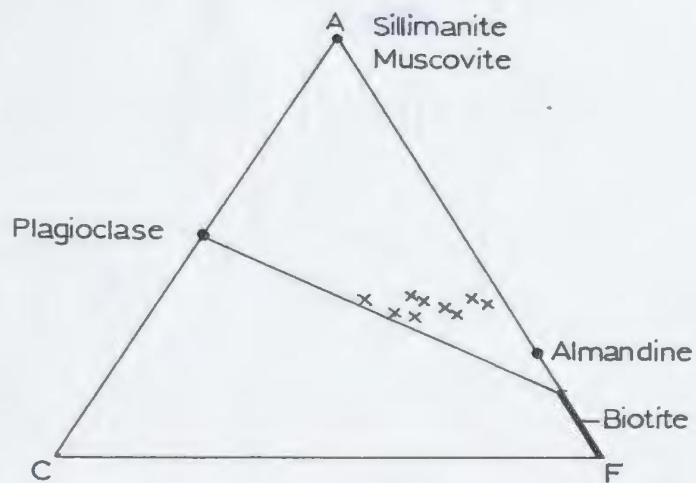


Fig. 2.30. ACF diagram for the Hare Bay Gneiss.  
x - chemical analyses of the Hare Bay Gneiss.

andalusite - sillimanite field boundary at 4.3 kb and 650°C (Figure 2.14, page 34). Therefore the pressure-temperature conditions of the metamorphism in the Hare Bay Gneiss must have been above 4.3 kb and 650°C.

#### 2.2.4. Geochemistry and Origin

Ten samples from the Hare Bay Gneiss were analysed for major, minor and trace elements. A sample location map is given in the back pocket. The samples contained both leucosome and melanosome. The analyses are listed in Table 2.4. Major and minor element compositions do not vary significantly among the individual analyses; Zr, Rb, Sr, Ba, Ni, Cr and V show a greater variation than the rest of the trace elements. This variation probably reflects slight differences in plagioclase, potassium feldspar, biotite, ilmenite and zircon contents in the samples.

The Hare Bay Gneiss is significantly different from the Square Pond Gneiss in chemical composition. The higher alumina, lime and alkali contents of the migmatites, relative to the Square Pond Gneiss (Figure 2.31), suggest that the protolith of the Hare Bay Gneiss was more pelitic than the latter. This fits well with the observation (p. 17) that the Square Pond Gneiss becomes more micaceous eastwards.

There are four main mechanisms that could produce migmatites. They are: (1) injection of igneous material into metamorphic rocks, (2) metasomatic replacement of metamorphic rocks, (3) anatexis and (4) metamorphic differentiation. The applicability of each of these mechanisms in the formation of the migmatite that constitutes the Hare Bay Gneiss is discussed below.



Table 2.4 Chemical analyses of the Hare Bay Gneiss

Sample #	54	70	75	224	227	234	307	311	413	$\bar{x}$	S
SiO <sub>2</sub> (wt.%)	72.6	72.9	72.9	70.0	70.7	76.4	75.1	73.2	64.7	72.0	3.4
TiO <sub>2</sub>	0.34	0.64	0.55	0.40	0.38	0.37	0.77	0.23	0.89	0.51	0.22
Al <sub>2</sub> O <sub>3</sub>	13.80	12.20	11.30	14.20	14.10	11.70	10.90	13.30	15.20	12.97	1.49
Fe <sub>2</sub> O <sub>3</sub>	0.00	0.69	1.65	0.19	0.03	0.65	0.79	0.20	1.26	0.61	0.57
FeO	2.24	3.04	2.84	2.81	2.59	2.21	3.35	2.30	4.92	2.92	0.84
MnO	0.05	0.10	0.07	0.12	0.12	0.06	0.10	0.06	0.13	0.09	0.03
MgO	0.78	1.45	1.59	0.97	0.75	1.02	1.57	0.69	2.02	1.20	0.47
CaO	1.49	1.14	1.43	1.47	1.31	1.30	1.09	2.00	0.93	1.35	0.31
Na <sub>2</sub> O	4.02	2.08	2.33	3.39	3.48	2.77	1.93	3.88	2.14	2.89	0.82
K <sub>2</sub> O	2.71	2.91	2.13	3.78	3.83	2.45	2.32	1.60	3.73	2.83	0.80
P <sub>2</sub> O <sub>5</sub>	0.04	0.11	0.06	0.12	0.10	0.07	0.09	0.03	0.14	0.08	0.03
H <sub>2</sub> O	1.17	1.35	1.43	1.36	0.79	1.29	1.21	0.89	2.24	1.30	
Total	99.24	98.61	98.28	98.81	98.18	100.29	99.22	98.38	98.30	98.75	
Zr	168	252	189	180	167	187	263	165	199	197	36
Sr	320	151	205	155	225	150	131	307	141	198	72
Rh	109	144	205	131	140	272	122	68	167	151	59
Zn	38	60	49	69	48	72	66	41	98	60	19
Ga	7	14	12	14	9	12	17	6	17	12	4
Ba	417	584	871	523	697	467	392	116	758	536	225
Nb	14	12	13	15	14	15	15	12	20	14	7
Ca	20	18	23	20	18	22	17	19	27	20	3
Pb	19	11	35	30	33	43	3	20	21	24	13
Ni	8	21	7	11	12	15	28	10	44	17	12
Cr	18	48	9	23	13	25	61	20	76	33	23
V	41	86	36	47	47	56	125	37	143	69	40
Y	35	37	48	34	38	48	39	31	41	39	6

 $\bar{x}$  - average composition; S - standard deviation

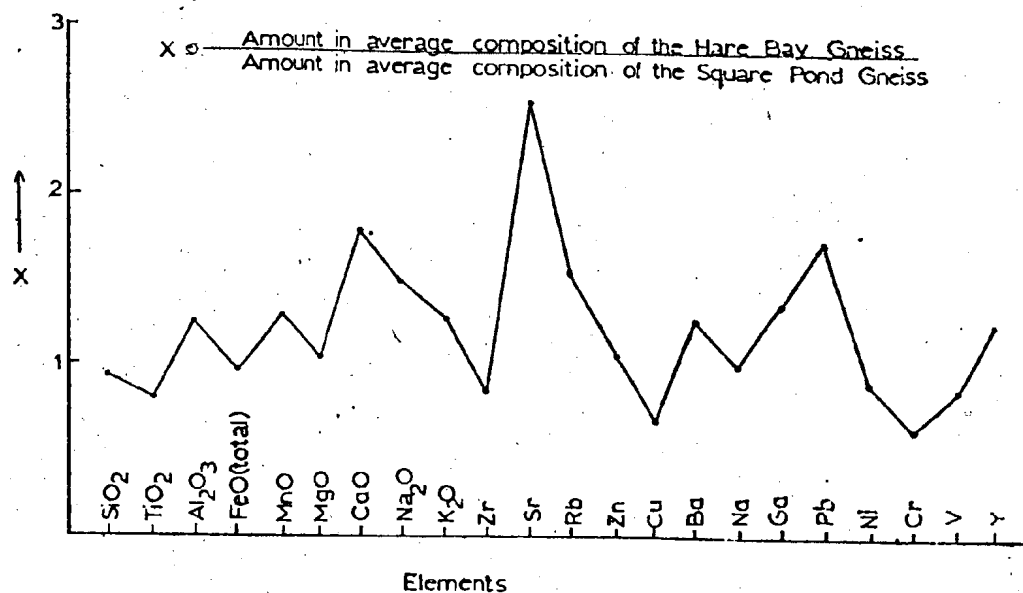


Fig. 2.31. Enrichment or depletion of major and minor element oxides and trace elements in the Hare Bay Gneiss relative to the Square Pond Gneiss.

It is difficult to disprove the proposition that injection of igneous material into metamorphic rocks produced the migmatite; a wide variety of igneous rock types can be injected into any type of country rock. Pitcher and Berger (1972) described the development of migmatites around the Thor and the Fanad plutons in the Donegal area, due to the injection of granitic material related to the plutons. However the granitic plutons in the present thesis area are rich in microcline and contain plagioclase with compositions ranging from  $An_{20}$  to  $An_{35}$ , whereas the leucosome in the migmatite is poor in potassium feldspar (<5%) and contain plagioclase with compositions between  $An_8$  to  $An_{14}$ . Also the granites post-date\* the migmatitic banding in the Hare Bay Gneiss. Therefore the leucosome in the latter is probably unrelated to the granitic intrusions in the area. Further, the plagioclase in the leucosome is similar in composition to that in the melanosome. This kind of relationship is unlikely to have been produced if the leucosome resulted from injection of igneous material into already existing metamorphic rocks.

Metasomatic replacement of metamorphic rocks to produce migmatites generally implies an addition of material from outside (external metasomatism). The presence of plagioclase (albite) porphyroblasts within the "migmatite front" suggests that metasomatism has contributed to the formation of the migmatite, but does not necessarily imply an influx of material from an external source. The available

---

\* The exact time difference between migmatization and granite emplacement in the area is not known as there are no radiometric dates available from the migmatite.

evidence does not completely rule out metasomatism as a mechanism at least partly responsible for the origin of the Hare Bay Gneiss.

A number of authors have attributed the origin of migmatites to anatexis (Brown and Fyfe, 1970; Mehnert et al., 1973; Busch et al., 1974; Ashworth, 1976). Winkler (1974) suggested that granitic, tonalitic to trondhjemitic melts can be produced by anatexis of gneissic rocks. However, Von Platen (1965) and Hoschek (1976) demonstrated that potassium feldspar crystallizes from early formed melts even if biotite is the only potassium-bearing mineral in the assemblage undergoing anatexis. Kilinc (1972) demonstrated that trondhjemitic melts could be produced by partial melting of greywacke but even these melts contained at least 15% potassium feldspar. Yoder et al. (1957), Winkler (1974) and Drake (1976) indicated that, during anatexis, the albite component of the plagioclase strongly fractionates into the coexisting melt phase. Therefore the plagioclase in the leucosome, formed by anatexis, must be more sodic than that in the melanosome. But the leucosome in the migmatite in the thesis area contains very little potassium feldspar and has plagioclase compositions similar to those in the melanosome. Therefore, despite the fact that the metamorphic conditions in the Hare Bay Gneiss have exceeded the "wet" granite solidus (Figure 2.14, page 34), anatexis was probably not the major mechanism that produced the migmatite.

Metamorphic differentiation involves "internal metasomatism" whereby quartzofeldspathic and mafic components are segregated within a closed system. Metamorphic differentiation has been found to occur

in both low grade and high grade metamorphic rocks (Hyndman, 1972) and has been cited as the principal mechanism for the origin of migmatites in a number of areas (Amit and Eyal, 1976; Yardley, 1978). Indeed the similarity in plagioclase composition between the leucosome and the melanosome in the Hare Bay Gneiss suggest local redistribution of material. According to Yardley (1978) the driving force of metamorphic segregation may include (1) already existing chemical gradients, (2) strain energy, and (3) hydraulic fracturing.

The evidence presented in the preceding sections indicates that metasomatism, anatexis and metamorphic differentiation contributed to the formation of the migmatite in the thesis area. The degrees of importance of these mechanisms relative to each other in producing the migmatite are not known.

### 2.3. Summary

The pre-granite rock types in the area are represented by two gneissic units: the Square Pond Gneiss and the Hare Bay Gneiss. These constitute the northward extensions of the Square Pond Gneiss and the Hare Bay Gneiss of Blackwood (1977). The Square Pond Gneiss consists dominantly of biotite gneiss. Associated with the gneiss are areas of schists and psammitic metasediments. Metamorphic grade in the Square Pond Gneiss increases eastwards from greenschist facies to amphibolite facies. The mineral parageneses and the garnet-biotite geothermometry indicate that the amphibolite facies metamorphism in the gneiss has occurred at pressures between 4.3 and 5.5 kb and temperatures between 550 and 650°C. The Hare Bay Gneiss consists of

migmatite and occurs to the east of the Square Pond Gneiss. It has been metamorphosed to amphibolite facies. Unlike in the Square Pond Gneiss, staurolite and andalusite are absent in the Hare Bay Gneiss, but sillimanite is common. Therefore the metamorphic conditions in the Hare Bay Gneiss must have exceeded 4.3 kb and 650°C.

There is evidence of at least three deformation events ( $D_1$ ,  $D_2$ ,  $D_3$ ) in the Square Pond Gneiss. The  $D_1$  and the  $D_2$  deformations have resulted in gneissic bandings  $S_1$  and  $S_2$ .  $S_2$  is the most ubiquitous structure in the gneiss.  $D_3$  has resulted in a steeply dipping, northeast-trending foliation ( $S_3$ ) that occurs axial planar to  $F_3$  minor folds of  $S_2$ . Microstructural relationships between garnet, staurolite, andalusite and fabrics in the Square Pond Gneiss indicate that the peak metamorphism in the latter is syntectonic with  $D_3$ . Migmatization in the area has occurred contemporaneously with the peak metamorphism. The migmatite layering (defined by the leucosome and the paleosome) in the Hare Bay Gneiss is believed to be partly inherited from  $S_2$  in the "parent rocks" of the migmatite.  $S_3$  occurs axial planar to minor folds of the migmatitic banding. In places, the Hare Bay Gneiss is cut by the  $D_4$  shear zones in the area, resulting in a mylonitic foliation ( $S_4$ ). The granitoids in the area post-date the migmatization.

## CHAPTER 3

### INTRUSIVE ROCKS: GRANITOIDS AND GABBRO

Intrusive rocks occupy approximately three-quarters of the thesis area. They comprise eight granitoid plutons, several gabbro bodies and a swarm of diabase dikes. The granitoid plutons are shown in the sketch map of Figure 2.1 (page 18). The gabbros are too small to be represented at the scale of Figure 2.1 but are shown together with the locations of the diabase dikes on the 1:50,000 scale geological map of the area (in back pocket). Of the eight granitoids, the Wareham, Lockers Bay, Cape Freels, Deadman's Bay and the Newport plutons are characterized by microcline megacrysts. The North Pond and the Business Cove plutons are non-megacrystic, muscovite-biotite two mica granites, with minor garnet. The Big Round Pond pluton consists of medium-grained biotite granite.

The purpose of this chapter is to describe the contact relationships, rock types and structures of the granitoids. Also included are a description of the deformation in the shear zones that affect the granitoids and a discussion of the ages of the intrusive rocks in the area. The diabase dikes have been studied in detail in a separate chapter.

In the following sections, the granitoids are described in the probable order of decreasing age of emplacement determined from field relationships. An unequivocal emplacement sequence cannot be established in the field mainly because they are not all in contact with each other. The mode of emplacement of the plutons in the area, except

for scanty evidence for forceful intrusion in the case of the North Pond and the Deadman's Bay plutons, is not clear.

### 3.1. Classification

Granitoids in the area<sup>1</sup> are classified according to Streckeisen (1976) and Hietanen (1963) (Figures 3.1 and 3.2). In Streckeisen's scheme, quartz, K-feldspar and plagioclase contents from modal analyses of the plutons (Table 3.1) were used (see Appendix 3.1 for techniques used in modal analysis). In Hietanen's scheme, molecular percentages of orthoclase, albite and anorthite from the mesonorms of the plutons (Appendix 3.2) were used. As there are more chemical analyses, from different parts, than modal analyses from each of the plutons, the nomenclature based on the mesonorms is more representative of the rock types of the plutons than that based on the modal analyses.

All the plutons plot in the granite field in the Streckeisen classification. In the Hietanen classification, analyses from the Lockers Bay, Deadman's Bay, Newport and Big Round Pond plutons plot in the granite field, as do those from the Cape Freels pluton except for the analyses from Greenspond, which fall in the quartz monzonite, monzonalite and granodiorite fields. In the Greenspond area, the Cape Freels pluton contains a large number of gneissic xenoliths, and the rock type there is more melanocratic than elsewhere in the pluton (see section 3.3.4b, page 101). This change in composition could be the result of assimilation

---

<sup>1</sup> Some of the granitoids extend beyond the limits of the present thesis area; however, the classification presented here refers only to the rock types that occur within the latter.



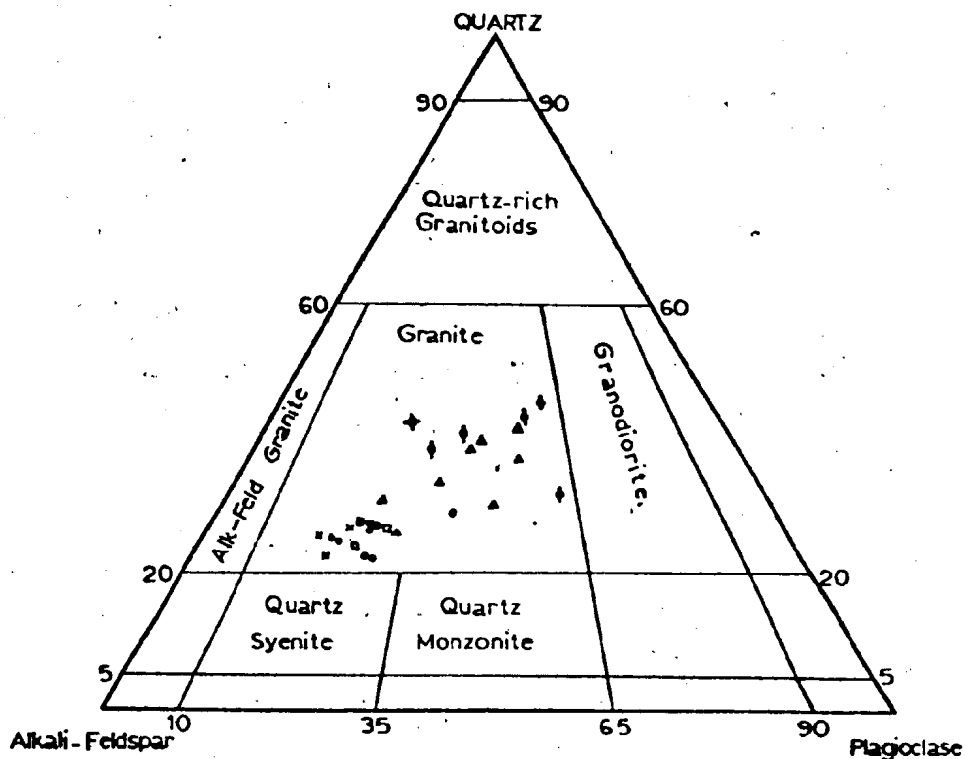
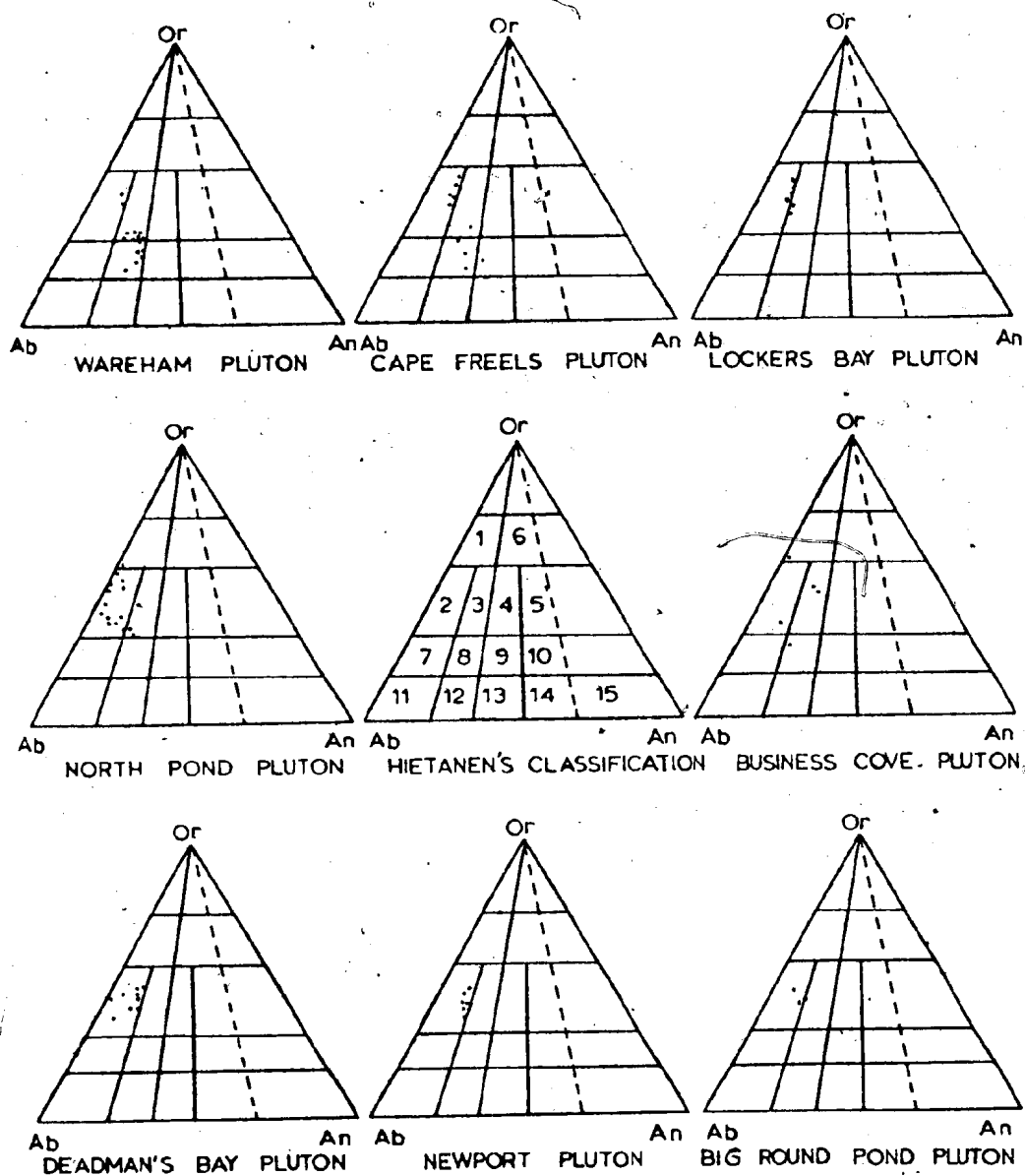


Fig. 3.1. Modal classification of the granitoids in the area according to Streckeisen (1973).  $\Delta$  - Wareham pluton, X - Cape Freels pluton,  $\square$  - Lockers Bay pluton,  $\diamond$  - North Pond pluton,  $\blacktriangle$  - Business Cove pluton,  $\circ$  - Deadman's Bay pluton,  $\bullet$  - Newport pluton, + - Big Round Pond pluton.



- |                     |                          |                  |                   |
|---------------------|--------------------------|------------------|-------------------|
| 1. Kaligranite      | 5. Calcimonzonite        | 9. Granodiorite  | 13. Quartzdiorite |
| 2. Granite          | 6. Calcigranite          | 10. Granogabbro  | 14. Gabbro        |
| 3. Quartz monzonite | 7. Granite trondhjemitic | 11. Trondhjemite | 15. Malic gabbro  |
| 4. Monzonite        | 8. Monzotonalite         | 12. Tonalite     |                   |

Fig. 3.2. Normative classification of the granitoids in the area according to Hietanen (1963).

TABLE 3.1 - Modal analyses of the granitic plutons in the thesis area.

Intrusion	Sample Number	Quartz	K-feldspar	Plagioclase	Biotite	Muscovite
Karelian Pluton	723	53.0	25.6	30.3	11.2	--
	877	51.6	37.7	24.2	6.5	--
	810	29.4	16.1	19.0	5.5	--
	911	25.8	30.0	29.2	15.0	--
	1034	24.4	15.7	22.2	7.7	--
North Pond Pluton (medium grained phase)	361	24.1	23.5	37.1	7.7	3.6
	369	41.2	19.9	29.8	6.9	1.8
	303	57.8	21.9	27.6	10.2	2.2
North Pond Pluton (porphyritic phase)	188	31.0	34.4	19.7	5.1	6.6
	915	33.6	28.0	21.0	5.3	11.1
Business Cove Pluton	182	35.6	29.3	25.1	6.2	5.3
	220	37.0	30.1	25.9	7.0	--
	222	38.1	25.1	29.5	1.2	5.3
Tide Falls Pluton	11	20.8	54.2	15.5	6.9	--
	115	22.9	52.5	15.2	9.3	--
	166	25.0	50.7	17.1	5.8	--
Deadman's Bay Pluton	1	23.3	53.9	15.6	7.3	--
	822	21.3	52.4	21.0	5.1	--
	921	27.2	38.5	27.9	6.1	--
	1091	25.2	49.5	20.3	4.6	--
	1095	25.6	49.4	19.3	5.7	--
Newport Pluton	190	25.0	19.0	10.8	5.3	--
	219	20.8	51.6	22.1	1.6	--
	306	22.9	52.5	16.9	7.0	--
Big Round Pond	131	40.9	38.1	18.0	3.0	--
Lockers Bay Pluton	L <sub>1</sub>	21.2	16.1	20.2	9.2	--
	L <sub>2</sub>	20.6	53.1	17.9	9.1	--
	L <sub>4</sub>	22.8	51.3	18.7	7.2	--

of country rocks, parts of which are now preserved as xenoliths. Therefore, the rock type in the Greenspond area is not considered representative of the intrusion.

The majority of the analyses from the North Pond pluton lie in the granite field, and the rest fall in the quartz monzonite field, in the normative classification. The analyses that plot in the quartz monzonite field come from a xenolith-free part of the pluton, and thus represent an original magmatic variation in the intrusion. This part has a different rock type from the rest of the pluton and has been described as a separate phase in the detailed description of the pluton (see section 3.3.2, page 87). However, based on the dominant rock type, the North Pond pluton is classified as a granite.

Most of the analyses (50 percent) from the Wareham pluton fall in the quartz monzonite field in the normative classification. The majority of the rest (36 percent of the total analyses) lie in the monzotonalite field and the remaining analyses (14 percent of the total number) plot in the granite field. Therefore, the Wareham pluton is classified as a quartz monzonite. This nomenclature is different from that obtained using the modal analyses; however, the chemistry of the pluton fits a quartz monzonite better than a granite (see Chapter 5).

Analyses from the Business Cove pluton are scattered in the Heitonen classification diagram and, thus, cannot be classified conclusively using the latter. This pluton contains numerous gneissic and megacrystic granite xenoliths and its highly variable composition probably resulted from assimilation of the xenoliths. However, the

Business Cove pluton is similar to the North Pond Granite in lithology (see section 3.3.3., page 94) and, thus, is classified as a granite.

The classification of the plutons shows that, except for the Wareham and the Business Cove plutons, they are largely similar in composition regardless of the presence or the absence of the microcline megacrysts.

### 3.2. Lithology of the Megacrystic Plutons

The megacrystic plutons in the area are largely similar in mineralogy. They are so similar that it is difficult to readily identify a hand specimen or a thin section as coming from one or another pluton. Therefore, instead of describing the rock type of each individual pluton, a general description<sup>1</sup> of the mineralogy and the microstructure of the megacrystic granitoids is given below. In the detailed descriptions of the individual plutons, deviations from this general description are discussed. The non-megacrystic plutons in the area, except for muscovite and garnet in the North Pond and the Big Round Pond plutons, consists of the same minerals as the groundmass of the megacrystic plutons. Also, many of the microstructures in the groundmass of the megacrystic granites apply to the non-megacrystic plutons. Therefore, in the microstructural descriptions of the latter, only the deviations from the microstructures in the groundmass of the megacrystic plutons will be given.

---

<sup>1</sup> Descriptions of microstructure in thin section apply only to areas outside the shear zones. Microstructures in the shear zones are described under the individual plutons affected by them.

The megacrystic plutons in the area consist of microcline megacrysts set in a medium-to coarse-grained groundmass of quartz, plagioclase, microcline and biotite. The size of the megacrysts and the megacrysts to groundmass ratio vary among the plutons. Accessory minerals in the plutons include apatite, zircon, sphene and pyrite.

Microcline megacrysts are pinkish in colour and are generally euhedral with rectangular or six-sided shapes (Figure 3.3). In places, the megacrysts occur in close clusters (Figure 3.4). Some of the megacrysts are mantled either partly or completely by plagioclase. The reverse, where large plagioclases (>2 cm in length) are mantled by microcline, also occurs. Carlsbad twins are widespread and are easily seen in outcrops as the two twins reflect light in different directions. Grid twinning in the megacrysts shows an uneven development from intrusion to intrusion. Megacrysts in the Wareham pluton show well-developed grid twinning. Those in the Cape Freels, Lockers Bay and the Deadman's Bay granites generally show well-developed grid twinning but in some of the crystals twinning is patchy. In the Newport Granite some of the megacrysts have grid twinning but in others the twinning is patchy or absent. In all the plutons, the megacrysts show a variably-developed microperthitic texture. The perthitic lamellae occur as veins or strings. Some of the megacrysts are zoned and are easily recognized by their oscillatory extinction (Figure 3.5). The zones are generally euhedral, few in number and are more common in the marginal part than in the central part of the crystals. Inclusions of plagioclase, quartz and biotite are common in the megacrysts. The inclusions may occur either randomly oriented or with their long direction parallel to the crystal outline of the



Fig. 3.3. Undeformed microcline megacrysts in the Cape Freels Granite. Location -86.

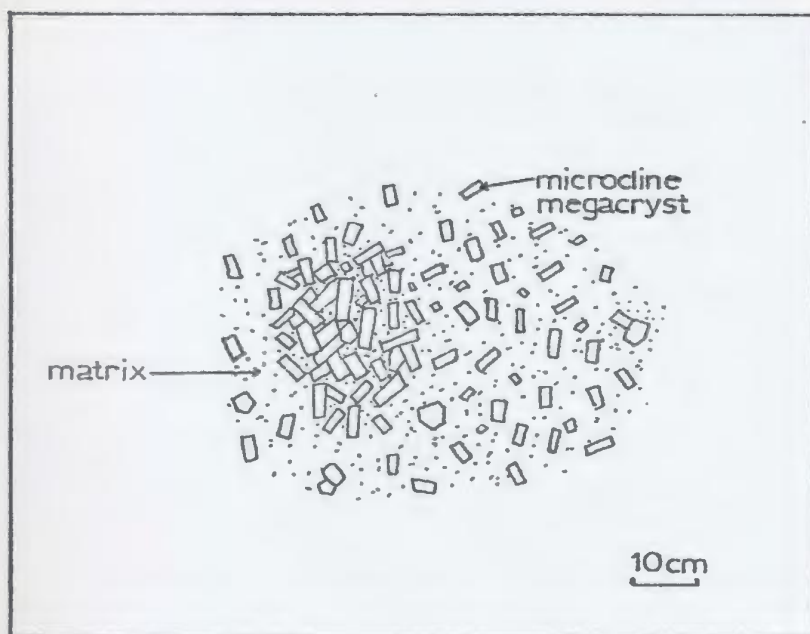


Fig. 3.4. Clusters of microcline megacrysts in the Deadman's Bay Granite. Location - 521.

host. Grain size of the inclusions is appreciably smaller than that in the groundmass. Plagioclase inclusions are generally similar in composition to the groundmass plagioclase; a few are more calcic than the latter (see Figure 4.3, page 152). Groundmass microclines are anhedral to subhedral and range from 0.2 to 1 cm in size. They have embayed and curved grain boundaries and a variably-developed microperthitic texture.

Plagioclase grains are mostly subhedral in shape and range from 0.2 to 8 mm in length; some are megacrystic (> 2 cm in length). Plagioclases have been altered in varying degrees to sericite and epidote. Some of the plagioclase grains have a more altered "dusty" core than the rest of the grain, indicating the more calcic nature of the former. Polysynthetic twinning is widespread and in some grains is accompanied by pericline twinning. Synneusis is common. Myrmekites are present in plagioclases adjacent to the microclines. Normal oscillatory zoning occurs in some of the plagioclases. Bulk composition\* of the plagioclases ranges from  $An_{22}$  to  $An_{30}$ .

Biotite flakes tend to occur in 3 to 6 mm wide clusters. Individual biotites range from 0.2 to 3 mm in length and are randomly oriented. They show pale brown to dark brown pleochroism. Quartz grains range from 0.4 to 5 mm in diameter. They are anhedral and have sutured and embayed grain boundaries. Undulatory extinction is common. Some of the quartzes have well-developed subgrains.

---

\* Determined optically by the extinction method. The compositions obtained by this method were found to be comparable with those calculated from the chemical analyses of the feldspars (see Figure 4.3, page 152).





Fig. 3.5. Compositional zones in a microcline megacryst. The zones are marked by oscillatory extinction, Newport Granite. Location - 304. (X10)



Fig. 3.6. An apophysis of the Wareham Quartz Monzonite truncating  $F_3$  folds in the Hare Bay Gneiss. Location - 793.

The significance and the origin of the microstructures described above will be discussed later (see Chapters 4 and 7).

### 3.3. Descriptions of the Individual Plutons

#### 3.3.1. Wareham Quartz Monzonite

##### a. Distribution and Contact Relationships

The Wareham Quartz Monzonite (Wareham Granite in Jayasinghe, 1978a and Bell *et al.*, 1979) occurs as a northeast-southwest elongated body between Big Round Pond and Northwest (First) Pond in the Wesleyville map area. Typical exposures of this pluton occur to the east of Parsons Pond and on Old Jingle at the western end of Indian Bay.

The Wareham Quartz Monzonite has been emplaced into the Hare Bay Gneiss, which occurs now adjacent to the southwestern, southern and the eastern margins of the pluton. The Business Cove, Deadman's Bay, Newport and Big Round Pond granites intrude it at places in the north and the northeast. In the west, it is intruded by the North Pond Granite. Its present outcrop shape has thus been determined largely by the younger granites which truncate it.

The contacts between the Wareham pluton and the granites intruding it are generally sharp; the contact with the Hare Bay Gneiss is either sharp or obliterated by 1 to 2 cm long microcline porphyroblasts. The pluton post-dates the gneissic layering and the  $S_3$  foliation in the migmatite since its apophyses can be seen truncating  $F_3$  folds in the latter (Figure 3.6).

The Wareham Quartz Monzonite contains numerous xenoliths of both the Square Pond Gneiss and the Hare Bay Gneiss. These may range up

to 10 to 15 m in size and are particularly abundant in places close to the western margin of the pluton (e.g. east of Parsons Pond). The pluton contains numerous pegmatitic and granitic minor intrusions. These probably represent late differentiates of the pluton itself as well as those of the other plutons that intrude it, especially the North Pond Granite.

b. Lithology and Structure

The Wareham Quartz Monzonite is a megacrystic pluton characterized by 2 to 4 cm long microcline crystals. The proportion of the megacrysts is variable and generally ranges from 10 to 30 percent of the rock, but in places, especially adjacent to the eastern margin of the pluton, the megacrysts are rare. Unlike in the other megacrystic plutons, the microcline megacrysts in the Wareham Quartz Monzonite are generally greyish white in colour. Furthermore, the Wareham pluton is richer in biotite than the other granitoids and is marked by yellowish green epidote and brownish sphene grains. The sphene grains range up to 7 mm in length and appear to have been corroded (Figure 3.7). Epidote is probably a secondary product because it generally encloses sphene crystals and contains inclusions of biotite which show extensive chloritization adjacent to the epidote grains.

The Wareham Quartz Monzonite contains mineral alignments<sup>1</sup> of two different ages. The older of these ( $W_1$ ) is the more commonly

---

<sup>1</sup>In this study, the term "mineral alignments" refers to the shape alignments produced by the parallelism of the long dimension of the minerals.



Fig. 3.7. A sphene grain in the Wareham Quartz Monzonite. Location - 374. (X10)

encountered structure in the intrusion and is formed by rectangular microcline megacrysts: the micas and the quartzes in the groundmass are randomly oriented. This mineral alignment, which probably formed with the emplacement of the pluton, is dominantly a northeast-striking, planar alignment with dips, gently to moderately, mostly to the west (Figure 3.8).

The second fabric ( $W_2$ ) is mylonitic and occurs in the southern part of the pluton, to the south of North West Pond. It is related to the western of the two shear zones in the area (see map in back pocket). The mylonitic foliation is defined by elongated quartzes and aligned biotite that curve in an anastomosing pattern around deformed feldspars. It strikes in a north-northeast direction and has steep dips (Figure 3.8). The mylonitic foliation has a shallowly plunging linear component because in horizontal outcrop surfaces the feldspars appear to be more elongated than in vertical surfaces at right angles to the foliation. Quartzes commonly show subgrains. Microcline megacrysts have rounded corners and may contain quartz filled fractures oriented at high angles to the foliation and the lineation. The significance of these fractures is described later (Section 3.4). The megacrysts generally have lensoid shapes and are fragmented. Some contain tails composed of fine-grained feldspar and quartz.

Away from and parallel to the shear zone, the Wareham Quartz Monzonite is cut by several narrow deformed zones. In these, the second fabric ( $W_2$ ) is only weakly developed and occurs axial planar to shallow, north-northeast trending open folds of  $W_1$ . The shear zones mark the  $D_4$  deformation in the area (see Section

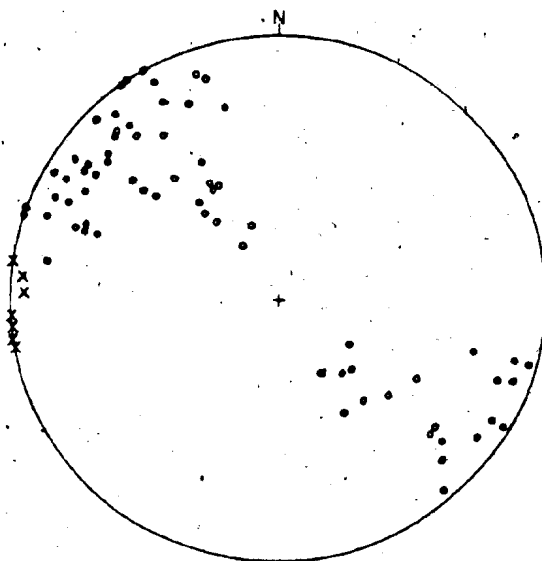


Fig. 3.8. Stereoplot showing poles to structures in the Wareham Quartz Monzonite. o -  $W_1$ , • -  $W_2$ , X - crenulation cleavage.

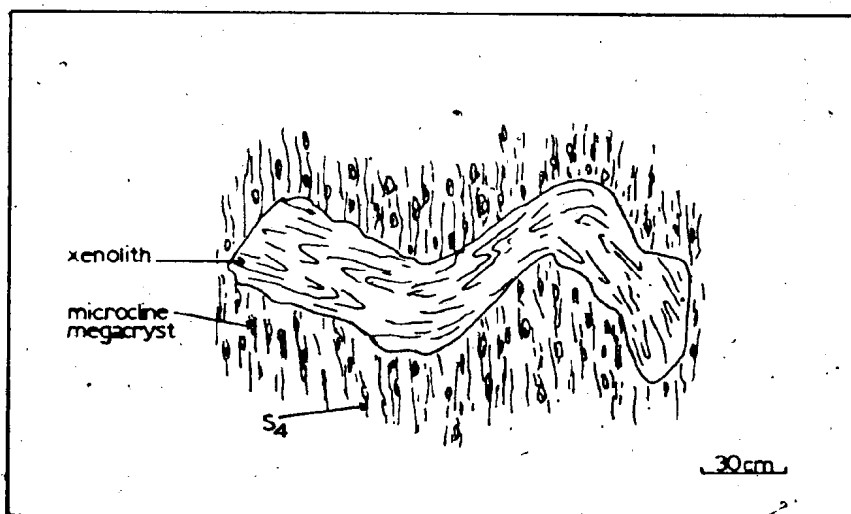


Fig. 3.9. Folded gneissic xenolith in Wareham Quartz Monzonite. Old Jingle.

2.2.1) and the mylonitic fabric ( $W_2$ ) in the Wareham pluton correlates with  $S_4$  in the gneisses (see page 54).

On Old Jingle south of Indian Bay, the Wareham Quartz Monzonite contains sheet-like xenoliths of the Square Pond Gneiss. These xenoliths have been folded with the mylonitic fabric in the host axial planar to the folds. Some of the xenoliths show tight to isoclinal folds of their internal banding ( $S_2$ ) with a foliation ( $S_3$ ) axial planar to them. These folds ( $F_3$ ) have been refolded during the folding of the xenoliths (Figure 3.9). The significance of these xenoliths is not very clear.

### 3.3.2. North Pond Granite

#### a. Distribution and Contact Relationships

The North Pond Granite<sup>1</sup> (Jayasinghe, 1978) occurs in the middle part of the thesis area. It is a northeasterly elongated body with a width ranging from 4 to 10 km. The widest part occurs close to the southern margin of the pluton around North West Pond, from where two large apophyses of the granite extend further south into the Square Pond Gneiss and the Hare Bay Gneiss.

The North Pond Granite intrudes the Square Pond Gneiss, the Hare Bay Gneiss and the Wareham pluton with a steep contact. It is intruded by the Deadman's Bay Granite to the north.

---

<sup>1</sup>The North Pond, Business Cove and Big Round Pond Granites (Jayasinghe, 1978a) are parts of the Powder Hill pluton of Jayasinghe and Berger (1976). Subsequent mapping by the writer showed that the granite underlying Powder Hill Pond is a separate intrusion from the earlier described Powder Hill pluton. Therefore, the term Powder Hill pluton was abandoned.

The North Pond Granite post-dates the  $S_3$  foliation in the gneisses. In the area to the north and west of North West Pond, it has deflected the layering ( $S_2$ ) and the  $S_3$  foliation in the Square Pond Gneiss to orientations that are more or less parallel to the granite contact. In places apophyses of the granite can be seen truncating the  $S_2$  and  $S_3$  structures in the gneiss (Figure 3.10).

Adjacent to the Wareham pluton, the North Pond Granite contains numerous angular xenoliths of the former. These often show a preferred alignment of rectangular microcline megacrysts ( $W_1$ ) that vary in trend from one xenolith to another, indicating that the xenoliths have been rotated to varying degrees. The North Pond Granite is cut by garnet-muscovite leucogranite<sup>1</sup> sheets, pegmatites and thin tourmaline-quartz veins.

b. Lithology

The North Pond Granite consists of two main rock types; namely, (1) medium-grained, muscovite-biotite granite, and (2) porphyritic, biotite-muscovite granite (Figure 3.11). Both are locally garnetiferous. The medium-grained granite is the dominant rock type in the western half of the pluton; the porphyritic variety is predominant in the south. For the most part, the two phases have a gradational boundary but in places both varieties intrude each other.

The porphyritic granite contains 1 to 2 cm long microcline

---

<sup>1</sup>In the sense of Streckeisen (1976).



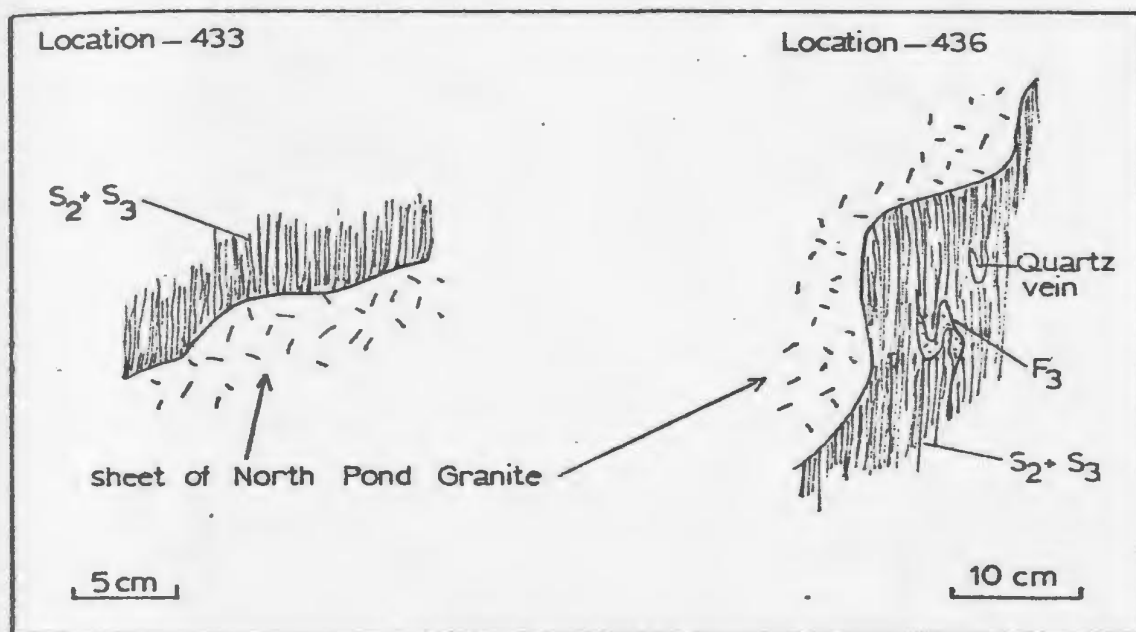


Fig. 3.10. Apophyses of the North Pond Granite truncating  $S_2$  and  $S_3$  in the Square Pond Gneiss.



Fig. 3.11. The porphyritic phase (A) and the medium-grained phase (B) of the North Pond Granite. Location - 856.

phenocrysts<sup>1</sup> in a medium-to coarse-grained matrix of quartz, plagioclase, microcline, biotite and muscovite. The microcline phenocrysts are subhedral and have straight to embayed grain boundaries. They exhibit patch perthitic and vein perthitic textures. The groundmass microclines, quartzes, plagioclases and biotites have sizes ranging from 0.1 to 1 mm, 0.2 to 2 mm, 0.2 to 3 mm and 0.1 to 0.8 mm, respectively. Apart from their smaller grain size, they are similar to the groundmass of the megacrystic plutons in microstructure. Plagioclase ( $An_8$  to  $An_{15}$ ) is more sodic than plagioclase in the megacrystic plutons. Muscovite grains range from 0.2 to 2 mm in length. The micas are randomly oriented.

The medium-grained granite consists of the same minerals as the porphyritic granite but is richer in plagioclase and biotite and poorer in K-feldspar and muscovite than the latter. The minerals in the medium-grained granite are largely similar to the matrix of the megacrystic granites in microstructure, but they are generally smaller in size (microcline, 0.2 to 0.8 mm; quartz, 0.1 to 1.5 mm; plagioclase, 0.2 to 2 mm; biotite and muscovite, 0.04 to 1 mm) than those in the porphyritic granite. Plagioclase in the medium-grained granite is similar to that in the porphyritic granite in composition.

Garnet grains in the North Pond Granite are not very common. They are subhedral to euhedral, reddish in colour, and generally less than 2 mm in diameter. Accessory minerals in the granite include

---

<sup>1</sup> These microclines are smaller than the microcline megacrysts in the area. Furthermore, unlike the megacrysts, they do not overgrow gneisses adjacent to the host granite or boundaries of minor intrusions or xenolith in the latter. Also, they are confined to a distinct phase of the intrusion. Thus they are considered as phenocrysts.

apatite, zircon, pyrite, epidote and, locally, fluorite.

c. Structure

Like the Wareham pluton, the North Pond Granite contains two fabrics. The first of these ( $NP_1$ ) is best seen in the northern and the eastern parts of the granite. The second fabric ( $NP_2$ ) occurs in the area affected by the shear zone which deformed the southwestern part of the Wareham pluton.

The older mineral alignment ( $NP_1$ ) trends in an east-northeast direction parallel to the length of the pluton. It is a  $L > S$  fabric defined by lath-shaped feldspars, elongated quartzes and, to a lesser degree, by micas. The lineation plunges at low angles ( $\approx 15^\circ$ ) to the north. The foliation dips at high angles ( $60-80^\circ$ ) mostly to the east (Figure 3.12). The fabric cuts across pegmatitic and granitic minor intrusions (Figure 3.13). It continues into the xenoliths of the Wareham pluton. In xenoliths with  $W_1$  at high angles to  $NP_1$ , the former is bent into open folds with  $NP_1$  axial planar to the folds (Figure 3.14).

The deformation that produced the older mineral alignment ( $NP_1$ ) in the North Pond Granite is also responsible for some of the structures seen in the Business Cove Granite and further discussion about it will be postponed until the latter granite has been described.

The shear zone mentioned above extends across the North Pond Granite, from west of Rocky Ridge Pond to the east end of the North West Pond. From there it continues to and beyond Northwest (First) Pond. It has deformed the southerly trending apophyses of the North Pond Granite, the eastern sheet more than the western sheet. It has

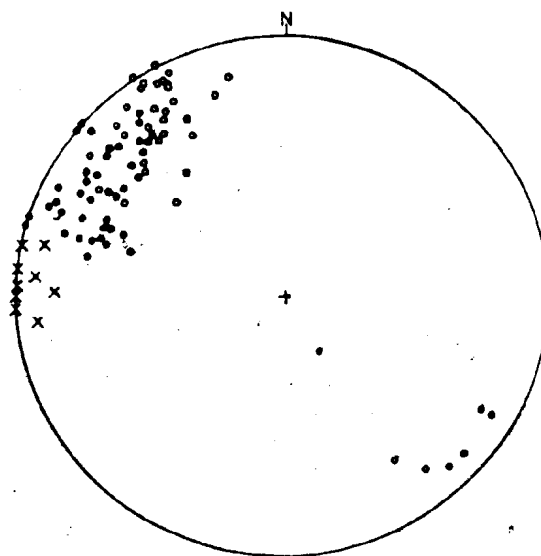


Fig. 3.12. Stereoplot showing poles to structures in the North Pond Granite. o -  $NP_1$ , • -  $NP_2$ , X - crenulation cleavage.

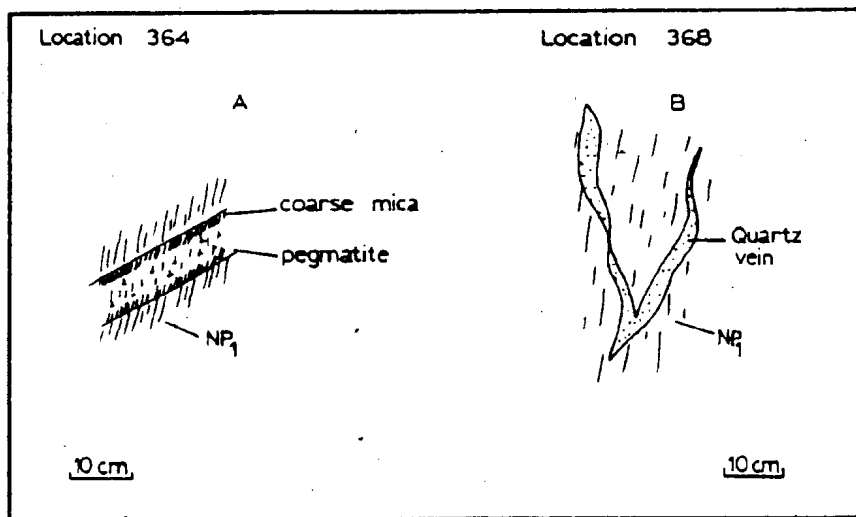


Fig. 3.13. (A)  $NP_1$  cutting across a pegmatite and (B)  $NP_1$  axial planar to a minor fold of a quartz vein in North Pond Granite.

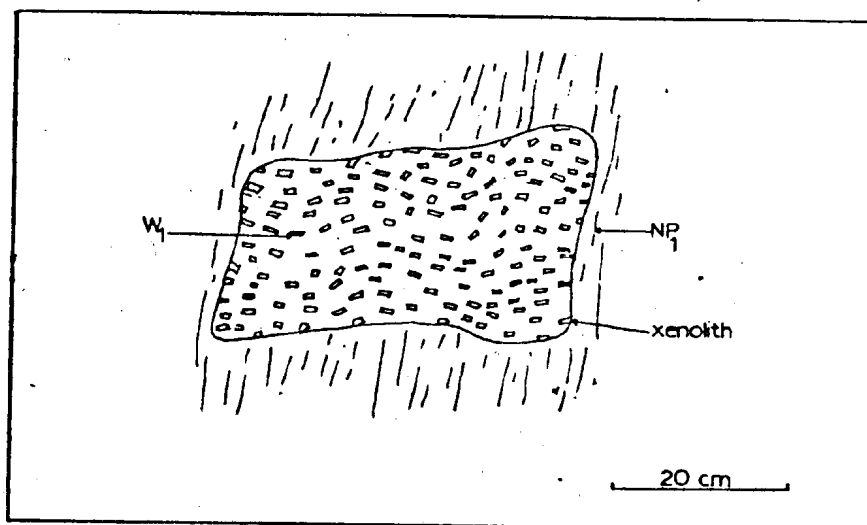


Fig. 3.14. A xenolith of the Wareham pluton in the North Pond Granite. Fabric in the xenolith is folded with  $NP_1$ , axial planar to the folds. Location - 352.

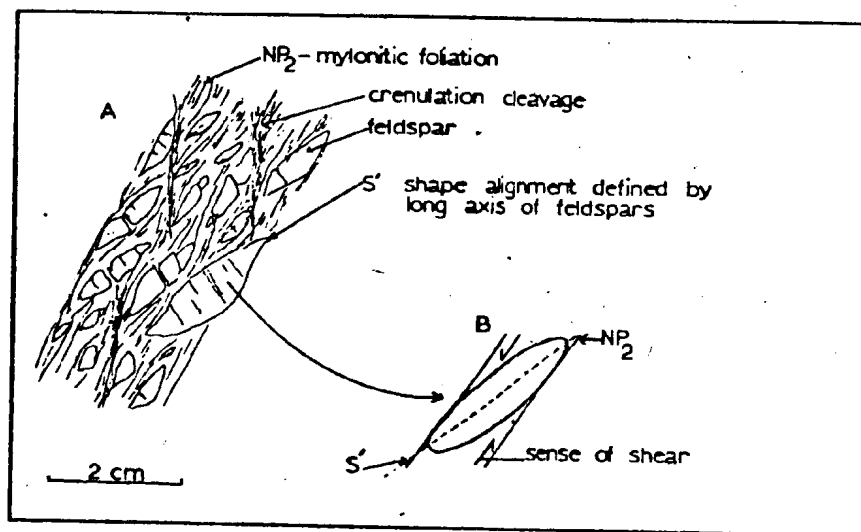


Fig. 3.15. (A) Feldspar alignment,  $NP_2$  and crenulation cleavage in the North Pond Granite. (B) Possible sense of shear along  $NP_2$ .

gradational contacts marked by alternating zones of deformed and relatively undeformed granite. These zones trend parallel to the length of the main shear zone. The fabric within the shear zone is mylonitic and is defined by "ribbon-like" quartz and films of mica that wrap around augen-shaped feldspars. It has a north-northeast strike and dips steeply (Figure 3.12). In places, curved traces of an earlier alignment of feldspars (probably  $NP_1$ ) can be recognized between the mylonitic foliation. The configuration of these traces shows that the earlier mineral alignment has been rotated anticlockwise within the shear zone (Figure 3.15). Therefore, the sense of movement in the shear zone is sinistral.

The mylonitic foliation is offset by a northerly trending, mostly vertical, discontinuous, crenulation cleavage marked by thin (<1 mm) biotite-rich zones. East-northeast trending, steeply dipping kink bands affect both the mylonitic fabric and the crenulation cleavage.

### 3.3.3. Business Cove Granite.

#### a. Distribution and Contact Relationships

The Business Cove Granite (Jayasinghe, 1978a) occurs in the eastern part of the thesis area. Excellent exposures of the granite are present along the side road leading to Valleyfield from the old road from Indian Bay to Wesleyville. To the east and to the north, the Business Cove Granite intrudes the Hare Bay Gneiss and, to the northwest, the Wareham Quartz Monzonite, though the actual contact is not exposed. In the west and in the south, it is cut by the Big Round Pond and the Newport granites.

The contact between the Business Cove Granite and the migmatite is sheeted with granite sheets intruding the migmatite parallel to the contact. Apophyses of the granite cut across the  $S_2$  banding,  $S_3$  foliation and the  $F_3$  folds of the migmatite (Figure 3.16). The contacts with the Big Round Pond and the Newport granites are sharp.

b. Lithology

The lithology of the Business Cove Granite is similar to the medium-grained part of the North Pond Granite and, thus, will not be described in detail. North of Big Round Pond, the Business Cove Granite is separated from the North Pond Granite by a kilometre wide area occupied by the Wareham pluton, which in this part is thoroughly intruded by sheets of medium-grained granite. These granite sheets are similar to the North Pond and the Business Cove plutons in rock type and it is most likely that the two granites are connected in subsurface.

The Business Cove Granite contains a large number of xenoliths of the Square Pond Gneiss, the Hare Bay Gneiss and the Wareham Quartz Monzonite. These range from a few centimetres to a few metres and are angular in shape. The pluton is cut by a plethora of felsic minor intrusions. These range from garnetiferous muscovite leucogranite sheets to aplites and pegmatites. The pegmatites are noted for their beryl and tourmaline (Gale, 1967; Jayasinghe, 1976).

c. Structure

The Business Cove Granite contains a variably developed northeast to east-northeast trending L-S fabric ( $BC_1$ ) defined by elongated quartz, rectangular feldspars and micas. In places, the

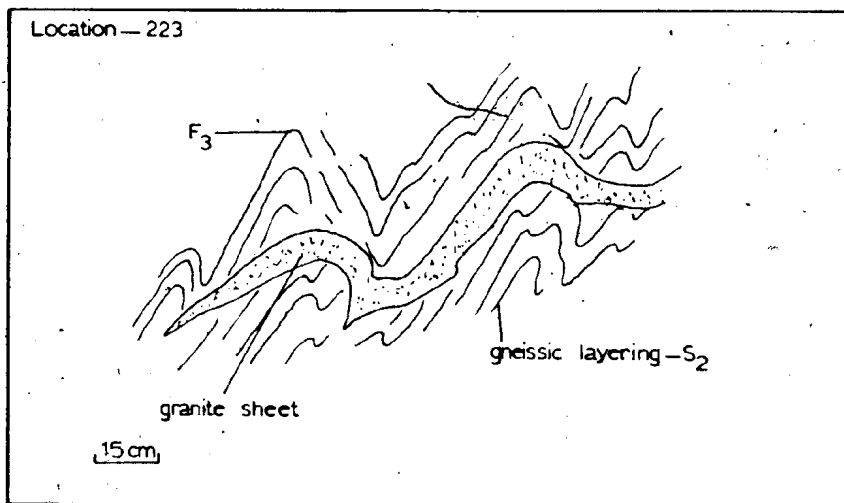


Fig. 3.16. An apophysis of the Business Cove Granite truncating  $D_3$  structures in the Hare Bay Gneiss.

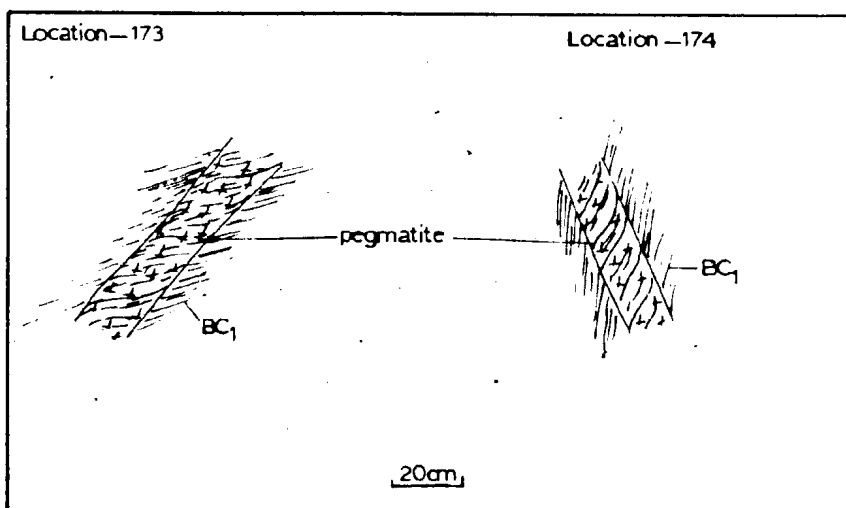


Fig. 3.17. Pegmatites in the Business Cove Granite cut by  $BC_1$ . Note the change in direction of  $BC_1$  within the pegmatite.



lineation, defined mainly by the elongated quartzes, is prominent and plunges at shallow angles to the southwest. For the most part, the planar fabric predominates. The foliation is vertical or dips at high angles mostly to the east. It is best seen in the pegmatitic veins in which coarse grained (up to 2 cm long) muscovite crystals can be seen arranged parallel to the fabric. The fabric generally changes slightly in orientation within the pegmatites (Figure 3.17). This might have been caused by differential movement along the pegmatites.

Commonly, thin (up to 15 cm wide) sheets of the granite cutting the xenoliths of the gneisses and the Wareham pluton are folded with the fabric in the host ( $BC_1$ ) axial planar to the folds (Figure 3.18). In the case of the megacrystic xenoliths, the megacrysts are augened by a quartz and mica alignment that is continuous with the external fabric.

Locally, the Business Cove Granite is cut by 0.5 to 1 m wide north-northeast striking shear zones with a strong mylonitic fabric ( $BC_2$ ). These minor shear zones are most probably related to the major shear zones that deform the Wareham, North Pond and the Cape Freels plutons.

d. Relationships between the fabrics in the Wareham, North Pond and Business Cove Plutons

Each of the above intrusions contains two distinct mineral alignments. They post-date the  $D_3$  structures in the gneisses as shown by apophyses from all three plutons truncating  $F_3$  folds in the gneisses.

Furthermore, adjacent to the North Pond Granite,  $S_3$  in the Square Pond Gneiss has been deflected to an orientation that more or less parallels the contact of the pluton either by forceful intrusion of the granite or by flattening of  $S_3$  against the granite during  $D_4$ . The second fabric ( $W_2$ ,  $NP_2$ ,  $BC_2$ ) in the plutons is mylonitic and is related to the shear zones that mark the  $D_4$  deformation in the area.

The inter-relationships among the first mineral alignments ( $W_1$ ,  $NP_1$ ,  $BC_1$ ) of the plutons is not very clear except for the fact that  $W_1$  pre-dates  $NP_1$ . The North Pond Granite contains xenoliths of the Wareham Quartz Monzonite and  $W_1$  in the xenoliths is commonly oriented oblique to  $NP_1$  in the host.  $W_1$ ,  $NP_1$  and  $BC_1$  are very unevenly developed. For example,  $NP_1$  is well developed in the North Pond Granite in outcrops north of Parsons Pond but is rare in outcrops around North West Pond. They are defined mainly by undeformed feldspars and tend to be parallel to  $S_3$  in the gneisses. In the North Pond and Business Cove granites, quartz grains are slightly elongated and some of the micas are aligned parallel to  $NP_1$  and  $BC_1$ .  $W_1$  and  $NP_1$  trend parallel to the length of their host plutons.  $BC_1$  trends oblique to the length of the Business Cove Granite but is parallel to  $NP_1$ . At places, apophyses of the plutons truncating the gneisses are folded with the first fabric in their "parent" plutons axial planar to the folds.

It is believed that  $W_1$ ,  $NP_1$  and  $BC_1$  were produced at the time of emplacement of their host plutons, in response to the late stages of regional stress field that caused  $D_3$  (Figure 3.19). This chronological relationship with  $D_3$  is based mainly on the parallelism between  $S_3$  in the gneisses and the above mineral alignments and the fact that the

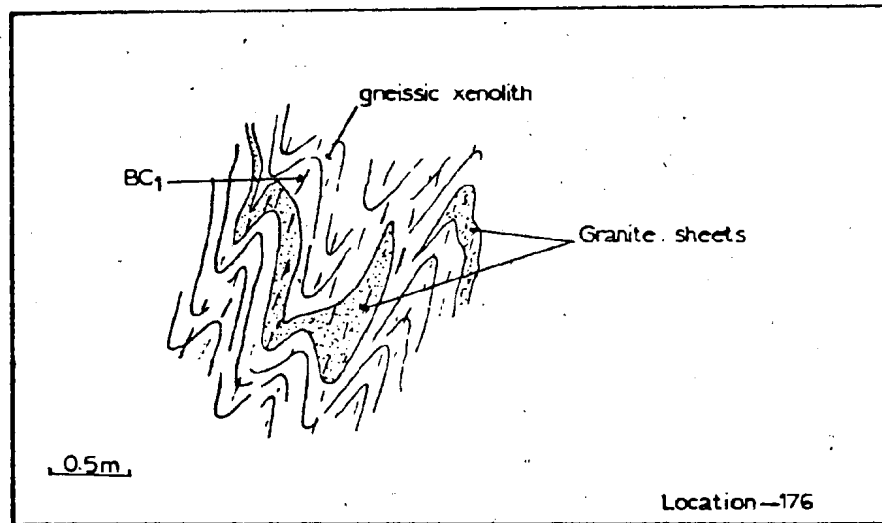


Fig. 3.18. Gneissic xenolith in the Business Cove Granite folded with sheets of the host.

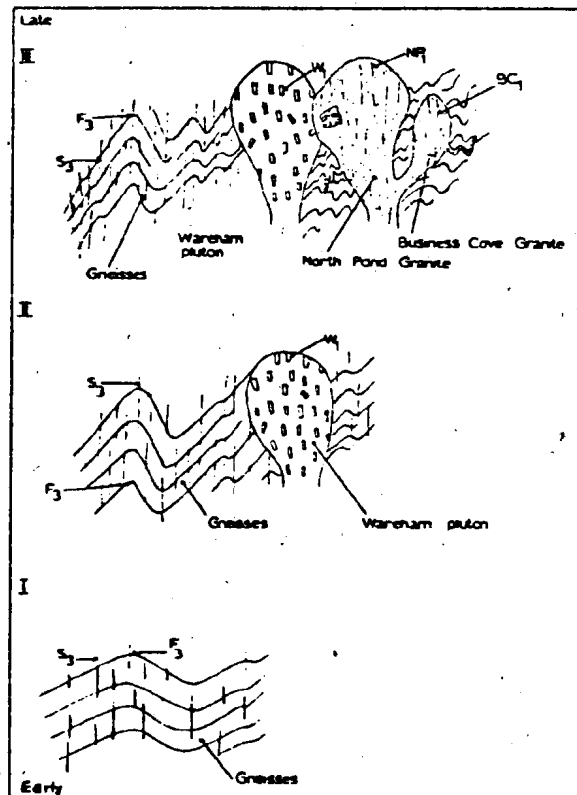


Fig. 3.19. Schematic illustration of the emplacement of the Wareham, North Pond and Business Cove plutons and the development of S<sub>3</sub>, W<sub>1</sub>, NP<sub>1</sub> and BC<sub>1</sub> during D<sub>3</sub>.

granites post-date  $D_3$  structures in the gneisses. An alternative mechanism would be a series of coaxial, coplanar deformation pulses resulting in  $S_3$ ,  $W_1$  and  $NP_1 + BC_1$ . The uneven distribution of  $W_1$ ,  $NP_1$  and  $BC_1$  may be a function of subsequent annealing controlled largely by the existing temperatures and the availability of pore fluids.

#### 3.3.4. Cape Freels Granite

##### a. Distribution and Contact Relationships

The Cape Freels Granite (Strong *et al.*, 1974; Jayasinghe, 1976) occupies most of the eastern coastal belt of the area. A major part of the pluton lies under the northwestern-most part of Bonavista Bay, as indicated by the aeromagnetic pattern of the region (Geological Survey of Canada, Aeromagnetic Map No. 73476, 1970) and by the granite outcrops on islands up to 8 km offshore (e.g. on Cabot Island -- A. R. Berger, personal communication, 1978). The pluton is well exposed both along the shoreline and inland. It is truncated by the Newport Granite in the south.

The Cape Freels Granite has been emplaced into the Hare Bay Gneiss. The original contact relationships between the two units have been largely obliterated by the more easterly of the two main shear zones in the area (Figure 2.1, page 18). This shear zone has intensely deformed both the granite and the gneiss adjacent to the contact. Locally, sheets of the granite occur within the gneiss adjacent to the contact. These trend parallel to the foliation in the shear zone. The gneisses adjacent to the granite show a profuse growth of microcline porphyroblasts.

In the southern part of Greenspond Island and in the nearby Newell Island and Puffin Island, layers of the Hare Bay Gneiss occur intercalated with sheets of the Cape Freels Granite. On Copper Island and Horse Island, sheets of the Cape Freels pluton intrude a gabbro.

b. Lithology

The Cape Freels pluton is a megacrystic granite with 2 to 8 cm long microcline (and in a few places plagioclase) crystals in a coarse grained matrix of quartz, plagioclase, microcline and biotite. Microcline megacrysts constitute 30 to 50 percent of the rock.

Xenoliths of the country rocks are rare in the pluton except at Newtown and on the southern part of Greenspond Island. There, xenoliths of migmatites, ranging from less than a metre to a few metres across, are common. The pluton is cut by a number of minor intrusions.

On Greenspond Island, Pouch Island, Flowers Island, Cabot Island and in the other small islands near them, the granite is darker than elsewhere in the pluton. The microcline megacrysts are smaller in size (2 to 4 cm long) and are more unevenly distributed. Locally, plagioclase content exceeds the microcline content and the rock type becomes a monzotonalite (see Figure 3.2 and page ). In addition to biotite, minor hornblende and sphene also occur. This difference in lithology may have been produced by assimilation of gneissic country rocks of which numerous xenoliths can be seen within this part of the pluton.

c. Structure

The Cape Freels Granite contains two mineral alignments. In the central part of the granite, undeformed megacrysts define an unevenly

developed S > L alignment (Figure 3.20). This fabric (CF<sub>1</sub>) has a variable orientation but for the most part it has a northerly strike and dips shallowly to the west. The minor intrusions in the central part of the granite trend in all directions and do not show any cross-cutting fabrics (Figure 3.21). Alignment of the undeformed megacrysts (CF<sub>1</sub>) may have resulted during the emplacement of the pluton.

The western part of the pluton is deformed by the more easterly of the two main shear zones in the area (Figure 2.1, page 18). The deformed area forms a marginal belt about 1.5 km wide in the north and wider in the south to encompass all of the onshore part of the pluton. The deformation in the pluton<sup>1</sup> increases gradually from east to west and has resulted in a complete gradation from undeformed megacrystic granite to mylonite.

In the less deformed part of the granite, the feldspar grains are undeformed. Quartz grains show undulose extinction and some are dimensionally oriented. The quartz grains along the boundaries of the feldspar crystals are finer-grained than those elsewhere. This decrease in grain size is probably a result of deformation and recrystallization in response to strain concentrated at the grain boundaries of the feldspars. Biotites show a random orientation.

In the more deformed part of the pluton away from the above, quartz grains are highly elongated and dimensionally oriented. Some of the quartz grains have been recrystallized to "ribbons" of fine

---

<sup>1</sup>See section 3.4 for a detailed description of deformation within the shear zone that cuts the Cape Freels Granite.



Fig. 3.20. Alignment of rectangular microcline megacrysts ( $CF_1$ ) in the Cape Freels Granite. Location - 168.

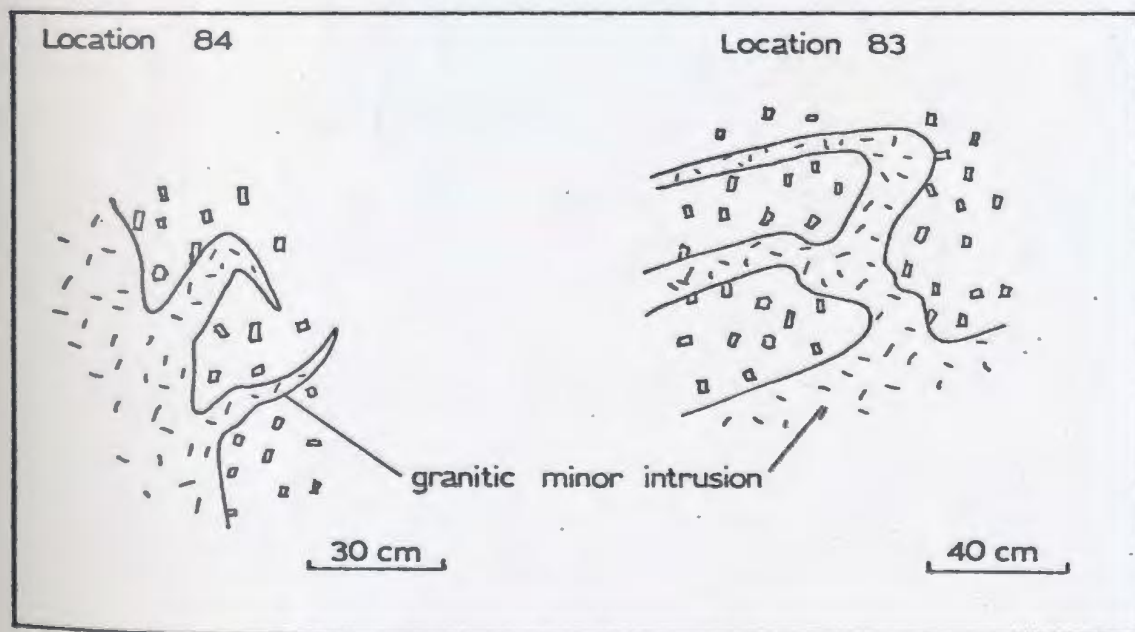


Fig. 3.21. Granitic minor intrusions in the Cape Freels Granite outside the shear zone. Location - 84.

polygonal grains. Quartz, along with micas that have been stretched to form streaks, defines a mylonitic fabric that forms augen around deformed feldspar grains (Figure 3.22). The megacrysts have rounded edges and are commonly lensoid in shape. Some have tails composed of fine-grained feldspar and quartz grains. Most of the megacrysts have quartz-filled fractures oriented at high angles to the mylonitic foliation, indicating extension in the plane of the foliation. The plagioclases have bent twin lamellae. Towards the western contact of the pluton, the feldspars become more fragmented and rounded and the overall grain size of the rock decreases.

The mylonitic foliation ( $CF_2$ ) in the shear zone strikes in a north-northeast direction and has steep to vertical dips (Figure 3.23). The fabric has a shallow L component marked by elongated quartz grains on the foliation surfaces; also, the feldspars appear to be extended more on horizontal surfaces than on vertical surfaces at right angles to the foliation (Figure 3.24). The minor intrusions in the deformed part of the granite occur mostly parallel to the mylonitic foliation, a few trend at high angles to the mylonitic foliation and have been folded with the foliation axial planar to the folds.

A northerly striking, steeply dipping crenulation cleavage similar to that in the North Pond Granite can be seen offsetting the mylonitic foliation. The significance of this structure is discussed together with the strain in the shear zones in a later section (Section 3.4, page 125).

The Cape Freels pluton on Greenspond Island, Flowers Island, Pouch Island, Cabot Island and on other small islands around them has



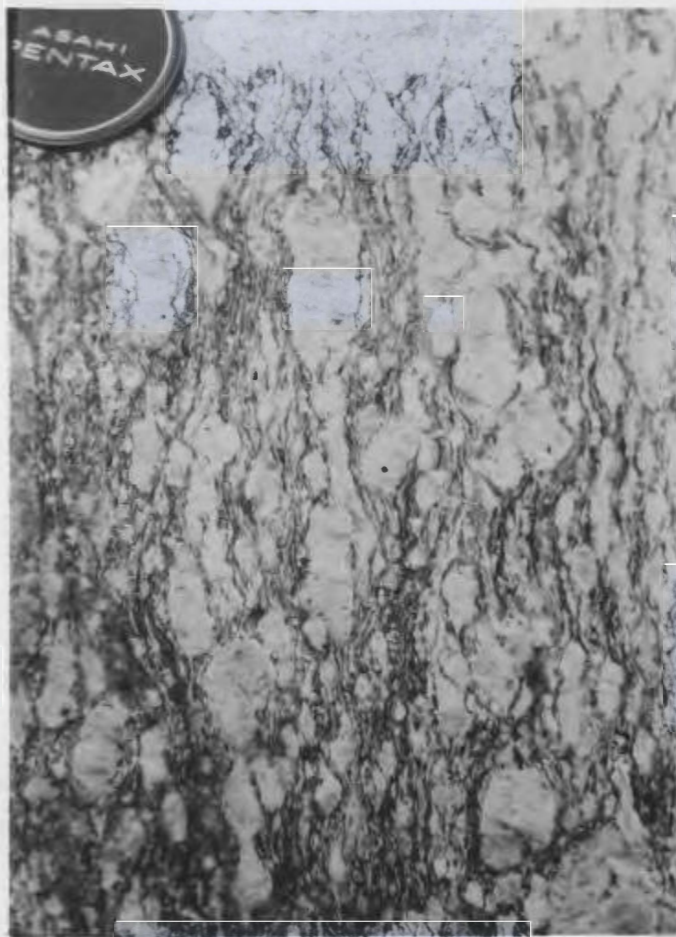
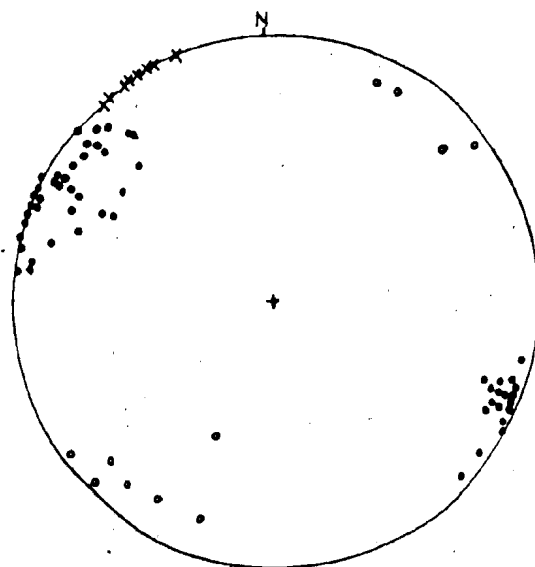


Fig. 3.22. Deformed Cape Freels Granite.  $CF_2$  defined by "ribbons" of quartz and mica forms augen around deformed feldspars. Location - 171.



- $CF_2$  x crenulation cleavage
- lineation related to  $CF_2$

Fig. 2.23. Stereoplot showing lineation related to  $CF_2$  and poles to  $CF_2$  and crenulation cleavage<sup>2</sup> in Cape Freels Granite.

an east-northeast trending mylonitic foliation defined by micas and elongated quartz grains. The foliation dips moderately to steeply, mostly to the northwest. On Puffin Island, Horse Island and Copper Island, the mylonitic foliation is very strong and affects the granite sheets as well as their host migmatite and the gabbro bodies. In places, the mylonitic migmatite has developed intrafolial folds of mylonitic banding with the foliation axial planar to the folds (Figure 3.25).

The chronological relationship between the fabric in this part of the pluton and the mylonitic foliation ( $CF_2$ ) in the shear zone described earlier is not known because the critical outcrops lie under water. It is believed that the east-northeast striking foliation is related to a movement along the Dover Fault which, when traced offshore, passes just to the south of the above islands (Jayasinghe, 1976; Jayasinghe and Berger, 1976).

### 3.3.5. Lockers Bay Granite .

#### a. Distribution and Contact Relationships

The Lockers Bay Granite (Blackwood and Kennedy, 1975) is an extensive linear intrusion whose northernmost portion occurs in the southern part of the thesis area. The granite was mapped and described by Blackwood (1977); only reconnaissance studies of the part within and just to the south of the thesis area were made for this work.

The Lockers Bay Granite has been emplaced into the Hare Bay Gneiss and truncates the gneissic banding in the gneiss. Adjacent to the contact, abundant microcline porphyroblasts overgrow the gneiss

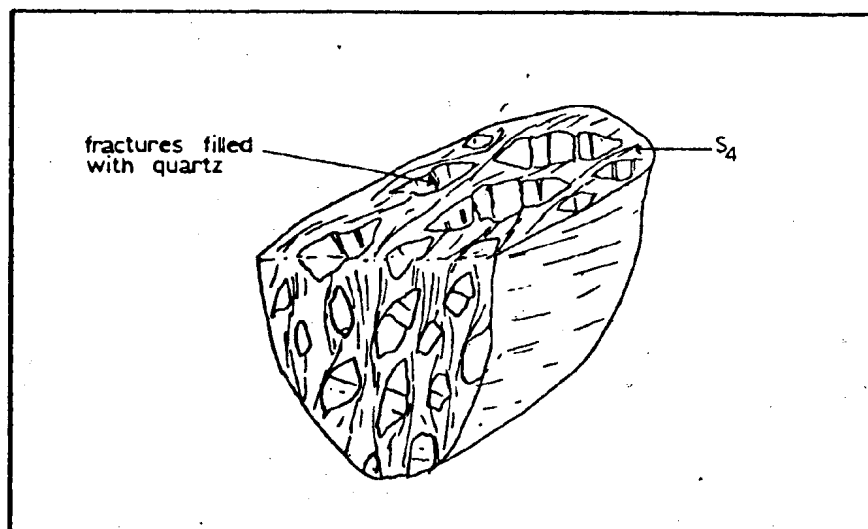


Fig. 3.24. Schematic diagram showing the difference in extension of feldspars on horizontal surfaces and vertical surfaces perpendicular to  $S_4$  in Cape Freels Granite.

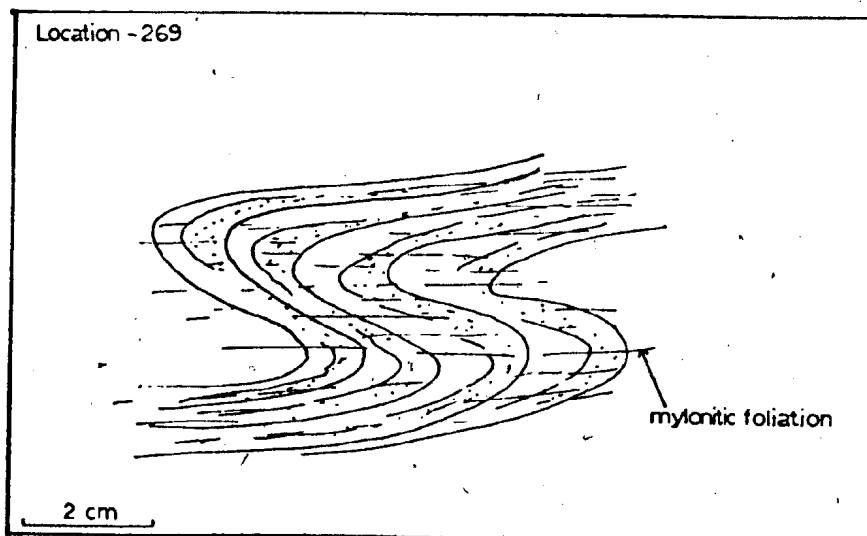


Fig. 3.25. Fold in mylonitized migmatite.

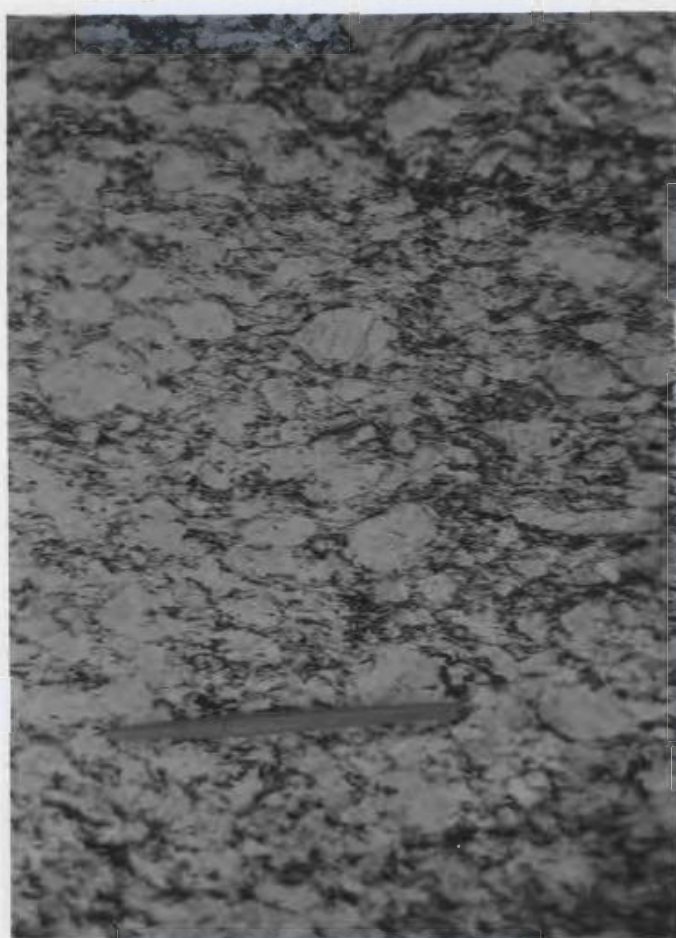


Fig. 3.26. Lockers Bay Granite. Mylonitic foliation defined by elongated quartz and streaked biotites form augen around deformed feldspar grains. Location - L2.

(e.g. at the North shore of Lewis Island). The Lockers Bay Granite is intruded by the Newport Granite in the northeast and is cut by the Dover Fault in the southeast (Blackwood, 1977).

b. Lithology and Structure

The Lockers Bay Granite resembles the deformed western marginal part of the Cape Freels Granite. It consists of deformed microcline crystals and plagioclases that are augened by a mylonitic foliation defined by elongated quartz and stretched biotites (Figure 3.26). The deformation in the pluton is heterogeneous; in places, the granite appears to be undeformed. In some outcrops the transition from undeformed granite to deformed granite occurs within a few tens of centimetres. In the northeastern part of the pluton the mylonitic foliation has an east-northeast strike, but elsewhere it strikes in a north-northeast direction. It has vertical or steep dips. This foliation could be related to a movement along the Dover Fault, as Blackwood (1977) argued, correlating the change in strike of the foliation in the granite with a change in trend of the fault in his area. But if the shear zone that deformed the North Pond Granite and the southern part of the Wareham pluton is extended southwards parallel to its trend, it continues into that part of the Lockers Bay Granite containing a north-northeast trending mylonitic foliation (Figure 2.1, see also geological map in back pocket). Indeed, the Lockers Bay Granite appears to have been stretched parallel to the shear zone, probably by deformation in the latter. It is thus possible that the north-northeasterly mylonitic foliation seen in the Lockers Bay Granite may be related to the same

shear zone that deformed the North Pond and the Wareham plutons in the area.

As in the case of the Cape Freels pluton, the age relationships between the two foliations in the Lockers Bay Granite are not known and further work is clearly required.

### 3.3.6. Deadman's Bay Granite

#### a. Distribution and Contact Relationships

The Deadman's Bay Granite (Fairbairn and Berger, 1974; Strong et al., 1974) occupies the northeastern part of the Wesleyville area and a large part of the eastern half of the Musgrave Harbour map area and extends onshore farther to the west of these areas. Regional aeromagnetic patterns (Geological Survey of Canada, aeromagnetic map No. 73476, 1970) indicate that a major part of the pluton lies offshore to the north of the present study area. The pluton is well exposed on the north shore of the study area; the inland exposure is poor.

The Deadman's Bay Granite intrudes the Square Pond and Hare Bay gneisses and the Wareham and North Pond plutons, with sharp contacts. The Square Pond Gneiss occurs adjacent to the southern-most contact of the granite. There, sheets of the granite truncate  $S_2$  layering and the  $S_3$  foliation in the gneiss (Figure 3.27). Within about half a kilometre from the granite, the gneiss has a spotted appearance (Figure 3.28). These spots are mostly aggregates of sericite, with scattered remnants of andalusite. Rarely, the andalusites and their sericite pseudomorphs overprint micro-crenulations (Figure 3.29) that probably represent  $F_2$  or  $F_3$  folds. Close to the granite contact (<1 km) the layering and

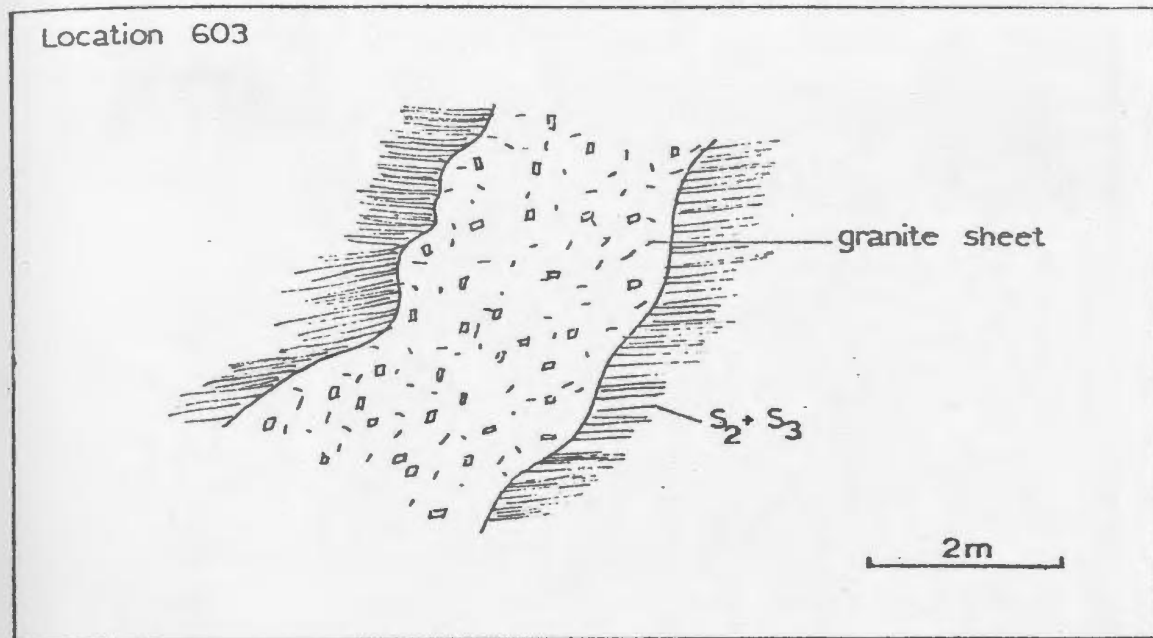


Fig. 3.27. An apophysis of the Deadman's Bay Granite truncating S<sub>2</sub> and S<sub>3</sub> structures in the Square Pond Gneiss.

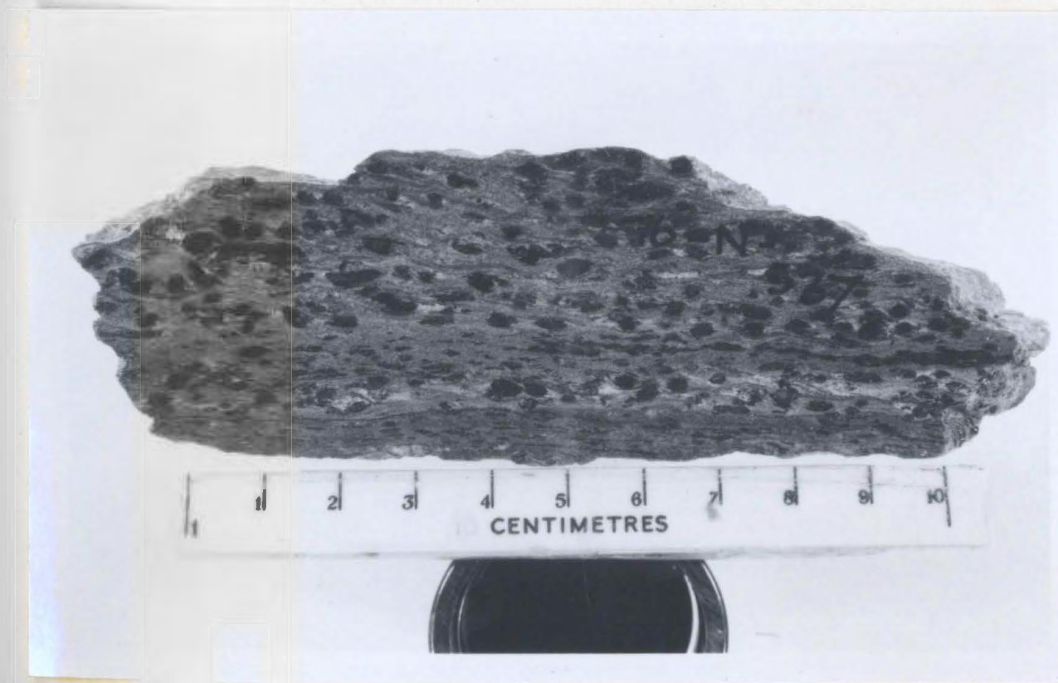


Fig. 3.28. "Spotted" metasediments adjacent to the Deadman's Bay Granite. Location - 537.



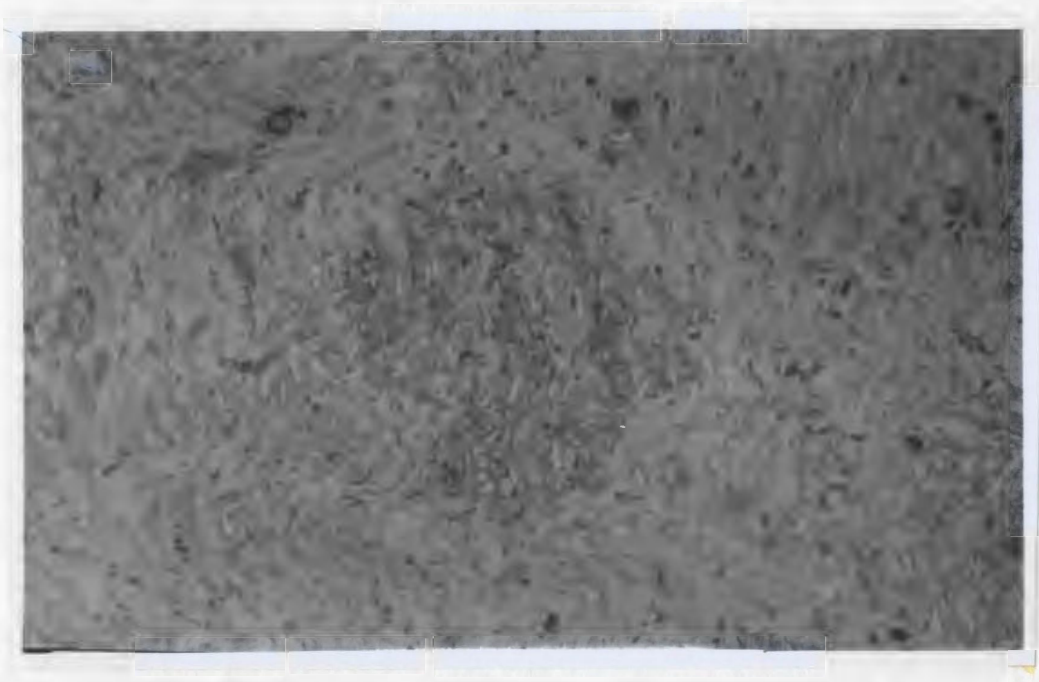


Fig. 3.29. Andalusite porphyroblast overprinting micro-crenulations ( $F_2$  or  $F_3$ ) in the Square Pond Gneiss adjacent to the Deadman's Bay Granite. (X40). Location - 538.

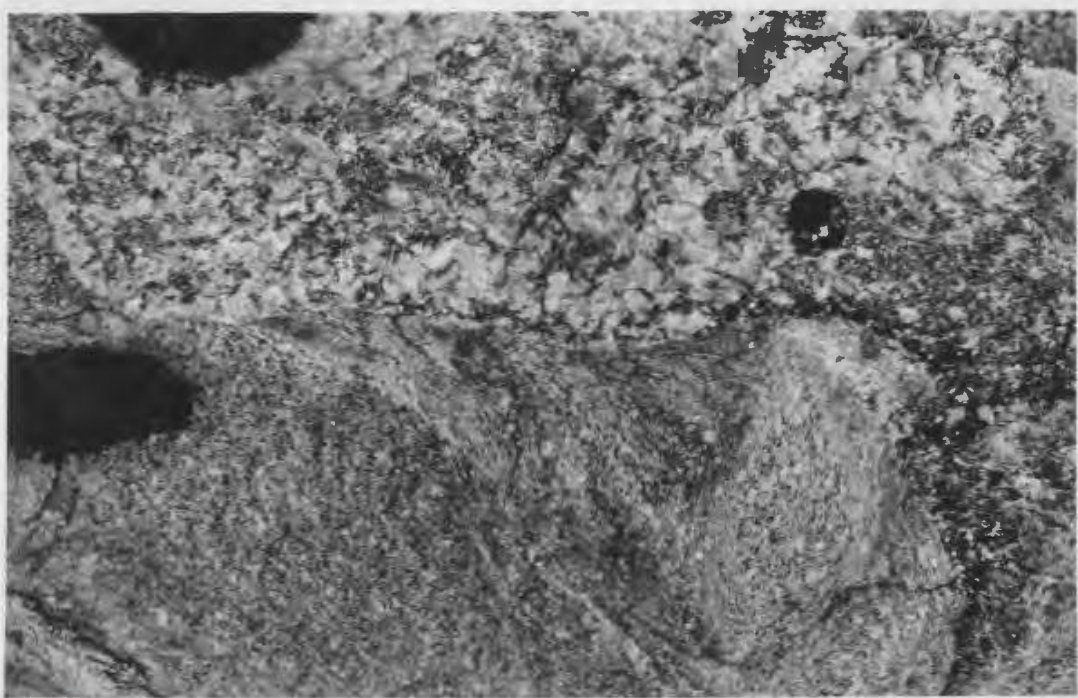


Fig. 3.30. An apophysis of the Deadman's Bay Granite cutting a deformed ( $D_4$ ) megacrystic granite sheet in the Hare Bay Gneiss. Windmill Bight.

the foliation in the gneiss show steeply plunging open folds with east-west trending axial planes and a weak axial planar fabric. The latter is marked by a widely-spaced crenulation cleavage. These folds may have been produced by the forceful intrusion of the pluton, the contact of which trends for the most part at high angles to the layering in the gneiss and parallel to the axial traces of the folds.

The alteration of the andalusites may have been caused by K-metasomatism related to the pluton because away from the granite the pre-S<sub>3</sub> regional metamorphic andalusites in the Square Pond Gneiss show very little or no sericitization. However, unlike the Cape Freels and the Lockers Bay granites, no extensive potassium-feldspar blastesis is present adjacent to the margin of the Deadman's Bay Granite.

The North Pond pluton occupies the southern contact of the Deadman's Bay Granite. There, Deadman's Bay Granite cuts across the shear zone that deformed the North Pond, Wareham and, probably, also the Lockers Bay plutons (Figure 2.1, page 18). The Wareham Quartz Monzonite probably also comes into contact with the Deadman's Bay pluton immediately to the east of North Pond Granite. The contact is not exposed but sheets of the Wareham pluton intruding the adjacent Hare Bay Gneiss are cut by the Deadman's Bay Granite. The Hare Bay Gneiss occupies most of the eastern contact of the Deadman's Bay pluton. The contact is best exposed at Windmill Bight. There sheets of the Deadman's Bay Granite truncate gneisses and megacrystic granite sheets containing S<sub>4</sub> mylonitic foliation (Figure 3.30). These deformed granite sheets could belong to either the Wareham Quartz Monzonite or the Cape Freels Granite. The

former is favoured because deformed megacrystic granite sheets similar to those at Windmill Bight occur in the Hare Bay Gneiss all the way from Windmill Bight to the northern contact of the Wareham pluton.

b. Lithology and Structure

The Deadman's Bay pluton is a megacrystic granite. Its megacrysts range up to 12 cm in length, exceeding those of the other plutons in the area in size. Megacrysts constitute about 45 to 55 percent by volume of the granite. Apart from minor variations in grain size and relative proportions of the constituent minerals, the Deadman's Bay Granite is rather homogeneous in rock type. Granitic minor intrusions are rare in the pluton.

In a few outcrops about 5 km from the contact with the North Pond Granite, the Deadman's Bay pluton contains sharply bounded inclusions of presumably chilled granite. These blocks consist of microcline megacrysts and coarse (up to 1.5 cm long) microcline, plagioclase, biotite and quartz, all set in a very fine grained granophyric matrix (Figure 3.31). Undeformed sheets of a similar lithology were found intruding sheared North Pond Granite at its contact with the Deadman's Bay pluton. The feldspars in the chilled rock are highly altered to chlorite and some of the biotite flakes are euhedral in shape. The quartzes have euhedral to subhedral shapes. This lithology may represent an early chilled "skin" of the granite that was disrupted during the emplacement of the pluton.

The pluton does not contain a penetrative fabric, the megacrysts are undeformed, quartzes occur as equigranular pods and the biotites are randomly oriented. In places, especially in the marginal parts of the



Fig. 3.31. Granophyric matrix in inclusions of chilled granite in the Deadman's Bay pluton, Q - quartz, F - alkali feldspar. (X40). Location - 509.



Fig. 3.32. Remobilized Cape Freels Granite near the contact of the Newport pluton at Loo Cove. Note the folds in the mylonitic foliation (CF<sub>2</sub>).

granite, rectangular microcline megacrysts define a planar alignment that generally trends parallel to the contact of the pluton. It dips either vertically or steeply towards the interior of the granite. This alignment is very distinct in the marginal part of the pluton to the north and west of Rocky Ridge Pond and to the west of Windmill Bight. Locally, the megacrysts define a southwest trending, moderately plunging L fabric.

The mineral alignment in the pluton could have formed at the time of the emplacement of the pluton as suggested by the general parallelism between the planar fabric and the contact of the pluton and the absence of evidence for large scale post-consolidation deformation.

### 3.3.7. Newport Granite

#### a. Distribution and Contact Relationships

The Newport Granite (Strong et al., 1974)<sup>1</sup> occurs in the southeastern part of the present study area. It is well exposed onshore and on offshore islands in the area.

The Newport Granite (Jayasinghe, 1978a; Bell et al., 1979) intrudes the Hare Bay Gneiss and the Wareham, Business Cove, Cape Freels and the Lockers Bay plutons, all with a sharp contact. In some areas (e.g. on the north shore of Indian Bay), apophyses of the granite truncate layering ( $S_2$ ) and foliation ( $S_3$ ) in the Hare Bay Gneiss. At Safe Harbour the contact between the granite and the gneiss is marked by a thin zone (<10 m wide) of medium-grained, granular, pinkish granite.

---

<sup>1</sup> During subsequent mapping the Newport Granite was found to occupy a larger area than that shown by Strong et al. (see Jayasinghe, 1978a).

Sheets of a similar lithology commonly intrude the host rocks near the contact elsewhere. The contact metamorphic effects of the Newport Granite are not pronounced and they are restricted to within 100 m of the granite margin.

The Newport pluton cuts the foliations ( $BC_1$  and  $BC_2$ ) in the Business Cove Granite. Close to the contact, the Business Cove Granite shows a development of large microcline grains (up to 2 cm long) and fibrolite.

Adjacent to the Newport Granite, the mylonitic foliations in the Cape Freels and Lockers Bay granites have been bent into open to close folds that are truncated by the Newport contact (Figure 3.32). These folds are believed to represent a "softening" or limited mobilization of the mylonitic foliations as a result of contact metamorphism by the Newport Granite. The elongated and highly strained quartz grains and the kinked and bent biotite flakes that define these foliations elsewhere have been recrystallized. Quartz grains occur as aggregates of polygonal grains with  $120^\circ$  triple junctions, and biotite flakes occur as straight strain-free grains.

b. Lithology

The Newport pluton is characterized by 2 to 3 cm long microcline megacrysts that make up close to 50 percent of the intrusion by volume. These megacrysts are distinctly smaller than those in the adjacent Cape Freels and Lockers Bay granites.

On Pork Island and Fair Islands, the Newport pluton contains sharply banded, angular blocks (some to several hundred metres long) of undeformed equigranular granite more leucocratic than the host





Fig. 3.33. A sheet-like xenolith of equigranular granite in the Newport pluton. Fair Islands.



Fig. 3.34. Banding in hornblende monzodiorite patches in the Newport Granite. Fair Islands. Location - 1140

(Bell et al., 1979) (Figure 3.33). Some of these blocks, which were earlier mapped incorrectly as long continuous sheets by Younce (1970), are cut by aplite and pegmatite dikes which are also truncated by the host Newport Granite. These granite blocks presumably represent fragments of a granitic body older than the Newport pluton. Representatives of the former have not been seen outside the Newport Granite. In a few small areas on these islands, the Newport Granite contains a few patches of hornblende monzodiorite. These patches range from a few metres to several tens of metres in length, are generally angular in shape, and have sharp to diffused margins. They consist mostly of hornblende and plagioclase ( $An_{24}$  to  $An_{34}$ ) with minor amounts of biotite, microcline and quartz. Commonly, these patches have a layering produced by alternating dark and light layers (Figure 3.34). The dark layers are rich in hornblende and poor in plagioclase and the light layers are poor in hornblende and rich in plagioclase. The width of the layers is variable and the contact between them is mostly gradational. In places, the hornblende monzodiorite shows a spectacular pattern of round whitish patches (up to 30 cm in diameter) in a dark matrix (Figure 3.35). This structure may have been produced by the diapiric rise of a plagioclase-rich layer through an overlying hornblende-rich layer and the diapirs then being truncated by the outcrop surface (Figure 3.36). These hornblende monzodiorite patches may be related to cumulates formed in a magma chamber or may represent rock fragments from source regions of the plutons. However, more work is needed before the origin of the granitic and the monzodioritic xenoliths in the Newport pluton



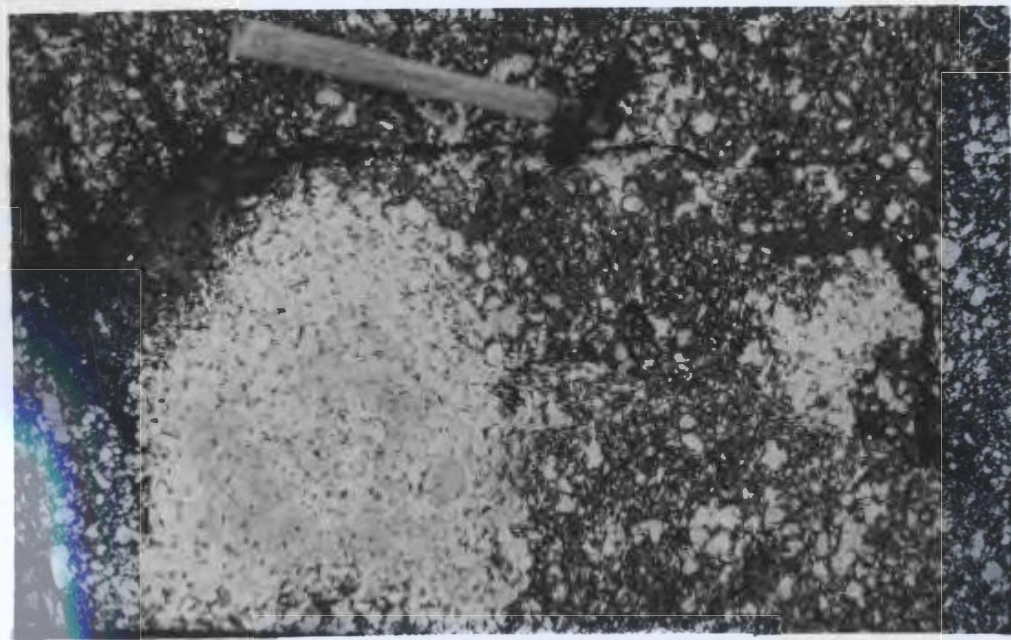


Fig. 3.35. Plagioclase-rich patches in hornblende monzodiorite, Newport pluton. South shore of Pork Island.

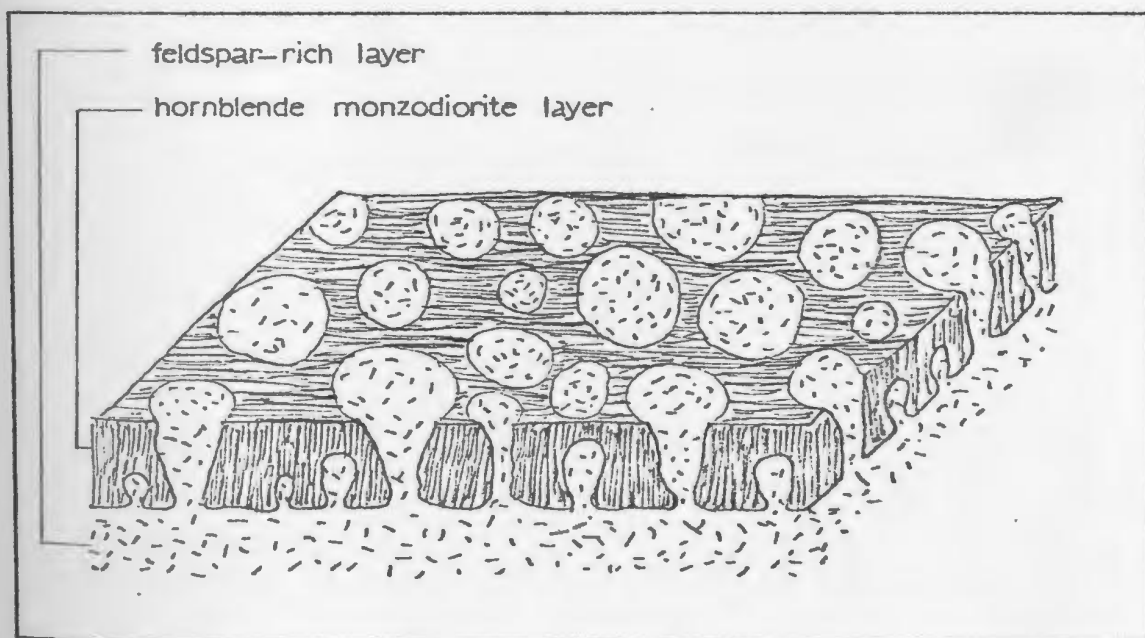


Fig. 3.36. Schematic interpretation of the development of round feldspar-rich patches shown in Fig. 3.35.

can be established because their distribution, petrography, structure and chemistry are not well known.

c. Structure

The Newport pluton does not contain a penetrative mineral alignment but, locally, the euhedral megacrysts define a variable L-S fabric. This is most pronounced in the southern part of the granite, where numerous small, elongated, mafic inclusions lie parallel to the alignment of the megacrysts. There, megacryst alignment strikes in an east-northeasterly direction and has moderate northwesterly dips.

In the southeast, on Fryingpan Island and on the outermost Fair Islands and on the eastern end of Lewis Island, the Newport Granite is highly brecciated. The feldspars are reddened, and the quartzes stand out as milky-white crystals. Veins of epidote and numerous northeasterly trending, steeply dipping fracture surfaces are present. The fracture surfaces contain slickensides plunging gently to the northeast. This deformation is probably related to movements along the Dover Fault Zone which may well have cut-off a part of the pluton in the south (Jayasinghe and Berger, 1976). It appears to be more brittle than the deformations that produced the mylonitic foliations in the Wareham, North Pond, Lockers Bay and Cape Freels plutons. Perhaps the brecciation of the Newport may have occurred at lower pressure and temperature conditions than those that prevailed during the formation of the mylonitic foliations in the plutons described earlier.

### 3.3.8. Big Round Pond Granite

#### a. Distribution and Contact Relationships

The Big Round Pond Granite (Jayasinghe, 1978a) occurs between Southwest Pond and Big Round Pond in the eastern part of the Wesleyville map area. It intrudes, with sharp contacts, the Hare Bay Gneiss and the Wareham, Business Cove and Newport plutons and truncates the foliations in the Hare Bay Gneiss ( $S_3$ ), and the Wareham ( $W_1$ ) and Business Cove ( $BC_1$  and  $BC_2$ ) plutons. In places, the Big Round Pond Granite contact truncates the megacrysts in the Newport Granite (Figure 3.37); indeed, this is the only way that the Big Round Pond Granite is recognized as a separate intrusion from the Newport.

#### b. Lithology and Structure

The Big Round Pond pluton consists of medium-grained biotite granite. Its principal mineral constituents are quartz, plagioclase ( $An_{13}$  to  $An_{30}$ ), microcline and biotite. Sphene, epidote, apatite, zircon and opaque minerals (probably pyrite) occur as accessory minerals.

The quartzes are mostly euhedral to subhedral in shape (Figure 3.38) and range from 0.5 to 2 mm in diameter. Some of the quartz grains show wavy extinction. The plagioclases range from 0.8 to 1.2 mm in size and have euhedral to subhedral shapes. The plagioclase grains are partly altered to sericite and epidote. They show normal zoning and Carlsbad and Albite twins are common. The microclines are subhedral to anhedral in shape and are generally between 2.4 to 5 mm in length; a few may reach up to 1.5 cm. The microcline grains show unevenly developed grid twinning; Carlsbad twins occur in the larger grains.

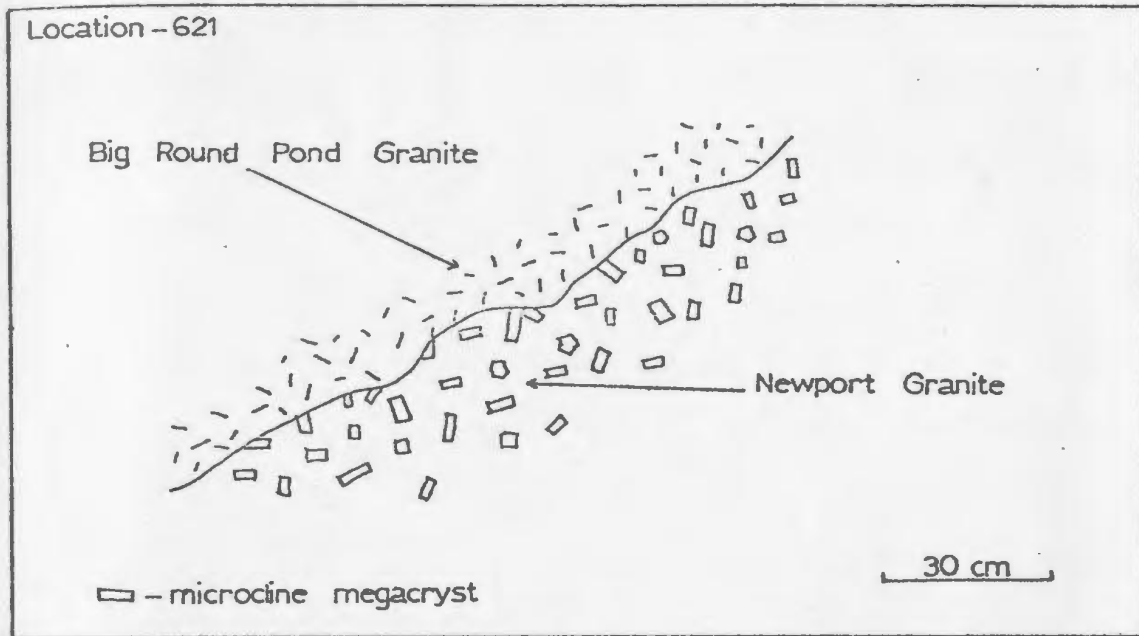


Fig. 3.37. Contact of the Big Round Pond Granite cutting across microcline megacrysts in the Newport Granite. Location - 621.

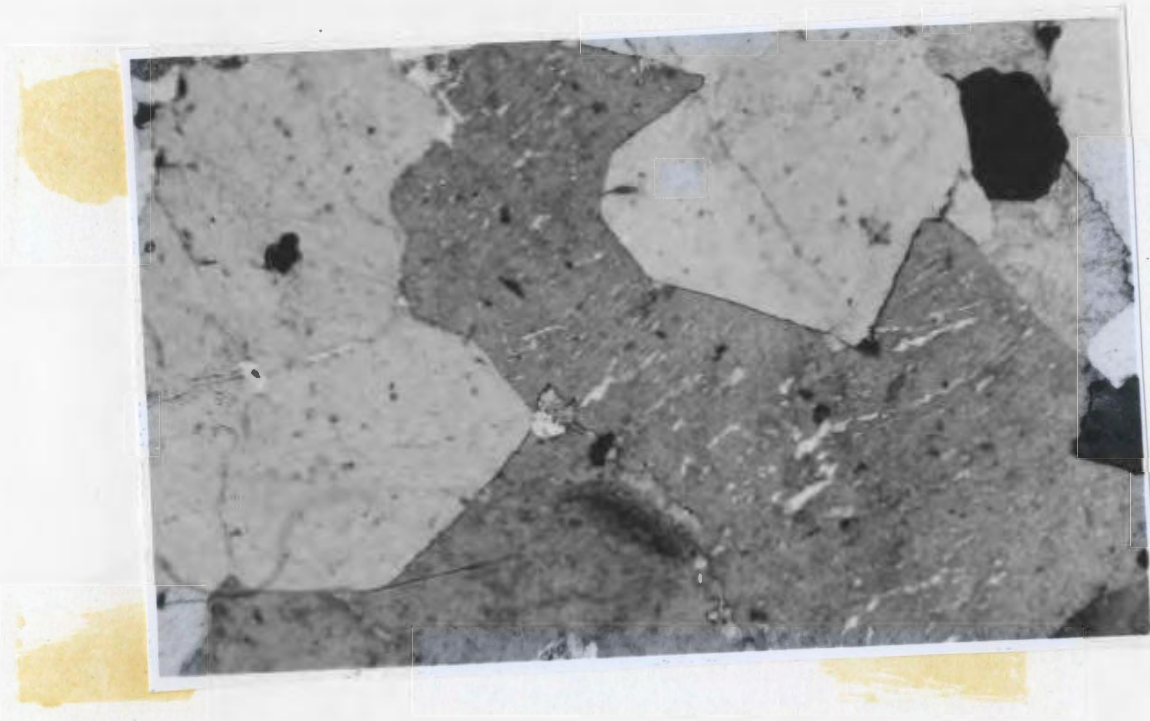


Fig. 3.38. Subhedral quartz grains (light coloured) in the Big Round Pond Granite. (X10). Location - 134.

Well-developed, vein-like microperthitic texture is common. Some of the microclines contain inclusions of quartz, plagioclase and biotite. The biotites are light brown to greenish brown pleochroic and range from 0.2 to 1.2 mm in length. They are randomly oriented. Some of the biotites are partly chloritized.

The Big Round Pond Granite contains numerous pegmatites and aplites which trend in all directions. No mineral alignment was seen in the granite.

#### 3.3.9. Gabbros

Several small bodies of gabbro occur in the central and southeastern parts of the Wesleyville map area. They are very poorly exposed and, thus, their contact relationships, lithology and structure are not well known. On Copper Island, Horse Island and Pigeon Island, a gabbro pre-dates sheets of the Cape Freels Granite.

The gabbro bodies consist of varying proportions of augite, plagioclase (labradorite) and their alteration products -- hornblende, biotite, chlorite and epidote. The gabbro on the above islands and the one immediately to the south of the Deadman's Bay Granite are highly deformed but the other gabbro bodies in the area appear massive. The deformed gabbro bodies show a foliation defined by flakes of greenish biotite and domains of granulated feldspar. Coarse grains of clinozoisite overgrow the foliation.

#### 3.4. Deformation in the Shear Zones

Detailed information on the deformation in the two major, north-northeasterly trending shear zones in the area could be obtained

by using structures in the plutons affected by them. Given below is a detailed account of a quantitative analysis of the deformed Cape Freels Granite, within the more easterly of the two shear zones. The aims of this analysis were to determine (1) the type of strain in the shear zones, (2) the distribution of strain within the shear zones, and (3) the stress pattern that produced them.

#### 3.4.1. Method

Dunnett (1969) related the final axial ratio ( $R_f$ ) of a homogeneously deformed elliptical particle and the angle ( $\phi$ ) between its long axis and the maximum principal strain direction to the initial axial ratio ( $R_i$ ) of the particle and to the finite strain axial ratio ( $R_s$ ) (Figure 3.39). Thus, he was able to calculate a series of curves relating  $R_f$  and  $\phi$  for specific values of  $R_i$  and  $R_s$  (Figure 3.40). For deformed particles both  $R_f$  and  $\phi$  are measurable in the field and  $R_f/\phi$  diagrams can be easily constructed. These diagrams can then be compared with the theoretical  $R_f/\phi$  curves and  $R_s$  and  $R_i$  for the deformed particles can be estimated. Dunnett demonstrated that his method can also be used to estimate the  $R_s$  and  $R_i$  values of rectangular, rhombic and pear-shaped particles, but in calculating the  $R_f$  values of these shapes the axes of ellipses of equivalent areas to the particles should be used (see also Coward, 1976). In the present study  $R_f$  and  $\phi$  measurements were made on deformed microcline megacrysts that are approximately elliptical in shape.

This method has a number of disadvantages: (1) it is only applicable to homogeneously deformed bodies; (2) for a given body the distribution of points in an  $R_f/\phi$  diagram is affected by earlier

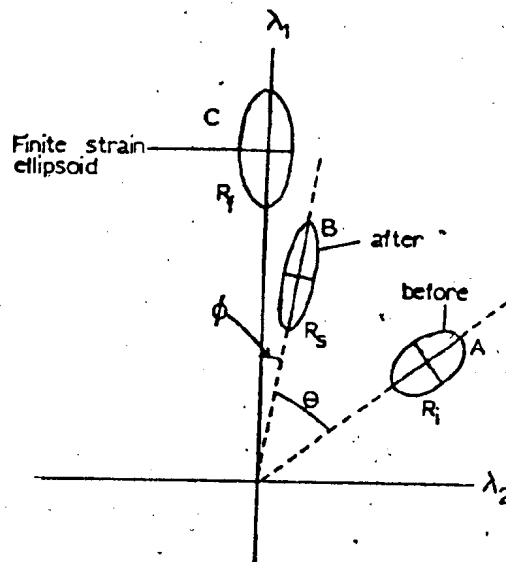


Fig. 3.39. The change in shape and orientation of an initial elliptical particle subject to a finite strain (after Dunnet, 1969).

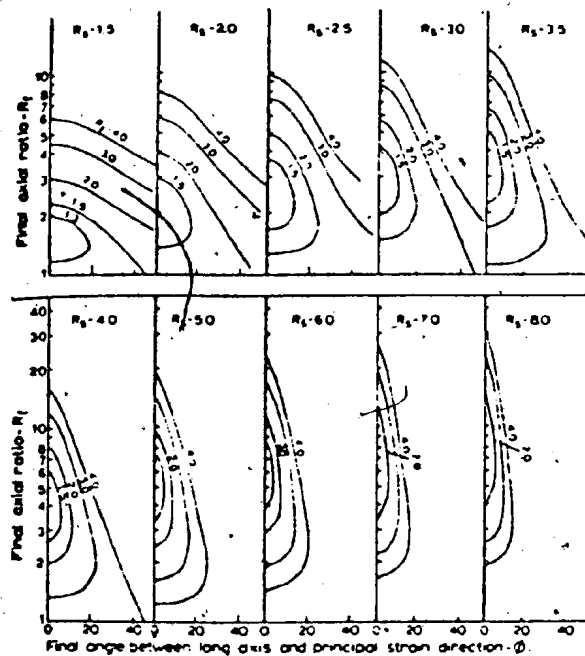


Fig. 3.40. Curves showing variation in  $R_f/\phi$  for initial elliptical ratios ( $R_1$ ) subject to various finite strain ratios ( $R_s$ ). The curves are symmetrical about the  $0^\circ \phi$  axis (after Dunnet, 1969).

alignments of the particles measured and by later superimposed deformations and, thus, may not give accurate  $R_s$  values; and (3) the ductility contrasts between the particles and the matrix may also give inaccurate  $R_s$  values for the body as a whole (if the matrix is more ductile than the particles, it will deform more than the latter (Gay, 1968).

#### 3.4.2. Results

Length and breadth of deformed megacrysts and the inclination of their long axes to the mylonitic foliation ( $\theta$ ) were measured at three locations (2, 4 and 5 in Figure 3.41) within the shear zones. The mylonitic foliation was taken to represent the ab plane of the finite strain ellipsoid ( $a \geq b \geq c$ ). Several authors (Johnson, 1967; Ramsay and Graham, 1970; Sinha Roy, 1977) have shown that mylonitic foliation in shear zones lies parallel to the ab plane of the finite strain ellipsoid. The approximately horizontal lineation in the rock (marked by the megacrysts that are more elongated on horizontal surfaces than on vertical surfaces at right angles to the foliation and by elongated quartz grains on the foliation surfaces) was considered to be parallel to the a direction of the strain ellipsoid. One hundred feldspars were measured at each location; fifty on ac plane (perpendicular to the foliation and parallel to the lineation) and fifty on bc plane (perpendicular to both foliation and lineation). To determine the strength of pre-shear zone alignments, the length and breadth of 100 microcline megacrysts were also measured at each of two locations (1 and 3 in Figure 3.41) in the undeformed megacrystic granite. There  $\theta$  was taken



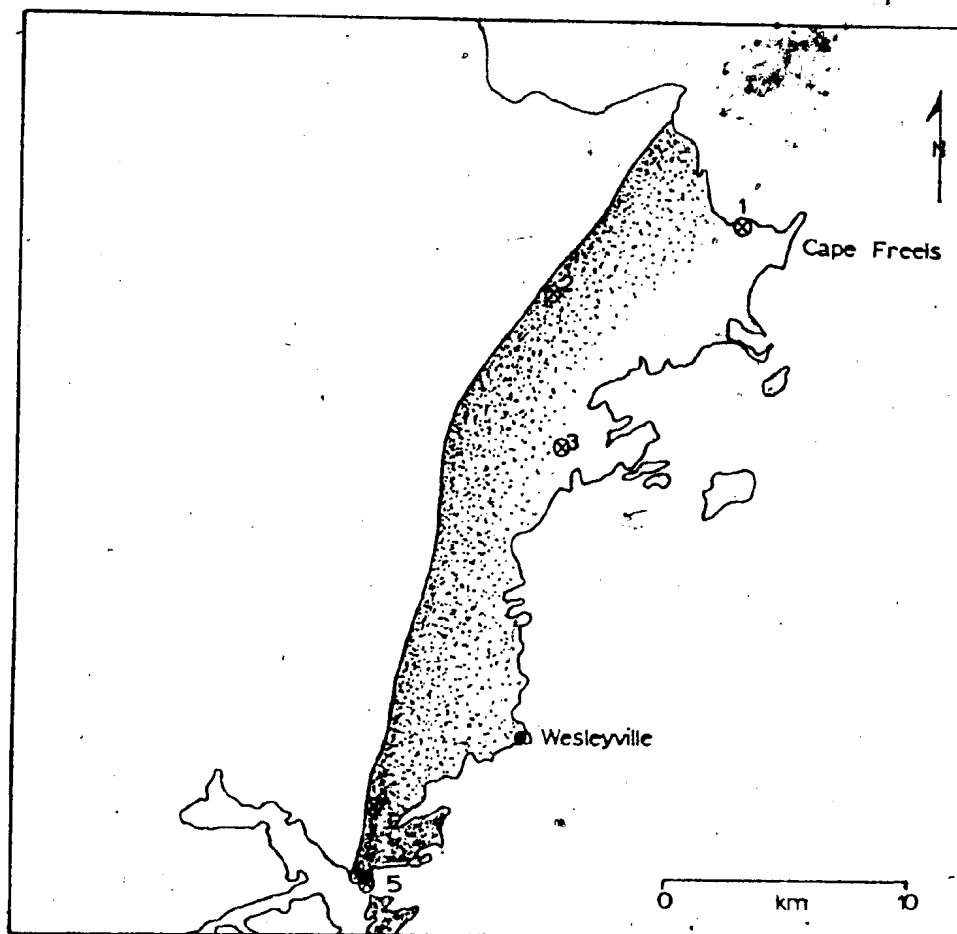


Fig. 3.41. Sketch map of the Cape Freels Granite (red). Dotted area marks the deformed part of the granite; dot density increases with increase in deformation. Numbers indicate locations at which measurements were made for strain analysis.

as the angle between the length of the crystals and the alignment defined by the rectangular megacrysts. Measurements were again made on two vertical planes at right angles to each other.

The individual measurements are listed in Appendix 3.3.

In all the localities the measurements on any one plane were restricted to an area of about  $0.5 \text{ m}^2$ . The deformation in such a small area was assumed homogeneous.

Figure 3.42a, b shows the  $R_f/\theta$  diagrams for the locations within the shear zone and in the granite outside. From these diagrams the axial ratios of the finite strain ellipsoids at the different localities can be estimated. The axial ratios of the strain ellipsoids at locations 2, 5, and 4 in the shear zone are 2.9:2.4:1, 2.8:2.7:1, and 3.5:2.8:1 respectively. In localities outside the shear zone the variation in axial ratios is independent of orientation thus indicating no strain. Location 4 lies more to the west of locations 2 and 5 and shows the greatest difference between a, b and c axes of the deformed ellipsoid. This supports the earlier conclusions (page 102, Jayasinghe and Berger, 1976) that the Cape Freels Granite is more deformed in the west than in the east and that the intensity of deformation in the shear zones increases with increasing distance from the margin.

The axial ratios of the strain ellipsoids at the three locations in the shear zone were plotted in the Flinn diagram of Figure 3.43. They plot close to the line  $K = 0$ . Therefore, the deformation in the shear zone has a flattening component (pure shear).

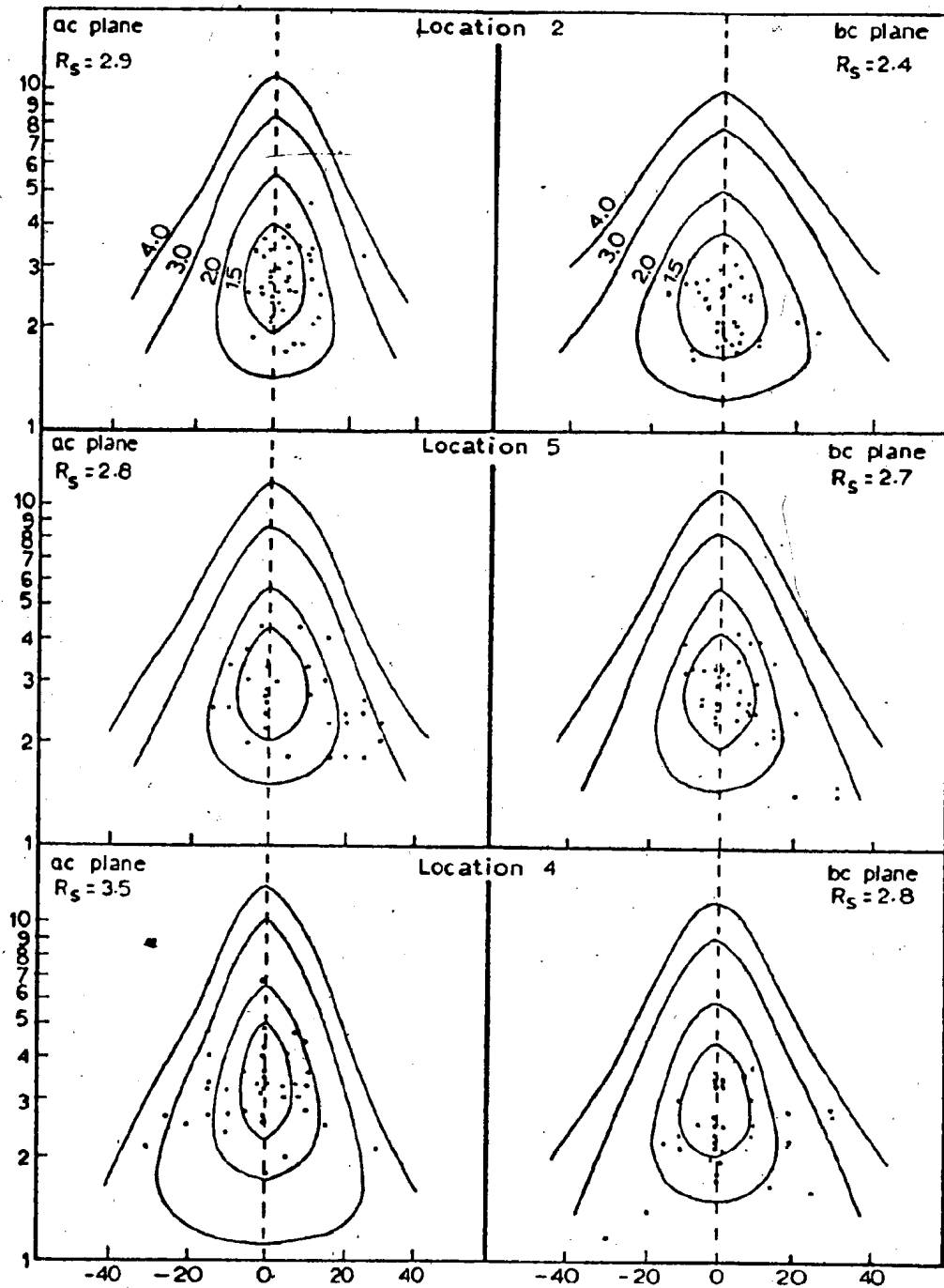


Figure 3.42 a

Fig. 3.42a.  $R_F/\theta$  diagrams for the locations within the shear zone.

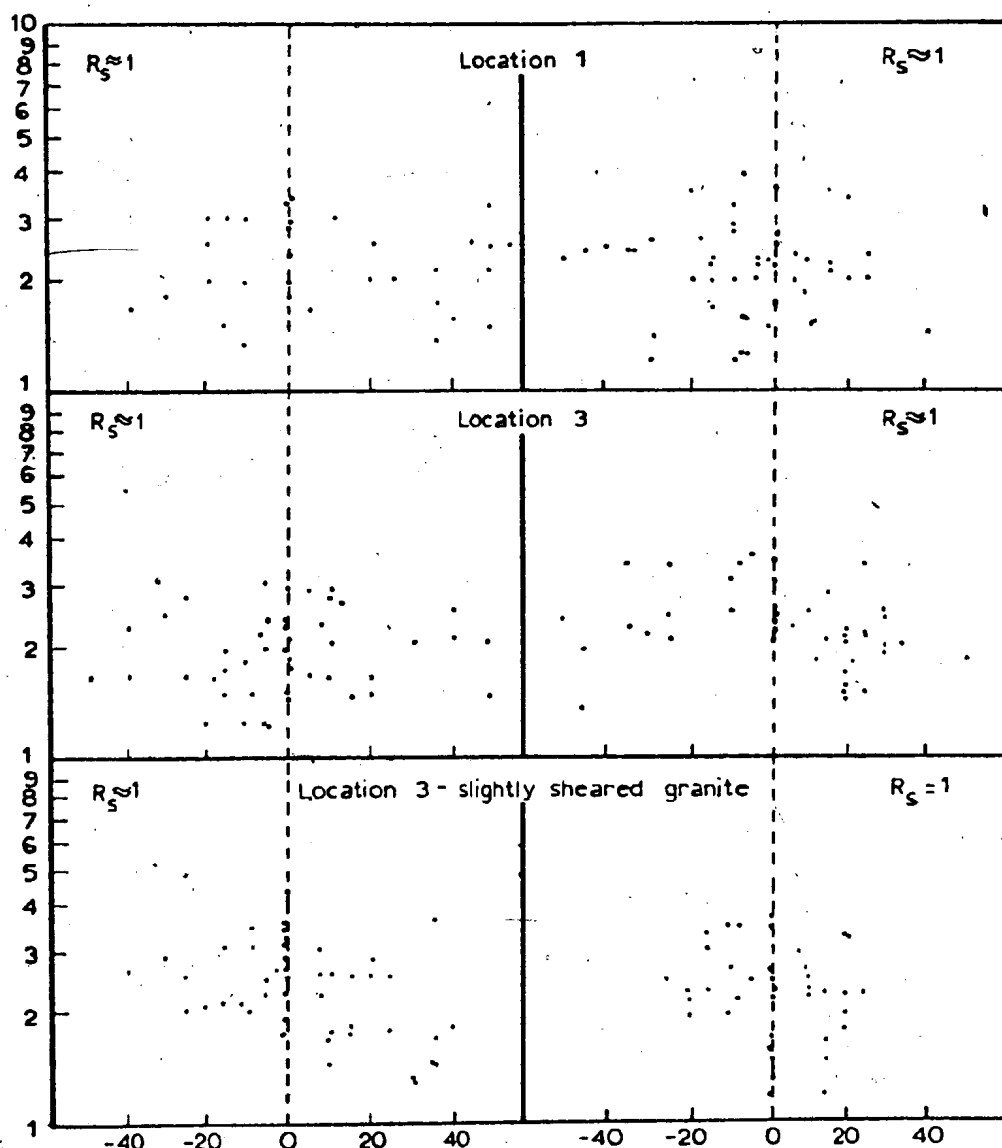


Figure 3.42b

Fig. 3.42b.  $R_f/\theta$  diagrams for the locations in the granite outside the shear zone.

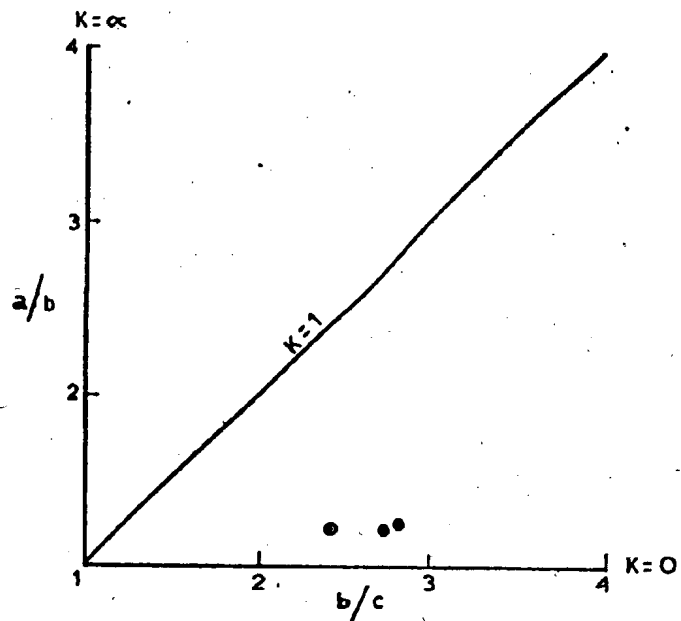


Fig. 3.43. Axial ratios of the strain ellipsoids (  $\odot$  ) for three locations within the shear zone plotted on the Flinn diagram.

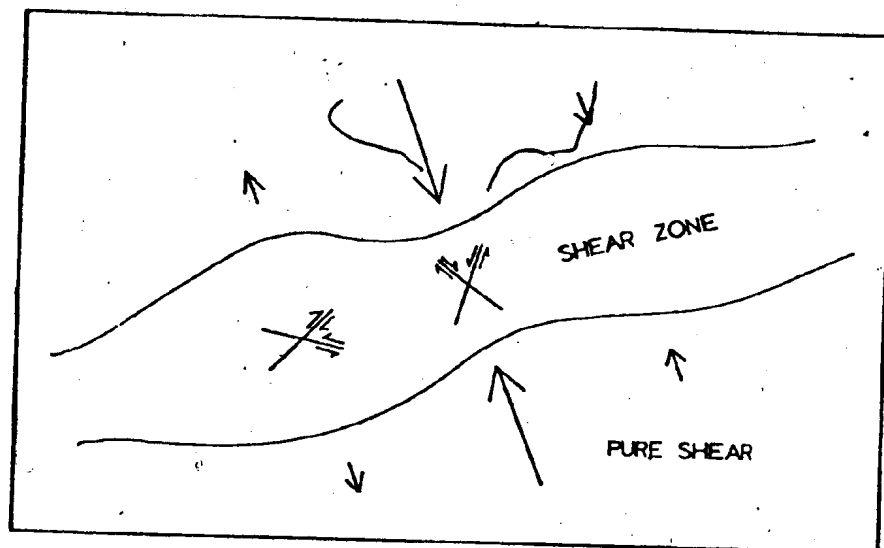


Fig. 3.44. Formation of conjugate shear fractures due to differences in lateral compression along a shear zone.

If the shear zone resulted entirely by simple shear, which by definition is a plane strain, the strain ellipsoids from localities within the shear zone should lie along the line  $K = 1$ .

Some authors (Coward, 1976; Sinha Roy, 1977) have suggested that shear zones are produced by a combination of pure shear and simple shear. The evidence presented above indicates that such a mechanism could have been responsible for the formation of the shear zones in the present study area. Once a shear zone forms, it progressively widens and its middle part gets more deformed as long as a sufficient stress is maintained (Mitra, 1978). Thereby it will take in the stress and the effects of the deformation that produced the shear zone will be localized within the latter. This may explain why  $D_4$  structures are not common outside the shear zones in the area.

In many places the mylonitic foliation in the shear zones is offset by a discontinuous, non-penetrative, crenulation cleavage (see pages 94 and 104). The origin of this cleavage is not clear. There are at least two possible ways by which it could have formed during  $D_4$ . (1) Conjugate sets of shear fractures could have resulted due to pure shear (Figure 3.44). Shear fractures that trend in one direction may have become more predominant than those that are inclined to them, thus resulting in the crenulation cleavage above<sup>1</sup>. (2) The crenulation cleavage may represent shear fractures (secondary shears) developed

---

<sup>1</sup>In fact, a weak crenulation cleavage occurs in places showing a conjugate relationship to the well-developed crenulation cleavage in the shear zones.

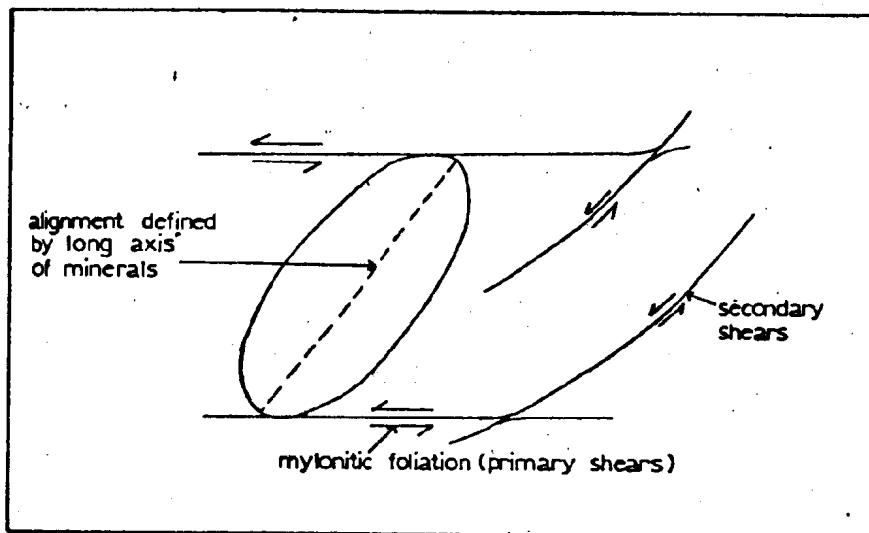


Fig. 3.45. Formation of secondary shear fractures oblique to primary shear fractures in a shear zone.

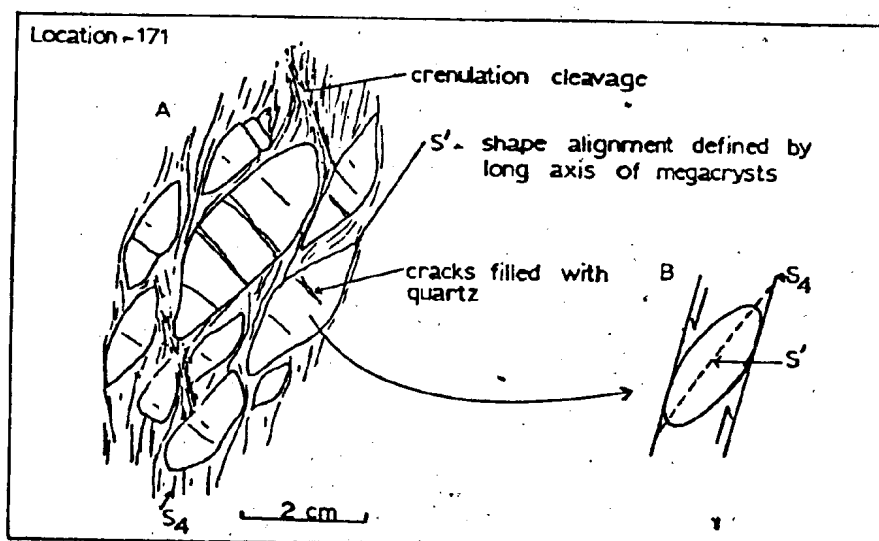


Fig. 3.46. (A) Diagram showing angular relationships between feldspar shape alignment, mylonitic foliation ( $S_4$ ) and crenulation cleavage in the Cape Freels Granite. (B) Possible sense of shear along  $S_4$ .

oblique to the mylonitic foliation (primary shears) as shown in Figure 3.45 (see Berthe, Choukroune and Jegouzo, 1979). However, more work is needed to establish the relationship between the mylonitic foliation and the crenulation cleavage in the shear zones.

The relationship between the direction of feldspar alignment and the mylonitic foliation indicates that the sense of movement in the shear zone that deformed the Cape Freels Granite is sinistral (Figure 3.46). Similar evidence indicates that sense of shear in the zone that deformed the North Pond and the Wareham plutons and the western part of the Lockers Bay Granite is also sinistral (page 94). However, the relationship between the feldspar alignment and the east-northeast trending mylonitic foliation in the eastern part of the Lockers Bay Granite indicates that the former has been rotated clockwise. The deformation in this part of the granite is related to movements along the Dover Fault (see page 110). Thus, the sense of shear within the Dover Fault Zone is dextral, and is opposite to that in the two major northeast trending shear zones in the area. This provides a tool to distinguish areas deformed by the above shear zones from areas affected by the Dover Fault related deformation.

### 3.5. Ages of the Granitoids

The relative ages of most of the granitoids in the area can be established from field relationships but radiometric dating is necessary to determine the absolute ages of the intrusions. The contact relationships and the structures of the granitoids have already been



discussed in detail in the present chapter. The diabase dikes in the area predate the Newport and Big Round Pond granites and postdate all the other granitoids in the area (see Chapter 5). They provide the only clue to establish the age relationship between the Newport Granite and the Deadman's Bay Granite in the field. The intrusive sequence determined from the field relationships is shown in Figure 3.47.

The small gabbro bodies in the area are not shown in the above sequence. The gabbro body on Copper Island, Horse Island and Pigeon Island is cut by sheets of the Cape Freels Granite. The gabbro that occurs in the Square Pond Gneiss, west of Rocky Ridge Pond, is older than the Deadman's Bay Granite immediately to its north because the gabbro is highly deformed whereas the granite is undeformed.

Blackwood and Kennedy (1975) suggested that the Lockers Bay Granite was deformed in the Precambrian times. They believed that the foliation that overprints the Lockers Bay Granite is of the same age as the main fabric in the Love Cove Group of the Avalon Zone. The Love Cove Group is a predominantly volcanic unit that was interpreted to occur stratigraphically below the molasse facies rocks of the Musgravetown Group (Jenness, 1963). The latter is considered to be of Late Hadrynian age as it is overlain by fossiliferous Lower Cambrian strata. Jenness (1963) related foliated acidic volcanic clasts in the basal conglomerates of the Musgravetown Group to the acidic volcanic rocks of the Love Cove Group and, hence, interpreted the foliation in the latter to be pre-Hadrynian. This was the criterion used by Blackwood

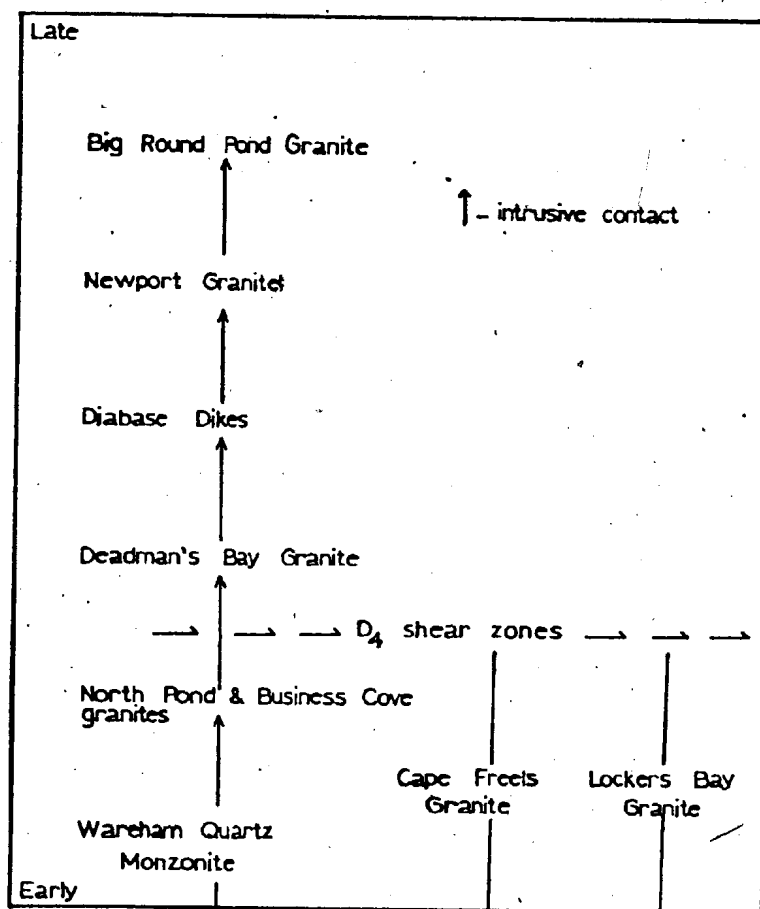


Fig. 3.47. The sequence of intrusive events in the area based on field relationships and structural evidence.

and Kennedy (1975) and Blackwood (1976, 1977) in suggesting a Precambrian age for the deformation in the Lockers Bay Granite.

However, Blackwood now doubts Jenness' idea that the conglomerates containing foliated acid volcanic clasts represent basal part of the Musgravetown Group (Blackwood, R. F., personal communication, 1979), and Hussey (1979) has demonstrated that the deformation in Love Cove Group can be as young as Devonian. These cast doubt on the proposed Precambrian age of the Lockers Bay Granite. Currie *et al.* (1979) studied the northwestern marginal part of the Deadman's Bay Granite, farther to the west of the present study area. They suggested that the Deadman's Bay pluton is possibly Carboniferous in age.

Radiometric dates from the granitoids in the area are shown in Table 3.3. The Rb/Sr whole-rock isochron dates in Table 3.2, except for the date from the Wareham Quartz Monzonite, were obtained by recalculating published dates\* (see Table 3.2 for references) using a decay constant ( $\lambda$ ) of  $1.42 \times 10^{-11} \text{ yr}^{-1}$  for  $\text{Rb}^{87}$ .

Samples from both the deformed and the undeformed parts of the Cape Freels Granite fit into a single isochron within analytical uncertainty (Bell *et al.*, 1977). Therefore, the Rb/Sr systematics in this intrusion appear to have been unaffected by the deformation. The K/Ar date from the Deadman's Bay Granite may be taken as closely representing the absolute age of the intrusion because similar K/Ar dates of a number of granitoids elsewhere in the Gander Zone were found to closely correlate with their Rb/Sr isochron ages (K. Bell, personal communication, 1979). The plutons are arranged in Figure 3.48, according to their radiometric dates.

---

\* The published Rb/Sr whole-rock isochron dates from the granitoids in the area have been calculated using a decay constant of  $1.47 \times 10^{-11} \text{ yr}^{-1}$  for  $\text{Rb}^{87}$ .

Table 3.2. Radiometric dates from the granitoids in the thesis area.

A. K/Ar date from the Deadman's Bay Granite

<u>Mineral</u>	<u>Location</u>	<u>Age Ma</u>	<u>Reference</u>
Biotite	49°13'20"N 54°03'25"W	335 ± 14	Wanless <u>et al.</u> , 1965

B. Rb/Sr whole rock isochron dates ( $\lambda = 1.42 \times 10^{-11} \text{yr}^{-1}$ )

<u>Intrusion</u>	<u>Age Ma</u>	<u>Initial <math>\text{Sr}^{87}/\text{Sr}^{86}</math> Ratio</u>	<u>Reference*</u>
Newport Granite	344 ± 44	0.7059 ± 0.0020	Bell <u>et al.</u> , 1979
Lockers Bay Granite	311 ± 18	0.7145 ± 0.0013	Bell and Blenkinsop, 1977
Cape Freels Granite	414 ± 05	0.7078 ± 0.008	Bell <u>et al.</u> , 1977
Wareham Quartz Monzonite	396 ± 16	0.7079 ± 0.007	K. Bell, personal communication, 1979

\* Published dates are based on a  $\lambda$  of  $1.47 \times 10^{-11} \text{yr}^{-1}$ .

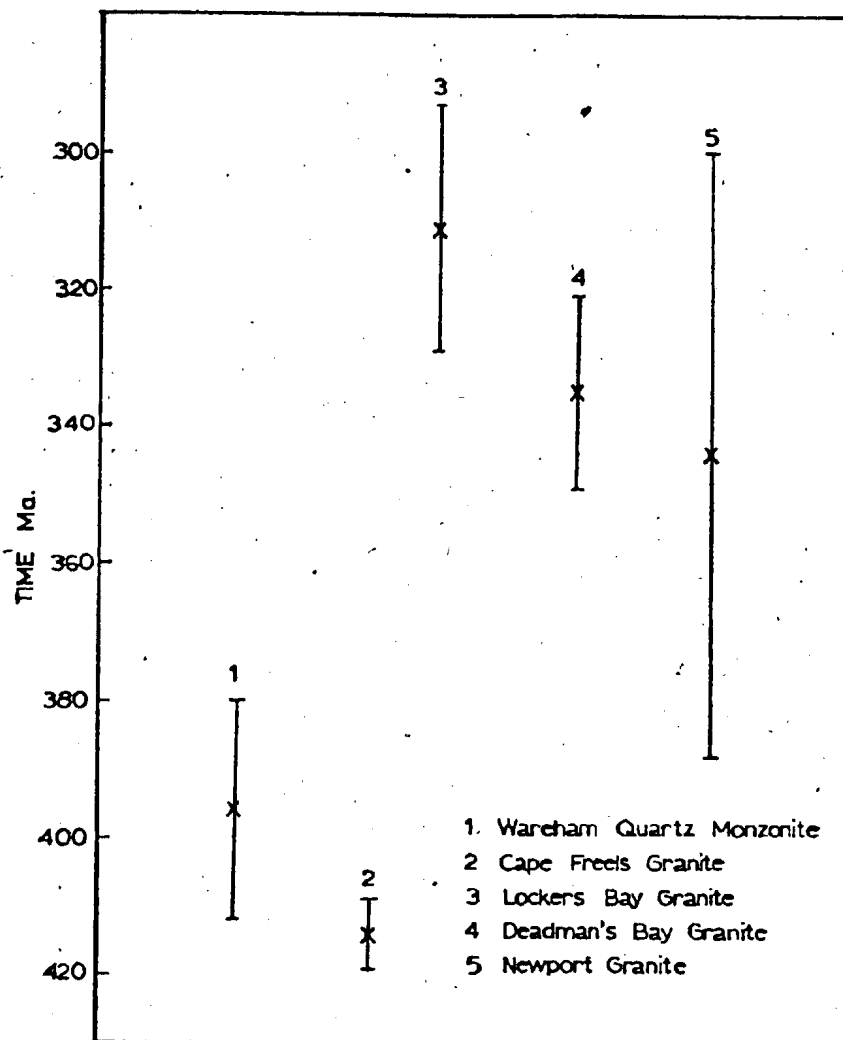


Fig. 3.48. Diagrammatic representation of the radiometric dates from the granitoids in the area. X - age, vertical bars denote the error margin. When the error margin is taken into account, the radiometric ages of the Lockers Bay, Deadman's Bay and the Newport plutons overlap between 330 and 320 Ma.

The radiometric dates indicate that the plutons have been emplaced in the Silurian-Carboniferous time interval (using Geologic Time Table compiled by Van Eysinga, 1975). The Wareham Quartz Monzonite and the Cape Freels Granite have similar ages of about 400 Ma. Their radiometric ages are higher than those of the Deadman's Bay and Newport granites and, therefore, are in agreement with the intrusive sequence obtained using field data. The K/Ar date from the Deadman's Bay Granite suggest a Carboniferous age for its emplacement (see also Currie *et al.*, 1979).

The Newport Granite has an older radiometric age than the Deadman's Bay Granite which in turn has an older radiometric age than the Lockers Bay Granite. This is the opposite to the age sequence obtained from the field relationships because the Newport Granite cuts the diabase dikes that post-date the Deadman's Bay Granite and the latter truncates the shear zone that deformed the western part of the Lockers Bay Granite. However, this is not the case when the error margin attached to the radiometric dates is considered (Figure 3.48). Taking into account the error margins of the dates and the field relationships, the above plutons should have been emplaced between 330 and 320 Ma in the following order, from old to young: Lockers Bay Granite -- (shear zones) -- Deadman's Bay Granite -- (diabase dikes) -- Newport Granite (see also Bell *et al.*, 1977). The radiometric dates invalidate, as does Hussey's recent work (see page 139), Blackwood and Kennedy's (1975) idea that the Lockers Bay Granite is of Precambrian age (see page 137).

Murthy (G. S. Murthy, personal communication, 1979), based on paleomagnetic data, proposed that the diabase dikes in the area have been emplaced in two episodes at 400 Ma and 380 Ma, respectively. He also suggests that the magnetization of the Lockers Bay Granite occurred at about 400 Ma. These dates do not agree with the radiometric dates from the Lockers Bay, Deadman's Bay and Newport plutons. However, Murthy admits that paleomagnetic data cannot be used to get conclusive emplacement ages for the dikes or the granite because of the absence of well-established Silurian-Devonian "polar-wandering" paths for eastern North America.

### 3.6. Summary

Granitoid plutons in the area include the Wareham, Cape Freels, Lockers Bay, Deadman's Bay and Newport megacrystic granitoids, the North Pond and Business Cove "two-mica" granites, and the Big Round Pond biotite granite. The field relationships indicate that the granitoids postdate the  $F_3$  folds and the  $S_3$  foliation in the gneisses. The mode of emplacement of the plutons is not known except for scanty evidence suggesting a forceful intrusion in the case of the North Pond and the Deadman's Bay granites.

All the granitoids, except the Big Round Pond Granite, contain a mineral alignment that could be related to their emplacement. In addition to this fabric, the Wareham, North Pond, Business Cove, Lockers Bay and Cape Freels plutons contain mylonitic foliations produced by the two major north-northeast trending shear zones in

the area. Furthermore, the southern part of the Cape Freels Granite and the eastern part of the Lockers Bay Granite contain a mylonitic foliation that is related to movements along the Dover Fault. A zone of brecciation in the southern-most part of the Newport Granite has also been attributed to movements along this fault.

The shear zones in the area resulted from a combination of pure shear and simple shear during the  $D_4$  deformation. The sense of movement within these shear zones is sinistral, whereas sense of shear in the Dover Fault-related deformation is dextral. The time relationships between  $D_4$  shear zones and the Dover Fault are not clear. It is possible that they represent complementary shears resulting from west northwest-east southeast compression. However, further work is clearly needed before the relationships between these structures can be established (see page 272).

The field relationships and the radiometric dates indicate that (1) the Wareham and Cape Freels plutons were emplaced at about 400 Ma and (2) the Lockers Bay Granite, Deadman's Bay Granite, diabase dikes and Newport Granite were intruded between 330 and 320 Ma ago; this interval also includes the  $D_4$  deformation.



## CHAPTER 4

### THE MICROCLINE MEGACRYSTS

The occurrence of microcline megacrysts is the most distinctive feature of the plutons in the thesis area and accordingly these plutons have been commonly referred to as megacrystic granites (Williams, 1968; Jayasinghe, 1976, 1978a; Blackwood, 1977; Bell *et al.*, 1979; Strong, 1979). The aim of this chapter is to determine the origin of the microcline megacrysts. The neutral term megacryst is preferred for these large crystals ( $> 2$  cm in length) over the terms such as phenocrysts, xenocrysts and porphyroblasts mainly because the latter terms have a genetic meaning. Phenocrysts are supposed to have crystallized from a magma. Xenocrysts are foreign to magma and have been incorporated by the magma after forming elsewhere. Porphyroblasts represent crystals that grew entirely in a solid medium. The distribution and the texture of the microcline megacrysts were discussed at length in the preceding chapter and thus will not be described here.

#### 4.1. Structural State of the Megacrysts

The structural state of the microcline megacrysts from three locations within each of the five megacrystic intrusions in the area were determined using the "three peak method" of Wright (1968). The sample locations, and the techniques used in determining the  $2\theta$  angles of the peaks are given in Appendix 4.1. The results are shown in Table 4.1. The  $2\theta$  angles were determined using  $\text{CuK}\alpha$  radiation.  $2\theta$  angles of the 060 and  $\bar{2}04$  diffractions of the megacrysts were plotted in a reference diagram taken from Wright (1968) (Figure 4.1). The

Table 4.1.  $2\theta$   $\text{CuK}\alpha$  values of the diffractions used in determining the structural state of the microcline megacrysts.

Intrusion	Sample #	$2\theta^{\circ}(\bar{2}01)$	$2\theta^{\circ}(060)$	$2\theta^{\circ}(\bar{2}04)$
Wareham Quartz Monzonite	NJ-355	21.01	41.76	50.55
	NJ-641	21.05	41.81	50.53
	NJ-723	21.03	41.81	50.53
Cape Freels	NJ-38	21.01	41.79	50.51
	NJ-96	21.05	41.82	50.52
	NJ-170	20.99	41.77	50.54
Lockers Bay Granite	NJ-L2	21.00	41.77	50.55
	NJ-L4	21.02	41.79	50.48
	NJ-L7	21.06	41.82	50.54
Deadman's Bay Granite	NJ-1	21.08	41.84	50.54
	NJ-828	21.08	41.80	50.55
	NJ-1094	21.08	41.81	50.52
Newport Granite	NJ-4	21.03	41.76	50.67
	NJ-205	21.03	41.78	50.88
	NJ-305	20.97	41.79	50.62

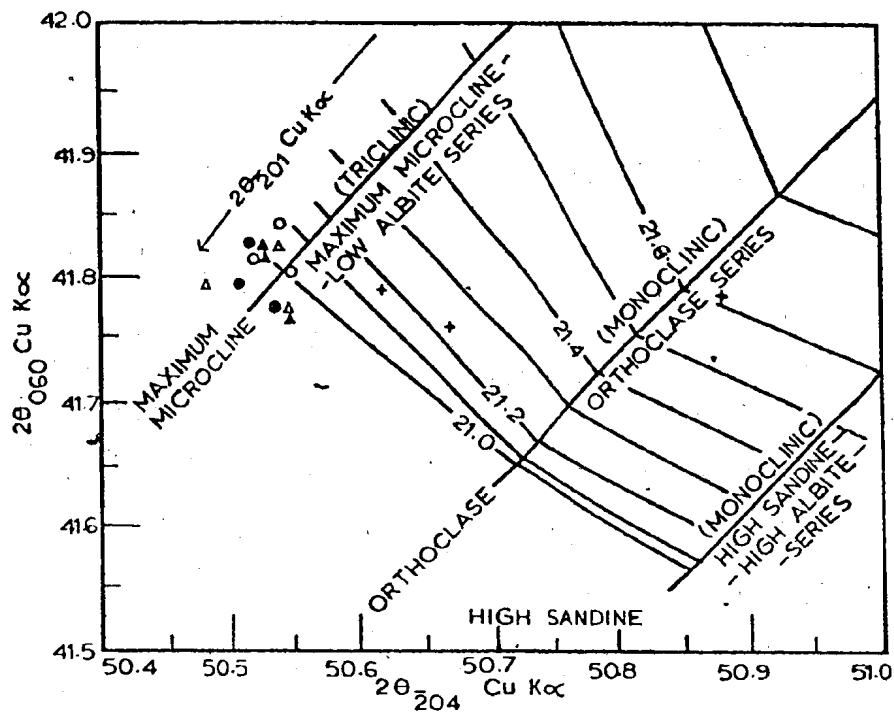


Fig. 4.1.  $2\theta$  angles of the 060 and  $\bar{2}04$  diffractions of the microcline megacrysts plotted on a reference diagram taken from Wright (1968)\*.  $\Delta$  - Wareham Quartz Monzonite,  $\Delta$  - Lockers Bay Granite,  $\bullet$  - Cape Freels Granite,  $\circ$  - Deadman's Bay Granite,  $+$  - Newport Granite.

\* In the case of the megacrysts from the Newport Granite,  $\bar{2}01$   $2\theta$  values determined from Fig. 4.1. exceed those obtained from diffractograms (Table 4.1) by more than  $0.1^\circ$ . Therefore, these megacrysts are anomalous and only their "apparent" structural state can be derived from Fig. 4.1. The extent this will depart from the true structural state is not known.

megacrysts from the Wareham, Cape Freels, Lockers Bay and the Deadman's Bay plutons plot near the maximum microcline member of the maximum microcline-low albite series. The megacrysts from the Newport Granite plot between the maximum microcline-low albite series and the high sanidine-high albite series.\*

Mackenzie (1954) used the splitting of the 130 diffraction of K-feldspars as an indicator of their structural state. In monoclinic K-feldspars, 130 diffraction is represented by a single peak, in triclinic K-feldspars it splits into two diffractions 130 and  $\bar{1}\bar{3}0$ , represented by two peaks. The 130 and  $\bar{1}\bar{3}0$  peaks of K-feldspars occur between  $23.18^\circ$  and  $24.03^\circ$   $2\theta$  for CuK radiation (Wright, 1968). Figure 4.2 shows diffractograms between  $22.5^\circ$  and  $24.5^\circ$   $2\theta$  for the megacrysts studied.

In the case of the Wareham, Cape Freels, Lockers Bay and the Deadman's Bay plutons the majority of the diffractograms show prominent 130 and  $\bar{1}\bar{3}0$  (triclinic) peaks with a smaller 130 (monoclinic) peak between them. In a few, the monoclinic 130 peak is the prominent diffraction. In the case of the Newport Granite all the diffractograms show only one prominent peak between  $23^\circ$  and  $24^\circ$   $2\theta$ , which is the 130 monoclinic peak.

These results indicate that both triclinic and monoclinic components occur within the megacrysts of the plutons. The possibility of the occurrence of domains with different degrees of ordering in a single feldspar has been suggested by a number of authors (see Smith, 1974). Thus, the megacrysts in the Wareham, Cape Freels, Lockers Bay

---

\* See footnote on page 147.

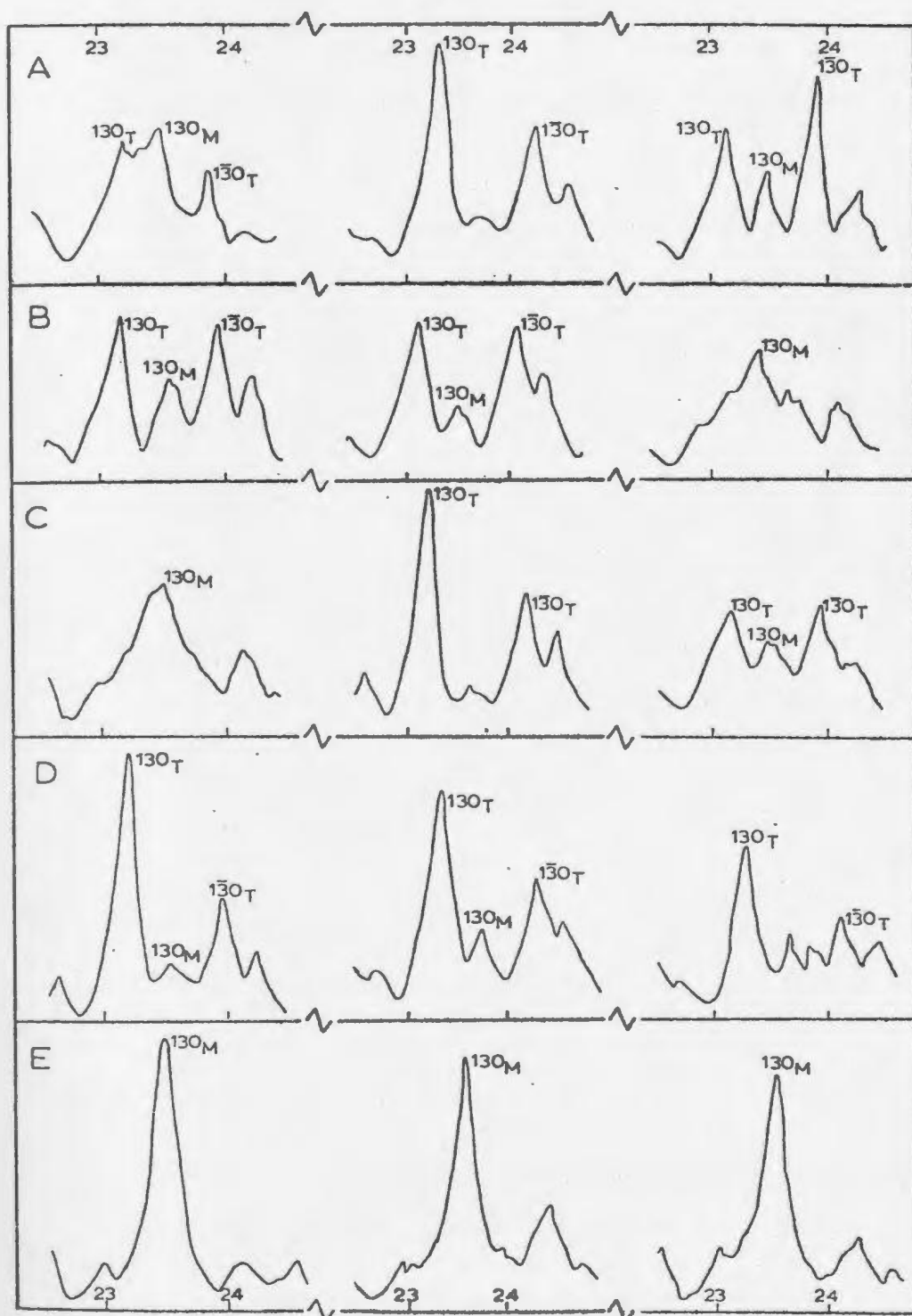


Fig. 4.2. Diffractograms between  $22.5^\circ$  and  $24.5^\circ$   $2\theta$  (CuK $\alpha$ ) for the megacrysts. Three samples from each megacrystic pluton were studied. A - Wareham Quartz Monzonite, B - Cape Freels Granite, C - Lockers Bay Granite, D - Deadman's Bay Granite, E - Newport Granite.

and the Deadman's Bay plutons appear to consist largely of domains with triclinic symmetry, whereas the megacrysts in the Newport Granite consist mostly of domains with monoclinic symmetry. Perhaps this may explain the lesser degree of development of grid twinning in the megacrysts in the Newport Granite compared to those in the other megacrystic granitoids in the area (see page 78). Such a correlation between structural state and grid twinning is not always valid because the interlocking nature of the twin lamellae could make a microcline appear untwinned when examined under a normal petrographic microscope (Smith, 1974).

#### 4.2. Chemical Composition

The chemical composition of the following feldspars were determined using a JEOL JXA-50A electron microprobe, using natural feldspars as standards:

##### (A) In megacrystic plutons

- 1) K-feldspar phase in megacrysts
- 2) K-feldspar phase in matrix microclines
- 3) perthitic lamellae in megacrysts
- 4) plagioclase inclusions in megacrysts
- 5) plagioclases in matrix

##### (B) In non-megacrystic plutons (the North Pond, Business Cove and the Big Round Pond granites)

- 1) K-feldspar phase in microclines
- 2) plagioclases

(C) In gneisses adjacent to the Cape Freels Granite

- 1) K-feldspar phase in microcline porphyroblasts
- 2) plagioclases

The individual analyses are given in Appendix 4.2 (see location map in back pocket for sample locations). The albite (Ab), anorthite (An) and orthoclase (Or) contents of the analysed feldspars were determined using a method described by Cawthorn (1974). They are plotted in the Ab-An-Or triangle in Figure 4.3 and are listed in Appendix 4.3.

Potassium-feldspar phase of the megacrysts and the matrix microclines in the granitoids and the gneisses have similar Ab-An-Or contents. These feldspars consist of more than 90 percent Or and 5 to 10 percent Ab. Some of the megacrysts analysed from the Newport Granite are zoned, due to a variation of K and Na contents (Figure 4.4). Plagioclase in the plutons is oligoclase except in the Wareham Quartz Monzonite where some of the plagioclase grains are andesines. Plagioclase inclusions in the megacrysts are similar in An content to the matrix plagioclases. Plagioclase in the gneiss is albite. Perthite lamellae in the megacrysts have more than 95 percent Ab.

In addition to the major elements, megacrysts and matrix microclines from the Newport Granite were also analysed for Ba and Sr. The results are shown in Figure 4.5 (Ba and Sr contents in potassium-feldspars from the other granitoids and the Hare Bay Gneiss were not determined). Neither Ba nor Sr vary systematically from core to rim of any of the feldspars. Most of the megacrysts analysed are richer in Ba than the groundmass microclines. The significance of this observation is discussed in the next section.

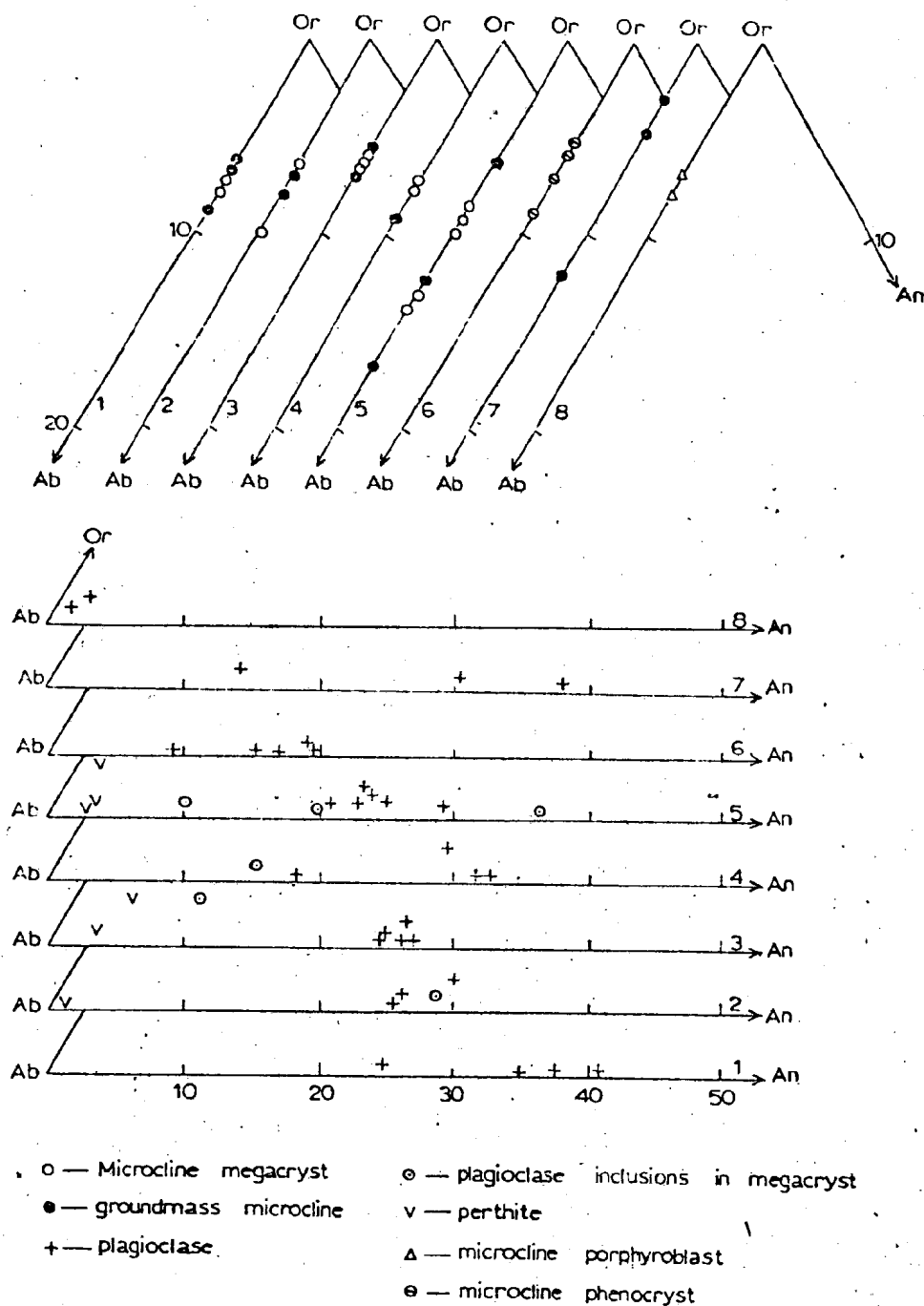


Fig. 4.3. Composition of feldspars from rock units in the area.  
 1. Wareham Quartz Monzonite, 2. Lockers Bay Granite, 3. Cape Freels Granite, 4. Deadman's Bay Granite, 5. Newport Granite, 6. North Pond Granite, 7. Big Round Pond Granite, 8. Hare Bay Gneiss adjacent to the Cape Freels Granite.



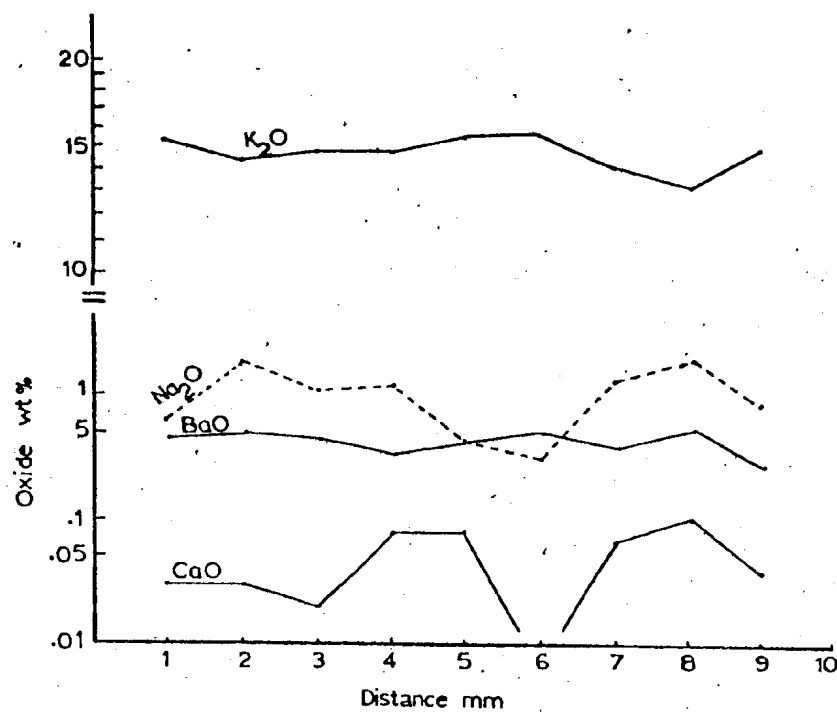


Fig. 4.4. Distribution of  $K_2O$ ,  $Na_2O$ ,  $BaO$  and  $CaO$  across a zoned microcline megacryst in the Newport Granite. Location - 205.

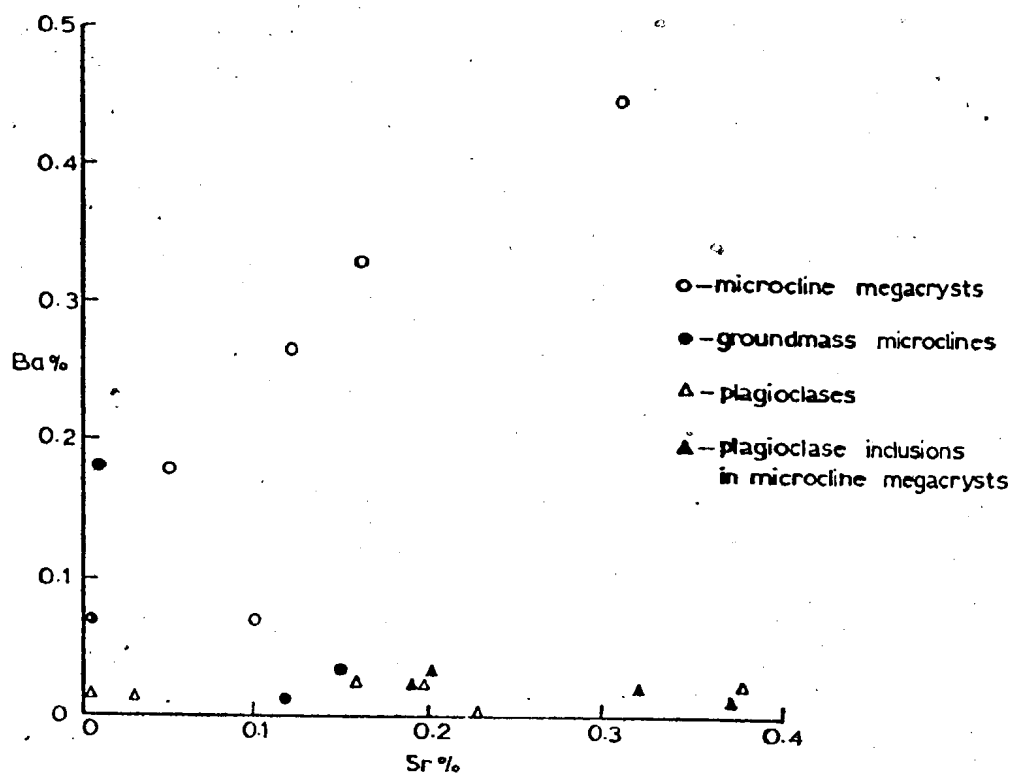


Fig. 4.5. Ba and Sr contents in feldspars from the Newport Granite.

#### 4.3. Origin of the Microcline Megacrysts

The microcline megacrysts in the plutons studied could have (1) crystallized from a magma; (2) grown metasomatically in a solid or near solid state; or (3) been produced by a combination of (1) and (2). Their widespread occurrence in a number of plutons of different ages and locations, plus the occurrence of microcline megacrysts overgrowing xenoliths and the boundaries of minor intrusions (Figures 4.6 and 4.7, see also page 107) as well as the gneisses suggest that they can hardly be xenocrysts.

Most of the textural evidence such as the zoning, inclusions of the matrix minerals, presence of plagioclase mantles and the clustering of the crystals are not unequivocal evidence for an origin for megacrysts either by crystallization from a magma or by metasomatic growth in a solid medium (Smith, 1974). Several authors have related the above features to metasomatic growth of potassium-feldspars (Booth, 1968; Dickson, 1968; Emmermann, 1969) while some others have attributed them to magmatic crystallization of potassium-feldspars (Hibbard, 1965; Smithson, 1965; Vance, 1969; see also discussion in Pitcher and Berger, 1972). However, some other features of the megacrysts are consistent with a magmatic origin for the latter.

The undeformed megacrysts define a fabric that may have a constant orientation in any one outcrop or a part of the plutons (see section 3.3. in the preceding chapter). The megacrysts in the marginal part of the Deadman's Bay Granite define an alignment parallel to the contact. These alignments are most likely to have been produced during the emplacement of the plutons.



Fig. 4.6. Microcline megacrysts (M) overgrowing a gneissic xenolith (G) in the Deadman's Bay Granite. Windmill Bight.



Fig. 4.7. Microcline megacrysts overgrowing a granitic minor intrusion in the Cape Freels Granite. Location - 86.

The plagioclase, biotite and quartz inclusions in the microcline megacrysts are smaller than the identical phases in the groundmass. Therefore these may have included at an early stage of their growth, whereas identical groundmass phases continued to grow.

Taylor et al. (1960) demonstrated that during the crystallization of a magma the early-formed potassium feldspars tend to be richer in Ba than the younger ones (see also Kerrick, 1969). The megacrysts in the Newport Granite tend to be richer in Ba than the groundmass microclines (page 154). Therefore the megacrysts in this pluton may have crystallized before the groundmass microclines. The fluctuation of the Ba content within the megacrysts and the matrix microclines were probably caused by changes in temperature and  $P_{H_2O}$  conditions which influence the diffusion coefficient of atoms in magmas to a large extent (Burnham, 1979).

The microcline megacrysts in the xenoliths and the Hare Bay Gneiss as well as those overgrowing the boundaries of the minor intrusions clearly grow in a solid medium. This indicates that there is a metasomatic component to the megacrysts. However, arguments in the preceding paragraphs indicate that most of the megacrysts have a magmatic origin. Their size may be a function of rates of nucleation and growth. Swanson (1977) estimated the nucleation density and growth rate of quartz, alkali feldspar and plagioclase in synthetic granite and granodiorite compositions of Whitney (1975). Whitney

studied the effects of pressure, temperature and  $H_2O$  content on the phase relations of these compositions. The  $SiO_2$ ,  $Al_2O_3$ ,  $CaO$ ,  $Na_2O$  and  $K_2O$  contents of the granitic composition studied by Whitney match those of the granitoids in the present study area. Thus, Swanson's (1977) results can be used directly to investigate the nucleation density and growth rate of quartz, microcline and plagioclase in these granitoids.

Figure 4.8 compiled from Swanson (1977) shows the nucleation density and rate of growth of quartz, alkali feldspar and plagioclase in the synthetic granite composition (Whitney, 1975) between  $400^{\circ}C$  and  $1000^{\circ}C$  at 8 kb. Based on reconnaissance studies at 2 kb, Swanson predicted that the form of the curves relating the nucleation density and growth rate with temperature will not be affected significantly by changes in pressure, though the absolute values may change noticeably.

Attempts to determine the temperature of crystallization of the feldspars in the granitoids using Whitney and Stormers' (1977) two-feldspar geothermometer were unsuccessful. These authors calculated the distribution curves for albite in potassium feldspars and plagioclases equilibrated at different temperatures based on thermodynamic data, which consider the effects of pressure and "non-ideal" behaviour in

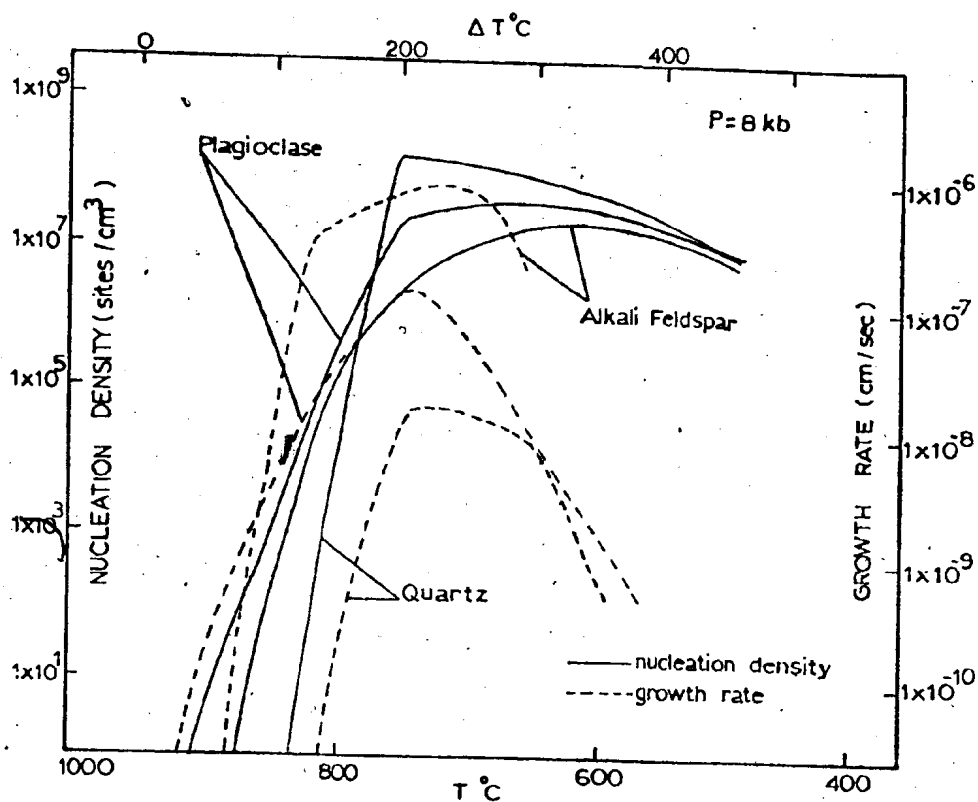


Fig. 4.8. Nucleation density and rate of growth of plagioclase, alkali feldspar and quartz in a synthetic granite composition (compiled from Swanson, 1977).

alkali feldspar on albite distribution. Only the potassium feldspars with structural states of sanidine - high albite series and microcline-low albite series have been used in the calculations, owing to the lack of sufficient thermodynamic data for potassium feldspars with intermediate structural states.

Figure 4.9 shows the molecular percentage of albite in coexisting microcline megacrysts, matrix microclines and plagioclases in the granitoids. Also shown in Figure 4.9 are the distribution curves from Whitney and Stormer (1977) showing albite contents in coexisting potassium feldspars and plagioclases for different temperatures of crystallization. The temperature of crystallization of potassium feldspars and plagioclases in the granitoids may be estimated by comparing their albite contents with the above distribution curves, taking into account the structural state of the potassium feldspars. The temperatures estimated for the crystallization of coexisting feldspars in the granitoids, by this method, range between 400 and 600°C. These temperatures are lower than those of the granite solidus (Wyllie, 1977) and thus do not represent the temperatures at which these feldspars crystallized, but they indicate that albite has been lost from the potassium feldspars as suggested by the widespread perthitic texture in the potassium feldspars of the granitoids, although care was taken to use only the feldspars that do not show perthites in this exercise.

However, there is evidence indicating that the granitoids in the area crystallized at temperatures between approximately 650°C and 850°C (see Chapter 7 for a detailed discussion). In the temperature



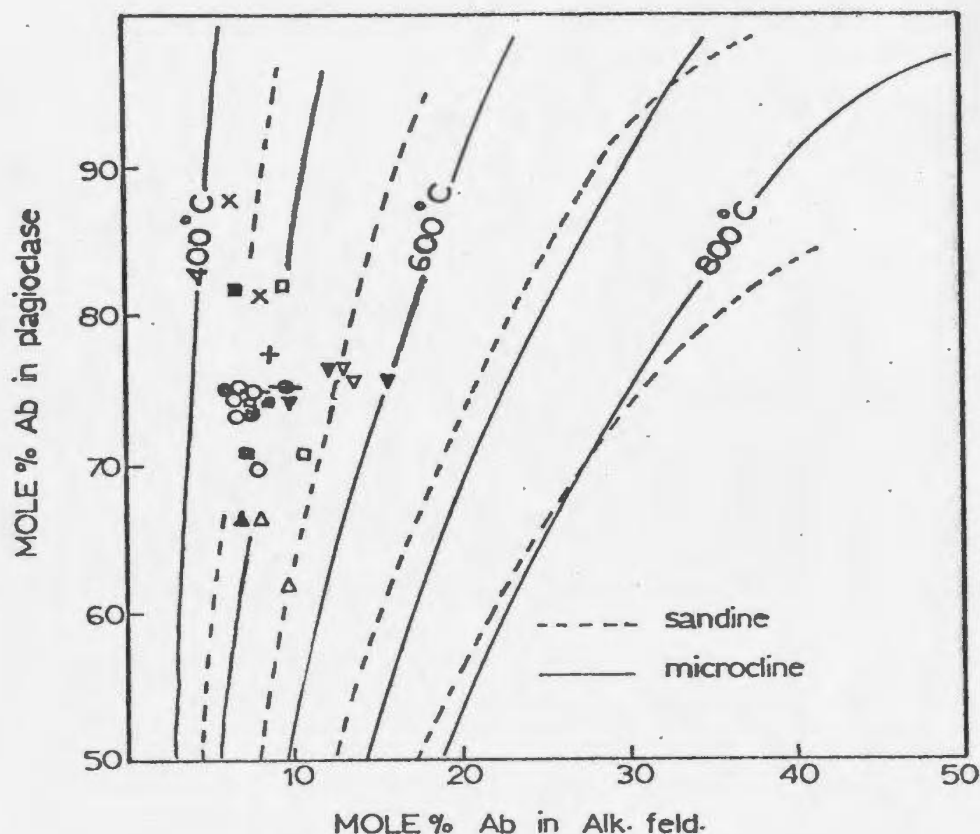


Fig. 4.9. Albite (Ab) content of plagioclase feldspars in the plutons plotted against that of coexisting potassium feldspars. Also shown are distribution curves for Ab in potassium feldspars and plagioclases equilibrated at different temperatures (after Whitney, 1977). Open symbols denote coexisting microcline megacryst-plagioclase pairs and closed symbols denote coexisting groundmass microcline-plagioclase pairs. Triangles - Wareham Quartz Monzonite, Squares - Lockers Bay Granite, Circles - Cape Freels Granite, Circles with horizontal bars - Deadman's Bay Granite, Inverted triangles - Newport Granite, Crosses - North Pond Granite, Plus signs - Big Round Pond Granite.

interval between 675°C and 850°C, the rate of growth of potassium feldspar exceeds the rate of nucleation, resulting in large potassium feldspar crystals (megacrysts). Below 675°C, the rate of nucleation of potassium feldspar is greater than the rate of growth and thus a large number of small potassium feldspar grains will be produced. Between 810°C and 850°C the rate of growth of plagioclase is greater than the rate of nucleation, but below 810°C the reverse is true. Thus with progressive decrease in temperature, initially a small number of large plagioclase crystals will form followed by a large number of smaller crystals. However, the large feldspar crystals will continue to grow until all the liquid is used. In the case of quartz, the rate of nucleation exceeds the rate of growth throughout the temperature interval between 650°C and 850°C resulting in a large number of small quartz crystals. The megacrystic granitoids in the area are characterized by a large number of microcline megacrysts (make up to approximately 50 percent by volume in most of the plutons), a few plagioclase megacrysts and a large number of smaller (< 2 cm) microcline, plagioclase and quartz grains. This microstructure could have resulted if the magmas of the granitoids were maintained at temperatures higher than 675°C for a sufficient time to crystallize a large number of potassium feldspar megacrysts. However, if the magmas were cooled rapidly to temperatures below 675°C, for example by rapid upward movement, a large number of megacrysts would not have formed. Also if a granitic magma was generated at a temperature close to 675°C, for example around 725 to 700°C, either by fractional crystallization of a "parent" magma or by partial melting of source rocks, it is unlikely for it to result in a megacrystic pluton because to produce

megacrysts it will have to be maintained in a small temperature interval ( $\approx 50$  to  $25^{\circ}\text{C}$ ) for a long time. Thus the origin of the megacrysts in the granitoids in the study area appears to be largely a function of rates of nucleation and growth of potassium feldspar and rate of cooling of the parent magmas of the plutons.

#### 4.4. Summary

Microcline megacrysts are the most striking feature in the majority of the plutons in the area, constituting up to 50 percent by volume in some of these bodies. Porphyroblastic microcline megacrysts occur in places in gneisses adjacent to some of the megacrystic plutons. But the distribution, chemistry and the alignments defined by undeformed crystals suggest a magmatic origin for the megacrysts. The origin of the magmatic megacrysts appears to be a function of rates of nucleation and growth of potassium feldspars and crystallization history of the plutons.

## CHAPTER 5

### THE DIABASE DIKES

Diabase dikes are common in the eastern half of the thesis area. Their locations are shown in the geological map in the back. They post-date all the granitic intrusions in the area except the Newport and the Big Round Pond plutons which truncate and contain xenoliths of the dikes. These dikes, representing an episode of basic magmatism breaking a longer episode of granite emplacement, are special and were investigated in detail (Jayasinghe, 1978b). This chapter is taken mostly from this paper, with minor modifications.

The dikes have a general north-south strike (Figure 5.1) and dip either vertically or steeply. The thickness ranges from less than a metre to approximately ten metres. In most cases, the dikes could not be traced for more than several metres along their length because of lack of continuous exposure. Commonly, the irregularities in the dike walls fit together along lines perpendicular to the dike attitudes, indicating simple dilation of fractures without any shear motion during the dike intrusion<sup>1</sup>. At places the dikes occur as multiple intrusions. Chilled margins are common. The central parts of most of the dikes carry 2 to 4 cm long plagioclase phenocrysts roughly

---

<sup>1</sup>The diabase dikes cross-cut the foliations in the host rocks. The angle between the strikes of the dikes and the foliation ranges from 10 to 20°. Since the dikes are dilational,  $\sigma_3$  at the time of intrusion of the dikes was probably oriented at right angles to the dikes and  $\sigma_1$  and  $\sigma_2$  were probably located in the planes of the dikes.

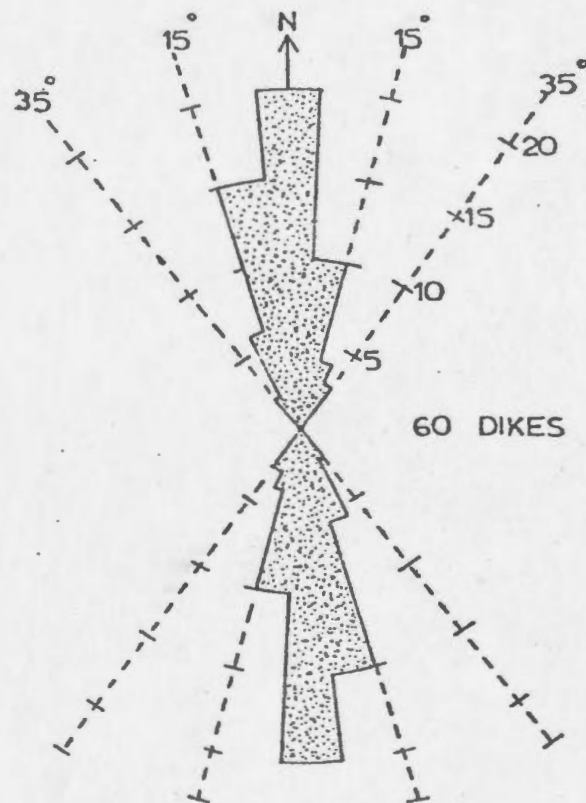


Fig. 5.1. Rose diagram showing dominant trend of the diabase dikes.

aligned with their long axis parallel to the length of the dikes (Figure 5.2). Some of the dikes have a knobby weathering due to the presence of plagioclase-rich knots.

The dikes post-date one of the post-tectonic granites, the Deadman's Bay Granite, in the area and do not show any sign of being deformed themselves.

#### 5.1. Petrography

The principal primary minerals in the dikes are augite and plagioclase. They exhibit a good subophitic texture. Titanomagnetite occurs as an accessory.

The augite shows weak purplish-brown to pale greenish-brown pleochroism. Commonly, the augite grains are altered at the margins and along cleavages to a bluish-green needle-like amphibole. Where the original grains are completely altered these needles occur in several clusters each with a radial pattern. Some of the fully altered grains have shapes of olivine crystals, but no fresh olivines were found in any of the thirty thin sections examined.

The plagioclases are slightly altered to sericite. The phenocrysts are more altered than the groundmass plagioclases. Their compositions range from  $An_{45}$  to  $An_{60}$  and  $An_{42}$  to  $An_{52}$ , respectively. A few flakes of secondary biotite occur associated with the pyroxenes and the opaques.

Within about 200 metres of the Newport Granite and the Big Round Pond Granite, augite is absent in the dikes. The amphibole,



Fig. 5.2. A diabase dike in the Deadman's Bay pluton. Note the central zone of plagioclase phenocrysts. Windmill Bight.

although still showing the same colours, is lath-shaped and has typical amphibole cross-sections, and the plagioclases are more altered. Biotite is abundant. Similar changes were observed in the dike xenoliths in these granites.

## 5.2. Chemistry

Fifteen diabase dikes were analysed for major, minor and trace elements using atomic absorption and X-ray fluorescence techniques. The results together with the CIPW norms are given in Table 5.1. Despite the high  $H_2O$  contents the  $Fe_2O_3$  and the  $FeO/Fe_2O_3$  ratios suggest that the major element chemistry of the dikes is not much affected by secondary alteration processes (Coombs, 1963). Except for the numbers 14 and 15, which are nepheline normative, all the other analyses are hypersthene normative. These two samples were taken adjacent to the Newport Granite, and their original compositions may have changed as a result of metasomatism related to granite intrusion.

In the plots of alkali versus silica (MacDonald and Katsura, 1964) and potash versus silica (Engel *et al.*, 1965), all the analyses fall in the alkali basalt field (Figure 5.3). In the  $TiO_2-K_2O-P_2O_5$  triangle (Pearce *et al.*, 1975), they plot in the continental basalt field (Figure 5.4). These diagrams indicate that the dikes consist of continental alkalic basalt.

When plotted in the (Ti/100)-Y-Zr diagram of Pearce and Cann (1973) all the dikes fall in the 'within-plate basalt' field (Figure 5.5). According to these authors within-plate alkalic basalts (both ocean



Table 5.1. Major and trace element contents and the CIPW norms of the diabase dikes.

	1	2	3	4	5	6	7	8	9	10	11	12	13	14	15
SiO <sub>2</sub> (wt.%)	44.8	44.1	44.8	46.3	46.2	46.0	45.0	47.1	49.2	47.6	46.0	45.8	51.0	44.7	46.8
TiO <sub>2</sub>	1.76	2.62	2.40	2.36	2.16	1.84	2.40	2.50	1.84	1.99	2.52	1.84	1.91	2.54	2.52
Al <sub>2</sub> O <sub>3</sub>	15.4	15.9	15.9	16.2	16.2	16.2	16.6	16.2	16.2	16.6	15.9	17.3	16.2	16.2	15.5
Fe <sub>2</sub> O <sub>3</sub>	3.68	4.13	4.25	3.36	4.03	3.17	3.69	3.96	2.84	2.30	3.64	4.30	2.39	2.90	4.12
FeO	8.22	9.63	9.14	9.10	8.37	8.47	9.40	9.28	8.34	9.15	10.28	8.08	8.34	10.58	8.01
MnO	0.18	0.20	0.20	0.18	0.18	0.18	0.21	0.19	0.17	0.22	0.21	0.19	0.16	0.20	0.22
MgO	8.28	6.38	6.06	5.32	6.34	7.80	6.60	5.20	5.88	5.43	5.42	6.56	5.15	5.92	5.24
CaO	9.62	7.58	6.10	7.64	8.02	9.54	8.66	7.56	7.58	7.20	7.46	8.18	6.83	7.04	9.98
Na <sub>2</sub> O	2.26	3.01	3.06	3.26	3.03	2.60	2.92	3.46	3.34	3.20	3.47	2.47	3.52	2.44	4.00
K <sub>2</sub> O	1.26	1.17	2.05	1.40	1.40	0.83	0.66	1.23	1.34	1.47	1.14	1.65	1.81	2.88	0.80
P <sub>2</sub> O <sub>5</sub>	0.26	0.36	0.40	0.54	0.34	0.42	0.44	0.74	0.30	0.74	0.56	0.44	0.52	0.50	0.50
H <sub>2</sub> O	3.90	3.11	4.26	2.97	2.81	2.40	2.69	2.19	2.21	2.62	2.55	2.26	1.84	2.72	1.88
Total	99.62	98.29	98.62	98.63	99.14	99.83	99.27	99.61	99.24	99.49	99.15	99.07	99.67	98.62	99.57
Ba (ppm)	216	210	227	273	212	155	143	274	261	284	184	214	296	369	245
Ce	36	55	69	78	53	75	58	90	56	64	62	50	64	63	137
Cr	178	16	16	28	33	126	12	4	32	13	12	14	11	9	34
Ga	17	19	22	20	21	17	18	19	19	21	22	19	20	18	21
La	21	33	47	43	34	27	38	49	39	37	42	29	37	34	47
Nb	6	12	12	13	12	6	12	14	10	10	13	10	11	11	16
Ni	199	111	114	77	116	175	102	46	88	92	56	97	79	81	54
Pb	6	6	6	7	7	6	7	7	8	8	6	7	8	7	7
Rb	92	55	195	58	42	17	34	34	41	92	38	68	48	197	25
Sr	327	452	395	470	446	427	502	531	444	491	423	494	450	366	483
V	229	238	236	252	219	213	248	219	209	218	225	217	196	246	274
Y	27	25	39	26	23	19	23	25	23	28	24	25	24	39	26
Zn	103	100	132	117	117	102	111	124	117	121	121	112	109	116	108
Zr	159	198	207	217	194	175	200	220	213	203	207	192	224	190	244
Q (wt.%)	0.0	0.0	0.0	0.0	0.0	0.0	0.0	0.0	0.0	0.0	0.0	0.0	0.0	0.0	0.0
Or	7.78	7.27	12.84	8.65	8.59	5.05	4.04	7.46	8.16	8.88	6.97	10.07	10.93	17.75	4.84
Ab	19.98	26.79	27.44	28.83	26.63	22.67	25.58	30.05	29.13	28.24	30.39	21.59	30.44	19.54	29.02
An	29.41	27.78	25.00	26.59	27.49	30.99	31.31	25.70	26.03	27.82	25.30	32.27	23.57	25.80	22.49
Ne	0.0	0.0	0.0	0.0	0.0	0.0	0.0	0.0	0.0	0.0	0.0	0.0	0.0	1.08	3.05
Di { Wo	7.80	3.89	1.80	3.92	4.82	6.25	4.27	3.29	4.48	1.85	3.87	2.80	3.18	3.02	10.39
En	5.00	2.25	1.05	2.12	2.93	3.86	2.47	1.79	2.53	0.95	1.99	1.73	1.70	1.55	6.23
Fs	2.30	1.46	0.67	1.66	1.63	2.03	1.60	1.38	1.77	0.85	1.78	0.91	1.39	1.39	3.61
Hy { En	1.41	1.71	2.19	3.85	3.53	4.56	4.37	6.07	8.19	7.87	2.47	6.58	10.52	0.0	0.0
Fs	0.65	1.11	1.40	3.01	1.97	2.40	2.83	4.69	5.73	7.00	2.22	3.47	8.60	0.0	0.0
Ol { Fo	10.61	8.93	8.94	5.52	6.97	8.13	7.13	3.80	3.06	3.70	6.67	6.00	0.63	9.68	4.99
Fa	5.38	6.39	6.32	4.76	4.28	4.72	5.09	3.23	2.36	3.62	6.59	3.48	0.57	9.56	3.18
Mt	5.57	6.30	6.53	5.09	6.07	4.74	5.54	5.89	4.24	3.48	5.46	6.44	3.54	4.38	6.11
Il	3.49	5.23	4.83	4.68	4.26	3.60	4.72	4.87	3.60	3.94	4.95	3.61	3.71	5.03	4.90
Ap	0.63	0.88	0.99	1.31	0.82	1.01	1.06	1.76	0.72	1.79	1.35	1.06	1.24	1.21	1.19

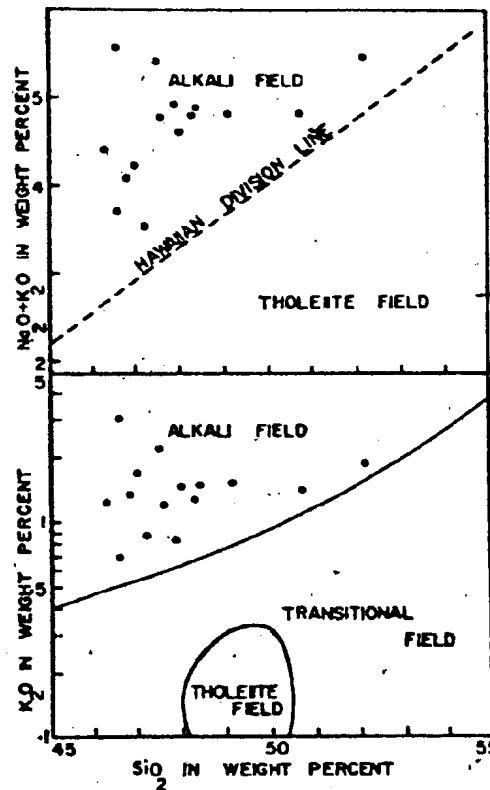


Fig. 5.3. Plots of (A) alkali versus silica, field boundaries from MacDonald and Katsura (1964), and (B) potash versus silica, field boundaries from Engel *et al.* (1965), of the diabase dikes.

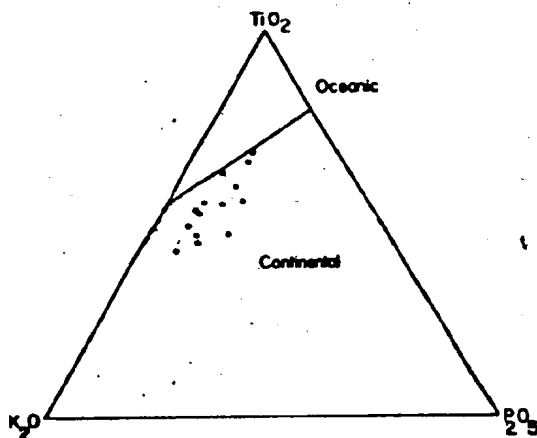
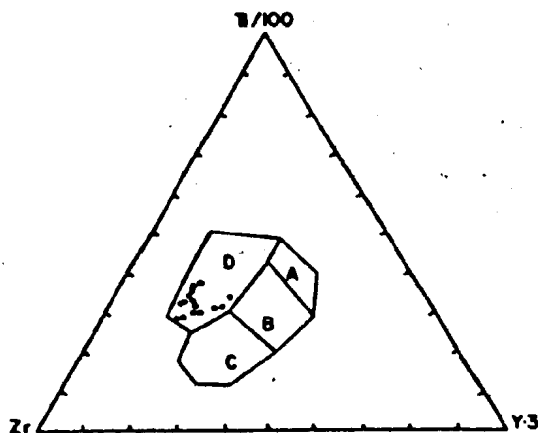


Fig. 5.4. Plot of the dikes in  $\text{TiO}_2$ - $\text{K}_2\text{O}$ - $\text{P}_2\text{O}_5$  diagram. Diagram from Pearce et al. (1975).



Plot 5.5. Plot of the dikes in the  $(\text{Ti}/100)$ - $\text{Y} \times 3$  -  $\text{Zr}$  triangle. Within plate basalts plot in field D. Diagram from Pearce and Cann (1973).

island and continental) are characterized by a Nb/Y ratio of less than 1. The diabase dikes discussed here have Nb/Y ratios greater than 2.

Thus the earlier classification of the dikes based on the major elements contradicts that based on the immobile trace elements.

To resolve this problem, pyroxenes from two of the dikes were analysed. Several authors have successfully related the composition of pyroxenes to the nature of their host rocks (Kushiro, 1960; Le Bas, 1962; Coombs, 1963). Twenty-three pyroxenes were analysed using a JEOL JXA-50A electron microprobe. Measurements were made at the rim, core and in between, and averaged for each grain (Table 5.2). Only analyses with totals between 98.5 and 101.5 were taken. No systematic difference in chemistry was seen between the rims and the cores of the individual grains. Figures 5.6 and 5.7 show plots  $\text{SiO}_2$  versus  $\text{Al}_2\text{O}_3$  and proportion of the z position filled by Al atoms ( $\text{Al}_2$ ) versus  $\text{TiO}_2$  of the pyroxenes. These diagrams indicate that the host rocks to the pyroxenes are alkalic basalts. This agrees with the conclusion drawn from the major and minor element contents of the dikes. Therefore, the Nb/Y ratios of the dikes are less diagnostic.

### 5.3. Origin and Tectonic Implication

It is difficult to establish a precise model for the origin of the alkalic basalts represented by the diabase dikes in the area from the available data. Alkalic basalt dikes are generally attributed to processes at mantle depths (Carmichael, Turner and Verhoogen, 1974). Based on higher contents of K, Rb, Ba and Sr in tholeiitic basalts

Table 5.2. Analyses of the pyroxenes from the diabase dikes, numbered 1 and 2 in Table 5.1.

	1	2	3	4	5	6	7	8	9	10	11	12
SiO <sub>2</sub>	48.80	49.01	47.24	47.91	48.74	48.53	49.54	49.31	48.84	47.06	48.25	47.63
TiO <sub>2</sub>	1.74	1.95	2.16	1.99	1.79	0.69	1.29	1.42	1.63	2.16	1.78	2.20
Al <sub>2</sub> O <sub>3</sub>	3.18	4.41	4.34	4.26	3.70	3.88	1.96	2.71	3.26	5.32	3.34	4.52
FeO <sub>total</sub>	9.92	9.18	9.96	9.34	9.28	9.09	10.38	9.15	9.93	9.70	11.42	10.05
MnO	0.23	0.17	0.22	0.23	0.25	0.23	0.32	0.24	0.21	0.32	0.29	0.26
MgO	14.11	13.88	13.53	13.86	14.09	14.04	14.28	14.61	13.35	13.53	12.93	13.34
CuO	21.43	20.59	20.55	20.78	21.05	20.97	21.03	20.89	20.91	20.79	20.01	20.74
Na <sub>2</sub> O	0.82	0.61	0.79	0.73	0.69	0.66	0.57	0.61	0.69	0.65	0.75	0.67
K <sub>2</sub> O	0.00	0.00	0.00	0.00	0.00	0.00	0.00	0.00	0.00	0.00	0.00	0.00
Total	100.23	99.81	98.79	99.10	99.59	98.09	99.37	98.94	98.82	99.53	98.77	99.41

	13	14	15	16	17	18	19	20	21	22	23
SiO <sub>2</sub>	48.66	48.82	49.25	48.89	47.65	49.55	49.73	48.14	47.06	49.12	48.04
TiO <sub>2</sub>	1.81	1.68	1.60	1.95	2.29	1.67	1.68	2.30	2.65	1.18	2.33
Al <sub>2</sub> O <sub>3</sub>	3.93	3.46	3.56	4.49	5.53	4.01	4.06	5.67	6.25	4.73	5.50
FeO	9.20	8.91	8.91	8.47	9.18	8.62	8.83	8.71	9.13	8.63	8.78
MnO	0.23	0.17	0.21	0.19	0.19	0.21	0.22	0.20	0.18	0.16	0.20
MgO	13.59	14.24	14.13	14.06	13.37	14.05	13.93	13.36	12.94	13.81	13.25
CuO	21.19	20.98	20.65	20.78	20.49	20.91	21.20	21.13	20.80	20.93	20.68
Na <sub>2</sub> O	0.61	0.57	0.61	0.64	0.77	0.66	0.71	0.72	0.77	0.70	0.71
K <sub>2</sub> O	0.00	0.00	0.00	0.00	0.00	0.00	0.00	0.00	0.00	0.00	0.00
Total	99.22	98.83	98.92	99.47	99.47	99.68	100.36	100.23	99.78	99.89	99.49

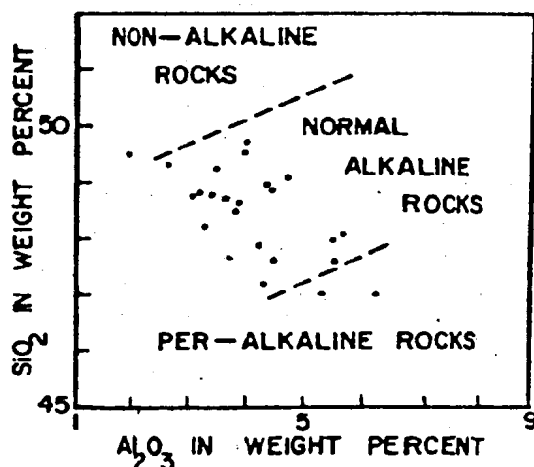


Fig. 5.6. Plot of silica versus alumina of the pyroxenes from the dikes. Field boundaries after Le Bas (1962).

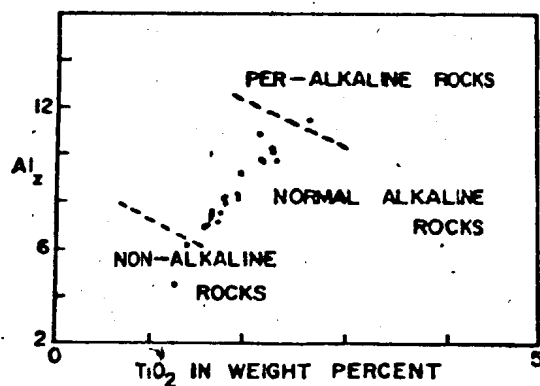


Fig. 5.7. Plot of  $Al_2$  versus  $TiO_2$  of the pyroxenes from the dikes. Field boundaries after Le Bas (1962). ( $Al_2$  = proportion of the 2 positions filled by Al atoms).

than in alkalic basalts, these authors argued that alkalic basalts cannot be produced by differentiation of tholeiitic basalts. Gast (1968) and Kay (1970) suggested that alkalic basalts could form by about 1 percent partial melting of garnet peridotite in the upper mantle and that partial melting in lesser degrees may produce potassic basalts. Gast concluded that in regions of extension the lithosphere may thin sufficiently to allow the formation of alkalic basalts by this mechanism. In fact, the extrusion and intrusion of alkaline rocks generally occur in zones of tension that mark the sites of continental rifting (Bailey, 1974; Scrutton, 1973).

The opening of the North Atlantic is considered to have occurred about 180 Ma ago (Ewing et al., 1970; Le Pichon and Fox, 1971; Dalrymple et al., 1975). In eastern North America peak magmatic activity related to this event occurred in early Mesozoic time (180-200 Ma, Armstrong and Besancon, 1970). The alkalic basalt dikes in the present study area were intruded between 330 and 320 Ma ago (page 142). These dikes thus mark a localized tensional event in the Carboniferous which could be an early sign of the major continental breakup that occurred later. In fact, alkalic basalt magmatism of similar age in Britain (MacDonald, 1975) marks the beginning of the opening of the northern North Atlantic (Russell, 1976).

## CHAPTER 6

### GEOCHEMISTRY OF THE GRANITOIDS: A MAGMATIC ORIGIN

The geochemistry of the granitic plutons in the thesis area was studied in order (1) to investigate the similarities and the differences between the compositions of the plutons, and (2) to gather evidence on their origin. Seventy samples were analysed for major and minor element oxides and Rb, Ba, Sr, Pb, Zr, Nb, Y, Ni, V, Cr, Cu, Zn and Ga. In addition to the above, eight analyses (major and minor element oxides and Rb, Sr, Ba, Zr, Cu and Zn) for the Cape Freels Granite were taken from Strong *et al.* (1974). Furthermore, composition of biotite in the Wareham Quartz Monzonite were also determined. The individual analyses are listed in Appendix 6.1 together with a description of the sample preparation, analytical techniques used and the precision and accuracy of the results.

#### 6.1. Major and Minor Element Oxides and Trace Elements

The average compositions of the plutons are given in Table 6.1. The major and minor element oxides and the trace element contents of the plutons are plotted against the Differentiation Index (Thornton and Tuttle, 1960) in Figures 6.1 and 6.2.

$\text{SiO}_2$  increases and  $\text{TiO}_2$ , FeO, MgO and V decrease along regular trends with increasing Differentiation Index (D.I.) in all the plutons except the Business Cove Granite.  $\text{Al}_2\text{O}_3$  and CaO show a systematic decrease with increasing D.I. in the Wareham, North Pond, Lockers Bay, Newport and the Big Round Pond plutons. MnO decreases along a regular trend with increasing D.I. in all the plutons excluding the Cape Freels



TABLE 6.1 - Average compositions of the granitoids.

	(1)	(2)	(3)	(4)	(5)	(6)	(7)	(8)	(9)	(10)	(11)	(12)
wt. %	61.37	4.32	70.32	1.61	71.76	1.62	67.41	2.00	70.15	3.61	69.36	2.28
SiO <sub>2</sub>	0.84	0.24	0.39	0.11	0.27	0.09	0.24	0.08	0.53	0.19	-0.48	0.19
TiO <sub>2</sub>	14.16	1.21	15.05	0.36	14.60	0.36	14.80	0.80	15.35	0.65	14.50	0.99
Al <sub>2</sub> O <sub>3</sub>	1.19	0.40	0.57	0.24	0.22	0.16	0.29	0.21	0.68	0.15	0.80	0.71
Fe <sub>2</sub> O <sub>3</sub>	3.15	0.98	1.75	0.46	1.42	0.55	1.24	0.42	1.94	0.07	1.59	0.79
FeO	0.19	0.05	0.09	0.02	0.07	0.02	0.05	0.01	0.06	0.02	0.07	0.03
MnO	2.04	0.48	0.53	0.31	0.55	0.25	1.19	1.55	0.94	0.15	1.00	0.43
MgO	3.41	9.92	1.71	0.64	1.56	1.79	1.99	1.38	2.35	0.28	1.77	0.69
CaO	3.12	0.18	3.34	0.26	3.19	0.27	5.27	0.58	3.21	0.23	3.25	0.39
Na <sub>2</sub> O	4.40	0.46	4.23	0.64	4.94	0.81	5.48	-0.39	5.28	0.48	5.05	0.57
K <sub>2</sub> O	0.34	0.20	0.26	0.11	0.27	0.08	0.14	0.09	0.21	0.03	0.12	0.04
P <sub>2</sub> O <sub>5</sub>	1.42	0.45	1.22	0.23	1.16	0.30	0.99	0.14	0.87	0.15	0.97	0.29
L.I.	217	18	240	41	296	46	260	73	208	19	240	43
ppm	869	266	407	104	299	123	410	358	713	169	613	107
Ba	371	70	180	66	90	58	127	88	148	25	123	26
Sr	22	10	20	4	29	6	31	5	27	5	30	7
Pb	256	52	192	35	124	26	115	51	257	13	284	25
Zr	14	3	9	3	14	5	14	3	17	2	15	3
Y	45	14	29	4	40	11	46	10	50	8	37	8
Yb	23	12	12	4	7	1	3	3	10	2	9	3
Yt	110	37	47	23	23	13	22	8	67	11	49	7
V	30	15	5	4	11	6	13	1	23	9	14	2
Cr	19	9	12	4	11	4	6	1	15	2	6	6
Cu	80	18	73	9	81	4	46	6	54	3	55	19
Zn	21	1	19	1	21	7	20	2	21	2	21	2
Ga												

(1) Vashan Quartz Monzonite; (2) North Pond Granite (medium grained phase); (3) North Pond Granite (porphyritic phase); (4) Business Cove Granite; (5) Lockers Bay Granite; (6) Cape Fria Granite; (7) Deadman's Bay Granite; (8) Vampere Granite; (9) Big Round Pond Granite; (10) Average composition of granite (After Nockolds (1954) and Taylor (1967)); (11) Average composition of granodiorite (After Nockolds (1954) and Taylor (1967)); (12) Average composition of basalt (After Unson (1967) and Peint (1967)).

L.I. = Loss on Ignition.  
n = No. of analyses  
x̄ = mean  
s = standard deviation  
7, 6, 5, and 3 = No. of analyses used to calculate the mean when different from n.

and the Business Cove granites.  $P_2O_5$  shows a systematic decrease with increasing D.I. in the Deadman's Bay and the Newport granites and Zr shows a systematic decrease with increasing D.I. in the latter. Ba and Sr decrease along regular trends with increasing D.I. in the North Pond, Cape Freels, Lockers Bay and the Newport granites but show an irregular distribution in the case of the rest of the plutons.  $Fe_2O_3$ ,  $Na_2O$ ,  $K_2O$ , Rb, Pb, Nb, Y, Ni, Cr, Cu and Zn do not show regular trends in the variation diagrams for all the plutons.

The range in composition within any one pluton, indicated by the different D.I. values and the trends in variation diagrams, may have been produced by mixing of varying amounts of early formed crystals with residual melts. For example, in the Wareham Quartz Monzonite, samples with D.I. greater than 80 contain significantly less biotite and more feldspars and quartz than samples with lower D.I. values ( $< 80$ ). Probably a large proportion of feldspars and quartz in the samples with high D.I. crystallized from residual melts, whereas in low D.I. samples most of the biotite and feldspars may represent early formed crystals.

None of the major and minor element oxides and the trace elements show a systematic variation with increasing D.I. in the Business Cove Granite. This reflects the highly variable composition of this granite. The Business Cove Granite contains a far greater number of large xenoliths of the country rocks than any other pluton in the area (see page 95) and may have been extensively contaminated by the assimilation of the country rocks.

Fig. 6.1 (a to k): Major and minor element variation diagrams. Weight percent oxides versus Thornton-Tuttle Differentiation Index.

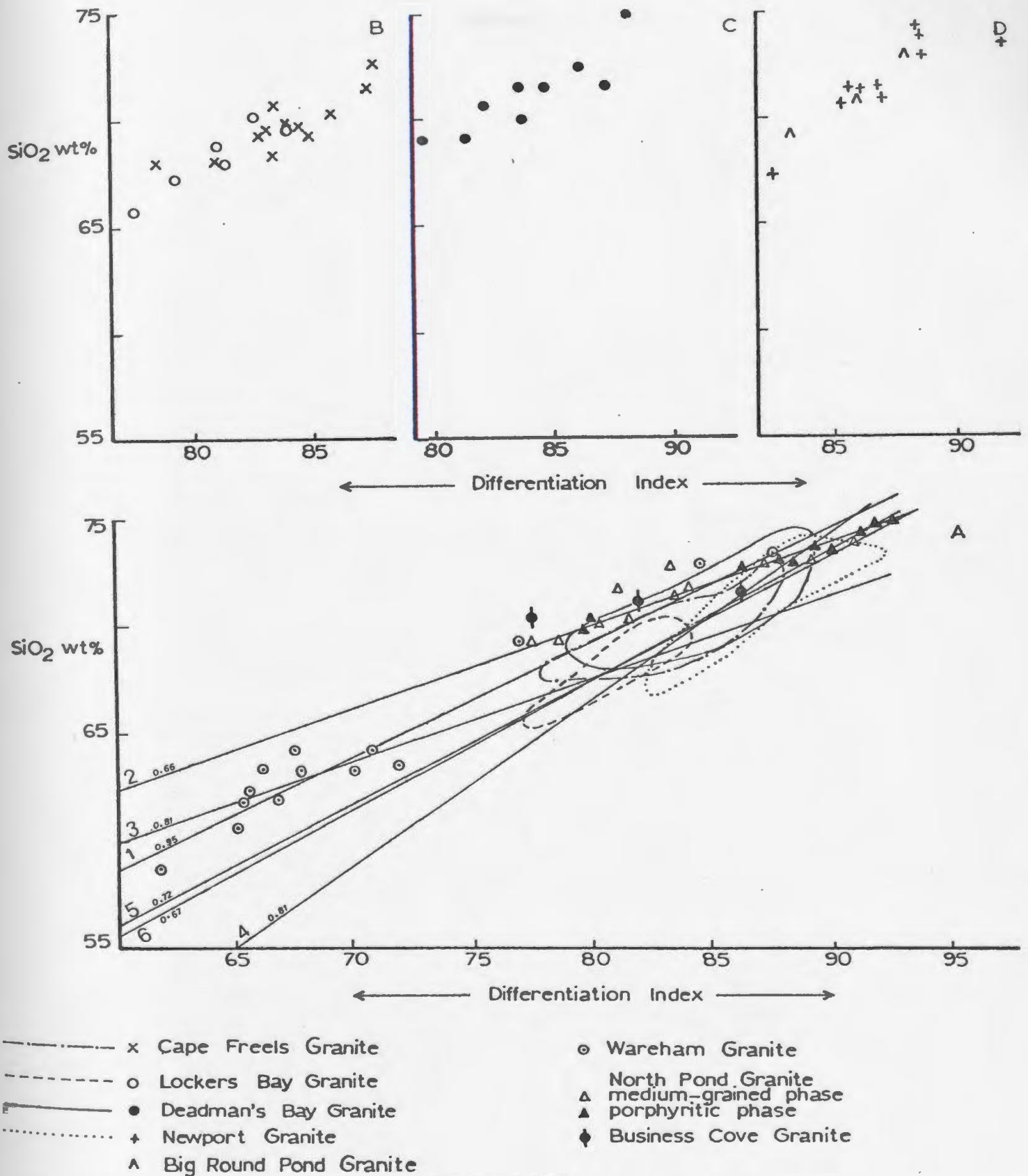
A - analyses from the Wareham, North Pond, and Business Cove plutons

B - analyses from the Lockers Bay and Cape Freels plutons

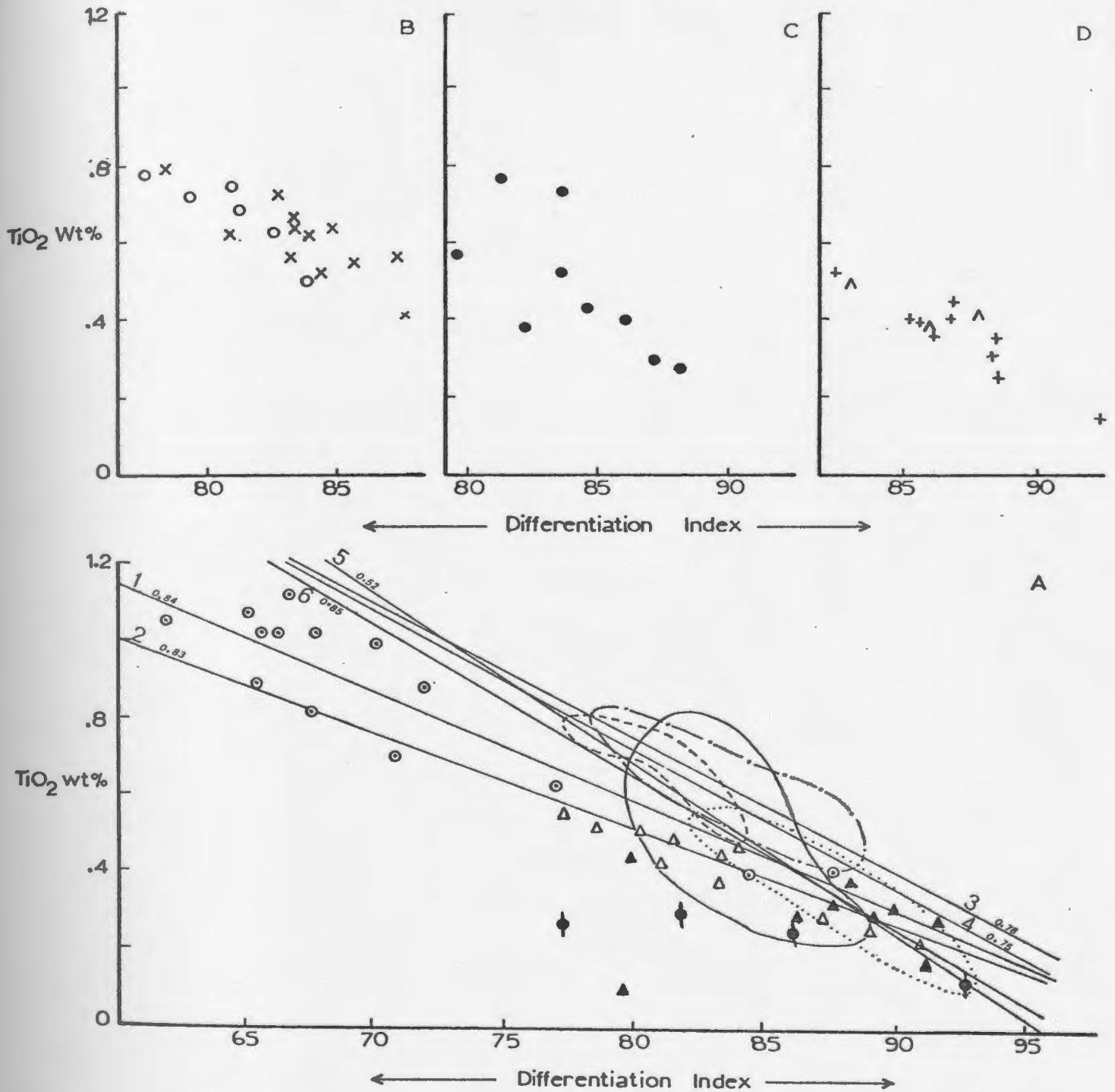
C - analyses from the Deadman's Bay pluton

D - analyses from the Newport and Big Round Pond plutons.

(Solid lines on  $\text{SiO}_2$ ,  $\text{TiO}_2$ ,  $\text{Al}_2\text{O}_3$ ,  $\text{FeO}$ ,  $\text{MgO}$  and  $\text{CaO}$  vs. D.I. plots represent linear regression lines. 1 - Wareham Quartz Monzonite, 2 - North Pond Granite, 3 - Cape Freels Granite, 4 - Lockers Bay Granite, 5 - Deadman's Bay Granite, 6 - Newport Granite. Small numbers along the lines are correlation coefficients. If all the points fit the line, the coefficient will be 1.)

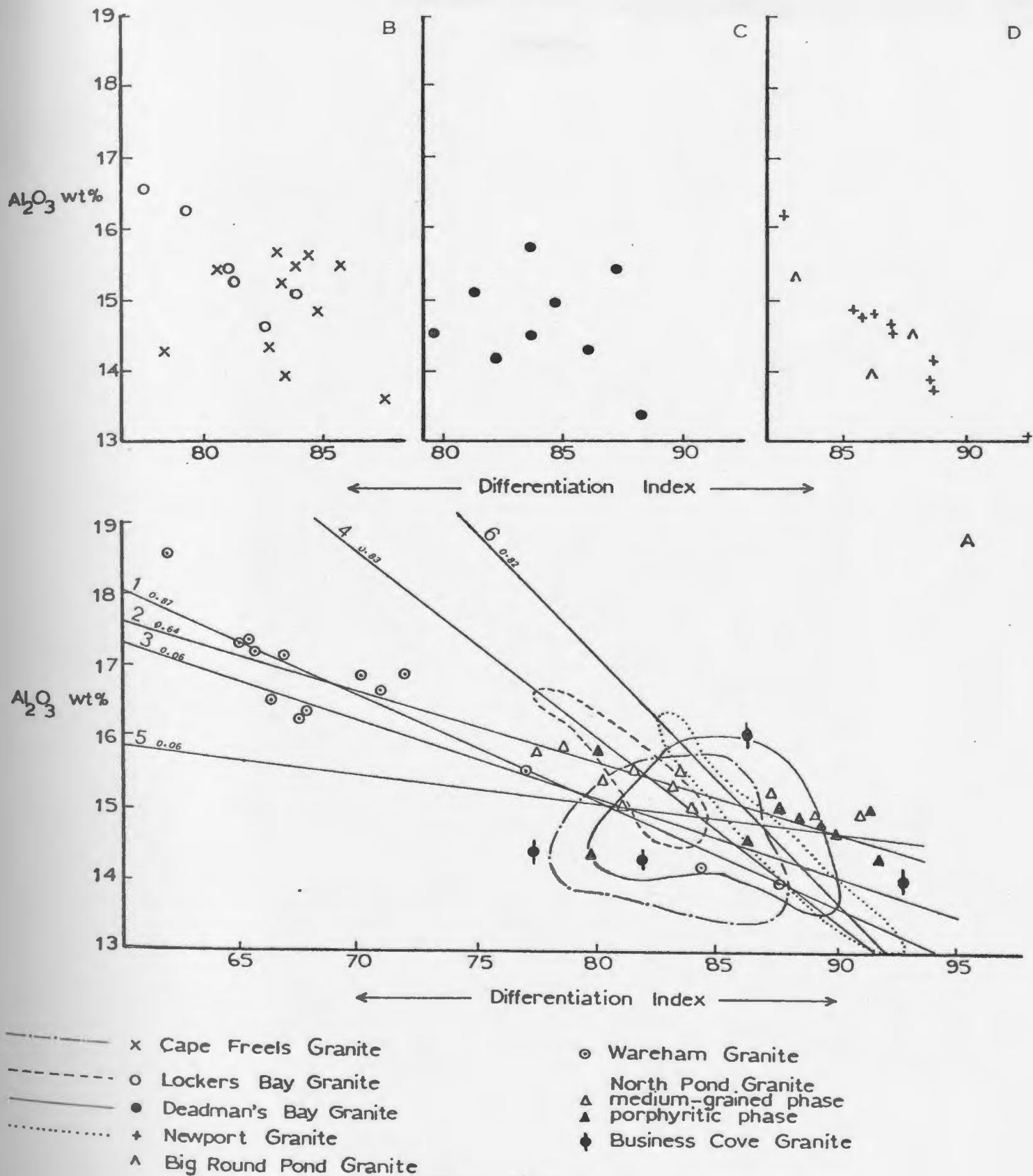


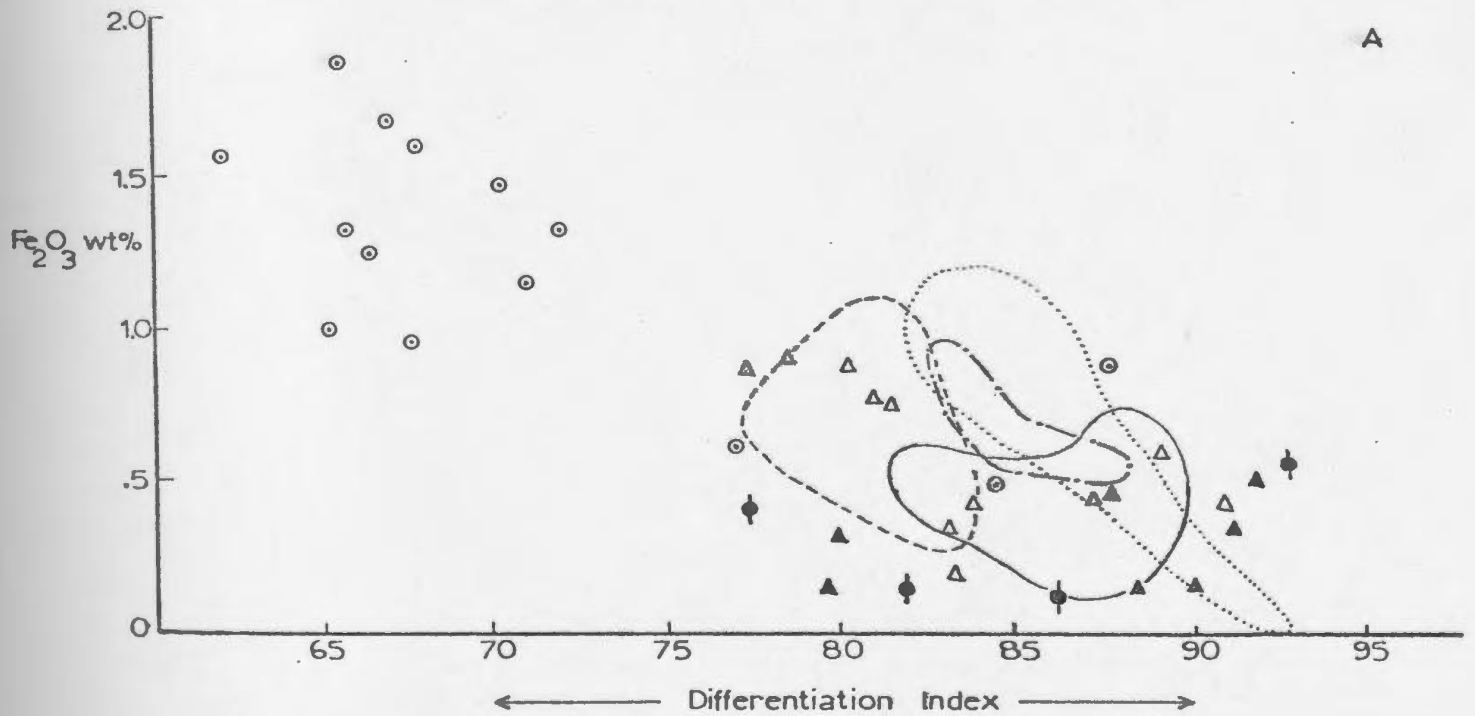
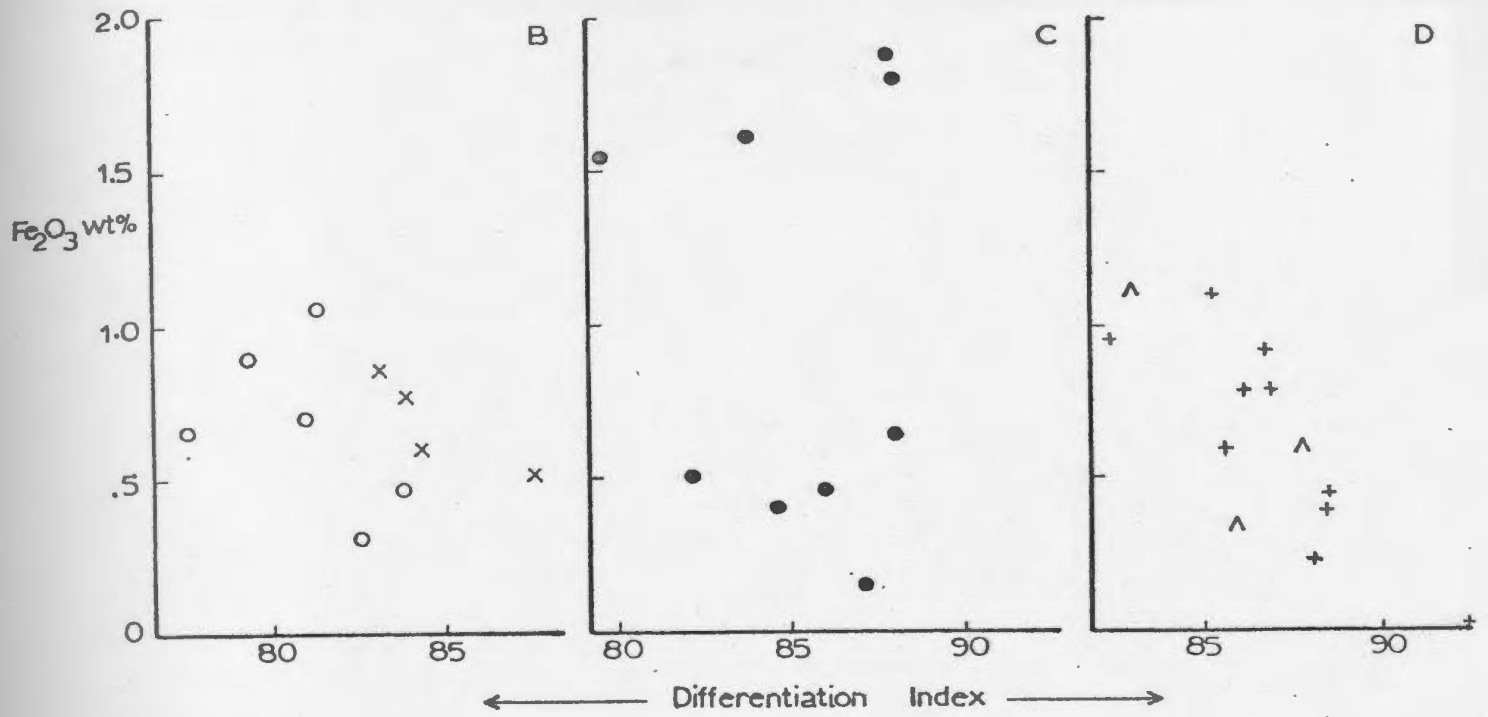
(Figure 6.1a)



- x Cape Freels Granite
- - - o Lockers Bay Granite
- • Deadman's Bay Granite
- - - + Newport Granite
- - - ^ Big Round Pond Granite
- o Wareham Granite
- Δ North Pond Granite
- ▲ medium-grained phase
- ▲ porphyritic phase
- ◆ Business Cove Granite

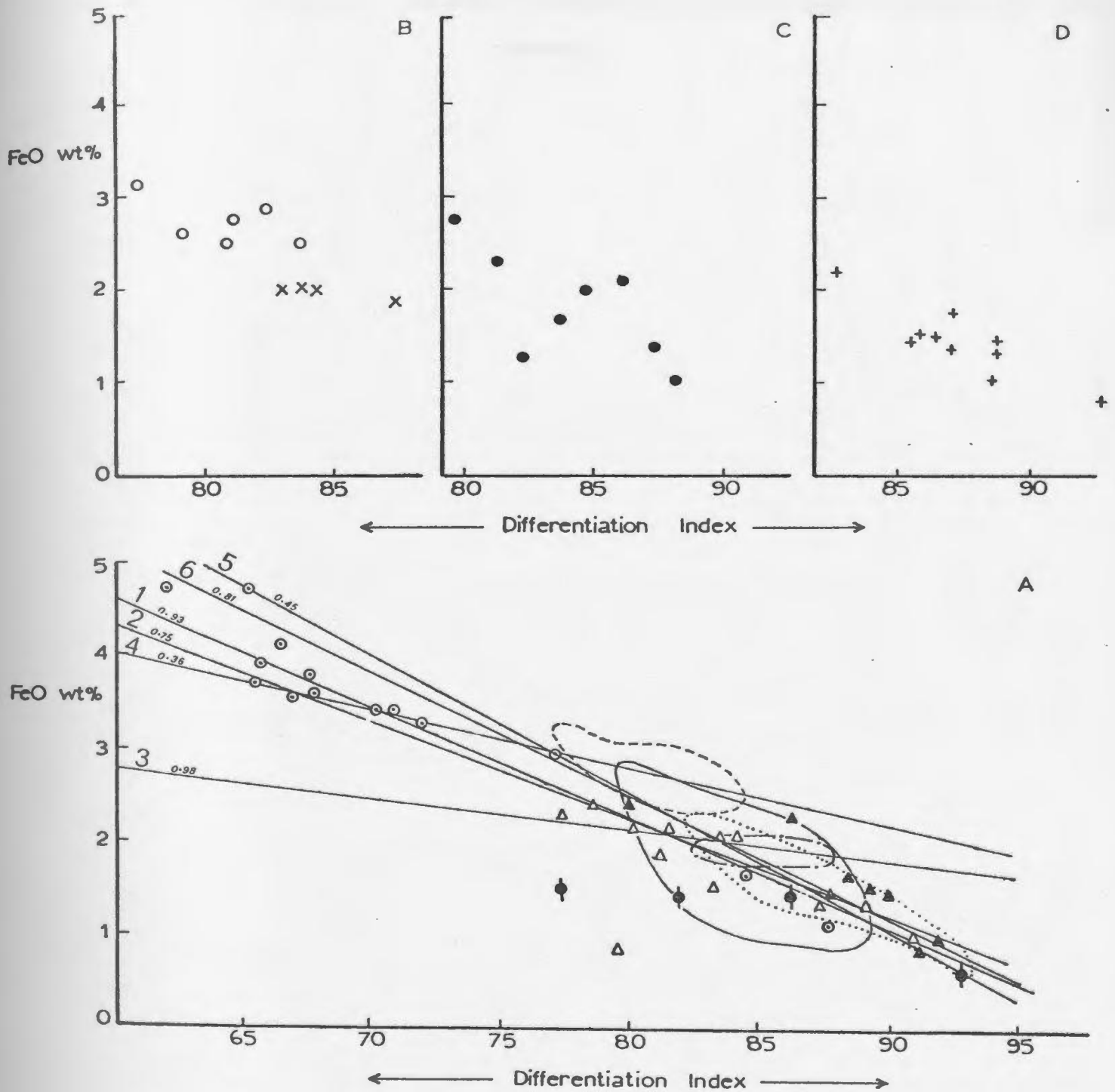
(Figure 6.1b)





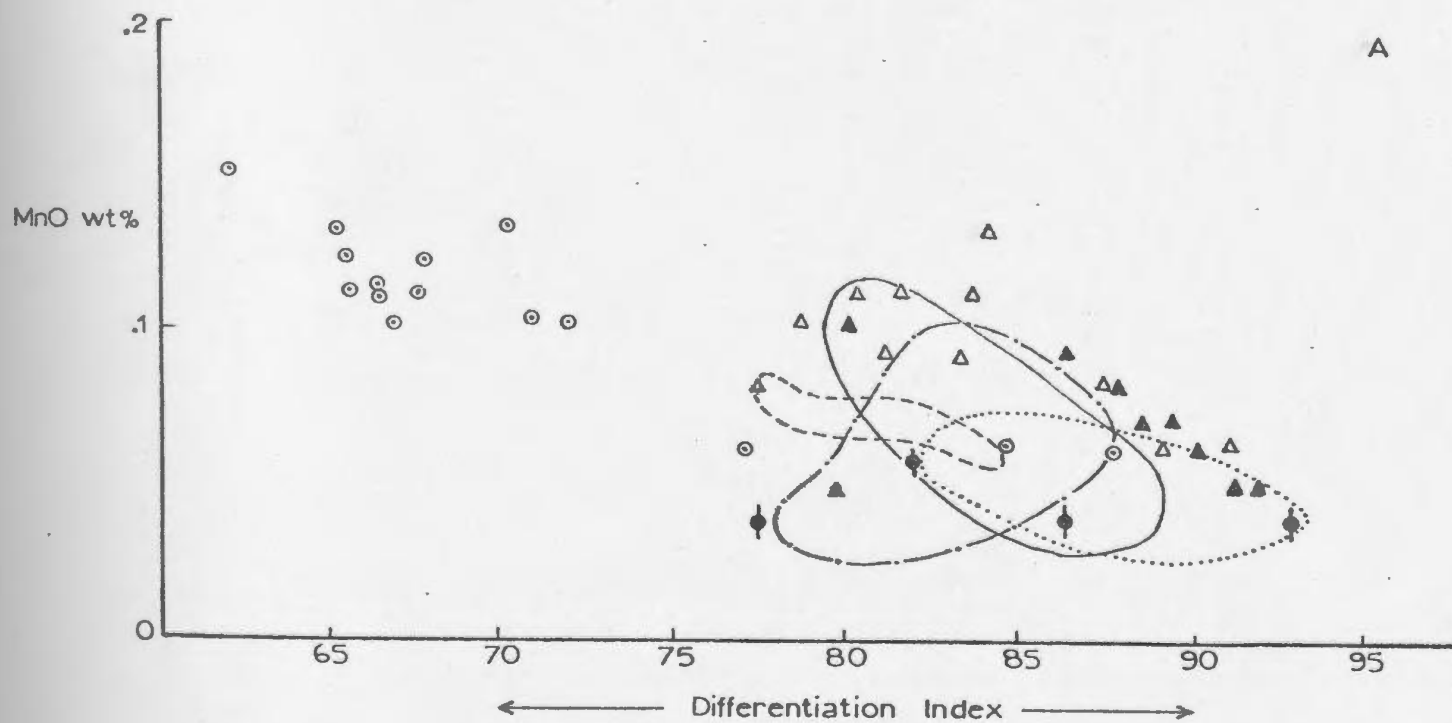
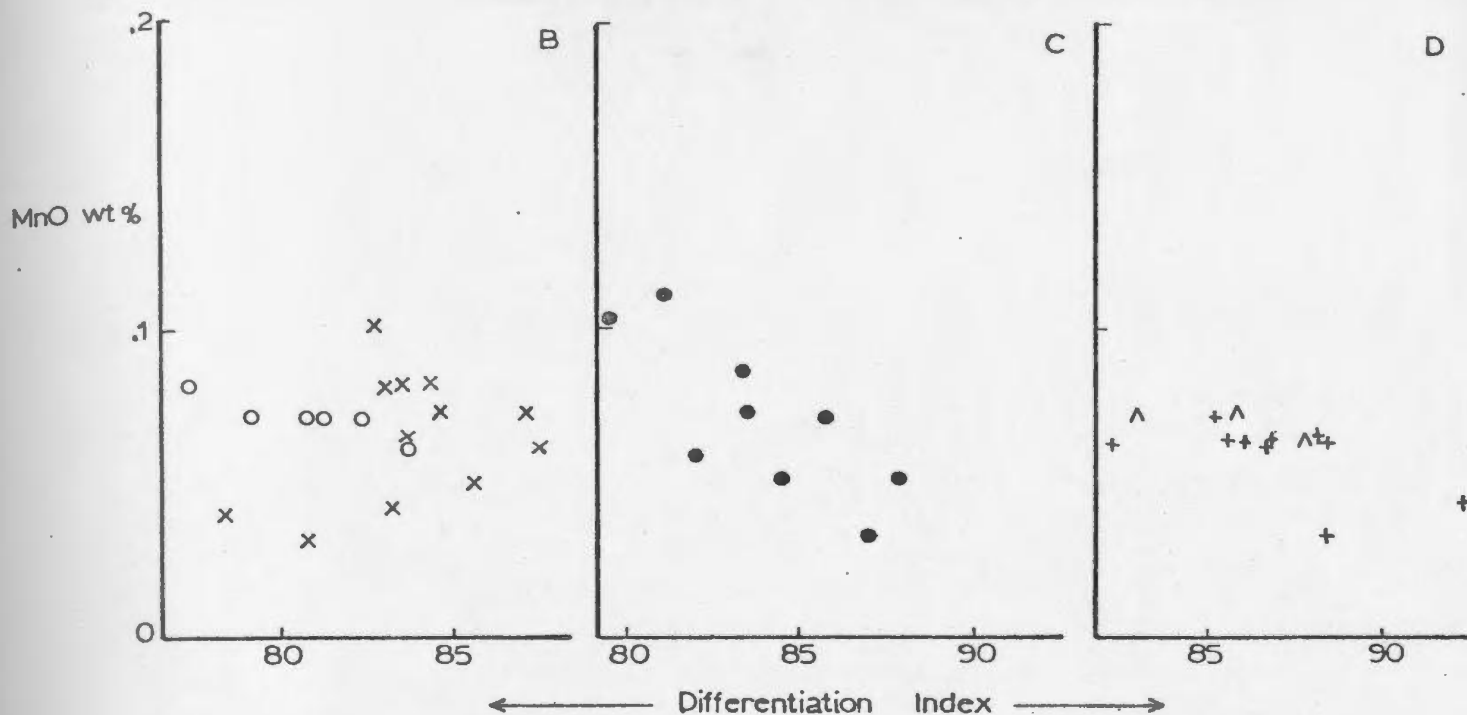
- |               |                        |   |                       |
|---------------|------------------------|---|-----------------------|
| — x —         | Cape Freels Granite    | o | Wareham Granite       |
| - - - o - - - | Lockers Bay Granite    | Δ | North Pond Granite    |
| — • —         | Deadman's Bay Granite  | ▲ | medium-grained phase  |
| ... + ...     | Newport Granite        | ◆ | porphyritic phase     |
| ^             | Big Round Pond Granite |   | Business Cove Granite |

(Figure 6.1d)



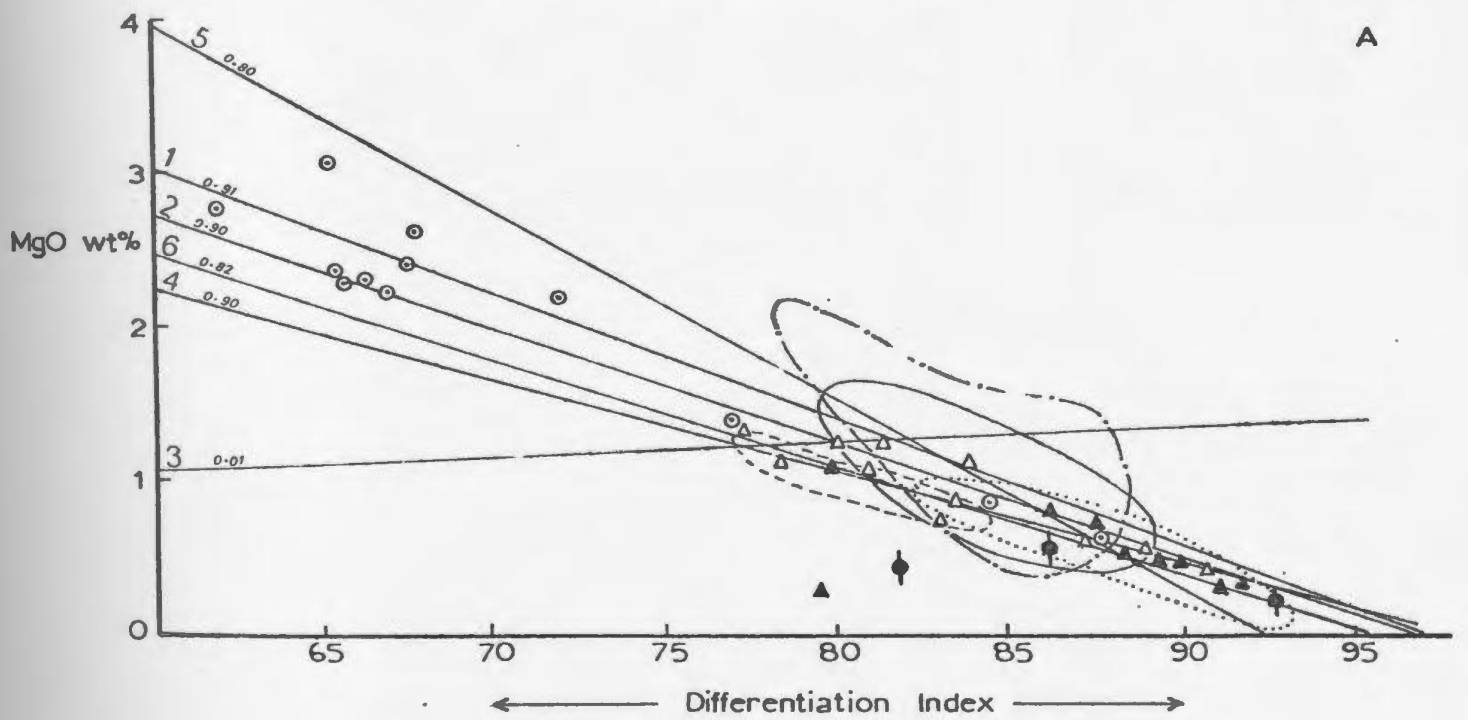
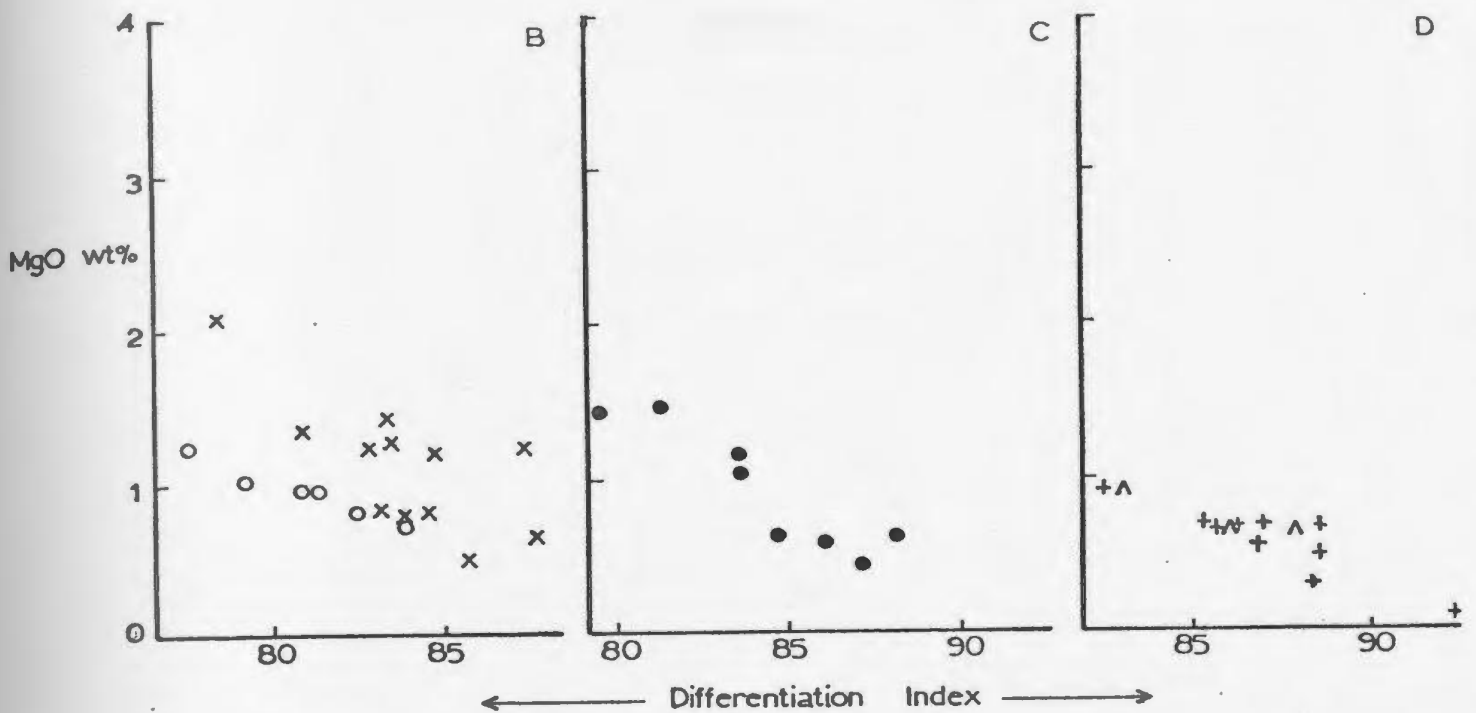
(Figure 6.1 e)



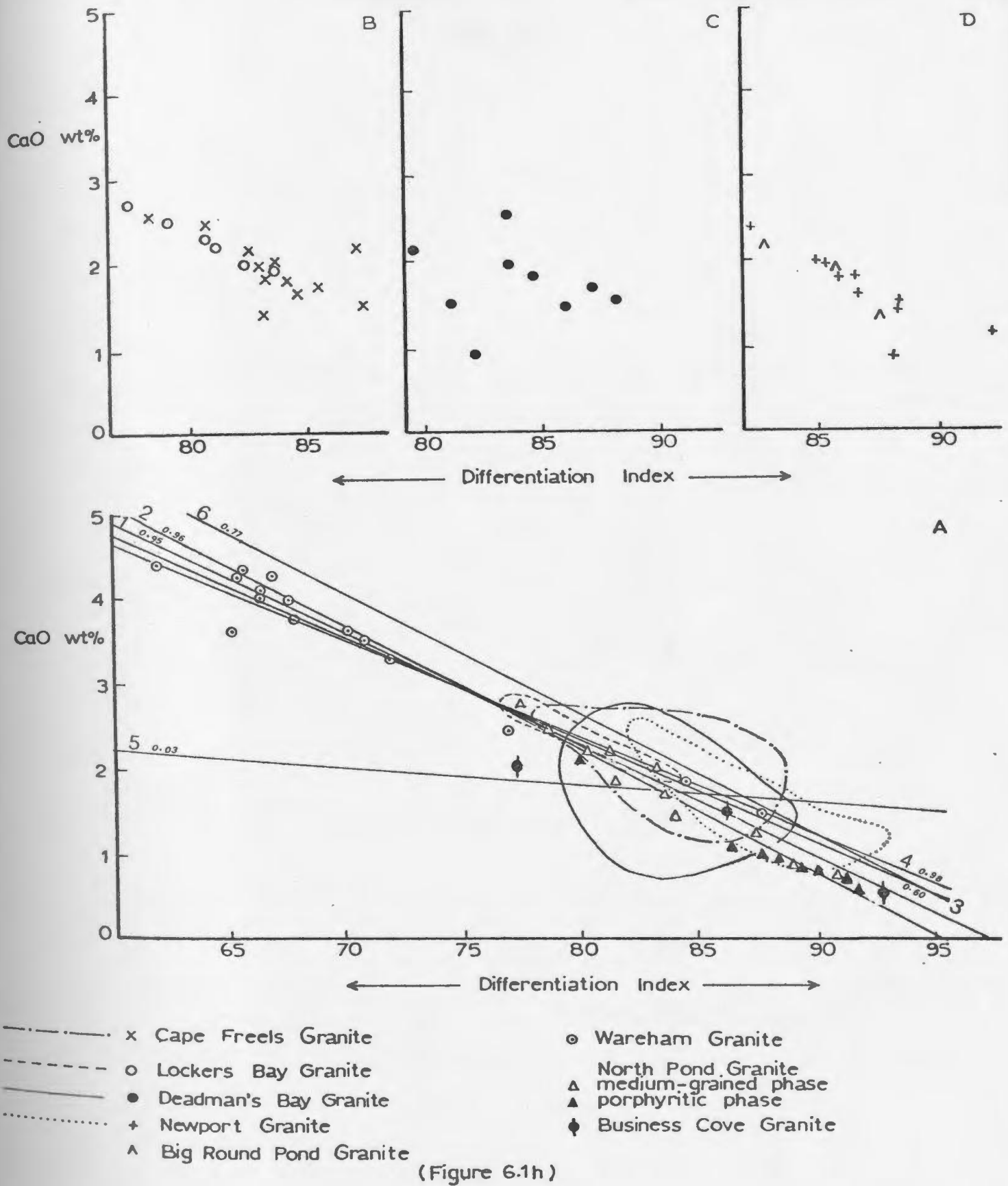


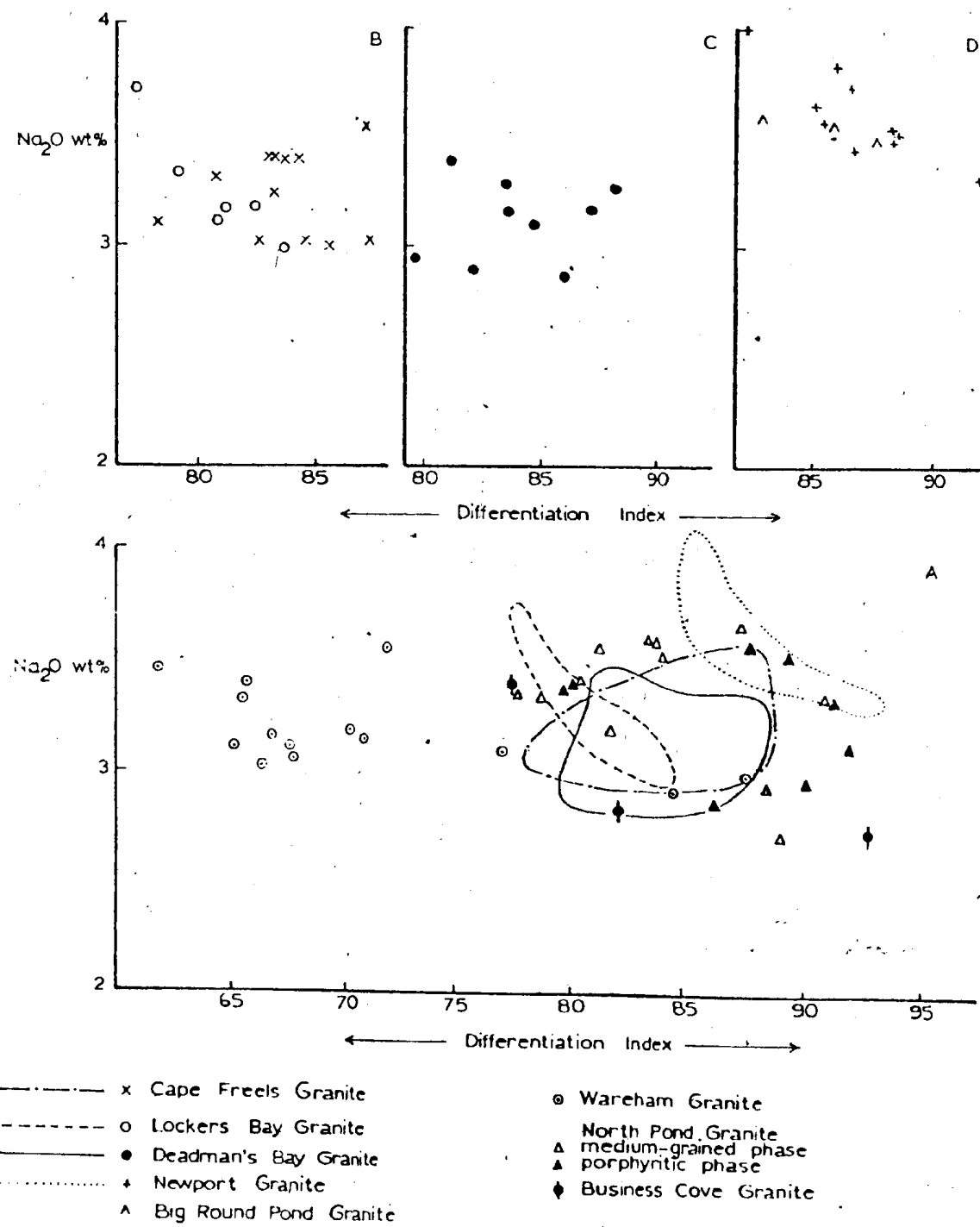
- x Cape Freels Granite
- o Lockers Bay Granite
- • Deadman's Bay Granite
- + Newport Granite
- ^ Big Round Pond Granite
- o Wareham Granite
- Δ North Pond Granite medium-grained phase
- ▲ North Pond Granite porphyritic phase
- ◆ Business Cove Granite

(Figure 6.1f)

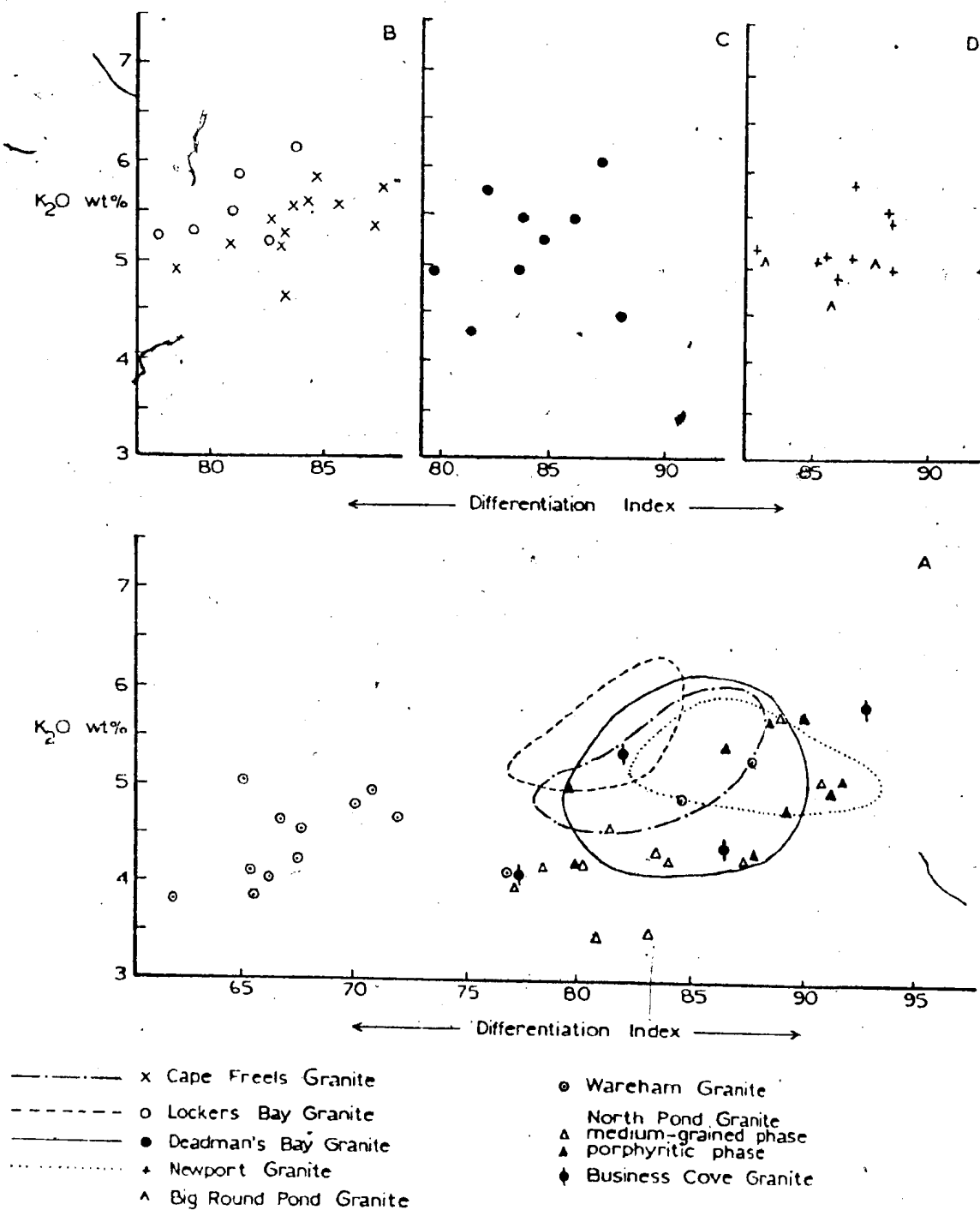


(Figure 6.1g)

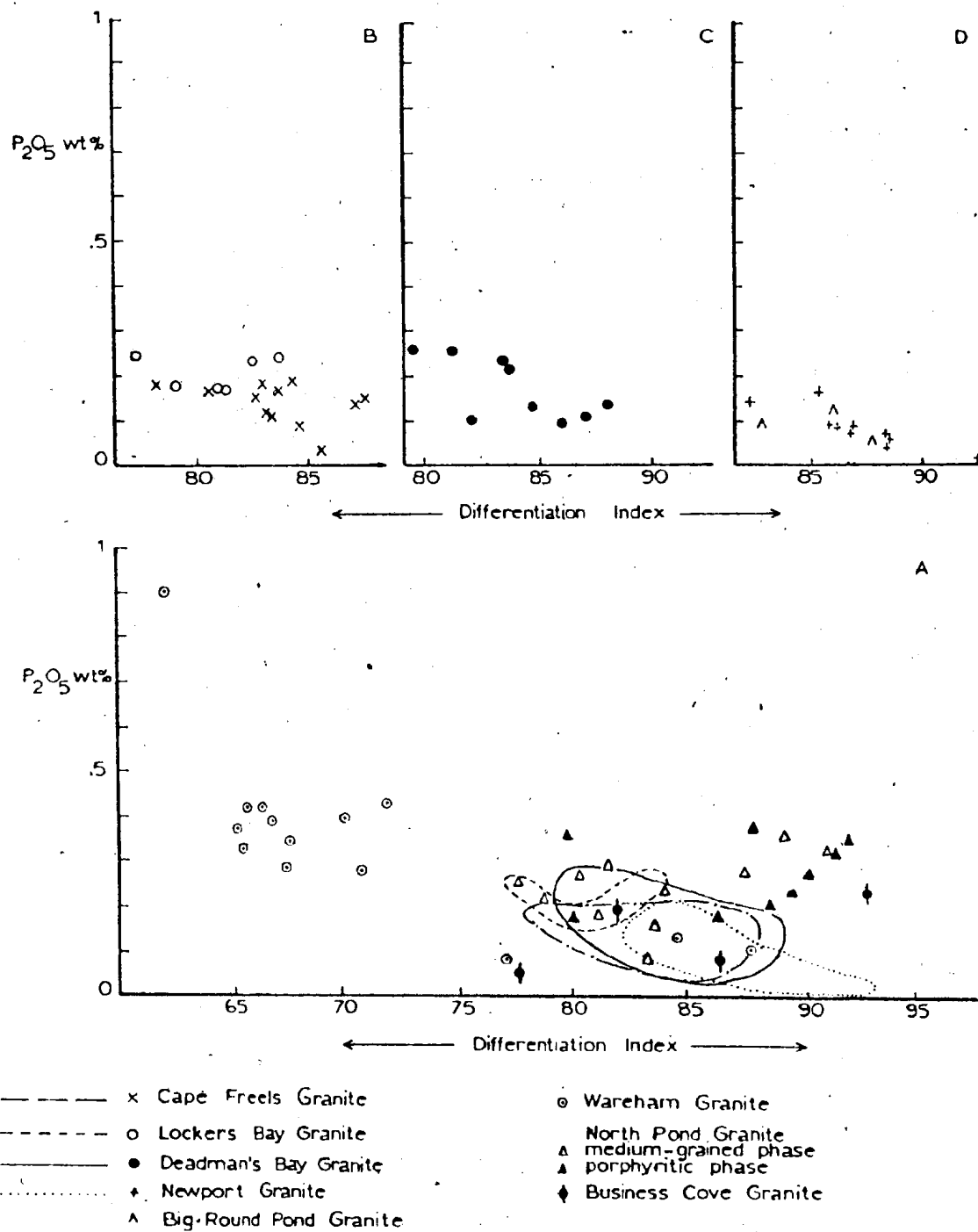




(Figure 6.1i)

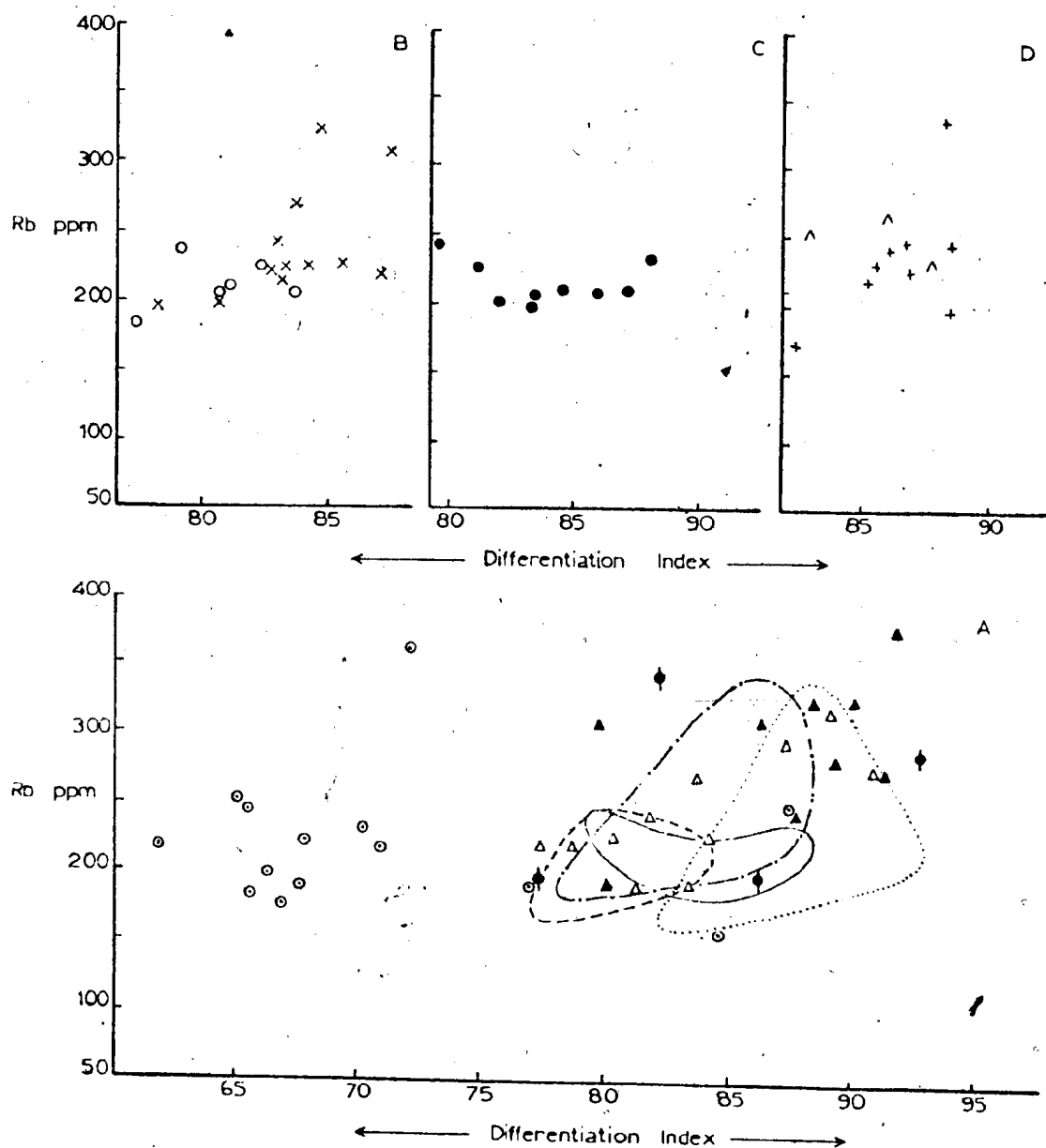


(Figure 6.1j)



(Figure 6.1k)

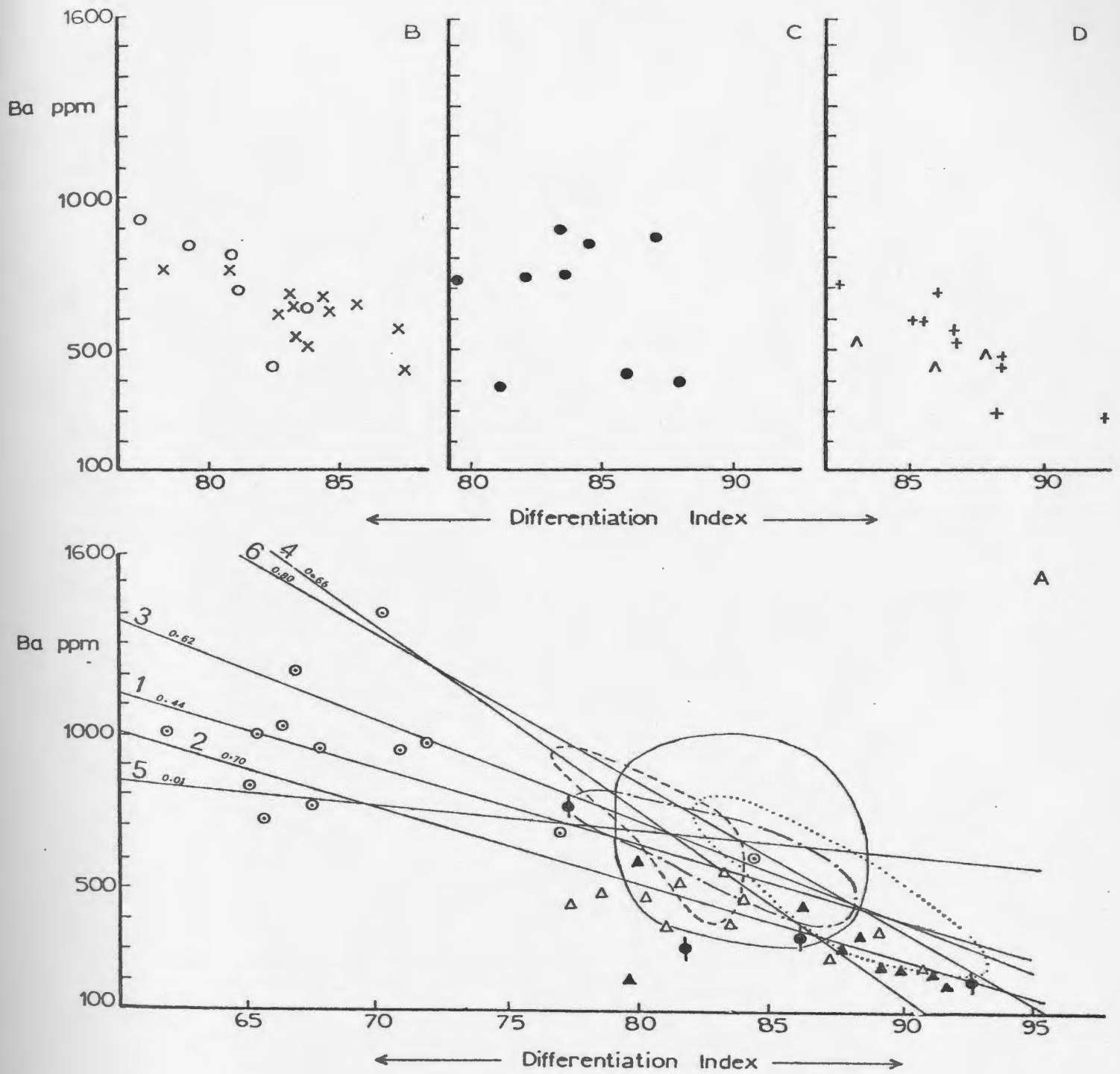
Fig. 6.2 (a to m). Trace element variation diagrams.  
Trace element concentrations versus  
Thornton-Tuttle Differentiation Index.  
A, B, C, and D as in Fig. 6.3.  
(Solid lines on Ba and V vs. D.I. plots  
represent linear regression lines 1, 2, 3,  
4, 5 and 6 as in Fig. 6.3. Small numbers  
along the lines are correlation coefficients.)



- |                                       |                         |
|---------------------------------------|-------------------------|
| — x — Cape Freels Granite             | ○ Wareham Granite       |
| - - - o - - - Lockers Bay Granite     | △ North Pond Granite    |
| — • — Deadman's Bay Granite           | △ medium-grained phase  |
| - · - · - + - · - · - Newport Granite | ▲ porphyritic phase     |
| - - - ^ - - - Big Round Pond Granite  | ◆ Business Cove Granite |

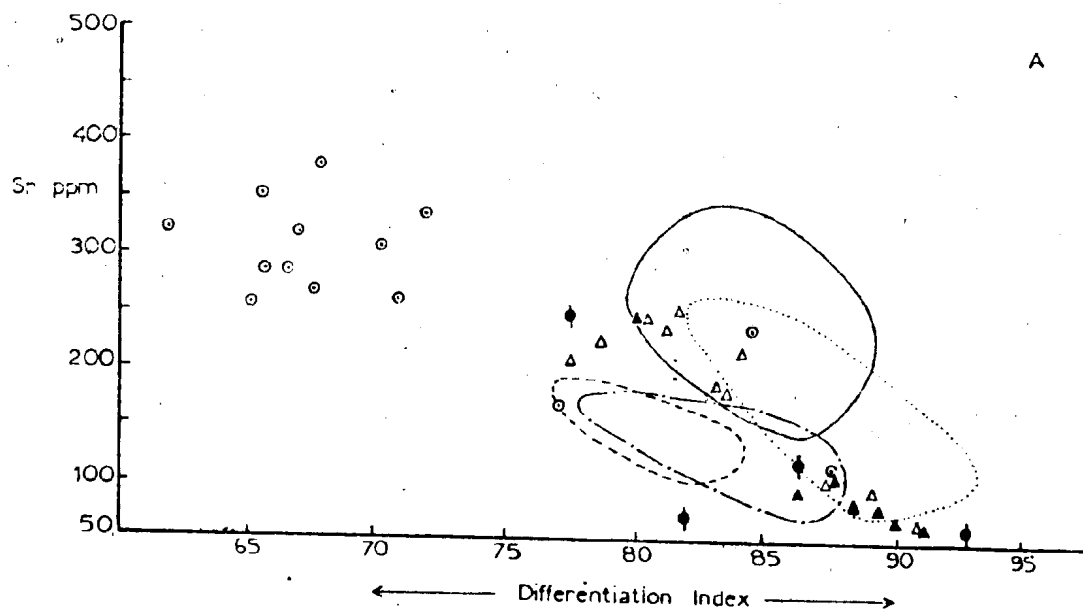
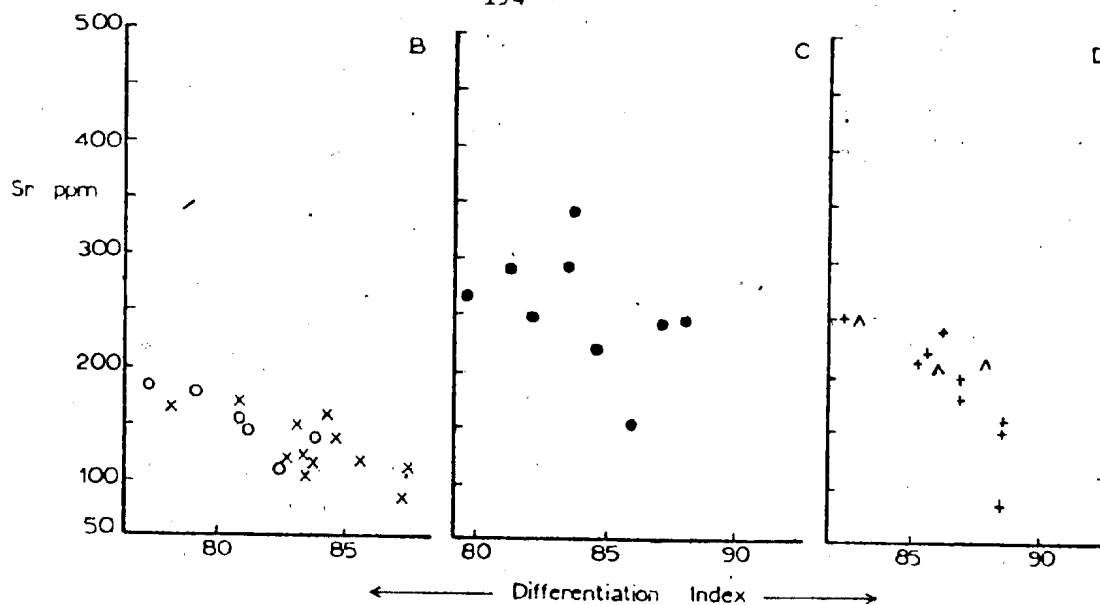
(Figure 6.2a)





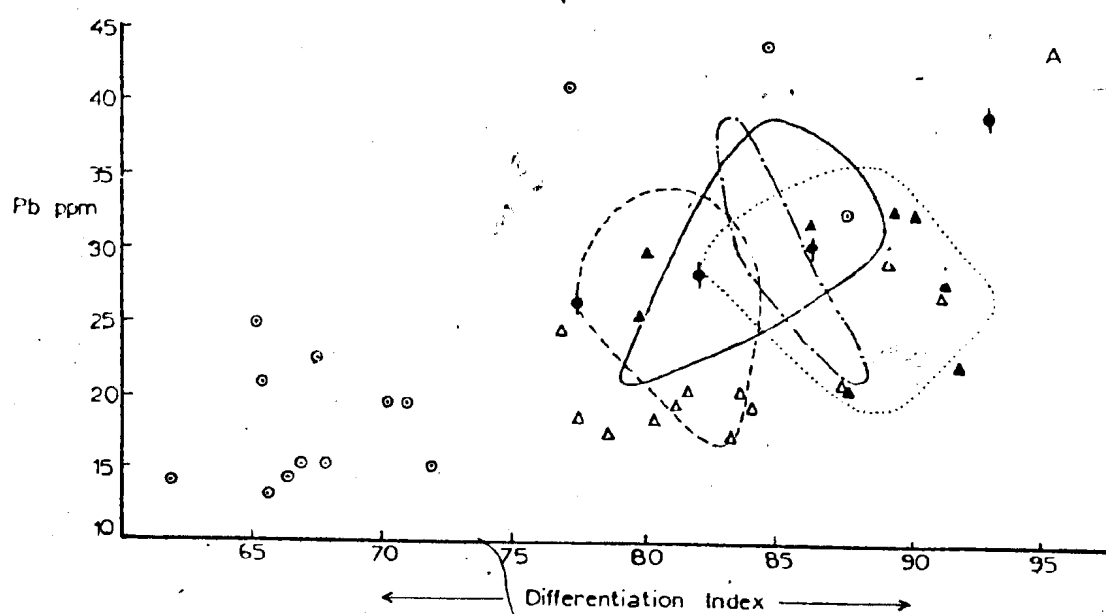
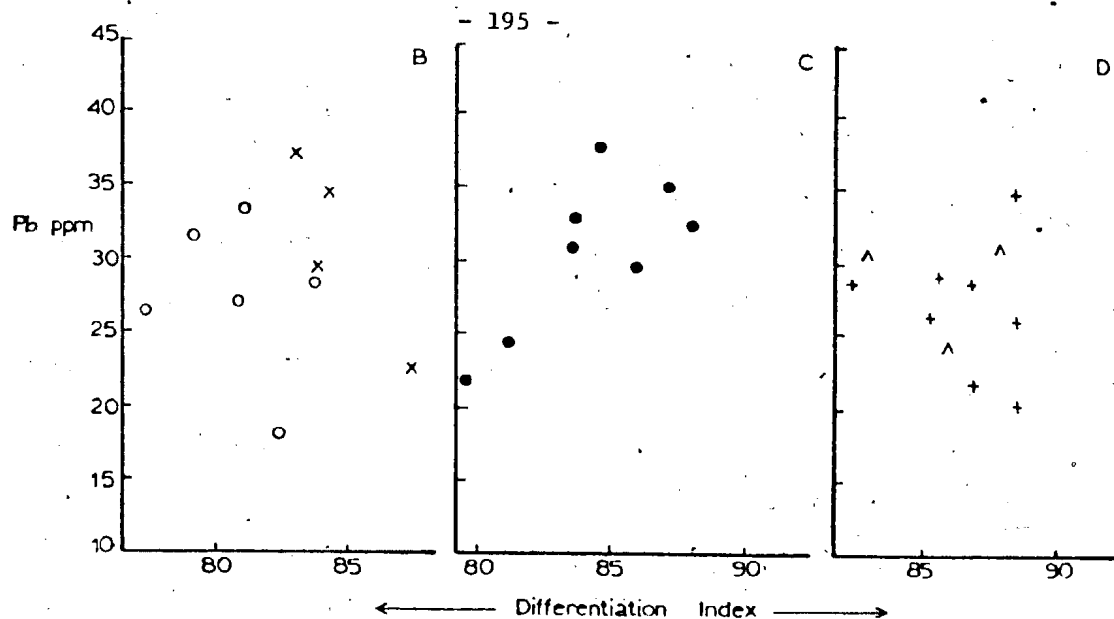
- x Cape Freels Granite
- o Lockers Bay Granite
- • Deadman's Bay Granite
- + Newport Granite
- Λ Big Round Pond Granite
- ○ Wareham Granite
- Δ North Pond Granite
- ▲ medium-grained phase
- ◆ porphyritic phase
- ◆ Business Cove Granite

(Figure 6.2 b)



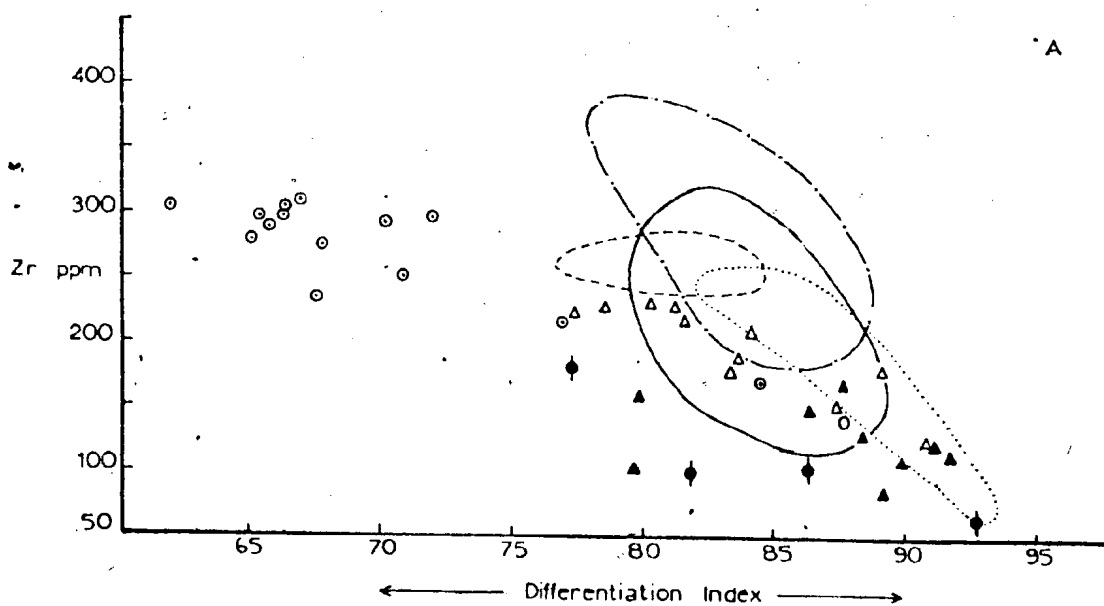
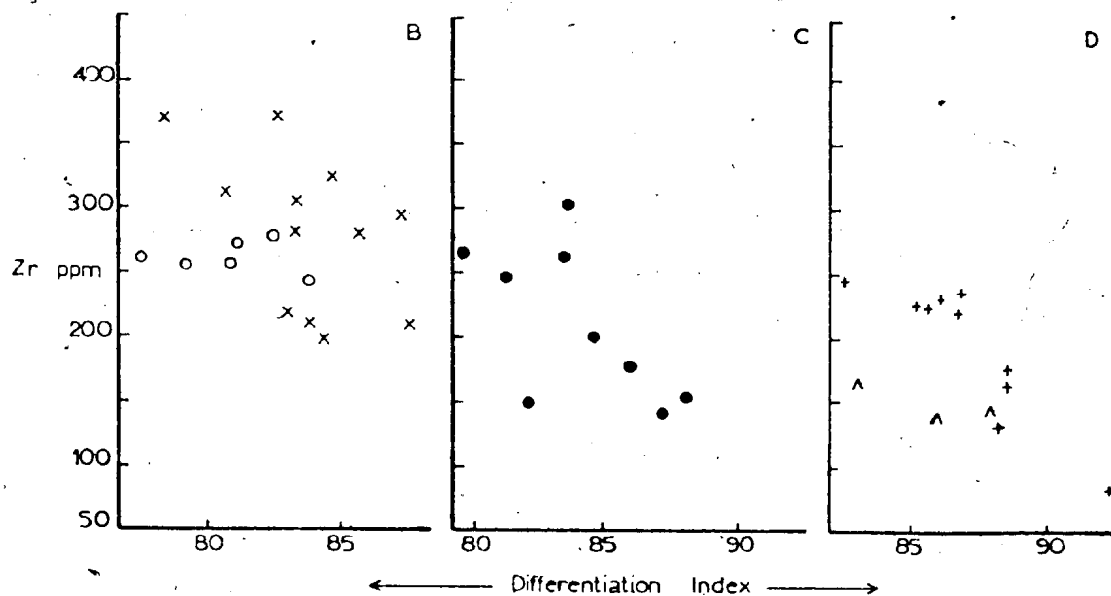
- x — Cape Freels Granite
- - - o - Lockers Bay Granite
- • — Deadman's Bay Granite
- - - + - Newport Granite
- - - ^ - Big Round Pond Granite
- o Wareham Granite
- North Pond Granite
- Δ medium-grained phase
- ▲ porphyritic phase
- ◆ Business Cove Granite

(Figure 6.2c)



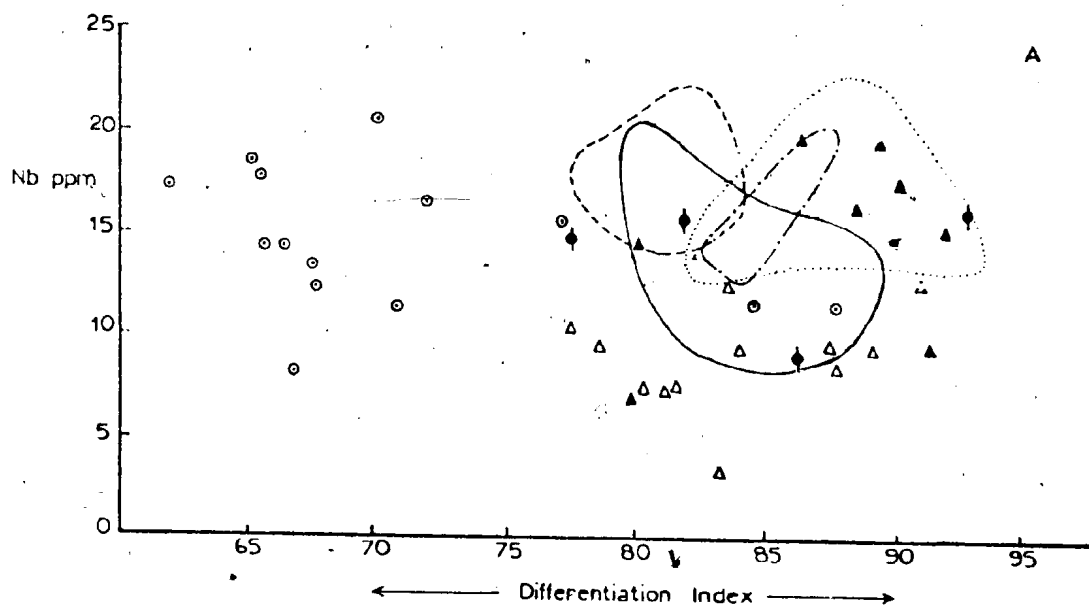
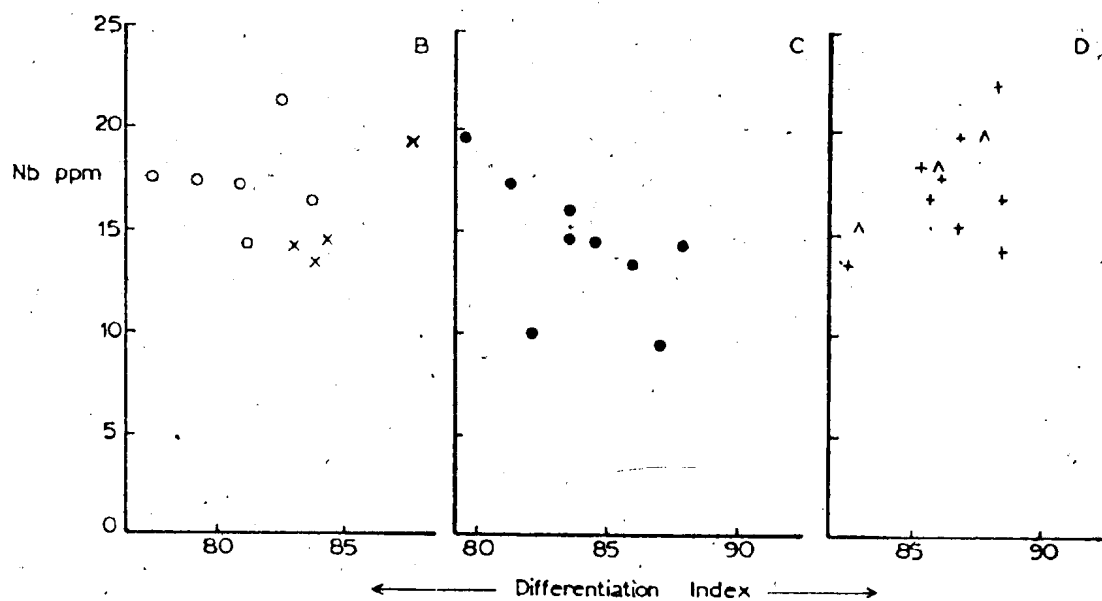
- x Cape Freels Granite
- - - o Lockers Bay Granite
- • Deadman's Bay Granite
- - - + Newport Granite
- - - Δ Big Round Pond Granite
- o Wareham Granite
- Δ North Pond Granite
- Δ medium-grained phase
- Δ porphyritic phase
- ◆ Business Cove Granite

(Figure 6.2d)



- x Cape Freels Granite
- - - o Lockers Bay Granite
- • Deadman's Bay Granite
- - - + Newport Granite
- - - ^ Big Round Pond Granite
- ◊ Wareham Granite
- Δ North Pond Granite medium-grained phase
- ▲ North Pond Granite porphyritic phase
- ◆ Business Cove Granite

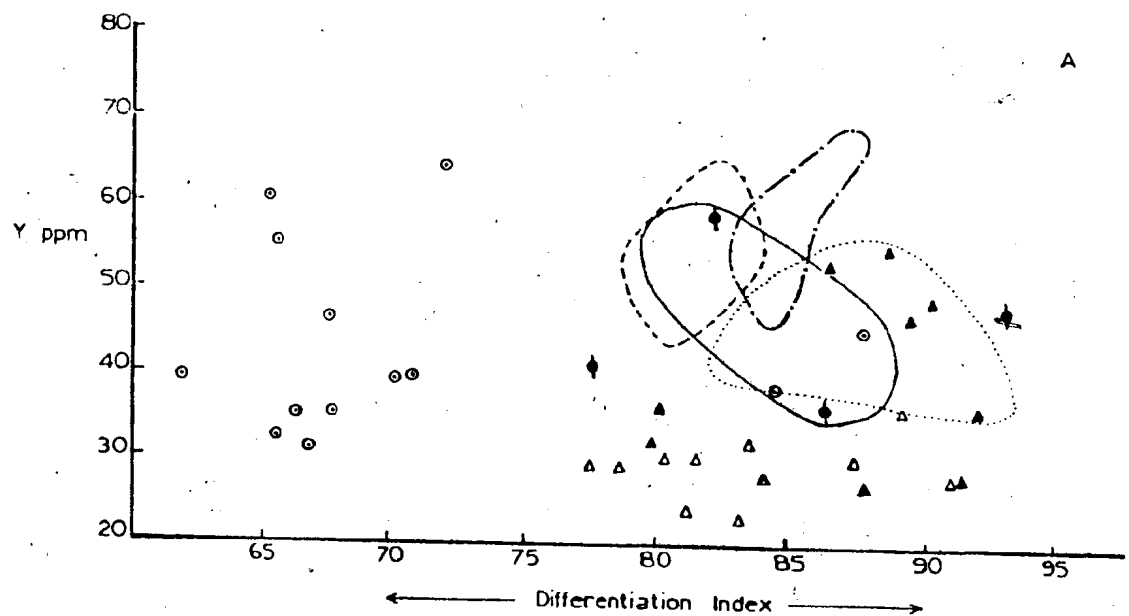
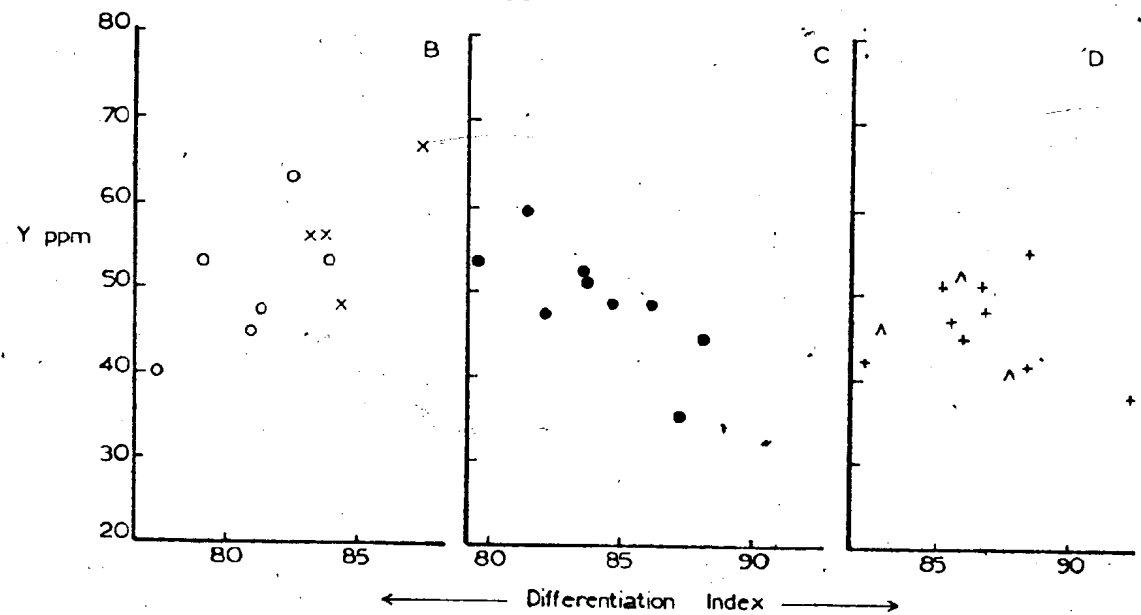
(Figure 6.2e)



- |               |                        |   |   |
|---------------|------------------------|---|---|
| — x —         | Cape Freels Granite    | o | Wareham Granite                         |
| - - - o - - - | Lockers Bay Granite    | Δ | North Pond Granite medium-grained phase |
| — • —         | Deadman's Bay Granite  | ▲ | North Pond Granite porphyritic phase    |
| - - - + - - - | Newport Granite        | ◆ | Business Cove Granite                   |
| - - - ^ - - - | Big Round Pond Granite |   |   |

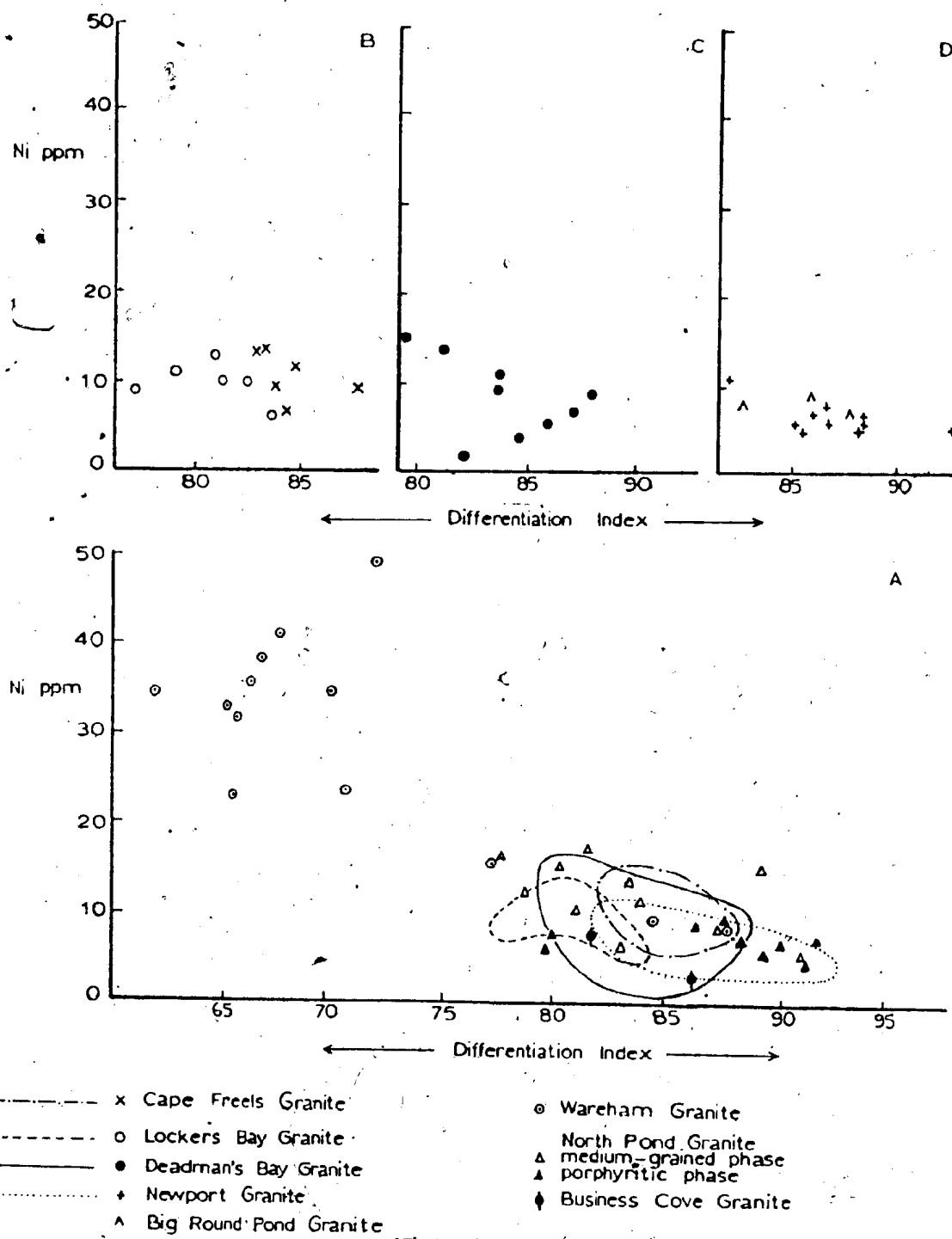
(Figure 6.2f)

- 198 -

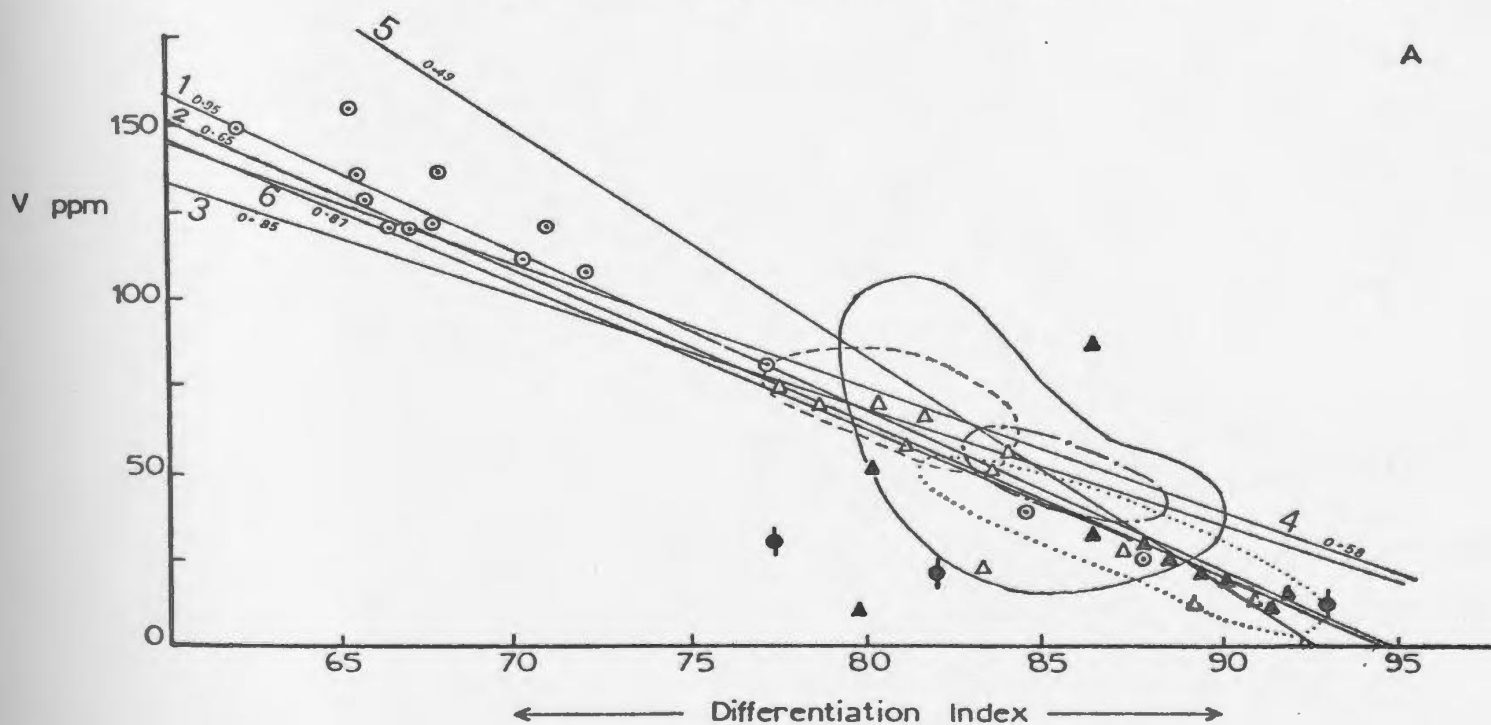
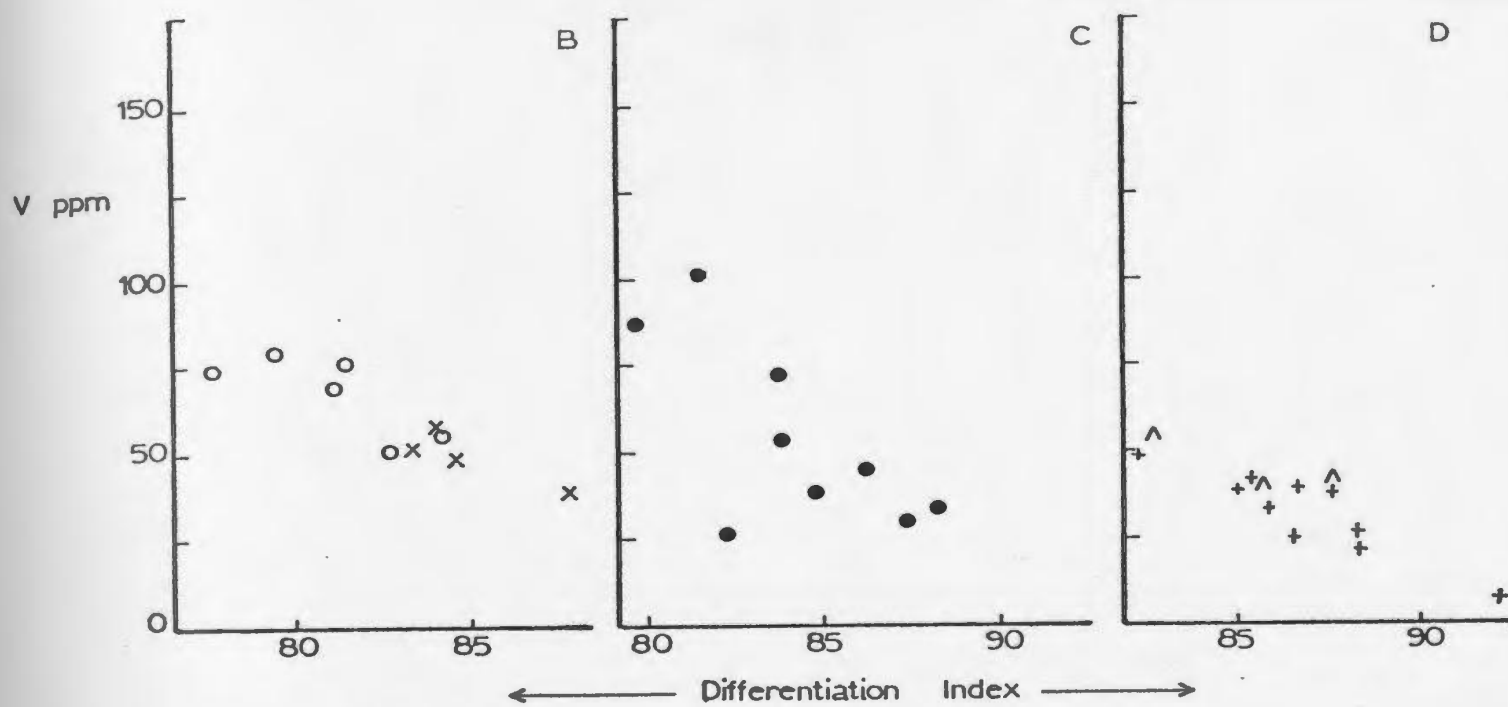


- |         |                        |   |                       |
|---------|------------------------|---|-----------------------|
| — x     | Cape Freels Granite    | ◉ | Wareham Granite       |
| - - - o | Lockers Bay Granite    | Δ | North Pond Granite    |
| — •     | Deadman's Bay Granite  | Δ | medium-grained phase  |
| - - - + | Newport Granite        | Δ | porphyritic phase     |
| ..... Λ | Big Round Pond Granite | ◊ | Business Cove Granite |

(Figure 6.2g)



(Figure 6.2h)



x Cape Freels Granite

o Lockers Bay Granite

• Deadman's Bay Granite

+ Newport Granite

^ Big Round Pond Granite

◊ Wareham Granite

North Pond Granite

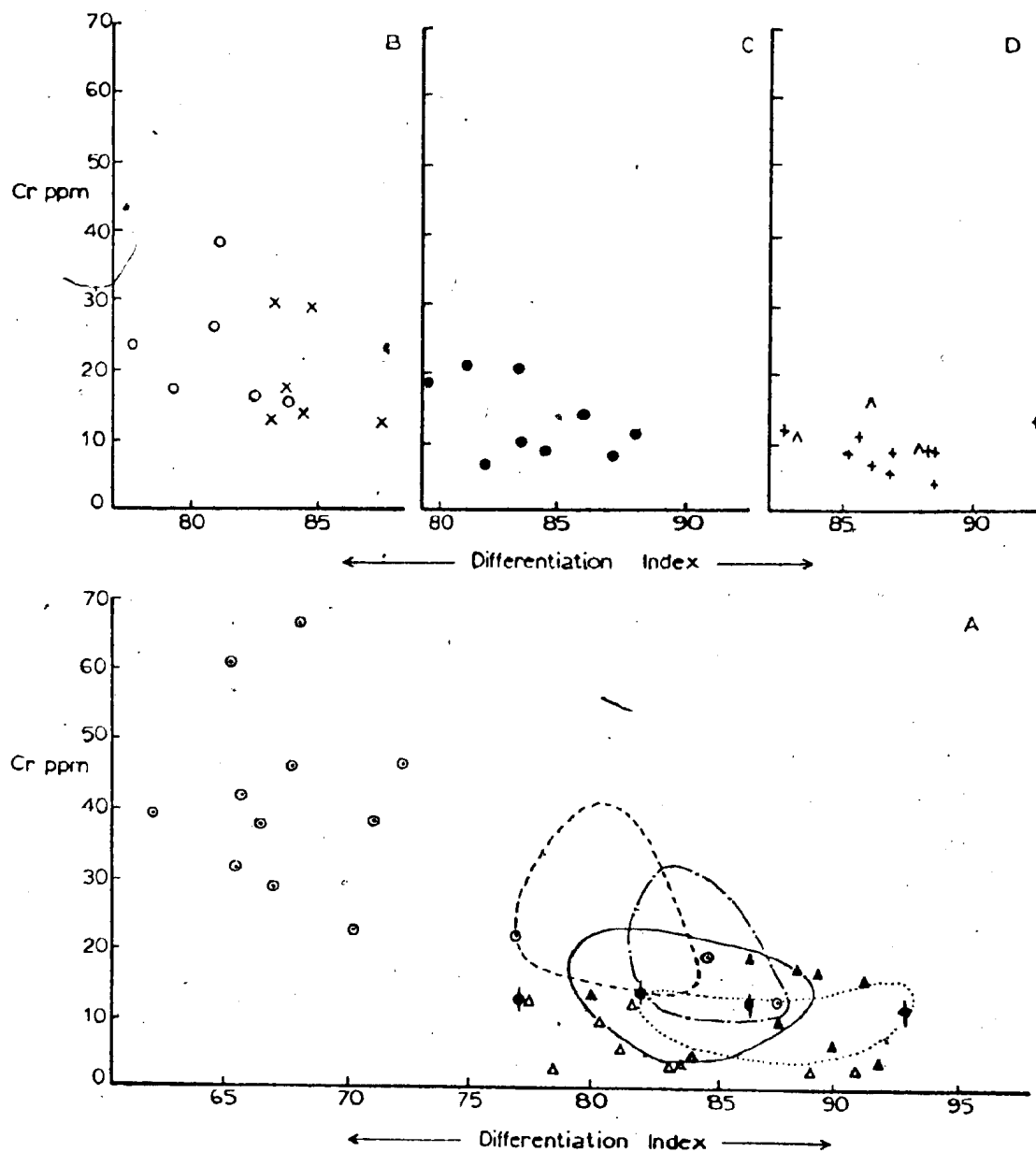
Δ medium-grained phase

▲ porphyritic phase

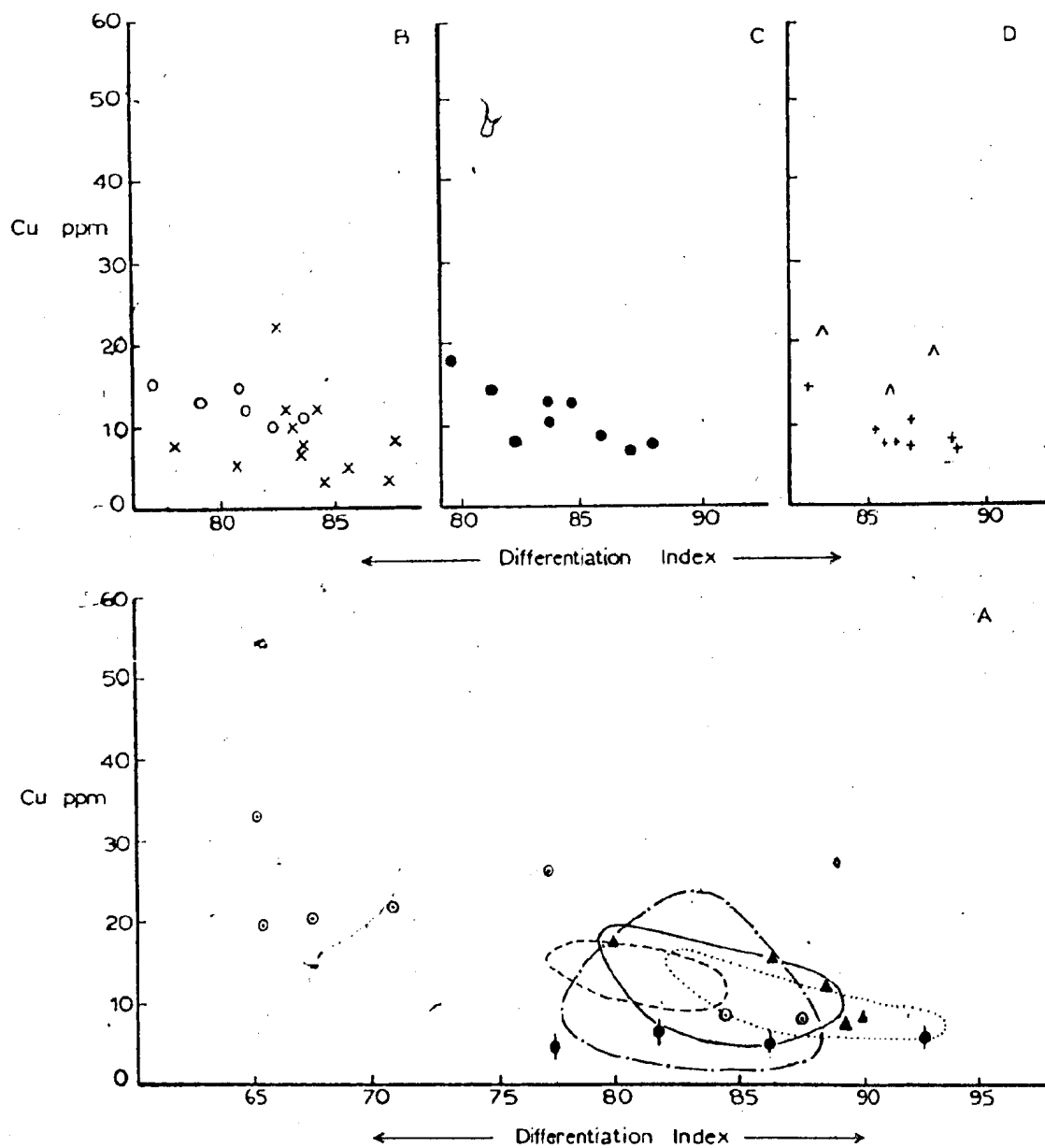
◊ Business Cove Granite

(Figure 6.2i)



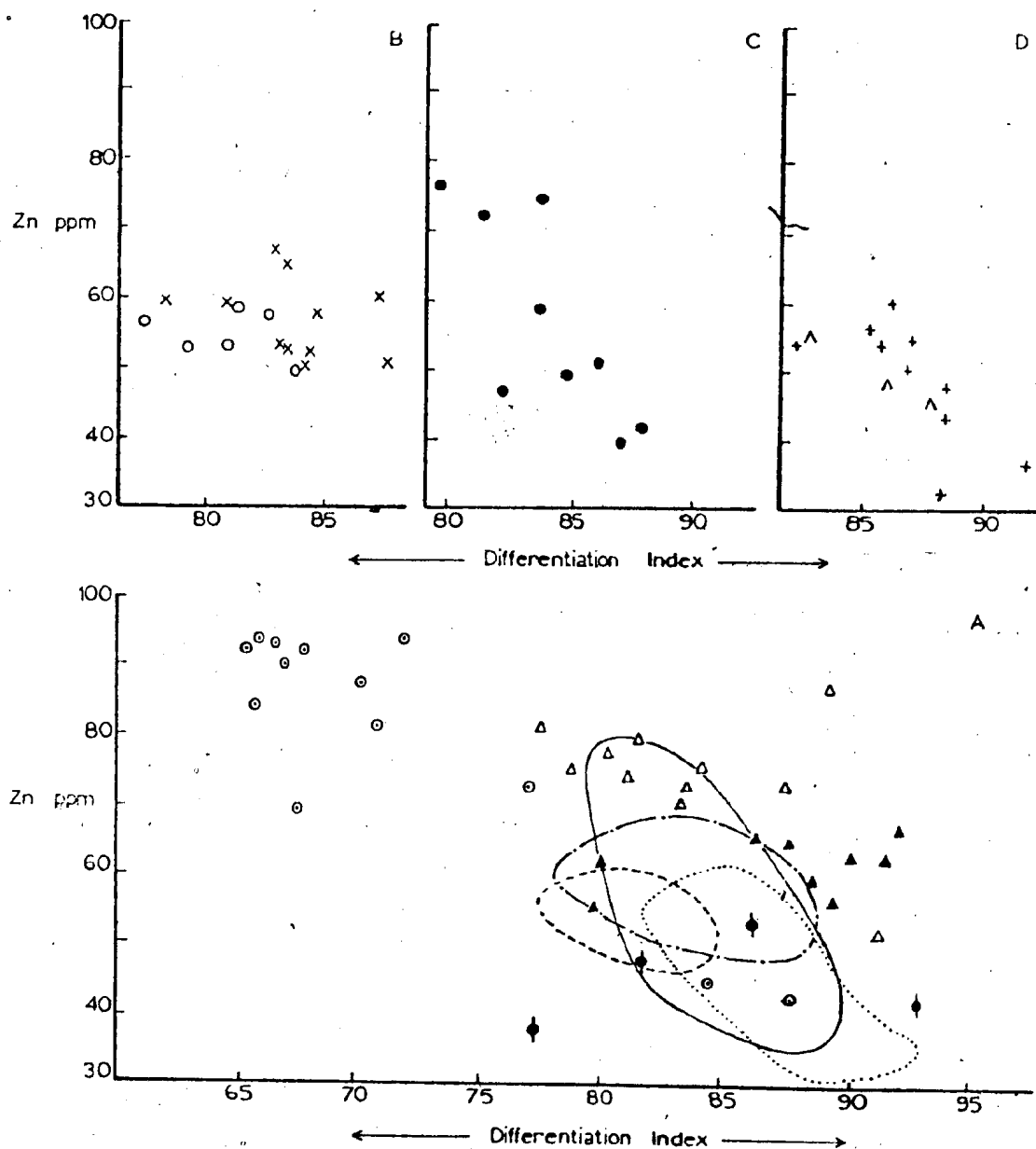


(Figure 6.2j)



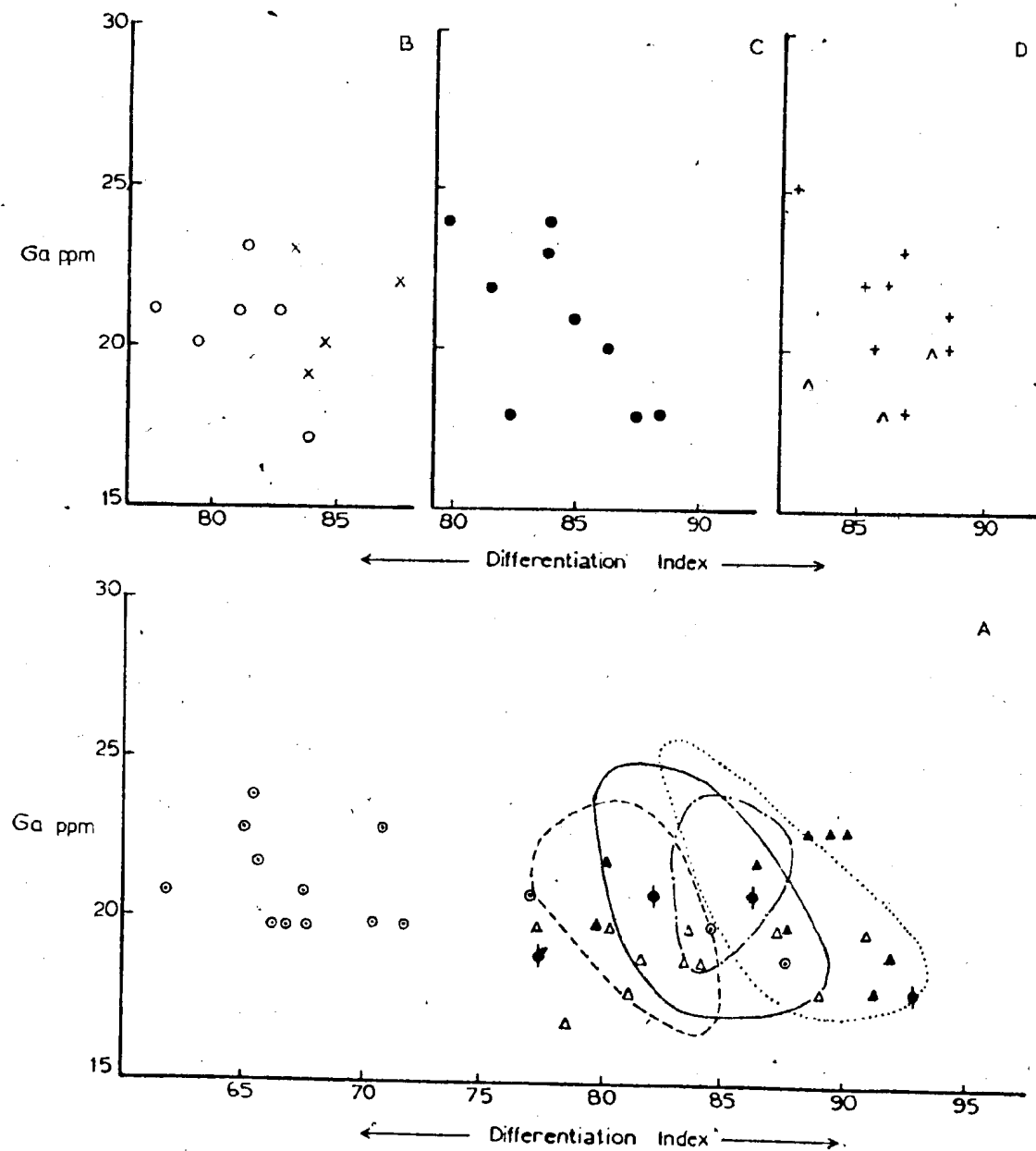
- |                                |                         |
|--------------------------------|-------------------------|
| ----- x Cape Freels Granite    | o Wareham Granite       |
| ----- o Lockers Bay Granite    | North Pond Granite:     |
| ----- • Deadman's Bay Granite  | Δ medium-grained phase  |
| ----- + Newport Granite        | ▲ porphyritic phase     |
| ----- Δ Big Round Pond Granite | ◆ Business Cove Granite |

(Figure 6.2k)



- x Cape Freels Granite
- o Lockers Bay Granite
- • Deadman's Bay Granite
- + Newport Granite
- ^ Big Round Pond Granite
- Wareham Granite
- North Pond Granite
- Δ medium-grained phase
- ▲ porphyritic phase
- ◆ Business Cove Granite

(Figure 6.21)



- |                                |                         |
|--------------------------------|-------------------------|
| ----- x Cape Freels Granite    | ◊ Wareham Granite       |
| ----- o Lockers Bay Granite    | North Pond Granite      |
| ----- • Deadman's Bay Granite  | Δ medium-grained phase  |
| ----- + Newport Granite        | Δ porphyritic phase     |
| ----- Δ Big Round Pond Granite | ◊ Business Cove Granite |

(Figure 6.2m)

The porphyritic phase of the North Pond Granite has higher D.I. values and  $\text{SiO}_2$ , Rb and Pb contents and lower  $\text{Al}_2\text{O}_3$ ,  $\text{TiO}_2$ , FeO,  $\text{Fe}_2\text{O}_3$ , CaO, MgO, MnO, Ba, Sr, Zr, and V contents than the medium-grained phase of the North Pond Granite and thus is more differentiated than the latter. This reflects the lower content of biotite and plagioclase and the higher content of muscovite and microcline in the porphyritic phase than in the medium-grained phase.

In the variation diagrams, the compositional fields of the plutons, except the Wareham Quartz Monzonite, overlap indicating that both the non-megacrystic granites and the majority of the megacrystic granites have a similar chemistry as was shown earlier by the normative classification of the plutons (see page 74). The Wareham Quartz Monzonite has lower D.I. values and  $\text{SiO}_2$  contents and higher  $\text{TiO}_2$ ,  $\text{Al}_2\text{O}_3$ , FeO,  $\text{Fe}_2\text{O}_3$ , CaO, MgO, MnO,  $\text{P}_2\text{O}_5$ , Ba, Sr, Ni, V, Cr, Cu and Zn concentrations than the other granitoids in the area. This bears out the earlier observation that the Wareham pluton is the most mafic intrusion among the granitoids in the area<sup>1</sup> (see page 83).

The trends defined by the analyses from the Wareham Quartz Monzonite and the North Pond Granite are close and subparallel to each other in a number of variation diagrams ( $\text{TiO}_2$ , FeO, CaO, MgO, Ba and V vs. D.I. plots). The trends defined by the other plutons generally do not show such a relationship with those of the Wareham pluton. It is common knowledge that genetically related rocks plot along a single

---

<sup>1</sup>Currie et al. (1979) reported an average of six chemical analyses from the western marginal part of the Deadman's Bay Granite. According to this average composition, the Deadman's Bay pluton, in their study area, is more mafic than the Wareham Quartz Monzonite.

regular trend in the variation diagrams (Taylor, 1967; Flinter, 1974). Therefore the fact that analyses from the Wareham pluton and the North Pond Granite tend to plot on a common trend in the variation diagrams, for a number of elements, may be taken as evidence of their consanguinity. Thus the Wareham and the North Pond plutons could have been produced by progressive differentiation of a parent magma or by progressive anatexis of source rocks. However, in progressive anatexis the older magma phases are more felsic than the younger phases; the reverse is true in progressive differentiation. It is clear from the field evidence that the Wareham Quartz Monzonite is the older of the two plutons. Therefore the medium-grained phase of the North Pond Granite and the porphyritic phase of the North Pond Granite could well have been resulted from increasing degrees of differentiation of a Wareham pluton-type magma.

#### 6.2. Element Ratios

The K/Rb, Ba/Rb, Rb/Sr, Ba/Sr and Sr/Ca ratios of the plutons are plotted against D.I. in Figure 6.3. K/Rb, Ba/Sr, Sr/Ca ratios do not show a systematic variation with increasing D.I. Rb/Sr ratios increase and Ba/Rb ratios tend to decrease with increasing D.I. The increase in Rb/Sr ratios is particularly pronounced going from the medium-grained phase of the North Pond Granite to the porphyritic phase of the North Pond Granite.

Theoretically, Rb enters the  $K^+$  positions in feldspars and micas because  $Rb^+$  and  $K^+$  ions are comparable in size and have smaller

Fig. 6.3. (a to e). K/Rb, Ba/Rb, Rb/Sr, Ba/Sr and Sr/Ca ratios versus Thornton-Tuttle Differentiation Index. Symbols as in Fig. 6.2 (page 192).

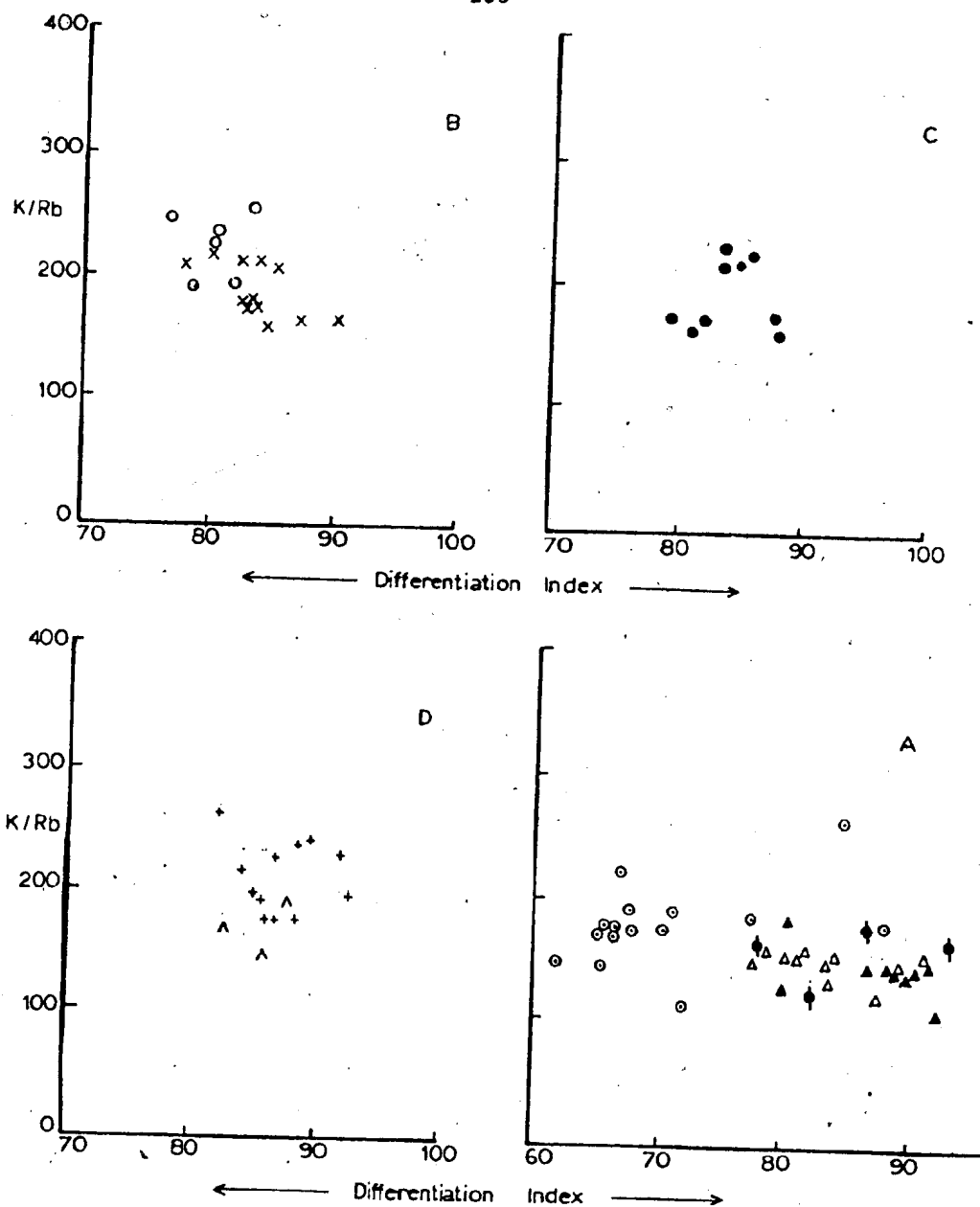


Fig 6.3a



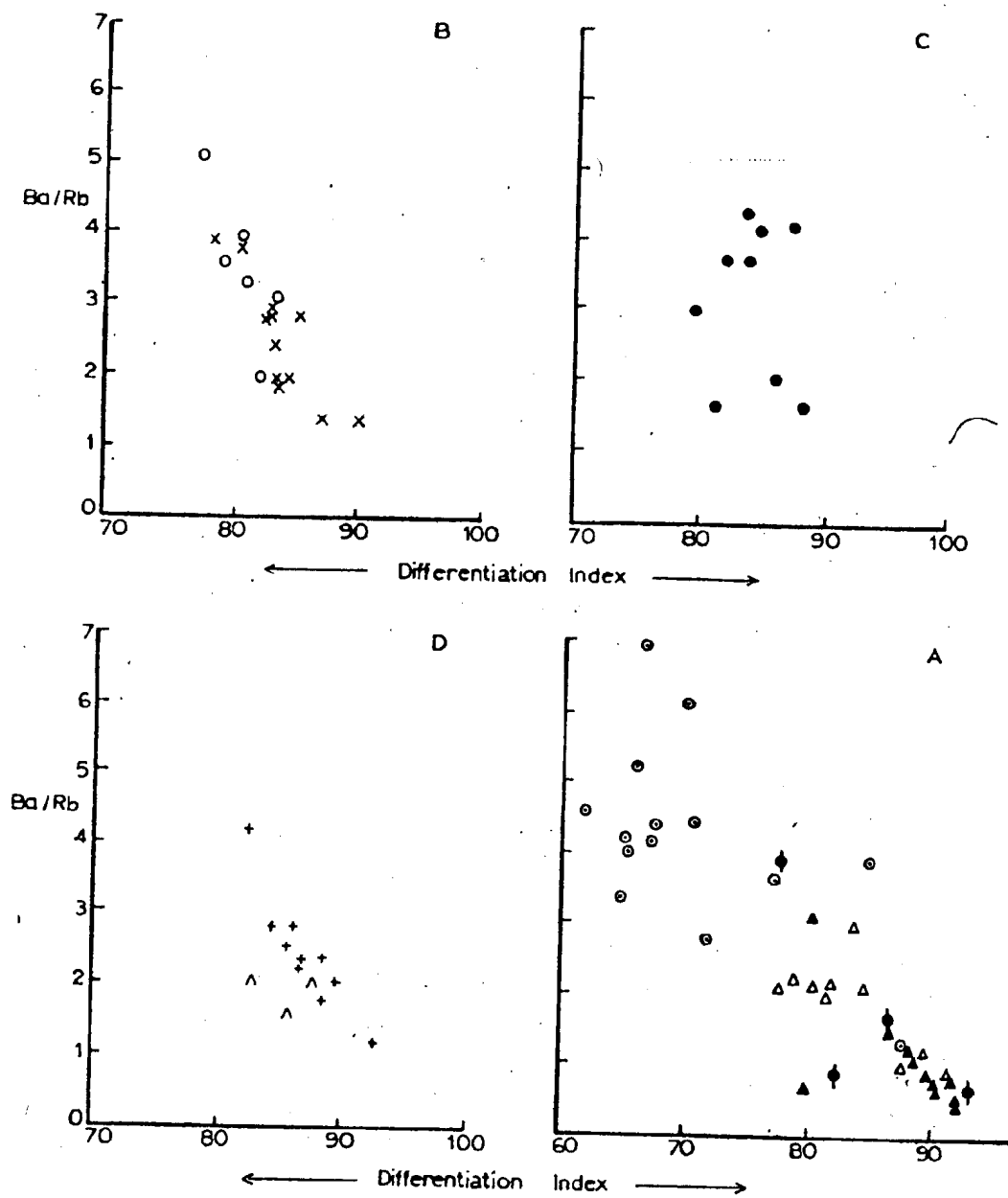


Fig. 63b

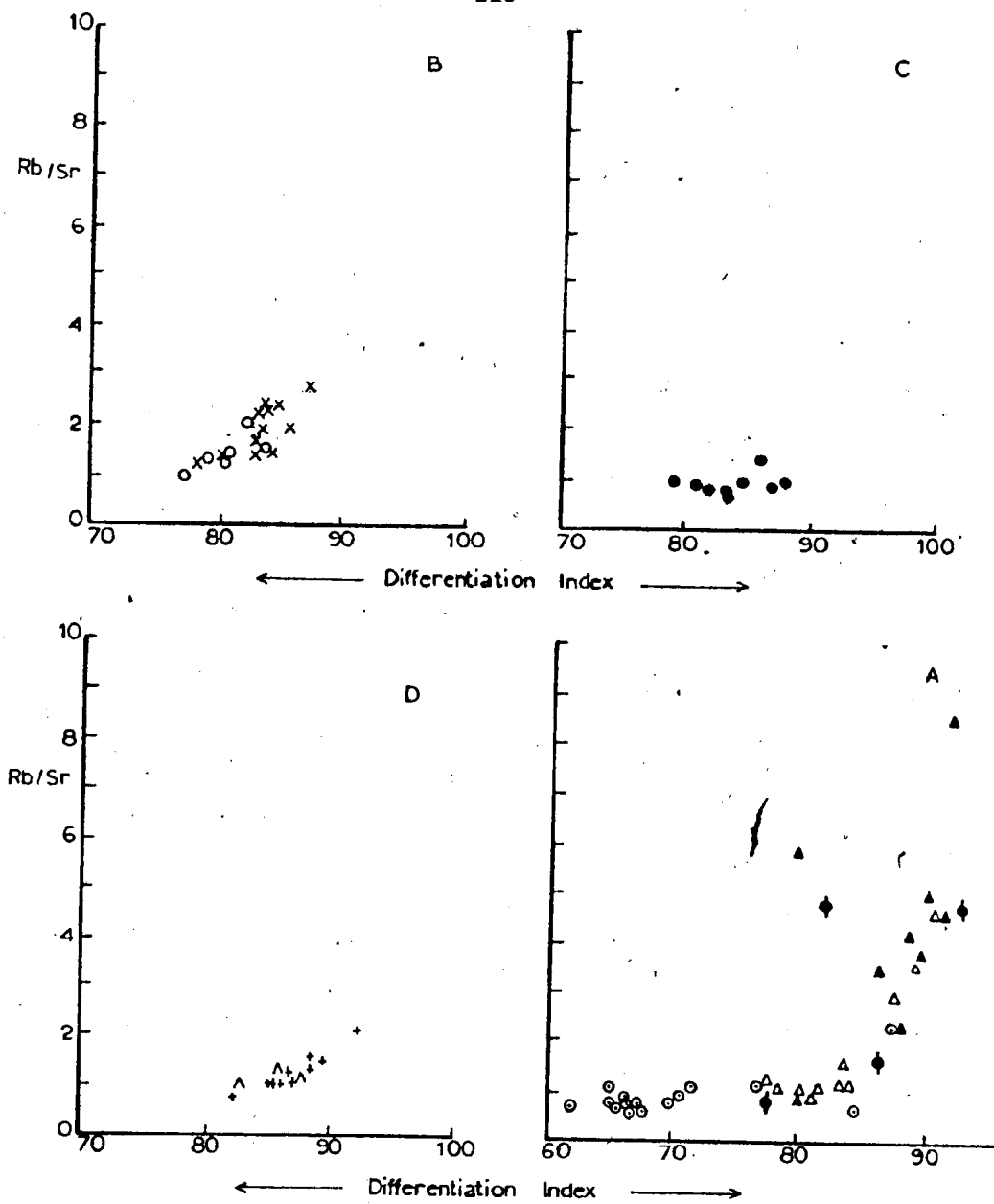


Fig.6.3c

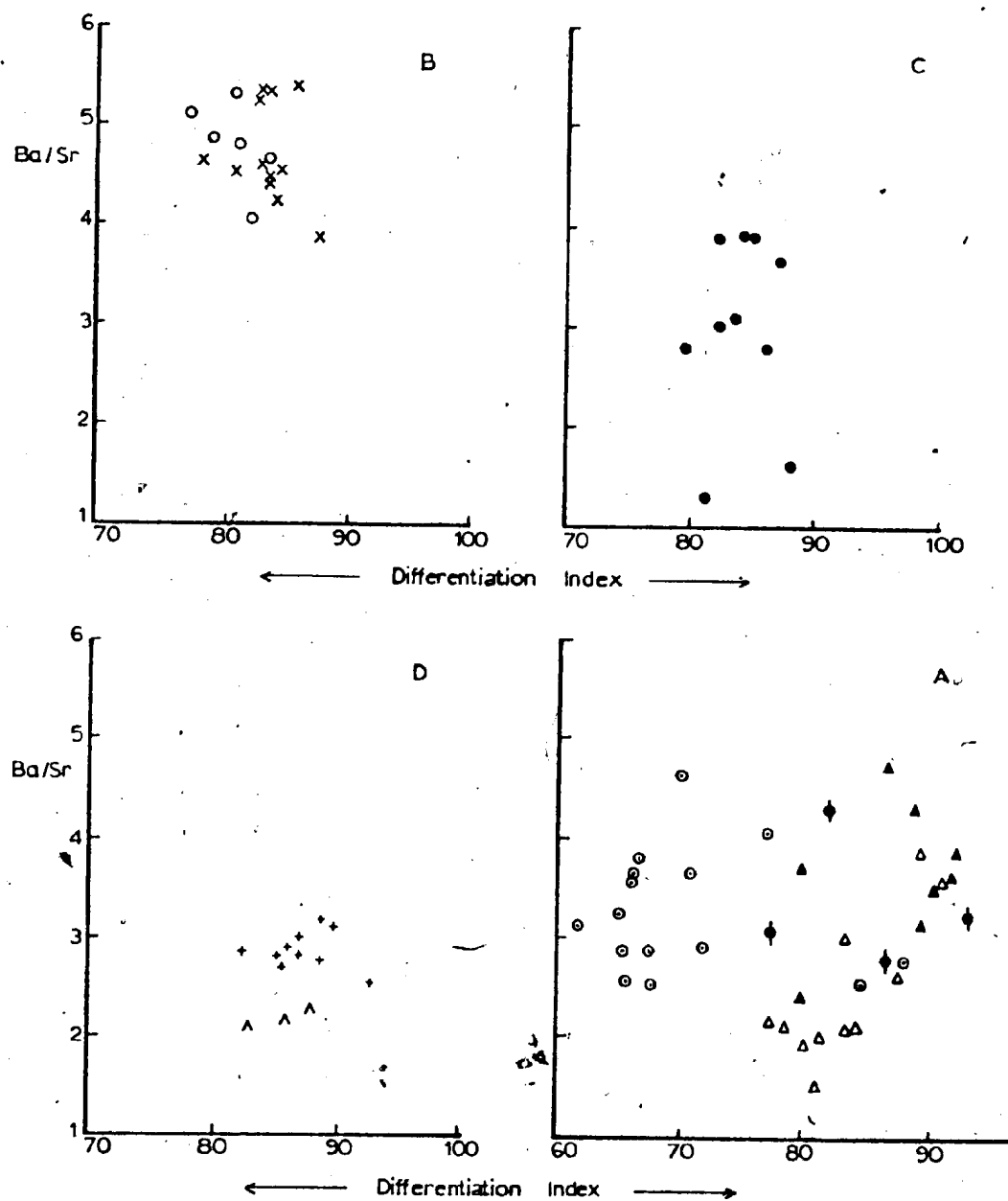


Fig. 6-3d

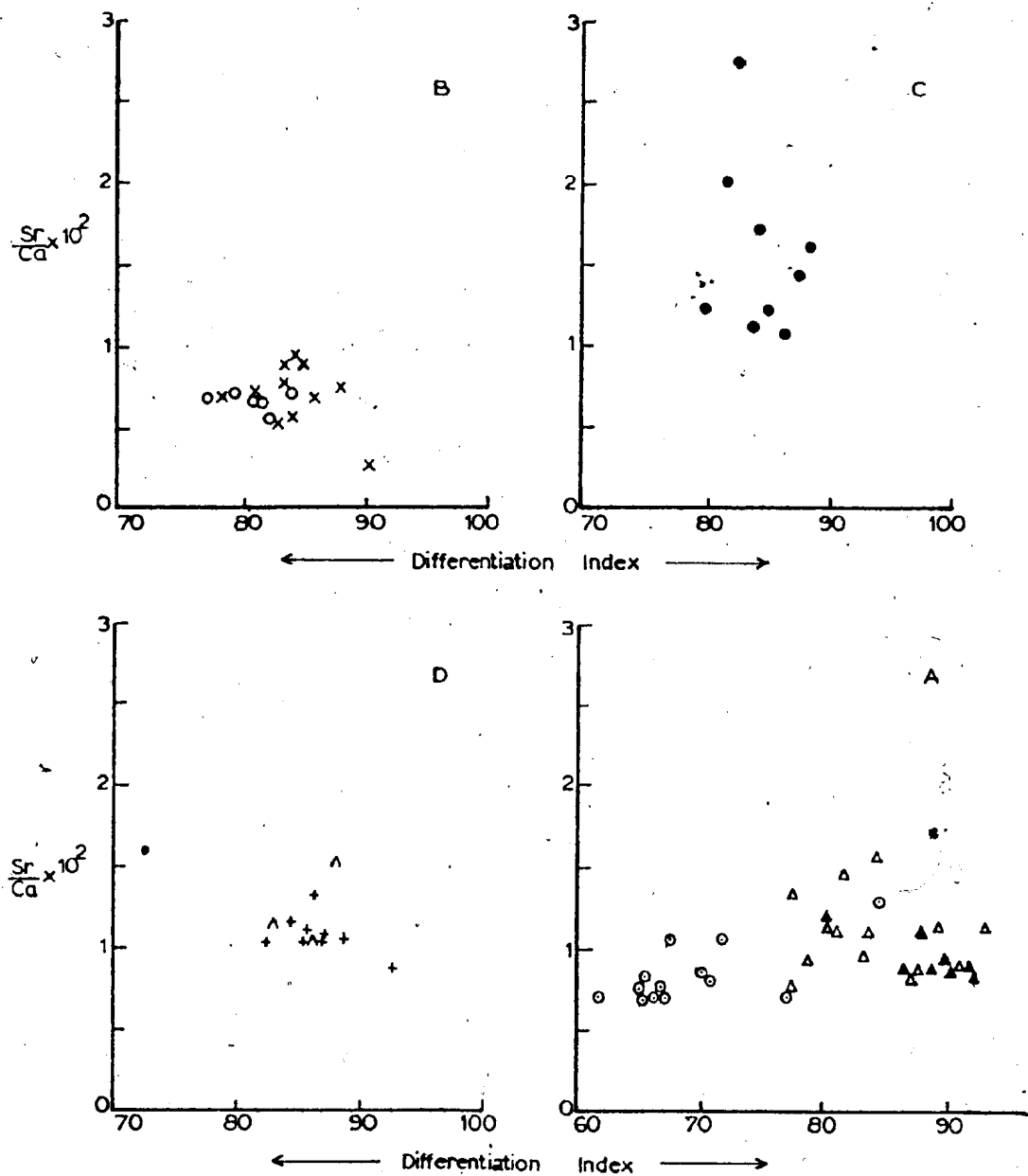


Fig. 6.32

electronegativities and ionization potentials. Rb favours micas over potassium feldspars.  $Ba^{2+}$  is identical in size to  $K^+$  and thus will be captured in the potassium feldspars and micas.  $Sr^{2+}$  enters the  $Ca^{2+}$  positions in plagioclase, apatite and sphene and the  $K^+$  positions in potassium feldspars. These  $Ca^{2+}$  and  $K^+$  positions have the right size to accommodate  $Sr^{2+}$ . The influence of apatite and sphene on the Sr content in coexisting melts is small, mainly because these minerals generally occur in very small percentages. Also the distribution coefficient<sup>1</sup> ( $K_d$ ) of Sr for apatite is small ( $\approx 1$ ). The distribution coefficient of Sr for sphene is not known. Therefore regardless whether the plutons represent melts derived by fractional crystallization of a more mafic magma or melts of crustal rocks, their K/Rb, Ba/Rb, Rb/Sr, Ba/Sr and Sr/Ca ratios are largely controlled by the proportions of plagioclase, potassium feldspar and biotite in the solid phase that coexisted with their parent melts. However, no conclusions as yet can be drawn from the observed variations of the K/Rb, Ba/Rb, Ba/Sr and Sr/Ca ratios of the plutons regarding their origin, apart from a suggestion that both feldspars and micas must have been involved. The variation of Rb/Sr with D.I. is significant as shown below.

The major and trace element variations discussed in the preceding section indicate that the Wareham Quartz Monzonite, the medium-

---

<sup>1</sup> $K_d$  = concentration in mineral/concentration in coexisting liquid.

grained phase of the North Pond Granite and the porphyritic phase of the North Pond Granite may be related through progressive differentiation. The Rb/Sr ratios show only a slight increase going from the Wareham pluton to the medium-grained North Pond Granite. Therefore both Rb and Sr must have been removed, more or less at a constant ratio, from the system during the differentiation of a Wareham-type magma to produce the medium-grained phase of the North Pond Granite. Thus, potassium feldspar and mica must have been present in significant amounts in the solid phase fractionated. From the medium-grained phase to the porphyritic phase of the North Pond Granite Rb/Sr ratios show a pronounced increase. Therefore during the differentiation that produced the porphyritic phase of the North Pond Granite from the medium-grained phase of the North Pond Granite, plagioclase must have constituted a large part of the solid phase fractionated.

### 6.3.. Wareham Quartz Monzonite - North Pond Granite Relationship

The analyses from the granitoids in the area are plotted in the  $\text{Na}_2\text{O} + \text{K}_2\text{O} - \text{FeO} - \text{MgO}$  (AFM),  $\text{Al}_2\text{O}_3 - \text{FeO} - \text{MgO}$  (A'FM) and the  $\text{CaO} - \text{FeO} - \text{MgO}$  (CFM) diagrams in Figures 6.4, 6.5 and 6.6. The analyses from the Wareham and the North Pond plutons plot along a linear trend in the AFM and the A'FM triangles and further strengthens the idea that the two intrusions are related by fractional crystallization. It also shows that the fractional crystallization has taken place keeping the Fe/Mg ratio of the parent magma constant. The analyses from the rest of the intrusions in the area do not define common trends. None of the plutons show a systematic variation in the CFM diagram.

Fig. 6.4. Analyses from the granitoids plotted in the  $(\text{Na}_2\text{O} + \text{K}_2\text{O}) - \text{FeO} - \text{MgO}$  (AFM) diagram. Also shown is the composition of biotites in the Wareham Quartz Monzonite (◇). Dashed line indicates trend defined by calc-alkaline rocks -- after Irvine and Baragar, 1971.

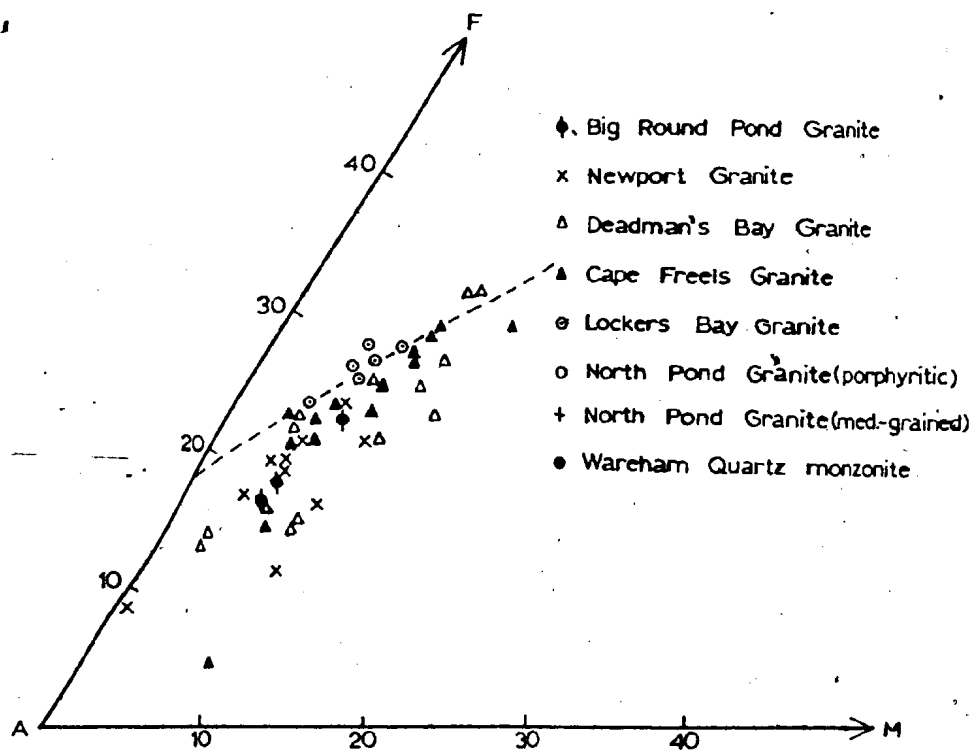
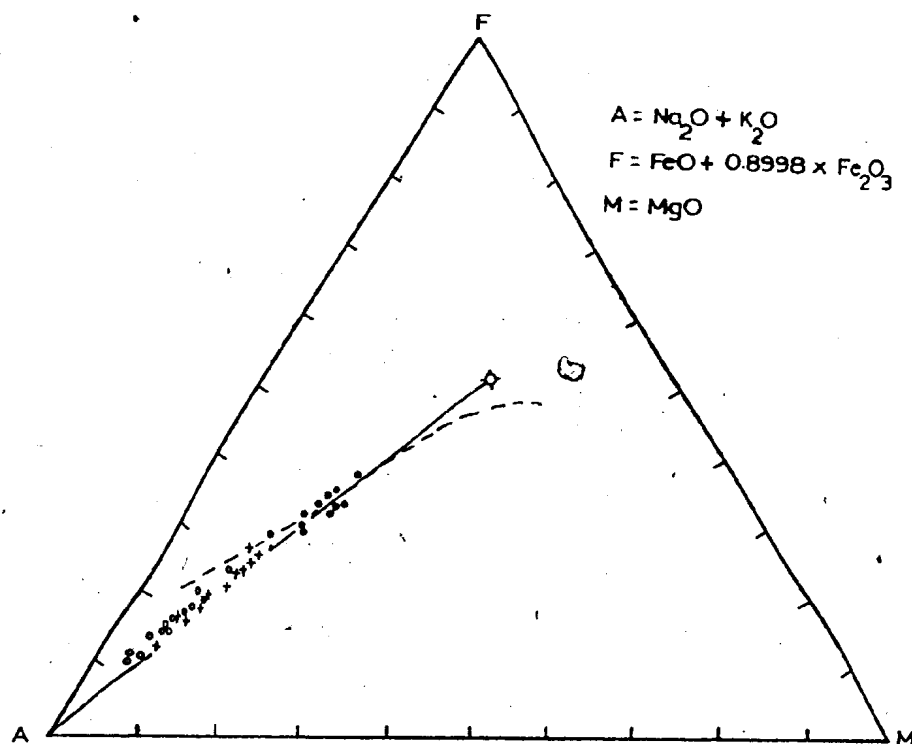




Fig. 6.5. Analyses from the granitoids plotted in the  $\text{Al}_2\text{O}_3$  - FeO - MgO, (A'FM) diagram. Symbols as in Fig. 6.4.

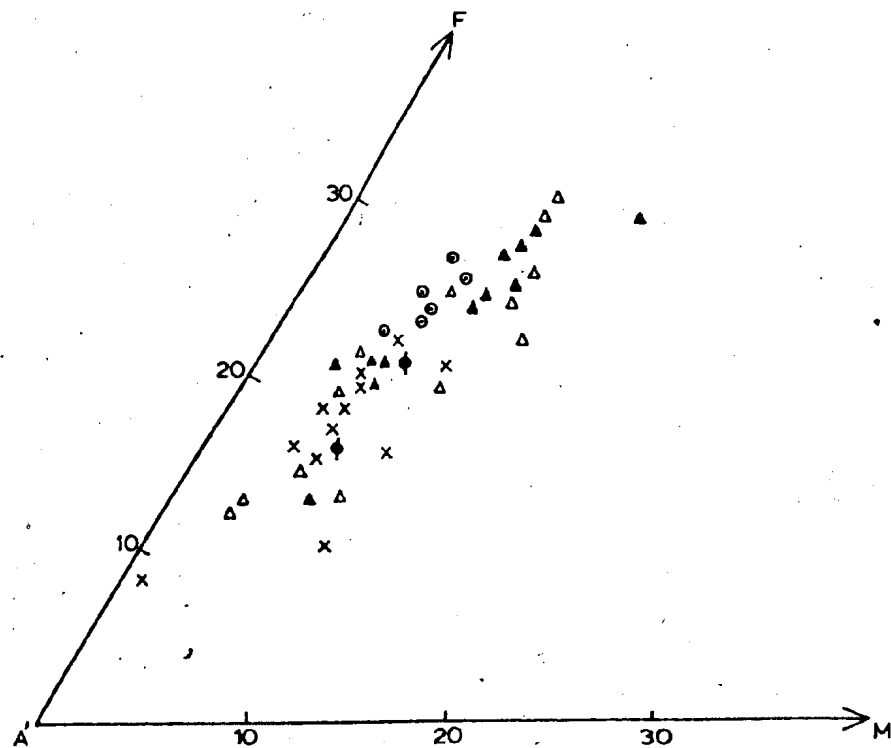
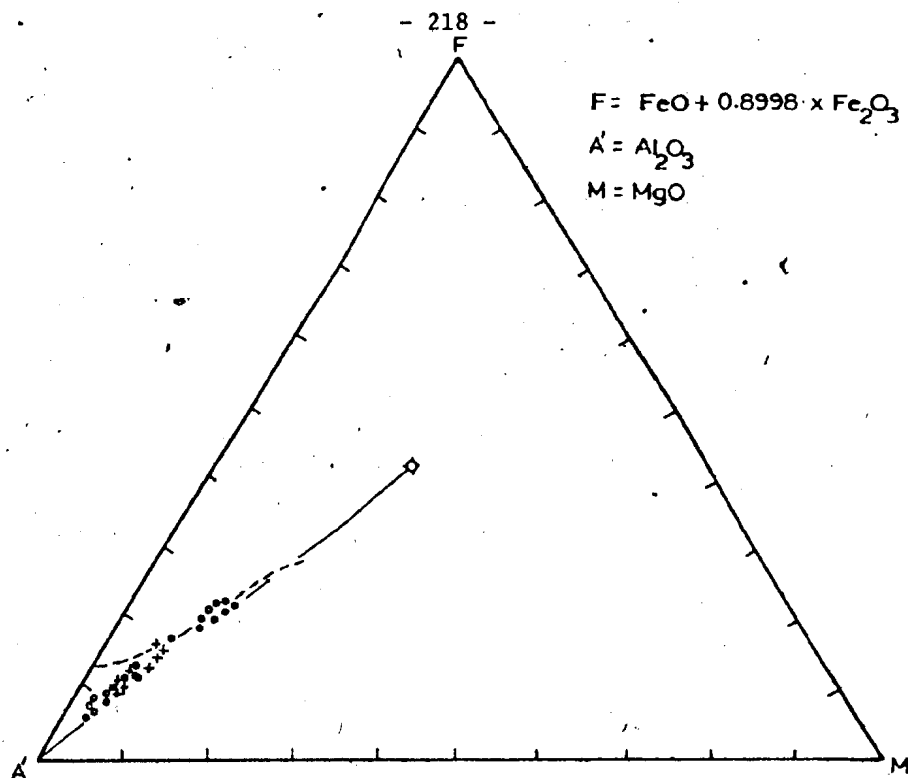
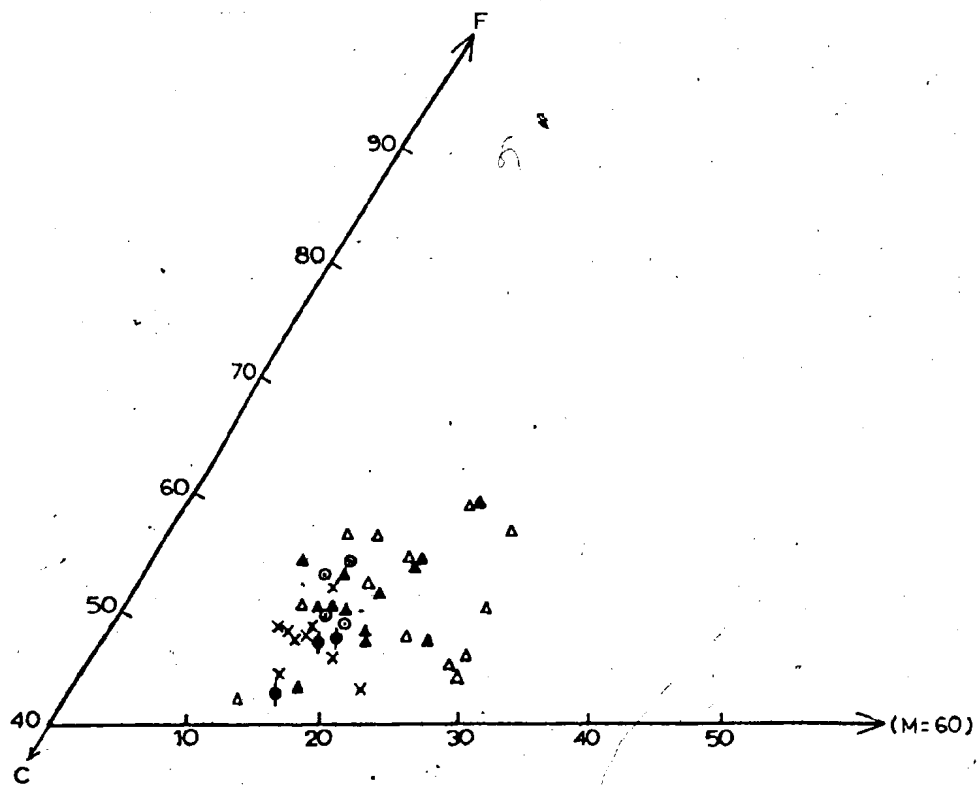
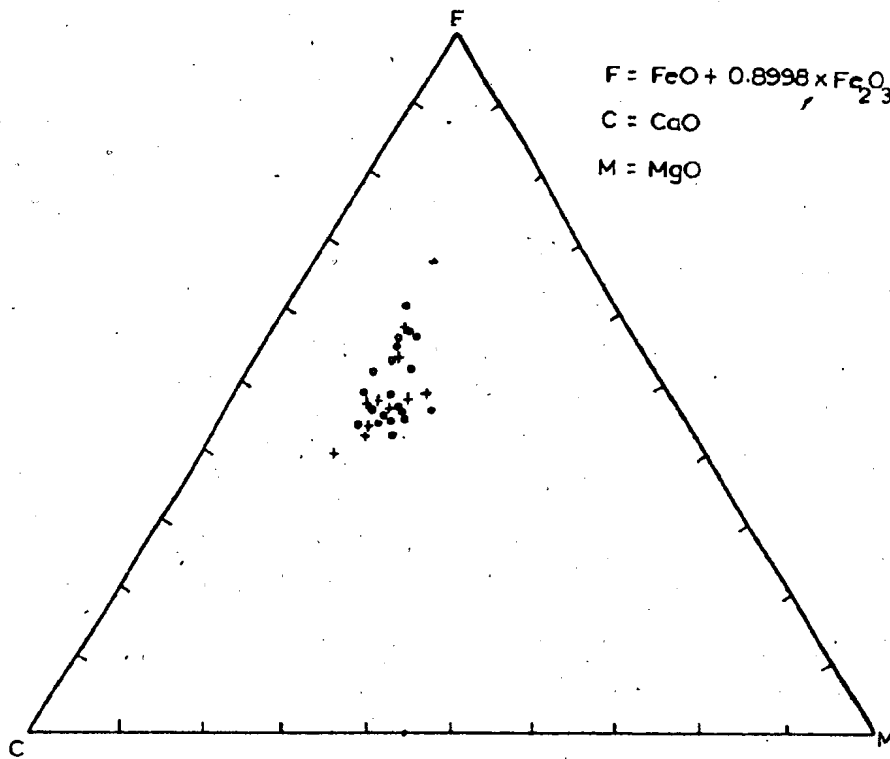


Fig. 6.6. Analyses from the granitoids plotted in the  
CaO - FeO - MgO, (CFM) diagram. Symbols as in  
Fig. 6.4.

- 220 -



Also shown in the AFM and the AFM diagrams are the compositions of biotite from the Wareham pluton. The feldspars from the same plot at the A apex and the A' apex of the above diagrams. If the differentiation which produced the North Pond Granite from a magma similar to the Wareham pluton in composition occurred by the fractional crystallization of biotite and feldspar, then the trend defined by these two plutons should lie along the line joining the feldspars and the biotite compositions. This is indeed the case because the trend defined by the analyses from the Wareham and the North Pond plutons mostly overlie this line.

A quantitative estimate of the percentage of the residual liquid and the nature of the solid phase involved in the differentiation of a Wareham-type magma to produce the two phases of the North Pond Granite can be obtained by geochemical modelling. This was done by comparing the Rb, Ba and Sr contents of the two phases of the North Pond Granite with hypothetical Rb, Ba and Sr abundances in various melts that may be produced by differentiation of the Wareham Quartz Monzonite. The average compositions of the Wareham pluton, the medium-grained phase of the North Pond Granite and the porphyritic phase of the North Pond Granite were used in the modelling. It was assumed that surface equilibrium was maintained between residual liquids and crystallizing solids during fractional crystallization. The distribution coefficients used in this study are given in Table 6.2. Petrochemical subtractions involved in the modelling were done using a computer programme developed by Evans (1978). The results of the geochemical

Table 6.2. Distribution coefficients used in geochemical modelling in this study.

	K-feldspar	Biotite	Plagioclase
Rb	0.34	3.26	0.048
Sr	3.87	0.12	2.84
Ba	6.12	6.36	0.36

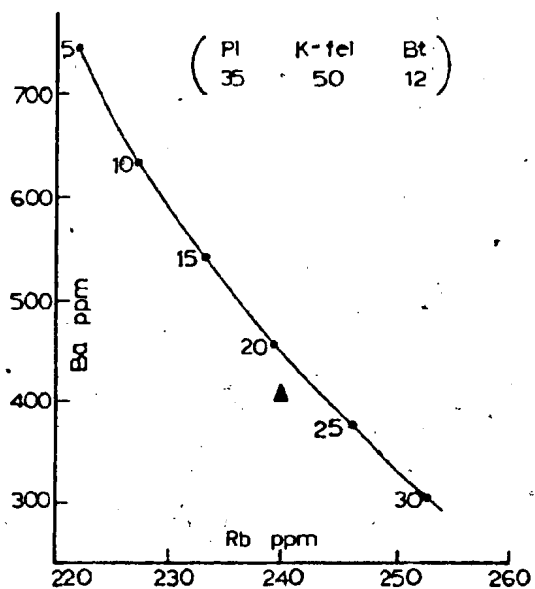
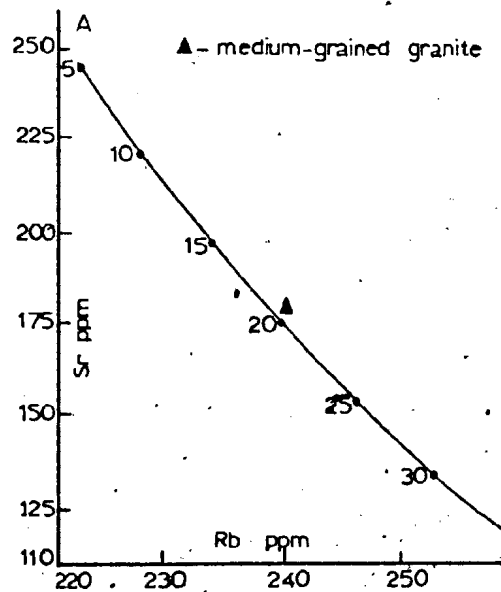
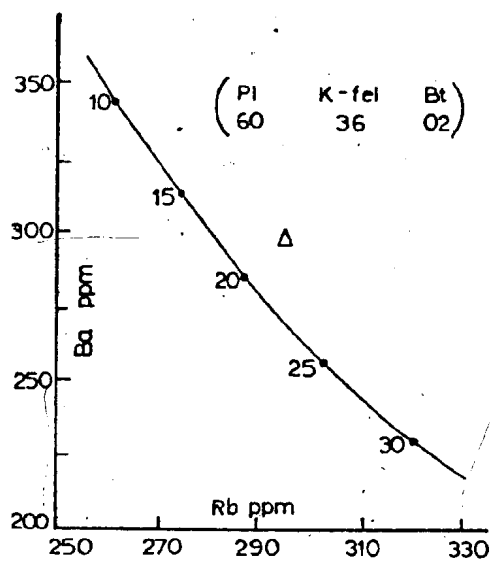
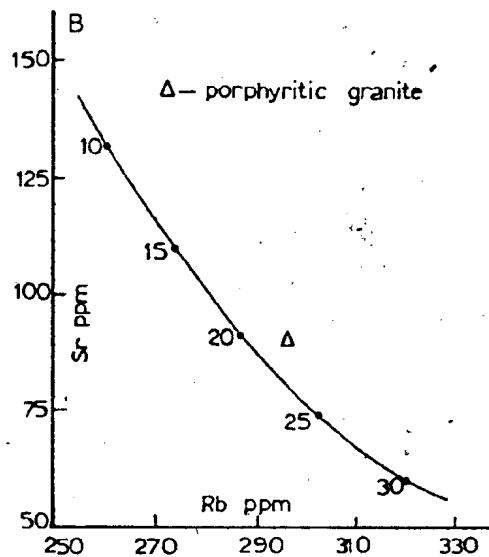
References: Schnetzler and Philpots (1970), Philpots and Schnetzler (1970), Noble and Hedge (1970), Arth (1976).

modelling are illustrated in Figure 6.7. They show that differentiation of a magma similar to the Wareham Quartz Monzonite in composition with the separation of a solid phase consisting of 25% plagioclase, 50% potassium feldspar, 12% biotite and 3% accessory minerals (probably apatite and magnetite) will produce a 20-25% liquid with the composition of the medium-grained phase of the North Pond Granite. Furthermore, separation of a solid phase with 60% plagioclase, 36% potassium feldspar, 2% biotite and 2% accessory minerals (probably apatite and magnetite) from a magma with the composition of the medium-grained North Pond Granite will result in a 20-25% melt having the chemistry of the porphyritic phase of the North Pond Granite. This differentiation sequence is illustrated in Figure 6.8.

The results obtained by geochemical modelling fit with the observed trace element variations in the Wareham - North Pond plutons. During the differentiation of a Wareham-type magma to produce the medium-grained phase of the North Pond Granite, all three phases, plagioclase, potassium feldspar and biotite, crystallized in significant amounts. Therefore, both Rb and Sr were actively removed keeping the Rb/Sr ratio of the residual liquids rather constant. During the differentiation of a melt similar to the medium-grained phase of the North Pond Granite to produce the porphyritic phase of the North Pond Granite, plagioclase was the dominant mineral in the solid phase crystallized. Therefore, Sr was rapidly removed (with respect to Rb) from the differentiating magma, giving rise to the observed increase in Rb/Sr ratios between the two phases in the North Pond Granite (Figure 6.3c, page 210).

Fig. 6.7 The distribution of Ba, Sr and Rb between solid phase and melt; (A) during the differentiation of a Wareham-type magma to produce the medium-grained phase of the North Pond Granite (▲), (B) during the differentiation of a medium-grained phase-type magma to produce the porphyritic-phase of the North Pond Granite (Δ). (Pl K-fel Bt) = approximate mineralogical composition of the solid phase fractionating. Numbers along the curved lines indicate weight percent melt in the system.





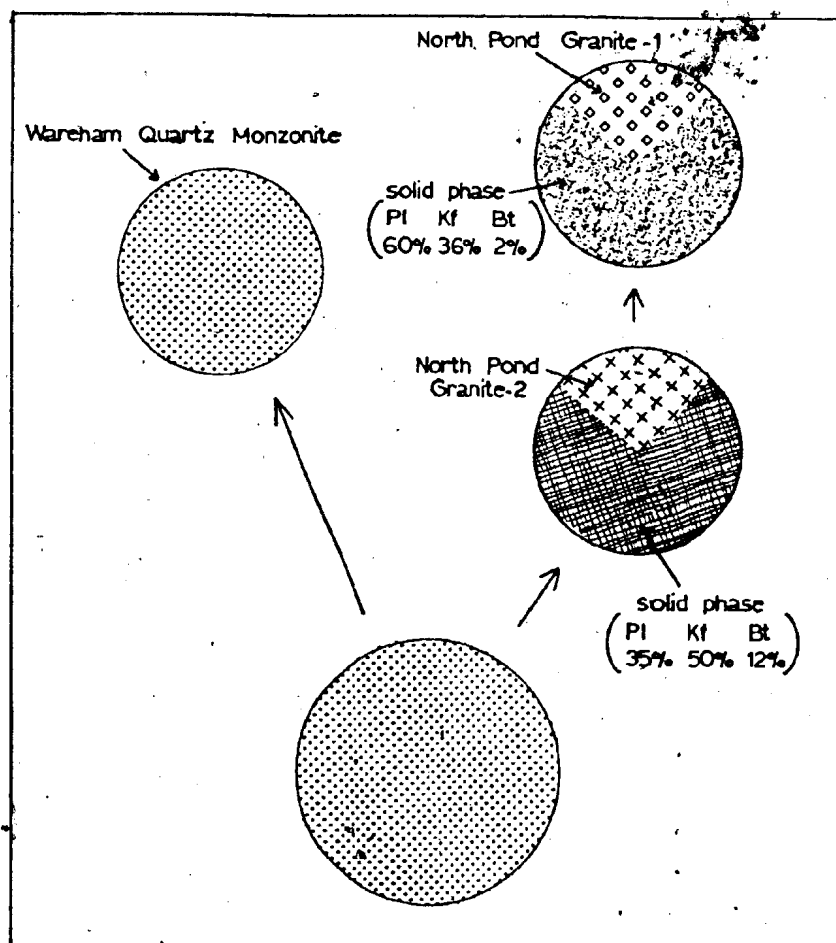


Fig. 6.8 Schematic representation of the possible differentiation sequence that produced the North Pond Granite from a magma similar to the Wareham Quartz Monzonite in composition. North Pond Granite -1 = medium-grained phase, -2 = porphyritic phase. Pl - plagioclase, Kf = potassium feldspar, Bt - biotite.

#### 6.4. Genetic Classifications of the Granitoids based on their Composition

##### 6.4.1. I-type and S-type Granitoids

Chappell and White (1974) recognized two types of granites in eastern Australia. They referred to these as I-type granitoids and S-type granitoids. The chemical and petrological characteristics of the two types as given by Chappell and White are:

1. I-type
  - a. Relatively high Na,  $\text{Na}_2\text{O}$  normally greater than 3.2% in felsic varieties and decreasing to 2.2% in more mafic types.
  - b. Mol.  $\text{Al}_2\text{O}_3/(\text{Na}_2\text{O} + \text{K}_2\text{O} + \text{CaO}) < 1.1$
  - c. C.I.P.W. normative diopside or less than 1% normative corundum
  - d. Broad spectrum of compositions from felsic to mafic lithologies
  - e. Linear trends in variation diagrams
  - f. Contain biotite + hornblende + sphene + magnetite.
2. S-type
  - a. Relatively low Na,  $\text{Na}_2\text{O}$  normally less than 3.2% in rocks with approximately 5%  $\text{K}_2\text{O}$ , decreasing to less than 2.2% in rocks with approximately 2%  $\text{K}_2\text{O}$ .
  - b. Mol.  $\text{Al}_2\text{O}_3/(\text{Na}_2\text{O} + \text{K}_2\text{O} + \text{CaO}) > 1.1$
  - c. Greater than 1% C.I.P.W. normative corundum
  - d. Relatively restricted in composition to high  $\text{SiO}_2$  types
  - e. Variation diagrams are more irregular
  - f. Contain biotite + muscovite + cordierite + garnet + ilmenite.

Based on these characteristics, Chappell and White (1974) concluded that the I-type granitoids were derived from igneous source

materials and that the S-type granitoids were derived from sedimentary source materials.

Most of the above features cannot be used to subdivide the granitic plutons in the thesis area into I and S types. On the average, they have 5%  $K_2O$ , 3.2%  $Na_2O$  and Mol.  $Al_2O_3/(Na_2O + K_2O + CaO)$  ratios of 1:1 (Figure 6.9). In variation diagrams of the plutons, both regular trends and scattered distributions occur. All the plutons contain biotite, sphene, ilmenite and magnetite; garnet and muscovite occur in the North Pond and the Business Cove granites. Thus the criteria a, b, c and f above fail to differentiate the plutons into I and S types. The plutons have greater than 1% C.I.P.W. normative corundum (Appendix 6.2) and most are rich in  $SiO_2$  (only the Wareham pluton has an intermediate composition). Therefore, according to the criteria c and d, the plutons are S-type granitoids derived from sedimentary source rocks.

However, Chappell and White's classification appears to be a rather oversimplified genetic subdivision of granitic rocks. They have ignored the effects of fractional crystallization or melting of different mineral phases in different proportions on the generation of magma. The  $Na_2O$ ,  $K_2O$ ,  $CaO$ ,  $Al_2O_3$  and  $SiO_2$  contents of magmas may be controlled largely by the phases fractionated or melted as well as by the degree of fractionation, melting and contamination by country rocks (see also Strong, 1979). Also they have completely ignored the trace elements that are equally, if not more, important as the major elements, in determining the origin of magmas. Thus, not much significance could be attached to the results obtained by using Chappell and White's scheme of classification.

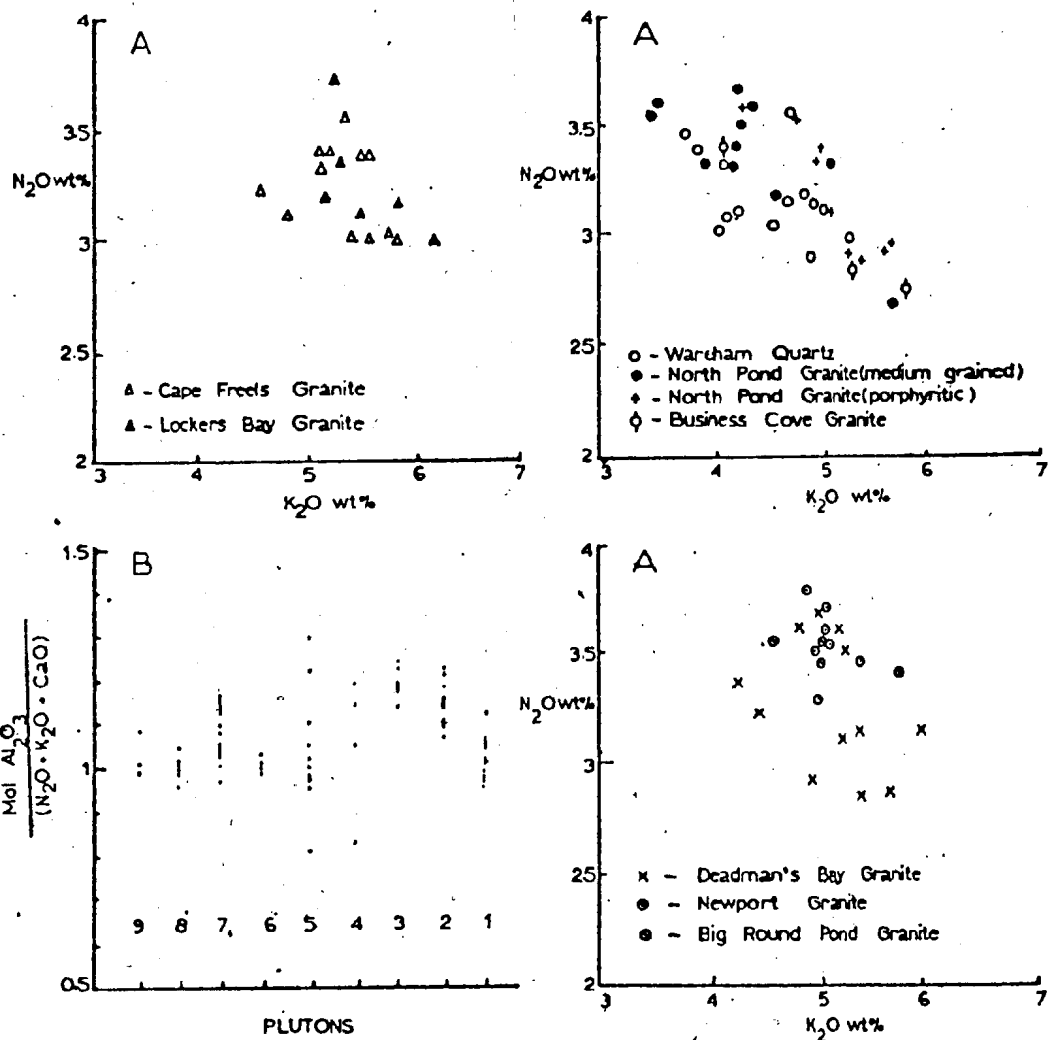


Fig. 6.9. Plots of (A)  $\text{Na}_2\text{O}$  vs  $\text{K}_2\text{O}$  and (B)  $\text{Mol Al}_2\text{O}_3 / (\text{Na}_2\text{O} + \text{K}_2\text{O} + \text{CaO})$  of the granitoids in the area. 1 - Wareham Quartz Monzonite, 2 - North Pond Granite (medium-grained), 3 - North Pond Granite (porphyritic), 4 - Business Cove Granite, 5 - Cape Freels Granite, 6 - Lockers Bay Granite, 7 - Deadman's Bay Granite, 8 - Newport Granite, 9 - Big Round Pond Granite.

#### 6.4.2. Orogenic and Non-orogenic Granitoids

Martin and Piwinski (1974) proposed a genetic subdivision of granitic plutons into orogenic granitoids and non-orogenic granitoids.

The orogenic granitoids were considered to form in areas of crustal shortening, i.e. associated with subduction zones. The non-orogenic granitoids were considered to form in areas of rifting, either continental or oceanic. They listed several differences in chemistry of plutons belonging to these two groups. They are:

1. Plots of  $\text{SiO}_2$ ,  $\text{Al}_2\text{O}_3$ ,  $\text{Na}_2\text{O}$  and  $\text{K}_2\text{O}$  against Differentiation Index define relatively good trends in orogenic granites and are more scattered in non-orogenic granites.
2. Within the Differentiation Index interval 90 to 95, orogenic granites typically contain 0.5 to 1% CaO and MgO almost as a trace content.
3. In orogenic granites CaO and MgO rise at a constant ratio as Differentiation Index decreases.
4. Orogenic granites have a nearly constant Fe/Mg ratio corresponding to a linear trend in the AFM diagram. The trend in AFM diagram for non-orogenic granites consists of two linear segments indicating an iron enrichment.

The variation diagrams in Figure 6.1 shows that criteria 1 and 2 cannot be used to subdivide the plutons in the area into orogenic and non-orogenic types. Plots of  $\text{SiO}_2$  and  $\text{Al}_2\text{O}_3$  against D.I. define regular trends but those of  $\text{Na}_2\text{O}$  and  $\text{K}_2\text{O}$  against D.I. show scattered

distribution. Most of the analyses (greater than 95% of the total number) have D.I. values less than 90. The few analyses with D.I. greater than 90 have CaO and MgO contents between 0.5 and 1%. The CaO and MgO contents of the plutons rise at a constant rate as D.I. decreases. Only the Wareham and the North Pond plutons define linear trends in an AFM diagram, the rest of the plutons in the area show scattered distributions and do not show any sign of iron enrichment. Thus the criteria given by Martin and Piwinski cannot be used to conclusively subdivide the plutons into orogenic and non-orogenic granites. However, there is evidence of a tensional event (intrusion of diabase dikes, see Chapter 5) in the area within the time interval defined by the emplacement of the plutons, but there is no direct evidence to relate their origin to a subduction zone (see Chapter 7).

Like Chappell and White's subdivision, the classification proposed by Martin and Piwinski appears to be oversimplified. Alkali-rich granites, though occurring commonly in areas of rifting, can easily form in other environments too (Burnham, 1967; Strong, 1979). The trends in AFM diagrams are controlled largely by the phases fractionating from a magma and there is no reason why linear trends in AFM diagrams cannot be produced in non-orogenic granites.

#### 6.5. Summary

With the exception of the Wareham Quartz Monzonite, the chemical compositions of the plutons are comparable despite the fact that the North Pond and the Big Round Pond granites are non-megacrystic.

The Wareham pluton is more mafic than the rest of the granitoids. The Business Cove Granite has a very inhomogeneous composition resulting from assimilation of country rocks.

The analyses from the Wareham and the North Pond plutons fall along a single regular trend in variation diagrams for a number of elements and the two plutons may be genetically related through fractional crystallization. Variations in Rb/Sr ratios indicate that during the differentiation of a Wareham-type magma to produce the medium-grained phase of the North Pond Granite, potassium feldspar must have formed a large percentage of the cumulate. During further differentiation, to produce the porphyritic phase of the North Pond Granite from the medium-grained phase-type magma, plagioclase must have been the dominant phase in the cumulate. This was verified by geochemical modelling.

It is believed that the genetic subdivisions of granitic rocks, proposed by Chappell and White (1974) and Martin and Piwinski (1974), are too generalized and are not of much use, at least in the present exercise.

Finally, it must be stated that even though no conclusions as to the origin of the megacrystic granites were drawn from their chemistry as yet, the chemical variations among these plutons are very significant and are discussed in the following chapter on the origin of the granites, where their meaning becomes clearer.



## CHAPTER 7

### ORIGIN OF THE GRANITOIDS

#### 7.1. Introduction

The following evidence indicates that the granitic plutons in the thesis area formed by crystallization of magmas rather than by granitization<sup>1</sup>: (1) The plutons have sharp intrusive contacts that commonly truncate structures in the country rocks. (2) The microcline megacrysts in the plutons, except for a few that may have grown metasomatically, appear to have crystallized from a magma. (3) The Deadman's Bay Granite contains blocks of a chilled lithology that probably represents fragments of an "early" rapidly cooled marginal part of the intrusion. (4) The Wareham pluton and the two phases of the North Pond Granite are related by fractional crystallization. It is the principal aim of this chapter to determine the origin of the parent magma of the granitoids in the area.

There are several possible ways of generating granitic magma. These include:

1. differentiation of basaltic magma;
2. partial melting of mantle lithologies;
3. contamination of basaltic magma by sialic crustal rocks;
4. partial or complete melting of sialic crustal rocks.

The validity of these four models to explain the production of granitic plutons concerned here is tested in the following sections.

---

<sup>1</sup>"Granitization includes any processes by which solid rocks of any composition or origin are transformed into rocks of granitic composition and texture" (Mehnert, 1968).

## 7.2. Differentiation of basaltic magma.

Granitic rocks constitute more than 95 percent of all the intrusive rocks in the area. Gravity studies (Weaver, 1967; Miller, 1977) suggest that there are no noticeable volumes of basaltic rocks within the first 15 kilometers (approximately) beneath the surface of the area. Therefore, by volume considerations alone, it is unlikely that the plutons were produced by differentiation of basalt.

Green and Ringwood (1968) proposed that crystallization of amphibole could produce magmas of intermediate composition (andesitic) which on further differentiation may yield granitic melts. However, fractionation of amphibole will strongly deplete the residual magma in Y with respect to the source, because of the high distribution coefficient ( $k_d$ ) of Y for amphibole in equilibrium with melts of intermediate composition (average dacitic  $k_d$  of Y for hornblende is 6.0; Ewart and Taylor, 1969). The Y contents of the plutons (Table 6.1, page 177) are greater than that of the average composition of basalts given by Prinz (1967). This supports the above conclusion that the plutons could not have been produced by differentiation of basaltic magma.

## 7.3. Partial Melting of Mantle Lithologies

Experimental studies by several authors have indicated that silica-rich melts could be produced by the partial fusion of hydrous mantle compositions. O'Hara (1965) demonstrated that andesitic magma could coexist with probable mantle assemblages composed of forsterite - spinel - orthopyroxene - clinopyroxene. Kushiro et al. (1968, 1972) and Kushiro (1973) showed that partial melting of hydrous peridotite

yields melts of andesitic and dacitic composition. In the olivine-diopside (clinopyroxene) - quartz - garnet tetrahedron (Figure 7.1), mantle composition plot in the olivine - diopside - enstatite (orthopyroxene) - garnet volume. Under anhydrous conditions melts formed by the partial fusion of mantle compositions lie on the olivine side of the diopside - garnet - enstatite plane. In the presence of water, the primary phase field of olivine expands and extends into the diopside - enstatite - garnet - quartz space, and silica-rich melts may be produced. The water necessary for the "wet" melting in the mantle is supposed to be supplied by subduction zones (either as pore fluids in subducted sediments or by breakdown of hydrous minerals).

Ringwood (1974) proposed a multistage model to explain the generation of andesitic magmas associated with subduction zones. It involved generation of rhyodacite - rhyolite magmas by partial melting of quartz eclogite in subduction zones, their reaction with overlying mantle wedge to form pyroxenites, diapiric uprise of pyroxenites followed by partial melting to produce basalt and andesite. Differentiation of the andesites may have resulted in more silicic melts. Huang and Wyllie (1973), based on phase relations in the system Ab - Or - Qz, disputed the possibility of generating rhyolitic melts in subduction zones. On the other hand, Burnham (1979) proposed that melts produced by the partial melting of subducted oceanic crust will rise into the overlying crustal rocks and undergo extensive assimilation resulting in calc-alkalic magmas.

The above models indicate that subduction of oceanic crust is a necessary part in the generation of granitic melts by partial

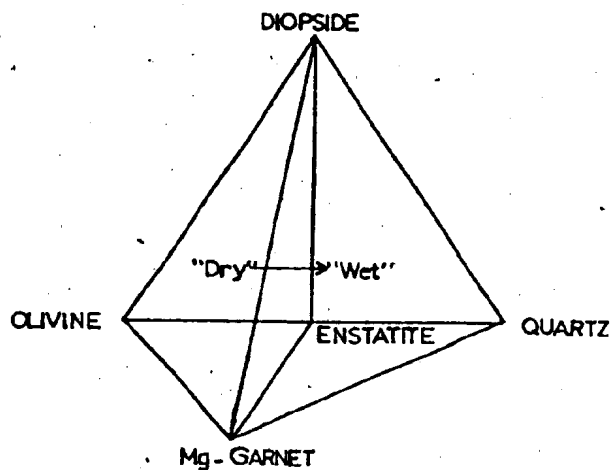


Fig. 7.1. Diagram showing the melting behaviour of mantle compositions. Under dry conditions melts formed by the partial fusion of mantle compositions lie on the olivine side (X) of the diopside-garnet-enstatite plane. In the presence of  $H_2O$ , primary fold of olivine extends into the diopside-enstatite-garnet-quartz space (Y) and silica-rich melts may be produced.

melting of mantle compositions. However it is very unlikely for large volumes of granitic magmas to be produced by partial melting of mantle rocks associated with subduction zones. Presnall and Batemann (1973) pointed out that even though andesites are common in oceanic environments, granitic batholiths are rarely found outside the continental regime. This implies that sialic crust is necessary for the formation of granitic melts. Also there is no evidence to relate the granitoids in the area to a subduction zone. The plutons have been emplaced in the Silurian-Carboniferous time interval (see section 3.5, page 136) and subduction that took place during the closure of the "proto-Atlantic Ocean" in Newfoundland had stopped by Middle Ordovician (Strong, 1977, 1979; Dean, 1978). Therefore the plutons do not represent magmas produced by the partial melting of mantle lithologies during subduction.

#### 7.4. Contamination of Basaltic Magma by Sialic Crustal Rocks

It was found that mixtures of basalt and material having average composition of the crust or mixtures of basalt and the migmatites in the area (Hare Bay Gneiss) cannot have produced the plutons. For example, Figure 7.2 shows the  $\text{SiO}_2$ ,  $\text{TiO}_2$ ,  $\text{MgO}$  and  $\text{Na}_2\text{O} + \text{K}_2\text{O}$  contents of the above mixtures in the range of 90% to 10% by weight of basalt in each mixture. The average composition of basalt used is that given by Manson (1967) and the average composition of granodiorite (Table 6.1, page 177) is taken as the average composition of the crust (Wedepohl, 1971). Comparison of the average compositions of the plutons (Table 6.1) with Figure 7.2 shows that even mixtures with 10% basalt to 90%

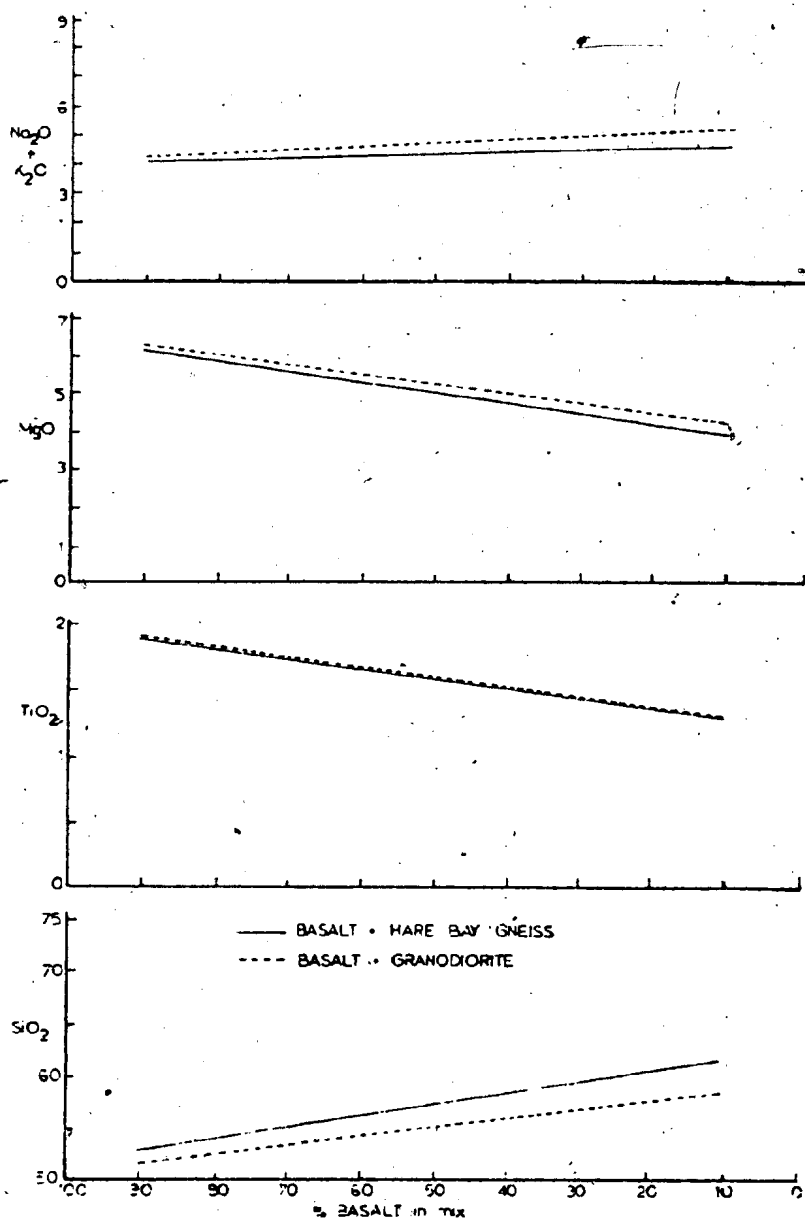


Fig. 7.2.  $(\text{Na}_2\text{O} + \text{K}_2\text{O})$ ,  $\text{MgO}$ ,  $\text{TiO}_2$ , and  $\text{SiO}_2$  contents in mixtures between (1) basalt and granodiorite, (2) basalt and Hare Bay Gneiss.

other component (granodiorite or Hare Bay Gneiss) are very much different in composition to the plutons. Therefore, the "parent" magmas of the granitoids in the area could not have been produced by this mechanism. Also, the fact that the majority of the plutons have a similar chemistry and the absence of intermediate compositions, except for the Wareham Quartz Monzonite, support this idea.

#### 7.5. Partial or Complete Melting of Crustal Rocks

The initial  $\text{Sr}^{87}/\text{Sr}^{86}$  ratios of the plutons (Cape Freels Granite - 0.7078, Lockers Bay Granite - 0.7145, Newport Granite - 0.7059, Wareham Quartz Monzonite - 0.7079; see Table 3.2, page 140 for details) suggest that they may have formed by the melting of crustal rocks. Even though these initial  $\text{Sr}^{87}/\text{Sr}^{86}$  ratios are higher than the  $\text{Sr}^{87}/\text{Sr}^{86}$  ratios in the mantle they are much lower than the average  $\text{Sr}^{87}/\text{Sr}^{86}$  ratio of 0.715 that Faure and Powell (1972) calculated would have existed in "typical" continental crust at the time of the intrusion of the plutons, i.e. about 400-300 Ma ago. This implies that the source rocks of the plutons were probably lower in Rb than such "typical" continental crust since the amount of radiogenic  $\text{Sr}^{87}$  depends on the Rb content.

Greywacke is a common crustal rock with low Rb contents. (Condle et al., 1970; Pettijohn, 1978). Greywacke and lithologies similar to greywacke in composition are common in the northern Gander Zone (Jenness, 1963; R. F. Blackwood, personal communication, 1979). Further, it has been demonstrated both experimentally and by petro-chemical considerations that partial melting of greywacke could yield

granitic melts (Harris et al., 1970; Kilinc, 1972; Albuquerque, 1977). Therefore it is possible that the plutons in the area may have been formed by partial melting of greywacke. This model can be tested by comparing the trace element contents in the plutons with calculated trace element abundances in liquids that may be produced by the partial melting of greywacke. This was done by geochemical modelling using Ba and Sr. It was shown earlier (page 214) that the North Pond and the Business Cove granites were produced by differentiation of a magma similar to the Wareham pluton in composition and thus they are not dealt with in this modelling.

The model employed is that of Shaw (1970) where the melt remains in equilibrium with the solid phase until removed. Under this condition, the concentration of any element in the melt ( $c^1$ ) is given by the expression:

$$\frac{c^1}{C_o} = \frac{1}{D_o + F(1-D_o)} \quad \text{where } C_o = \text{original concentration of the element in the source.}$$

$D_o$  - bulk distribution coefficient of the element for the solid phase.

$D_o = K_\alpha X^\alpha + K_\beta X^\beta + \dots$ , where  $K_\alpha, K_\beta \dots$  are the distribution coefficients of the element for the minerals  $\alpha, \beta, \dots$  whose proportions in the solid phase are  $X^\alpha, X^\beta, \dots$  etc.

$F$  - proportion of the melt.

The distribution coefficients used in this study are given in Table 6.2., page 222. They have been calculated for minerals coexisting with



lavas, and their behaviour at P, T conditions of melting of crustal rocks at depth is not known. Also, the source composition used in the modelling is an assumed one based on little evidence (the initial  $\text{Sr}^{87}/\text{Sr}^{86}$  ratios of the plutons and the low Rb contents in typical greywacke; see page 239). Therefore, the result obtained by the modelling is only an approximation to the processes that may have taken place during the generation of the parent magmas of the plutons.

The composition of the source rocks of the plutons is assumed to be the same as the average composition of greywacke by Wedepohl (1978)\*. Initially, for each pluton, the composition of the solid phase after 5%, 10%, 15% .... up to 50% melting of the source rocks to produce melts similar in composition to the intrusion concerned was determined using a method described by Cawthorn (1974). It was found that greywacke does not have sufficient  $\text{K}_2\text{O}$  to produce a magma similar to the Wareham Quartz Monzonite in composition at melting greater than 45% and to produce magmas similar to the other granitoids in composition at melting beyond 35%. Therefore the Wareham Quartz Monzonite may have been produced by less than 45% melting of the source rocks and each of the rest of the intrusions by less than 35% melting of the source rocks. Thus, the mesonorm of the solid phase, at each 5% increase in degree of melting was determined up to 45% melting of the source rocks in the case of the Wareham pluton and up to 35% melting for the rest of the intrusions.

---

\*  $\text{SiO}_2$  - 66.7,  $\text{TiO}_2$  - 0.6,  $\text{Al}_2\text{O}_3$  - 13.5,  $\text{FeO}_{\text{total}}$  - 4.95,  $\text{MnO}$  - 0.1,  $\text{MgO}$  - 2.1,  $\text{CaO}$  - 2.5,  $\text{Na}_2\text{O}$  - 2.0,  $\text{K}_2\text{O}$  - 2.0,  $\text{P}_2\text{O}_5$  - 0.2, Rb - 80, Ba - 380, Sr - 200, oxide contents in wt%, trace elements in ppm.

The results are given in Appendix 7.1 and were used as a guide to the mineralogy of the solid phase in the modelling.

It was found that for all the plutons, the solid phase after more than 15% melting of the source rocks consists of quartz, plagioclase, biotite, hypersthene, corundum, sphene, magnetite and apatite. Except for biotite, the distribution coefficients of Ba for the rest of the minerals in the residue are very small. In the case of Sr, only plagioclase and apatite have significant distribution coefficients. The distribution coefficients of Ba and Sr for sphene are not known. But both apatite and sphene occur only in accessory quantities in the residue. Therefore the Ba and the Sr concentrations of the parent magmas, of the plutons, if they were produced by greater than 15% melting of the greywacke, depend strongly on the biotite and the plagioclase contents in the residue, respectively. Figure 7.3 shows the distribution of Ba and Sr in the more significant models, among the large number of models tested. Table 7.1 shows the approximate degree of melting of greywacke and the plagioclase and the biotite contents in the residue corresponding to each of the plutons concerned, deduced from Figure 7.3.

Table 7.1 -- The degree of melting (F) of the source rocks (greywacke) and the plagioclase (Pl) and the biotite (Bt) contents in the residue required to produce the parent magmas of the plutons.

<u>Intrusion</u>	<u>F%</u>	<u>Pl wt%</u>	<u>Bt wt%</u>
Wareham Quartz Monzonite	40	10-15	0-1
Lockers Bay Granite	30-35	30-40	2
Cape Freels Granite	30	20-25	4
Deadman's Bay Granite	25	15-20	4
Newport Granite	15	15-20	7
Big Round Pond Granite	25	20	7

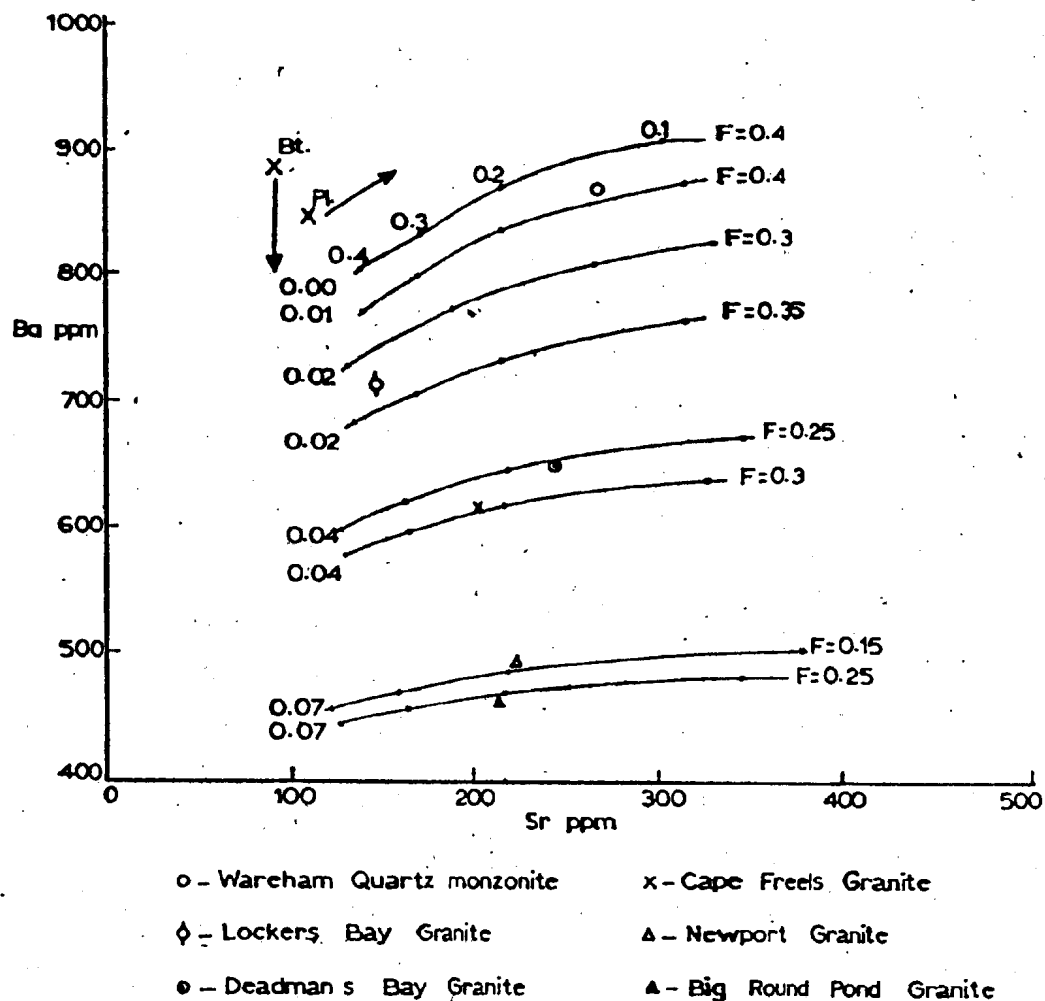


Fig. 7.3. Hypothetical Ba and Sr contents of partial melts derived from the "average" greywacke in equilibrium with a solid phase containing plagioclase and biotite,  $X$  = weight fraction of mineral-plagioclase (Pl) or biotite (Bt) - in the solid phase,  $F$  = degree of melting. Computed using average rhyolitic distribution coefficients (Table 6.2, page 222).

The higher degree of melting and the lower contents of biotite in the residual solid phase should make the Wareham Quartz monzonite more mafic than the rest of the intrusions. This conclusion fits well with the major and trace element chemistry and the lithology of the plutons. Again, based mainly on the degree of melting and the biotite content in the residual solid phase, the Lockers Bay Granite should be slightly more mafic than the Cape Freels, Deadman's Bay, Newport and the Big Round Pond granites. On the same grounds, the Newport Granite must be more felsic than the other intrusions shown in Figure 7.3. Both these facts are reflected in the variation diagrams for the major and trace elements, particularly in those with regular trends. The fact that the conclusions drawn on the basis of the geochemical modelling are reflected in the overall chemistry of the plutons lends support to the idea that the granitoids may have been produced by partial melting of greywacke according to the conditions shown in Figure 7.3 and Table 7.1.

The modelling illustrates another interesting feature of the plutons. That is the older (pre-shear zone) Wareham, Lockers Bay and the Cape Freels plutons were produced by greater degrees of melting of the source rocks than were the younger (post-shear zones) Deadman's Bay, Newport and the Big Round Pond granites. It can be speculated that perhaps the older plutons may have formed by melting in a deeper level than in the case of the younger plutons.

In summary, out of the four mechanisms proposed in the introduction, only the fourth one -- the partial melting of sialic crustal rocks, appears to have been capable of producing the granitoids

in the area. The parent magmas of the plutons were probably produced by 15 to 40% melting of greywacke leaving behind a residue with quartz, plagioclase, biotite, hypersthene, corundum, sphene, magnetite and apatite; the last three minerals occur in accessory amounts.

#### 7.6. Cause of the Melting of the Source Rocks

The regional metamorphic grade in the area, as recorded by the mineral assemblage in the Square Pond and the Hare Bay Gneisses (page 30) is of the low pressure-high temperature type. This suggests that the geothermal gradient in the area was in excess of  $25^{\circ}\text{C}/\text{km}$ . The gabbros and the diabase dikes in the area are indicative of mafic magmas intruded into crustal rocks at depth. The shear zones imply that shear heating may also have contributed to the heat budget in the area along with the ambient geothermal gradient and the heat supplied by crystallizing mafic magmas.

The granitoids studied have formed by the partial melting of sialic crustal rocks. Therefore they must have formed at pressures less than 10 kb, but above 3.5 kb, because primary muscovite occurs in some of the intrusions (the North Pond and the Business Cove granites) and the muscovite solidus intersects the "hydrous" granite solidus at approximately 3.5 kb and  $650^{\circ}\text{C}$  (Figure 7.4). The geochemical modelling indicates that a part of the biotites in the source rocks of the plutons was melted while the rest of the biotites remained as a residual phase in producing the parent magmas of the plutons. Therefore, the melting of the source rocks has occurred within the temperature interval defined by the biotite solidus and the biotite

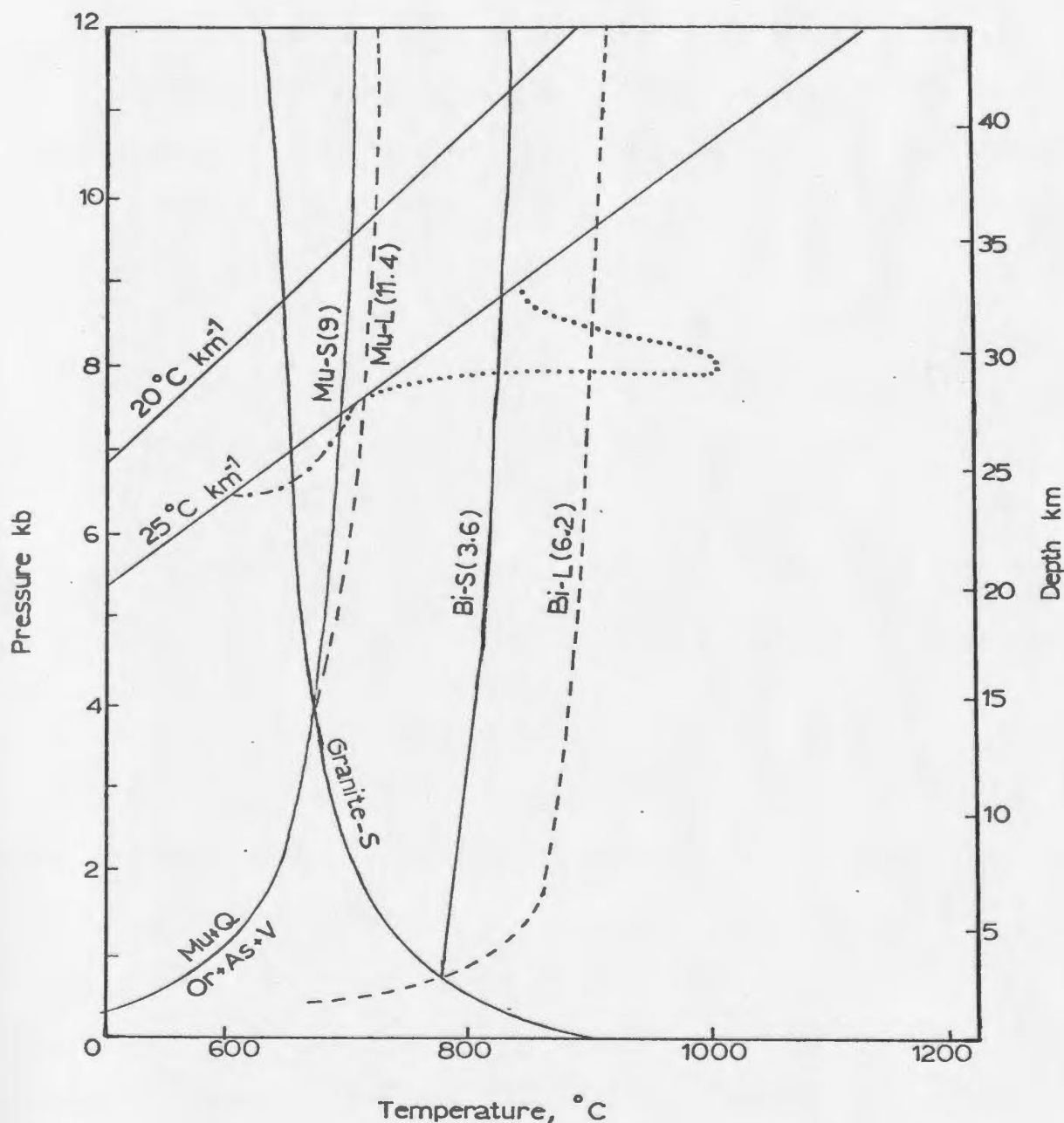


Fig. 7.4. Pressure and temperature grid of some melting and reaction relations pertinent to the generation of the granitoids. The solid line labelled "granite-s" is the "wet" granite solidus as shown by Wyllie (1977). The solid and dashed lines labelled Mu and Bi are solidus and liquidus for muscovite and biotite as given by Burnham (1979). The dotted line and the dashed dotted line indicate possible modifications of the  $25^{\circ}\text{C km}^{-1}$  geotherm by intrusion of mafic magma and by frictional heating, respectively. The equilibrium curve muscovite (Mu) + quartz (Q)  $\rightleftharpoons$  orthoclase (Or) + aluminum silicate (As) +  $\text{H}_2\text{O}$  (V) is after Day (1973).

liquidus; that is, between 800°C and 900°C (Figure 7.4). Under a geothermal gradient of 25°C/km these temperatures could be attained at pressures of 9 to 10 kb (Figure 7.4). Burnham (1979) showed that intrusion of mafic magma into crustal rocks at 600°C would bring the surrounding country rocks to a temperature close to 1000°C. Therefore, intrusion of mafic magma could have caused melting in the source rocks of the plutons even at pressures less than 9 kb. The possible change in an ambient geothermal gradient of 25°C/km, due to intrusion of mafic magmas into crustal rocks at a depth of 30 km is shown in Figure 7.4, which clearly illustrates that the necessary heat for the melting of source rocks of the plutons could have readily been supplied by this mechanism.

Reitan (1968a, 1968b) demonstrated that frictional heating could raise the temperature in crustal rocks by about 100°C. But once melting occurs, even at 1 to 2% melting of the rocks, heating through this mechanism ceases. Therefore, frictional heating will not increase the temperature of crustal rocks much above the solidus. A possible modification of the 25°C/km geothermal gradient by frictional heating at about 7 kb is shown in Figure 7.4. It is probable that this kind of heating may give rise to melting in muscovite bearing assemblages, but it is not capable of producing temperatures needed for the breakdown of biotite. Therefore, the heat supplied by mafic magmas intruded at depths within a relatively high ambient geothermal gradient (which appears to have been greater than 25°C/km) may have caused the partial melting in the source rocks of the plutons.

### 7.7. H<sub>2</sub>O Content: Crystallization Sequence

Biotite is a liquidus phase in all the granitic plutons in the area. According to Burnham (1979) for biotite and muscovite to crystallize from granitic melts, the H<sub>2</sub>O content in the latter must be above approximately 3.6 wt% and 9 wt% respectively. Therefore, the parent magmas of the plutons must have had in excess of 3.6 wt% H<sub>2</sub>O and in the North Pond and the Business Cove granites it must have exceeded 9 wt%.

As shown earlier, the plutons have crystallized between 10 kb and 3.5 kb. Several authors have investigated the phase relations in granitic melts at pressures within this pressure interval and at varying temperatures and H<sub>2</sub>O contents of the melts (Figure 7.5). However, the crystallization sequence in granitic melts at the above pressure range and at a given H<sub>2</sub>O content, as deduced from the experimental work by different authors, vary considerably as shown in Table 7.2.

Winkler et al. (1975, 1978) described a method of determining the crystallization sequence of quartz and feldspars in a pluton by its position in the quartz-albite-orthoclase-anorthite-H<sub>2</sub>O system\*. The composition of the pluton represented by the quartz (Qz), albite (Ab), orthoclase (Or), anorthite (An) contents in the mesonorm with Qz + Ab + Or + An calculated to 100% is plotted on the Qz-Ab-Or projection and the An-Ab-Or projection. The crystallization sequence is then inferred by considering the position of the plot of the composition of the pluton relative to the three cotectic surfaces

---

\* with excess H<sub>2</sub>O.



Fig. 7.5 Phase assemblage diagram for a synthetic granite -  $H_2O$  system showing the minerals that would crystallize, (A) at differing temperatures and water contents at 8 kb and 5 kb (after Namey, 1979) and (B) at differing pressures and water contents at  $750^\circ C$  (after Whitney, 1975). Abbreviations are: opx or o - orthopyroxene, cpx or c - clinopyroxene, Q - quartz, Bt - biotite, Pl - plagioclase, Af - alkali feldspar, Ep - epidote, Hb - hornblende, L - liquid, V - vapour. The phase diagram for 5 kb was constructed by linear extrapolation between Namey's data for 8 and 2 kb pressures.

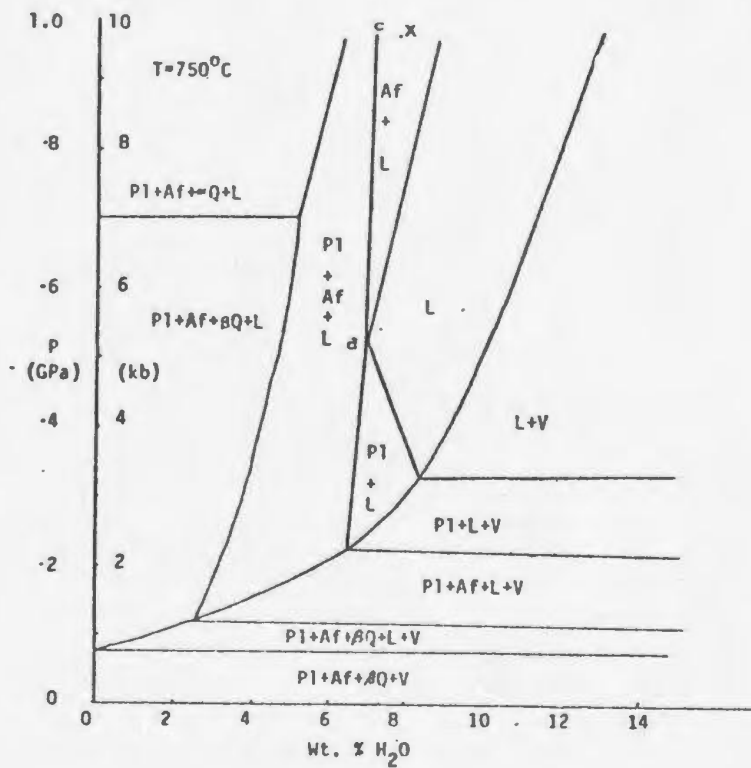
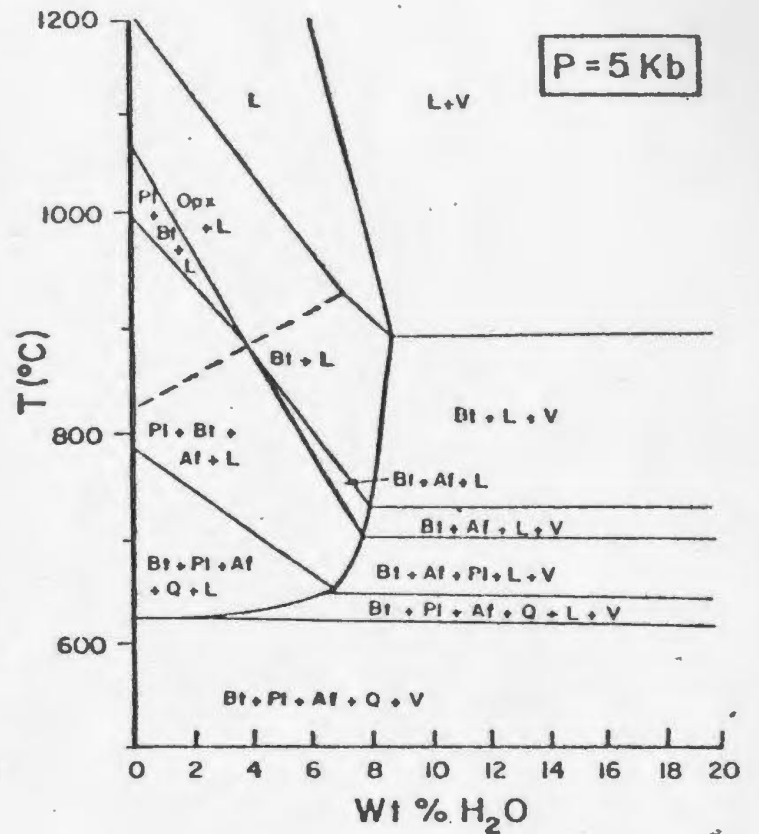
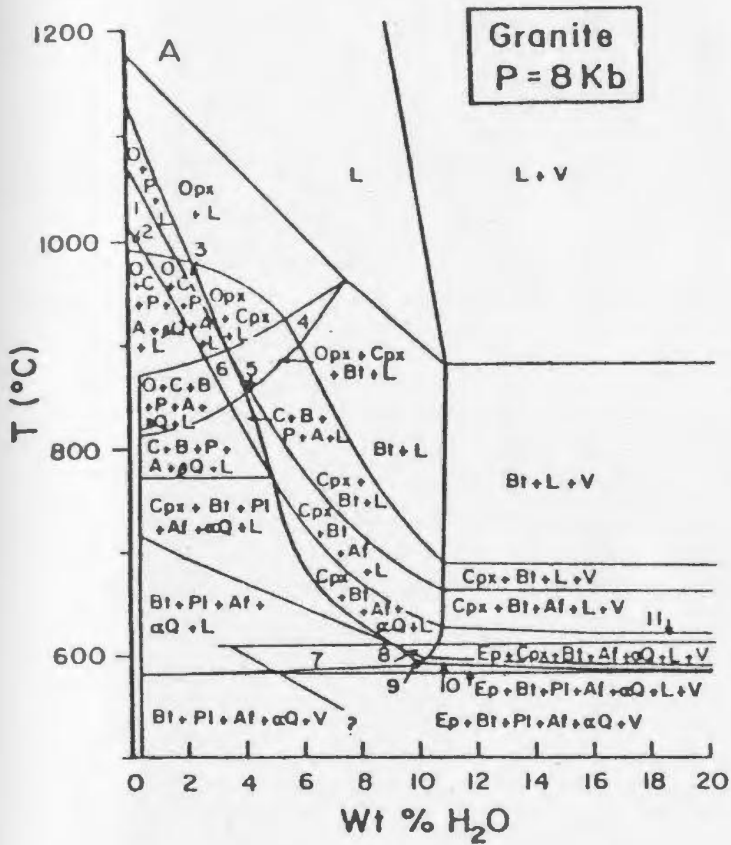


TABLE 7.2 Crystallization sequence in granitic melts. (Abbreviations as in Fig. 7.5).

A. After Naney (1979)\*

P	H <sub>2</sub> O wt. %	Crystallization Sequence →			
8	3.6 - 5	Bt	Af	P1	Q
8	5	Bt	Af	Q	P1
5	3.6	Bt	Af	P1	Q

\*phases that will be crystallized and then resorbed are now shown.

B. After Whitney (1925)

P	H <sub>2</sub> O wt. %	Crystallization Sequence →		
8	3.6	P1	At	Q
8	6 - 9	Af	P1	Q
8	9 - 13	Af	Q	P1

liquid (L) + plagioclase (Pl) + quartz (Qz) + Vapour (V), L + Pl + alkali feldspar (Alk) + V and L + Qz + Alk + V and the cotectic line in the system. The position of the cotectic surfaces and the cotectic line in the system Qz-Ab-Or-An-H<sub>2</sub>O at 5 kb determined by Winkler *et al.* (1975) are used to evaluate the crystallization sequence of the plutons concerned here. The average compositions of the plutons expressed in terms of normative Qz+An+Ab+Or = 100 (Table 7.3) are plotted in the Qz-Ab-Or and the An-Ab-Or projections in Figure 7.6 which also show the projections of the cotectic surfaces and the cotectic line in the Qz-Ab-An-Or-H<sub>2</sub>O system.

The method will be described in detail for the Wareham Quartz Monzonite but for the other plutons only the results will be given. Limitations of this method include: (1) it applies for H<sub>2</sub>O saturated melts, and (2) it assumes that the crystallization has taken place under a fixed pressure. However, the plutons in the area are highly unlikely to have remained saturated with H<sub>2</sub>O during their crystallization and they did not crystallize at a constant pressure. It is interesting to compare the crystallization sequence of the plutons as deduced by this method with those given in Table 7.2.

The Wareham pluton lies approximately at 11% An above the L + Pl + Qz + V cotectic surface in the Qz-Ab-Or projection. In the An-Ab-Or projection it has about 10% less quartz than it would have if it lay on the L + Pl + Qz + V cotectic surface. This indicates that the composition of the pluton is situated within the plagioclase space in the Qz-Ab-An-Or tetrahedron and the plagioclase is the first

Table 7.3. Average compositions of the plutons expressed in terms of their normative (mesonorm) quartz (Qz), anorthite (An), albite (Ab) and orthoclase (Or) contents. (Qz + An + Ab + Or = 100)

Intrusion	Qz	An	Or	Ab
Wareham Quartz Monzonite	29.65	15.47	20.36	34.52
Cape Freels Granite	30.34	6.69	31.83	31.14
Lockers Bay Granite	28.08	8.75	31.51	31.66
North Pond Granite (1)	37.00	6.29	24.58	32.13
North Pond Granite (2)	35.33	6.19	28.53	29.95
Deadman's Bay Granite	34.60	6.35	29.34	29.71
Newport Granite	31.46	7.04	29.63	31.87
Big Round Pond Granite	32.16	32.45	27.80	32.45

(1) - medium-grained phase; (2) - porphyritic phase.

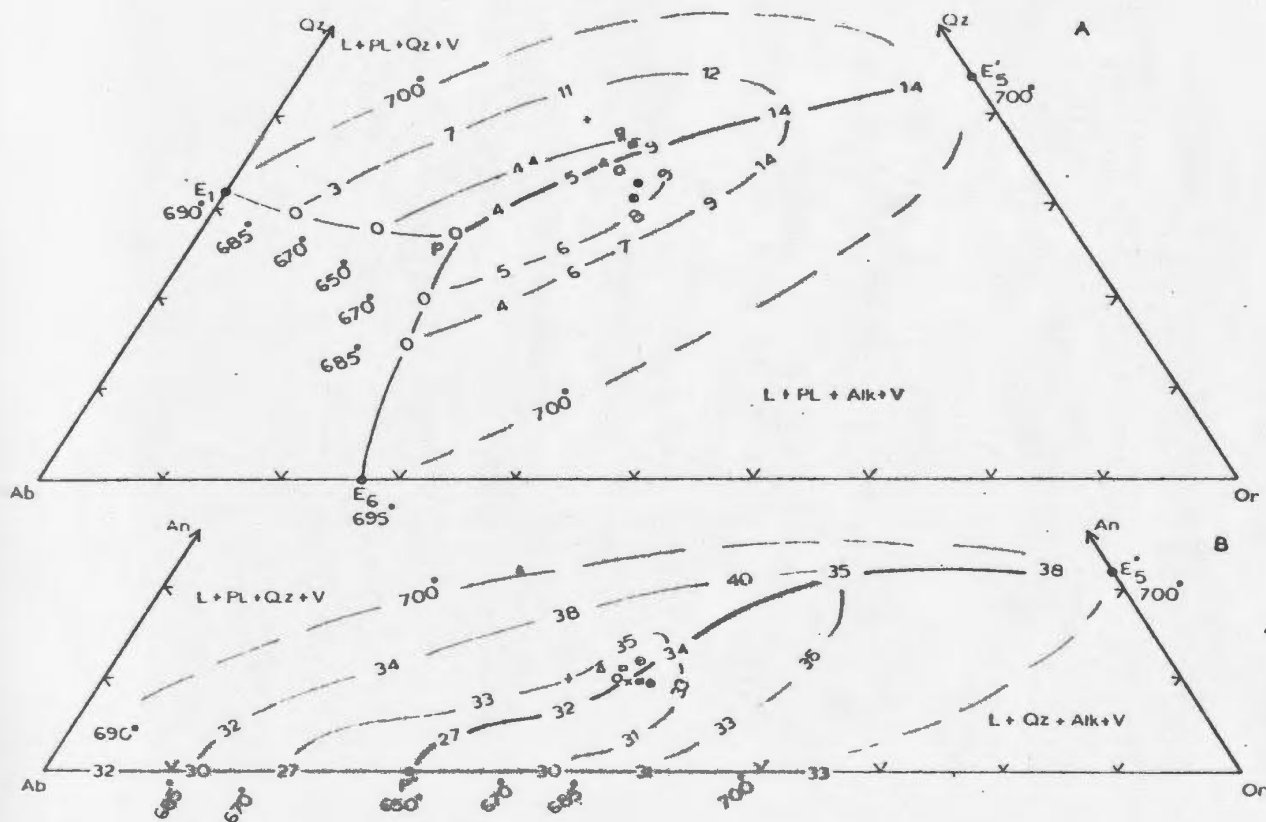


Fig. 7.6 The granitoids in the area represented in the granitic system  $Q_3$ -Ab-Or-An- $H_2O$ - (Skb).  $L + Q_3 + Alk + V$ ,  $L + Q_3 + Alk + V$  and  $L + Pl + Q_3 + V$  all the three cotectic surfaces. Dashed lines on cotectic surfaces are isotherms. Numbers indicate An content at places on the isotherms.  $\blacktriangle$  - Wareham Quartz Monzonite,  $\circ$  - Cape Freels Granite,  $\odot$  - Lockers Bay Granite,  $+$  - North Pond Granite (medium-grained),  $\times$  - North Pond Granite (porphyritic),  $\square$  - Business Cove Granite,  $\blacksquare$  - Deadman's Bay Granite,  $\circ$  - Newport Granite,  $\Delta$  - Big Round Pond Granite.

phase to crystallize. With the crystallization of plagioclase the liquid composition moves away from the An-Ab side in the tetrahedron and will reach the L + Pl + Qz + V cotectic surface. Then quartz will crystallize together with plagioclase and the liquid composition will move towards the cotectic line. From the projections it can be seen that the cotectic line will be reached probably with a drop of 20 - 30°C after quartz starts crystallizing. Along the cotectic line alkali feldspars will crystallize together with quartz and plagioclase.

The crystallization sequences of the plutons as determined by this method are summarized below except for the Business Cove Granite. This pluton was not considered in the above scheme due to its extremely inhomogeneous chemical composition.

	Progressive crystallization		
Wareham Quartz Monzonite	plagioclase	quartz	K-feldspar
North Pond Granite (medium grained)	quartz	plagioclase	K-feldspar
North Pond Granite (porphyritic)	quartz	plagioclase	K-feldspar
Lockers Bay Granite	plagioclase	K-feldspar	quartz
Cape Freels Granite	K-feldspar	plagioclase	quartz
Big Round Pond Granite	plagioclase	quartz	K-feldspar

The crystallization sequences for the plutons, obtained by using the phase relations in granitic systems published by different authors do not agree. The difference among them cannot be tested by the textural criteria such as inclusion of mineral in another because these features themselves have no clear and unambiguous genetic meaning. Therefore the crystallization sequences in the plutons remain undetermined.

#### 7.8. The Garnets and the Muscovites: Leucogranites and Megacrystic Granites

Garnets and primary muscovites occur in the North Pond and the Business Cove granites. They are also common in most of the pegmatites, aplites and minor intrusions that truncate the plutons in the area. The garnetiferous muscovite granites in the Gander Zone have been commonly referred to as leucogranites (see page , see also Strong, 1979). The genetic relationships between the leucogranites and the megacrystic granites in the Gander Zone have not been well understood (Strong and Dickson, 1978; Strong, 1979). The leucogranites have been generally regarded as partial melts of crustal rocks (Kennedy, 1975; Currie and Pajari, 1977). The purpose of this section is to determine the origin of garnets and muscovites in the North Pond and the Business Cove granites and to reflect upon the leucogranites - megacrystic granites relationships.

Green (1976) reported that garnets generally crystallize from granitic melts at depths greater than or equal to 25 km. However, several other authors (Green and Ringwood, 1972; Huang and Wyllie, 1973) suggested that garnets may crystallize from granitic liquids at depths less than 25-30 km. Green (1977) experimentally demonstrated that Mn-rich garnets could crystallize from granitic melts even at depths of about 12 km. The composition of garnets in the intrusions in the thesis area is not known. Nevertheless, it was shown before that the North Pond and the Business Cove granites could have been produced by differentiation of a magma similar to the Wareham pluton in composition (see section 6.3, page 214). This plus the fact that



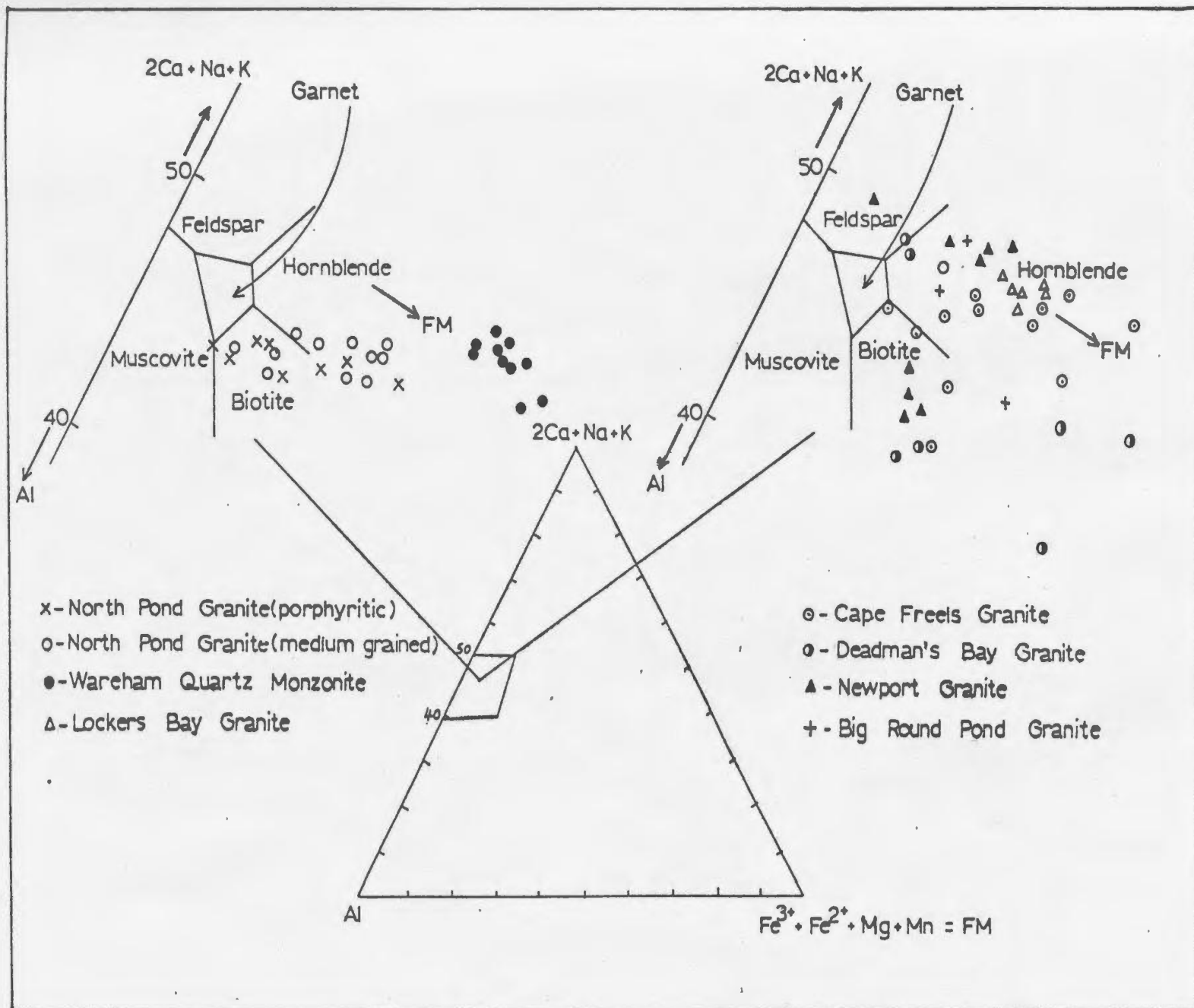
garnets and muscovites are common in pegmatites and aplites that truncate the granitoids in the area rule out the possibility that these garnets may have formed at deep levels ( $\geq 25$  km) but indicate that the garnet and the muscovite were crystallized at shallower levels as a result of differentiation of the parent magmas of the plutons. Currie and Pajari (1977) proposed a similar origin for garnets and muscovites in the Ragged Harbour complex; a granitic body farther to the west of the thesis area and largely similar to the North Pond and the Business Cove granites in rock type. Also, Pitcher and Berger (1972) attributed the origin of garnets in Donegal granites to a similar mechanism.

Cawthorn and Brown (1976) explained the origin of garnets and muscovites in granites by means of hypothetical phase relationships in part of the system  $(2Ca + Na + K) - Al - (Fe^{3+} + Fe^{2+} + Mn + Mg)$ . It should be noted that the phase relationships given by these authors are just a guide based on very limited experimental data and may not represent the actual crystallization paths in the P, T range in which the plutons have crystallized. The compositions of the plutons are plotted in the  $(2Ca + Na + K) - Al - FM^*$  triangle in Figure 7.7. The analyses from the Lockers Bay, Cape Freels, Deadman's Bay, Newport and the Big Round Pond granites plot to the FM-rich side of the schematic garnet and the muscovite fields of Cawthorn and Brown. This suggests that these plutons would not have produced garnets and muscovites, but their differentiated liquids will plot further away from the FM corner

---

\*  $FM = (Fe^{3+} + Fe^{2+} + Mn + Mg)$

Fig. 7.7 Compositions of the plutons plotted in the  $(2\text{Ca} + \text{Na} + \text{K}) - \text{Al} - \text{FM}$  diagram. Phase relations are after Cawthorn and Brown (1976).



than the "parent" granites and thus could crystallize garnets and muscovites.

The analyses from the Wareham and the two phases of the North Pond Granite define a regular trend in Figure 7.7. This trend indicates that the residual liquids of the Wareham pluton, represented by the North Pond Granite, move closer to the garnet and the muscovite fields with progressive differentiation and thus could have crystallized garnets and the muscovites. The garnets and the muscovites in the Business Cove Granite probably formed in the same way because this pluton appears to be comagmatic with the North Pond Granite. It is interesting that most of the analyses that plot close to the muscovite field belong to the porphyritic phase of the North Pond pluton because this phase is richer in muscovite than the medium-grained phase of the pluton. The results obtained by using the hypothetical phase relationships given by Cawthorn and Brown support the idea that the garnets and the muscovites in the plutons and their minor intrusions are a product of differentiation and did not form by melting at deep levels.\*

The above evidence and the geochemical modelling discussed earlier (page 214) clearly indicate that the garnetiferous muscovite "leucogranites" can be produced by differentiation of magmas similar to the megacrystic granites in composition. Thus the megacrystic granites may be the precursor to at least some of the leucogranites in the Gander Zone.

---

\* Most of the analyses from the granitoids in the area plot in the hornblende field, but the majority of the rocks contain biotite. This may be due to a reaction relationship between amphibole and liquid once biotite becomes stable (see Cawthorn and Brown, 1976).

#### 7.9. Summary

The granitoids in the area were produced probably by partial melting of greywacke with the older, deformed granites representing 30 to 40% melting and the younger, undeformed granites representing 15 to 25% melting of the source rocks. The residue consisted mainly of quartz, plagioclase, biotite and hypersthene. The heat for the melting in the source rocks was probably supplied by mafic magma intruded at depths within a relatively high ambient geothermal gradient ( $\geq 25^{\circ}\text{C}/\text{km}$ ).

The  $\text{H}_2\text{O}$  contents in the parent magmas of the plutons were above 3.6 wt%, but were higher ( $\geq 9$  wt%) in the case of the North Pond and the Business Cove granites. The crystallization sequences in the plutons are hard to establish. The garnets and the muscovites in the North Pond and the Business Cove granites and in numerous pegmatites, aplites and granitic minor intrusions in the area are a result of magmatic differentiation and do not indicate melting at deeper levels. This fact and the geochemical modelling indicate that the megacrystic granites may have produced garnetiferous muscovite "leucogranites" by differentiation.

## CHAPTER 8

### SUMMARY, PLATE TECTONIC MODELS AND FUTURE WORK

#### 8.1. Summary

##### 8.1.1. Field Relationships, Rock Types, Metamorphism and Structure

Granitoid rocks underlie approximately three-fourths of the thesis area and comprise eight separate intrusions. They are the Wareham Quartz Monzonite and the Cape Freels, Lockers Bay, Deadman's Bay, Newport, North Pond, Business Cove and the Big Round Pond granites. The first five of these are megacrystic plutons characterized by microcline crystals greater than 2 cm in length set in a finer-grained matrix. The remaining intrusions are non-megacrystic. The North Pond and the Business Cove plutons are garnetiferous two-mica granites and the Big Round Pond pluton is a medium-grained biotite granite. The North Pond pluton consists of two distinct phases; a porphyritic phase with microcline phenocrysts ranging up to 2 cm in length and a medium-grained phase.

The country rocks to the intrusions consist of two gneissic units: the Square Pond Gneiss and the Hare Bay Gneiss. The Square Pond Gneiss is the oldest rock unit in the area. It consists of psammitic to semi-pelitic gneiss, schists and minor psammitic metasediments. Its metamorphic grade increases from greenschist facies in the west to amphibolite facies in the east. The mineral parageneses and garnet-biotite geothermometry indicate that the amphibolite facies metamorphism of the gneiss has taken place at pressures between 4.3 and 5.5 kb and temperatures between 550 and 650°C.

There is evidence of at least three main deformation events ( $D_1$ ,  $D_2$  and  $D_3$ ) in the Square Pond Gneiss.  $D_1$  has resulted in a fine gneissic layering ( $S_1$ ). In places,  $S_1$  occurs axial-planar to minor folds of thicker compositional layering, which probably represent original sedimentary bedding.  $S_1$  is not commonly seen in outcrops, as it has been largely obliterated by the later deformation events.  $D_2$  has resulted in a second gneissic layering ( $S_2$ ).  $S_2$  is produced by alternating 0.5 to 1 cm wide quartz-rich layers and thinner micaceous horizons and is the most ubiquitous structure in the gneiss. In a few outcrops,  $S_2$  occurs axial-planar to minor folds of  $S_1$  or gives rise to microlithons with curved traces of  $S_1$  in them.  $S_2$  generally strikes in an east-northeast direction and dips at moderate to steep angles mostly to the northwest.  $D_3$  has produced a northeast-trending, steeply dipping schistosity,  $S_3$ .  $S_3$  commonly occurs axial-planar to tight minor folds of  $S_2$  and numerous quartz veins that truncate  $S_2$ . Microstructural relationships between the garnet, staurolite and andalusite porphyroblasts and the fabrics in the Square Pond Gneiss indicate that the peak metamorphism in the gneiss has occurred during the early part of  $D_3$ .

The Hare Bay Gneiss occurs to the east of the Square Pond Gneiss and consists mostly of migmatite. The contact between the two gneiss terrains is gradational and is marked by a "migmatite front", a 0.5 to 1 km wide zone within which the Square Pond Gneiss shows increasing amounts of granitic material and feldspar blastesis and passes into migmatite. The migmatite has a crude to well-developed

layering that it has inherited, at least partly, from the  $S_2$  of its "parent" gneiss terrain.  $S_2$  in the migmatite is defined by alternating quartz-rich layers (leucosome) and micaceous layers (melanosome). The  $S_2$  layering has been folded by the  $D_3$  deformation in the area with the development of a northeast-trending, steeply dipping foliation,  $S_3$ .

The Hare Bay Gneiss shows metamorphism of the amphibolite facies. It commonly contains sillimanite but not staurolite or andalusite. Therefore, the P, T conditions in the Hare Bay Gneiss must have been higher than those at which the "staurolite stability curve" intersects the andalusite-sillimanite field boundary, i.e. above 4.3 kb and 650°C. These P, T conditions are above the "wet" granite solidus. However, petrographical considerations indicate that anatexis was not the principal mechanism responsible for the formation of the migmatite in the area. It is believed that metamorphic differentiation was probably the dominant process that produced the migmatite.

The granitoids in the area post-date  $D_3$  in the gneisses. An unequivocal emplacement sequence cannot be established for the plutons because they are not all in contact with each other and furthermore, only a few of the plutons have been dated radiometrically. The mode of emplacement of the plutons, except for scanty evidence for forceful intrusion in the case of the North Pond and the Deadman's Bay plutons, is not clear. All the plutons in the area show variably developed mineral alignments that may be related to their emplacement. In addition, the Wareham, North Pond, Lockers Bay and the Cape Freels plutons have been deformed during the  $D_4$  deformation in the area.



D<sub>4</sub> has resulted in two north-northeast trending shear zones. The westerly of these cuts through the North Pond, Wareham and the Lockers Bay plutons and the gneisses between them. The easterly shear zone deforms the western marginal part of the Cape Freels Granite and the adjoining Hare Bay Gneiss. The shear zones are characterized by an intense mylonitic foliation (S<sub>4</sub>) defined by micas and dimensionally elongated quartz grains. S<sub>4</sub> strikes parallel to the length of the shear zones and dips either steeply or vertically. The sense of movement in the shear zones, as determined from the sense of rotation of feldspars, is sinistral. An east-northeast trending, steeply-dipping mylonitic foliation in the southern part of the Cape Freels Granite and the northeastern part of the Lockers Bay Granite is believed to be related to movements along the Dover Fault. The age relationships between this foliation and S<sub>4</sub> are not known.

The Deadman's Bay, Newport and the Big Round Pond plutons post-date D<sub>4</sub>. However, the Newport Granite in the extreme south of its outcrop has been shattered and cut off by further reactivations of the Dover Fault. A swarm of north-south trending, alkalic basalt dikes pre-date the Newport and the Big Round Pond plutons and post-date all the other granitoids in the area. These dikes mark a localized event in the Carboniferous, which could be an early sign of the major continental breakup that occurred later. Figure 8.1 summarizes the metamorphic, deformational and intrusive events in the area and the probable chronological relationships between them.

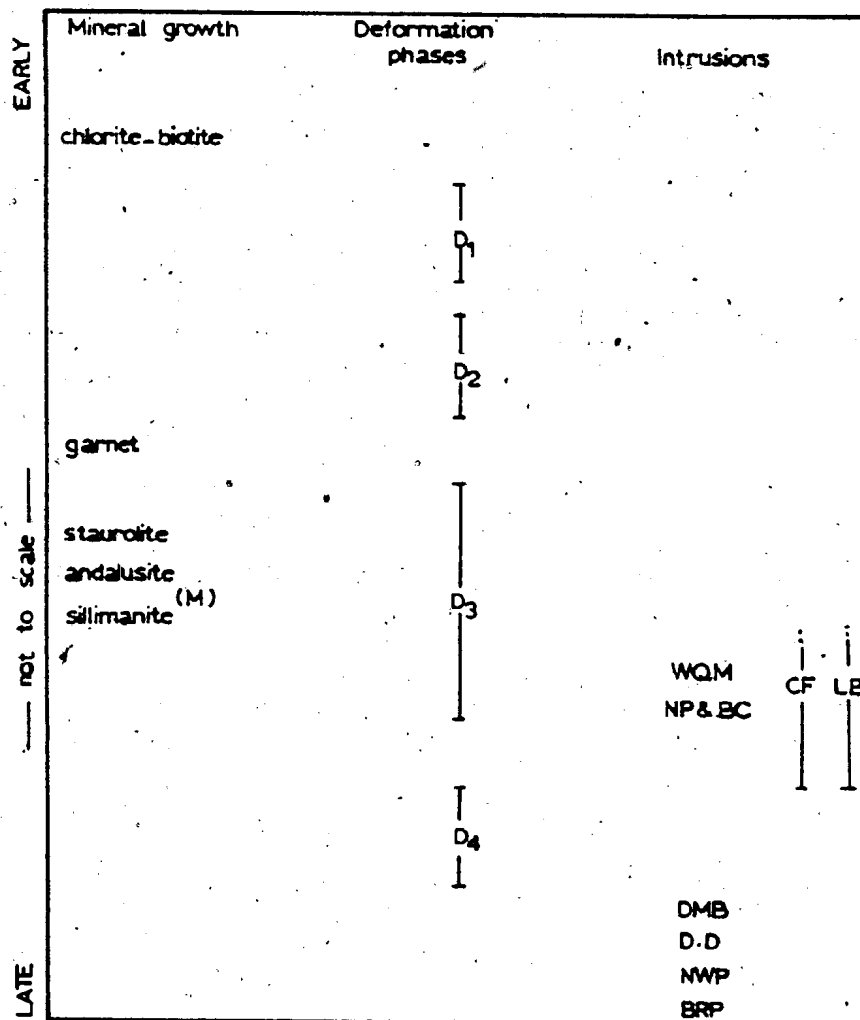


Fig. 8.1 Relative time relationships between progressive metamorphism (indicated by the index minerals), deformation phases, and intrusive events in the area. M - migmatization, WQM - Wareham Quartz Monzonite, NP - North Pond Granite, BC - Business Cove Granite, CF - Cape Freels Granite, LB - Lockers Bay Granite, DMB - Deadmans Bay Granite, D.D - Diabase dikes, NWP - Newport Granite, BRP - Big Round Pond Granite.

### 8.1.2. Geochemistry and the Origin of the Granitoids

Except for the Wareham Quartz Monzonite, the plutons in the area are largely similar in chemical composition. The Wareham pluton is more mafic than the rest of the granitoids. The analyses from the Wareham and the North Pond plutons plot along regular trends in the variation diagrams and the  $(\text{Na}_2\text{O} + \text{K}_2\text{O}) - \text{FeO} - \text{MgO}$  and the  $\text{Al}_2\text{O}_3 - \text{FeO} - \text{MgO}$  diagrams. The trends in the latter diagrams lie along the line joining the compositions of feldspars and biotites in the Wareham pluton. Thus, these two plutons are probably related by fractional crystallization of feldspars and biotite. Geochemical modelling indicates that (1) medium-grained phase of the North Pond Granite could be derived by fractional crystallization of a solid phase with approximately 35% plagioclase, 50% potassium feldspar, 12% biotite and 3% accessory minerals from a magma similar to the Wareham Quartz Monzonite in composition, and (2) porphyritic phase of the North Pond Granite could have formed by fractionation of a solid phase with approximately 60% plagioclase, 36% potassium feldspar, 2% biotite and 2% accessory minerals from a magma similar to the medium-grained phase in composition (Figure 6.8, page 226).

The initial  $\text{Sr}^{86}/\text{Sr}^{87}$  ratios of some of the megacrystic plutons in the area indicate that they could have been produced by the partial melting of greywacke. Comparison of Ba and Sr concentrations of the plutons with hypothetical abundances of Ba and Sr in melts that may be produced by the partial melting of "typical" greywacke indicate that the parent magmas of the plutons may indeed have formed by different

degrees of partial melting of "typical" greywacke (Figure 7.3, page 243). The older (pre-D<sub>4</sub>) Wareham, Lockers Bay and the Cape Freels plutons appear to have been produced by 30-40% melting of greywacke and the younger (post-D<sub>4</sub>), Deadman's Bay, Newport and the Big Round Pond granites by 15-25% melting of greywacke.

The genetic relationships between the Wareham Quartz Monzonite and the garnetiferous, muscovite-bearing North Pond Granite and the common occurrence of garnet and muscovite in pegmatites, aplites and granitic minor intrusions in the area suggest that these two minerals are a result of differentiation of parent magmas of the megacrystic plutons in the area. Results obtained by the application of hypothetical phase relationships in the system (2Ca + Na + K) - Al - (Fe<sup>3+</sup> + Fe<sup>2+</sup> + Mn + Mg), proposed by Cawthorn and Brown (1976), to the plutons confirm this idea. Thus, the megacrystic plutons in the Gander Zone could be the forerunners of at least some of the garnetiferous, two-mica "leucogranites" associated with them.

#### 8.2. Plate-tectonic Models

The purpose of this section is to discuss the pros and cons of some of the plate-tectonic models that deal directly with the geology of the Gander Zone. It is not an aim of this study to propose a detailed plate-tectonic model for the geological evolution of the thesis area or to make regional correlations of its lithologies with other similar rock types along the Appalachian-Caledonian Orogen. A number of regional correlations of the Gander Zone lithologies have already been proposed by several authors (Williams *et al.*, 1972, 1974;

Williams and Stevens, 1974; Kennedy, 1975; Rast et al., 1976; Schenk, 1978; Phillips, 1978) including a lithofacies map showing the distribution of the various elements of the Appalachian Orogen (Williams, 1978). Also, numerous plate-tectonic models have been coined to explain the development of the Newfoundland Appalachians (Bird and Dewey, 1970; Strong et al., 1974; Stevens et al., 1974; Kennedy, 1975; Williams, 1975; Blackwood, 1976; Strong, 1977; Dean, 1978; Haworth et al., 1979).

Strong and others (1974) argued for the existence of an east-dipping Appalachian subduction zone in Newfoundland on geochemical grounds. Their evidence included: (1) an eastward increase in the average potassium content of the plutons in the Central, Gander and Avalon zones of Newfoundland, and (2) similarity between zonation of Newfoundland mineral deposits and the metal zoning in areas of active orogenic zones. They attributed the metamorphism in the Gander Zone to metamorphism along a continental margin above the subduction zone and the granites to melting associated with the subduction zone. But Strong subsequently rejected the idea that the granitoids in the Gander Zone were produced by melting along a subduction zone (Strong, 1977; Strong and Dickson, 1977; Strong, 1979).

Kennedy (1975) related the metamorphism and the granite intrusion in the Gander Zone to opening and closing of a marginal basin within the western continental margin of the Iapetus Ocean, in Late Precambrian (Hadrynian) times. He referred to this event as the Ganderian Orogeny but stated that because of the absence of detailed information it is hard to propose a conclusive plate mechanism for the development of the Gander Zone. However, no Precambrian ages

have been obtained from any of the granitoids in the Gander Zone during recent Rb/Sr dating (Bell and Blenkinsop, 1975; Bell et al., 1977). Also, Hussey (1979) convincingly showed that the deformation in the Love Cove Group may have occurred as late as Devonian and not during Kennedy's Precambrian Ganderian Orogeny. This conflicting evidence makes Kennedy's plate model for the Gander Zone less attractive, and the existence of the Ganderian Orogeny highly doubtful.

Blackwood (1976) believed that the metamorphism, deformation and granitic intrusions in the Gander Zone were largely a product of Late Precambrian Cadomian Orogeny. He proposed the following sequence of events for the development of the Gander-Avalon zones.

1. 800 Ma - Cadomian Ocean which separated the Paleo-North America from the Paleo-Eur-Africa being subducted under the North American Continent.
2. 800-700 Ma - Formation of a small back-arc basin and thus isolation of a micro-plate now represented by the Avalon Zone. Gander Group is being deposited in the back-arc basin.
3. 700-600 Ma - Closing of the Cadomian Ocean. The Avalon micro-plate is being pushed back against the North American continent, thus closing the back-arc basin. This results in the Cadomian Orogeny. The Dover Fault makes the Gander Zone-Avalon Zone boundary.
4. 600-500 Ma - Development of the Iapetus Ocean.
5. Before 450 Ma - Ophiolite obduction on to the Gander Zone.

Blackwood's model is based on the same evidence as Kennedy's model involving Precambrian metamorphism, granite intrusion and deformation and does not stand up to scrutiny in the light of the recent work in the Gander Zone (Bell et al., 1977; Currie et al., 1979).

In fact, none of the plate-tectonic models so far proposed adequately explain the development of the Gander Zone. Any future tectonic models dealing with the Gander Zone in Newfoundland should explain some of the observations and conclusions of the present study, i.e.:

1. eastward prograding metamorphism, and the complex deformation history of the gneisses;
2. the relatively high geothermal gradient ( $25^{\circ}\text{C}/\text{km}$ ) which existed during the peak metamorphism of the gneisses;
3. generation of a number of granitoids of crustal origin during Silurian-Carboniferous time; and
4. formation of the major sinistral shear zones and the intrusion of alkalic basalt dikes during the emplacement of the granitoids.

### 8.3. Future Work

A number of problems that came to light during this study call for further work. Some of these are mentioned in the preceding chapters and the more important ones are listed below with suggestions for future work.

1. The exact age difference between the formation of the migmatites and the intrusion of the granitoids is not known. Furthermore, there are no radiometric dates available for a number of plutons in the area. Thus, a detailed geochronological study directed at dating the gneisses as well as the "undated" granitoids and the diabase dikes is needed for a proper understanding of the timing of the geological events in the area.
2. The relative timing between  $D_4$  and the Dover Fault-related deformation in the Cape Freels and Lockers Bay granites and the Hare Bay Gneiss is not clear. Detailed structural studies, especially in the area south of Indian Bay, should provide important clues to solve this problem.
3. Further geochemical work such as the analysis of additional samples from the granitoids and REE studies is needed to adequately test the origin of the granitoids and the leucogranites-megacrystic granites relationships proposed here.



REFERENCES

- Ahlin, S. 1976. The compositional relationships of biotite and garnet in the Goteborg area of south-western Sweden and their thermometric implications. *Geol. Foren. Stockholm, Foth.*, V. 98, pp. 337-342.
- Albuquerque, C.A.R. de. 1977. Geochemistry of the tonalitic and granitic rocks of the Nova Scotia southern plutons. *Geochim. Cosmochim. Acta*, V. 41, pp. 1-13.
- Amit, O. and Eyal, Y. 1976. The genesis of Wadi Mārgish migmatites (N-E Sinai). *Contrib. Mineral. Petrology*, V. 59, pp. 95-110.
- Armstrong, R.L. and Besancon, J. 1970. A Triassic time scale dilemma: K-Ar dating of Upper Triassic mafic igneous rocks of eastern U.S.A. and Canada and post-Upper Triassic plutons of western Idaho, U.S.A. *Ecologiae Geol. Helv.*, V. 68, pp. 15.- 38.
- Arth, J.G. 1976. Behaviour of trace elements during magmatic processes - a summary of the theoretical models and their applications. *U.S. Geol. Surv., J. Res.*, V. 4, pp. 41-47.
- Ashworth, J.R. 1976. Petrogenesis of migmatites in the Huntly-Portsoy area, northeast Scotland. *Mineral. Mag.*, V. 40, pp. 661-682.
- Bailey, D.K. 1974. Continental rifting and alkaline magmatism. In: Sorensen, H. (ed.), *The Alkaline Rocks*. Wiley & Sons, N.Y., pp. 148-159.
- Bell, K. and Blenkinsop, J., 1977. Geochronological evidence of Hercynian activity in Newfoundland. *Nature*, V. 265, pp. 616-618.
- Bell, K. and Blenkinsop, J. 1975. Geochronology of eastern Newfoundland. *Nature*, V. 254, pp. 410-411.

- Bell, K., Blenkinsop, J. and Strong, D.F. 1977. The geochronology of some granitic bodies from eastern Newfoundland and its bearing on Appalachian Evolution. *Can. J. Earth Sci.*, V. 14, pp. 456-476.
- Bell, K., Berger, A.R., Blenkinsop, J. and Jayasinghe, N.R., 1979. The Newport Granite: its age, geological setting and implications for the geology of northeastern Newfoundland. *Can. J. Earth Sci.*, V. 16, pp. 264-269.
- Berger, A.R. and Naylor, C.R. 1974. Isotopic data on zircons from the Deadmans Bay pluton, Northeastern Newfoundland and their geologic implications. *Abstr. Program of 1974. GAC/MAC Meeting, St. John's*, p. 9.
- Bird, J.M. and Dewey, J.F. 1970. Lithospheric plate-continental margin tectonics and the evolution of the Appalachian Orogen. *Geol. Soc. Amer., Bull.*, V. 81, pp. 1031-1060.
- Blackwood, R.F. 1978. Northwestern Gander Zone Newfoundland. In: Gibbons, R.V. (ed.), Report of Activities for 1977; Newfoundland Department of Mines and Energy, Mineral Development Division, Report 78-1, pp. 72-79.
- Blackwood, R.F. 1977. Geology of the east half of the Gambo (2D/16) map area and the northwest portion of the St. Brendan's (2C/13) map area, Newfoundland. Newfoundland Department of Mines and Energy, Mineral Development Division, Report 77-5, 20 p.
- Blackwood, R.F. and O'Driscoll, C.F. 1976. The Gander-Avalon boundary in southeastern Newfoundland. *Can. J. Earth Sci.*, V. 13, pp. 1155-1159.

- Booth, B. 1968. Petrogenetic significance of alkali feldspar megacrysts and their inclusions in Cornubian Granites. *Nature*, V. 217, pp. 1036-1038.
- Brown, E.H. 1971. Phase relations of biotite and stilpnomelane in the greenschist facies. *Contrib. Mineral. Petrology*, V. 31, pp. 275-299.
- Brown, G.C. and Fyfe, W.S. 1970. The production of granitic melts during metamorphism. *Contrib. Mineral. Petrology*, V. 28, pp. 310-318.
- Burnham, C.W. 1979. Magmas and Hydrothermal Fluids. In: Barnes, H.L. (ed), *Geochemistry of Hydrothermal Ore Deposits*, Chapter 2, 2nd Edition (in press). John Wiley and Sons, N.Y.
- Busch, W., Schneider, G. and Mehnert, K.R. 1974. Initial melting at grain boundaries, Part II: Melting in rocks of granodioritic, quartzdioritic and tonalitic composition. *Neues Jahrb. Mineral. Monatsh.*, Bd. 8, pp. 345-370.
- Carmichael, I.S.E., Turner, F.J., and Verhoogen, J., 1974. *Igneous Petrology*. McGraw-Hill, New York, 739 p.
- Cawthorn, R.G. 1974. Computer programs available for geological calculations. Unpublished report. Department of Geology, Memorial University of Newfoundland, pp. E1-F10.
- Cawthorn, R.G. and Brown, P.A. 1976. A model for the formation and crystallization of corundum-normative calc-alkaline magmas through amphibole fractionation. *J. Geol.*, V. 84, pp. 467-476.
- Chappell, B.W. and White, A.J.R. 1974. Two contrasting granite types. *Pacific Geology*, V. 8, pp. 173-174.

- Colman-Sadd, S.P. 1979. Geology of South-Central Newfoundland and evolution of the proto-Atlantic's eastern margin. (Manuscript in preparation).
- Condie, K.C., Macke, J.E. and Reiner, T.O. 1970. Petrology and Geochemistry of Early Precambrian greywackes from the Fig Tree Group, South Africa. Geol. Soc. Amer. Bull, V. 81, pp. 2759-2775.
- Coombs, D.S. 1963. Trends and affinities of basaltic magmas and pyroxenes as illustrated on the diopside-olivine-silica diagram. Mineralogical Society of America, Special Paper 1, pp. 227-250.
- Coward, M.P. 1976. Strain within ductile shear zones. Tectonophysics, V. 34, pp. 181-197.
- Currie, K.L. and Pajari, G.E. 1977. Igneous and metamorphic rocks between Rocky Bay and Raggad Harbour, northeastern Newfoundland. In: Report of Activities, Part A, Geol. Surv. Can. Paper 77-1A, pp. 341-346.
- Currie, K.L., Pajari, G.E. and Pickerill, R.K. 1979. Tectonic-stratigraphic problems in the Carmanville area, northeastern Newfoundland. In: Current Research, Part A, Geol. Surv. Can. Paper 79-1A, pp. 71-76.
- Dalrymple, G.B., Gromme, C.S. and White, R.W. 1975. Potassium-argon age and paleomagnetism of diabase dikes in Liberia: Initiation of central Atlantic rifting. Geol. Soc. Amer. Bull., V. 86, pp. 399-411.
- Day, H.W. 1973. The high temperature stability of muscovite plus quartz. Amer. Mineral., V. 58, pp. 255-262.
- Dean, P.L. 1978. The volcanic stratigraphy and metallogeny of Notre Dame Bay, Newfoundland. Memorial University of Newfoundland, Geology Report 7, 177 p.

- Dickson, F.W. 1968. Exsolution origin of zoned, twinned, preferentially concentrated plagioclase inclusions in K-feldspar crystals. *Progr. Geol. Soc. Amer., Mexico City*, p. 74.
- Dickson, W.L. 1974. The general geology and geochemistry of the granitoid rocks of the northern Gander Lake Belt, Newfoundland. Unpublished M.Sc. thesis, Memorial University of Newfoundland.
- Drake, M.J. 1976. Plagioclase-melt equilibria. *Geochim. Cosmochim. Acta.*, V. 40, pp. 457-466.
- Emmerring, R. 1969. Genetic relations between two generations of K-feldspar in a granitic pluton. *Neues Jahrb. Mineral. Abh.*, Bd. 111, pp. 289-313.
- Engel, A.E.J., Engel, C.G. and Havens, R.G. 1965. Chemical characteristics of oceanic basalt and the upper mantle. *Geol. Soc. Amer. Bull.*, V. 76, pp. 719-734.
- Eugster, H.P. 1959. Reduction and oxidation in metamorphism. In: Abelson, P.H. (ed.), *Researches in Geochemistry*. John Wiley, N.Y., pp. 397-426.
- Evans, J. 1978. An alkali volcanic suite of the Labrador Trough, Labrador. Unpublished M.Sc. thesis, Memorial University of Newfoundland.
- Ewart, A. and Taylor, S.R. 1969. Trace element geochemistry of the rhyolitic rocks, Central North Island, New Zealand; phenocryst data. *Contrib. Mineral. Petrology*, V. 22, pp. 127-146.
- Ewing, J., Hollister, C., Hathaway, J., Paulus, F., Lancelot, Y., Habib, D., Poag, C.W., Luterbacher, H.P.; Worstell, P. and Wilcoxon, S.A., 1970. Deep sea drilling project: Leg II. *Geotimes*, V. 15, pp. 14-16.

- Fairbairn, H.W. and Berger, A.R. 1969. Preliminary geochronological studies in northeast Newfoundland. 17th Ann. Prog. Rept. Mass. Inst. Technol., A.E.C. 1381-17, pp. 19-20.
- Faure, G. and Powell, J.L. 1972. Strontium isotope geology. Springer-Verlag, N.Y., 188 p.
- Ferry, J.M. and Spear, F.S. 1978. Experimental calibration of the partitioning of Fe and Mg between biotite and garnet. Contrib. Mineral. Petrology, V. 66, pp. 113-117.
- Flinter, B.H. 1974. Differentiation Index applied to the New England Igneous Complex, New South Wales, Australia: A preliminary study. Pacific Geology, V. 7, pp. 45-63.
- Gale, G.H. 1967. Economic assessment of pegmatites. Unpublished Report, Newfoundland Department of Mines, Mineral Resources Division, 70 p.
- Gast, P.W. 1968. Trace element fractionation and the origin of tholeiitic and alkaline magma types. Geochim. Cosmochim. Acta, V. 32, pp. 1057-1086.
- Gay, N.C. 1968. Pure shear and simple shear deformation of inhomogeneous viscous fluids: 2. The determination of the total finite strain in a rock from objects such as deformed pebbles. Tectonophysics, V. 5, pp. 295-302.
- Goldman, D.S. and Albee, A.L. 1977. Correlation of Mg/Fe partitioning between garnet and biotite with  $^{18}\text{O}/^{16}\text{O}$  partitioning between quartz and magnetite. Amer. J. Sci., V. 277, pp. 750-767.
- Green, T.H. 1977. Garnet in silicic liquids and its use as a P-T indicator. Contrib. Mineral. Petrology, V. 65, pp. 59-67.

- Green, T.H. 1976. Experimental generation of cordierite - or garnet-bearing granitic liquids from a pelitic composition. *Geology*, V. 4, pp. 85-88.
- Green, T.H. and Ringwood, A.E. 1972. Crystallization of garnet-bearing rhyolite under high pressure hydrous conditions. *Geol. Soc. Austral. J.*, V. 19, pp. 203-212.
- Green, T.H. and Ringwood, A.E. 1968. Genesis of the calc-alkaline igneous rock suite. *Contrib. Mineral. Petrology*, V. 18, pp. 105-162.
- Harris, P.G., Kennedy, W.Q. and Scarfe, C.M. 1970. Volcanism versus plutonism - the effect of chemical composition. In: Newell, G. and Rast, N. (eds.) *Mechanism of Igneous Intrusion*. Liverpool, Gallery Press, pp. 187-200.
- Harland, W.B. and Gay, R.A. 1972. The Arctic Caledonides and earlier oceans. *Geol. Mag.*, V. 109, pp. 289-314.
- Harte, B. and Johnson, M.R.W. 1969. Metamorphic history of Dalradian rocks in Glens Cova, Esk and Lethnot, Angus, Scotland. *Scott. J. Geol.*, V. 5, pp. 54-80.
- Haworth, R.T., Lefort, J.P. and Miller, H.G. 1978. Geophysical evidence for an east-dipping Appalachian subduction zone beneath Newfoundland. *Geology*, V. 6, pp. 522-526.
- Hietanen, A. 1963. Idaho batholith near Pierce and Bungalow Clearwater Country, Idaho. *U.S. Geol. Survey., Prof. Paper 344D*, 42p.
- Hibbard, M.J. 1965. Origin of some alkali feldspar phenocrysts and their bearing on petrogenesis. *Amer. J. Sci.*, V. 263, pp. 245-261.
- Hollister, L.S. 1966. Garnet zoning: An interpretation based on the Rayleigh fractionation model. *Science*, V. 154, pp. 1647-1651.

- Hoschek, G. 1926. Melting relationships of biotite + plagioclase + quartz. Neues Jahrb. Mineral. Monatsh., Bd. 2, pp. 79-83.
- Hoschek, G. 1969. The stability of staurolite and chloritoid and their significance in metamorphism of pelitic rocks. Contrib. Mineral. Petrology, V. 22, pp. 208-232.
- Hsu, L.C. 1968. Selected phase relationships in the system Al-Mn-Fe-Si-O; a model for garnet equilibria. J. Petrol., V. 9, pp. 40-83.
- Huang, W. and Wyllie, P.J. 1973. Melting relations of muscovite-granite to 35 kb as a model for fusion of metamorphosed subduction oceanic sediments. Contrib. Mineral. Petrology, V. 42, pp. 1-14.
- Hussey, E.M. 1979. Geology of the Clode Sound map area, eastern Newfoundland. Unpublished M.Sc. thesis, Memorial University of Newfoundland.
- Hyndman, D.W. 1972. Petrology of igneous and metamorphic rocks. McGraw-Hill, N.Y.
- Jayasinghe, N.R. 1978a. Geology of the Wesleyville (2F/4) and the Musgrave Harbour East (2F/5) map areas, Newfoundland. Newfoundland Department of Mines and Energy, Mineral Development Division, Report 77-5, 11p.
- Jayasinghe, N.R. 1978b. Devonian alkaline basalt dikes of northeastern Newfoundland: evidence of a tensional environment. Can. J. Earth Sci., V. 15, pp. 848-853.
- Jayasinghe, N.R. 1976. Geology of the Wesleyville area, Newfoundland. Unpublished M.Sc. thesis, Memorial University of Newfoundland.
- Jayasinghe, N.R. and Berger, A.R. 1976. On the plutonic evolution of the Wesleyville area, Bonavista Bay, Newfoundland. Can. J. Earth Sci., V. 13, pp. 1560-1570.



- Jenness, S.E. 1963. Terra Nova and Bonavista map areas, Newfoundland. Geological Survey of Canada, Memoir 327, 184 p.
- Jenness, S.E. 1954. Geology of the Gander River Ultrabasic belt, Newfoundland. Unpublished Ph.D. thesis, Yale University.
- Johnson, M.R.W. 1967. Mylonite zones and mylonite banding. *Nature*, V. 213, pp. 246-247.
- Kay, R.W. 1970. The rare earth geochemistry of alkaline basaltic volcanics. Unpublished Ph.D. thesis, Columbia University.
- Kean, B.F., Dean, P.L. and Strong, D.F. (in press). Regional geology of the Central Volcanic Belt of Newfoundland. In: Geol. Surv. Canada, Special Paper.
- Kennedy, M.J. 1975. Repetitive orogeny in the northeastern Appalachians - new plate models based upon Newfoundland examples. *Tectonophysics*, V. 28, pp. 39-87.
- Kennedy, M.J. and McGonigal, M.H. 1972. The Gander Lake and Davidsville groups of northeastern Newfoundland: new data and geotectonic implications. *Can. J. Earth Sci.*, V. 9, pp. 452-459.
- Kerrick, D.M. 1969. K-feldspar megacrysts from a porphyritic quartz monzonite, central Sierra Nevada, California. *Amer. Mineral.*, V. 54, pp. 839-848.
- Kilinc, I.A. 1972. Experimental study of partial melting of crustal rocks and formation of migmatites. *Internat. Geol. Cong.*, 24th, Montreal, Sect. 2, pp. 109-113.
- Kushiro, I. 1973. Origin of some magmas in oceanic and circum oceanic regions. *Tectonophysics*, V. 17, pp. 211-222.
- Kushiro, I. 1960. Si-Al relation in clinopyroxenes from igneous rocks. *Amer. J. Sci.*, V. 258, pp. 548-554.

- Kushiro, I., Shimazn, N., Nakamura, Y. and Akimoto, S. 1972. Compositions of coexisting liquid and solid phases formed upon melting of natural garnet and spinel Iherzolites at high pressure: A preliminary report. *Earth Planet Sci. Letters*, V. 14, pp. 19-25.
- Kushiro, I., Syomo, Y. and Akimoto, S. 1968. Melting of a peridotite at high pressure and high water pressures. *J. Geophys. Res.*, V. 73, pp. 6023-6029.
- LeBas, M.J. 1962. The role of aluminium in igneous clinopyroxenes with relation to their parentage. *Amer. J. Sci.*, V. 360, pp. 267-288.
- LePichon, X. and Fox, P.J. 1971. Marginal offsets, fracture zones, and the early opening of the North Atlantic. *J. Geophys. Res.*, V. 76, pp. 6294-6308.
- MacDonald, R. 1975. Petrochemistry of the Early Carboniferous (Dinantian) Lavas of Scotland. *Scott. J. Geol.*, V. 11, pp. 269-314.
- MacDonald, G.A. and Katsura, T. 1964. Chemical composition of Hawaiian lavas. *J. Petrology*, V. 5, pp. 82-133.
- MacKenzie, W.S. 1954. The orthoclase-microcline inversion. *Mineral Mag.*, V. 30, pp. 354-366.
- Martin, R.F. and Piwinski, A.J. 1974. The contrasting origin of orogenic and non-orogenic granitoid rocks. In: *Proceedings of the Symposium on "Andean and Antarctic volcanology problems.* Santiago.
- Manson, V. 1967. Geochemistry of basaltic rocks: major elements. In: Hess, H.H. and Poldervaart, A. (eds.), *Basalts: the Poldervaart treatise on rocks of basaltic composition*. V. 1, Interscience Publications, N.Y., pp. 215-269.

- Mehnert, K.R. 1968. Migmatites and the origin of granitic rocks. Elsevier, Amsterdam, 393 p.
- Mehnert, K.R., Busch, W. and Schneider, G. 1973. Initial melting at grain boundaries of quartz and feldspar in gneisses and granulites. Neues Jahrb. Mineral. Monatsh. Bd. 4, pp. 165-183.
- Miller, H.G., 1977. Gravity zoning in Newfoundland. Tectonophysics, V. 38, pp. 317-326.
- Mitra, G. 1978. Ductile deformation zones and mylonites: The mechanical processes involved in the deformation of crystalline basement rocks. Amer. J. Sci., V. 278, pp. 1057-1084.
- Miyashiro, A. 1973. Metamorphism and metamorphic belts. George Allen & Unwin, London, 492 p.
- Naney, M.T. 1978. Stability and crystallization of ferromagnesian silicates in water-vapor undersaturated melts at 2 and 8 kb pressures. Unpublished Ph.D. thesis, Stanford University.
- Noble, D.C. and Hedge, C.E. 1970. Distribution of rubidium between sodic sanidine and natural silicic liquid. Contrib. Mineral. Petrology, V. 29, pp. 234-241.
- O'Hara, M.J. 1965. Primary magmas and the origin of basalts. Scott. J. Geol., V. 1, pp. 19-40.
- Olsen, N.O. 1978. Distinguishing between inter-kinematic and syn-kinematic porphyroblastic. Geol. Rundsch., Bd. 67, pp. 288-305.
- Pearce, J.A. and Cann, J.R. 1973. Tectonic setting of basic volcanic rocks determined using trace element analyses. Earth Planet. Sci. Lett., V. 19, pp. 290-300.
- Pearce, T.H., Gorman, B.C. and Pickett, T.C. 1975. The  $TiO_2$ - $K_2O$  -  $P_2O_5$  diagram: a method of discriminating between oceanic and non-oceanic basalts. Earth Planet Sci. Letters, V. 24, pp. 419-426.

- Perchuk, L.L. 1970. Equilibrium of biotite with garnet in metamorphic rocks. *Geochem. Int.*, V. 1, pp. 157-179.
- Pettijohn, F.J., Potter, P.W. and Siever, R. 1972. Sand and sandstones. Springer-Verlag, N.Y., 618 p.
- Phillips, W.E.A. 1978. The Caledonide Orogen in Ireland. In: Caledonian-Appalachian Orogen of the North Atlantic. *Geol. Surv. Canada Paper* 78-13, pp. 97-109.
- Philpotts, J.A. and Schnetzler, C.C. 1970. Phenocryst-matrix partition coefficients for K, Rb, Sr and Ba, with application to anorthosite and basalt genesis. *Geochim. Cosmochim. Acta*, V. 34, pp. 307-322.
- Pitcher, W.S. and Berger, A.R. The Geology of Donegal: A study of granite emplacement and unroofing. Wiley-Interscience, N.Y., 425 p.
- Presnall, D.C. and Bateman, P.C. 1973. Fusion relations in the system  $\text{Ab-An-Or-Q}_3\text{-H}_2\text{O}$  and generation of granitic magmas in the Sierra Nevada batholith. *Geol. Soc. Amer. Bull.*, V. 84, pp. 2583-2610.
- Prinz, M. 1967. Geochemistry of basaltic rocks-minor elements in basalts. In: Hess, H.H. and Poldervaart A. (eds.), Basalts- the Poldervaart treatise on rocks of basaltic composition, V. 1. Interscience, pp. 271-323.
- Ramsay, J.G. 1967. Folding and fracturing of rocks. McGraw-Hill, 568 p.
- Ramsay, J.G. and Graham, R.H. 1970. Strain variation in shear belts. *Can. J. Earth Sci.*, V. 7, pp. 786-813.
- Rast, N. 1958. Metamorphic history of the Schichallion complex Perthshire. *Trans. R. Soc. Edinb.*, V. 63, pp. 413-431.

- Rast, N. and Sturt, B.A. 1957. Crystallographic and geological factors in the growth of garnets from Central Perthshire. *Nature*, V. 179, pp. 215-230.
- Rast, N., Kennedy, M.J. and Blackwood, R.F. 1976. Comparison of some tectonostratigraphic zones in the Appalachians of Newfoundland and New Brunswick. *Can. J. Earth Sci.*, V. 13, pp. 868-875.
- Reitan, P.H. 1968a. Frictional heat during metamorphism. 1. Quantitative evaluation of concentration of heat generation in time. *Lithos*, V. 1, pp. 151-163.
- Reitan, P.H. 1968b. Frictional heat during metamorphism. 2. Quantitative evaluation of concentration of heat generation in space. *Lithos*, V. 1, pp. 268-274.
- Richardson, S.W., Gilbert, M.C. and Bell, P.M. 1969. Experimental determination of kyanite-andalusite and andalusite-sillimanite equilibria; the aluminum silicate triple point. *Amer. J. Sci.*, V. 267, pp. 259-272.
- Ringwood, A.E. 1974. The petrological evolution of island arc systems. *J. Geol. Soc.*, V. 130, pp. 1-204.
- Schenk, P.E. 1978. Synthesis of the Canadian Appalachians. In: *Caledonian-Appalachian Orogen of the North Atlantic*. Geological Survey of Canada Paper 78-13, pp. 111-136.
- Schnetzler, C.C. and Philpots, J.A. 1970. Partition coefficients of rare-earth elements between igneous matrix material and rock-forming mineral phenocrysts - II. *Geochim. Cosmochim. Acta*, V. 34, pp. 331-340.

- Scrutton, R.A. 1973. The age relationship of igneous activity and continental breakup. *Geol. Mag.*, V. 110, pp. 227-234.
- Shaw, D.M., 1970. Trace element fractionation during anatexis. *Geochim. Cosmochim. Acta*, V. 34, pp. 237-243.
- Sinha, Ray, S. 1977. Mylonitic structures and their bearing on the development of mylonites - an example from deformed trondhjemites of the Bergen Arc region, SW Norway. *Geol. Mag.*, V. 114, pp. 445-458.
- Smith, J.V. 1974. *Feldspar Minerals*, Volumes 1 & 2. Springer-Verlag, N.Y.
- Smithson, S.B. 1965. Oriented plagioclase grains in K-feldspar porphyroblasts. *Contr. to Geology, Univ. Wyoming* 4, pp. 63-68.
- Spry, A. 1963. Chronological analysis of crystallization and deformation of some Tasmanian Precambrian rocks. *J. Geol. Soc. Aust.*, V. 10, pp. 193-210.
- Streckeisen, A. 1976. To each plutonic rock its proper name. *Earth-Sci. Rev.*, V. 12, pp. 1-33.
- Stevens, R.K., Strong, D.F. and Kean, B.F. 1974. Do some eastern Appalachian ultramafic rocks represent mantle diapirs produced above a subduction zone? *Geology*, V. 2, pp. 175-178.
- Storre, B. and Karotke, E. 1971. An experimental determination of the upper stability limit of muscovite + quartz in the range 7-20 kb water pressure. *Neues Jahrb. Mineral. Monatsh.*, pp. 237-240.
- Strong, D.F. 1979. Metallogeny of North Atlantic granitoid rocks (ms. under review).
- Strong, D.F. 1977. Volcanic regimes in the Newfoundland Appalachians. In: Baragar, W.R.A., Coleman, L.C. and Hall, J.M. (eds.), *Volcanic Regimes in Canada*. *Geol. Assoc. Canada Spec. Paper* 16, pp. 61-90.

- Strong, D.F. and Dickson, W.L. 1978. Geochemistry of Paleozoic granitoid plutons from contrasting tectonic zones of northeast Newfoundland. *Can. J. Earth Sci.*, V. 15, pp. 145-156.
- Stukas, V. and Reynolds, P.H. 1974.  $^{40}\text{Ar}/^{39}\text{Ar}$  dating of the Long Range Dikes, Newfoundland. *Earth Planet. Sci. Letters*, V. 22, pp. 256-266.
- Swanson, S.E. 1977. Relation of nucleation and crystal-growth rate to the development of granitic textures. *Amer. Mineral.*, V. 62, pp. 966-978.
- Taylor, S.R. 1967. Geochemistry of andesites. In: Ahrens, L.H. (ed.), *Origin and distribution of elements*. Pergamon Press, London, pp. 559-582.
- Taylor, S.R., Heier, K.S. and Svendrup, T.L. 1960. Trace element variations in three generations of feldspar from the Landoverk I pegmatite, Evje-southern Norway. *Novsk Geologist Tidsskrift*, V. 40, pp. 136-156.
- Thornton, C.P. and Tuttle, O.F., 1960. Chemistry of igneous rocks. I. Differentiation Index. *Amer. J. Sci.*, V. 258, pp. 664-684.
- Upadhyay, H.D., Dewey, J.F. and Neale, E.R.W. 1971. The Betts Cove Ophiolite complex, Newfoundland: Appalachian oceanic crust and mantle. *Proc. Geol. Assoc. Can.*, 24, pp. 27-34.
- Van.Eysinga, F.W.B. (compiler) 1975. *Geological Time Table*. Elsevier, Amsterdam.
- Vance, J.A. 1969. On Syneusis. *Contrib. Mineral. Petrology*, V. 24, pp. 7-29.
- Vernon, R.H. 1978. Porphyroblast-matrix microstructural relationships in deformed metamorphic rocks. *Geol. Rundsch.*, Bd. 67, pp. 288-305.

- Wanless, R.K., Stevens, R.D., Lachance, G.R. and Rimsaite, J.Y.H. 1965. Age determinations and geological studies, Part I. Isotopic ages. Geol. Surv. Canada Paper 64-IX, 126 p.
- Weaver, D.F. 1967. A geological interpretation of the Bouguer anomaly field of Newfoundland. Dom. Obs. Can. Publ., V. 35, pp. 223-251.
- Wedepohl, K.H. 1971. Geochemistry. Holt, Rinehart and Winston, Inc., N.Y., 231 p.
- Whitney, J.A. 1975. The effects of P, T and  $X_{H_2O}$  on phase assemblages in four synthetic rock compositions. J. Geol., V. 83, pp. 1-31.
- Whitney, J.A. and Stormer, J.C. Jr. 1977. The distribution of  $NaSiSi_3O_8$  between coexisting microcline and plagioclase and its effect on geothermometric calculations. Amer. Mineral., V. 62, pp. 687-691.
- Williams, H. 1979. Appalachian Orogen in Canada. Can. J. Earth Sci., V. 16, pp. 792-807.
- Williams, H. (compiler) 1978). Tectonic-Lithofacies Map of the Appalachian Orogen. Memorial University of Newfoundland, Map. No. 1.
- Williams, H. 1975. Structural succession, nomenclature and interpretation of transported rocks in western Newfoundland. Can. J. Earth Sci., V. 12, pp. 1874-1894.
- Williams, H. 1968. Wesleyville, Newfoundland. Geol. Surv. Can., Map 1227A.
- Williams, H. 1964. The Appalachians in Northwestern Newfoundland - A two-sided symmetrical system. Amer. J. Sci., V. 262, pp. 1137-1158.
- Williams, H. and St. Julien, P. 1978. The Baie Verte - Brompton Line in Newfoundland and regional correlations in the Canadian Appalachians. Geol. Surv. Canada Paper 75-1A, pp. 225-229.



- Williams, H. and Stevens, R.K. 1974. The ancient continental margin of eastern North America. In: Burk, C.A. and Drake, C.L. (eds.), The geology of continental margins. Springer-Verlag, N.Y., pp. 781-796.
- Williams, H., Kennedy, M.J. and Neale, E.R.W. 1974. The northeastward termination of the Appalachian Orogen. In: Nairn, S.E.M. and Stehli, F.G. (eds.), The ocean basins and margins. Plenum Press, N.Y., pp. 79-123.
- Williams, H. and Stevens, R.K. 1969. Geology of Belle Isle - Northern extremity of the deformed Appalachian miogeosynclinal belt. Can. J. Earth Sci., V. 6, pp. 1145-1157.
- Wilson, J.T. 1966. Did the Atlantic close and then re-open? Nature, V. 211, pp. 676-681.
- Winkler, H.G.F. 1974. Petrogenesis of metamorphic rocks (3rd ed.). Springer Verlag, N.Y., 320 p.
- Winkler, H.G.F. and Breitbart, R. 1978. New aspects of granitic magmas. Neus Jahrb. Mineral. Monatsh., pp. 463-480.
- Winkler, H.G.F., Borse, M. and Marcopoulos, T. 1975. Low temperature granitic melts. Neus Jahrb. Mineral. Monatsh., pp. 145-268.
- Wright, T.L. 1968. X-ray and optical study of alkali feldspars: II an X-ray method for determining the composition and structural state from measurement of 2 $\theta$  values for three reflections. Amer. Mineral., V. 53, pp. 88-104.
- Wyllie, P.J. 1977. Crustal anatexis: an experimental review. Tectonophysics, V. 43, pp. 41-71
- Yardley, B.W. 1978. Genesis of the Skagit Gneiss migmatites, Washington, and the distribution between possible mechanisms of migmatization. Geol. Soc. Amer. Bull., V. 89, pp. 941-951.

- Yoder, H.S. Jr., Stewart, D.B. and Smith, J.R. 1957. Ternary feldspars. Carnegie Inst. Washington Yearb., 56, pp. 206-214.
- Younce, G.B. 1970. Structural geology and stratigraphy of the Bonavista Bay region, Newfoundland. Unpublished Ph.D. thesis, Cornell University.
- Zwart, H.J. 1962. On the determination of polymetamorphic mineral associations and its application to the Bosot area (Central Pyrenees). Geol. Rundsch., V. 52, pp. 38-65.
- Zwart, H.J. and Calon, T.J. 1977. Chloritoid crystals from Curaglia; Growth during flattening or pushing aside? Tectonophysics, V. 29, pp. 477-486.
- Dunnet, D., 1969. A technique of finite strain analysis using elliptical particles. Tectonophysics, V. 7, pp. 117-136.
- Mueller, R.F. and Saxena, S.K., 1977. Chemical Petrology. Springer-Verlag, New York, 394 p.
- Berthe, D., Choukroune, P. and Jegouzo, P., 1979. Orthogneiss, Mylonite and now coaxial deformation of granites: the example of the South American Shear zone. J. Struct. Geol., V. 1, pp. 31-42

Appendix 1.1 Definition of the terms metasediment, schist, gneiss and migmatite as given in "Glossary of Geology" published by the American Geological Institute (1972).

Gneiss - A foliated rock formed by regional metamorphism in which bands or lenticles of granular minerals alternate with bands or lenticles in which minerals having flaky or elongate prismatic habits predominate. Generally less than 50 percent of the minerals show preferred parallel orientation. Although a gneiss is commonly feldspar - and quartz-rich, the mineral composition is not an essential factor in its definition. Varieties are distinguished by texture, characteristic minerals or general composition and/or origins.

Schist - A strongly foliated crystalline rock formed by dynamic metamorphism which can be readily split into their flakes or slabs due to the well developed parallelism of more than 50 percent of the minerals present, particularly those of lamellar or elongate prismatic habit, e.g. mica, hornblende. The mineral composition is not an essential factor in its definition unless specifically included in the rock name. Varieties may also be based on general composition or on texture (e.g. spotted schist).

Migmatite - A composite rock composed of igneous or igneous looking and/or metamorphic materials which are generally distinguished megascopically.

Appendix 2.1 Composition of garnets and muscovites from the Square Pond Gneiss.

- Gi-R = Composition of the rim of garnet Gi
- Gi-R = Composition of the core of garnet Gi
- B-1 = Composition of biotite adjacent to garnet Gi
- B-1A = Composition of biotite from the same specimen as Gi but away from Gi

Analyses were done using a JEOL JXA-50A electronmicroprobe.

COMPOSITION OF GARNETS FROM LOCATION 422

SAMPLE	* G1-C	* G1-R	* G2-C	* G2-R	* G3-C	* G3-R	* G4-C	*
SiO2	* 37.32	* 36.05	* 36.25	* 35.69	* 34.11	* 36.62	* 37.50	*
TiO2	* 0.0	* 0.01	* 0.07	* 0.0	* 0.04	* 0.02	* 0.0	*
Al2O3	* 21.50	* 21.43	* 21.24	* 21.92	* 22.14	* 21.13	* 21.57	*
Cr2O3	* 0.02	* 0.02	* 0.0	* 0.02	* 0.02	* 0.11	* 0.0	*
FeO	* 30.45	* 30.57	* 27.21	* 32.90	* 32.12	* 32.19	* 30.71	*
MnO	* 5.33	* 5.18	* 9.40	* 4.66	* 6.78	* 4.44	* 5.99	*
MgO	* 1.53	* 1.81	* 1.19	* 1.07	* 1.50	* 1.99	* 1.84	*
CaO	* 1.31	* 1.53	* 2.08	* 1.91	* 1.55	* 1.88	* 1.68	*
Na2O	* 0.09	* 0.03	* 0.27	* 0.04	* 0.02	* 0.02	* 0.0	*
K2O	* 0.01	* 0.01	* 0.07	* 0.01	* 0.0	* 0.01	* 0.01	*
TOTAL	* 98.27	* 97.09	* 97.78	* 100.12	* 98.38	* 98.38	* 99.30	*

SAMPLE	* G4-R	* G5-C	* G5-R	* G6-C	* G6-R	*
SiO2	* 37.35	* 36.22	* 37.20	* 38.36	* 36.72	*
TiO2	* 0.07	* 0.02	* 0.0	* 0.01	* 0.0	*
Al2O3	* 21.46	* 22.15	* 22.89	* 21.99	* 21.50	*
Cr2O3	* 0.04	* 0.0	* 0.02	* 0.0	* 0.03	*
FeO	* 31.18	* 28.96	* 30.52	* 31.95	* 34.34	*
MnO	* 5.56	* 8.26	* 7.90	* 6.84	* 5.20	*
MgO	* 1.96	* 1.36	* 1.26	* 1.70	* 2.21	*
CaO	* 0.87	* 1.30	* 1.17	* 1.80	* 0.66	*
Na2O	* 0.05	* 0.0	* 0.0	* 0.07	* 0.02	*
K2O	* 0.02	* 0.01	* 0.0	* 0.03	* 0.02	*
TOTAL	* 98.56	* 98.28	* 100.96	* 102.75	* 100.70	*

# COMPOSITION OF GARNETS FROM LOCATION 547

SAMPLE	* G7-R	* G8-C	* G8-R	* G9-C	* G9-R
SiO2	36.78	39.03	38.85	37.77	37.90
TiO2	0.02	0.02	0.03	0.01	0.0
Al2O3	21.36	22.46	22.51	21.98	22.25
Cr2O3	0.02	0.02	0.02	0.02	0.06
FeO	33.82	29.92	30.03	29.85	30.18
MnO	5.06	6.58	6.60	7.05	6.80
MgO	1.97	1.88	1.91	1.43	1.47
CaO	1.80	1.24	1.49	1.14	1.02
Na2O	0.03	0.03	0.02	0.0	0.02
K2O	0.03	0.0	0.0	0.0	0.0
TOTAL	100.89	101.18	101.46	99.25	99.70

# COMPOSITION OF BIOTITES FROM LOCATION 422

SAMPLE	* B-1	* B-1A	* B-2	* B-2A	* B-3	* B-4	* B-6
SiO2	34.66	32.86	34.38	34.89	33.62	35.22	34.73
TiO2	1.96	1.78	1.93	1.44	1.69	1.42	1.51
Al2O3	20.78	20.71	22.03	20.77	19.84	21.24	20.43
Cr2O3	0.05	0.09	0.08	0.09	0.05	0.07	0.09
FeO	20.28	23.83	21.68	21.41	20.60	20.20	22.52
MnO	0.13	0.13	0.13	0.05	0.14	0.12	0.13
MgO	7.52	8.12	8.02	7.59	7.78	8.30	7.92
CaO	0.0	0.02	0.0	0.04	0.0	0.0	0.0
Na2O	0.28	0.26	0.24	0.27	0.29	0.31	0.25
K2O	7.41	7.02	6.58	7.19	7.28	7.41	7.12
TOTAL	92.59	91.62	95.07	93.78	91.29	94.29	94.70

POOR COPY  
COPIE DE QUALITEE INFERIEURE

# COMPOSITION OF BIOTITES FROM LOCATION 422

SAMPLE	* B-5A	* B-23	* B-24	* B-25	* B-25	*
SiO2	33.37	37.73	38.57	36.98	37.13	*
TiO2	1.43	1.27	1.60	1.57	1.74	*
AL2O3	21.59	21.83	21.78	21.61	21.31	*
CR2O3	0.05	0.0	0.02	0.04	0.02	*
FeO	21.83	21.11	23.20	23.04	24.02	*
MNO	0.08	0.09	0.06	0.11	0.13	*
MGO	8.41	8.32	8.12	7.91	7.78	*
CAO	0.0	0.0	0.0	0.0	0.0	*
NA2O	0.32	0.30	0.24	0.27	0.21	*
K2O	7.37	5.91	6.07	6.05	5.82	*
TOTAL	94.94	96.56	99.66	97.58	98.73	*

# COMPOSITION OF BIOTITES FROM LOCATION 547

SAMPLE	* B-7	* B-9	* B-14	* B-16	*
SiO2	36.08	35.60	36.41	35.15	*
TiO2	1.66	1.41	1.46	1.35	*
AL2O3	21.73	20.71	21.21	21.13	*
CR2O3	0.09	0.01	0.02	0.04	*
FeO	19.77	25.50	25.38	25.74	*
MNO	0.09	0.14	3.11	0.15	*
MGO	7.59	6.78	6.55	6.47	*
CAO	0.0	0.0	0.0	0.0	*
NA2O	0.23	0.19	0.25	0.24	*
K2O	7.27	6.91	6.75	6.54	*
TOTAL	94.51	97.25	101.14	96.82	*



### Appendix 3.1 Modal Analysis.

#### a. Megacrystic granites.

Modal analysis was done on flat slabs of rock each about  $10 \times 10 \text{ cm}^2$  in area. The face to be analyzed was ground to a rough polish and then stained for potassium-feldspar. The staining was done using sodium cobaltinitrite according to method described by Hutchinson (1974). A sheet of transparent graph paper with a 10 m grid was laid on the polished and stained surface and the points of intersection of the lines on the graph paper were counted for quartz, potassium-feldspar, plagioclase and biotite. Modal analysis was done on at least two rock slabs from each location.

In addition, the ratio of megacrysts to matrix was obtained at several places by using a fishing net with an approximately 2.5 cm grid. At least 500 points were counted at each location.

#### b. Non-megacrystic plutons.

Modal analysis was done on standard size thin sections stained for potassium-feldspar with sodium cobaltinitrite. The analysis was carried out using a polarizing microscope with a Swift automatic point-counter stage unit attached to its stage and an electronic control box with 7 non-resetting counters. The horizontal traverses were done with a  $1/3 \text{ mm}$  step and the vertical traverses with a

1/2 mm step. At least 750 points were counted on each thin section.

Reference:

Hutchinson, C.S. (1974). Laboratory Handbook of Petrographic Techniques. Wiley-Interscience, N.Y., 527 p.

Appendix 3.2 Molecular percentages of quartz (Q), albite (Ab), orthoclase (Or) and anorthite (An) in the mesonorms (Barth, 1959) of the granitoids in the area. (Q+Ab+An+Or has been normalized to 100).

	Sample #	Q	Ab	Or	An
Wareham Quartz Monzonite	NJ-353	39.17	15.12	6.42	9.70
	354	49.53	18.46	6.41	7.34
	355	54.22	16.18	11.30	6.78
	373	54.62	19.28	7.40	8.57
	637	51.45	17.66	9.96	11.66
	641	53.16	18.31	10.96	5.96
	642	26.50	15.20	9.35	7.15
	700	52.57	17.42	8.71	9.28
	763	67.19	13.06	7.69	5.41
	723	49.72	17.15	10.41	7.25
	1084	55.50	16.45	10.90	9.05
	914	58.58	15.28	8.14	8.22
	877	69.80	11.51	11.30	3.05
	374	68.68	12.00	12.82	2.30
North Pond Granite (medium-grained)	NJ-364	66.52	13.07	9.86	2.53
	368	68.07	14.07	8.86	1.76
	369	66.30	14.86	9.60	2.69
	370	69.55	14.09	7.43	3.55
	352	69.09	10.44	13.33	0.45
	510	68.29	14.41	9.60	1.49
	567	65.33	14.21	8.35	4.85
	592	68.90	12.90	11.99	0.31
	601	65.97	14.28	8.97	3.44
	601A	69.18	14.10	7.01	3.69
	503	65.05	14.12	9.08	4.24

	Sample #	Q	Ab	Or	An
North Pond Granite (porphyritic)	NJ-891	69.13	11.36	11.98	1.41
	512	53.65	16.03	15.44	4.92
	488	71.06	11.49	11.63	0.00
	597	69.59	12.66	11.60	0.38
	598	69.23	13.70	9.35	0.61
	648	66.14	14.13	8.81	3.62
	845	68.56	11.62	13.48	0.47
	856	68.01	11.66	13.27	0.92
	1172	68.92	13.80	10.73	0.74
Cape Freels Granite	38	60.31	15.56	14.71	3.39
	41	61.87	15.17	13.01	3.26
	96	60.71	15.44	14.61	2.93
	170	66.84	12.80	14.34	2.36
	80	55.31	15.26	15.14	2.92
	NJ-FI*	55.44	17.85	6.40	10.55
	271*	46.42	21.13	11.78	7.67
	272*	37.80	21.97	15.76	9.89
	273*	54.78	15.44	6.72	9.85
	267*	44.63	24.04	8.19	11.69
*From Greenspond variant.					
Lockers Bay Granite	NJ-L1	52.70	19.29	14.13	5.30
	L2	57.57	16.01	13.98	4.67
	L3	60.91	14.29	14.01	3.94
	L4	60.98	13.83	16.25	3.17
	L5	64.68	13.88	12.26	3.07
	L6	58.25	15.29	15.82	4.04
Business Cove Granite	NJ-173	67.79	14.35	6.86	4.15
	219	63.62	17.36	10.85	2.90
	266	70.74	10.35	14.06	0.36
	1070	72.52	11.97	14.75	4.96

	Sample #	Q	Ab	Or	An
Big Round Pond Granite	NJ-621	67.64	14.69	10.99	3.43
	134	60.87	16.32	13.28	4.35
	1163	66.53	14.32	12.31	2.28
Deadman's Bay Granite	509	65.61	13.71	9.08	1.38
	819	71.87	12.47	9.98	2.90
	822	62.23	13.85	13.96	3.14
	824	62.45	14.08	16.30	3.25
	828	66.62	12.18	11.35	1.19
	993	65.62	12.54	10.89	3.23
	1094	65.90	13.07	12.69	3.01
	1095	68.25	11.59	12.69	2.24
	1	64.48	13.89	12.42	3.99
Newport Granite	205	67.81	14.49	12.15	2.63
	302	65.43	14.91	13.95	2.75
	304	61.66	15.60	15.72	3.02
	260	63.07	16.85	12.69	3.49
	1001	63.61	15.70	13.22	3.78
	1003	62.91	16.50	13.58	3.51
	1004	62.32	16.23	13.45	3.75
	1005	72.22	12.59	11.90	2.17
	1140	50.94	22.89	15.51	5.42

Reference:

Barth, T.F., 1959. Principles of classification and norm calculations of metamorphic rocks. J. Geol., V. 67, pp. 135-152.

Appendix 3.3

Length (l) and breadth (b) of megacrysts and the angle ( $\phi$ ) between the long axis of the megacrysts and the mineral alignment at five locations in the Cape Freels Granite.

Location 1:- Near wharf on north shore of Cape Freels Island. Undeformed megacrystic granite. Measurements on a vertical plane striking at  $150^{\circ}$ .

l cm	b cm	l/b	$\phi$	l cm	b cm	l/b	$\phi$
2.1	0.7	3.0	0	1.2	0.8	1.5	50
0.9	0.6	1.5	-15	0.9	0.6	1.5	70
0.7	0.9	0.78	-05	0.3	0.4	2.0	-10
1.3	0.4	3.25	0	1.3	0.6	2.17	-60
1.7	0.6	2.83	0	1.3	0.4	3.25	50
0.7	0.3	2.33	30	1.0	0.4	2.5	50
1.3	0.6	2.17	50	1.1	0.6	1.83	30
1.0	0.4	2.5	55	1.3	0.7	2.57	45
1.0	0.6	1.67	-40	2.0	1.6	1.25	60
0.9	0.6	1.5	70	0.8	0.3	2.67	0
1.2	0.4	3.0	-10	1.5	0.6	2.5	-20
0.9	0.4	2.25	0	1.1	0.3	1.33	35
1.1	0.4	2.75	70	1.0	0.3	3.33	0
1.1	0.3	3.67	75	0.8	0.4	2.0	0
1.2	0.4	3.0	-15	0.8	0.4	2.0	25
1.5	0.5	3.0	10	1.0	0.7	1.43	75
1.4	0.9	1.56	40	1.7	0.9	1.89	60
0.6	0.4	1.5	-15	0.9	0.5	1.8	-30
0.8	0.4	2.0	-20	1.5	0.7	2.14	35
0.9	0.4	2.25	30	1.0	0.4	2.5	20
0.9	0.5	1.8	0	1.6	0.6	2.67	65
0.7	0.4	1.75	35	1.4	0.6	2.33	0
1.3	0.9	2.0	20	0.8	0.6	1.33	-10
0.8	0.4	2.0	20	1.2	0.5	2.4	-30
1.0	0.6	1.67	05	1.3	0.6	3.0	-20

Location 1:- Undeformed megacrystic granite. Measurements on a vertical plane striking at  $60^{\circ}$ .

l cm	b cm	l/b	$\phi$	l cm	b cm	l/b	$\phi$
1.7	0.6	2.83	-10	0.8	0.4	2.0	05
1.2	0.5	2.4	-35	1.6	0.7	2.29	-50
0.9	0.4	2.25	-15	1.3	0.6	2.17	-05
2.0	0.9	2.22	-15	1.2	0.6	2.0	-10
1.3	0.7	2.57	-30	1.1	0.7	1.57	-08
1.7	1.2	1.42	40	1.1	0.5	2.2	0

Continued .....

l cm	b cm	1/b	$\phi$	l cm	b cm	1/b	$\phi$
1.4	0.4	3.5	-20	1.0	0.5	2.0	-05
0.3	0.4	2.0	20	1.3	1.3	1.33	-30
1.4	0.7	2.0	25	0.3	0.3	2.67	0
0.7	0.3	2.33	0	2.0	0.5	4.0	-08
1.1	0.6	2.17	15	0.3	0.3	1.0	0
1.2	0.5	2.4	-45	0.6	0.3	2.0	0
0.3	0.4	2.0	-20	0.6	0.3	2.0	0
1.0	0.5	2.0	-15	1.3	0.5	2.6	-18
0.9	0.4	2.25	-02	1.1	0.6	1.83	03
1.5	0.9	1.67	-15	0.6	0.5	1.2	-30
1.0	0.4	2.5	0	0.9	0.6	1.5	-02
1.7	0.3	2.13	15	0.9	0.4	2.25	-05
1.0	0.3	3.33	20	0.7	0.2	3.5	15
1.5	1.2	1.25	-03	1.4	0.6	2.33	05
1.3	0.4	3.25	-10	0.9	0.4	2.25	03
1.1	0.4	2.75	-10	0.7	0.2	3.5	0
0.7	0.3	2.33	0	0.6	0.4	1.5	10
0.7	0.2	3.5	0	0.6	0.3	2.0	0
0.7	0.4	1.75	0	1.0	0.5	2.0	-15

Location 2:- Quarry 1.5 kilometers south of the turnoff to Cape Freels.  
Deformed megacrystic granite. Measurements on a plane  
perpendicular to foliation (30,85 NW) and parallel to  
lineation (horizontal).

l cm	b cm	1/b	$\phi$	l cm	b cm	1/b	$\phi$
3.5	1.0	3.5	07	1.4	0.6	2.33	0
4.3	2.5	1.72	04	6.5	2.6	2.5	0
3.0	0.9	3.33	10	2.7	1.2	2.25	08
4.2	1.5	2.3	10	5.6	2.2	2.55	-06
3.0	3.9	2.05	10	1.4	0.6	2.33	0
3.8	1.0	3.8	12	3.3	1.2	2.75	0
4.0	1.2	3.33	-04	3.2	1.1	2.91	0
2.5	0.8	3.13	10	3.3	1.4	2.36	02
3.0	1.1	2.73	0	3.0	1.0	3.0	02
2.3	1.1	2.09	0	2.5	0.8	3.13	05
2.9	1.3	2.23	85	4.3	1.7	2.53	02
3.0	0.9	3.33	0	4.2	1.5	2.8	0
2.3	0.9	2.56	06	5.3	1.3	4.08	0
3.3	1.0	3.3	25	1.8	1.0	1.8	06
4.5	1.3	3.46	10	2.2	0.9	2.44	0
4.4	1.7	2.59	05	5.2	1.4	3.71	03
3.2	1.0	3.2	-02	2.7	1.2	2.25	03
2.5	0.9	2.78	04	2.5	1.1	2.27	0
3.0	1.2	2.5	0	4.3	1.7	2.53	-02

Continued.....

l cm	b cm	l/b	$\phi$	l cm	b cm	l/b	$\phi$
3.0	1.2	2.5	12	1.2	0.7	1.71	0
3.6	1.0	3.6	-02	5.0	1.0	5.0	0
9.0	5.0	1.8	03	1.5	0.7	2.14	0
4.0	1.0	4.0	04	5.0	1.8	2.78	03
4.2	0.9	4.67	10	4.3	2.0	2.15	12
3.2	1.7	1.88	-04	2.2	1.0	2.2	03

Location 2:- Deformed megacrystic granite. Measurements in a plane perpendicular to foliation and lineation.

l cm	b cm	l/b	$\phi$	l cm	b cm	l/b	$\phi$
2.0	1.1	1.82	10	2.3	1.1	2.09	04
4.5	1.3	2.5	0	3.2	1.1	2.91	05
4.0	2.5	1.6	0	2.1	1.0	2.1	20
2.7	1.0	2.7	02	3.0	1.1	2.73	-03
3.8	2.2	1.73	04	1.1	0.9	1.22	-02
5.0	3.0	1.67	-03	2.3	0.9	2.55	-06
2.2	1.2	1.83	05	1.4	0.7	2.0	-02
1.8	1.0	1.8	0	4.4	1.8	2.56	-15
3.3	1.2	2.75	-10	2.0	0.8	2.5	0
3.0	1.5	2.0	05	1.5	0.6	2.5	0
4.0	1.3	3.03	0	2.5	1.0	2.5	08
3.0	1.2	2.5	-05	2.5	0.8	3.13	03
2.3	1.3	2.15	0	2.0	1.0	2.0	25
3.3	1.5	2.53	06	3.5	1.3	2.69	-20
3.2	1.2	2.67	0	2.0	1.0	2.0	25
4.0	1.7	2.35	-04	1.3	0.6	2.17	0
3.5	1.0	3.5	0	1.7	1.0	1.7	0
3.2	1.5	2.13	0	2.3	1.3	1.77	-02
3.5	1.0	3.5	0	1.3	0.7	1.96	10
2.7	1.5	1.8	0	3.5	1.6	2.19	0
4.7	2.7	1.74	-03	3.8	1.5	2.53	08
3.2	1.7	1.88	0	1.4	0.5	2.8	-05
3.5	1.7	2.06	04	2.0	1.0	2.0	0
3.0	1.5	2.0	-02	1.4	0.7	2.0	0
2.0	1.1	1.82	02	2.1	0.9	2.63	0

Location 3:- Big quarry at the side road to Newtown water supply. Undeformed megacrystic granite. Measurements on a vertical plane striking at 140°.

l cm	b cm	l/b	$\phi$	l cm	b cm	l/b	$\phi$
3.5	1.2	2.92	05	1.5	1.0	1.5	-15
3.3	2.0	1.65	10	2.2	0.8	2.75	-25
4.0	2.0	2.0	0	3.5	1.2	2.92	10
2.2	1.2	1.83	-10	2.0	1.0	2.0	-15

Continued.....



l cm	b cm	1/b	$\phi$	l cm	b cm	1/b	$\phi$
3.0	1.3	2.31	-40	3.0	2.0	1.5	20
5.0	2.5	2.0	0	3.5	1.5	2.33	0
2.2	1.5	1.47	0	1.2	0.8	1.5	-08
1.5	0.9	1.33	0	1.5	1.2	1.25	-10
3.2	3.0	1.07	30	2.3	1.3	1.77	0
1.2	0.8	1.5	0	2.5	1.7	1.47	15
7.6	3.2	2.33	-05	5.0	1.7	2.94	0
4.2	2.5	1.68	-25	1.7	1.7	1.0	0
4.5	2.2	2.05	10	2.5	1.2	2.03	30
2.0	1.0	2.0	-05	2.1	1.0	2.1	50
2.5	1.5	1.67	-50	3.7	2.5	1.48	50
1.7	0.8	2.13	0	3.0	1.3	2.31	0
1.5	1.2	1.25	-20	3.2	1.8	1.77	-15
1.5	1.2	1.25	-05	1.5	0.5	3.0	-05
2.3	1.7	1.65	-18	2.3	1.0	2.3	0
4.0	2.2	1.82	-10	4.0	1.5	2.67	12
2.0	1.2	1.67	05	5.0	2.0	2.5	40
2.8	1.0	2.8	10	5.0	2.5	2.0	75
2.5	1.5	1.67	20	2.8	1.2	2.33	08
3.0	1.8	1.67	-40	3.0	1.4	2.14	40
2.5	1.0	2.5	-30	3.7	1.7	2.18	-06

Location 3:- Undeformed granite. Measurements on a vertical plane striking at  $45^\circ$ .

l cm	b cm	1/b	$\phi$	l cm	b cm	1/b	$\phi$
5.0	1.5	3.33	-08	3.5	1.5	2.33	0
2.5	1.0	2.5	-10	2.5	1.0	2.5	0
4.0	1.2	3.33	-25	4.0	1.2	3.33	0
2.5	0.7	3.57	-05	2.5	1.2	2.08	20
2.0	1.0	2.0	30	4.8	2.0	2.4	30
5.0	2.2	2.27	05	2.0	1.5	1.33	-45
3.2	3.0	1.07	0	2.0	1.0	2.0	35
2.0	0.8	2.5	0	3.0	1.5	2.0	0
3.0	1.3	2.31	0	1.5	1.5	1.0	0
1.7	1.2	1.42	20	4.2	2.2	1.91	-45
5.5	2.2	2.2	-35	2.0	1.2	1.67	20
1.2	0.6	2.0	35	3.3	1.5	2.2	20
1.2	0.5	2.4	-25	5.0	1.5	3.33	-35
2.3	1.2	1.92	90	2.2	1.0	2.2	0
1.1	0.6	1.83	12	2.3	1.0	2.3	0
2.4	1.1	2.18	-30	3.7	1.8	2.06	0
2.0	1.3	1.54	20	4.2	1.5	2.8	15
1.5	1.3	1.15	-70	2.3	1.2	1.92	30
4.5	1.5	3.0	-10	2.2	1.2	1.83	50

Continued.....

l cm	b cm	l/b	$\phi$	l cm	b cm	l/b	$\phi$
4.0	1.7	2.35	-50	2.2	1.0	2.2	0
3.5	1.7	2.06	15	1.5	1.0	1.5	20
3.5	1.4	2.5	30	5.0	1.5	3.33	25
3.5	1.7	2.06	20	2.5	1.0	2.5	10
2.5	1.2	2.08	-25	1.5	1.0	1.5	25
4.5	2.5	1.8	22	1.5	0.7	2.14	25

Location 3:- Slightly sheared megacrystic granite. Measurements on a plane perpendicular to foliation and parallel to lineation.

l cm	b cm	l/b	$\phi$	l cm	b cm	l/b	$\phi$
5.0	2.0	2.5	20	1.5	0.6	2.5	0
1.8	0.5	3.6	35	2.5	1.1	2.27	0
2.0	1.2	1.67	35	3.7	1.8	2.06	-20
2.0	1.0	2.0	0	1.7	0.5	3.4	-08
3.0	2.3	1.30	30	4.2	1.4	3.0	-08
1.8	0.3	2.25	0	1.0	0.6	1.67	0
2.5	1.4	1.79	40	2.5	1.0	2.5	10
2.0	1.4	1.43	35	2.5	1.2	2.08	-15
1.7	0.7	2.43	-05	1.7	0.7	2.43	-05
2.8	1.0	2.8	20	1.5	0.5	3.0	0
3.0	1.2	2.5	-25	4.0	1.3	3.08	0
1.5	0.5	3.0	-15	4.2	1.0	4.2	0
1.8	1.0	1.8	15	5.0	1.7	2.94	03
3.0	1.2	2.5	0	3.5	1.4	2.5	15
2.8	1.0	2.8	-30	1.7	0.9	1.89	0
1.0	0.6	1.67	10	1.8	0.7	2.57	-02
1.2	0.7	1.71	10	3.0	1.2	2.5	08
2.0	0.9	2.22	-05	1.8	0.7	2.57	-40
1.3	0.6	2.17	08	2.0	0.8	2.5	25
1.2	0.7	1.71	15	4.2	1.2	3.5	0
1.0	0.7	1.43	10	2.3	0.7	3.29	0
5.5	1.8	3.06	0	1.8	0.8	2.25	0
3.3	1.2	2.75	0	2.5	1.2	2.08	-10
2.6	1.0	2.6	0	2.0	1.0	2.0	-08
3.8	1.2	3.17	0	2.0	1.0	2.0	-25

Location 3:- Slightly sheared megacrystic granite. Measurements on a plane perpendicular to foliation and lineation.

l cm	b cm	l/b	$\phi$	l cm	b cm	l/b	$\phi$
2.0	0.9	2.22	-20	0.6	0.5	1.2	0
0.9	0.4	2.25	-08	0.2	0.15	1.33	0
0.6	0.4	1.5	0	1.0	0.3	3.33	-15
1.0	0.4	2.5	-25	0.7	0.3	2.33	0
0.9	0.4	2.25	15	0.4	0.2	2.0	-10

Continued.....

l cm	b cm	1/b	$\phi$	l cm	b cm	1/b	$\phi$
1.4	0.3	4.67	-15	0.8	0.3	2.67	-25
2.0	1.0	1.0	0	1.3	0.6	2.17	-30
1.6	0.6	2.67	-15	2.0	0.5	4.0	0

Location 4:- Deformed megacrystic granite. Measurements on a plane perpendicular to foliation and lineation.

l cm	b cm	1/b	$\phi$	l cm	b cm	1/b	$\phi$
1.2	0.4	3.0	10	1.1	0.4	2.75	35
0.7	0.6	1.17	-30	2.1	1.0	2.1	02
1.2	0.4	3.0	10	1.1	0.4	2.75	30
0.9	0.2	4.5	0	1.4	3.5	0.4	0
1.0	0.3	3.33	0	1.1	0.5	2.2	-15
1.5	0.4	3.5	02	1.0	0.3	3.33	0
1.0	0.4	2.5	10	1.2	0.3	4.0	0
1.0	0.4	2.5	0	1.1	0.4	2.75	20
0.7	0.5	1.4	-20	1.0	0.6	1.67	15
1.1	0.3	3.67	10	0.9	0.4	2.25	0
2.9	0.8	3.63	0	1.7	0.8	2.13	-10
1.0	0.4	2.5	0	0.9	0.3	3.0	0
1.0	0.5	2.0	-02	1.0	0.4	2.5	0
0.7	0.3	2.33	0	0.9	0.4	2.25	20
1.3	0.6	2.17	0	0.7	0.5	1.4	70
0.7	0.3	2.33	-10	0.9	0.5	1.8	0
1.0	0.4	2.5	0	1.3	0.4	3.25	02
0.3	0.5	1.6	25	1.5	0.6	2.5	-05
0.2	0.7	0.29	0	1.1	0.6	1.83	0
1.0	0.5	2.0	02	0.6	0.2	3.0	0
0.7	0.2	3.5	0	0.8	0.3	2.67	30
1.4	0.6	2.33	10	0.7	0.3	2.33	0
1.0	0.5	2.0	0	1.0	0.4	2.5	02
1.6	0.4	4.0	0	1.2	0.3	4.0	0
0.8	0.3	2.67	0	1.2	0.4	3.0	-10

Location 5:- Southeast corner of Main Pools Island. Deformed megacrystic granite. Measurements on a plane perpendicular to foliation ( $30^\circ$ ,  $90^\circ$ ) and parallel to lineation (horizontal).

l cm	b cm	1/b	$\phi$	l cm	b cm	1/b	$\phi$
2.0	0.8	2.5	-15	0.8	0.3	2.67	0
0.9	0.5	1.8	20	1.2	0.3	4.0	0
1.7	0.7	2.43	0	1.3	0.6	2.17	0
1.0	0.3	3.33	0	1.0	0.5	2.0	0
1.3	0.5	2.6	0	1.3	0.5	2.6	0
0.8	0.4	2.0	0	1.6	0.5	3.2	0

Continued.....

l cm	b cm	1/b	$\phi$	l cm	b cm	1/b	$\phi$
0.3	0.5	1.6	0	0.2	0.1	2.0	0
0.9	0.4	2.0	0	0.7	0.3	2.33	70
0.8	0.3	2.67	10	0.6	0.3	2.0	-20
0.6	0.5	1.2	15	2.0	0.5	4.0	0
1.0	0.4	2.5	10	0.5	0.2	2.25	10
1.9	1.0	1.8	20	0.6	0.2	3.0	0
0.9	0.4	2.25	20	1.0	0.4	2.5	-05
0.7	0.4	1.75	0	0.7	0.3	2.33	10
2.1	0.6	3.5	-08	0.6	0.2	3.0	03
2.0	0.8	2.5	10	0.3	0.1	3.0	0
0.7	0.3	2.33	0	1.3	0.4	3.25	20
0.8	0.3	2.67	-60	0.8	0.3	2.67	0
1.0	0.4	2.5	0	0.7	0.2	3.5	-10
1.4	0.4	3.5	0	0.3	0.1	3.0	0
0.7	0.3	2.33	-15	0.5	0.3	1.67	15
0.3	0.2	1.5	15	0.6	0.2	3.0	-15
0.3	0.15	2.0	20	0.7	0.3	2.33	0
1.5	0.9	1.67	75	0.5	0.2	2.25	0
0.7	0.3	2.33	-20	0.8	0.3	2.67	-10
0.5	0.2	2.25	25	0.5	0.2	2.25	0

Location 4:- Outcrop behind Goodview Hotel at Badger's Bay. Deformed megacrystic granite. Measurements on a plane perpendicular to foliation (30,85 NW) and lineation (horizontal).

l cm	b cm	1/b	$\phi$	l cm	b cm	1/b	$\phi$
1.9	0.6	3.17	0	1.6	0.4	4.0	-15
1.3	0.3	4.33	0	2.5	0.3	3.13	0
0.3	0.3	2.67	-10	2.5	0.5	5.0	0
1.1	0.6	1.83	0	1.0	0.3	3.33	-02
1.9	0.6	3.17	-10	1.0	0.5	2.0	0
0.4	0.2	2.0	05	1.2	0.4	3.0	05
1.6	0.5	3.2	-15	1.3	0.4	3.25	10
2.3	0.7	3.29	0	2.2	0.6	3.67	0
1.5	0.5	3.0	08	1.4	0.5	2.8	10
1.0	0.4	2.5	15	1.0	0.4	2.5	0
1.2	0.3	4.0	0	2.4	0.6	4.0	0
2.0	0.3	6.67	0	1.1	0.4	2.75	-05
1.8	0.7	2.57	0	1.9	0.4	4.75	0
1.9	0.4	4.75	08	1.2	0.3	4.0	0
1.0	0.4	2.5	-20	1.2	0.3	4.0	05
1.3	0.4	3.25	-15	3.6	1.6	2.25	40
1.3	0.3	4.33	10	1.7	0.8	2.13	45
1.2	0.3	4.0	0	1.7	0.4	4.25	0
1.3	0.4	3.25	05	1.4	0.4	3.5	-35
1.0	0.3	3.33	0	1.3	0.4	3.25	08
1.7	0.7	2.43	-10	1.4	0.4	3.5	10
1.0	0.4	2.5	50	2.8	1.3	2.15	30

Continued.....

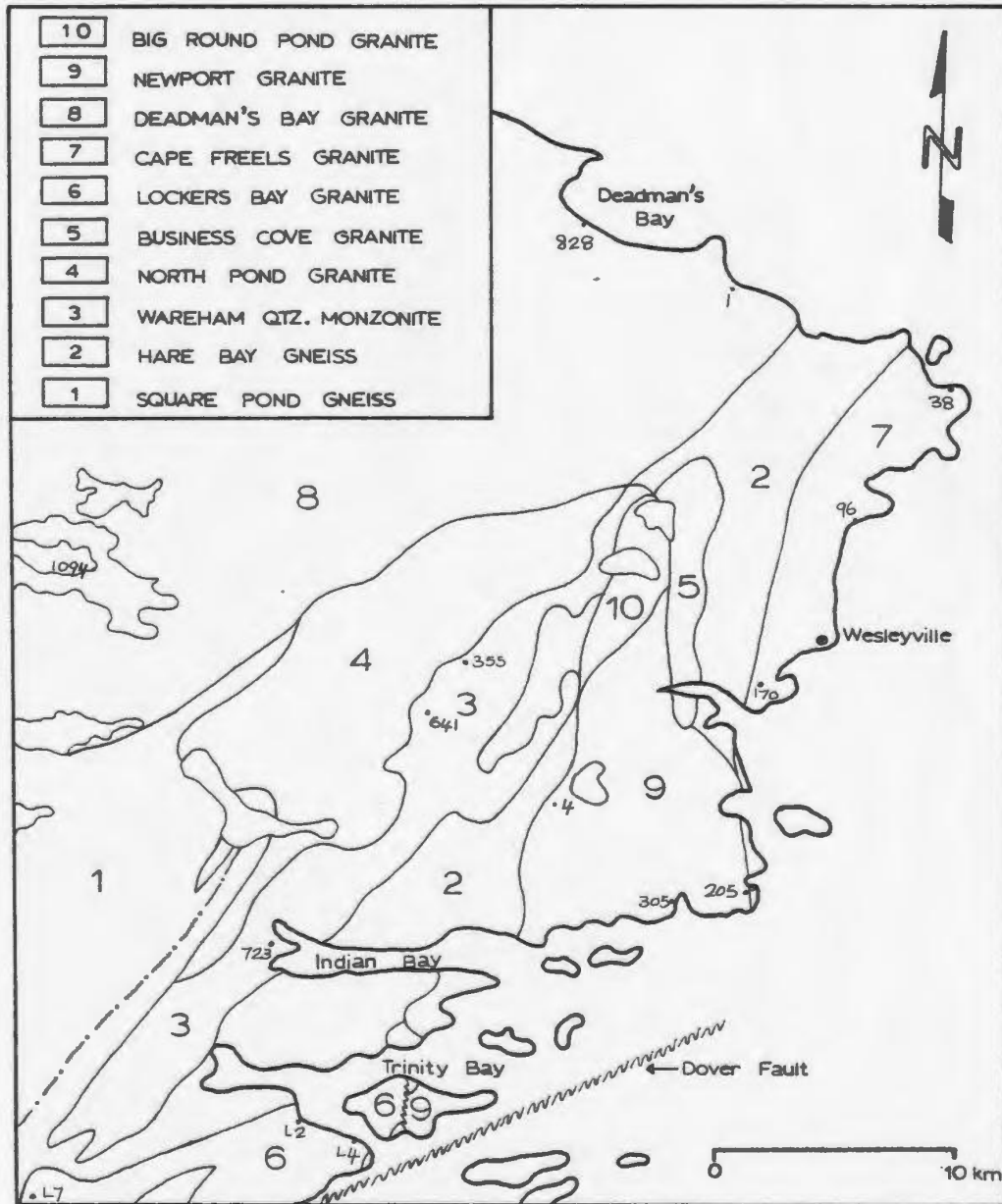
l cm	b cm	1/b	$\phi$	l cm	b cm	1/b	$\phi$
0.3	0.3	2.67	25	1.5	0.5	3.0	0
1.0	0.4	2.5	-10	1.2	0.3	4.0	0
2.1	1.2	1.75	75	1.5	0.5	3.0	0
0.9	0.4	2.25	15	1.2	0.5	2.4	25
1.0	0.3	3.33	-10	1.2	0.4	3.0	15
0.9	0.5	1.8	25	1.1	0.3	3.67	-05
0.9	0.4	2.25	30	0.9	0.4	2.25	15
2.1	0.3	2.63	0	1.3	0.3	4.33	08
1.2	0.5	2.4	20	1.0	0.3	3.33	0
1.4	0.7	2.0	0	0.9	0.3	3.0	-05
0.9	0.5	1.8	15	0.9	0.5	1.8	05
1.2	0.3	4.0	0	0.9	0.4	2.25	20
1.2	0.2	6.0	0	1.3	0.3	4.33	-02
0.8	0.2	4.0	15	2.0	1.0	1.0	0
1.4	0.5	2.8	0	1.1	0.4	2.75	10
0.6	0.3	2.0	-05	1.0	0.5	2.0	0
1.5	0.5	3.0	02	0.9	0.4	2.25	08
1.3	0.4	3.25	0	1.3	0.4	3.25	10
1.0	0.5	2.0	30	1.3	0.7	1.86	50

Location 5:- Deformed megacrystic granite. Measurements on a plane perpendicular to foliation and lineation.

l cm	b cm	1/b	$\phi$	l cm	b cm	1/b	$\phi$
1.3	0.6	3.0	02	1.3	0.3	4.33	05
1.4	0.5	2.8	40	2.0	1.4	1.43	30
1.0	0.6	1.67	70	1.4	0.4	3.5	15
0.9	0.3	3.0	0	1.3	0.4	3.25	-10
0.7	0.2	3.5	05	1.0	0.3	3.33	-05
1.7	0.7	2.43	0	1.3	0.3	4.33	0
0.7	0.7	1.0	-60	1.6	0.8	2.0	10
1.0	0.3	3.33	-02	2.0	0.5	4.0	0
1.0	0.7	1.43	20	1.0	0.4	2.5	20
1.6	0.7	2.43	-65	1.5	0.6	2.5	10
0.8	0.3	2.67	0	0.9	0.3	3.0	0
1.0	0.3	3.33	-08	1.2	0.4	3.0	-10
1.5	0.7	2.14	15	2.7	1.8	1.5	30
1.2	0.3	4.0	08	0.8	0.3	2.67	-05
1.2	0.3	4.0	0	1.2	0.3	4.0	-10
1.1	0.4	2.75	-05	0.7	0.3	2.33	0
1.0	0.3	3.33	0	0.6	0.4	1.5	05
1.1	0.5	2.0	15	0.8	0.3	2.67	05
1.4	0.7	2.0	30	0.8	0.3	2.67	08
1.5	0.6	2.5	0	2.0	1.0	1.0	12
1.2	0.3	4.0	10	1.8	0.9	2.0	10
2.0	0.7	2.86	05	1.9	0.8	2.38	05
1.3	0.4	3.25	02	0.8	0.3	2.67	05
1.3	0.4	3.25	0	1.0	0.4	2.5	08
1.1	1.0	1.1	-80	1.2	0.6	2.0	0

Appendix 4.1 Determination of  $2\theta_{CuK}$  values of 201, 060 and 204 diffractions of the microcline megacrysts.

The rock samples were sawed into approximately 5 mm thick slabs from which fragments of potassium feldspar megacrysts were broken-off by tapping with a small hammer. The feldspar fragments were examined for any visible mineral inclusions and the inclusion free fragments were separated. These were then ground in an agate mortar with an agate pestle until the grittiness disappeared. The powder was mixed with analytical grade  $CaF_2$  that was kept in an oven at  $500^{\circ}C$  for 12 hrs before using.  $CaF_2$  was used as an internal standard. The sample was loaded into an aluminium sample holder and a diffractogram from  $12^{\circ}$  to  $54^{\circ} 2\theta$  was obtained using a Phillips X-ray diffractometer. Scanning was done at a rate of  $1/2^{\circ} 2\theta$  per minute. The  $2\theta$  values of the 201, 060 and 204 "peaks" of the microcline were measured from the diffractogram. These values were compared with the  $2\theta$  values of the  $CuF_2$  "peaks" and necessary corrections were made to eliminate errors due to changes in chart speed.



Map showing locations of the samples used to obtain the structural state of the potassium feldspar megacrysts.

Appendix 4.2 Compositions of feldspars from the granitoids in the area.

NJ XXX	-	Sample number
MM	-	Microcline megacryst
GM	-	Groundmass microcline in megacrystic plutons
MI	-	Microcline in non-megacrystic plutons
PL	-	Plagioclase
PI	-	Plagioclase inclusion in microcline megacryst
PG	-	Perthite lamella in microcline megacryst



# COMPOSITION OF FELDSPARS FROM THE WAREHAM QUARTZ MONZONITE

SAMPLE	* NJ374 MM *	* NJ374 GM *	* NJ374 PL *	* NJ374 PE *
SiO2	* 64.77 *	* 67.48 *	* 62.05 *	* 65.30 *
Al2O3	* 18.59 *	* 18.51 *	* 24.26 *	* 22.95 *
CaO	* 0.0 *	* 0.0 *	* 5.32 *	* 0.93 *
Na2O	* 1.75 *	* 0.74 *	* 9.46 *	* 13.85 *
K2O	* 15.44 *	* 16.43 *	* 0.20 *	* 1.27 *
TOTAL	* 99.94 *	* 103.16 *	* 101.32 *	* 101.00 *

SAMPLE	* NJ541 MM *	* NJ641 MM *	* NJ641 GM *	* NJ641 PL *	* NJ353 MM *	* NJ353 PL *	* NJ353 PL *
SiO2	* 64.24 *	* 65.25 *	* 65.51 *	* 58.54 *	* 64.39 *	* 57.91 *	* 57.61 *
Al2O3	* 18.48 *	* 18.69 *	* 19.55 *	* 26.43 *	* 19.00 *	* 27.72 *	* 27.49 *
CaO	* 0.0 *	* 0.0 *	* 0.0 *	* 7.17 *	* 0.0 *	* 9.57 *	* 7.95 *
Na2O	* 7.91 *	* 0.87 *	* 0.77 *	* 7.99 *	* 1.05 *	* 7.31 *	* 7.71 *
K2O	* 15.36 *	* 15.44 *	* 15.36 *	* 0.11 *	* 15.42 *	* 0.14 *	* 0.14 *
TOTAL	* 98.99 *	* 100.25 *	* 100.19 *	* 100.13 *	* 99.77 *	* 101.65 *	* 100.99 *

# COMPOSITION OF FELDSPARS FROM THE NORTH POND GRANITE

SAMPLE	* NJ369 PL *	* NJ369 PL *
SiO2	* 63.19 *	* 63.31 *
Al2O3	* 23.31 *	* 23.32 *
CaO	* 4.13 *	* 3.86 *
Na2O	* 10.11 *	* 10.59 *
K2O	* 0.21 *	* 0.09 *
TOTAL	* 100.86 *	* 101.17 *

# COMPOSITION OF FELDSPARS FROM THE NORTH POND GRANITE

SAMPLE	* NJ856 MI	* NJ856 MI	* NJ856 PL	* NJ856 PL	* NJ369 MI	* NJ369 MI	* NJ369 PL	*
SIC2	* 64.97	* 64.34	* 64.00	* 65.43	* 65.35	* 65.19	* 63.55	*
AL2O3	* 13.44	* 18.97	* 22.66	* 21.39	* 13.94	* 18.71	* 23.16	*
CAO	* 0.0	* 0.0	* 3.35	* 2.04	* 3.0	* 0.0	* 4.33	*
NA2O	* 0.66	* 0.89	* 11.00	* 11.76	* 1.14	* 0.72	* 10.24	*
K2O	* 16.92	* 16.65	* 0.15	* 0.10	* 15.99	* 16.48	* 0.13	*
TOTAL	* 101.95	* 100.84	* 101.16	* 100.71	* 101.41	* 101.09	* 101.41	*

# COMPOSITION OF FELDSPARS FROM THE LOCKERS BAY GRANITE

SAMPLE	* NJ L2 MM	* NJ L2 GM	* NJ L2 PL	* NJ L2 PI	* NJ L6 MM	* NJ L6 GM	* NJ L6 PL	*
SIO2	* 63.94	* 64.09	* 60.10	* 60.98	* 64.64	* 64.09	* 61.61	*
AL2O3	* 18.77	* 18.70	* 24.59	* 24.58	* 18.82	* 18.44	* 24.52	*
CAO	* 0.01	* 0.0	* 6.21	* 6.08	* 0.0	* 0.0	* 5.52	*
NA2O	* 1.24	* 0.87	* 8.52	* 8.99	* 3.91	* 2.99	* 9.45	*
K2O	* 15.59	* 16.30	* 0.52	* 0.24	* 16.62	* 15.96	* 0.15	*
TOTAL	* 99.55	* 99.96	* 100.04	* 100.87	* 100.39	* 99.48	* 101.25	*

SAMPLE	* NJ L6 FL	* NJ L6 PE	*
SIO2	* 61.11	* 67.61	*
AL2O3	* 24.48	* 20.24	*
CAO	* 5.74	* 0.33	*
NA2O	* 9.38	* 12.36	*
K2O	* 0.25	* 0.02	*
TOTAL	* 100.96	* 100.56	*

COMPOSITION OF FELDSPARS FROM THE CAPE FREELS GRANITE

SAMPLE	* NJ 41 MM *	* NJ 41 PL *	* NJ 41 PL *	* NJ 41 PE *	* NJ 41 PI *	* NJ 96 MM *	* NJ 96 GM *
SiO2	* 64.83 *	* 61.48 *	* 61.96 *	* 68.35 *	* 65.38 *	* 65.28 *	* 64.08 *
Al2O3	* 19.96 *	* 22.03 *	* 24.05 *	* 21.39 *	* 22.13 *	* 18.88 *	* 18.85 *
CaO	* 0.01 *	* 5.88 *	* 5.29 *	* 0.58 *	* 1.90 *	* 0.01 *	* 0.02 *
Na2O	* 0.73 *	* 9.32 *	* 9.58 *	* 11.12 *	* 10.53 *	* 0.91 *	* 0.85 *
K2O	* 16.64 *	* 0.17 *	* 0.15 *	* 0.19 *	* 0.72 *	* 16.57 *	* 16.47 *
TOTAL	* 101.17 *	* 98.79 *	* 100.93 *	* 101.33 *	* 100.56 *	* 101.55 *	* 100.27 *

SAMPLE	* NJ 96 PL *	* NJ 96 PL *	* NJ 96 FE *	* NJ166 MM *	* NJ166 MM *	* NJ166 MM *	* NJ166 GM *
SiO2	* 65.21 *	* 61.79 *	* 66.36 *	* 64.62 *	* 64.38 *	* 64.77 *	* 64.85 *
Al2O3	* 22.53 *	* 24.13 *	* 21.97 *	* 18.85 *	* 18.95 *	* 19.96 *	* 18.59 *
CaO	* 0.92 *	* 5.53 *	* 0.87 *	* 0.0 *	* 0.01 *	* 0.01 *	* 0.0 *
Na2O	* 11.52 *	* 9.14 *	* 11.13 *	* 1.12 *	* 0.77 *	* 0.76 *	* 0.81 *
K2O	* 3.72 *	* 0.40 *	* 0.66 *	* 16.28 *	* 16.16 *	* 16.27 *	* 16.43 *
TOTAL	* 100.90 *	* 100.99 *	* 100.99 *	* 100.87 *	* 100.27 *	* 100.77 *	* 100.67 *

SAMPLE	* NJ166 GM *	* NJ166 PL *	* NJ166 PL *
SiO2	* 63.76 *	* 61.96 *	* 61.94 *
Al2O3	* 19.73 *	* 23.97 *	* 24.43 *
CaO	* 0.01 *	* 5.34 *	* 5.73 *
Na2O	* 0.70 *	* 9.58 *	* 9.45 *
K2O	* 16.76 *	* 0.20 *	* 0.11 *
TOTAL	* 99.96 *	* 101.05 *	* 101.66 *

COMPOSITION OF FELDSPARS FROM THE DEADMANS BAY GRANITE

SAMPLE	* NJ812 MM *	* NJ819 GM *	* NJ819 PL *	* NJ819 PL *	* NJ819 PI *	* NJ822 MM *	* NJ922 PL *
SiO2	* 55.05 *	* 54.63 *	* 64.18 *	* 60.76 *	* 64.35 *	* 64.37 *	* 61.18 *
Al2O3	* 18.81 *	* 19.09 *	* 22.28 *	* 22.95 *	* 22.42 *	* 18.86 *	* 24.24 *
CaO	* 0.02 *	* 0.04 *	* 4.05 *	* 7.51 *	* 3.23 *	* 0.02 *	* 6.98 *
Na2O	* 0.88 *	* 1.12 *	* 10.52 *	* 9.02 *	* 10.69 *	* 0.95 *	* 8.56 *
K2O	* 16.45 *	* 16.03 *	* 0.18 *	* 0.15 *	* 0.24 *	* 16.30 *	* 0.13 *
TOTAL	* 101.21 *	* 101.11 *	* 101.21 *	* 100.29 *	* 100.93 *	* 100.50 *	* 101.39 *

SAMPLE	* NJ822 PL *
SiO2	* 61.72 *
Al2O3	* 24.05 *
CaO	* 6.23 *
Na2O	* 8.93 *
K2O	* 0.56 *
TOTAL	* 101.49 *

COMPOSITION OF FELDSPARS FROM THE NEWPORT GRANITE

SAMPLE	* NJ305 PL *	* NJ305 PI *	* NJ305 PI *	* NJ305 PE *	* NJ305 PE *	* NJ305 PE *	* NJ2002MM *
SiO2	* 51.82 *	* 54.04 *	* 50.42 *	* 65.61 *	* 67.39 *	* 57.59 *	* 64.15 *
TiO2	* 9.0 *	* 0.0 *	* 0.0 *	* 0.32 *	* 0.31 *	* 0.0 *	* 0.03 *
Al2O3	* 23.72 *	* 20.07 *	* 22.01 *	* 21.79 *	* 21.15 *	* 20.71 *	* 18.65 *
FeO	* 0.11 *	* 0.06 *	* 9.00 *	* 0.36 *	* 3.33 *	* 3.92 *	* 3.37 *
MnO	* 0.0 *	* 0.0 *	* 600.01 *	* 0.0 *	* 0.0 *	* 0.0 *	* 0.0 *
MgO	* 0.0 *	* 0.0 *	* 0.01 *	* 0.0 *	* 0.01 *	* 0.01 *	* 0.0 *
CaO	* 4.56 *	* 4.19 *	* 8.03 *	* 1.99 *	* 0.45 *	* 0.53 *	* 0.0 *
Na2O	* 9.09 *	* 9.99 *	* 8.14 *	* 10.77 *	* 11.46 *	* 11.79 *	* 1.57 *
K2O	* 0.20 *	* 0.10 *	* 0.11 *	* 0.17 *	* 0.12 *	* 0.20 *	* 14.01 *
BaO	* 0.32 *	* 0.02 *	* 0.01 *	* 0.32 *	* 0.0 *	* 0.03 *	* 0.94 *
SrO	* 0.38 *	* 0.32 *	* 0.19 *	* 0.19 *	* 0.20 *	* 0.20 *	* 0.17 *
TOTAL	* 99.90 *	* 98.79 *	* 707.93 *	* 100.62 *	* 101.65 *	* 101.08 *	* 99.59 *

COMPOSITION OF FELDSPARS FROM THE NEWPORT GRANITE

SAMPLE	* NJ2002MM	* NJ2002MM	* NJ2002GM	* NJ2002GM	* NJ2002PL	* NJ2002PL	* NJ2002PL
SiO2	64.52	64.00	64.46	64.73	62.67	61.80	61.35
TiO2	0.5	0.01	0.01	0.01	0.01	0.0	0.01
Al2O3	18.52	18.42	18.61	19.20	23.62	24.01	23.96
FeO	0.11	0.05	0.10	0.03	0.11	0.13	0.14
MnO	0.0	0.0	0.0	0.0	0.0	0.0	0.0
MgO	0.0	0.0	0.01	0.0	0.0	0.01	0.01
CaO	0.02	0.01	0.02	0.0	4.18	4.75	5.04
Na2O	1.37	1.07	1.51	0.73	9.41	9.09	8.87
K2O	14.70	15.15	15.45	15.61	0.21	0.36	0.29
BaO	0.08	0.27	0.12	0.07	0.01	0.02	0.02
SrO	0.10	0.12	0.01	0.0	0.0	0.30	0.20
TOTAL	99.42	99.10	100.36	99.38	100.21	100.47	99.89

SAMPLE	* NJ305 MM	* NJ305 PL	* NJ305 PL	* NJ305 MM	* NJ305 MM	* NJ305 GM	* NJ305 PL
SiO2	65.54	61.89	62.09	64.58	63.74	64.17	61.58
TiO2	0.01	0.01	0.01	0.01	0.0	0.01	0.0
Al2O3	18.79	23.75	23.94	18.46	19.45	18.69	24.12
FeO	0.07	0.18	0.10	0.07	0.17	0.06	0.13
MnO	0.0	0.0	0.0	0.0	0.01	0.0	0.0
MgO	0.0	0.01	0.01	0.0	0.0	0.01	0.0
CaO	0.02	4.51	5.21	0.0	0.0	0.06	6.02
Na2O	1.50	8.98	9.16	0.99	1.14	1.98	8.62
K2O	14.37	0.46	0.25	15.27	14.82	14.36	0.22
BaO	0.19	0.01	0.03	0.33	0.45	0.01	0.02
SrO	0.15	0.14	0.15	0.15	0.31	0.11	0.21
TOTAL	100.63	99.94	100.95	99.99	99.34	99.46	100.92

COMPOSITION OF FELDSPARS FROM THE NEWPORT GRANITE

SAMPLE	* NJ2002PE	* NJ2002PE *
SiO2	68.23	68.31
TiO2	0.0	0.0
AL2O3	20.29	20.34
FeO	0.0	0.06
MNO	0.0	0.0
MGO	0.0	0.0
CAO	0.19	0.66
NA2O	10.80	10.89
K2O	0.77	1.02
BAO	0.0	0.0
SRO	0.48	0.16
TOTAL	100.56	101.43

COMPOSITION OF FELDSPARS FROM THE BIG ROUND POND GRANITE

SAMPLE	* NJ134 MI	* NJ134 MI	* NJ134 FL	* NJ134 PL	* NJ134 PL *
SiO2	64.34	65.39	60.97	64.95	58.75
AL2O3	19.54	18.66	24.90	21.55	26.44
CAO	0.0	0.09	6.72	2.84	8.17
NA2O	0.56	1.47	8.83	10.67	7.71
K2O	16.74	15.51	0.23	0.34	0.19
TOTAL	99.98	101.42	101.65	100.35	101.26

#### Appendix 6.1 Chemical analyses of the granitoids.

##### a. Sample collection and preparation.

The sampling program was designed to obtain a representative composition of each of the granitoids based on the availability of suitable outcrops. At each location a six pound sledge hammer was used to collect 2 kg rock samples consisting of unweathered pieces. The collected pieces were subsequently crushed to 1-2 cm fragments in a Denver steel jaw crusher. A representative sample of these fragments was crushed in a tungsten carbide Siebtechnik Swing mill for three minutes producing a rock powder of -100 mesh.

##### b. Analytical techniques.

b.1.  $\text{SiO}_2$ ,  $\text{TiO}_2$ ,  $\text{Al}_2\text{O}_3$ ,  $\text{Fe}_2\text{O}_3$  (total),  $\text{CaO}$ ,  $\text{MgO}$ ,  $\text{Na}_2\text{O}$ ,  $\text{K}_2\text{O}$  and  $\text{MnO}$  were determined by a Perkin Elmer 370 Atomic Absorption Spectrometer using solutions prepared by the following method:

1. 0.1000 g of rock powder was weighed into a digestion flash (Nalgene Catalogue #3122 polycarbonate centrifuge bottle).
2. 5 ml conc. HF acid was added by a automatic pipette, the screw top was tightened, and the bottle was placed for 30 minutes on a steam bath. At the end of 30 minutes no black residue was found in any of the bottles.
3. After being removed from heat and let cool 50 ml of saturated boric acid solution was added by pipette and the bottle again placed on a steam bath until the solution was clear.

4. After being let cool the solution was made up to a 200 ml volume by addition of distilled water from a precise volume dispenser. This solution was then stored in polyethylene bottles and used for all analyses.

All elements except CaO and MgO were analysed on the solutions by comparison to a range of standards 90%, 80%, 70% .....10% prepared from a standard granite stock solution employing the settings given in the A.A.S. instrument book for each element. CaO and MgO were determined on solutions prepared by pipetting 5 ml of sample solution into a 50 ml volumetric flask, adding 5 ml conc. Hcl, 10 ml of lanthanum oxide solution and making the solution up to 50 ml with distilled water. Standard solutions were treated in the same manner.

A granitic rock standard (G-1) was analyzed four times in the above manner to determine the accuracy and precision of the major element analyses (see Table below).

Precision of A.A.S. analysis (n=4)

Element	Published* value	$\bar{X}$	S	Range	
				low	high
SiO <sub>2</sub>	69.11	69.70	0.57	68.20	69.96
Al <sub>2</sub> O <sub>3</sub>	15.40	15.10	0.24	14.75	15.60
Fe <sub>2</sub> O <sub>3</sub>	2.65	2.60	0.02	2.64	2.74
MgO	0.76	0.80	0.05	0.75	0.82
CaO	1.94	2.00	0.10	1.92	2.14
Na <sub>2</sub> O	4.07	4.30	0.02	4.07	4.21
K <sub>2</sub> O	4.51	4.56	0.02	4.50	4.57
TiO <sub>2</sub>	0.50	0.50	0.01	0.47	0.51
MnO	0.03	0.03	0.0		
Total	98.97	99.59			

S - standard deviation  $\bar{X}$  - mean

\*Flanagan, F.J., 1970. Sources of geochemical standards - 11. Geochim. Cosmochim. Acta, V34, pp. 121-125.



b.2.  $P_2O_5$  and loss on ignition determinations.

$P_2O_5$  was determined by colorimetry using a Bausch & Lomb colorimeter. Loss on ignition was calculated by measuring a known amount of powder into a porcelain crucible, heating at  $1050^{\circ}C$  for two hours, weighing again and expressing the difference in percent.

b.3. Trace element analysis.

Thirteen trace elements (Rb, Ba, Sr, Pb, Zr, Nb, Y, Ni, V, Cr, Cu, An and Ga) were determined on pressed powder discs using a Phillips X-Ray Spectrometer.

The sample discs were prepared in the following manner.

1. 10 gm of rock powder were thoroughly mixed with 1 gm of binding agent.
2. This powder was pressed into a disc for one minute at 20 tons per sq. in. and baked in an oven for 10 minutes at  $200^{\circ}C$ .

The precision and accuracy of the trace element analyses were determined by analysing standard rock samples and are shown below.

	V	Cr	Ni	Cu	Zn	Ga	Rb	Sr	Y	Zr	Nb	Ba	Pb
W-1	240	92	70	117	85	20	22	189	24	98	8	171	7
S	5	6	3	4	2	2	2	6	2	2	1	12	3
N	13	13	13	13	13	13	13	13	11	13	13	13	13
P	240	120	78	110	86	16	21	190	25	105	9.5	160	8
G-2	43	13	2	17	85	24	166	477	11	292	10	1865	27
S	3	3	2	1	2	1	2	7	2	3	1	30	2
N	10	10	10	10	10	10	10	10	11	10	10	10	10
P	34	9	6	11	85	23	170	480	12	300	14	1850	29

S = standard deviation  
 N = number of determinations  
 P = published values

# CHEMICAL ANALYSES OF THE WAREHAM QUARTZ MONZONITE

SAMPLE	* NJ	303 * NJ	354 * NJ	355 * NJ	373 * NJ	537 * NJ	641 * NJ	642 *
SiO2	62.60	58.30	62.20	61.40	61.30	62.40	62.10	*
TiO2	1.00	1.04	0.90	1.00	1.10	0.85	1.00	*
Al2O3	16.30	18.40	16.50	16.90	16.90	16.50	16.00	*
Fe2O3	1.21	1.54	1.43	1.29	1.65	1.29	1.56	*
FeO	4.05	4.65	3.31	3.84	3.48	3.16	3.51	*
MnO	0.11	0.15	0.13	0.11	0.10	0.10	0.12	*
MgO	2.24	2.73	2.00	2.25	2.19	2.13	2.56	*
CaO	4.00	4.37	3.54	4.23	4.23	3.20	3.68	*
Na2O	2.98	3.43	3.12	3.33	3.12	3.48	2.99	*
K2O	3.04	3.77	4.10	3.78	4.58	4.58	4.43	*
P2O5	0.41	0.39	0.39	0.41	0.38	0.42	0.33	*
LOI	1.32	1.41	1.25	1.01	1.32	1.57	1.68	*
TOTAL	100.20	100.68	99.52	99.54	100.35	99.68	100.16	*
Zr	297	303	285	282	305	290	268	*
Sr	242	318	297	279	310	429	371	*
Ba	195	216	228	131	175	355	216	*
Zn	92	100	20	92	89	92	90	*
Cu	0	0	0	0	0	0	0	*
Ra	1011	985	1375	713	1199	950	934	*
Nb	14	17	20	14	3	15	12	*
Ga	20	21	20	22	20	20	20	*
F9	14	14	19	13	15	15	15	*
Ni	35	34	34	31	38	48	40	*
Co	37	39	22	41	28	45	65	*
V	120	145	110	127	119	105	135	*
Y	35	30	39	32	31	64	35	*

POOR COPY  
COPIE DE QUALITEE INFERIEURE

# CHEMICAL ANALYSES OF THE WAREHAM QUARTZ MONZONITE

SAMPLE	* NJ	700	* NJ	723	* NJ	763	* NJ	914	* NJ	1064	* NJ	877	* NJ	374	*
SiO2	*	59.50	*	59.36	*	58.00	*	63.00	*	63.00	*	71.60	*	72.50	*
Al2O3	*	0.55	*	1.04	*	0.60	*	0.30	*	0.58	*	0.38	*	0.40	*
FeO	*	16.70	*	16.90	*	15.20	*	15.90	*	16.30	*	13.90	*	13.80	*
MnO	*	1.70	*	0.97	*	0.50	*	0.93	*	1.12	*	0.46	*	0.85	*
MgO	*	2.57	*	4.59	*	2.86	*	3.63	*	3.29	*	1.58	*	1.11	*
CaO	*	0.12	*	0.13	*	0.00	*	0.11	*	0.10	*	0.06	*	0.06	*
Na2O	*	2.25	*	2.98	*	1.34	*	2.37	*	2.00	*	0.87	*	0.60	*
K2O	*	4.08	*	3.53	*	2.37	*	3.89	*	3.42	*	1.79	*	1.44	*
Sum	*	3.10	*	3.04	*	3.02	*	3.04	*	3.08	*	2.85	*	2.96	*
SiO2	*	3.93	*	4.90	*	4.24	*	4.12	*	4.80	*	4.79	*	5.21	*
Al2O3	*	0.31	*	0.36	*	0.08	*	0.28	*	0.27	*	0.12	*	0.10	*
FeO	*	1.73	*	1.84	*	1.43	*	1.19	*	2.41	*	0.96	*	0.59	*
Sum	*	98.02	*	99.58	*	99.58	*	99.31	*	100.53	*	99.29	*	99.52	*
SiO2	*	285	*	272	*	210	*	229	*	246	*	167	*	139	*
Al2O3	*	335	*	253	*	163	*	264	*	257	*	229	*	107	*
FeO	*	234	*	246	*	186	*	185	*	215	*	153	*	245	*
MnO	*	91	*	91	*	71	*	68	*	80	*	44	*	42	*
MgO	*	10	*	32	*	26	*	20	*	21	*	5	*	8	*
CaO	*	965	*	311	*	652	*	751	*	937	*	580	*	298	*
Na2O	*	17	*	19	*	15	*	13	*	11	*	11	*	11	*
K2O	*	24	*	23	*	21	*	21	*	23	*	20	*	19	*
Sum	*	20	*	24	*	20	*	22	*	19	*	43	*	32	*
SiO2	*	22	*	32	*	15	*	0	*	23	*	9	*	8	*
Al2O3	*	30	*	59	*	21	*	45	*	37	*	18	*	12	*
FeO	*	135	*	150	*	80	*	120	*	112	*	45	*	26	*
Sum	*	55	*	50	*	77	*	46	*	39	*	38	*	45	*

POOR COPY  
COPIE DE QUALITEE INFERIEURE

# CHEMICAL ANALYSES OF THE NORTH POND GRANITE (MEDIUM GRAINED PHASE)

SAMPLE	* NJ	352	* NJ	364	* NJ	368	* NJ	369	* NJ	370	* NJ	503	* NJ	510
SiO2	*	72.50	*	69.35	*	70.90	*	70.50	*	72.50	*	67.69	*	70.80
TiO2	*	0.24	*	0.47	*	0.44	*	0.44	*	0.36	*	0.50	*	0.27
Al2O3	*	14.50	*	15.30	*	14.80	*	15.30	*	15.20	*	15.50	*	14.80
Fe2O3	*	0.58	*	0.72	*	0.40	*	0.18	*	0.33	*	0.87	*	0.42
FeO	*	1.28	*	2.05	*	1.37	*	2.00	*	1.48	*	2.30	*	1.24
MnO	*	0.06	*	0.11	*	0.13	*	0.11	*	0.09	*	0.19	*	0.08
MgO	*	0.55	*	1.23	*	1.11	*	0.95	*	0.73	*	1.12	*	0.61
CaO	*	0.84	*	1.80	*	1.40	*	1.67	*	2.00	*	2.40	*	1.20
Na2O	*	2.69	*	3.15	*	3.46	*	3.55	*	3.60	*	3.25	*	3.57
K2O	*	5.67	*	4.49	*	4.18	*	4.23	*	3.88	*	4.06	*	4.10
P2O5	*	0.35	*	0.28	*	0.23	*	0.15	*	0.08	*	0.21	*	0.26
LOI	*	1.24	*	1.42	*	1.30	*	1.10	*	0.71	*	1.19	*	1.22
TOTAL	*	100.50	*	100.32	*	100.34	*	100.11	*	100.56	*	99.31	*	98.67
Zn	*	178	*	213	*	203	*	194	*	175	*	221	*	146
Se	*	91	*	251	*	214	*	177	*	155	*	220	*	101
Rb	*	319	*	240	*	225	*	269	*	192	*	217	*	287
Zn	*	57	*	79	*	75	*	72	*	70	*	74	*	71
CU	*	0	*	0	*	0	*	0	*	0	*	0	*	0
BA	*	355	*	505	*	457	*	376	*	559	*	472	*	264
Nb	*	99	*	7	*	9	*	12	*	0	*	9	*	9
GA	*	18	*	19	*	19	*	20	*	19	*	17	*	20
PR	*	29	*	20	*	19	*	20	*	17	*	17	*	20
NI	*	15	*	17	*	11	*	13	*	6	*	12	*	8
CR	*	2	*	11	*	4	*	3	*	3	*	2	*	0
V	*	12	*	65	*	56	*	50	*	31	*	58	*	27
Y	*	36	*	30	*	28	*	32	*	23	*	29	*	30

POOR COPY  
COPIE DE QUALITEE INFERIEURE

CHEMICAL ANALYSES OF THE NORTH POLO GRANITE (MEDIUM GRAINED PHASE)

SAMPLE	NJ	567	NJ	592	NJ	501	NJ	501A
SiO2	*	68.00	*	71.60	*	69.20	*	70.40
TiO2	*	0.53	*	0.20	*	0.49	*	0.40
AL2O3	*	15.50	*	14.40	*	15.20	*	12.70
Fe2O3	*	0.94	*	0.39	*	0.85	*	0.74
FeO	*	2.18	*	0.89	*	2.09	*	1.73
MnO	*	0.78	*	0.06	*	0.11	*	0.09
MgO	*	1.31	*	0.40	*	1.25	*	1.02
CaO	*	2.72	*	0.69	*	2.16	*	2.10
Na2O	*	3.29	*	3.24	*	3.38	*	3.50
K2O	*	3.86	*	4.90	*	4.11	*	3.37
P2O5	*	0.24	*	0.31	*	0.26	*	0.17
LOI	*	1.53	*	1.03	*	1.21	*	1.51
TOTAL	*	100.08	*	98.11	*	100.31	*	99.41
Zr	*	218	*	119	*	220	*	221
SP	*	203	*	60	*	243	*	232
SB	*	216	*	269	*	224	*	186
ZN	*	80	*	50	*	77	*	73
CU	*	0	*	0	*	0	*	0
BA	*	439	*	217	*	471	*	359
NB	*	10	*	12	*	7	*	7
GA	*	20	*	20	*	20	*	19
PB	*	18	*	26	*	18	*	19
NI	*	16	*	5	*	15	*	10
CR	*	12	*	2	*	9	*	5
V	*	74	*	12	*	59	*	53
Y	*	29	*	28	*	30	*	24

POOR COPY  
COPIE DE QUALITEE INFERIEURE

CHEMICAL ANALYSES OF THE NORTH POND GRANITE (PORPHYRITIC PHASE)

SAMPLE	* NJ	433	* NJ	512	* NJ	557	* NJ	598	* NJ	648	* NJ	845	* NJ	850	*
SiO2	*	74.60	*	71.60	*	72.40	*	71.30	*	68.20	*	72.10	*	72.40	*
TiO2	*	0.27	*	0.10	*	0.15	*	0.30	*	0.42	*	0.29	*	0.35	*
Al2O3	*	14.30	*	14.60	*	14.60	*	14.70	*	15.40	*	14.40	*	14.90	*
Fe2O3	*	0.48	*	0.15	*	0.31	*	0.44	*	0.30	*	0.13	*	0.13	*
FeO	*	0.90	*	0.84	*	0.77	*	1.39	*	2.32	*	1.37	*	1.59	*
MnO	*	0.05	*	0.05	*	0.05	*	0.08	*	0.10	*	0.06	*	0.07	*
MgO	*	0.33	*	0.27	*	0.32	*	0.70	*	1.06	*	0.46	*	0.53	*
CaO	*	0.55	*	0.82	*	0.69	*	0.98	*	2.05	*	0.77	*	0.93	*
Na2O	*	3.10	*	3.49	*	3.25	*	3.49	*	3.30	*	2.90	*	2.91	*
K2O	*	5.04	*	5.11	*	4.80	*	4.17	*	4.00	*	5.59	*	5.59	*
P2O5	*	0.34	*	0.37	*	0.31	*	0.37	*	0.17	*	0.27	*	0.26	*
LOT	*	0.94	*	0.74	*	0.90	*	1.29	*	1.71	*	1.37	*	1.30	*
TOTAL	*	100.92	*	98.54	*	98.55	*	99.21	*	99.07	*	99.71	*	100.81	*
Si	*	116	*	104	*	120	*	165	*	153	*	105	*	129	*
Ti	*	45	*	55	*	50	*	105	*	233	*	65	*	80	*
Al	*	380	*	316	*	266	*	238	*	186	*	322	*	325	*
Fe	*	67	*	37	*	61	*	54	*	60	*	62	*	59	*
Cu	*	0	*	0	*	0	*	0	*	17	*	3	*	12	*
Ba	*	176	*	202	*	218	*	292	*	571	*	228	*	345	*
Nb	*	15	*	7	*	9	*	5	*	14	*	17	*	16	*
Ga	*	19	*	20	*	18	*	20	*	22	*	23	*	23	*
Pb	*	22	*	26	*	27	*	20	*	29	*	32	*	42	*
Ni	*	7	*	6	*	4	*	9	*	7	*	6	*	7	*
Cr	*	4	*	1	*	15	*	9	*	13	*	6	*	17	*
V	*	15	*	10	*	11	*	28	*	51	*	13	*	24	*
Y	*	35	*	32	*	28	*	27	*	36	*	49	*	55	*

POOR COPY  
COPIE DE QUALITE INFERIEURE

# CHEMICAL ANALYSES OF THE NORTH POND GRANITE (POPPHYRITIC PHASE)

SAMPLE	* NJ	991	* NJ	1172	*
SiO2	*	73.90	*	72.20	*
TiO2	*	0.27	*	0.27	*
Al2O3	*	14.20	*	14.50	*
Fe2O3	*	0.08	*	0.0	*
FeO	*	2.16	*	1.44	*
MnO	*	0.09	*	0.07	*
MgO	*	0.75	*	0.49	*
CaO	*	1.04	*	0.33	*
Na2O	*	2.79	*	3.46	*
K2O	*	5.25	*	4.61	*
P2O5	*	0.17	*	0.23	*
LOI	*	0.97	*	1.25	*
TOTAL	*	98.57	*	99.36	*
Zr	*	143	*	84	*
SR	*	39	*	75	*
RB	*	394	*	276	*
ZN	*	54	*	55	*
CU	*	15	*	7	*
BA	*	423	*	234	*
NB	*	19	*	19	*
GA	*	22	*	23	*
Pb	*	31	*	32	*
NI	*	8	*	5	*
CR	*	18	*	16	*
V	*	31	*	20	*
Y	*	53	*	47	*

## CHEMICAL ANALYSES OF THE BUSINESS COVE GRANITE

SAMPLE	* NJ	173	* NJ	219	* NJ	266	* NJ	1070	*
SiO2	*	71.00	*	71.00	*	74.80	*	72.60	*
TiO2	*	0.27	*	0.25	*	0.12	*	0.30	*
Al2O3	*	14.70	*	15.90	*	14.00	*	14.60	*
Fe2O3	*	0.40	*	0.10	*	0.53	*	0.14	*
FeO	*	1.51	*	1.41	*	0.61	*	1.23	*
MnO	*	0.04	*	0.04	*	0.04	*	0.06	*
MgO	*	3.51	*	0.55	*	0.24	*	0.47	*
CaO	*	2.09	*	1.49	*	0.56	*	0.83	*
Na2O	*	3.46	*	4.00	*	2.73	*	2.90	*
K2O	*	4.12	*	4.32	*	5.82	*	5.43	*
P2O5	*	0.04	*	0.08	*	0.23	*	0.20	*
LOI	*	0.46	*	1.00	*	0.24	*	1.19	*
TOTAL	*	102.07	*	100.14	*	100.62	*	100.15	*
Zr	*	186	*	104	*	65	*	104	*
SR	*	254	*	120	*	51	*	73	*
RB	*	202	*	199	*	289	*	350	*
ZN	*	39	*	53	*	42	*	40	*
CU	*	5	*	5	*	6	*	7	*
BA	*	787	*	339	*	199	*	317	*
NB	*	15	*	9	*	16	*	15	*
GA	*	19	*	21	*	18	*	21	*
Pb	*	27	*	30	*	39	*	29	*
NI	*	1	*	3	*	0	*	3	*
CR	*	13	*	12	*	11	*	14	*
V	*	30	*	24	*	11	*	22	*
Y	*	41	*	36	*	46	*	59	*

POOR COPY  
COPIE DE QUALITE INFERIEURE

# CHEMICAL ANALYSES OF THE CAPE FREELS GRANITE

SAMPLE	* NJ	38 * NJ	41 * NJ	95 * NJ	170	LD000180 *				
SiO2	*	68.70	*	69.30	*	68.40	*	71.00	67.49	*
TiO2	*	0.50	*	0.56	*	0.51	*	0.40	0.63	*
AL2O3	*	15.30	*	15.60	*	15.30	*	13.30	14.28	*
FE2O3	*	0.75	*	0.85	*	0.59	*	0.51	3.49	*
FEO	*	1.99	*	1.99	*	1.95	*	1.84	0.0	*
MNO	*	3.35	*	0.08	*	0.06	*	0.06	0.07	*
MGO	*	0.74	*	0.80	*	0.79	*	0.62	1.14	*
CAO	*	1.05	*	1.95	*	1.75	*	1.45	1.56	*
NA2O	*	3.34	*	3.39	*	3.32	*	2.93	2.93	*
K2O	*	5.46	*	5.10	*	5.67	*	5.63	5.77	*
P2O5	*	3.16	*	0.16	*	0.19	*	0.14	0.08	*
LOI	*	0.45	*	0.95	*	1.07	*	1.24	0.97	*
TOTAL	*	99.50	*	100.75	*	99.42	*	99.14	98.61	*
Zr	*	205	*	217	*	194	*	205	316	*
SO	*	112	*	147	*	156	*	107	133	*
RB	*	264	*	240	*	220	*	301	314	*
ZN	*	49	*	53	*	51	*	49	56	*
CU	*	7	*	12	*	12	*	3	3	*
BA	*	493	*	674	*	651	*	414	569	*
NB	*	13	*	14	*	14	*	19	0	*
GA	*	10	*	23	*	20	*	22	0	*
PB	*	20	*	37	*	34	*	22	0	*
NI	*	0	*	13	*	6	*	9	11	*
CF	*	17	*	12	*	13	*	12	28	*
V	*	56	*	52	*	49	*	39	0	*
Y	*	56	*	56	*	48	*	67	0	*

POOR COPY  
COPIE DE QUALITEE INFERIEURE



# CHEMICAL ANALYSES OF THE CAPS FREELS GRANITE

SAMPLE	* LD000184	* LD000185	* LD000186	* LD000187	* LD000188	* LD 239	* LD000240
SiO2	71.83	67.02	76.02	68.13	66.61	70.80	69.72
TiO2	0.23	0.65	0.05	0.79	0.61	0.55	0.71
Al2O3	15.26	14.94	13.37	14.35	15.19	15.60	14.18
Fe2O3	1.73	4.34	0.47	4.49	3.72	2.92	3.87
FeO	0.0	0.0	0.0	0.0	0.0	0.0	0.0
MnO	0.02	0.04	0.01	0.04	0.03	0.05	0.10
MgO	0.78	1.37	0.82	2.03	1.28	0.50	1.19
CaO	0.75	1.37	0.38	2.54	2.37	1.72	2.12
Na2O	4.32	3.33	2.56	3.12	3.25	3.01	3.00
K2O	4.37	5.14	6.22	4.90	5.06	5.62	5.35
P2O5	0.04	0.11	0.03	0.15	0.17	0.03	0.15
LOI	0.89	1.80	0.66	0.91	0.85	0.0	0.0
TOTAL	100.22	100.11	100.66	101.51	99.34	100.80	99.39
Zr	119	275	25	369	365	278	367
Sr	20	116	122	165	165	118	115
Rb	230	208	196	195	195	228	218
Zn	31	63	21	60	58	104	66
Cu	0	0	0	0	0	0	0
Ba	306	615	783	758	739	634	601
Nb	0	0	0	135	135	141	140
Ga	0	0	0	387	407	419	404
Pb	0	0	0	379	406	416	404
Ni	0	130	0	0	0	0	0
Cr	21	29	17	0	0	0	0
V	0	0	0	0	0	0	0
Y	0	0	0	0	0	0	0

POOR COPY  
COPIE DE QUALITEE INFERIEURE

# CHEMICAL ANALYSES OF THE LOCKERS BAY GRANITE

SAMPLE	* NJ	L1 * NJ	L2 * NJ	L3 * NJ	L4 * NJ	L6 * NJ	L7 *
SiO2	64.30	66.20	68.50	69.50	69.66	67.20	*
TiO2	0.76	0.70	0.74	0.50	0.62	0.67	*
Al2O3	16.20	16.00	15.40	14.90	14.50	15.10	*
Fe2O3	3.64	0.88	0.70	0.47	0.32	1.05	*
FeO	3.10	2.58	2.51	2.46	2.85	2.72	*
MnO	0.08	0.07	0.07	0.05	0.07	0.07	*
MgO	1.20	0.99	0.94	0.77	0.81	0.93	*
CaO	2.65	2.46	2.23	1.83	2.00	2.19	*
Na2O	3.62	3.28	3.10	2.95	3.15	3.13	*
K2O	5.13	5.23	5.48	6.07	5.15	5.75	*
P2O5	0.24	0.18	0.17	0.24	0.23	0.17	*
LOI	0.82	1.04	1.01	0.85	0.64	0.84	*
TOTAL	98.74	99.61	100.91	99.75	100.00	99.86	*
Zn	254	251	256	233	275	268	*
SP	178	172	183	135	109	143	*
PB	178	233	224	203	223	209	*
ZN	55	52	53	49	57	58	*
CU	15	13	15	11	10	12	*
BA	904	830	805	622	438	691	*
NB	17	17	17	16	21	14	*
GA	21	20	21	17	21	23	*
PB	26	31	27	23	18	33	*
NI	9	11	13	6	10	10	*
CR	23	17	26	15	16	33	*
V	75	80	69	59	53	77	*
Y	40	53	45	53	63	47	*

POOR COPY  
COPIE DE QUALITEE INFERIEURE

# CHEMICAL ANALYSES OF THE DEADMANS BAY GRANITE

SAMPLE	* NJ	1 * NJ	509 * NJ	819 * NJ	322 * NJ	524 * NJ	625 * NJ	993 *
SiO2	67.50	68.30	74.30	69.20	69.60	71.00	67.40	
TiO2	0.69	0.76	0.27	0.51	0.29	0.30	0.56	
AL2O3	14.90	15.00	13.30	14.20	18.10	14.30	14.20	
FE2O3	0.62	2.01	0.63	1.58	0.14	0.52	1.51	
FEO	2.51	2.25	1.01	1.65	1.34	1.32	2.69	
MNO	0.08	0.11	0.05	0.07	0.03	0.05	0.10	
MGO	1.09	1.43	1.52	1.59	1.52	3.55	1.36	
CAO	2.38	1.47	0.59	0.98	0.40	0.92	2.06	
NA2O	3.09	3.34	3.21	3.06	3.68	2.90	2.87	
K2O	4.64	4.22	4.41	5.29	5.86	5.74	4.78	
P2O5	0.22	0.25	0.13	0.21	0.10	0.10	0.25	
LOI	0.54	1.76	0.69	0.69	0.83	1.26	0.88	
TOTAL	98.73	100.00	100.11	98.33	98.61	102.08	98.66	
ZE	247	240	150	293	134	140	254	
SS	273	284	240	328	230	247	254	
RB	192	221	232	196	202	199	235	
ZN	70	71	41	57	38	47	74	
CU	12	14	7	10	6	8	17	
BA	939	364	399	720	845	736	706	
NR	15	17	14	14	9	10	19	
GA	23	22	18	24	18	14	24	
PR	29	24	32	32	34	50	21	
NI	5	13	8	10	6	1	14	
CE	16	20	10	9	7	5	17	
V	72	101	34	54	30	25	96	
Y	52	59	44	51	35	47	53	

POOR COPY  
COPIE DE QUALITE INFERIEURE

# CHEMICAL ANALYSES OF THE DEADMANS BAY GRANITE

SAMPLE	* NJ	1094	* NJ	1095	*
SiO2	*	70.50	*	71.70	*
TiO2	*	0.43	*	0.40	*
Al2O3	*	14.80	*	14.20	*
Fe2O3	*	0.40	*	0.45	*
FeO	*	1.97	*	2.10	*
MnO	*	0.05	*	0.07	*
MgO	*	0.59	*	0.57	*
CaO	*	1.75	*	1.39	*
Na2O	*	3.06	*	2.83	*
K2O	*	5.15	*	5.36	*
P2O5	*	0.13	*	0.09	*
LOI	*	0.92	*	0.91	*
TOTAL	*	99.75	*	100.07	*
Zr	*	197	*	171	*
Sr	*	213	*	148	*
Pb	*	203	*	203	*
Zn	*	48	*	50	*
Cu	*	12	*	8	*
Ba	*	835	*	412	*
Nb	*	14	*	13	*
Ga	*	21	*	20	*
Pb	*	37	*	29	*
Ni	*	3	*	5	*
Co	*	8	*	13	*
V	*	38	*	45	*
Y	*	48	*	48	*

POOR COPY  
COPIE DE QUALITEE INFERIEURE

# CHEMICAL ANALYSES OF THE NEWPORT GRANITE

SAMPLE	* NJ	205	* NJ	210	* NJ	260	* NJ	302	* NJ	304	* NJ	1140	* NJ	2001	*
SiO2	*	71.80	*	72.70	*	69.40	*	72.60	*	69.20	*	65.50	*	69.60	*
TiO2	*	0.35	*	0.30	*	0.35	*	0.20	*	0.43	*	0.51	*	0.38	*
Al2O3	*	13.40	*	13.60	*	14.40	*	14.10	*	14.20	*	16.00	*	14.40	*
Fe2O3	*	0.33	*	0.24	*	0.76	*	0.43	*	0.76	*	0.93	*	0.57	*
FeO	*	1.39	*	1.04	*	1.48	*	1.35	*	1.72	*	2.19	*	1.51	*
MnO	*	0.05	*	0.06	*	0.06	*	0.03	*	0.06	*	0.05	*	0.06	*
MgO	*	0.45	*	0.28	*	0.63	*	0.64	*	0.64	*	0.89	*	0.61	*
CaO	*	1.43	*	0.86	*	1.73	*	1.41	*	1.57	*	2.35	*	1.89	*
Na2O	*	3.41	*	3.44	*	3.68	*	3.44	*	3.32	*	4.22	*	3.25	*
K2O	*	4.80	*	5.44	*	4.72	*	5.43	*	5.65	*	5.09	*	4.04	*
P2O5	*	0.05	*	0.04	*	0.06	*	0.06	*	0.08	*	0.14	*	0.09	*
LOI	*	0.84	*	0.74	*	1.18	*	0.72	*	0.79	*	0.24	*	0.86	*
TOTAL	*	98.36	*	98.74	*	98.47	*	100.44	*	96.42	*	99.11	*	98.36	*
Si	*	156	*	124	*	221	*	173	*	228	*	239	*	214	*
Al	*	151	*	79	*	228	*	147	*	170	*	243	*	211	*
Fe	*	235	*	327	*	232	*	192	*	216	*	165	*	221	*
Zn	*	46	*	32	*	59	*	43	*	53	*	53	*	52	*
Cu	*	7	*	5	*	7	*	8	*	10	*	14	*	7	*
Ba	*	416	*	267	*	654	*	461	*	505	*	691	*	563	*
Nb	*	16	*	22	*	17	*	14	*	19	*	13	*	16	*
Ga	*	20	*	21	*	22	*	21	*	18	*	25	*	20	*
Ge	*	25	*	34	*	24	*	20	*	21	*	28	*	28	*
Ni	*	5	*	4	*	6	*	5	*	5	*	10	*	4	*
Co	*	3	*	8	*	6	*	3	*	8	*	11	*	10	*
V	*	27	*	17	*	33	*	22	*	39	*	50	*	420	*
Y	*	55	*	66	*	45	*	42	*	40	*	42	*	47	*

POOR COPY  
COPIE DE QUALITEE INFERIEURE

# CHEMICAL ANALYSES OF THE NEWPORT GRANITE

SAMPLE	* NJ	2003	* NJ	2004	* NJ	2005	*
SiO2	*	71.20	*	70.70	*	74.40	*
TiO2	*	0.40	*	0.40	*	0.14	*
Al2O3	*	14.60	*	14.90	*	14.50	*
Fe2O3	*	0.90	*	1.09	*	0.00	*
FeO	*	1.36	*	1.46	*	0.78	*
MnO	*	0.06	*	0.07	*	0.04	*
MgO	*	0.53	*	0.68	*	0.08	*
CaO	*	1.79	*	2.00	*	1.00	*
Na2O	*	3.68	*	3.61	*	3.16	*
K2O	*	5.03	*	5.04	*	4.78	*
R2O5	*	0.07	*	0.16	*	0.00	*
LCI	*	0.76	*	0.69	*	0.37	*
TOTAL	*	100.38	*	100.80	*	98.36	*
Zr	*	217	*	225	*	75	*
Sr	*	192	*	209	*	100	*
Rb	*	241	*	214	*	211	*
Zn	*	50	*	56	*	28	*
Cu	*	7	*	9	*	6	*
Ba	*	541	*	583	*	249	*
Nb	*	15	*	18	*	13	*
Ga	*	23	*	22	*	19	*
Pb	*	29	*	26	*	26	*
Ni	*	7	*	5	*	4	*
Cr	*	5	*	8	*	12	*
V	*	25	*	39	*	7	*
Y	*	51	*	51	*	38	*

POOR COPY  
COPIE DE QUALITE INFERIEURE

# CHEMICAL ANALYSES OF THE BIG POUND POND GRANITE

SAMPLE	* NJ	134	* NJ	621	* NJ	1153	*
SiO2	*	59.40	*	72.90	*	71.00	*
TiO2	*	0.49	*	0.38	*	7.40	*
Al2O3	*	15.30	*	14.00	*	14.20	*
Fe2O3	*	1.12	*	0.34	*	0.58	*
FeO	*	1.74	*	1.59	*	1.26	*
MnO	*	0.07	*	0.07	*	0.06	*
MgO	*	0.69	*	0.64	*	0.60	*
CaO	*	2.17	*	1.91	*	1.32	*
Na2O	*	3.54	*	3.52	*	3.37	*
K2O	*	5.01	*	4.58	*	4.87	*
P2O5	*	0.03	*	0.12	*	0.05	*
LOI	*	0.95	*	0.64	*	0.97	*
TOTAL	*	100.77	*	100.69	*	98.68	*
Zn	*	163	*	137	*	137	*
SP	*	243	*	200	*	202	*
RB	*	248	*	262	*	222	*
ZN	*	55	*	48	*	44	*
CU	*	21	*	14	*	18	*
BA	*	509	*	428	*	456	*
MB	*	15	*	18	*	19	*
GE	*	19	*	18	*	20	*
RB	*	30	*	24	*	30	*
NI	*	7	*	8	*	6	*
CP	*	10	*	15	*	8	*
V	*	54	*	40	*	39	*
Y	*	45	*	52	*	41	*

Poor Copy  
Copie de qualitee inferieure

Appendix 6.2 - C.I.P.W. norms of the granitoid plutons  
- Wareham Pluton.

Sample No.	Q	Or	Ab	An	C	H <sub>2</sub> O	K <sub>2</sub> O	Il	Py	Ap
76-NJ-353	17.05	23.77	25.48	17.67	0.69	10.68	1.77	1.92	0.00	0.96
76-NJ-354	10.26	22.42	29.21	16.33	2.75	12.70	2.25	1.99	0.00	2.08
76-NJ-355	15.03	23.24	26.84	15.74	0.62	8.67	2.11	1.85	0.00	0.90
76-NJ-373	14.32	22.66	23.58	18.83	0.53	10.29	1.88	1.93	0.00	0.97
76-NJ-637	12.84	27.31	26.64	13.75	0.00	8.81	2.41	2.11	0.00	0.89
76-NJ-641	14.30	27.57	29.99	13.70	0.90	8.98	1.90	1.64	0.00	0.99
76-NJ-642	15.40	26.62	25.72	16.70	0.27	10.26	2.30	1.93	0.00	0.78
76-NJ-700	13.25	24.10	23.01	19.24	0.42	9.85	2.69	1.68	0.00	0.75
77-NJ-763	26.75	24.31	26.03	11.64	1.70	7.36	0.86	1.16	0.00	0.19
77-NJ-723	9.16	29.61	26.30	15.77	0.96	13.87	1.44	2.02	0.00	0.86
77-NJ-1084	15.33	28.89	26.54	15.78	0.37	9.48	1.65	1.32	0.00	0.64
77-NJ-914	16.43	24.80	26.20	17.90	0.00	10.91	1.37	1.55	0.00	0.66
77-NJ-877	31.54	23.72	24.51	8.43	1.01	4.09	0.68	0.73	0.00	0.28
76-NJ-374	31.54	31.08	25.29	6.65	0.88	2.30	1.24	0.77	0.00	0.23



- North Pond Pluton (medium-grained phase).

Sample No.	Q	Or	Ab	An	C	Hr	Mt	Il	Py	Ap
76-NJ-364	27.92	26.82	26.94	7.38	2.61	5.72	1.06	0.90	0.00	0.66
76-NJ-368	29.57	24.93	29.72	5.67	2.52	5.62	0.59	0.94	0.00	0.54
76-NJ-369	27.96	25.42	30.33	7.52	2.14	5.17	0.26	0.84	0.00	0.35
76-NJ-370	32.28	20.58	30.49	9.21	2.14	3.84	0.48	0.68	0.00	0.19
76-NJ-352	32.88	33.65	22.86	2.01	3.52	2.97	0.84	0.46	0.00	0.82
76-NJ-510	31.71	24.86	30.99	4.47	2.97	3.23	0.62	0.53	0.00	0.62
76-NJ-567	26.10	23.14	28.14	12.27	1.50	5.93	1.24	1.02	0.00	0.57
76-NJ-592	33.23	29.82	28.24	1.53	3.32	2.15	0.58	0.39	0.00	0.74
76-NJ-601	27.05	24.50	28.85	9.29	1.83	5.69	1.24	0.94	0.00	0.61
76-NJ-601	30.96	20.25	30.12	9.93	1.75	4.73	1.09	0.77	0.00	0.40
76-NJ-503	26.18	24.44	28.10	10.91	1.85	5.76	1.29	0.97	0.00	0.50

- North Pond Pluton (porphyritic phase).

Sample No.	Q	Or	Ab	An	C	Hy	Mt	Il	Py	Ap
77-NJ-891	30.63	31.78	24.18	4.28	2.46	5.62	0.12	0.53	0.00	0.40
76-NJ-512	22.00	29.26	28.62	9.33	0.00	0.00	0.21	0.18	0.00	0.83
76-NJ-488	36.05	29.90	26.23	0.58	3.51	1.72	0.70	0.51	0.00	0.79
76-NJ-597	34.35	29.04	28.16	1.52	3.60	1.84	0.46	0.29	0.00	0.74
76-NJ-598	32.72	25.16	30.15	2.62	3.58	3.66	0.65	0.58	0.00	0.88
76-NJ-648	27.07	24.51	28.67	9.51	2.26	6.31	0.45	0.82	0.00	0.41
77-NJ-845	31.82	33.59	24.95	2.18	2.84	3.24	0.19	0.56	0.00	0.64
77-NJ-856	30.89	33.19	24.74	3.43	2.72	3.68	0.19	0.69	0.00	0.47
77-NJ-172	32.08	27.77	29.84	2.75	2.88	3.61	0.00	0.52	0.00	0.54

- Business Cove Pluton.

Sample No.	Q	Or	Ab	An	C	H <sub>y</sub>	Mt	Il	Py	Ap
75-NJ-173	24.67	24.18	28.66	9.96	0.74	10.58	0.57	0.50	0.00	0.14
75-NJ-219	26.60	25.75	34.13	7.04	2.10	3.57	0.15	0.48	0.00	0.19
75-NJ-266	35.56	34.50	23.17	1.35	2.72	1.16	0.77	0.23	0.00	0.54
77-NJ- 70	26.58	31.47	24.06	10.57	0.00	0.30	0.20	0.56	0.00	0.46

- Lockers Bay Pluton.

Sample No.	Q	Or	Ab	An	C	H <sub>y</sub>	Mt	Il	Py	Ap
77-NJ- L1	15.17	30.94	31.26	12.08	0.36	7.19	0.95	1.47	0.00	0.57
77-NJ- L2	19.68	31.34	28.14	11.42	0.83	5.52	1.29	1.35	0.00	0.42
77-NJ- L3	22.24	32.40	26.24	10.48	0.53	5.28	1.02	1.41	0.00	0.40
77-NJ- L4	22.29	36.25	25.23	8.08	0.55	5.39	0.69	0.96	0.00	0.56
77-NJ- L6	25.02	30.62	26.82	8.61	0.61	6.13	0.47	1.18	0.00	0.54
77-NJ- L7	19.90	34.54	26.74	10.04	0.04	5.51	1.54	1.28	0.00	0.40

- Cape. Freels Pluton.

Sample No.	Q	Or	Ab	An	C	Hy	Mt	Il	Py	Ap
75-NJ- 38	22.71	32.57	28.52	8.86	0.69	4.03	1.10	1.15	0.00	0.38
75-NJ- 41	24.16	30.19	28.73	8.71	1.32	4.17	1.23	1.07	0.00	0.42
75-NJ- 96	22.95	32.85	28.55	7.76	1.14	4.44	0.87	0.98	0.00	0.45
75-NJ- FI	14.02	24.23	28.41	18.15	0.75	11.76	0.36	2.19	0.00	0.12
75-NJ-170	28.09	33.98	25.49	6.54	0.01	4.03	0.76	0.78	0.00	0.33
75-NJ-271	11.06	26.63	32.18	16.50	0.60	7.48	3.21	1.96	0.00	0.38
75-NJ-272	4.83	32.49	29.11	16.93	0.00	10.28	2.51	2.14	0.00	0.38
75-NJ-273	14.16	22.04	25.56	21.41	0.00	10.15	3.66	2.34	0.00	0.33
75-NJ-267	9.99	20.63	34.95	19.90	0.00	7.18	3.32	1.96	0.00	0.36
75-NJ-30A	17.53	40.01	25.71	6.80	1.23	6.67	0.54	0.76	0.00	0.75
169*	28.82	27.30	27.29	7.72	0.76	3.07	-	0.17	-	0.23
171*	25.89	31.56	29.81	2.74	0.00	1.19	-	0.15	-	0.33
180*	24.40	34.88	25.36	6.67	1.05	2.90	-	0.15	-	0.19
184*	27.62	25.99	36.78	3.18	2.28	1.95	-	0.04	-	0.09
185*	23.81	30.88	28.64	3.90	1.80	3.47	-	0.08	-	0.26
186*	35.11	36.74	21.90	1.71	1.75	2.14	-	0.02	-	0.07
187*	23.32	28.76	26.22	10.63	-	3.07	-	0.08	-	0.42
188*	22.53	30.33	27.90	10.39	0.62	3.23	-	0.07	-	0.40
239*	27.52	32.91	25.24	7.50	1.77	1.23	-	0.11	-	0.07
240*	25.41	31.77	25.51	8.68	0.79	2.98	-	0.21	-	0.35

\* indicates analyses from Strong et.al. 1974.

- Deadman's Bay Pluton.

Sample No.	Q	Or	Ab	An	C	Ky	Mt	Il	Py	Ap
76-NJ-509	27.65	25.14	28.49	5.89	2.82	5.01	2.94	1.46	0.01	0.59
77-NJ-819	34.65	26.20	27.31	6.89	0.74	2.45	0.92	0.52	0.01	0.30
77-NJ-822	25.25	32.00	26.50	8.46	0.42	3.52	2.34	0.99	0.01	0.50
77-NJ-824	25.24	35.40	26.64	7.80	0.97	2.97	0.21	0.56	0.01	0.24
77-NJ-828	24.21	33.64	24.33	4.11	1.78	10.20	0.75	0.73	0.01	0.23
77-NJ-99F	33.58	28.22	30.38	1.69	2.47	1.79	0.74	0.41	0.01	0.62
77-NJ-99C	25.79	28.87	24.82	9.02	1.09	6.47	2.24	1.09	0.01	0.59
77-NJ- 94	27.72	30.78	26.19	8.17	1.25	4.18	0.59	0.83	0.01	0.31
77-NJ- 95	29.99	31.93	24.14	6.50	1.39	4.40	0.66	0.77	0.01	0.21
75-NJ- 1	26.99	28.97	27.62	11.24	0.95	2.87	0.00	0.17	0.01	0.54

- Newport Pluton.

Sample No.	Q	Or	Ab	An	C	Hx	Mt	Il	Py	Ap
75-NJ-210	17.67	19.13	17.32	2.43	0.33	0.41	1.58	0.34	0.01	0.06
75-NJ-302	27.33	31.99	29.18	6.76	0.12	3.34	0.62	0.50	0.01	0.14
75-NJ-304	23.84	34.19	28.76	7.33	0.00	3.48	1.13	0.84	0.01	0.19
75-NJ-260	25.36	28.66	31.99	8.50	0.21	3.27	1.13	0.68	0.01	0.19
75-NJ-305	22.05	31.60	24.91	9.98	0.07	7.00	2.05	1.66	0.00	0.66
76-NJ- 1	25.66	29.93	29.93	9.20	0.09	3.38	0.85	0.74	0.01	0.21
76-NJ- 3	25.61	29.83	31.25	8.49	0.00	2.47	1.31	0.76	0.01	0.16
76-NJ- 4	24.88	29.74	30.50	9.06	0.18	2.93	1.58	0.76	0.01	0.37
76-NJ- 5	35.61	29.12	27.74	5.66	0.09	1.51	0.00	0.27	0.01	0.00
77-NJ-140	15.72	30.41	36.10	9.79	0.00	4.22	1.36	0.98	0.01	0.33
76-NJ-205	29.87	29.08	29.58	7.08	0.07	2.96	0.56	0.68	0.01	0.12

- Big Round Pond Pluton.

Sample No.	Q	Or	Ab	An	C	Hx	Mt	Il	Py	Ap
75-NJ-621	29.12	27.04	29.76	8.84	0.01	3.73	0.49	0.72	0.00	0.28
76-NJ-134	23.14	29.65	30.00	10.38	0.26	3.81	1.63	0.93	0.00	0.21
77-NJ-163	29.18	29.44	29.17	6.53	1.07	2.84	0.86	0.78	0.00	0.12

Appendix 7.1 Mesonorm of the solid phase at each of 5 wt.% increment of melt during the partial melting of the "average" greywacke to produce the parent magmas of the megacrystic plutons and the Big Round Pond Granite in the area.

F - wt.% melt in the system, Q - Quartz, Ab - Albite  
Or - orthoclase, An - anorthite, C - corundum,  
Bt - biotite, Hy - hypersthene, Sp - sphene,  
Mg - magnetite, Ap - apatite.

Wareham Quartz Monzonite

F	Q	Ab	Or	An	C	Bt	H <sub>y</sub>	Sp	Mg	Ap
5	39.30	28.03	2.51	8.07	4.37	12.48	0.0	1.48	3.37	0.37
10	40.22	28.03	1.64	7.87	4.53	12.44	0.0	1.46	3.46	0.35
15	41.24	28.11	0.64	7.61	4.63	12.42	0.0	1.41	3.56	0.33
20	42.07	28.20	0.0	7.31	4.85	11.77	0.43	1.38	3.68	0.31
25	42.56	28.30	0.0	7.00	5.04	9.91	1.76	1.33	3.81	0.29
30	43.13	28.41	0.0	6.69	5.24	7.77	3.29	1.26	3.95	0.26
35	46.44	28.37	0.0	6.36	7.90	5.25	5.04	1.21	4.10	0.26
40	44.28	28.80	0.0	5.81	5.87	2.34	7.20	1.15	4.35	0.20



Cape Freels Granite

F	Q	Ab	Or	An	C	Bt	Hr	Sp	Mg	Ap
5	39.08	27.96	2.01	8.39	4.45	12.79	0.0	1.53	3.42	0.38
10	39.62	28.04	0.58	8.54	4.61	13.15	0.0	1.53	3.55	0.38
15	39.68	28.06	0.0	8.64	4.82	12.05	1.06	1.56	3.73	0.40
20	39.38	28.09	0.0	8.75	5.06	9.92	2.90	1.58	3.88	0.42
25	38.95	28.14	0.0	9.01	5.30	7.43	5.08	1.59	4.07	0.42
30	38.52	28.18	0.0	9.23	5.61	4.48	7.61	1.61	4.30	0.44
35	37.96	28.32	0.0	9.45	5.96	1.17	10.47	1.64	4.56	0.46

Lockers Bay Granite

F	Q	Ab	Or	An	C	Bt	Hy	Sp	Mg	Ap
5	39.28	27.95	1.98	8.34	4.43	12.74	0.0	1.51	3.42	0.37
10	40.04	28.03	0.55	8.38	4.58	13.00	0.0	1.51	3.55	0.37
15	40.34	28.05	0.0	8.42	4.77	11.78	1.09	1.48	3.70	0.37
20	40.29	28.08	0.0	8.48	4.99	9.38	3.04	1.48	3.88	0.37
25	40.21	28.11	0.0	8.58	5.23	6.71	5.26	1.46	4.07	0.37
30	39.91	28.22	0.0	8.94	5.39	3.67	7.76	1.46	4.29	0.37
35	37.96	28.32	0.0	9.45	5.96	1.17	10.47	1.64	4.56	0.46

Deadman's Bay Granite

F	Q	Ab	Or	An	C	Bt	Hy	Sp	Mg	Ap
5	40.02	28.53	6.84	8.64	4.52	6.00	0.0	1.57	3.48	0.39
10	39.58	27.88	0.75	8.65	4.52	13.15	0.0	1.56	3.52	0.38
15	39.78	27.81	0.0	8.87	4.69	12.41	0.81	1.58	3.65	0.38
20	39.46	27.76	0.0	9.05	4.90	10.37	2.62	1.63	3.80	0.40
25	39.09	27.71	0.0	9.38	5.08	8.06	4.64	1.66	3.99	0.40
30	38.71	27.59	0.0	9.76	5.30	5.38	6.99	1.69	4.18	0.40
35	38.20	27.55	0.0	10.09	5.57	2.34	9.67	1.74	4.41	0.42

Newport Granite

F	Q	Ab	Or	An	C	Bt	Hy	Sp	Mg	Ap
5 <sup>W</sup>	39.02	27.87	1.97	8.40	4.46	12.93	0.0	1.56	3.42	0.38
10	39.64	27.70	0.52	8.50	4.67	13.41	0.0	1.58	3.56	0.40
15 <sup>•</sup>	39.60	27.55	0.0	8.62	4.93	12.32	1.19	1.63	3.73	0.42
20	40.53	25.68	0.0	8.77	5.57	10.22	3.19	1.69	3.92	0.44
25	38.82	27.21	0.0	8.93	5.53	7.79	5.42	1.74	4.11	0.46
30	38.31	27.00	0.0	9.12	5.89	5.12	7.93	1.81	4.35	0.48
35	37.76	26.72	0.0	9.37	6.31	1.89	10.94	1.89	4.62	0.50

Big Round Pond Granite








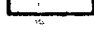



F	Q	Ab	Or	An	C	Bt	Hy	Sp	Mg	Ap
5	38.98	27.87	2.11	8.35	4.44	12.89	0.0	1.56	3.42	0.38
10	39.50	27.79	0.81	8.40	4.64	13.33	0.0	1.58	3.55	0.40
15	39.71	27.63	0.0	8.50	4.86	12.86	0.72	1.61	3.70	0.42
20	39.34	27.58	0.0	8.61	5.09	10.91	2.51	1.63	3.88	0.44
25	38.95	27.45	0.0	8.69	5.38	8.78	4.52	1.69	4.07	0.46
30	38.55	27.63	0.0	8.92	5.76	6.35	7.53	1.76	3.01	0.48
35	37.96	27.12	0.0	9.00	6.10	3.41	9.55	1.79	4.56	0.50

Appendix 8    Published papers which include results pertinent to  
this thesis.

Papers by the author and colleagues appear listed in the references  
cited. Copies of these papers may be secured by contacting the  
author in the Department of Geology, Memorial University of Newfound-  
land.

GEOLOGY OF THE WESLEYVILLE (2F/4), MUSGRAVE HARE  
AND THE NORTHWEST PORTION OF THE ST. BRENDANS (2)

LEGEND

	Big Round Pond Granite: Massive, medium grained, biotite granite.	Mylonitic foliation
	Newport Granite: Massive, coarse grained, megacrystic, biotite granite.	Crenulation cleavage
	Deedman's Bay Granite: Massive, coarse grained, megacrystic, biotite granite.	First recognizable
	Lockers Bay Granite: Foliated, coarse grained, megacrystic, biotite granite.	Lineation (L <sub>1</sub> ): related
	Cape Freels Granite: Foliated to massive, coarse grained, megacrystic, biotite granite.	Lineation (L <sub>2</sub> ): related
	Foliated, medium grained, gabbro.	Minor fold axis: related
	Business Cove Granite: Foliated, medium grained, muscovite-biotite granite with minor garnet.	Minor fold axis: related
	North Pond Granite: a, Foliated, medium grained, muscovite-biotite granite with minor garnet; b, foliated (locally massive), medium grained, porphyritic granite with minor garnet.	Location and trend
	Wareham Quartz Monzonite: Foliated (locally massive), coarse grained, megacrystic, quartz monzonite.	Shear zone
	Hare Bay Gneiss: Migmatite containing enclaves of paragneiss.	Fault (defined, approximate)
	Square Pond Gneiss: Psammitic and semipeliteic, paragneiss, schist and metasediments.	

SYMBOLS

Geological boundary (defined, approximate, assumed, gradational)

First recognizable gneissic banding (S<sub>1</sub>) (inclined, vertical)

Second recognizable gneissic banding (S<sub>2</sub>) (inclined, vertical)

Foliation (S<sub>3</sub>): regionally developed (inclined, vertical)

Scale 1:50,000

Kilometres 0 1 2 3 Kilometres

1 of 1

# GEOLOGY OF THE WESLEYVILLE (2F/4), MUSGRAVE HARBOUR EAST (2F/5)

## AND THE NORTHWEST PORTION OF THE ST. BRENDANS (2C/13) MAP AREAS

red, biotite granite

acrystic, biotite granite

d. megacrystic, biotite granite

megacrystic, biotite granite

grained, megacrystic, biotite granite

red, muscovite-biotite granite with minor

red, muscovite-biotite granite with minor  
grained, porphyritic granite with minor

massive), coarse grained, megacrystic,

of paragneiss

paragneiss, schist and metasediments

ational)

Mylonitic foliation ( $S_0$ ): related to the shear zones (inclined; vertical)

Crenulation cleavage (inclined, vertical)

First recognizable planar fabric in the granitoids (inclined, vertical)

Lineation ( $L_1$ ): related to the regional foliation

Lineation ( $L_2$ ): related to the mylonitic foliation

Minor fold axis: related to the regional foliation

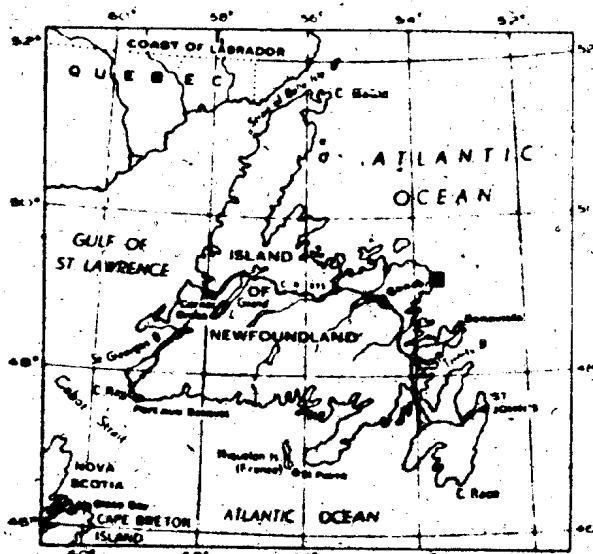
Minor fold axis: related to the mylonitic foliation

Location and trend of diabase dike

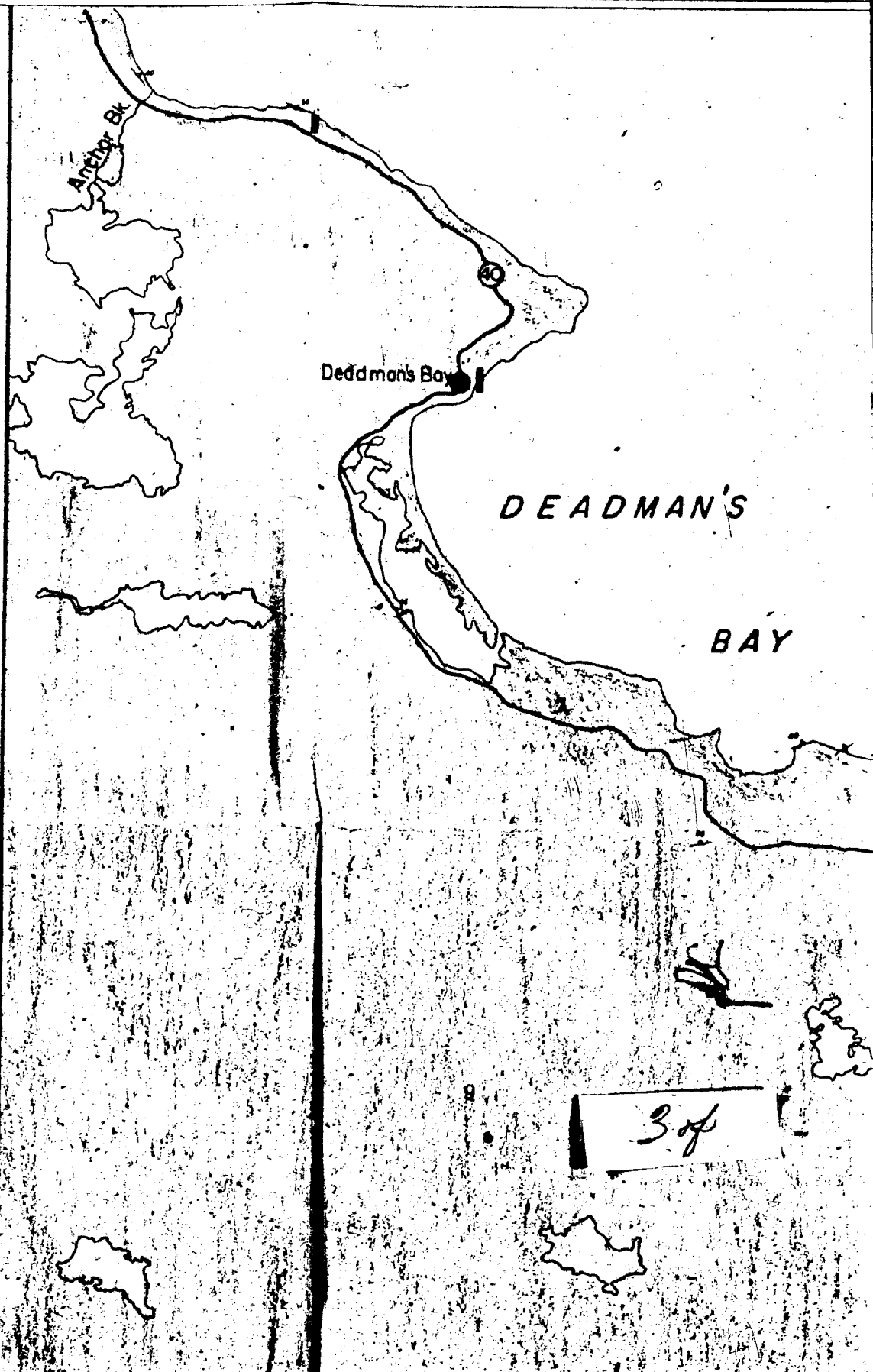
Shear zone

Fault (defined, approximate, assumed)

Memorial University of Newfoundland  
May 1979







Deadman's Bay

DEADMAN'S

BAY

3 of

D'EADMAN'S

BAY

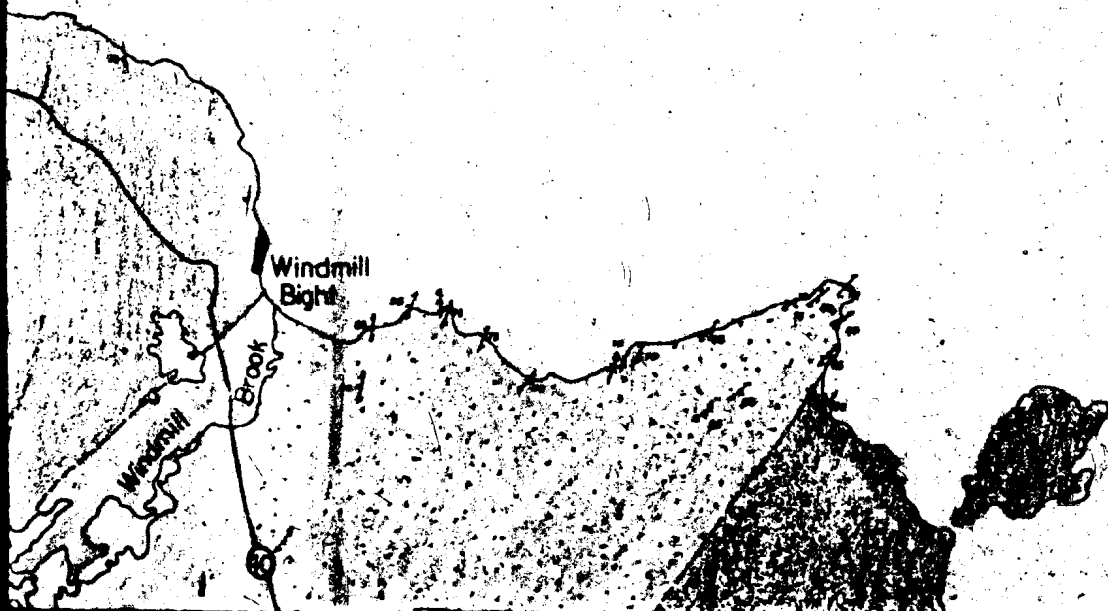
on's Bay

Lumsden

Windmill  
Bight

Windmill  
Brook

4 of 4



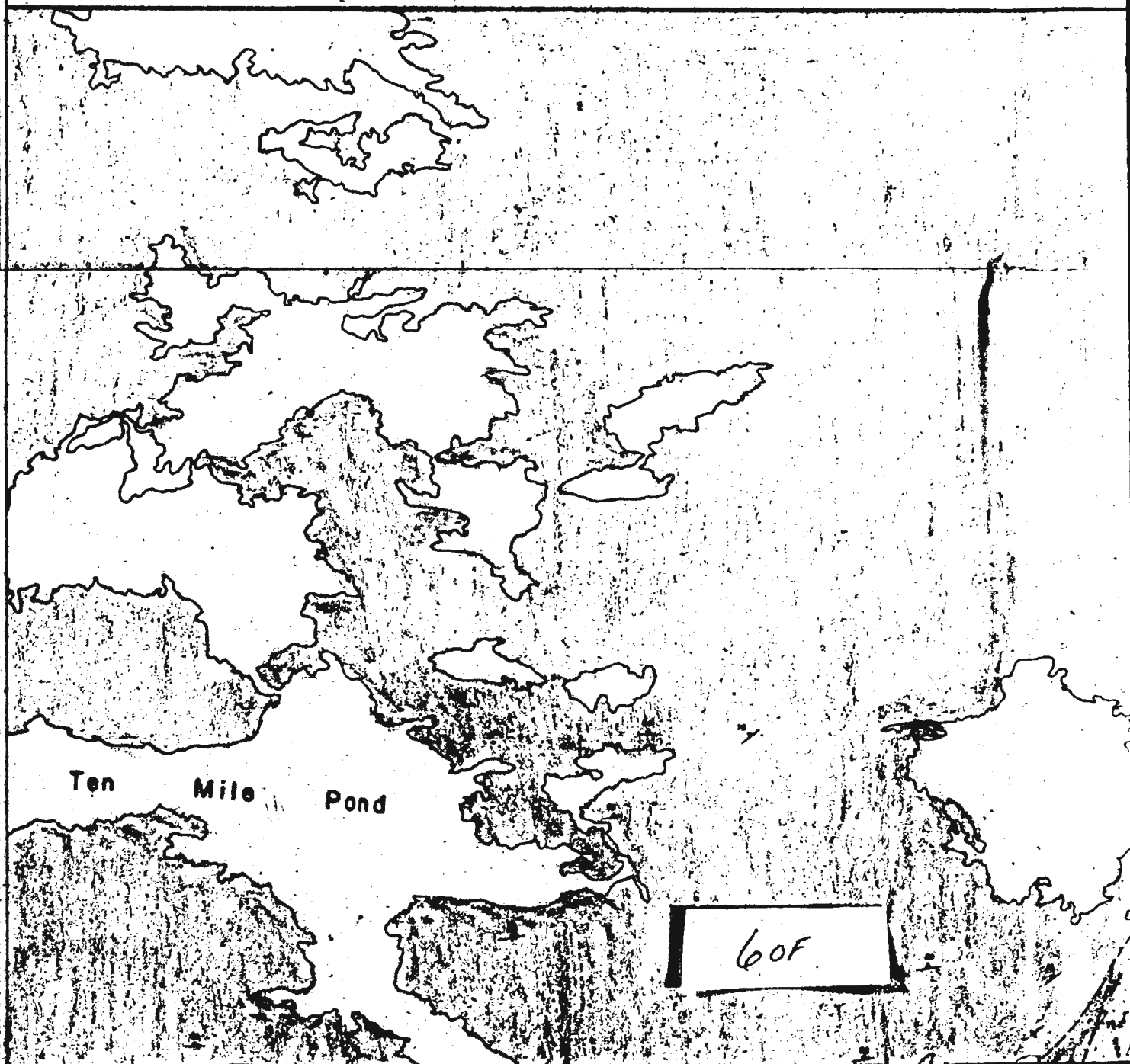
50f

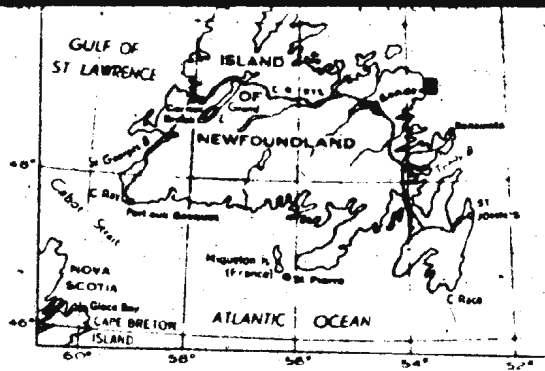
Second recognizable gneissic banding ( $S_2$ ) (inclined, vertical) //

Foliation ( $S_3$ ): regionally developed (inclined, vertical) //

Scale 1:50,000

Kilometres 0 1 2 3 Kilometres

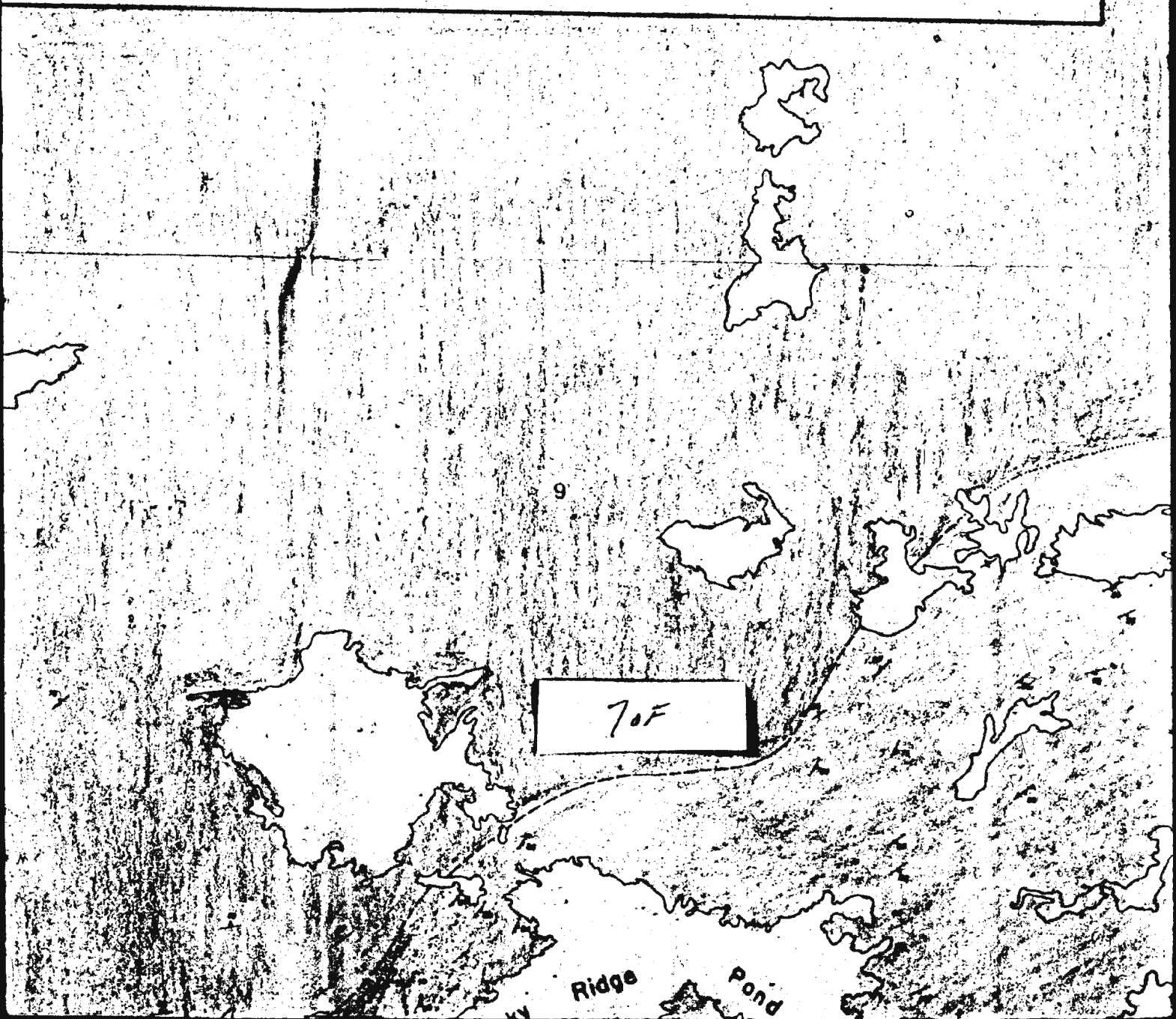




INDEX MAP

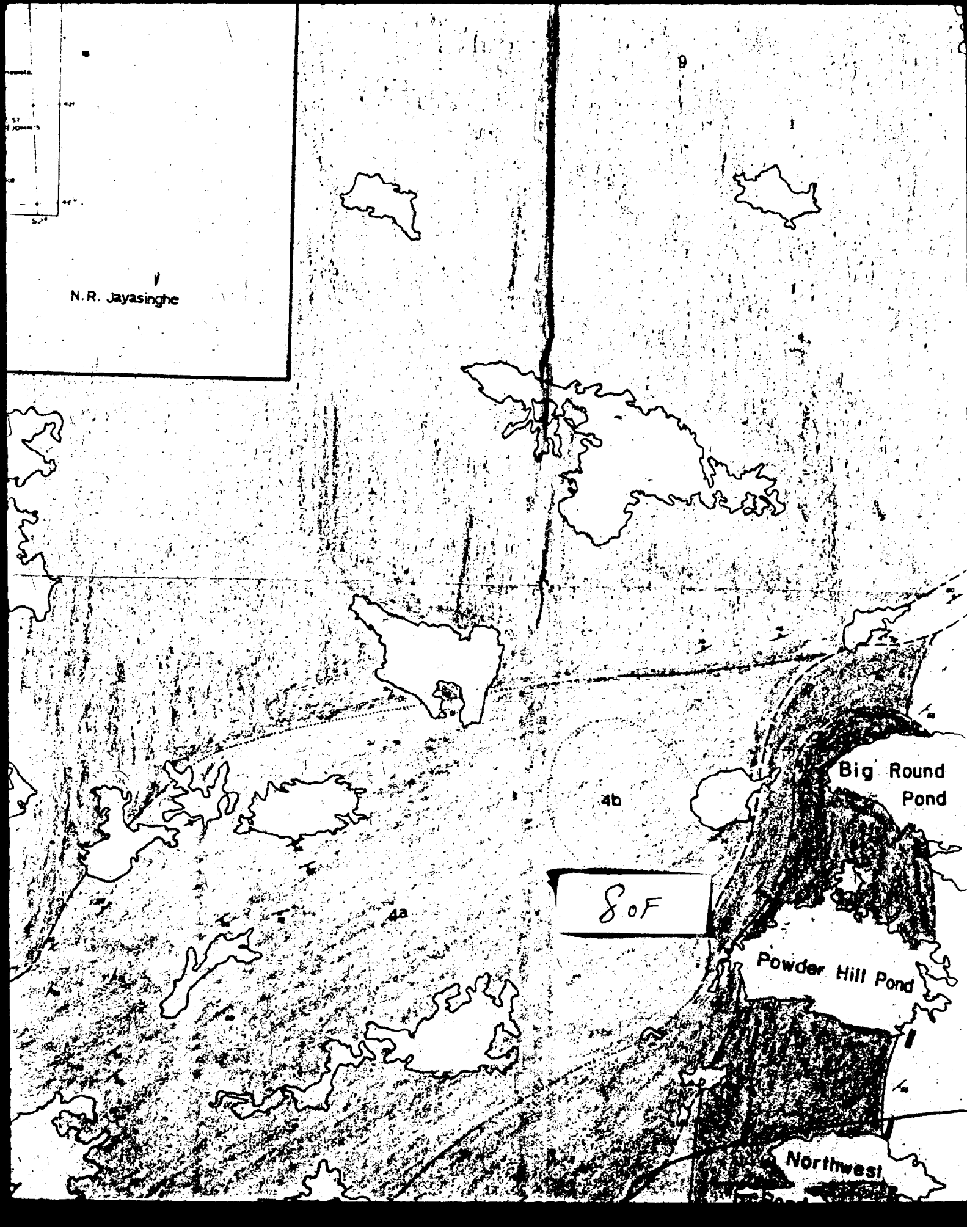
3 Kilometres

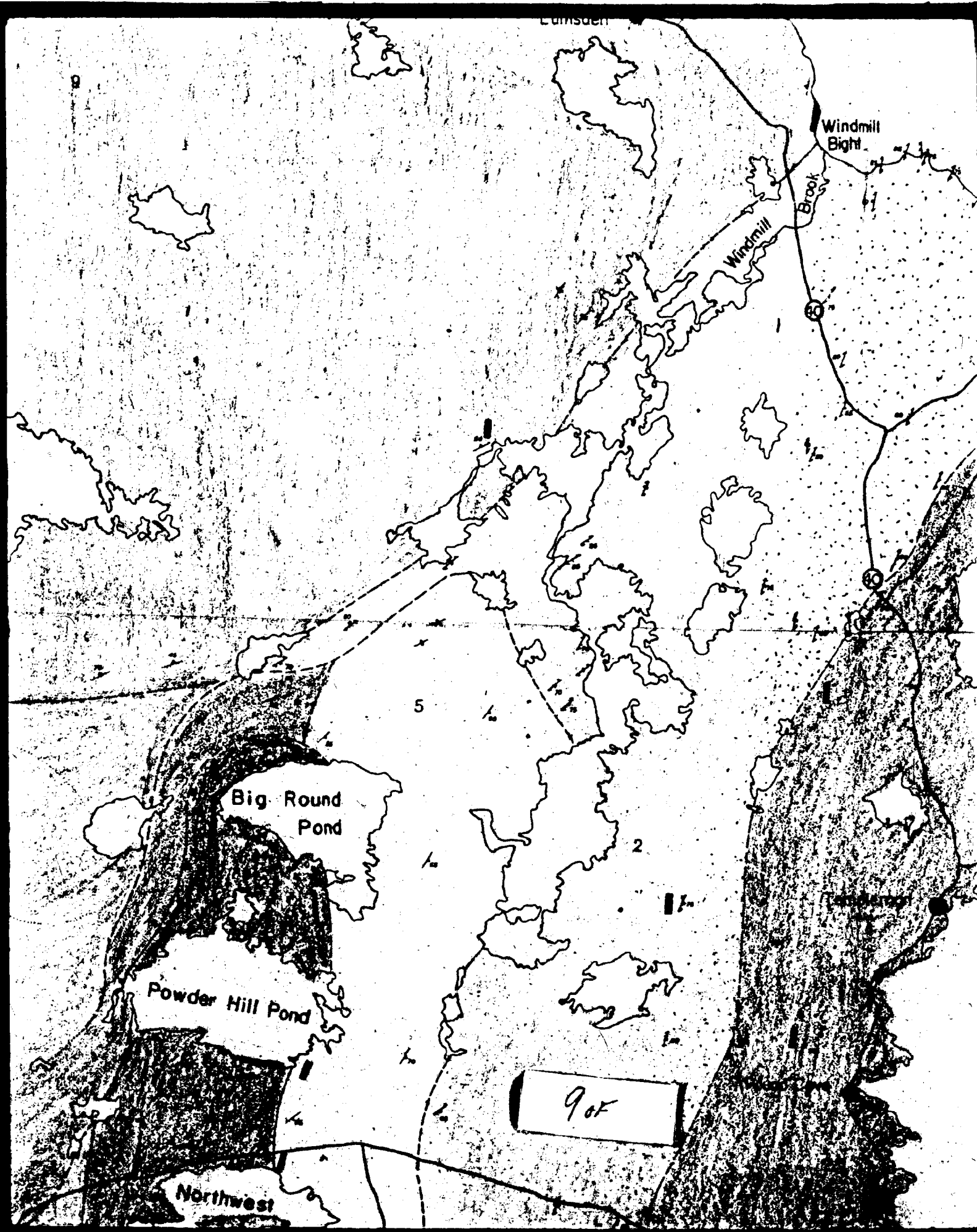
N.R. Jayasinghe



51  
52  
53  
54  
55  
56  
57  
58  
59  
60  
61  
62  
63  
64  
65  
66  
67  
68  
69  
70  
71  
72  
73  
74  
75  
76  
77  
78  
79  
80  
81  
82  
83  
84  
85  
86  
87  
88  
89  
90  
91  
92  
93  
94  
95  
96  
97  
98  
99  
100

N. R. Jayasinghe





Lumsden

Windmill Bight

Brook

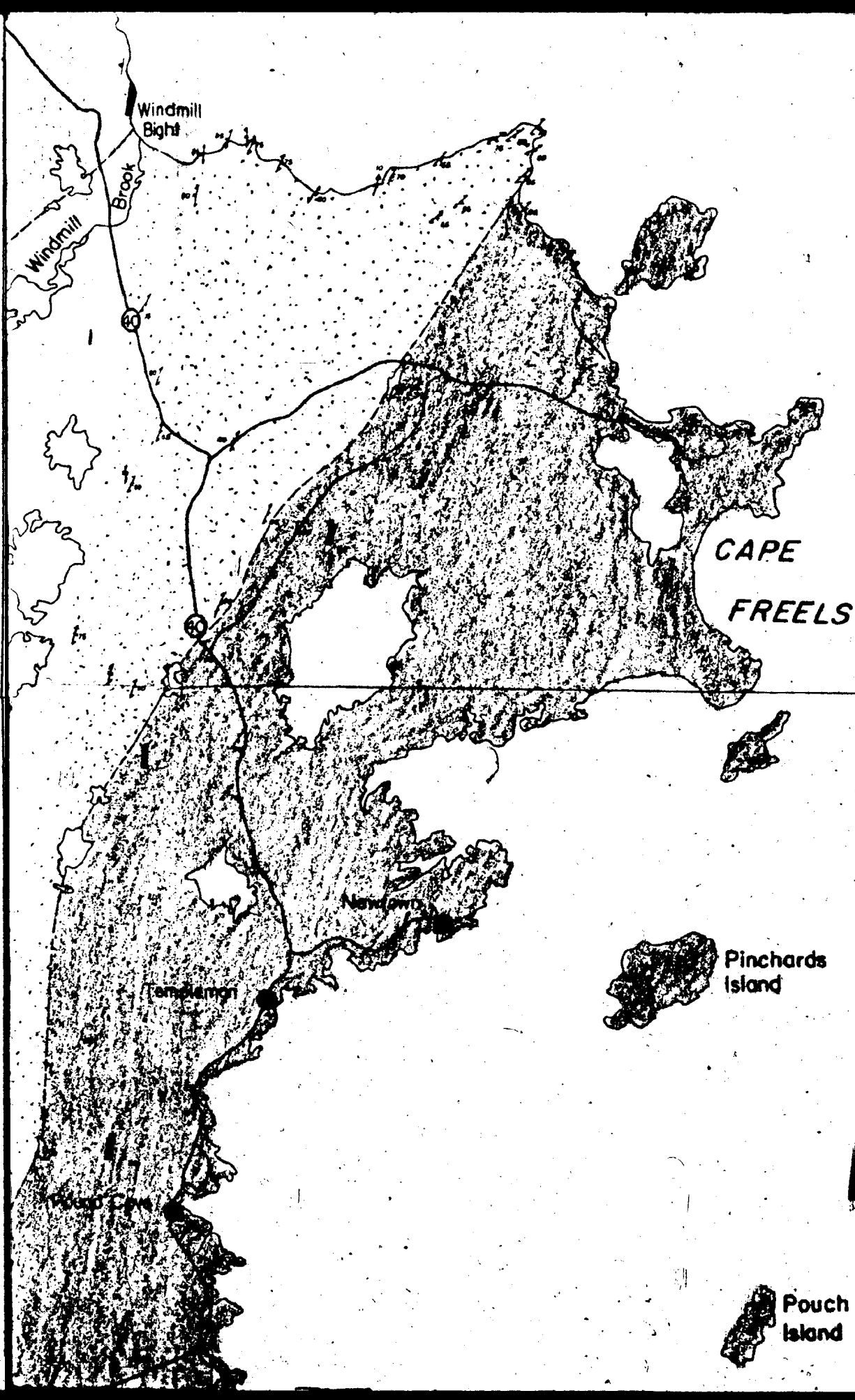
Windmill

Big Round Pond

Powder Hill Pond

Northwest

9 of



275  
274

CAPE  
FREELS

Pinchards  
Island

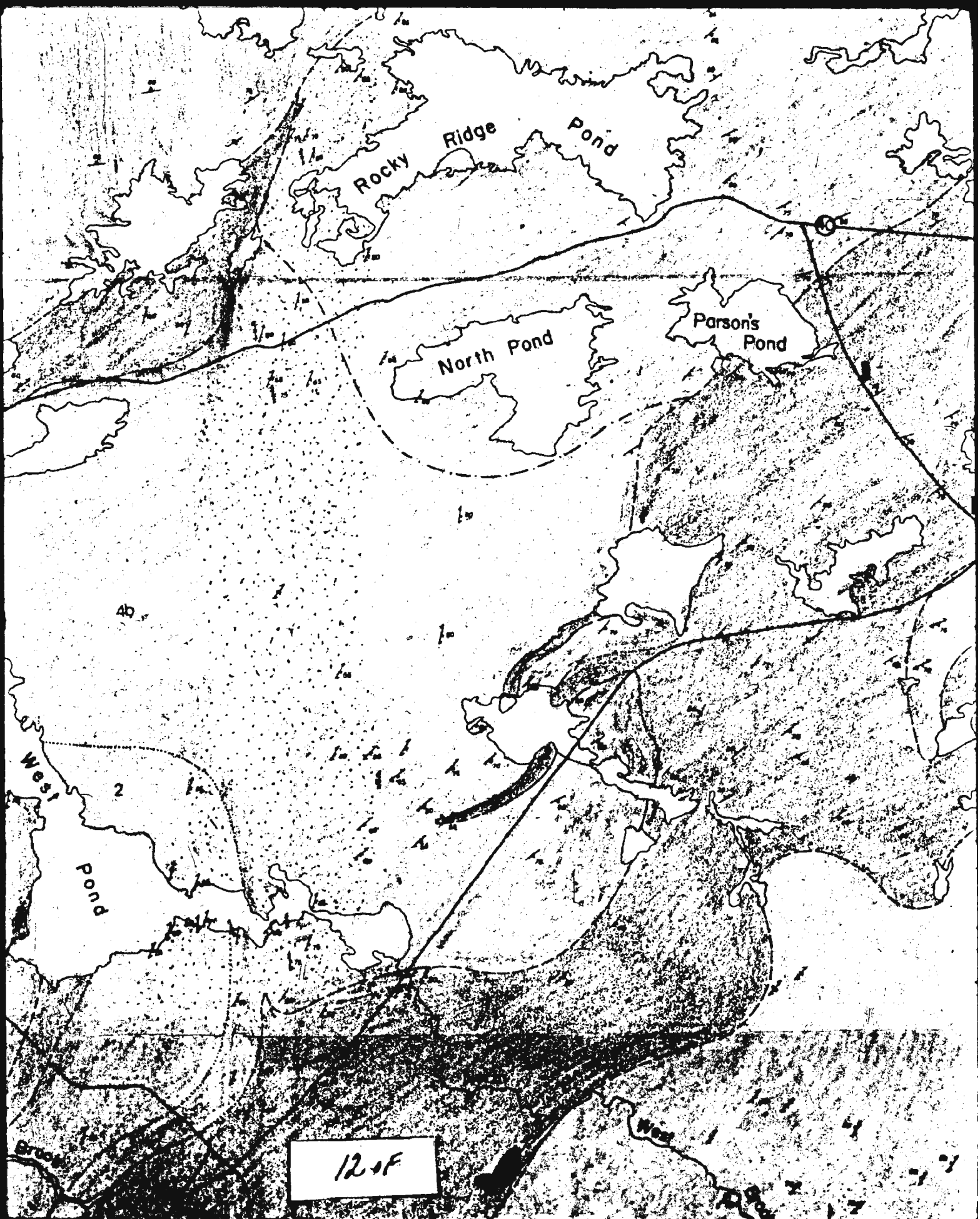
10 of

Pouch  
Island

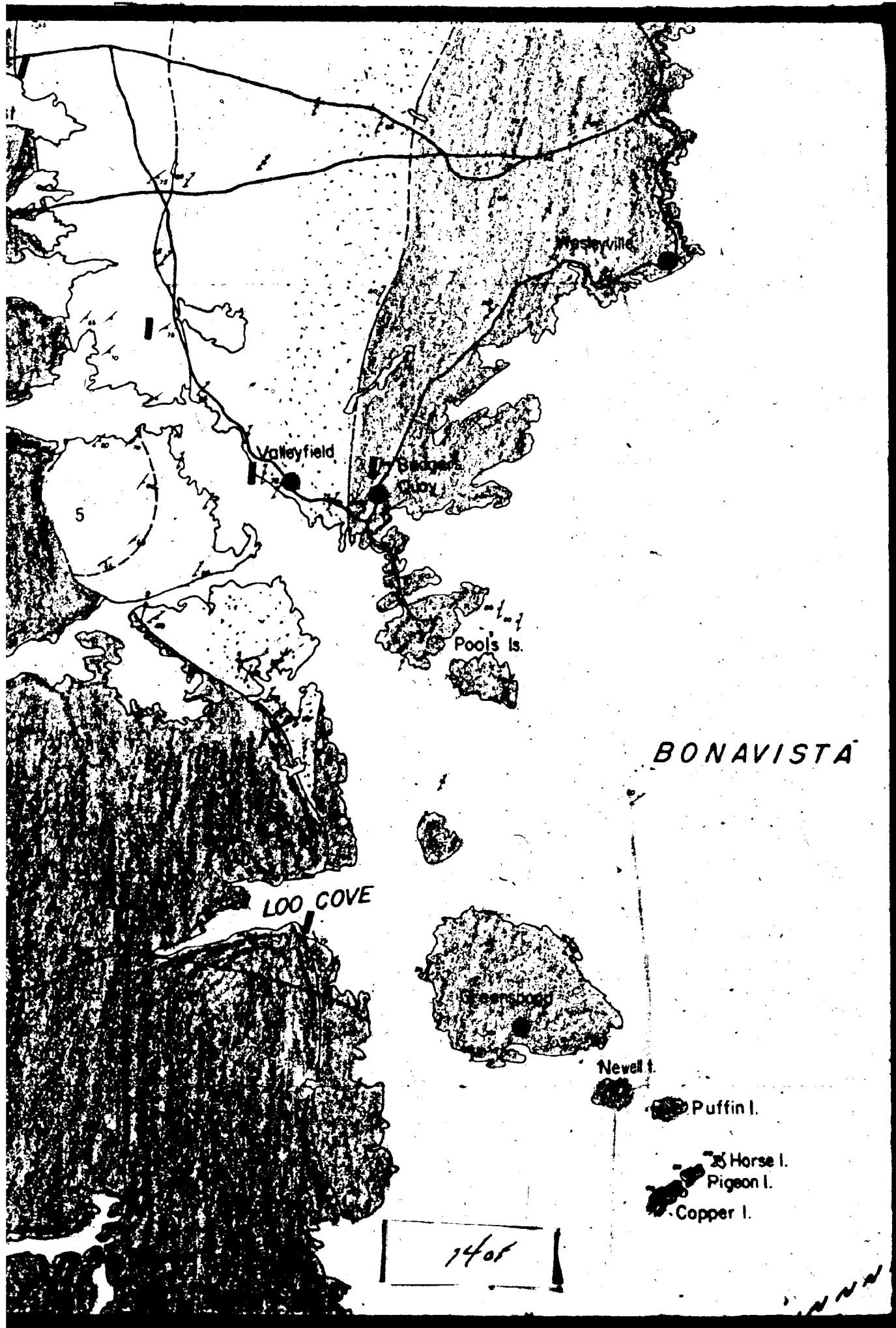




11 OF







Pouch  
Island

Flowers  
Island

BONAVISTA

BAY

New I.

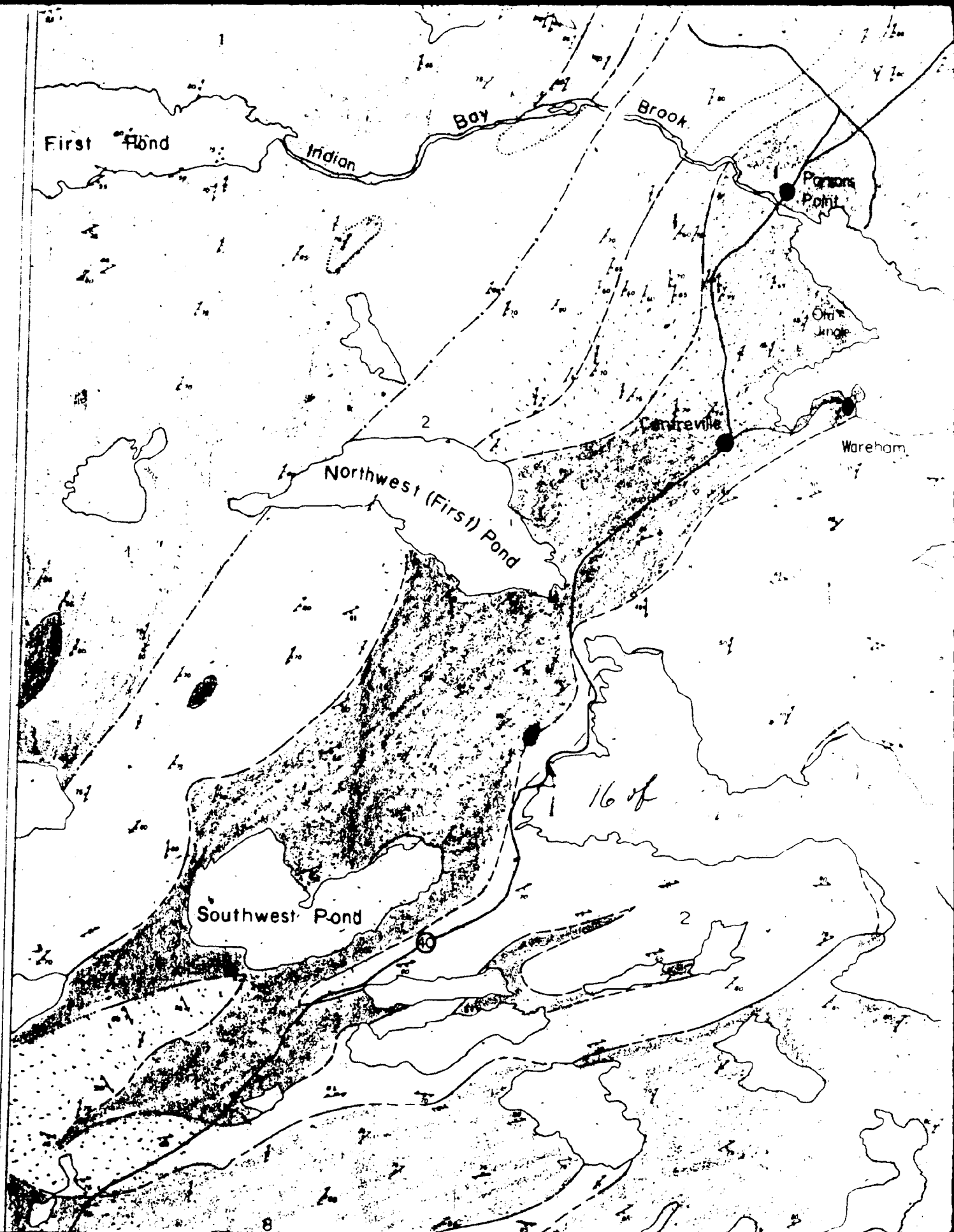
Puffin I.

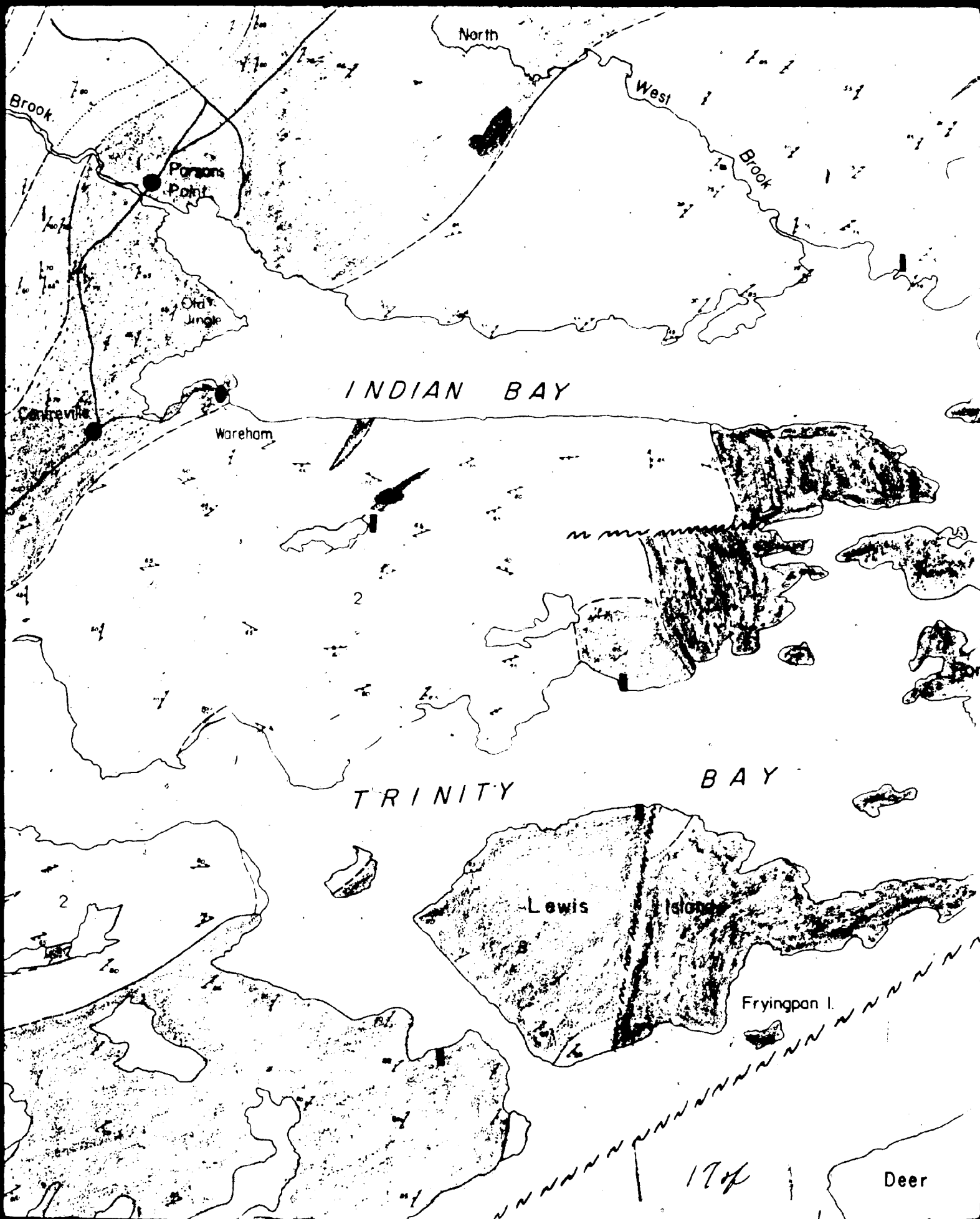
Horse I.

Pigeon I.

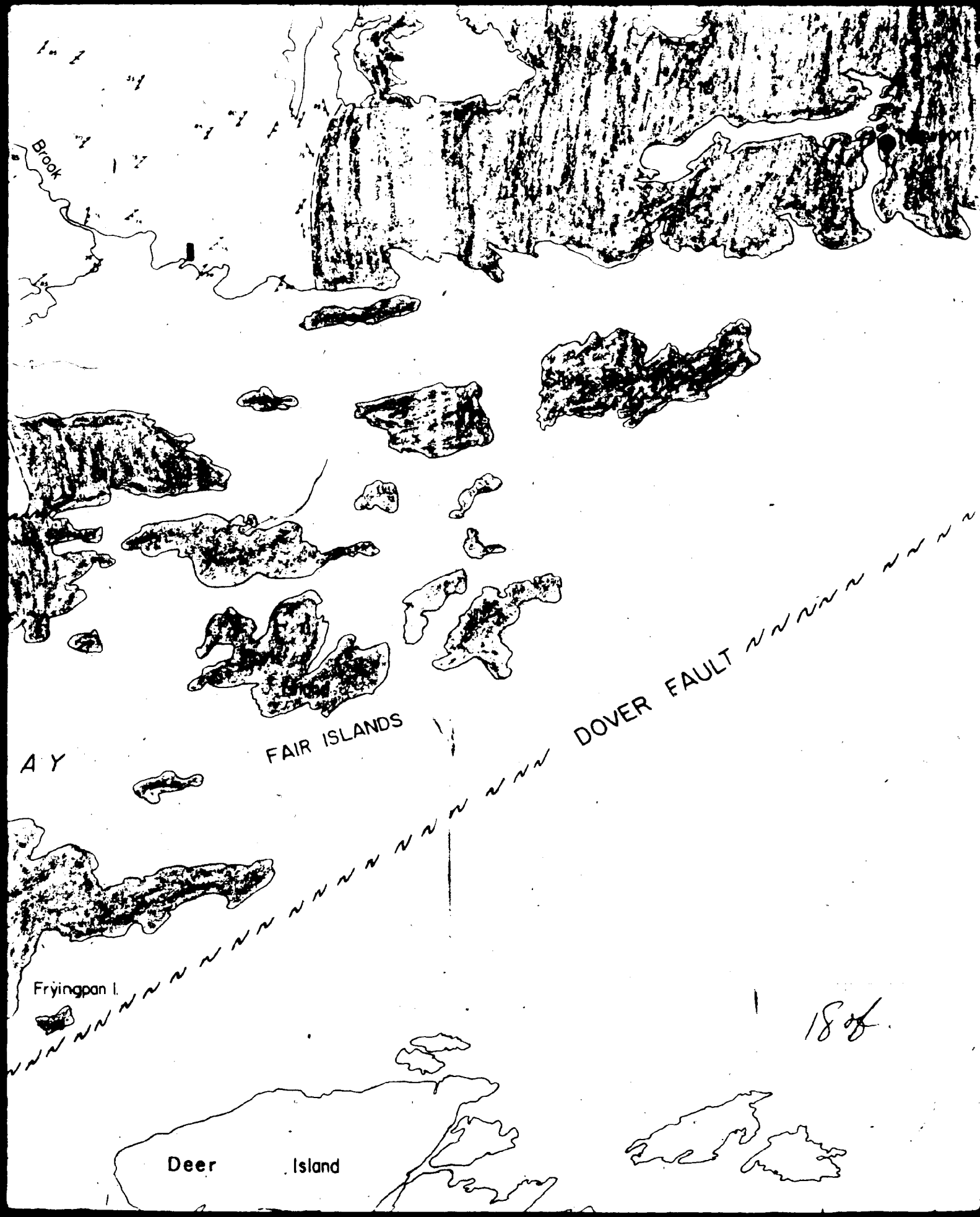
Copper I.

1505







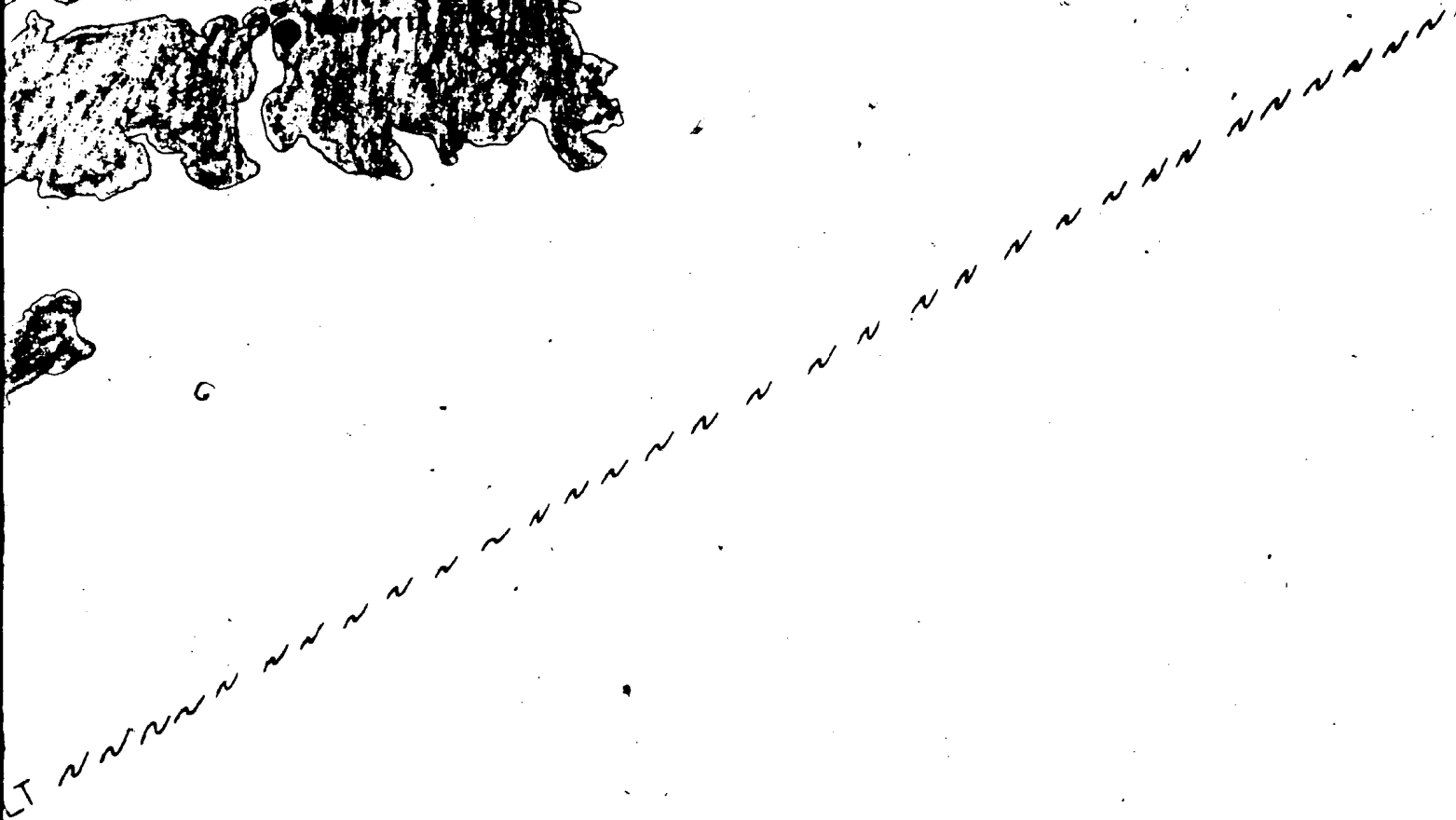


1808





Horse I.  
Pigeon I.  
Copper I.



1905



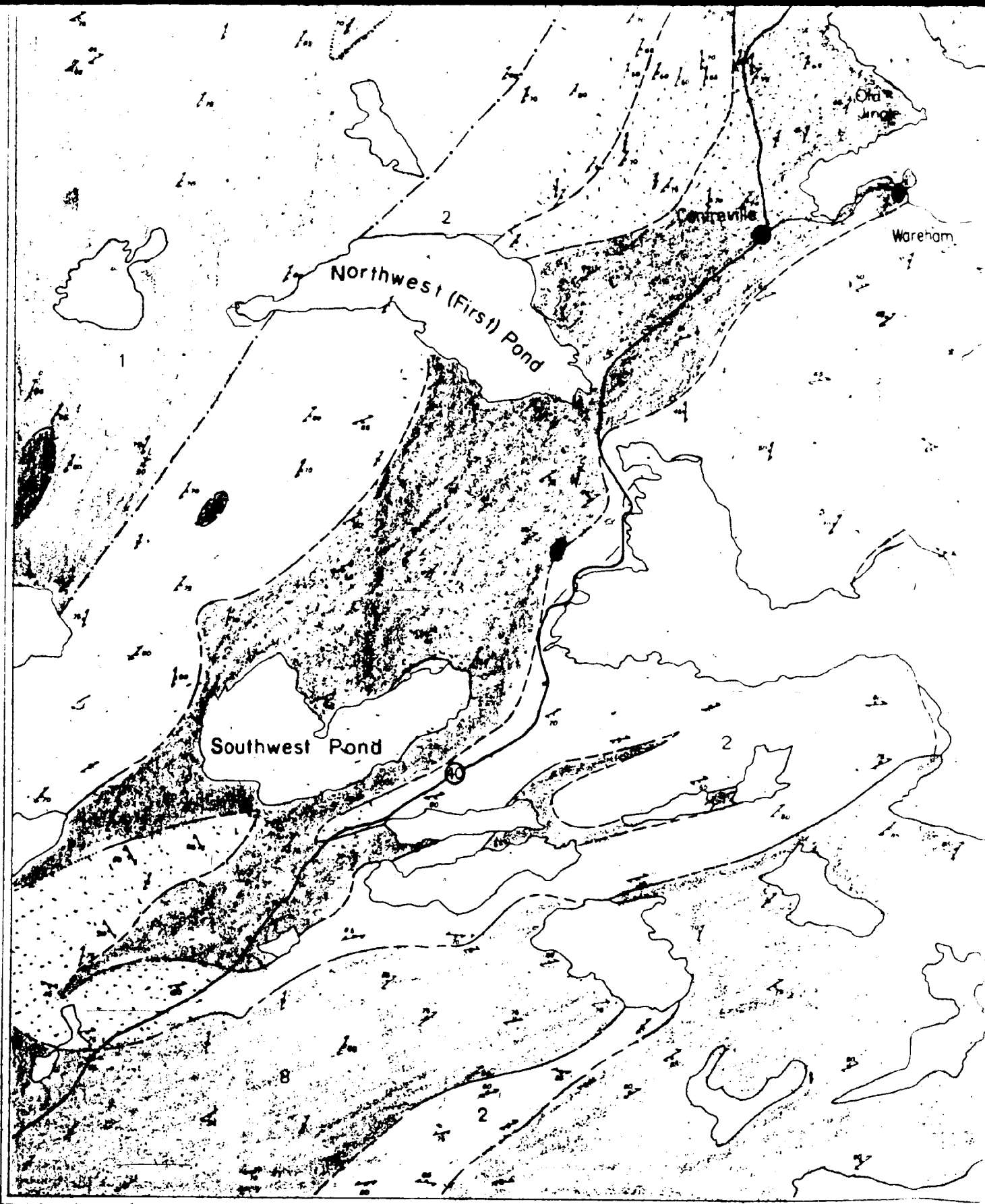
Horse I.  
Pigeon I.  
Copper I.

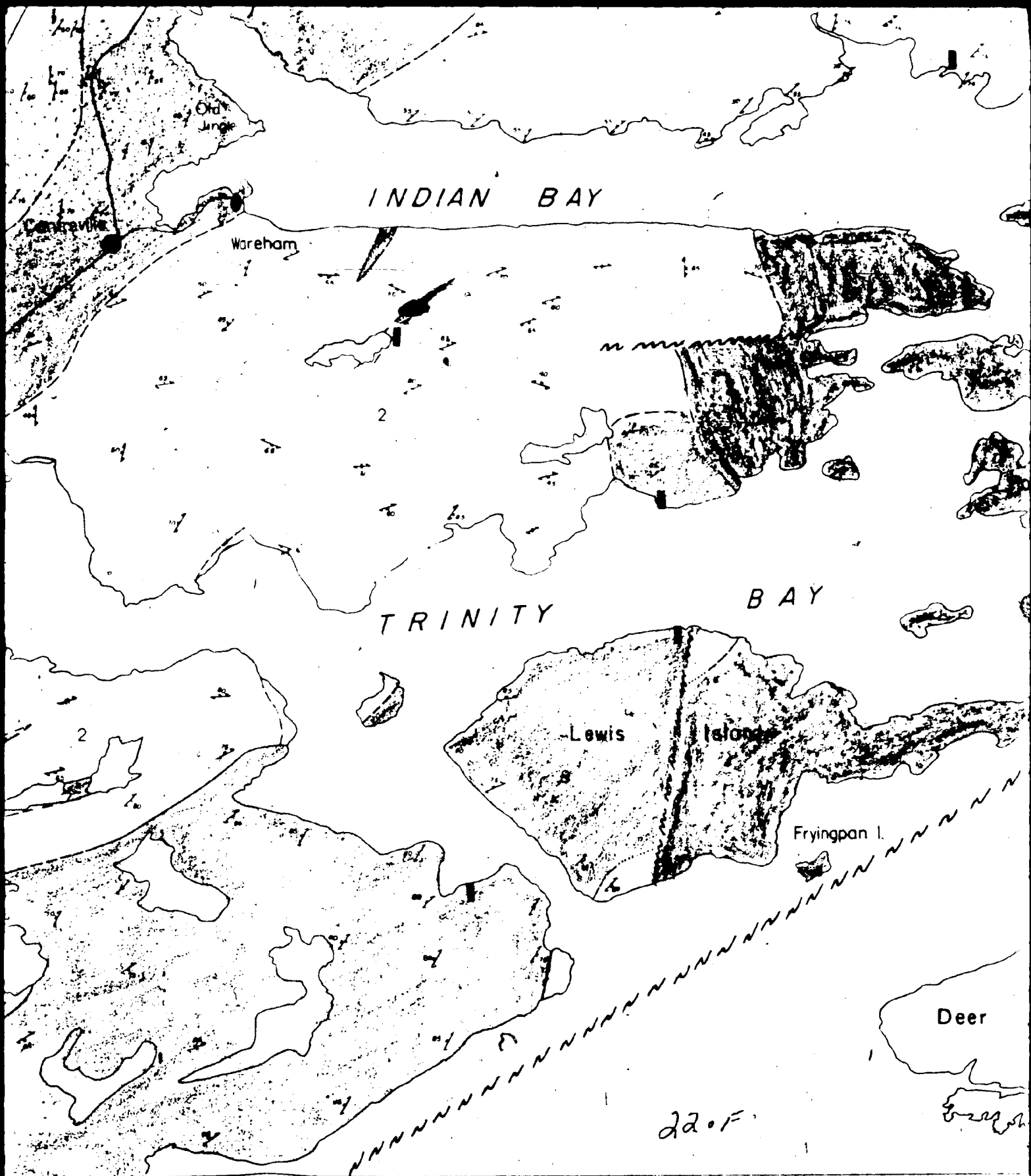
~~~~~

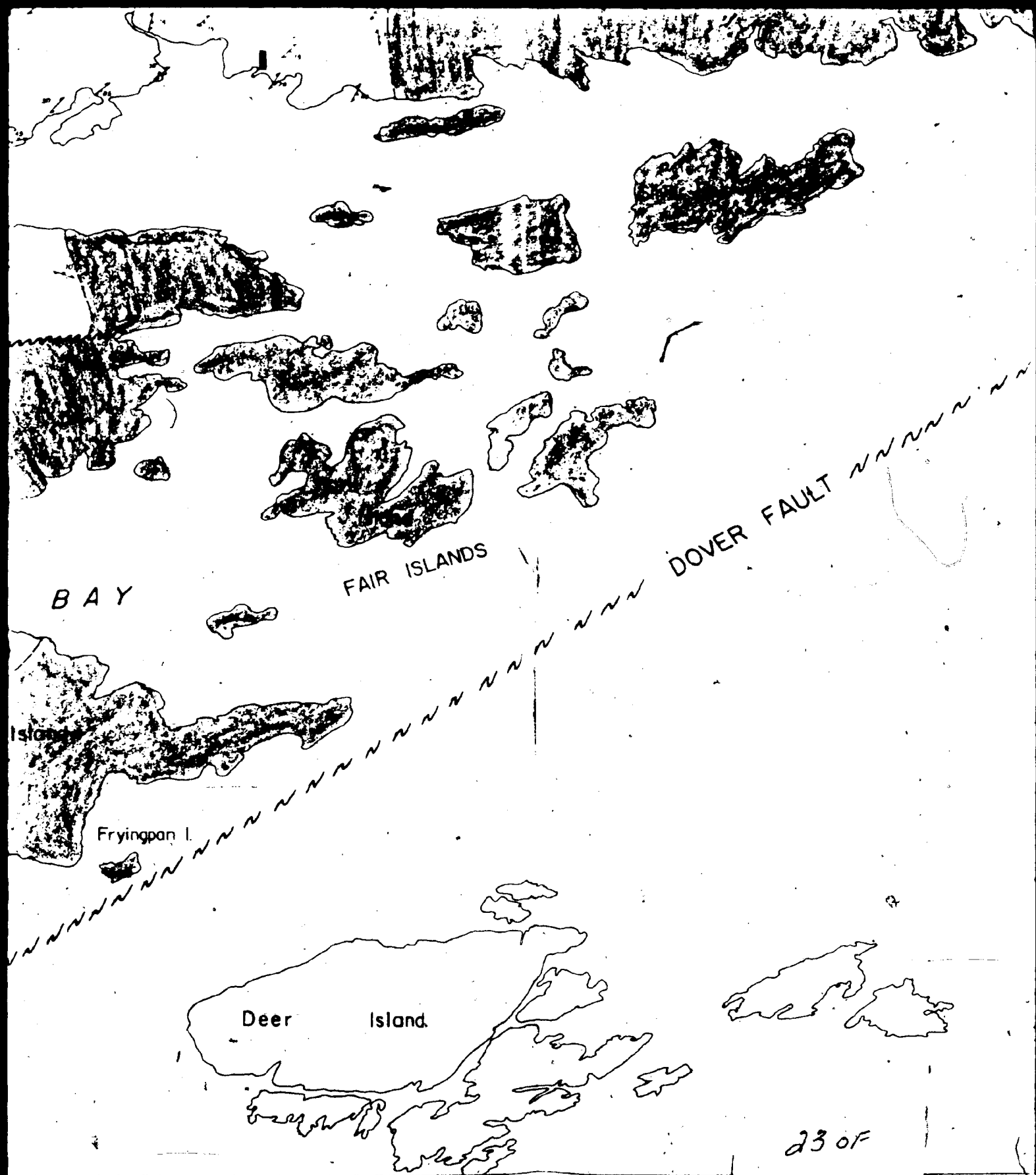
27/4  
20/13

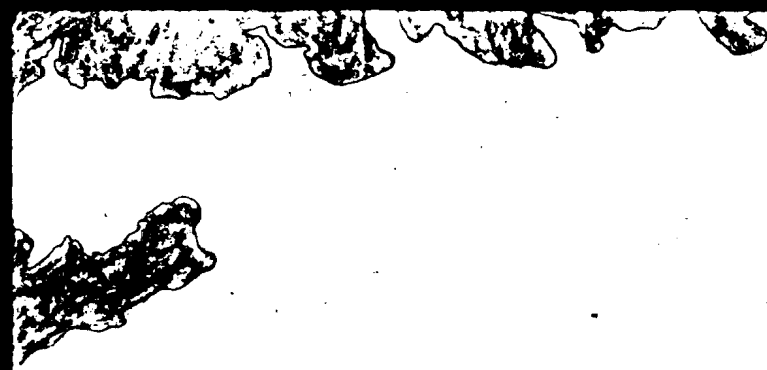


200F









R FAULT ~~~~~



24 or

~~~~~



2F/4  
2C/13



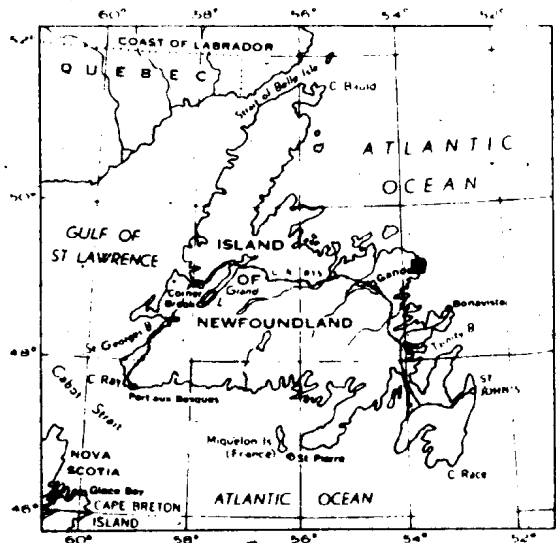
25 of 25

54°00'  
49°23'

55°

20'

10



1 of 1

LO  
**WESLEYVILLE-N**  
ST. BENDAS (Northwest)



50'

45'

LOCATION MAP

WESLEYVILLE—MUSGRAVE HARBOUR (East)  
ST. BENDAS (Northwest)

Scale 1:50,000 Echelle

45'

40'

813

814

815

816

817

818

Deadman's Bay

821

Deadman's Bay

822

DEADMAN'S

BAY

823

824

825

9

9

9

9

9

3 of 1

OUR (East)

40'

35'

D E A D M A N ' S

B A Y

Lumsden

Lumsden Harbour

Lumsden South

Lumsden

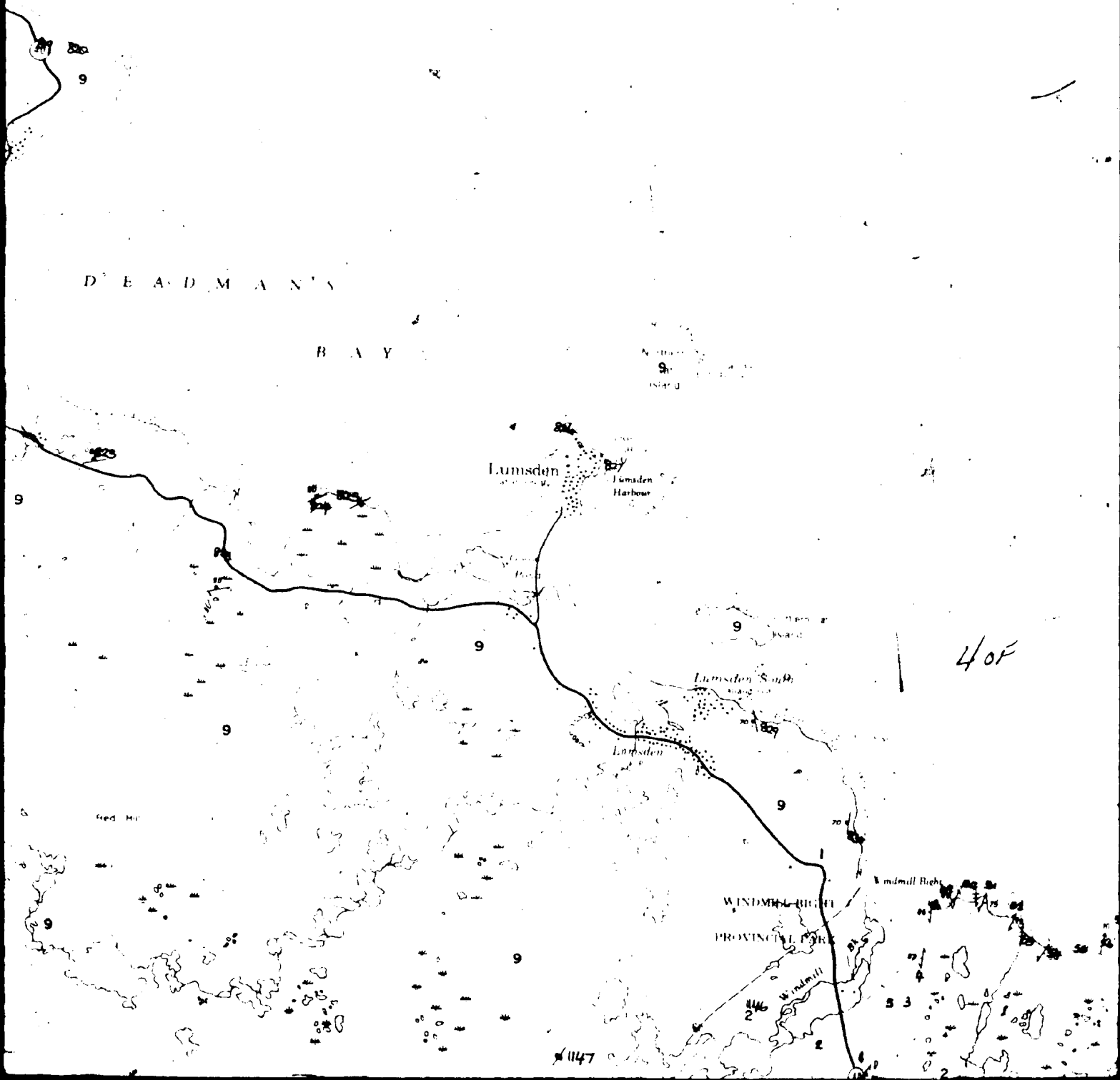
WINDMILL RIDGE

PROVINCIAL PARK

Windmill Ridge

1147

40F



35'

 $53^{\circ}30'$  $+49^{\circ}23'$ 

20'

South

~~ADMINISTRATIVE~~

WINN-DIXIE

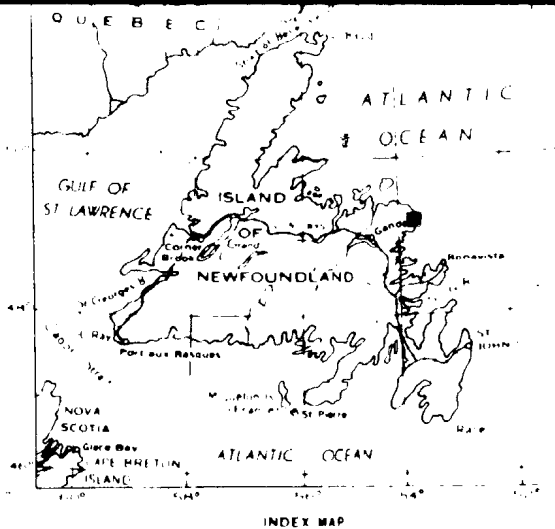
Windmill Bigh

North B...

### Branches

News is

50F



LOCA

**WESLEYVILLE-MU**  
ST. BENDAS (Northwest)

### Scale

**Abstract**

Metres 1 000

\* **arabidopsis** **100%**

60F

9

6

1089

996

५१

C

838

837

839

840

9

90

974

94

gbc

48

926

97

975

974

97

•

6

520

2

/ 59

20/03

Ten Mile Pond

1096

9

1092

156

50  


83

8

832

829

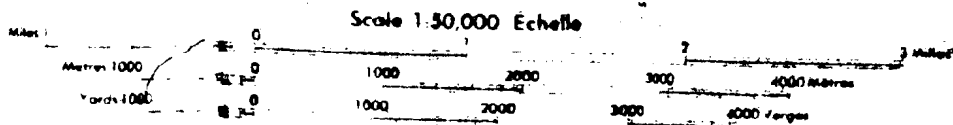
128

51

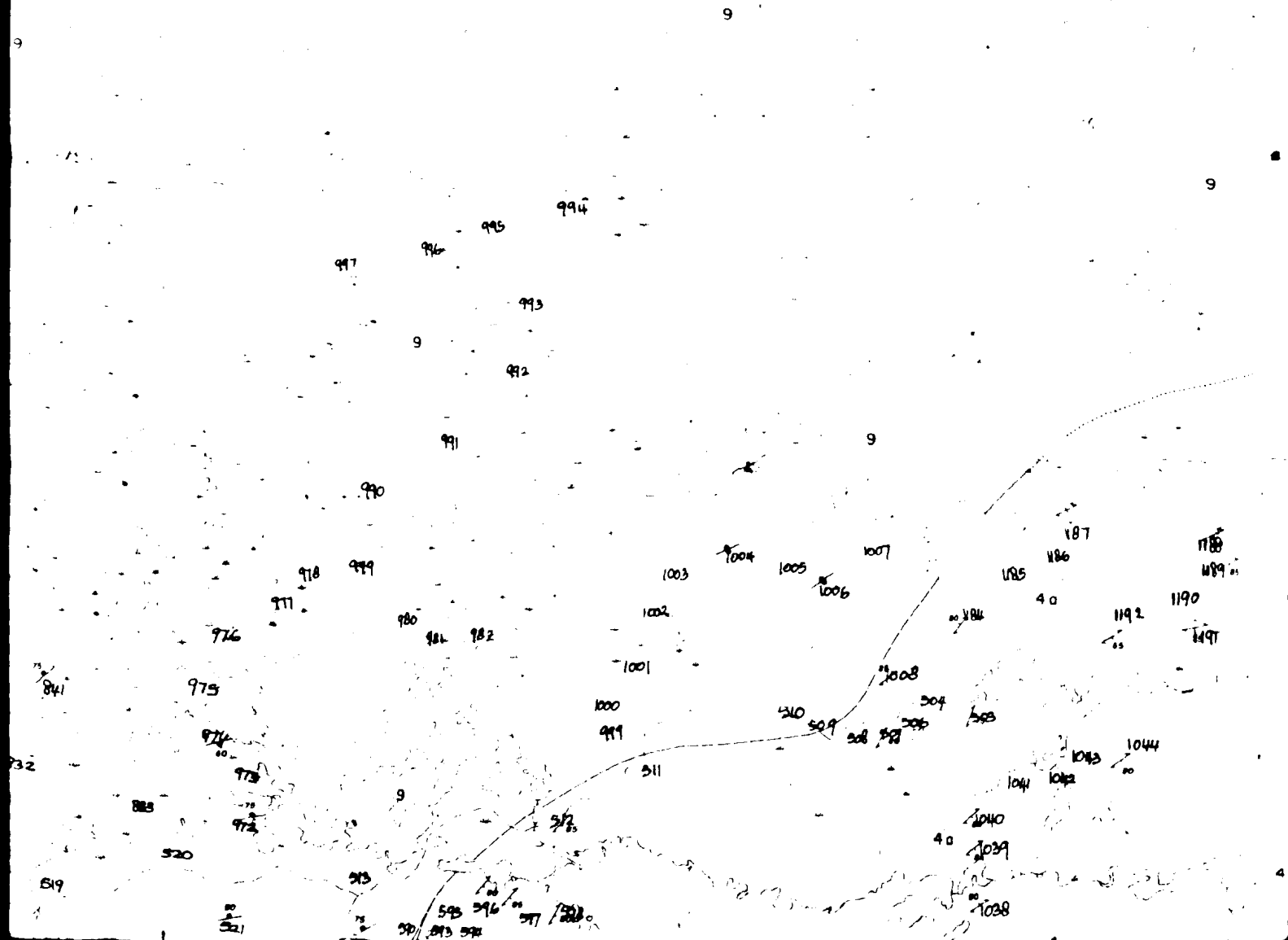
8

LOCATION MAP

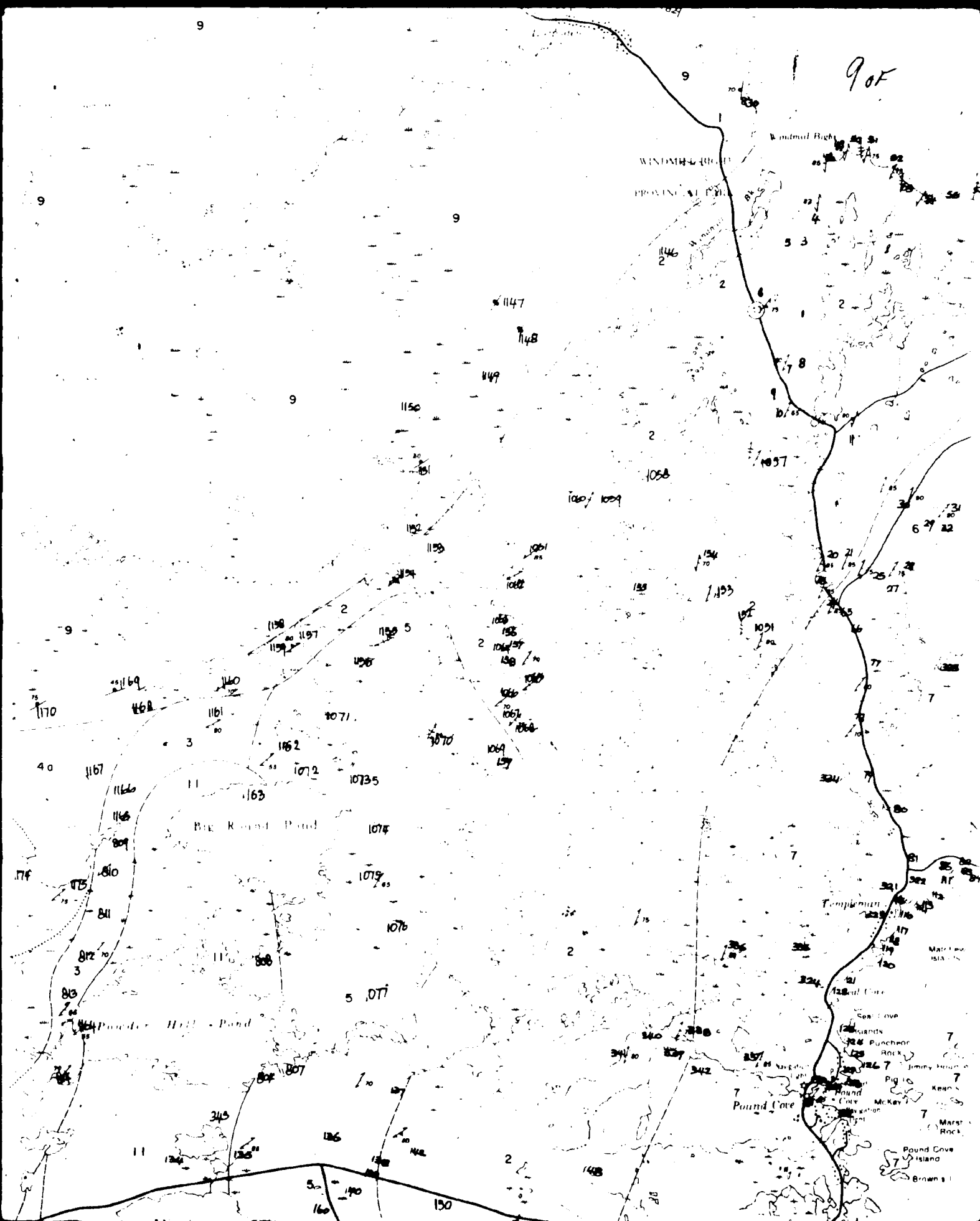
WESLEYVILLE-MUSGRAVE HARBOUR (East)  
ST. BENDAS (Northwest)



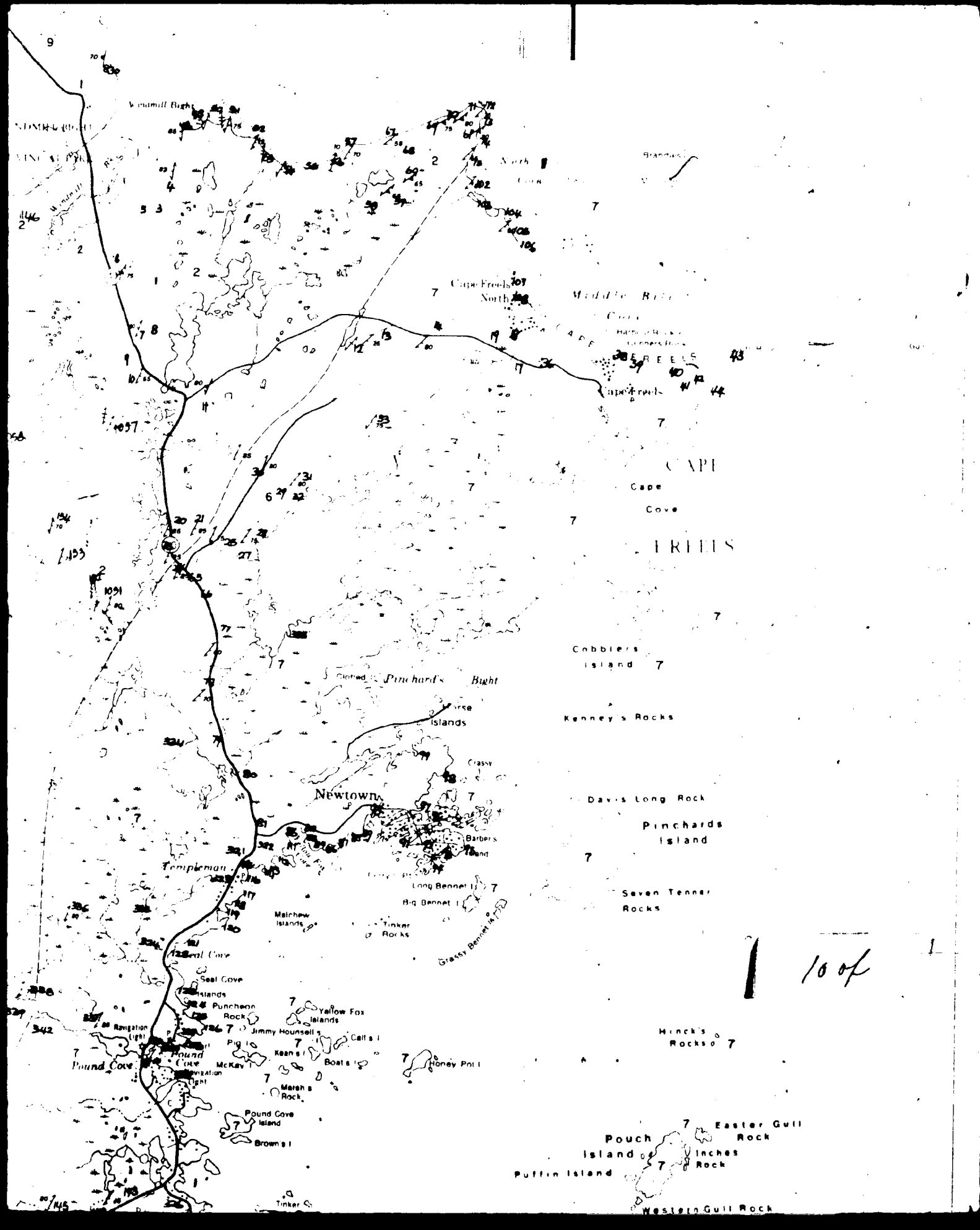
70F



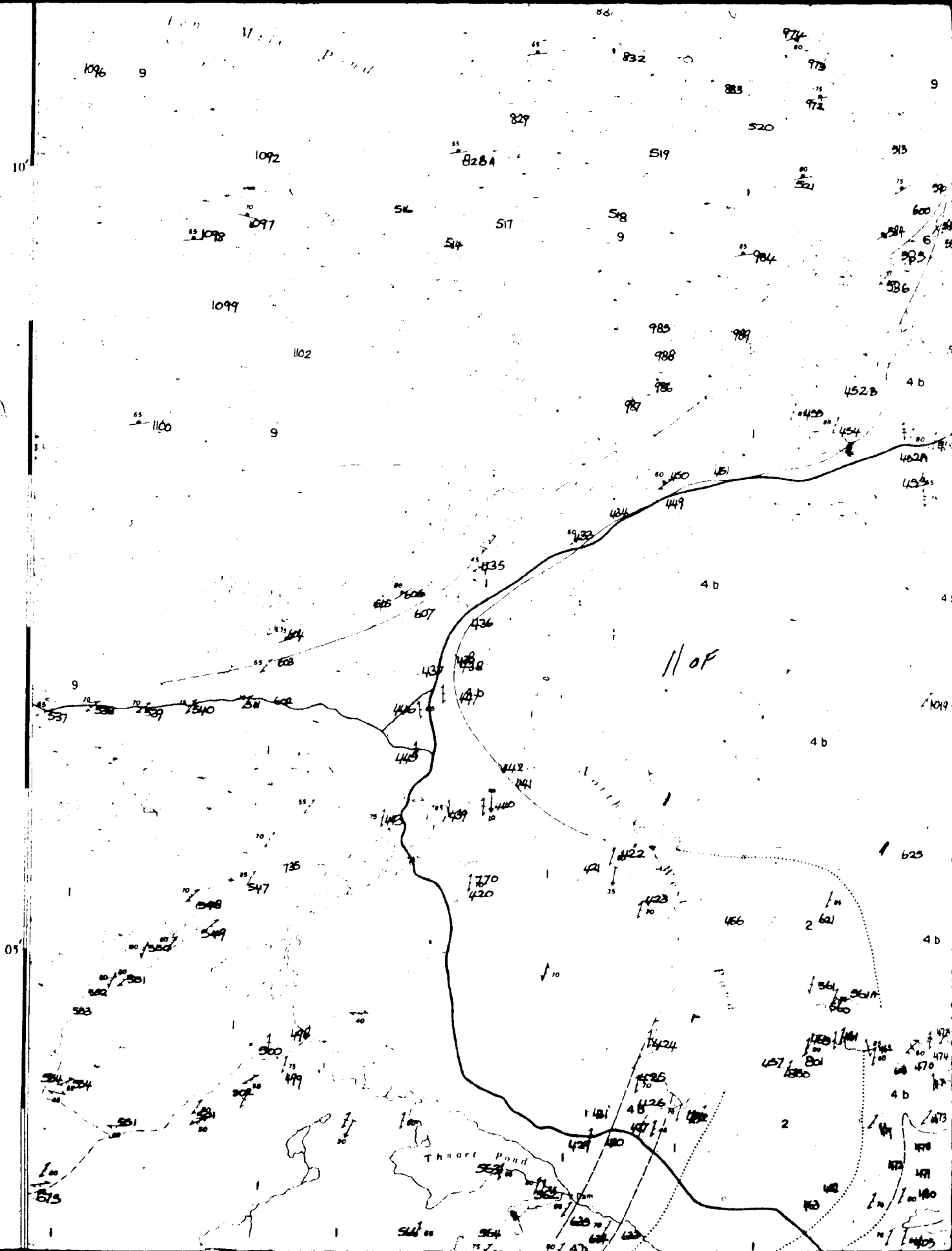
**OUR (East)**

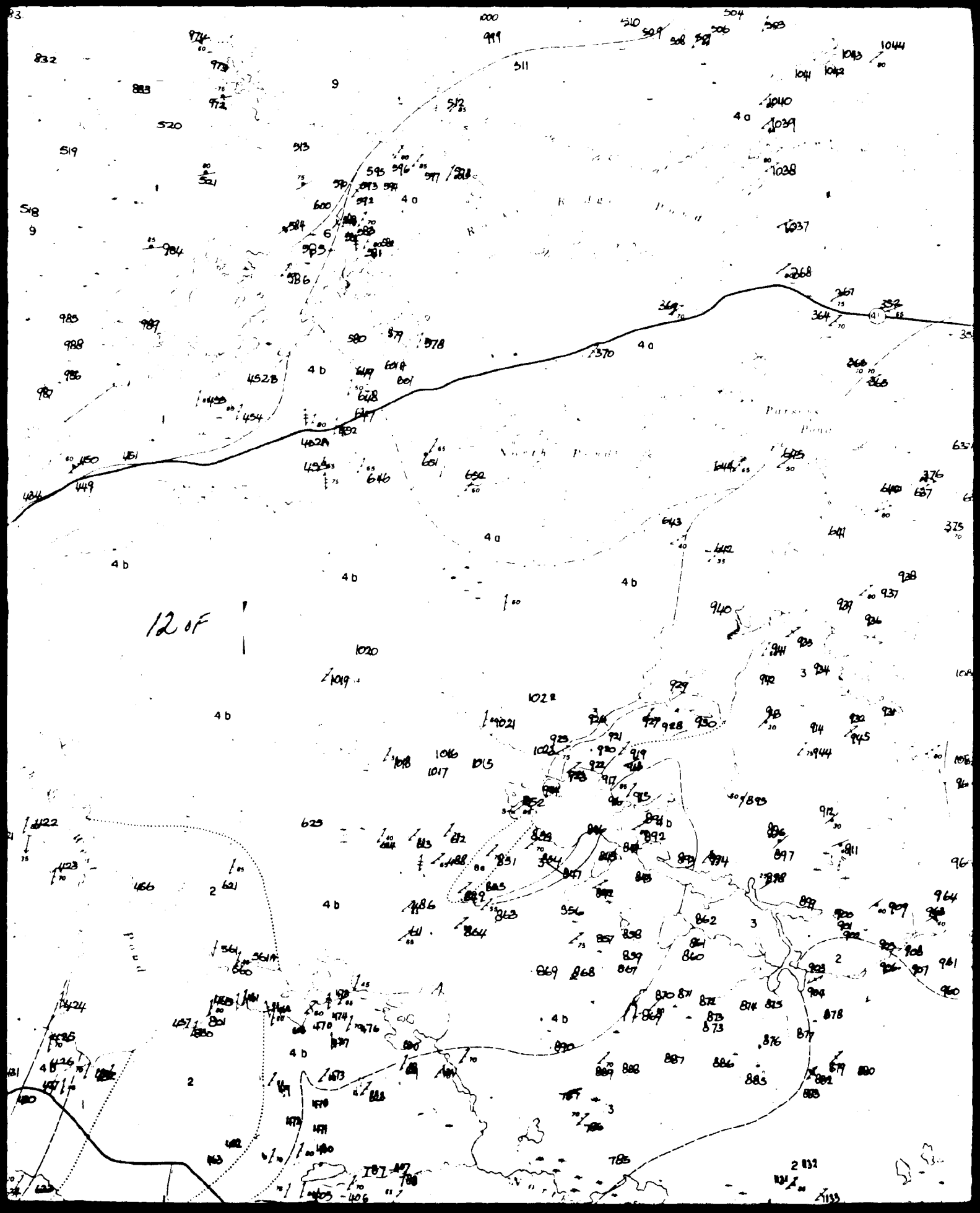


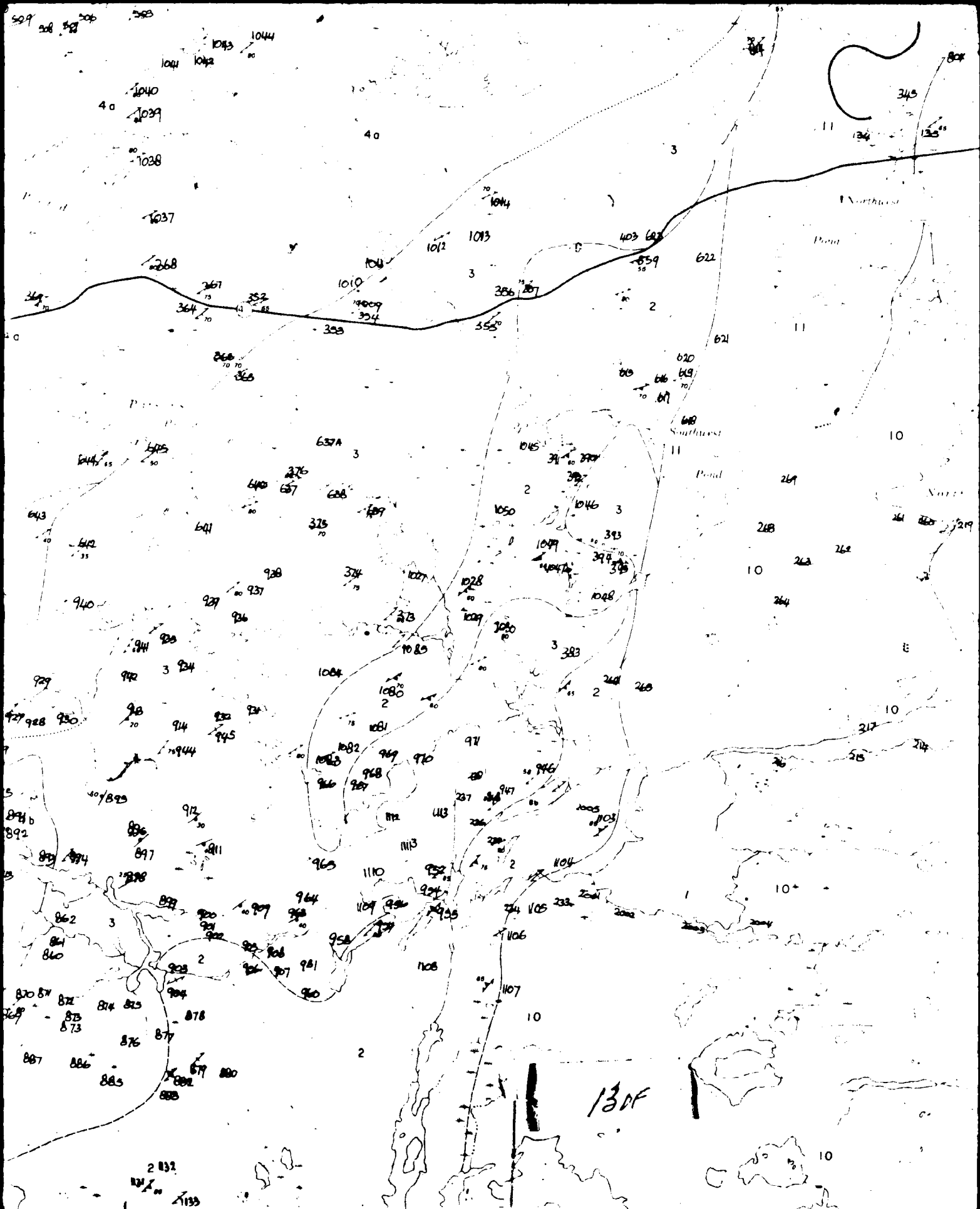


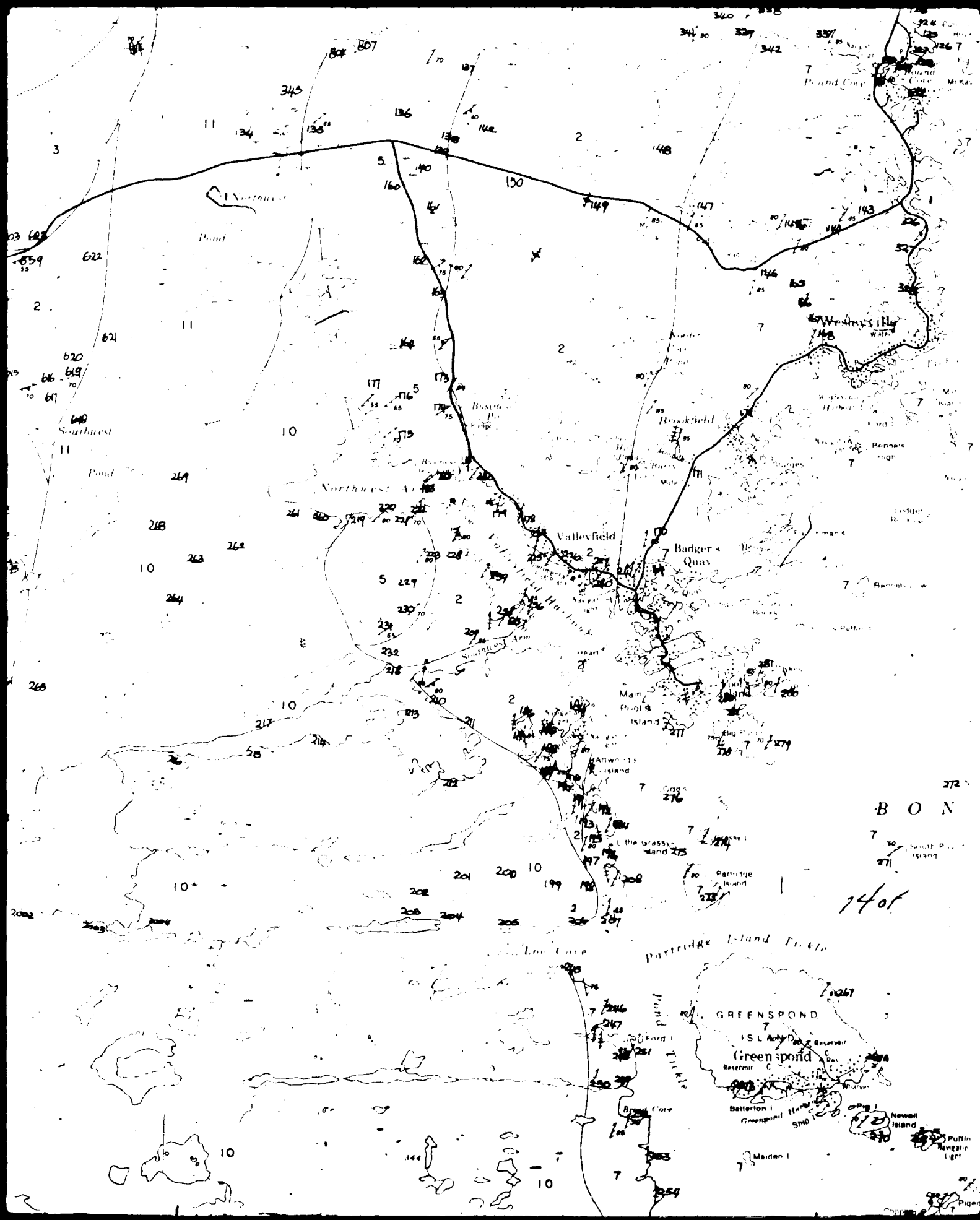


10 of



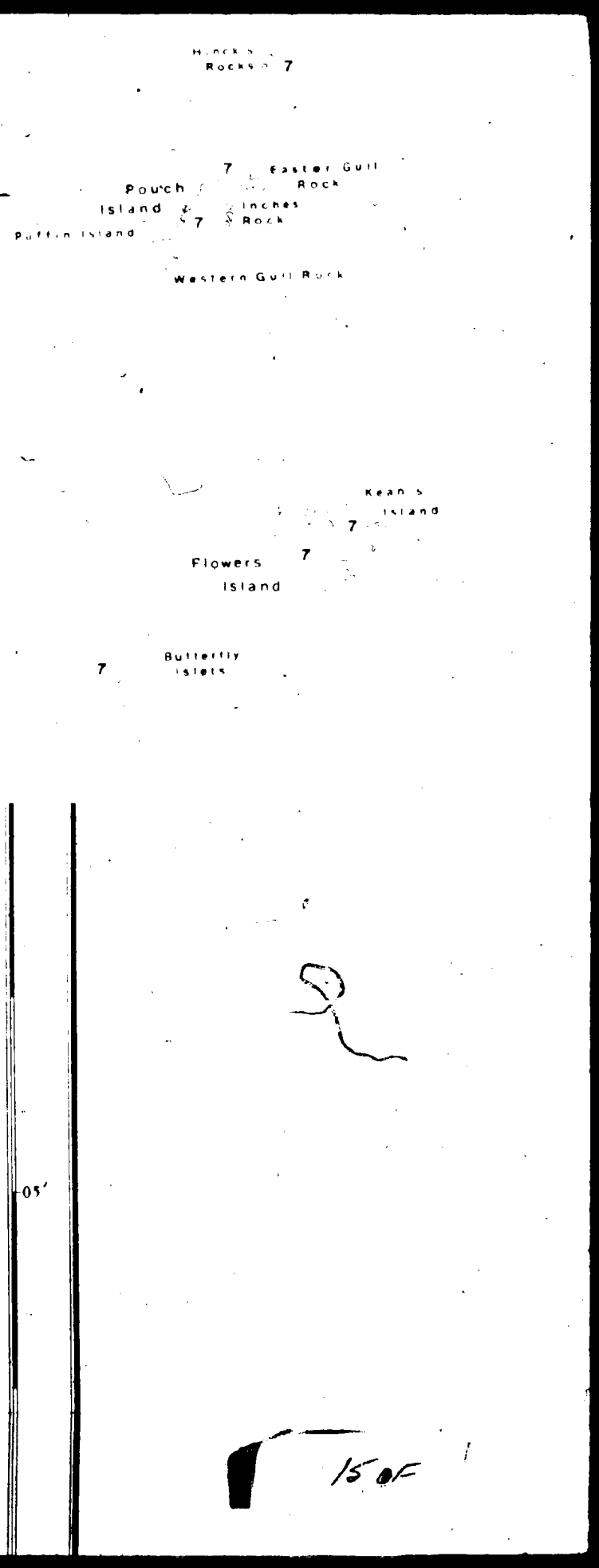
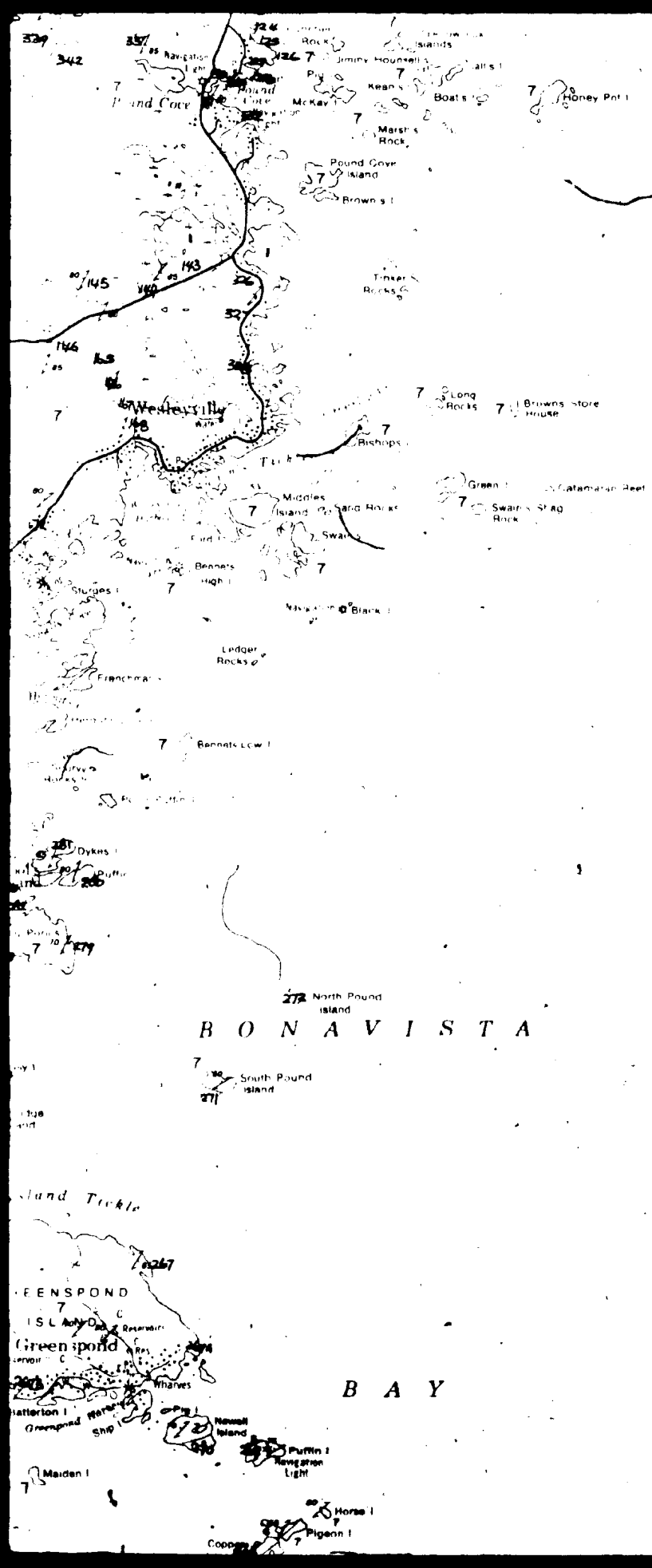


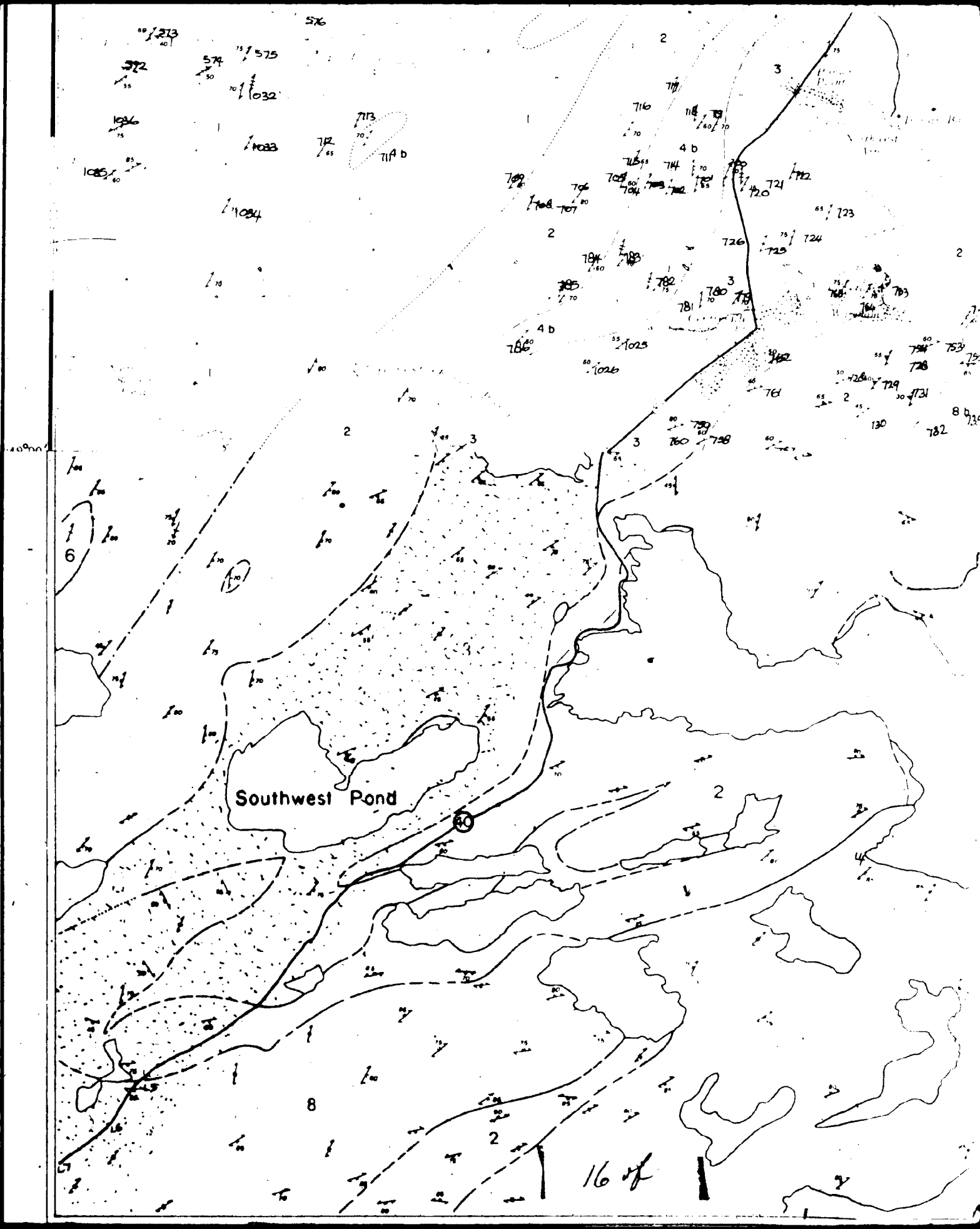


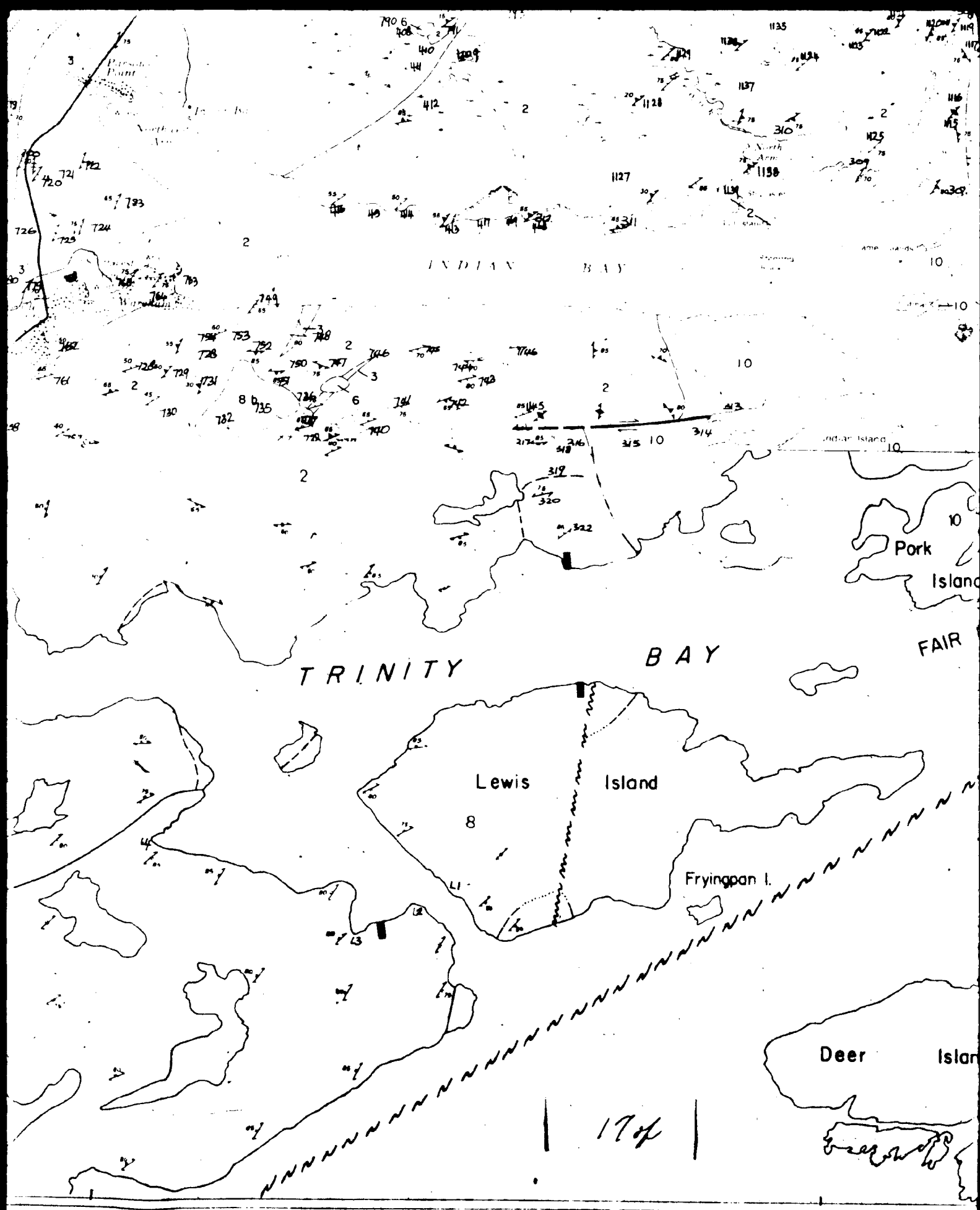


B O N

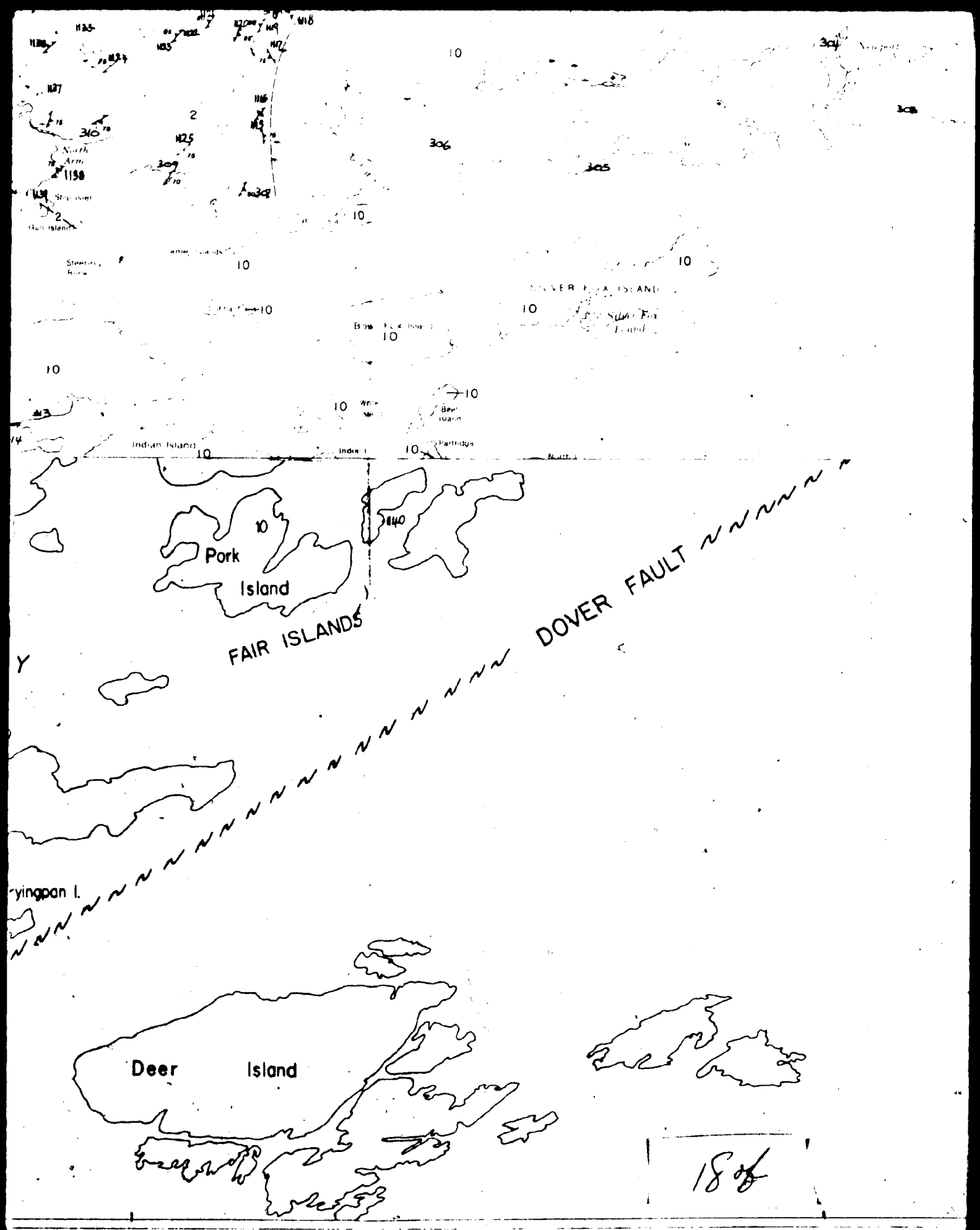
1405











1808

268A 255

Black  
Hicks  
Black Feet

Newport

300

100

202

300

Low Price

10

ULT ~~~~~



1905



20 of 20



